Synthesis, characterization and biological activities of heterocycles: Peptides, O, N and S based small molecules

This work is submitted in fulfilment of the requirements for the degree of Doctor of Philosophy in Chemistry, in the Faculty of Applied Sciences, at Durban University of Technology

Mr. Muthu Thangaraj

2018

Supervisor: Prof. Robert Moonsamy Gengan

DECLARATION

This thesis is being submitted to the Durban University of Technology for the degree of Doctor of Philosophy in Chemistry. I declare that this work is my own and has not been submitted before for any degree or examination to this or any other university or institution for this or any other degree or award.

Student Number: **21356991**

Student: [redacted] Date: 30/07/2018

Mr. Muthu Thangaraj

Supervisor: [redacted] Date: 30/07/2018

Prof. Robert Moonsamy Gengan

Acknowledgement

I still remember the occasion, when I was only three years old, my mother took me in front of Goddess with my father, gave me a slate and chalk and taught me to write the letters அ, ஆ, இ, ஈ… etc. Today, I have finished writing my Ph.D. thesis. Since then it has been a long journey, and my father is always beside me keeping his hand on my shoulder to give me all the support that a father can give to his dearest son to see him on top of the world. My mother's unconditional love, care and prayers have always been with me. She wanted to see me achieve the apex of education; and I am proud that I am still climbing the apex because of her love and wishes. My parents were the first and last to believe that I can achieve my dreams. I don't like to thank my mother and father by means of just a few words. Today, I bow down in front of them for everything.

I am grateful to the lord almighty for his abundant blessings that have lifted me up to this level. I feel immense pleasure in expressing my deep sense of gratitude and indebtedness to my esteemed Gurunathar, Professor **Robert Moonsamy Gengan**, Department of Chemistry, Durban University of Technology, Durban, for his outstanding guidance, constructive criticism, motivation, valuable advice, untiring support and constant encouragement throughout the study holding me strong in all the places I faltered. I express my heartfelt thanks to Dr. D.H. Pienaar, Dr. Charlette Tiloke, Professor K.G. Moodley, Professor G.G. Redhi, Professor K. Bisetty and Dr. K. Ramluckan, Head of Department, Department of Chemistry, for their timely help and support.

I extend my thanks to Professor P. S. Mohan, Head of Department of Chemistry, Bharathiar University, for his motivation and encouragement for my higher studies. It is my pride and pleasure to seize the opportunity to record my deep sense of gratitude to Dr. K. J. Rajendra Prasad, former Professor and Head (UGC-Emeritus Professor), Dr. S. Govindarajan (UGC-Emeritus Professor), Dr. S. P. Rajendran, Professor (Retd), Dr. M. Ilanchelian, Asst. Professor and Dr. R. Prabhakaran, Asst. Professor, Department of Chemistry, Bharathiyar University. I sincerely thank Dr. K. Natarajan, the CSIR-Emeritus Scientist for his kind encouragement.

I express my profound thanks to Professor, Reji Varghese, Scientist, Indian Institute of Science Education and Research, Thiruvananthapuram, Kerala, India.

I also express my sincere thanks to Mr. Dilip Jagjivan, University of KwaZulu-Natal, Westville campus. Without him, a major part of my thesis would have remained blank. Thanks for filling the gap and training me in NMR spectral data acquisition. Words seem to be inadequate to express my heartfelt thanks to my colleagues Mr. M. Arul, Mr. A. Vasanthakumar, Mr. A. Nandhakumar, Dr. Deepak Gussain, Dr. Abishek Guldhe, Dr. G. Yathirajan and Mr. Ajay

Vasudeo Rane for providing food, spending money all the time, their limitless care and support during the stay and their countless help to compile this dissertation successfully.

I am greatly indebted to Mr. G. Sateesh Kumar, Govt. Arts College, Nandanam, Dr. P. Govindaraj, Associate Professor and Head, Mrs. S. Radha, Mr. P. Ramasamy and Mr. C. Sathya Kumar, Department of Chemistry. I also thank Mr. Venkata Subbian, Department of Physics for his guidance. I wish to extend my thanks to Dr. D. Jacqueline Periyanayakam, Associate Professor and Head, Dr. P. Rajendran, former Head and Professor, Mrs. A. Kamaleswari, Department of English, Dr. K. Sellathai and Mrs. Kaliyanantham, Department of Tamil, SBK College for their support and motivation.

I wish to thank my senior Dr. K. Anand for introducing Durban University of Technology in my life. I extend my thanks to Research seniors Dr. R. Selvakumar, Dr. A. Selvasharma, Dr. K. Shanmugaraj and Dr. P. Manivel, Dr. S. Packiyaraj, Bharathiar University, for their advice and motivation. I wish to extend my thanks to Mr. Jimmy Chetty, Dr. Thishana Singh and Mr. Rajein, other non-teaching staff members of the department for their encouragement and support.

I express my sincere thanks to Mr. Talent Makhanya for letting me to go forward and his motivation in all the time, Mr. M. Sureshkumar for supporting and motivating me in all the time and his mother for her wishes, Dr. Sivanandhan, Ms. Nikisha Rajkoomar and Ms. Kaunda Thabisile for their care, discussion and support. I also thank Dr. M. Shree Ramesh, Dr. B. Ravindran, Mr. Faiz Ahmad, Dr. Sanjay Kumar Gupta, Mrs. Poonam Singh, Dr. Gulshan Singh, Dr. Venkat, Dr. Mithilkumar, Mr. Bibhuti Ranjan, Ms. Deepthi and Mr. Srinivasan for their support in tough times.

Acknowledgement will be unsound if I fail to thank my friends Mr. K. Neppoliyan and his family, Mr. N. Hariharan and his family, Mr. G. Naveen Vasu, Mr. M. Manikandan (Remo) and his mother, Mr. S. Suman, Mr. Senthilkumar, Mr. Kashi Viswanath and his family, Mr. B. Tamilarasan, Mr. S. Samraj, Mr. B. Alagarsamy, Dr. Deepak Raja (MBBS, Russia), Ms. A. Gnanasundari and her family, Mrs. Gnanadeepam and her family, Mrs. Karthigai Priya, Ms. Jeyadevi, Mrs. K. Suganya, Mrs. Bavani, Mrs. Revathy, Mrs. K. Suryakala, Mrs. R. Muthu Priya and her family, Ms. Chitra, Ms. Ajantha, Mrs. K. Suriya Praba, undergraduate and post-graduate friends.

In addition, several people have knowingly and unknowingly helped me in the successful completion of this project. My sincere gratitude goes to Professor Sibusiso Moyo, Deputy Vice-Chancellor and Dr. Bloodless Dzwario, Grants Administrator, for their help and my fellowship arrangements for research project. I acknowledge the Durban University of Technology and National Research Foundation for the financial support. My sincere gratitude goes to Professor Suren Singh, Executive Dean, Ms. Gill Shackleford, Faculty officer of the Faculty of Applied

Science, Durban University of Technology. I take this golden opportunity to express my heartfelt thanks to mother Mrs. Shirley Gengan and sisters Dr. Kerena and Ms. Trinisha for their affection and help.

I take this golden opportunity to express my heartfelt thanks to my parents Mr. V. Thangaraj and Mrs. T. Pandiyammal @ Parimala (late), my brothers Mr. T. Thirumurugan, Mr. T. Elangeswaran and his wife Mrs. E. Kanaga, my sisters Ms. T. Sivanandhini, Mrs. S. Krishnaveni and her husband Mr. S. Saravanan for their everlasting love, support, motivation and endless help.

I also widen my thanks to my uncle Mr. Mariyappan, Police Inspector Mr. Chinnathambi @ Selvaraj (late), Mrs. Chinnathayee, Mrs. Parvati (late), Mr. K.P. Karuppu and his family, Mr. Ravikumar and his wife, Mr. Jegan, Mr. Suresh, Mr. Ganesh and his family, Thandiyampatti Mr. Prabhu and his family, brother Mr. Muthupandi and his family, uncle Mr. Bose and his family, Mr. Ilaiyaraja and other relatives for their care and support.

I am deeply indebted to many, who helped me in different ways throughout this dissertation and without whom it could not have been achieved.

Muthu Thangaraj.

தான் கஷ்டப்பட்டாலும் தான் பட்ட கஷ்டங்களை தன்னோட பசங்க படக்கூடாதுனு மழையிலும் வெயில்லையும் கஷ்டப்பட்டுக் கூலி வேலை பார்த்து எங்க எல்லோரையும் படிக்க வைச்சு பெரியாளாக்குன என்னோட அப்பாவுக்கும், தன் பிள்ளைங்க பெரிய இடத்துல இருக்கணும்னு உசுரையே எங்க மேல வச்சு இருந்த என்னோட அம்மாவுக்கும், தன்னைப்போல என்னை நினைச்சு கஷ்டத்துலயும், சந்தோஷத்துலயும் எப்பவும் கூட நிக்கிற என்னோட அன்புத் தம்பி, தங்கச்சிக்கும், அக்காவுக்கும், அன்பான மாமாவோடு, கனகாவுக்கும் இந்த ஆராய்ச்சியை அர்ப்பணிக்கிறேன்...

அன்புடன், **த. முத்து.**

Dedicated to my lovable Family and Friends

General remarks

The numbers representing the structure are for the particular chapter only. Each chapter contains a separate experimental section. The following abbreviations are used in text:

MDR	: multiple drug resistance
SAR	: structure-activity relationship
SBDD	: structure-based drug design
TOF	: time of flight
MS	: mass spectra
m.p	: melting point
℃	: Centigrade
mmol	: Milli mole
HASIL	: humic acid supported ionic liquid
nm	: Nano meter
BN	: boron nitride
Fe/BN	: iron loaded boron nitride
I/BN	: iodine loaded boron nitride
Ca/BN	: calcium loaded boron nitride
min	: minutes
TLC	: thin layer chromatography
XRD	: X-ray diffraction
SEM	: scanning electron microscopy
EDX	: Energy Dispersive X-ray
BET	: Brunauer-Emmett-Teller
TEM	: transmission electron microscopy
DSC	: differential scanning calorimetry
TGA	: thermogravimetric analysis
FTIR	: Fourier transform infrared spectroscopy
NMR	: nuclear magnetic resonance
$POCl_3$	: phosphoryl chloride
EtOAc	: ethyl acetate
PE	: petroleum ether
$CHCl_3$	: chloroform

DMSO	: dimethyl sulfoxide
DCM	: dichloromethane
MeOH	: methanol
EtOH	: ethanol
THF	: tetrahydrofuran
US	: Unites States of America
CHF	: congestive heart failure
HIV	: human immunodeficiency virus
Et_3N	: triethylamine
IC_{50}	: half maximal inhibitory concentration
THAM	: tris-hydroxymethylaminomethane
TB	: tuberculosis
Topo-I	: topoisomerase-I
DNA	: deoxyribonucleic acid
1,4-DHPs	: 1,4-Dihydropyridines
mGlu 1	: metabotropic glutamate receptor 1
DLA	: dihydrolipoic acid
AChE	: acetylcholinesterase
ROS	: reactive oxygen species
AIDS	: acquired immune deficiency syndrome
MCRs	: multicomponent reactions
Ugi-4CR	: Ugi four component reaction
UDC	: Ugi-Deprotection-Cyclization
PTSA	: *p*-Toluenesulfonic acid
HCl	: hydrochloric acid
DMAP	: dimethylamino pyridine
HMTA	: hexamethylenetetramine
CTABr	: cetyl trimethyl ammonium bromide
MW	: microwave
Cs_2CO_3	: Cesium carbonate
Pd/BN	: palladium loaded on boron nitride
DETA	: diethylenetriamine
h	: hours
ILs	: ionic liquids

S. aureus	: *Staphylococcus aureus*
B. cereus	: *Bacillus cereus*
E. faecalis	: *Enterococcus faecalis*
P. aeruginosa	: *Pseudomonas aeruginosa*
E. coli	: *Escherichia coli*
C. albicans	: *Candida albicans*
UTI	: urinary tract infections
DPPH	: 2,2-diphenyl-1-picrylhydrazyl-hydrate
QLPs	: quinolinyl-lipoyl peptides
QOLP	: quinolonyl-lipoyl peptide
rt	: room temperature
[bmim]BF_4	: 1-butyl-3-methylimidazolium tetrafluoroborate
LB	: Luria Bertani
PD	: potato dextrose
MIC	: minimal inhibitory concentration
QPs	: quinolinyl-*4H*-pyrans
QOPs	: quinolonyl-*4H*-pyrans
HASIL	: humic acid supported ionic liquid
IPs	: indolyl-4*H*-pyrans
HEAA	: 2-hydroxyethyl ammonium acetate
BAIL	: Brønsted acid ionic liquid
HA	: humic acid
[bmim]SCN	: 1-butyl-3-methylimidazolium thiocyanate
CFQ	: 2-chloroquinoline-3-carbaldehyde
CMFQ	: 2-chloro-6-methylquinoline-3-carbaldehyde
CFFQ	: 2-chloro-7-fluoroquinoline-3-carbaldehyde
MQC	: 2-methoxyquinoline-3-carbaldehyde
IOPN	: 3-(3*H*-indol-3-yl)-3-oxopropanenitrile
BTQPs	: α-aminobenzylthioquinolinyl phosphonates
APs	: α-aminophosphonates
h-BN	: hexagonal boron nitride
B_2O_3	: boron trioxide
BTQC	: 2-(benzylthio)quinoline-3-carbaldehyde
BTQ-DHPs	: benzylthioquinolinyl-1,4-dihydropyridines

CAN	: cerium ammonium nitrate
PPh_3	: triphenylphosphine
ASA	: alumina-sulphuric acid
N_2	: nitrogen gas
DMAD	: dimethyl acetylene dicarboxylate
APCs	: 2-amino-*4H*-pyran-3-carbonitrile derivatives
TEBA	: benzyltriethylammonium chloride
2D	: two-dimensional
$[RE(PFO)_3]$	: Rare earth perfluoro octanoate
TMSCN	: trimethylsilyl cyanide

A Labcon Ultrasonic 5019U was used to generate ultrasonic irradiation and homogenize the reaction mixture. CEM discover microwave reactor was used for the reaction.

All chemicals were purchased from Sigma-Aldrich and used without further purification. Solvents used were of synthesis grade. The X-Ray diffraction analysis was conducted with a Philips PW 1050 diffractometer set at 1 minute with a scanning step size of 0.02º from 40º to 100º 2θ using monochromated CoK_α irradiation. Data was captured with a sietonics 122D automated microprocessor linked to a diffractometer. A Carl Zeiss Ultra Plus scanning electron microscope with EDX detector was also used. The TGA and DSC analysis were conducted with TA instruments. TEM analysis was conducted with a JEOL 1010 TEM (Korea, Japan) and images were captured with iTEM Images capture software (v5.0). Melting points were determined by Stuart SMP10 and were uncorrected. The IR spectra were recorded on Perkin Elmer 537 spectrophotometer instrument, using ATR disc and the absorption frequencies were expressed as ν_{max} cm^{-1}. ^{1}H-NMR and ^{13}C-NMR spectra were recorded on BRUKER 400 MHz spectrometer using tetramethylsilane (TMS) as an internal standard. The chemical shifts were quoted in parts per million (ppm). The following abbreviations are used:

s	: singlet
brs	: broad singlet
d	: doublet
dd	: doublet of doublet
dt	: doublet of triplet
t	: triplet

td	: triplet of doublet
q	: quartet
m	: multiplet
J	: coupling constant in Hertz (Hz)

The chemical shift values were recorded on δ scale and the coupling constants (*J*) were expressed in hertz. The progress of the reaction was monitored by TLC using aluminium plates with silica gel (Sigma-Aldrich and Fluka). Columns packed with activated silica gel (60-120 mesh) were used to purify the crude products. Petroleum ether used was of boiling range 60-80℃.

For some of the compounds especially for ^{1}H-NMR values, splitting patterns, integral values and the intensity of peaks were ascertained from its expanded version of the spectrum and the copies are not produced in the thesis. *J* values were averaged. The elemental analyses (C, H and N) were obtained from a Perkin Elmer precisely 2400 analyzer.

CONTENTS

Abstract

This study is based on the synthesis and characterization of quinoline based peptides and heterocycles containing oxygen, nitrogen and sulfur atoms by using new catalysts. In addition, the biological activities of the novel small molecules is evaluated. A total of 71 small molecules were prepared by using multi-component reactions including Ugi and Kabachnik-Fields reaction. The Ugi four-component reaction was implemented for the synthesis of medicinally important 13 new quinolinyl-lipoyl peptides (QLPs) and one quinolonyl-lipoyl peptide (QOLP) by microwave irradiation using methanol as medium. A series of 12 new quinolinyl-*4H*-pyrans (QPs), two quinolonyl-4*H*-pyrans (QOPs) and one indolyl-4*H*-pyran (IP) were successfully synthesized *via* a three-component reaction using ethanol as solvent in the presence of a new catalyst: humic acid supported 1-butyl-3-methylimidazolium thiocyanate ionic liquid catalyst (HASIL) under microwave irradiation. By using Kabachnik-Fields reaction, a total of 14 novel α-aminobenzylthio-quinolinyl phosphonates (BTQPs) were synthesized in the presence of a catalytic amount of iron-loaded boron nitride (Fe/BN) catalyst by using water as medium. A series of 14 novel benzylthioquinolinyl-1,4-dihydropyridines (BTQ-DHPs) were synthesized with high yields in short reaction time by a four-component reaction in the presence of iodine-loaded boron nitride (I/BN) catalyst by using water as solvent. A total of 14 derivatives of 2-amino-*4H*-pyran-3-carbonitrile derivatives (APCs) were prepared by using calcium loaded boron nitride (Ca/BN) in ethanol as solvent. This transformation transpired via a Knoevenagel condensation, Michael addition and intra-molecular cyclization. The prepared catalysts: HASIL, Fe/BN, I/BN and Ca/BN were characterized by XRD, SEM with EDX, TEM, DSC, TGA, BET, Raman spectra and FTIR analysis. All the synthesized molecules (QLPs, QOLP, QPs, QOPs, IP, BTQPs, BTQ-DHPs and APCs) were confirmed by FTIR, ^{1}H-NMR, ^{13}C-NMR and elemental analysis. Moreover, ^{19}F-NMR, ^{31}P-NMR and TOF-MS analysis were included for some selected compounds. In every chapter, one model compound was selected and discussed with two-dimensional spectra such as HSQC, DEPT 90º, DEPT 135º (selected), COSY, NOESY and HMBC. Among the synthesized compounds, a total of 48 compounds (8 QLPs, 15 (QPs, QOPs and IP), 10 BTQPs, 10 BTQ-DHPs and 5 APCs) were subjected to antimicrobial activities with *Bacillus cereus, Staphylococcus aureus, Escherichia coli, Enterococcus faecalis, Pseudomonas aeruginosa, Candida albicans* and *Candida utilis* and antioxidant studies were observed by the radical scavenging assay. The toxicity studies were

evaluated using the brine shrimp assay and the mortality rate was noted. Among them, 4 peptides, 7 pyrans, 8 aminophosphonates, 7 dihydropyridines and 5 carbonitriles showed good antimicrobial activity whilst 3 peptides, 9 pyrans, 6 aminophosphonates and 4 dihydropyridines showed antioxidant potential. Also, 4 peptides, 5 pyrans, 8 aminophosphonates and 5 dihdyropyridines showed mortality rate less than 50 % upto 48 h. The molecular docking studies were performed by Libdock score with DNA gyrase, Mtb gyrase and *Staphylococcus aureus* gyrase. A docking score of 183.24 kcal/mol and 165.01 kcal/mol were recorded for 2 peptides compared to ciprofloxacin. Among quinolinyl pyrans, one QP showed higher binding affinity of 96.96 kcal/mol with Mtb DNA gyrase. One BTQP showed more potency towards *Staphylococcus aureus* gyrase with 149.97 kcal/mol and one BTQ-DHP showed a strong ligand-protein interaction toward *Staphylococcus aureus* gyrase with Libdock score of 125.27 kcal/mol. The advantages of the synthetic methodology of this project are its green approach, easy work up, mild reaction conditions, the use of an inexpensive solvent, short reaction times with higher yields and recyclability of the catalyst.

Chapter-I

Introduction

Chapter One: Introduction

Heterocyclic chemistry is an interesting branch of organic chemistry with practical and theoretical importance. It is a vast and expanding area of chemistry due to heterocyclic compounds being used in pharmacy, medicine, agriculture, plastic, polymer and several other fields. Many heterocyclic compounds are either synthesized or derived from natural sources which display therapeutic properties as they are employed in the treatment of diseases such as infection by multidrug-resistant bacteria, viral influenza, leishmaniasis, coccidiosis and infectious septic shock. There are millions of heterocycles already available however studies on heterocycles are in-exhaustive. More efficient and effective synthesis of new heterocycles is an on-going aim of synthetic chemists. Furthermore, their biological properties require investigation so that new drugs are developed and made available to improve human health.

An important structural feature of heterocycles is their ability to manifest substituents around a core scaffold in defined three dimensional representations. This is an advantage that can enable skilled researchers to strategically manipulate the molecule thereby leading to a variety of new compounds with multi-functional groups which can even be further modified. To accomplish this task, new synthetic strategies need to be implemented including the use of new catalysts, non-conventional heating protocols, new substrates, multi-component reactions, new reagents and reaction conditions.

The aim of this study is to prepare quinoline based peptides and synthesis of novel heterocycles containing oxygen, nitrogen and sulfur atoms by using new catalysts. In addition, the biological activities of the novel small molecules will also be evaluated.

The objectives were to synthesize and characterize:

1. Quinolinyl-lipoyl and quinolonyl-lipoyl peptides and determine their antimicrobial and antioxidant potential, evaluate toxicity and assess their binding with DNA-gyrase by molecular docking.
2. Humic acid-supported ionic liquid catalyst and quinolinyl-*4H*-pyrans, quinolonyl-*4H*-pyrans and indolyl-*4H*-pyran and determine their antimicrobial and antioxidant potential, evaluate toxicity and assess their binding with *Mycobacterium tuberculosis* (Mtb) gyrase by molecular docking.

3. Iron-loaded boron nitride catalyst and α-aminobenzylthioquinolinyl phosphonates and determine their antimicrobial and antioxidant potential, evaluate toxicity and assess their binding with *Staphylococcus aureus* gyrase by molecular docking.

4. Iodine-loaded boron nitride catalyst and benzylthioquinolinyl-1,4-dihydropyridines and determine their antimicrobial and antioxidant potential, evaluate toxicity and assess their binding with *Staphylococcus aureus* gyrase by molecular docking.

5. Calcium-loaded boron nitride catalyst and 2-amino-4*H*-pyran-3-carbonitriles and assess their anti-bacterial potential.

The **second chapter** of the thesis discusses and presents the literature on the heterocyclic system, in particular, the synthesis and utilization of oxygen, nitrogen and sulfur heterocyclic molecules. The advantages of multi-component synthesis, multi-disciplinary of organic synthesis, green and sustainable methods via microwave and ultrasonic irradiation are also described. The necessity of a green catalyst in one-pot multi-component reactions is proposed. The importance of synthesizing drugs which can be used against infections from pathogenic bacteria and fungi such as *Bacillus cereus, Staphylococcus aureus, Escherichia coli, Enterococcus faecalis, Pseudomonas aeruginosa, Candida albicans* and *Candida utilis* is also discussed. Relevant literature on antioxidants, toxicity and molecular docking studies are described and discussed.

The **third chapter** reports a simple, cost effective, catalyst-free and eco-friendly synthesis of quinolinyl-lipoyl peptides and quinolonyl-lipoyl peptide through an Ugi four-component condensation reaction under microwave irradiation.

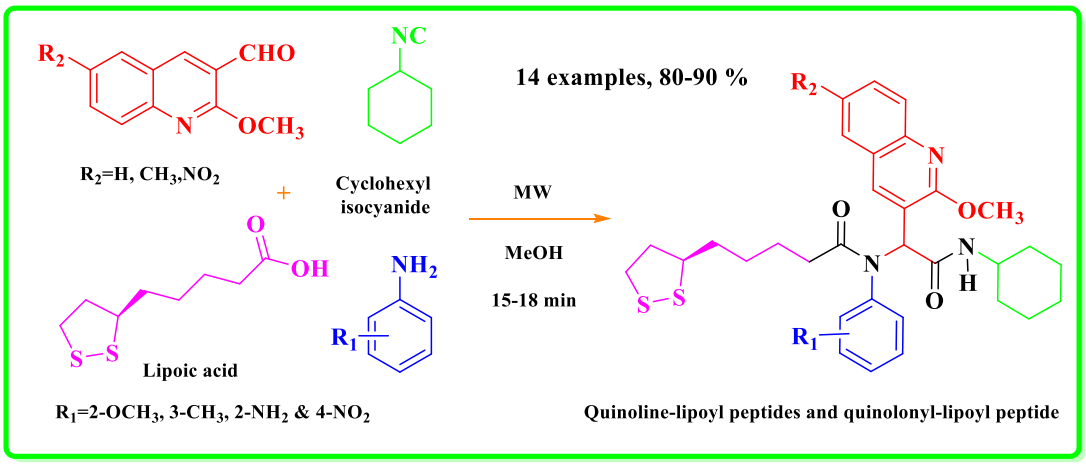

Lipoic acid, 2-methoxyquinoline-3-carbaldehyde derivatives, aniline derivatives and cyclohexyl isocyanide were employed to synthesize quinolinyl-lipoyl peptides. Quinolonyl-lipoyl peptide was synthesized from 2-oxo-1,2-dihydroquinoline-3-carbaldehyde, *o*-anisidine and cyclohexyl isocyanide. A total of 14 peptides were synthesized within 15-18 minutes. All synthesized peptides were characterized by FTIR, ^{1}H-NMR, ^{13}C-NMR and elemental analysis. A total of eight peptides were subjected to antimicrobial, antioxidant and toxicity evaluation. In addition, toxicity of all peptides was evaluated using the brine shrimp test. Molecular docking studies were also conducted to determine the binding with DNA gyrase based on Libdock score.

The **fourth chapter** discusses the synthesis and applications of quinolinyl-*4H*-pyrans, quinolonyl-*4H*-pyrans and indolyl-*4H*-pyran. A series of 2-methoxyquinoline bearing 4*H*-pyrans were synthesized under microwave irradiation using 2-methoxyquinoline-3-carbaldehyde derivatives, malononitrile and 1,3-diketones.

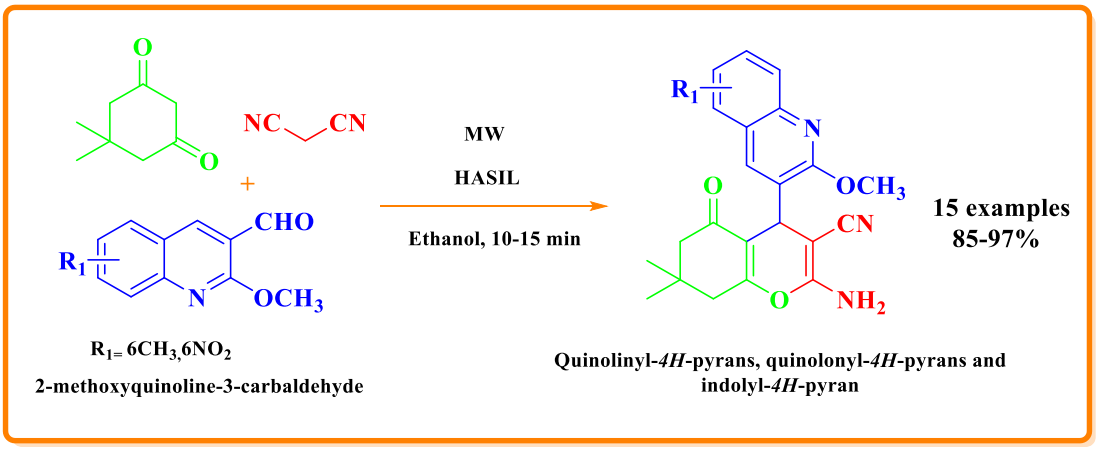

Two quinolonyl-4*H*-pyrans were synthesized from substrates 2-oxo-1,2-dihydroquinoline-3-carbaldehyde derivatives, malononitrile and 1,3-diketone and one indolyl-4*H*-pyran was synthesized from substrates 4-methylbenzaldehyde, malononitrile and 3-(3*H*-indol-3-yl)-3-oxopropanenitrile. A new humic acid-supported 1-butyl-3-methyl-imidazolium thiocyanate ionic liquid (HASIL) was used. The catalyst was characterized by XRD, SEM with EDX, TEM, TGA, DSC and FTIR analysis. All the synthesized *4H*-pyrans were characterized by FTIR, ^{1}H-NMR, ^{13}C-NMR and elemental analysis. A total of 15 compounds were subjected to antimicrobial, antioxidant and toxicity evaluation. Also, the toxicity of all pyrans was evaluated using the brine shrimp test. Molecular docking studies were undertaken to determine binding with Mtb DNA gyrase based on Libdock score.

The **fifth chapter** discloses the synthesis of α-aminobenzylthioquinolinyl phosphonates (BTQPs) and their applications. A series of α-aminobenzylthioquinolinyl phosphonates were synthesized within 5-10 min by using a new iron-loaded boron nitride catalyst under microwave irradiation in water. The catalyst was characterized by XRD, SEM with EDX, TEM, TGA, DSC and FTIR. 2-(benzylthio)quinoline-3-carbaldehyde, various aniline derivatives and diethylphosphite were used to synthesize the phosphonates.

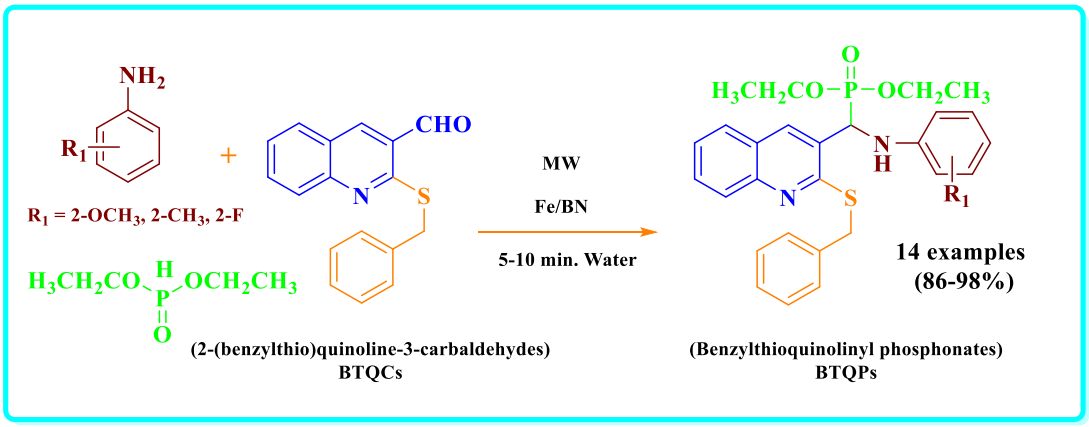

All synthesized α-aminobenzylthioquinolinyl phosphonates were characterized by FTIR, ^{1}H-NMR, ^{13}C-NMR and elemental analysis. A total of 10 compounds were subjected to antimicrobial, antioxidant testing and toxicity was assessed using the brine shrimp test. Molecular docking studies were conducted to determine binding with *Staphylococcus aureus* gyrase based on Libdock score.

The **sixth chapter** discusses the synthesis of benzylthioquinolinyl-1,4-dihydropyridines (BTQ-DHPs) and their applications.

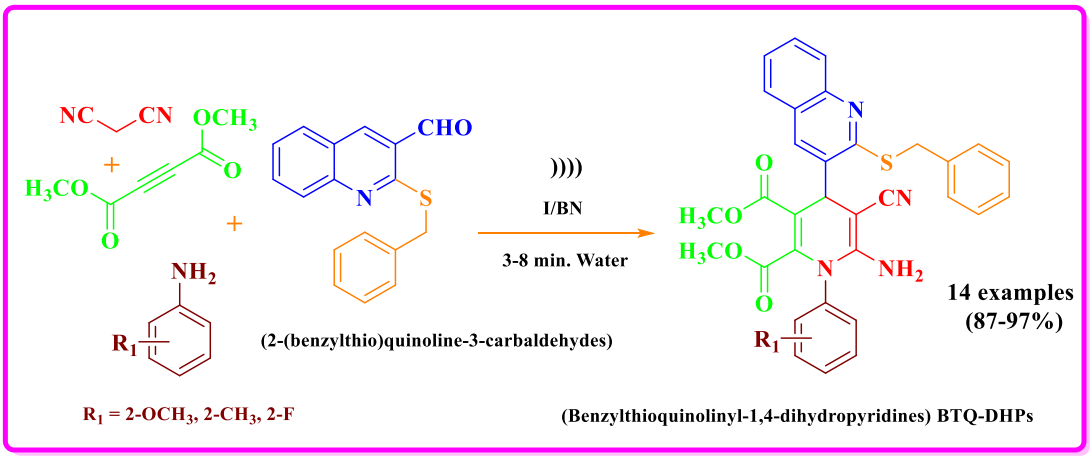

A novel iodine-loaded boron nitride heterogeneous catalyst was used. The catalyst was characterized by XRD, SEM with EDX, TEM, TGA, DSC and FTIR. 2-(benzylthio)quinoline-3-carbaldehyde, dimethyl acetylenedicarboxylate, malononitrile and aniline derivatives were used as substrates. All synthesized benzylthioquinolinyl-1,4-dihydropyridines were characterized by FTIR, ^{1}H-NMR, ^{13}C-NMR and elemental analysis. A total of 10 compounds were subjected to antimicrobial, antioxidant and toxicity evaluation. Also, the toxicity of all pyrans was evaluated using the brine shrimp test. Molecular docking studies were used to determine the binding with *Staphylococcus aureus* gyrase based on Libdock score.

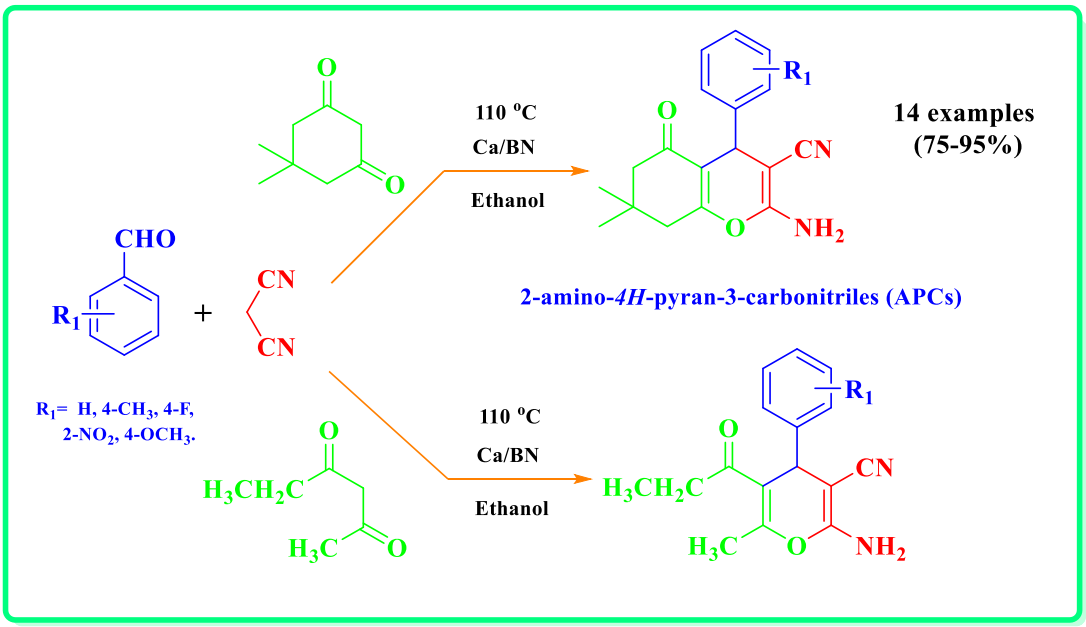

The **seventh chapter** of the thesis presents the synthesis of 2-amino-4*H*-pyran-3-carbonitriles by a cheap alkaline earth metal calcium-loaded boron nitride catalyst. This transformation proceeds via a Knoevenagel condensation, Michael addition and intramolecular cyclization. An alkaline earth metal-based green catalyst was successfully prepared and characterized by XRD, SEM with EDX, Raman spectroscopy, BET, DSC-TGA and FTIR. All synthesized 2-amino-4*H*-pyran-3-carbonitriles were characterized by FTIR, ^{1}H-NMR, ^{13}C-NMR and elemental analysis. A total of 5 compounds were subjected to antimicrobial evaluation against pathogenic bacteria *Staphylococcus aureus*, *Escherichia coli* and *Pseudomonas aeruginosa* and the results are discussed.

Chapter-II

Literature survey

Chapter Two

Literature survey

Every living organism is made up of organic molecules. The proteins that constitute our hair, skin and muscles; the DNA that controls our genetic heritage; the foods that nourish us; the clothes that keep us warm; and the medicines that heal us are all made up of organic molecules (McMurry, 1999). Chemistry has played an important role in our understanding of the universe. It is the science of molecules. However, organic chemistry is more complexed. It evolves and re-creates itself as it grows. It is imperative that we study the various molecules in nature because they are interesting in their own right and their functions are important to our lives.

Organic chemistry often studies life by developing new and novel molecules that provide information which is not readily available from existing molecules that are present in living organisms. The creation of new molecules has led to new materials and products such as plastics, dyes to colour clothes, perfumes and drugs to treat and cure various diseases. Early Asian civilization (2500-3000 BC) extensively used natural materials from herbal extracts (Ayurveda) for treating illnesses (Patwardhan *et al*., 2005). One such extract was "ma huang" *(Ephedra sinica)* which reduced elevated blood pressure (Chan *et al*., 2016). It was found that it contained ephedrine, an organic compound similar in structure and physiological activity to adrenaline, a hormone secreted by the adrenal gland. Currently, almost all drugs that are prescribed for treatment of diseases are organic compounds. However, some are derived from natural sources; but many are the products of synthetic organic chemistry.

Morphine was isolated from opium produced from seed pods of the poppy plant *(Papaver somniferum)* (Da Cheng *et al*., 2015). Inspired by the discovery of penicillin, pharmaceutical research was expanded to include a massive screening of micro-organisms for new antibiotics. Over the centuries there has been a long list of drugs discovered, however the ones obtained from natural sources which have undoubtedly revolutionized medicine include antibiotics **(Fig. 1)** such as penicillin (**1**), tetracycline, and erythromycin, antiparasitics such as avermectin (**4**), antimalarials such as quinine and artemisinin (**2**), lipid control agents such as lovastatin (**3**) and its analogs,

immunosuppressants such as cyclosporine and rapamycin (**6**) and anticancer drugs such as paclitaxel (**7**) and irinotecan (**5**) (Harvey, 2008).

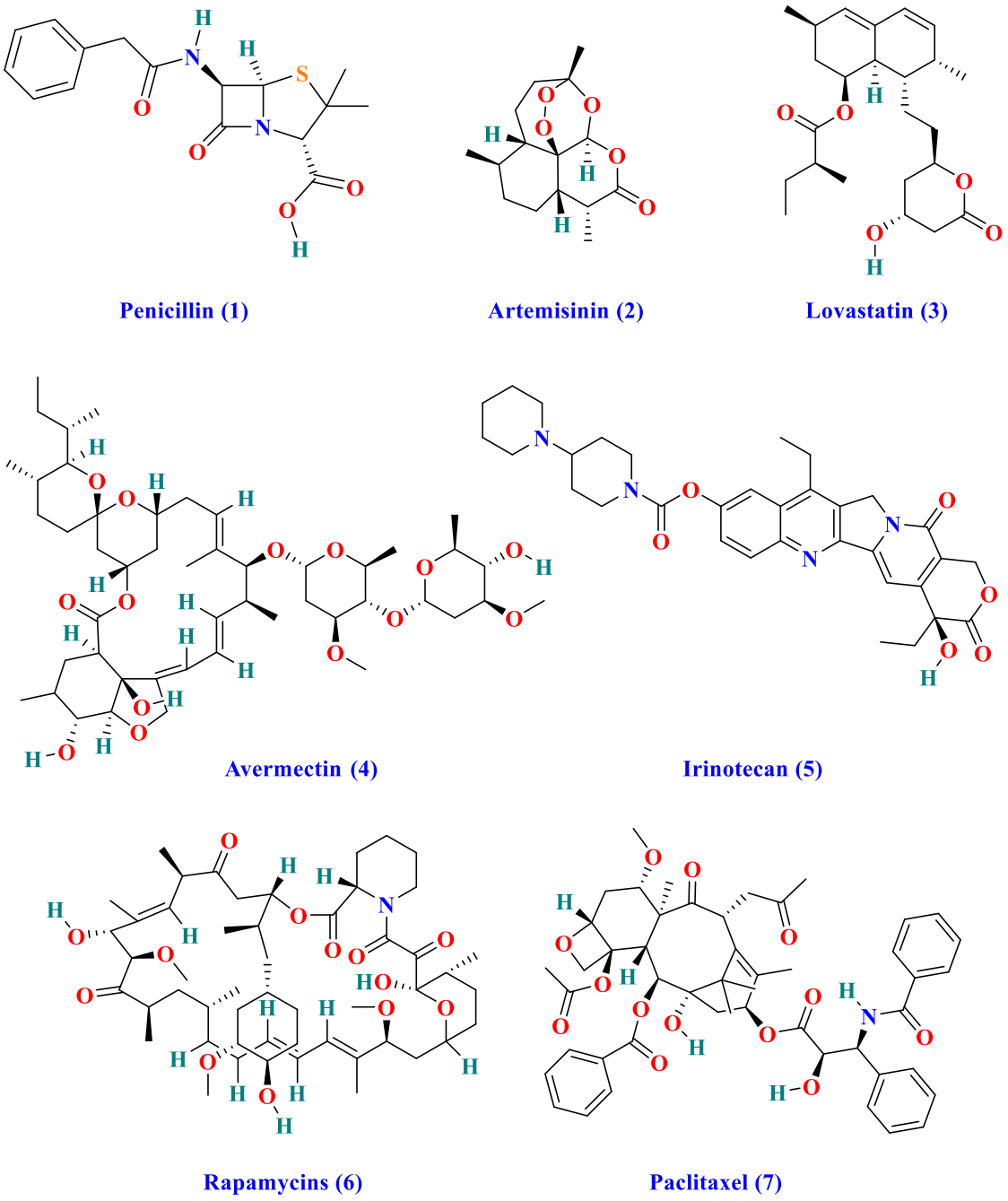

Fig. 1. Important drugs extracted from natural sources

Modern synthetic organic chemists can synthesize some of the most intriguing natural molecules in the laboratory by new synthetic strategies and technologies. These

molecules improve various fields of study including biology and medicine due to their potent biological activity and can serve as new drug candidates for clinical development. In addition, by employing sophisticated catalytic reactions and appropriately designed synthetic processes, organic chemists can synthesize a myriad of organic molecules for potential applications in many areas of science, technology and in everyday life (Nicolaou, 2014).

The field of total synthesis continues to serve as the ultimate testing ground for new methodologies and strategies. Organic synthesis has experienced a remarkable increase in quality thereby empowering synthetic chemists to construct molecules of any degree of structural complexity. In 1975, Hendrickson defined the "ideal synthesis" as one which: "...creates a complex molecule...in a sequence of only construction reactions involving no intermediary re-functionalizations, and leading directly to the target, not only its skeleton but also its correctly placed functionality" (Hendrickson, 1975). This prescient statement encompassed and epitomized the "economies" of synthesis design (Newhouse *et al*., 2009). The field of total synthesis has a rich history and a vibrant future. Landmark advances and revolutionary strides in the approach to synthesis of compounds have placed the synthetic chemist in an enviable position of being able to create almost any molecule given sufficient time and resources. The stage is now set for organic chemists to aim for "ideality" in the way molecules are synthesized **(Fig. 2)**.

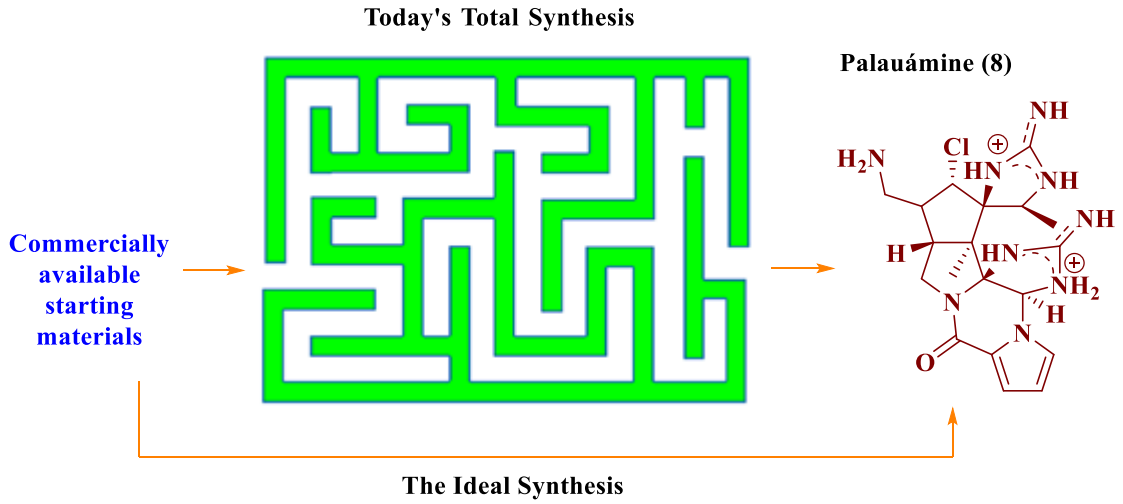

Fig. 2. A schematic diagram showing a footpath of ideal synthesis

2.1. Heterocyclic chemistry: oxygen, nitrogen and sulfur heterocycles

Heterocyclic chemistry deals exclusively with the synthesis, properties and applications of heterocycles. The synthesis of heterocycles is arguably one of the oldest and most promising disciplines of organic chemistry (Cabrele and Reiser, 2016). Nitrogen, oxygen and sulfur are the most common heteroatoms but heterocyclic rings containing other heteroatoms are also widely known (Franzén, 2000). An enormous number of heterocyclic compounds are known and this number is increasing rapidly. The heterocycle scaffold, present in most medicinal drugs, reflects its central role in modern drug design. These scaffolds can be functionalised with appropriate groups to influence the lipophilicity, polarity and hydrogen bonding capacity of organic compounds, which may lead to improved pharmacological, pharmacokinetic, toxicological and physicochemical properties of new and existing medicinal drugs. Over 80% of the important drugs that were retailed by US (Lindsley, 2015) in 2014, were heterocycles **(Fig. 3)**.

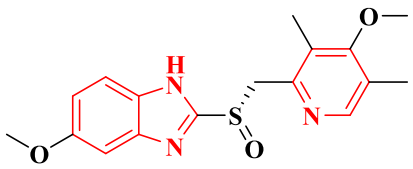

Esomerprazol (9)

Treats: dyspepsia, peptic ulcer disease, gastroesophageal reflux disease

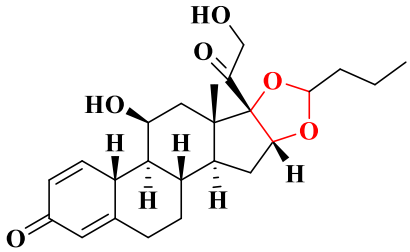

Budesonide (10)

Treats: asthma, chronic obstructive pulmonary disease

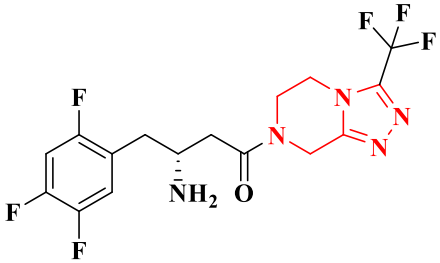

Sitagliptin (11)

Treats: diabetes mellitus type 2

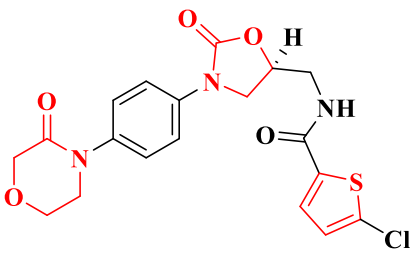

Rivaroxaban (12)

Treats: venous thromboembolism

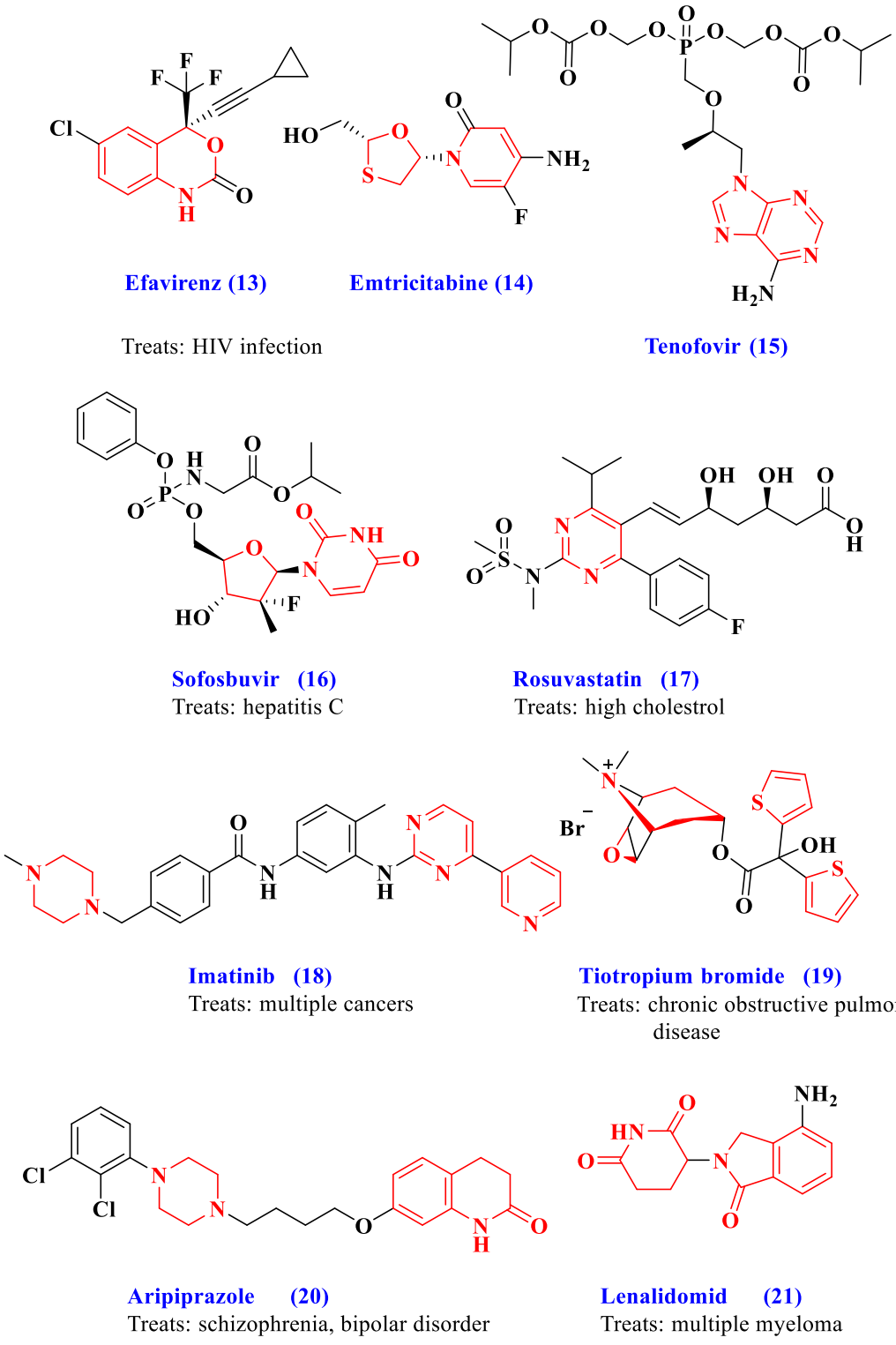

Fig. 3. Important drugs containing the heterocyclic scaffold.

The heterocyclic architecture allows chemists to devise innovative ways for the synthesis of complex structures. Such targets often require difficult transformations that appear impossible to achieve. This challenge is the major driving force for the development of

new and better synthetic methodologies that can subsequently lead to great value-based organic compounds. Moreover, the aim of the synthesis should include sustainable and green principles such as atom and step economy, convergent and cascade strategies, fragment coupling with high functional group tolerance, selective C, H-bond activations with minimal involvement of protecting groups, or catalytic transformations with environmentally benign and cost economic reagents.

2.1.1. The synthesis and importance of oxygen heterocycles

Oxygen heterocycles are an important class of heterocyclic compounds mainly due to their natural abundance and diverse biological functions. Many naturally occurring oxygen heterocycles such as sugars, vitamins, hormones, antibiotics and pigments are biologically active compounds (Xu *et al*., 2006). Saturated five-membered oxygen heterocycles occur widely in nature, especially as simple sugars. Most naturally occurring sugars are monosaccharides but they also serve as building blocks for other molecules. The anti-arrhythmic drug, amidarone, contains benzene fused furan nucleus (Anderson and Prystowsky, 1999). Six-membered fused pyran nuclei are found in essential natural products such as Vitamin E (α-tocopherol). Generally, heterocyclic compounds are either aliphatic or aromatic in nature. The aliphatic heterocycles are cyclic analogs of amines, ethers, amides etc. while the aromatic heterocyclic compounds behave like benzene. Another sub-class of heterocycles is the benzene fused heterocycles in which the heterocyclic N-ring is fused to one or more benzene rings (Chan, 1974).

Natural products also serve as lead compounds in the development of new drugs. Many natural and semi-synthetic oxygen heterocyclic compounds such as Taxol (Willenbring and Tantillo) as an anti-cancer drug, Digoxin for Congestive Heart Failure (CHF) treatment, Cyclosporine A as an immunosuppressant and Lovastatin as a hypolipidemic agent, are well known for their therapeutic effects (Koehn and Carter, 2005). Several studies have shown that 2-amino-4*H*-pyrans with amino and nitrile functions at the 2nd and 3rd positions **(Fig. 4)** are known to possess diverse pharmaceutical properties such as cytotoxic, myorelaxant, antioxidant, anti-proliferative, anti-microbial, anti-HIV, anti-rheumatic and anti-cancer activities (Raj *et al*., 2010; Saundane *et al*., 2013; Paliwal *et al*., 2013; Venkatesham *et al*., 2012; Makawana *et al*., 2012; Patil *et al*., 1993; Smith *et al*., 1995; Patil *et al*., 2012).

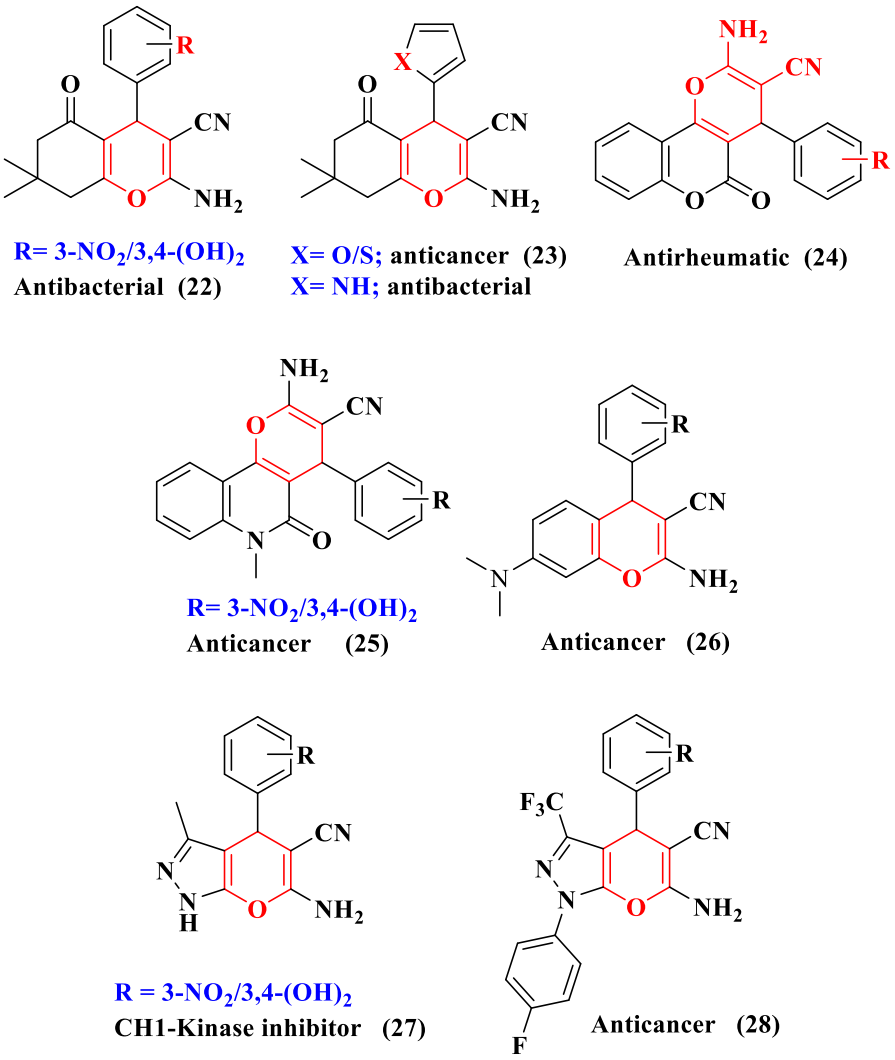

Fig. 4. The medicinal applications of 4*H*-pyrans

Many compounds containing pyran, as the structural unit, have an application as a cognitive enhancer in the treatment of neuro-degenerative diseases like Alzheimer's and Parkinson's (Bonsignore *et al*., 1993; Konkoy *et al*., 2001). Apart from their medicinal applications, compounds belonging to this class are customarily used in the field of cosmetics (Schweizer and Meeder-Nycz, 1977; Abd El-Rahman *et al*., 2007; Darbarwar and Sundaramurthy, 1982), agrochemicals (Sofan *et al*., 1989; Abdel-Galil *et al*., 1982) as well as dyes (Ellis, 1977; Armesto *et al*., 1989). Due to their wide range of applications, the development of efficient protocols for the synthesis of compounds containing 2-amino-3-cyano-4*H*-pyrans as the structural motif is highly desirable.

The synthesis of 4*H*-pyrans involves a one-pot, three-component condensation between an aldehyde, malononitrile and an enolizable C-H acid. The commonly used acids are dimedone, barbituric acid, naphthol (α and β), 4-hydroxycoumarin, resorcinol, 2-

hydroxy-1,4-naphthoquinone and kojic acid (Han and Xia, 2010). Furthermore, this reaction is known to proceed via a Knoevenagel-Carba-Michael-Throbe-Ziegler type cascade pathway (Han and Xia, 2010).

Shestopalov *et al*., 2012 reported the synthesis of a series of 4*H*-pyrans (**32, 33** and **34**), with poly alkoxy substituents (**29**), in the presence of triethylamine (Et_3N) as a catalyst by a Knoevenagel-Michael-hetero-Thorpe-Ziegler three-component domino reaction. The overall yield of the series of compounds was in the range of 45-82 %. The targeted molecules were evaluated in a phenotypic sea urchin embryo assay for anti-mitotic and microtubule destabilizing activity (Tsyganov *et al*., 2014). The selected compounds of this investigation exhibited strong cytotoxicity in the NC160 human tumor cell line. The results suggested that poly alkoxy substituted 2-amino-4-phenyl-4*H*-chromene-3-carbonitriles could be feasible as an anti-cancer agent (Shestopalov *et al*., 2012).

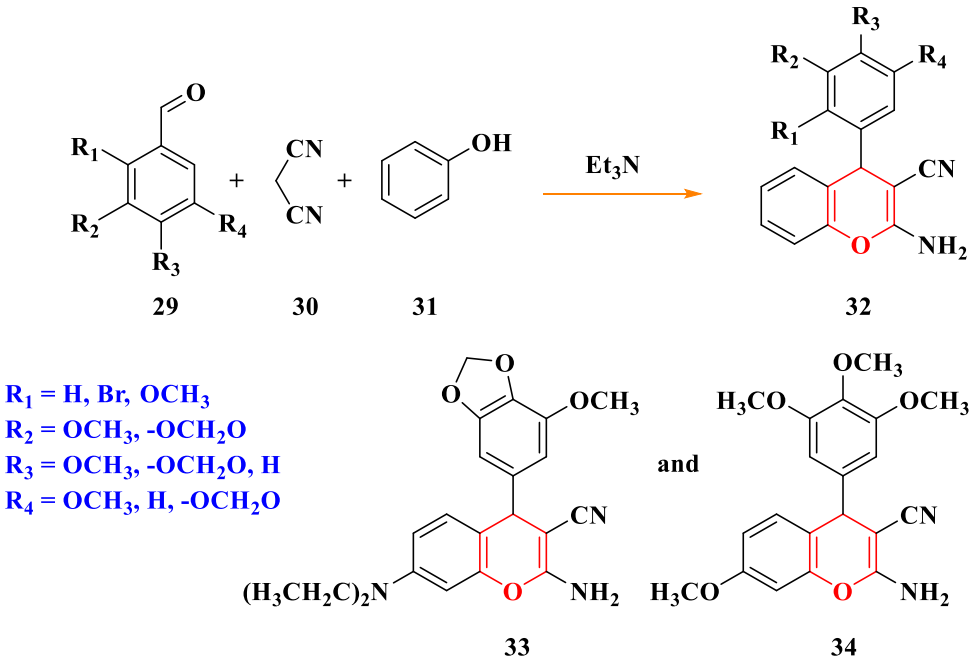

29 30 31 32 33 34

Mahmoodi *et al*., 2010 synthesized a new series of 2-amino-4*H*-chromene-3-carbonitriles (**37**) bearing a 2-aryl thiazole-4-yl (**35**) moiety and their *in-vitro* activity was investigated in comparison with etoposide, a well-known anti-cancer drug, using 3-(4,5-Dimethylthiazol-2-Yl)-2,5-Diphenyltetrazolium Bromide (MTT) colorimetric assay.

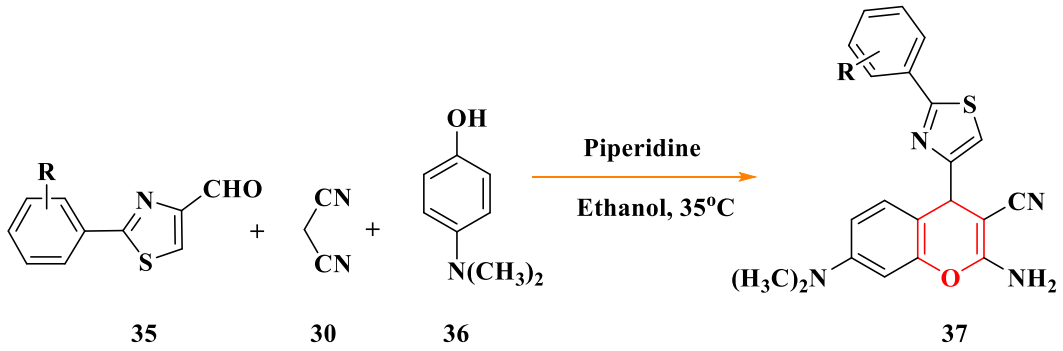

35 30 36 37

R= H, 2-Cl, 3-Cl, 4-Cl, 4-Br

Among them, 2-(2-chlorophenyl)thiazole-4-yl-4*H*-chromene-3-carbonitrile showed the most potent activity against nasopharyngeal epidermoid carcinoma KB, medulloblastoma DAOY and astrocytoma 1321N1. A 4*H*-chromene viz. 2-(4-chlorophenyl)thiazole-4-yl moiety exhibited the best growth inhibitory activity against breast cancer cells MCF-7, lung cancer cells A549, colon and adenocarcinoma cells SW480 with IC_{50} values less than 5µM (Lee *et al*., 2011).

Salama *et al*., 2017 reported an efficient and eco-friendly procedure for the synthesis of bis(4*H*-chromene-3-carbonitrile) derivatives (**40**) using chitosan with piperidine as a catalyst. The reaction was carried out under microwave irradiation conditions. The maximum yield of 88 % was obtained within ten minutes under reflux.

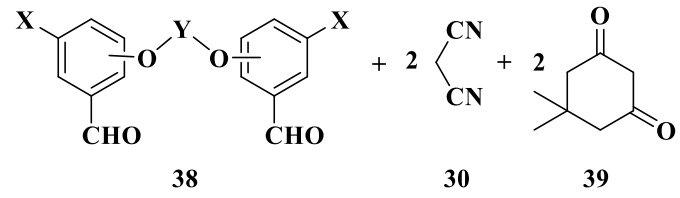

38 30 39

X = H
Y = CH_2-CH_2

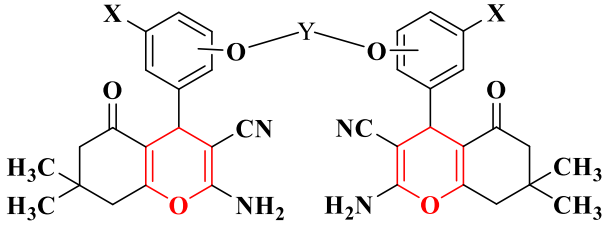

40

Gong *et al*., 2009 designed an efficient and convenient method for the synthesis of polyfunctionalized 4*H*-pyrans (**43**, **45** and **46**) through the condensation of aldehydes (**41**), malononitrile (**30**), 4-hydroxycoumarin (**42**), phenols (**44**) or active methylene carbonyl compounds such as 1, 3-cyclohexanedione and dimedone (**39**) in the presence of 1-butyl-3-methylimidazolium hydroxide ([bmim]OH) as a catalyst in aqueous media. In this reaction, 10 mol % of the catalyst was used to attain maximum yield. Also, the synthesized compounds were compared with previous studies. Although the procedure was simple and higher product yields were obtained, recyclability of the catalyst was not determined.

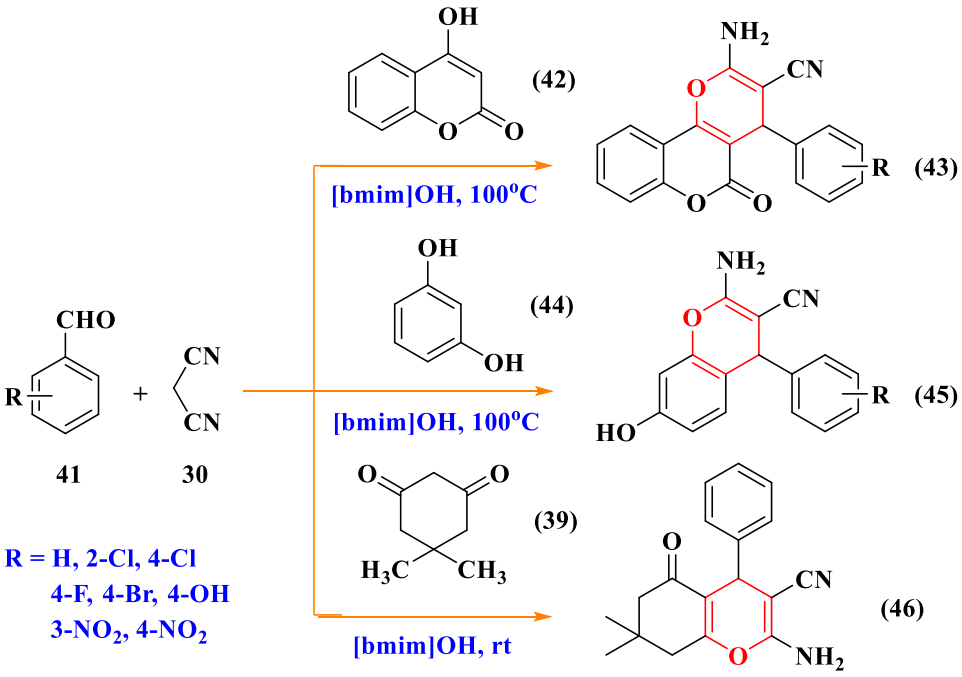

Pandit *et al*., 2015 developed an efficient protocol for the synthesis of medicinally important tetrahydro[*b*]pyrans (**46**, **49**, **51** and **53**) and pyran-annulated heterocycles using a commercially available and non-toxic tris-hydroxymethylaminomethane (THAM) as an organocatalyst. A 30 mol % of the catalyst was used in the reaction to attain the best yield. The avoidance of conventional isolation, the recyclability of the catalyst for five consecutive runs were advantages which improved the practical utility of this reaction protocol.

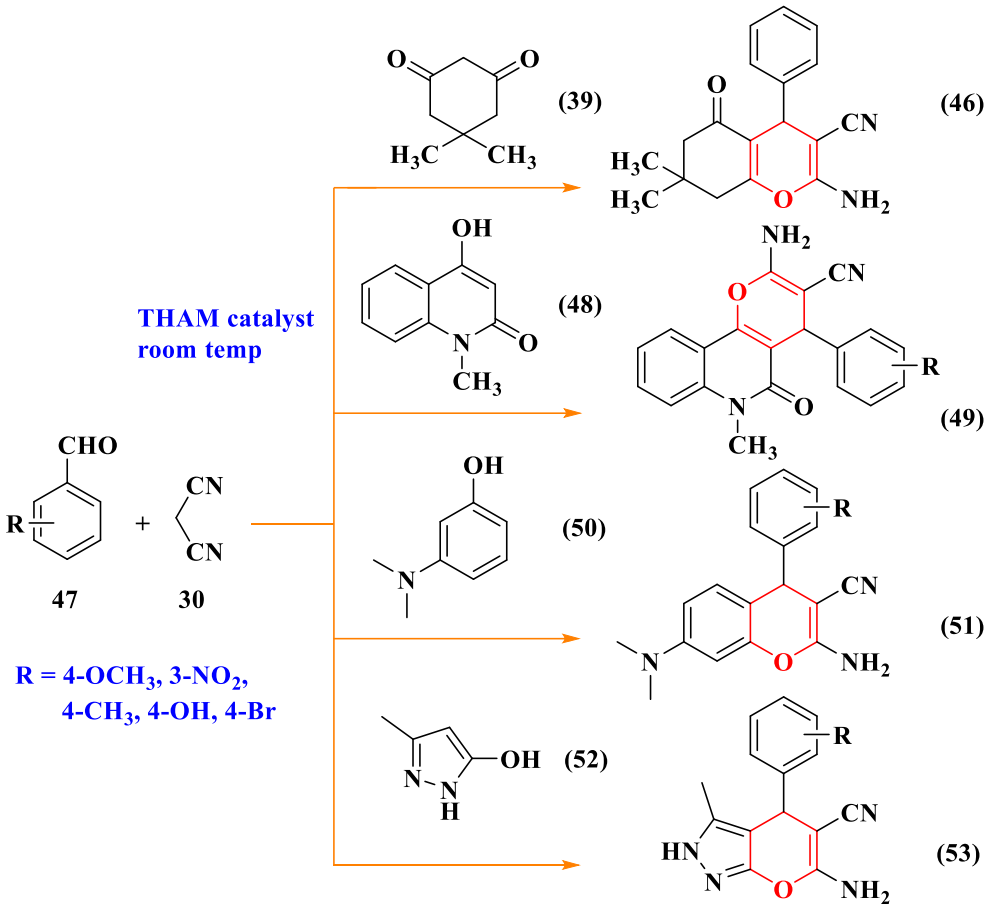

2.1.2. The synthesis and importance of nitrogen heterocycles

Nitrogen heterocycles are ubiquitous in natural products (Joule, 2016), pharmaceuticals (Joule and Mills, 2010) and materials science (Anton and Baird, 2006; Baxter and Dali-Youcef, 2005; Hab and Mlostoń, 2017). Their preparation has always been an important aspect of organic synthesis. Over the past few decades, great efforts have been made to develop novel and efficient methods for the construction of nitrogen-containing heterocycles (Li and Gribble, 2000; Husson and Royer, 2009; Orru *et al*., 2010; Eicher *et al*., 2013; Wolfe, 2013; Vo and Bode, 2014; Allais *et al*., 2014; Yamamoto, 2014).

Quinoline, a well-known nitrogen heterocyclic compound, and its derivatives are widely used as “parental” compounds to synthesize molecules with medical benefits including anti-malarial and antimicrobial activities. The quinoline scaffold has been reported to possess a diverse range of pharmacological activities (Orhan *et al*., 2013; Solomon and Lee, 2011; Lavrado *et al*., 2010; Kumar *et al*., 2009; Michael, 2002; Michael, 1999; Kharwar *et al*., 2011; Singh and Bodiwala, 2010; Williams *et al*., 2011; Chauhan and

Srivastava, 2001; Chen *et al*., 2001; Roma *et al*., 2000) including anti-protozoal (Bawa *et al*., 2010; Gryzlo and Kulig, 2014; Kaur *et al*., 2010; Gorka *et al*., 2013; Bongarzone and Bolognesi, 2011; Reynolds *et al*., 2013), anti-tubercular (Keri and Patil. 2014; Singh *et al*., 2015), anti-cancer (Solomon and Lee, 2011; Afzal, 2015; Vlahopoulos *et al*., 2014), anti-psychotics (Zajdel *et al*., 2014), anti-inflammatory (Mukherjee and Pal, 2013; Mukherjee and Pal, 2013), antioxidant (Vo *et al*., 2014; Allais *et al*., 2014; Yamamoto, 2014), anti-HIV (Musiol, 2013), anti-fungal (Musiol, 2010), efflux pump inhibitors (Mahamoud *et al*., 2006), treatment of neuro-degenerative diseases (Bongarzone and Bolognesi, 2011) and lupus (Costedoat-Chalumeau *et al*., 2014).

The quinoline moiety also contributes to the effect of drugs used for several other diseases. This includes the fluoroquinoline antibiotic ciprofloxacin (**57**), pitavastatin (**58**) as a cholesterol lowering agent, lenvatanib (**59**) as a kinase inhibitor for cancer and its structural analogs such as cabozantinib and bosutinib, tipifarnib (**60**) as a farnesyl transferase inhibitor for leukaemia, saquinavir (**61**) as an antiretroviral and bedquiline (**62**) as an anti-tuberculosis drug (Mahajan, 2013).

The 2-(2-fluorophenyl)-6,7-methylene-dioxy quinoline-4-one monosodium phosphate (CHM-1-P-Na) (**63**) is a pre-clinical anti-cancer agent, showing anti-tumor activity in a SKOV-3 xenograft nude mice model (Chou *et al*., 2010; Chou *et al*., 2010). Several quinoline-based compounds (**64**-**69**) also showed the inhibition of kinases which are involved in cancer progression (Solomon and Lee, 2011). The chemical structures of various quinoline-based drugs (a) and kinase inhibitors (b) are shown in **Fig. 5**.

Quinoline and its analogs have recently been examined for their mode of function in the inhibition of tyrosine kinases, proteasome, tubulin polymerization, topoisomerase and DNA repair. Substitution of a group in a suitable position of a bioactive molecule is found to exert a profound pharmacological effect (Gasparotto *et al*., 2006). The quinoline nucleus is present in many naturally occurring alkaloids with anti-tumor activity such as camptothecin (Wall *et al*., 1966). Buta *et al*., 1978 isolated camptothecin, a quinoline analogous from *Camptotheca acuminata*. It was the first compound identified which directly blocks the topoisomerase (Topo-I), a DNA replication enzyme, thus stopping cell division.

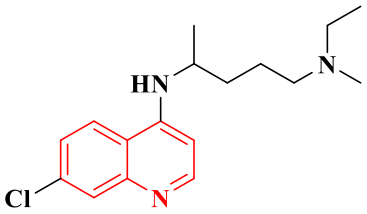

Chloroquine (54)

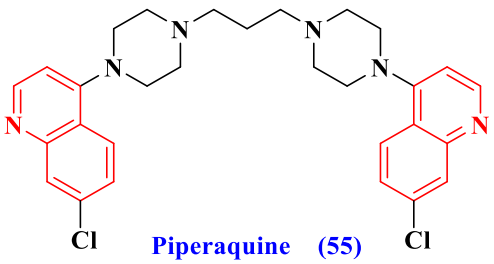

Piperaquine (55)

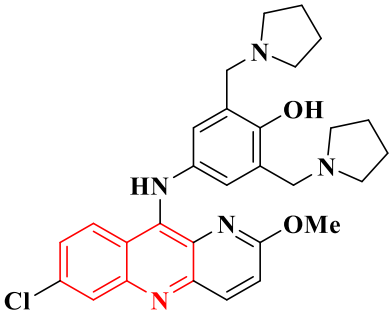

Pyronaridine (56)

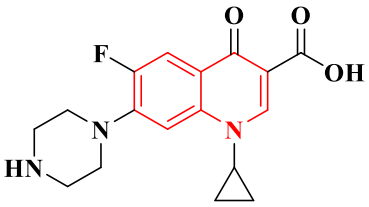

Ciprofloxacin (57)

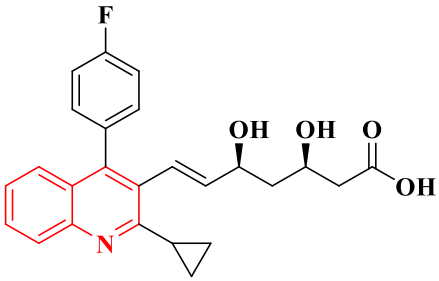

Pitavastatin (58)

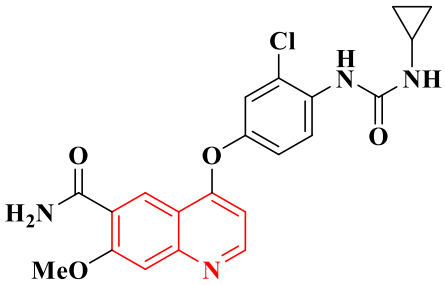

Lenvatinib (59)

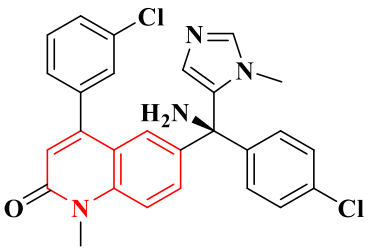

Tipifarnib (60)

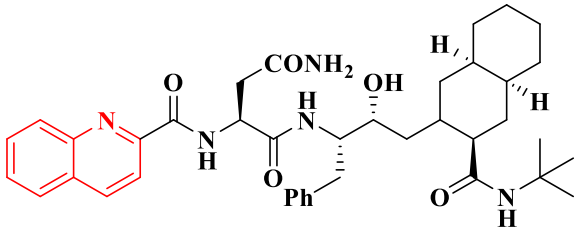

Saquinavir (61)

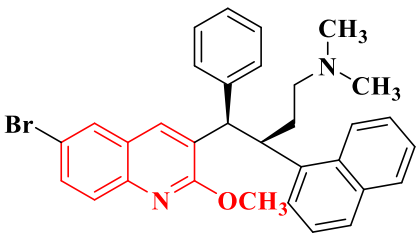

Bedaquiline (62)

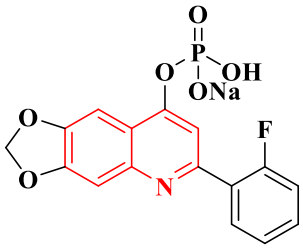

CHEM-1,P-Na (63)

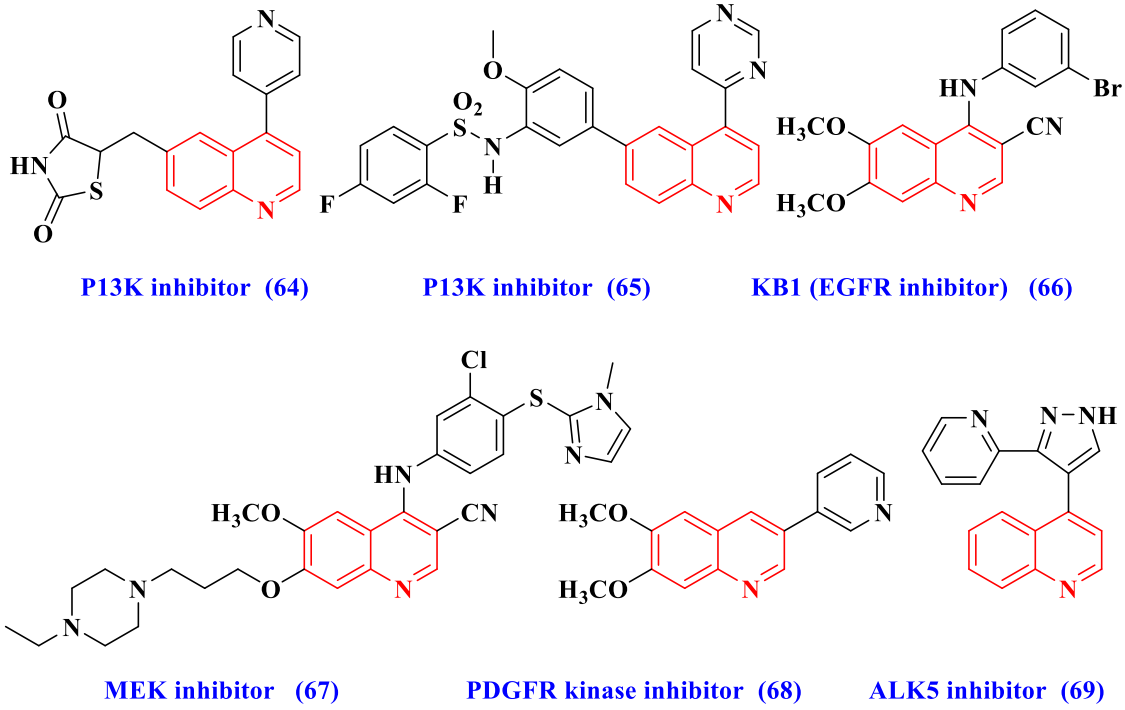

Fig. 5. Chemical structures of quinoline-based kinase inhibitors

Aravinda *et al*., 2009 presented a simple approach for the accession of quinoline peptide (**72**) analogs: 1,4-disubstituted 1,2,3-triazoles using 3-(azidomethyl)-2-chloroquinoline (**70**) as a building block. Their synthesis and applications including DNA binding and photonuclease activity were reported. DNA binding studies have shown a good interaction with quinoline peptides and peptidomimetics when it binds with base pairs of calf thymus-DNA.

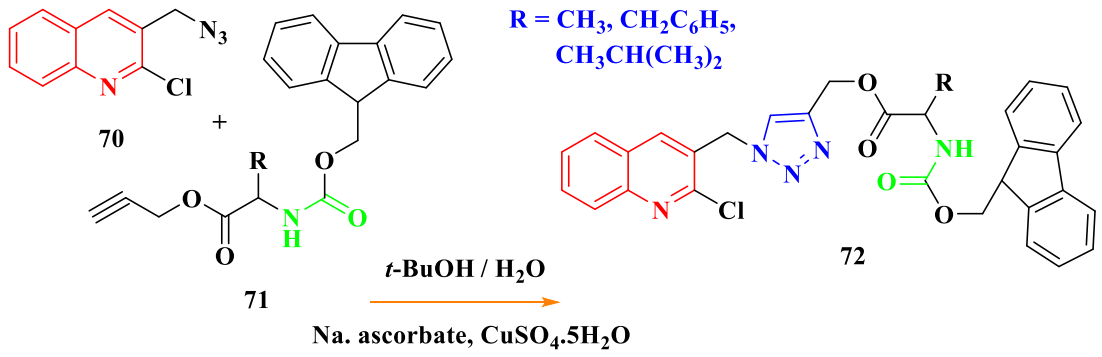

Ghandi *et al*., 2017 described a successful synthesis of novel tetrazole based quinoline (**76**) derivatives via a one-pot reaction in moderate to good yields. These reactions proceeded presumably through Ugi-azide or Ugi-azide/Pictet-Spengler processes.

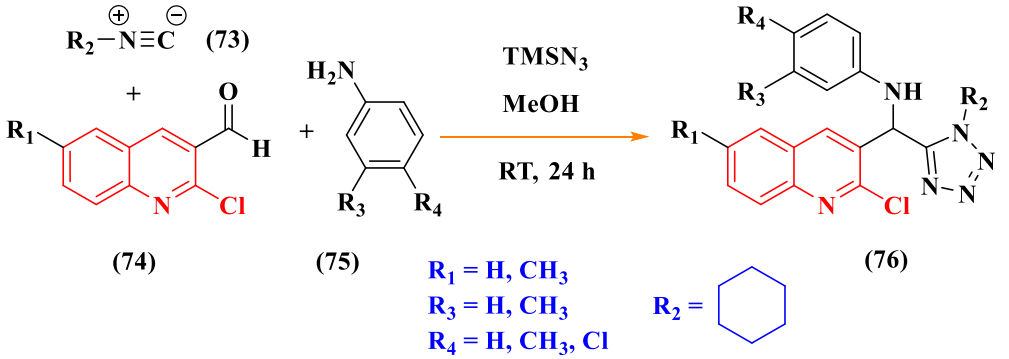

El-Gamal, 2016 reported the synthesis and antimicrobial activity of polyfunctionalized heterocyclic systems especially quinoline-based 2-cyano-*N*-(3-cyano quinoline-2-yl) acetamide moiety (**81**).

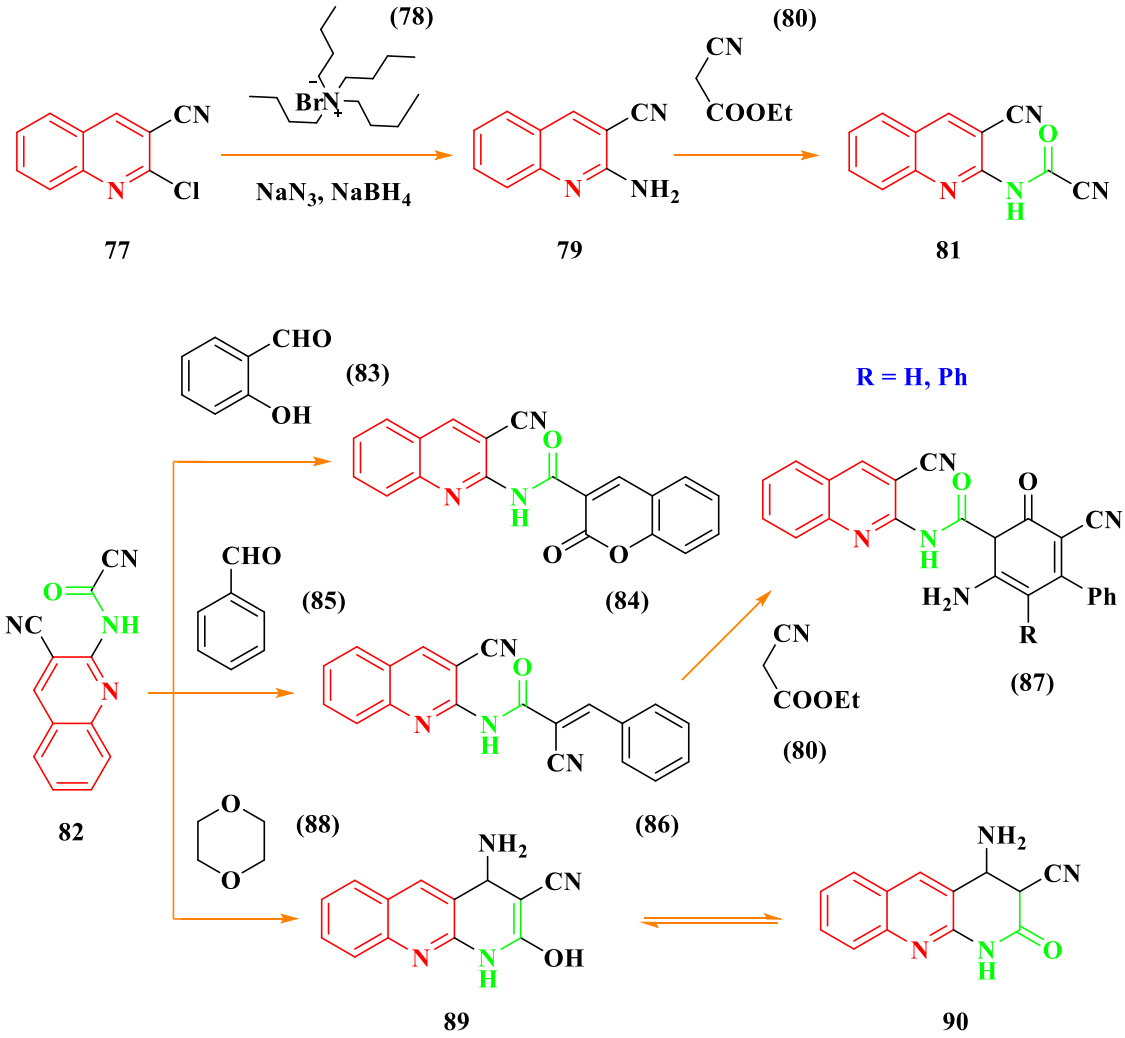

The synthetic methods depended on region-selective attack and/or cyclization by the cyanoacetamide moiety of quinoline. All synthesized compounds were characterized by

spectral data and elemental analysis. It was further screened for their antimicrobial activity.

1,4-Dihydropyridines (1,4-DHPs) as privileged pharmacophores, have gained a vital place in the field of pharmaceuticals. Valuable commercial drugs such as nifedipine (**91**) (Murphy *et al*., 1983; Masotti *et al*., 1985; Janis *et al*., 1983; Morad *et al*., 1983; Loev *et al*., 1974), cilnidipine (**92**) (Pajouhesh *et al*., 2010; Yamamoto and Takahara, 2009; Oike *et al*., 1990; Takahara *et al*., 2003), nicardipine (**93**) (Nobili *et al*., 2006; Sorkin and Clissold, 1987), and nimodipine (**95**) (Lavilla *et al*., 2002; Varache-Lembège *et al*., 1996; Janis *et al*., 1987) are calcium channel blockers with useful effects on cardiovascular disorders including hypertension or cardiac arrhythmias (Edraki *et al*., 2009; Safak and Simsek, 2006; Shan *et al*., 2004; Velázquez and Knaus, 2004; Gaudio *et al*., 1994; Goldmann *et al*., 1991; Triggle *et al*., 1989; Bossert and Vater, 1989; Bossert *et al*., 1981; Janis and Triggle, 1984).

In addition, functionalized 1,4-DHPs are common to numerous bioactive compounds, which exhibit a broad range of biological activities such as antidiabetic (Briede *et al*., 2008; Kharkar *et al*., 2002), antitumor (Abbas *et al*., 2010; Swarnalatha *et al*., 2011), antitubercular (Sriram *et al*., 2010; Nayyar *et al*., 2006), radioprotective (Ivanov *et al*., 1990), neuroprotective (Klimaviciusa *et al*., 2007; Klusa *et al*., 1995), bronchodilator (Suresh *et al*., 2007) and anti-ischemic for the treatment of Alzheimer's disease (Khadilkar and Borkar, 1998; Priego *et al*., 1992; Cooper *et al*., 1992) amongst several others (Trivedi *et al*., 2011; Hilgeroth, 2002; Vijesh *et al*., 2011; Mai *et al*., 2009; Hilgeroth, 2002; Kawase *et al*., 2002; Gullapalli and Ramarao, 2002; Tasaka *et al*., 2001; Zhu *et al*., 2001; Zhao and Cheng, 2000).

Replacement of the aryl group of the DHPs with the bioactive heterocyclic compounds leads to the formation of scaffolds with various biological properties. Isoxazolyl dihydropyridine (**95**) inhibits the multidrug resistance transporter (Hulubei *et al*., 2012). Moreover, coumarin and pyrazole-based 1,4-DHPs such as (**97**) and (**98**) are known as bone anabolic (Sashidhara *et al*., 2012) and potential antitubercular (Trivedi *et al*., 2011) agents, respectively **(Fig. 6)**.

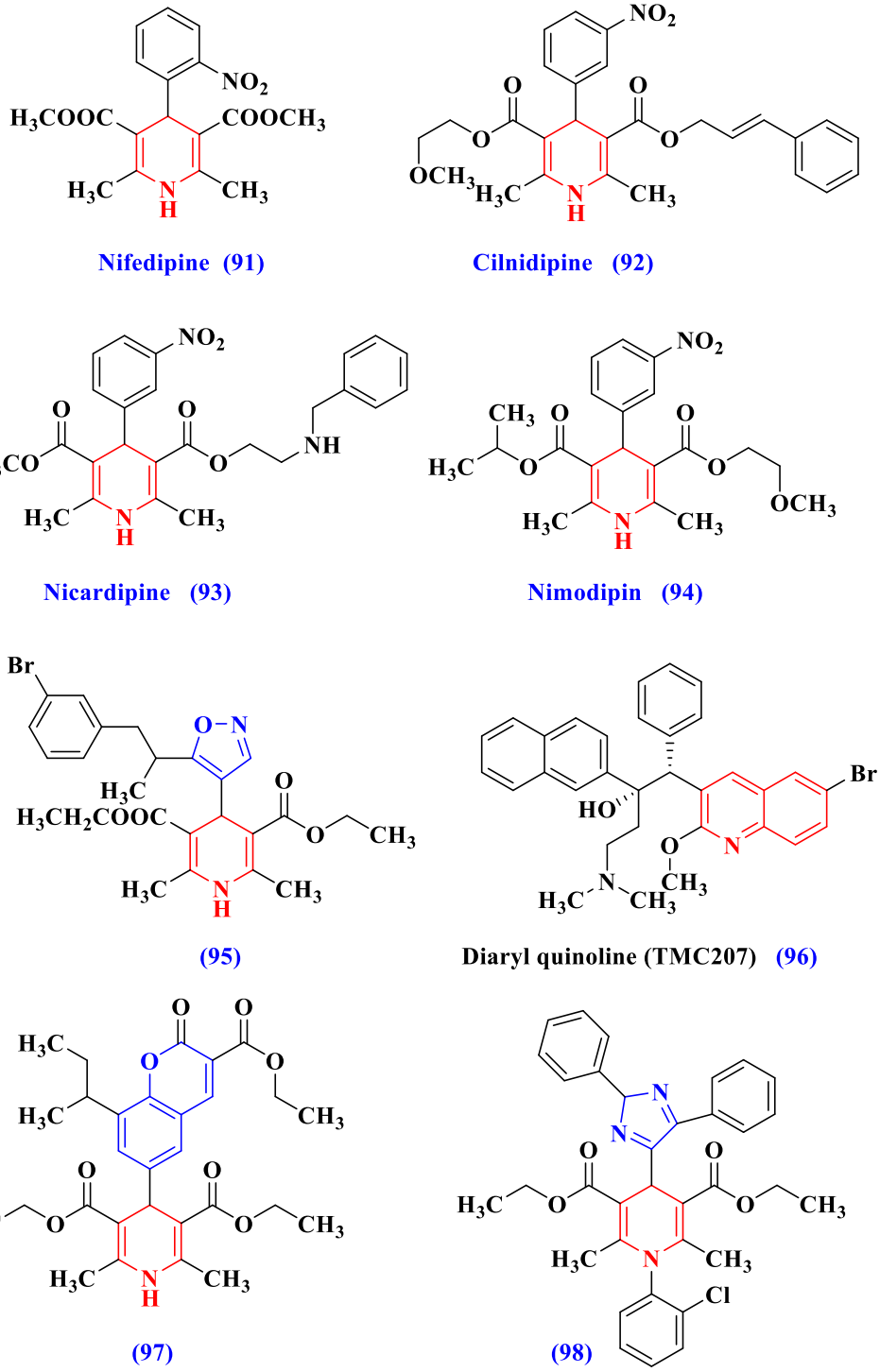

Fig. 6. Examples of 1,4-DHPs and quinoline derivative as potential antitubercular agents.

Niraj *et al.*, 2011 demonstrated a microwave-assisted Hantzsch reaction for the synthesis of tetrazolo[1,5-a]quinolone-based 1,4-dihydropyridines (**101**), acridine-1,8-diones (**104**) and polyhydroquinolines via a three-component coupling reaction of tetrazolo[1,5-*a*]-quinoline-4-carbaldehyde (**99**, **102** and **105**), dimedone (**103**) and ethyl/methyl

acetoacetate (**107**) in the presence of ammonium acetate as a catalyst. All synthesized compounds were screened for their antimicrobial activity against bacteria and fungi.

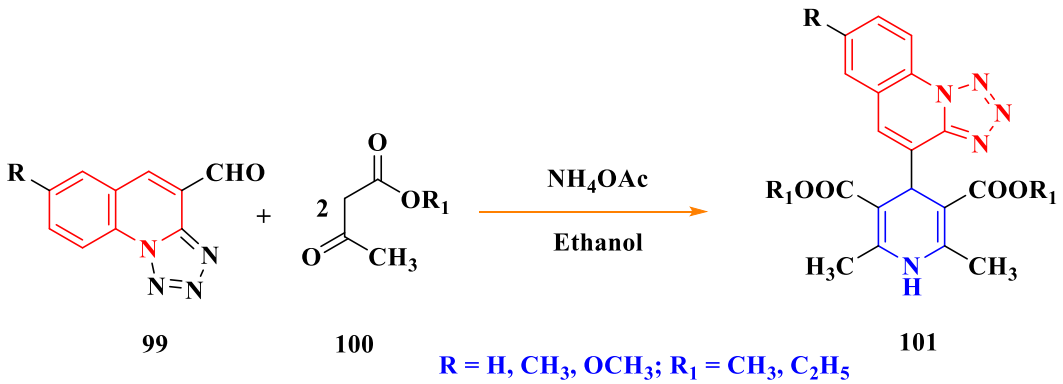

99 **100** **101**

R = H, CH_3, OCH_3; R_1 = CH_3, C_2H_5

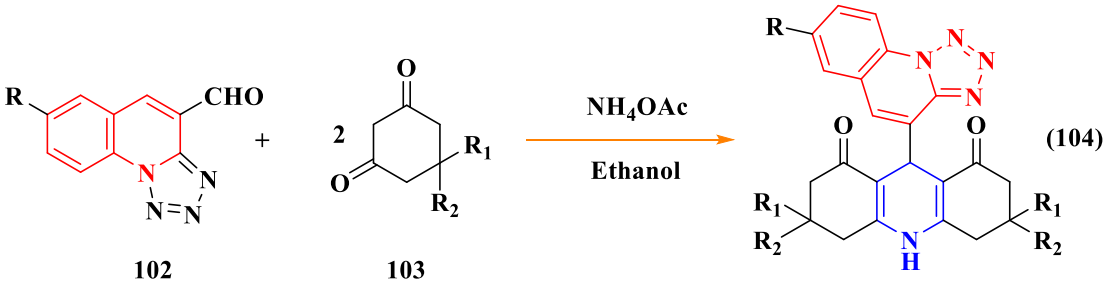

102 **103**

R = H, CH_3, OCH_3; R_1 = H, CH_3; R_2 = CH_3, C_2H_5

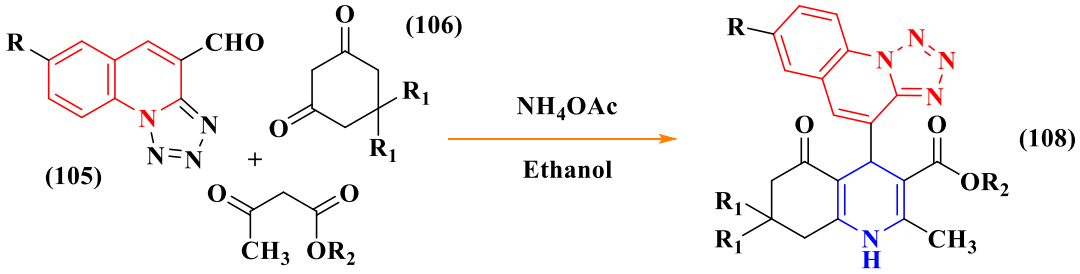

R = H, CH_3, OCH_3; R_1 = H, CH_3; R_2 = CH_3, C_2H_5

Gandhi and Zarezadeh, 2015 reported quinolinyl 1,4-dihydropyridines (**112**) in a facile and efficient protocol via a one-pot four-component condensation of 2-chloroquinoline-3-carbaldehydes (**109**), aryl amines (**110**), acetylenedicarboxylates (**111**) and malononitrile (**30**) in moderate to excellent yields. Triethylamine was used as a catalyst, ethanol as the solvent under reflux condition for 10 h: a maximum of 92 % yield was obtained.

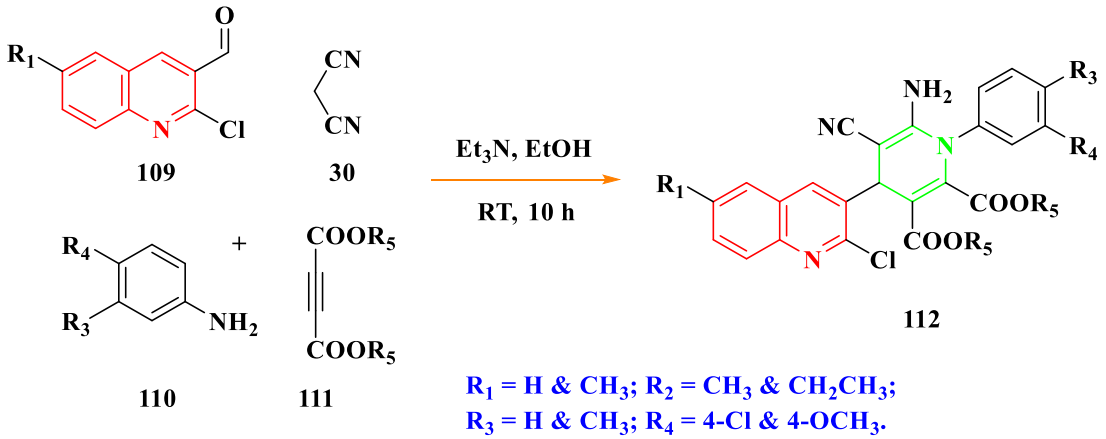

Kathrotiya and Patel, 2013 described a one-pot three-component cyclocondensation of β-aryloxyquinoline-3-carbaldehydes (**113**) and beta enaminones (**114**). Piperidine was used as a catalyst in ethanol. Anti-tuberculosis activity were evaluated against *Mycobacterium tuberculosis* H37Rv.

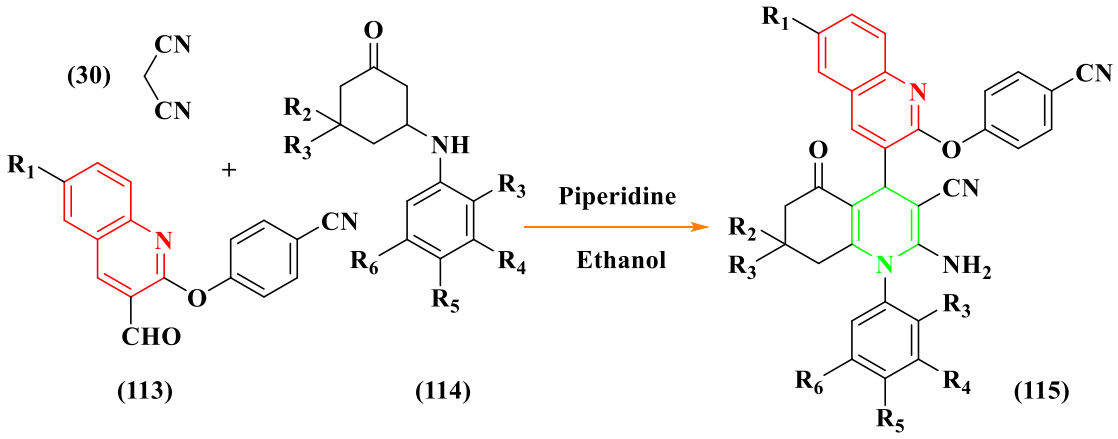

2.1.3. The synthesis and importance of sulfur based heterocycles

The synthesis of sulfur-based molecules has attracted significant attention due to their application in industry, medicine and organic chemistry (Metzner and Thuillier, 1994; Nagao, 1977; Nudelman, 1984; Chatgilialoglu and Asmus, 2013). Thiolic precursors are fundamental substrates for the synthesis of many organosulfur compounds (Koval. 2007). Alicyclic thiols (benzyl mercaptans) are considered as masked thiols as they can be readily transformed by hydrolysis or acyl group transfer reactions under mild conditions (Wuts and Greene, 2006; Koval, 1994; Mukaiyama *et al*., 1973; McGarvey *et al*., 1986; Conrow and Portoghese, 1986). The presence of sulfur atoms result in

significant changes to the cyclic molecular structure due to the availability of unshared pairs of electrons and the difference in electronegativity between heteroatoms and carbon. As a result, these heterocycles are considered as promising materials in different areas of pharmaceutical and agrochemical research, and also more recently as compounds with interesting physical properties for magnetism and conductivity. Sulfur-based heterocycles are common constituents of petroleum and liquids derived from coal, and they are found in various secondary metabolites of micro-organisms and plants. For example, penicillins and cephalosporins have sulfur-containing rings.

Simple thiol favoring agents are the alkyl, alicyclic, and aromatic thiols which may be metabolized along several pathways. Simple aliphatic and aromatic thiols undergo S-methylation in mammals to produce the corresponding methyl thioether or sulfide. Methylation is catalyzed by thiopurine methyltransferase in the cytoplasm and thiol methyltransferase in microsomes (Glauser *et al*., 1993). Quinoline containing fused sulfur heterocycles, such as 3,4-dihydro-2*H*-thiopyrano[2,3-*b*]quinoline (**116**) showed metabotropic glutamate receptor antagonistic activity, in particular, mGlu 1 receptor activity (Xiao *et al*., 2006), and 2*H*-thiopyrano[2,3-*b*]quiunoline-2-carboxylic acid (**117**) could be used as a strong antioxidant to protect against oxidative DNA damage from harmful free radicals and inhibitors of protein kinase casein kinase II **(Fig. 7)** (Syniugin *et al*., 2016).

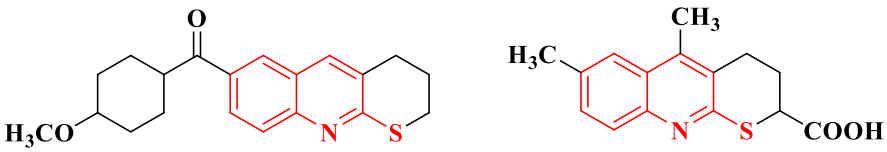

mGlu 1 receptor antagonist (116) **antioxidant (117)**

Fig. 7. Biologically active molecules containing 2*H*-thiopyrano[2,3-*b*] quinoline ring systems.

Wu *et al*., 2013 reported an efficient procedure for the stereo controlled construction of 2H-thiopyran[2,3-*b*]quinoline (**120**) starting from simple compounds. The domino Michael/Aldol reaction between 2-mercapto benzaldehydes (**118**) and 3-phenylprop-2-enal (**119**), promoted by chiral diphenylprolinol TMS ether, proceeded with excellent chemo- and enantioselectivity. Synthetically useful and pharmaceutically valuable 2H-thiopyrano-[2,3-*b*]quinolines (**120**), high yields of 90-99 %, were obtained.

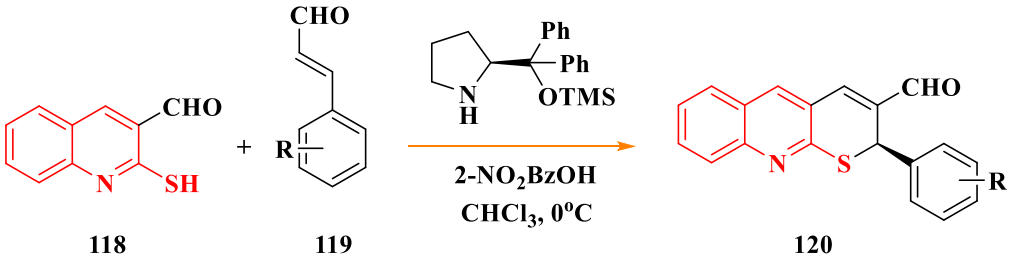

118 119 120

R = 2-F, 4-F, 3-Cl, 2-Br

Hagrs *et al.*, 2015 presented a series of new 6-methoxy quinoline-3-carbonitrile derivatives (**125, 127** and **129**) and evaluated their antimicrobial activity against Gram-positive bacteria, *Streptococcus pneumonia*, *Bacillus subtilis* and fungi *Aspergillus fumigatus*, *Syncephalastum racemosum*, *Geotriucum candidum* and *Candida albicans*.

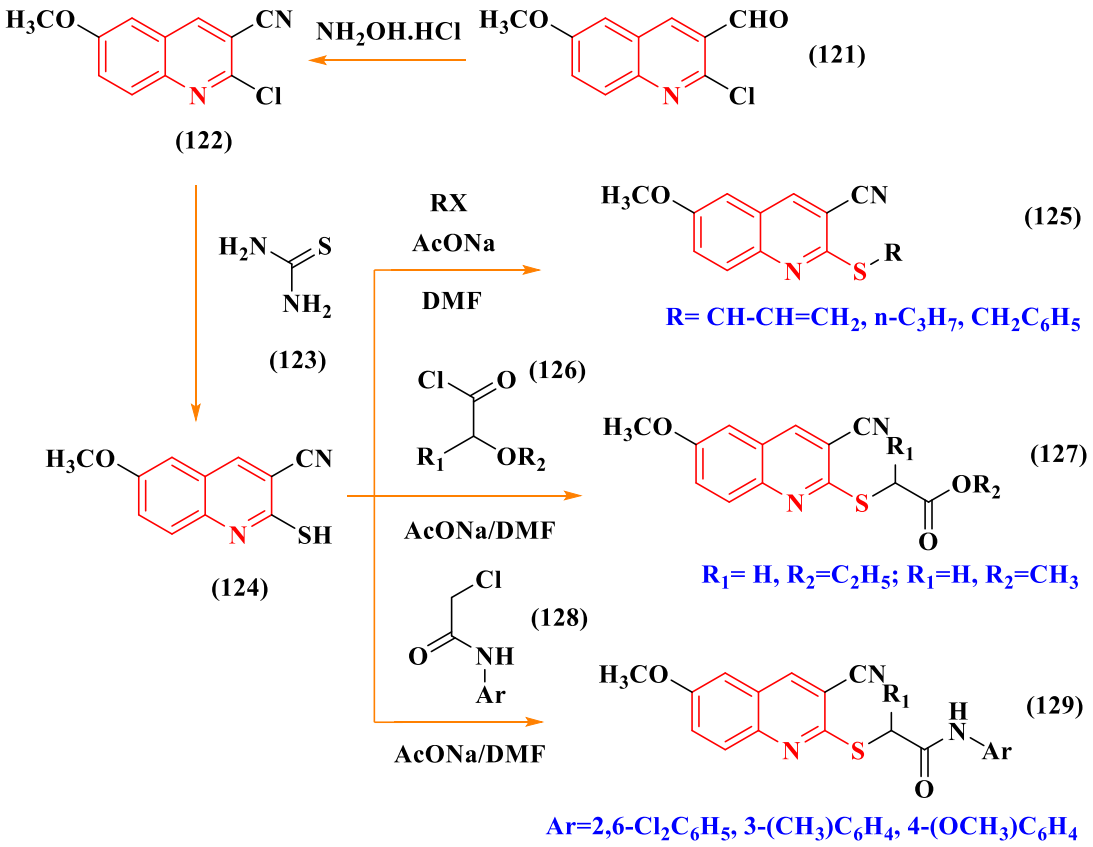

Amongst the sulfur heterocycles, interestingly lipoic acid is known as a universal antioxidant (Biewenga *et al.*, 1997; Packer, 1998; Packer *et al.*, 1995; Tirosh *et al.*, 1999). Its antioxidant activity is attributed to the capacity to scavenge free radicals in both membrane and aqueous domains. By chelating transition metals in biological systems, lipoic acid prevents membrane lipid peroxidation and protein damage through the redox regeneration of endogenous antioxidants such as vitamin E (α-tocopherol (**132**)), vitamin

C (ascorbic acid (**131**)) and glutathione (**130**) **(Fig. 8)**, thus maintaining an intracellular antioxidant balance (Harnett *et al*., 2002). They have also been extensively studied as useful neuroprotective agents (Boldyrev *et al*., 2004; Roghani and Behzadi, 2001; Stamford *et al*., 1999). Lipoic acid (**133**) is readily absorbed by diet, transported, taken up by cells, and reduced to dihydrolipoic acid (DLA) (**134**) in various tissues, including the brain.

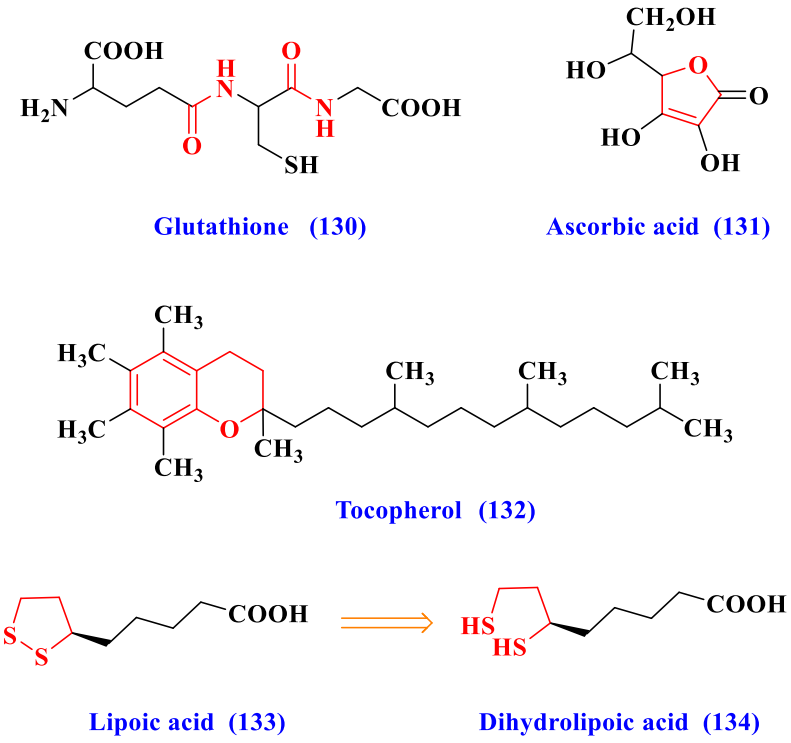

Fig. 8. Chemical structure of natural antioxidants glutathione, ascorbic acid (vitamin C) and α-tocopherol (vitamin E), lipoic acid and its reduced metabolite dihydrolipoic acid

Recently, focus has been placed on pharmacological tools that are able to act as far upstream as possible in the neurodegenerative cascade which are able to reach different selected targets. Therefore the structure of lipoic acid (**133**) was combined with a pharmacophore with well-established biological properties such as the ability to inhibit acetylcholinesterase (AChE) activity. The design strategy leading to these compounds is outlined by linking the structure of lipoic acid to that of an appropriate pharmacophore. Lipoic acid represents a privileged structure on which the selected pharmacophore is inserted to achieve selectivity for given targets.

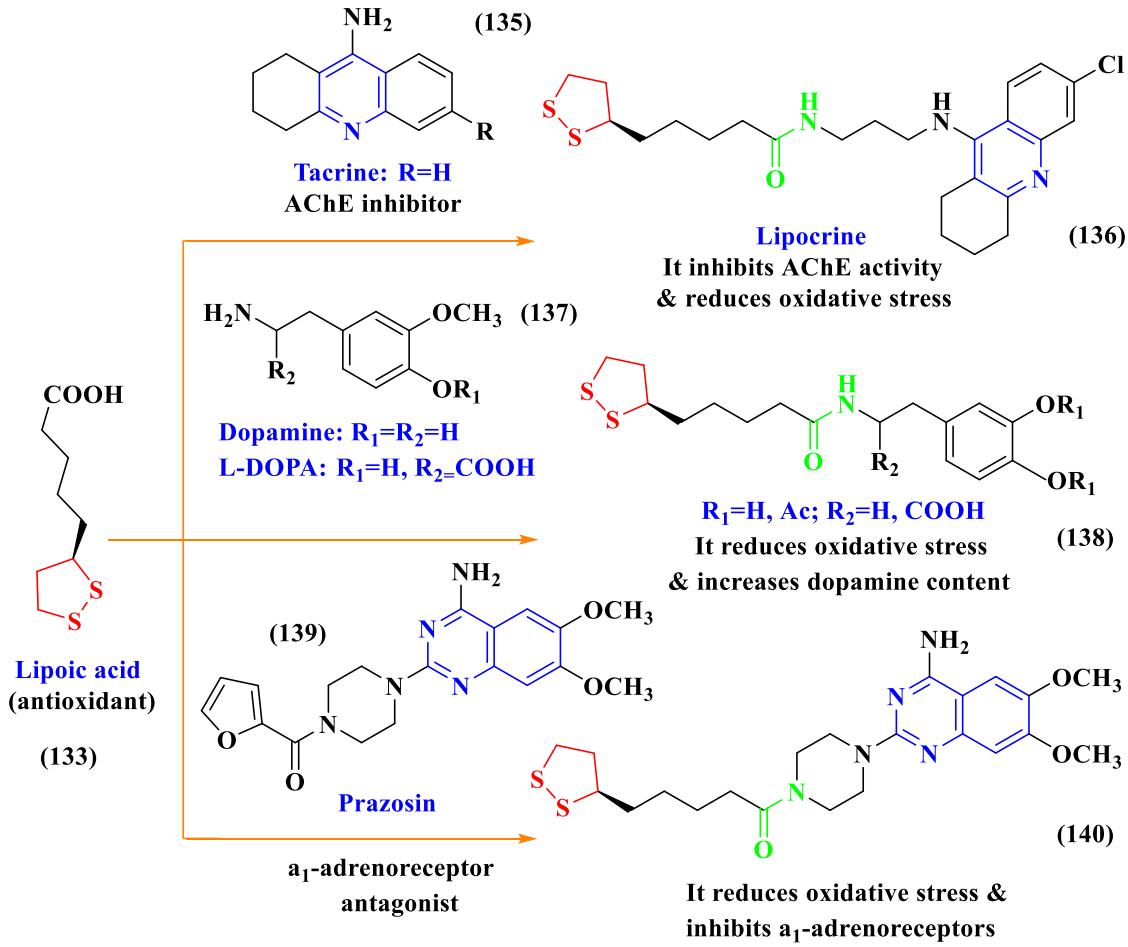

Fig. 9. Examples of multi-target directed compounds.

Lipocrine (**136**) emerged as a candidate for drug development, displaying multiple biological properties such as inhibition of AChE activity, inhibition of AChE induced Aβ aggregation, ability to protect cells against reactive oxygen species (ROS) (Rosini *et al*., 2005) and as promising lead compounds for treatment of Alzheimer (**Fig. 9**).

Benchekroun *et al*., 2016 reported the synthesis of novel multifunctional tacrines (**114**) for the treatment of Alzheimer's disease, by Ugi reaction of a lipoic acid (**133**), melatonin like isocyanide (**143**), formaldehyde (**142**) and tacrine derivatives (**141**). One of the synthesized compounds was identified as a promising permeable agent which showed excellent antioxidant properties, strong cholinesterase inhibitory activity, less hepatotoxicity and best neuroprotective capacity.

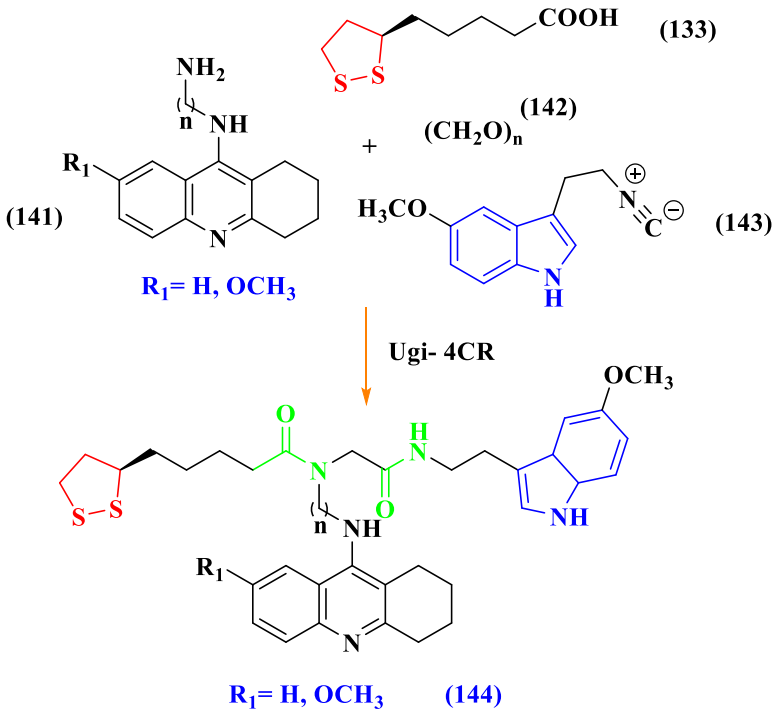

There is a rise in the number of publications confirming the beneficial effect of lipoic acid in the therapy of many diseases, including diabetes mellitus, atherosclerosis, degenerative processes in neurons, diseases of joints, or acquired immune deficiency syndrome (AIDS). An interest in contemporary medicine of this compound results from the unique reductive power of lipoic acid (Roy and Packer, 1998).

2.2. Multi-component reactions

Multi-component reactions (MCRs) are generally defined as one-pot reactions where more than two starting materials react to form a product, incorporating essentially all of the atoms of the educts. MCRs have gained considerable popularity in the field of contemporary organic synthesis. They represent ideal synthetic tools to generate structures of great complexity and diversity from simple starting materials and therefore are extensively applied by medicinal chemists to construct diverse chemical libraries of "drug-likeness" (Domling *et al*., 2012; Akritopoulou-Zanze, 2008; Weber, 2002; Hulme and Gore, 2003). The rapid, easy access to biologically relevant compounds and the scaffold diversity of MCRs has been recognized by the "synthetic" community and academia as a preferred method to design and discover biologically active compounds. MCRs chemistry has been reviewed multiple times in the past, focusing mostly on diverse synthetic and structural aspects (Dömling, 2006; Simon *et al*., 2004; Ugi, 1962; Ugi, 1982; Armstrong *et al*., 1996; Montgomery, 2000; Dömling and Ugi, 2000;

Ulaczyk-Lesanko and Hall, 2005; Mironov, 2006; Tempest, 2005; Ramón and Yus, 2005; Kappe, 2003; Orru, and de Greef, 2003; Ugi, 2003; Balme *et al*., 2003; Zhu, 2003; Hulme and Gore, 2003; Masciadri *et al*., 2003; Dömling, 2002; Lockhoff and Frappa, 2002; Orru and Ruijter, 2010; Toure and Hall, 2009; Kalinski *et al*., 2010). The biological chemistry of MCRs is very rich and provides great opportunities for investigation of small molecular weight compounds with biological activity. Generally, there are different classification schemes of MCRs according to the reaction mechanisms, the components involved, or their intrinsic variability (Zhu and Bienayme, 2005). Many basic MCRs are named reactions, for example, Ugi (Ugi, 1959), Passerini (Passerini, 1921), Van Leusen (Van Leusen *et al*., 1977), Strecker (Strecker, 1854), Hantzsch (Hantzsch, 1881), Bignelli (Biginelli, 1891) or one of their many variations.

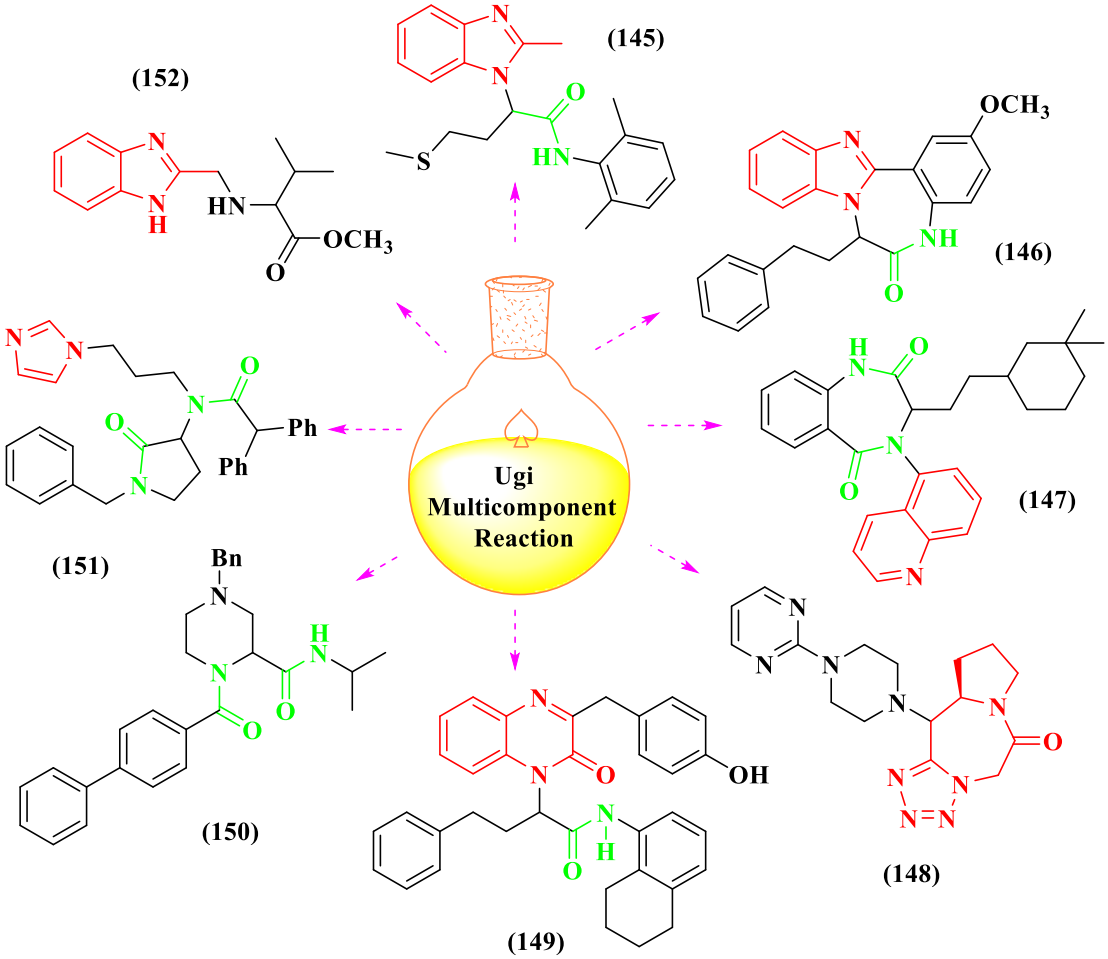

Fig. 10. UDC strategy allows for great scaffold diversification of an initial Ugi reaction by using orthogonal protected bifunctional starting materials.

The four-component Ugi reaction (Ugi-4CR) has attracted enduring attention owing to its broad input scope, high diversity of products, unmatched versatility and simple operation (Ugi *et al*., 1965). It is noteworthy that the Ugi-4CR provides a linear dipeptide-like skeleton rather than a more valuable heterocyclic ring. A versatile example for the libraries of drug-like advanced compounds is the Ugi-Deprotection-Cyclization (UDC) procedures leading to great scaffold diversity, e.g., benzimidazoles (**145**, **146** and **152**), benzodiazepindione (**147** and **148**), tetrazolodiazepinone (**151**), quinozalinones (**149**), γ-lactams and piperazines (**150**) **(Fig. 10)** (Keating and Armstrong, 1996; Szardenings *et al*., 1997; Hulme *et al*., 2000; Hulme *et al*.,1999; Golebiowski *et al*., 2000; Tempest *et al*., 2001; Nixey *et al*., 2002; Faggi *et al*., 2002; Zhang and Tempest, 2004; Hulme and Dietrich, 2009; Tejedor and Garcia-Tellado, 2007; Isambert and Lavilla, 2008; Willy and Mueller, 2008; Simon *et al*., 2004).

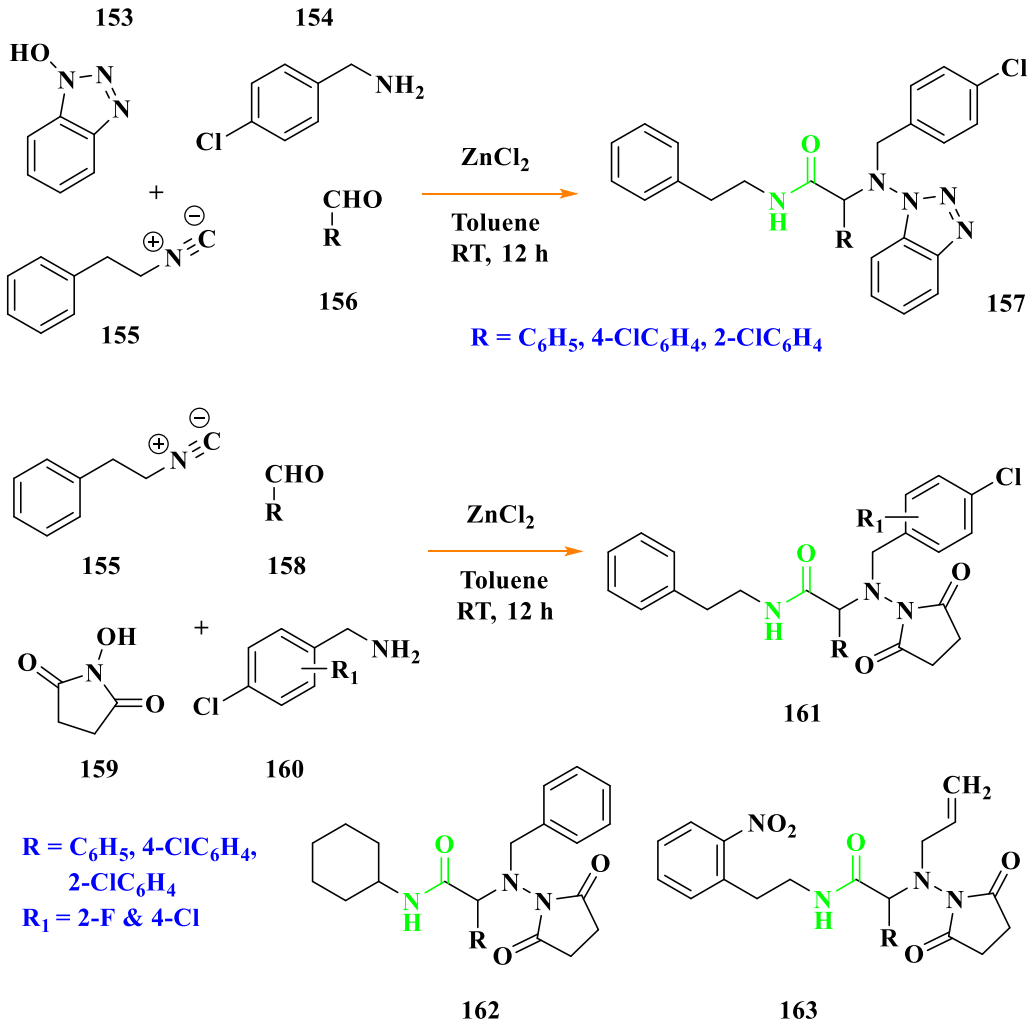

Recently, Chandgude and Dömling, 2017 reported Ugi-4CR with *N*-hydroxyimides (**154**) as a novel carboxylic acid isostere (**153**) towards one-pot synthesis of α-hydrazino amides (**157**). The reaction required 30 mol % of $ZnCl_2$ and toluene at room temperature for 12 h. The readily available *N*-hydroxyimides, which replaced the toxic and unstable hydrazines/oxaziridine is used for the synthesis of α-hydrazino amides.

Venkata Prasad *et al*., 2017 described the novel synthesis of pyrrole[2,3-c]pyridone (**168**) by Ugi-4CR. At 50℃, 50 mol % of PTSA was used as a catalyst in methanol for one h and the Ugi adducts were formed with a maximum yield of 91 %. The methodology was successfully employed to the electron deficient anilines (**167**) and phenyl glyoxylic acids (**166**) having a CF_3 group.

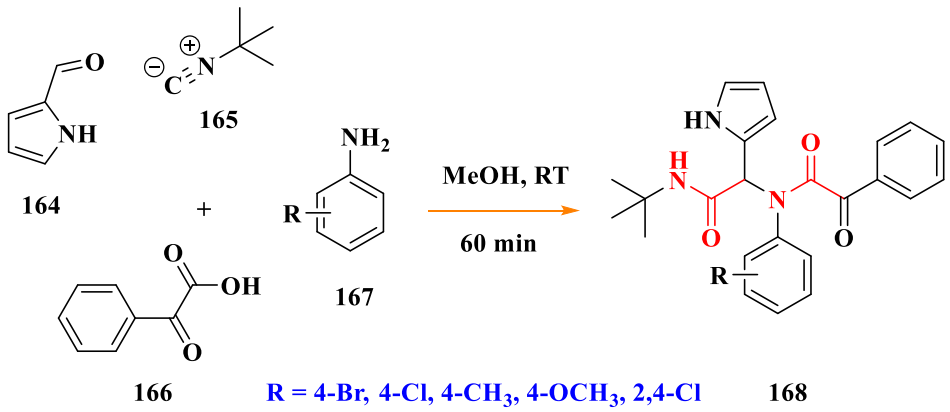

The Kabachnik-Fields reaction (Kabachnik and Medved, 1952) is an important multi-component reaction using aldehydes, amines and dialkyl phosphites in the presence of a Brønsted or Lewis acid, to produce α-amino phosphonates. In recent years, much attention has been made on the α-amino phosphonates. They can be considered as structural analogs of the corresponding α-amino acids and transition state mimics of peptide hydrolysis. α-Amino phosphonates have several biological activities, such as an antibiotic, an enzyme inhibitor, HIV protease and anti-tumor agents (Atherton *et al*., 1986; Paige *et al*., 1989; Peyman *et al*., 1994; Jin *et al*., 2006).

Sambath *et al*., 2013 described a facile method for the synthesis of novel α-amino phosphonates (**172**) by Kabachnik-Fields reaction. The reaction was carried out with equimolar quantities of 4-amino-*N*-2-thiazolyl-benzenesulfonamide (**171**) (Sulfathiazole), dimethyl phosphite (**169**) and aldehydes in dry toluene at reflux conditions. 70-80 % product yield was obtained at 50℃ between 5-6 h. Antibacterial and antifungal applications were further investigated for the synthesized compounds.

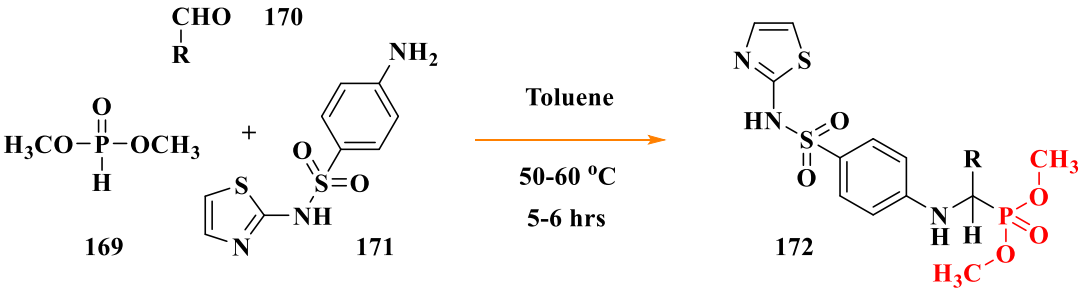

R = 4-NO_2, 3-OCH_3, 3-CF_3, 3-Cl, 4-Cl, 3-F

Amulrao *et al*., 2012 presented a convenient, one-pot three-component Kabachnik-Fields reaction of novel *N*-phenyl isoquinolone-1-phosphonates (**176**) from ethyl 2-(2-formyl-4,5-dimethoxyphenyl) acetate (**173**) and anilines (**174**). The reaction was successfully carried out by using trifluoroacetic acid as a catalyst in acetonitrile: 64-74 % yield was obtained. Antibacterial studies were investigated for the synthesized compounds.

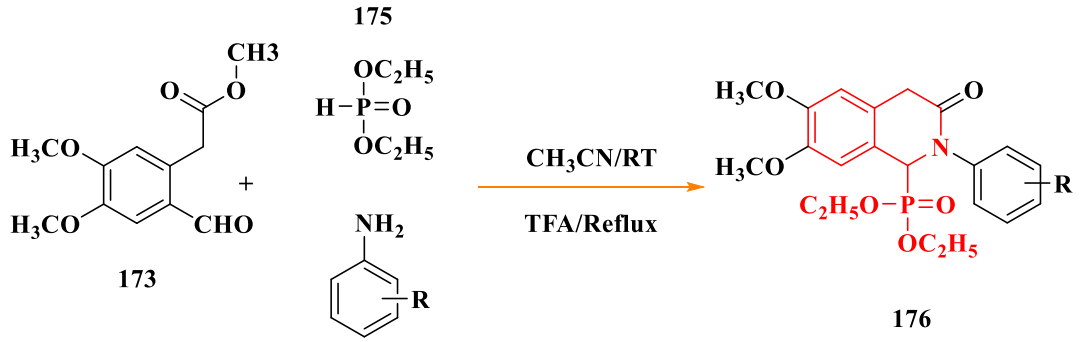

R = 4-F, 4-Cl, 4-Br, 3-Cl, 4-CH_3

Badadhe *et al*., 2011 reported the synthesis and antibacterial activity of novel α-amino phophonates (**179**). The reaction was achieved by reacting 1-phenyl-3-(pyridine-4-yl)-1*H*-pyrazole-4-carbaldehyde (**177**) with various anilines (**178**), in ethanol, in the presence of glacial acetic acid. Further treatment with diethyl phosphite (**175**) in the presence of conc. HCl at room temperature resulted in the product.

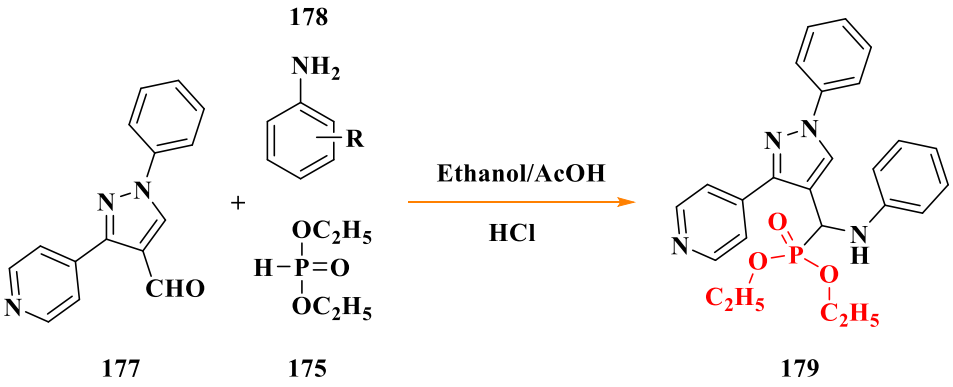

R = 2-F, 2-Cl, 2-CH_3, 4-OCH_3

Hantzsch reaction is a well-known three-component MCR, which affords 1,4-dihydropyridine derivatives (**91**) using β-ketoesters (**180**), aldehydes (**181**) and ammonia. A calcium channel blocker, "Nifedipine" was synthesized by this reaction (Khadilkar and Chitnavis, 1995; Khadilkar *et al*., 1995).

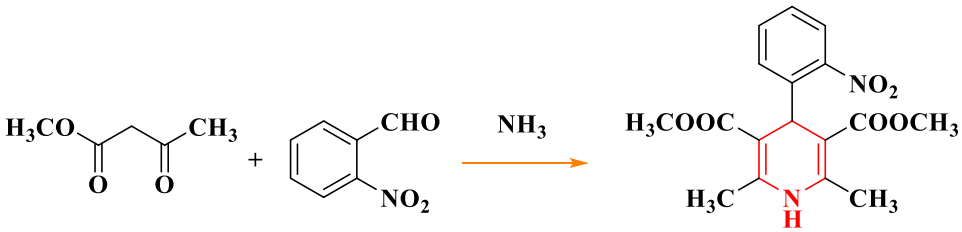

Rao and Parthiban, 2014 reported the simple, convenient one-pot synthesis of a library of highly functionalized hexa-substituted 1,4-dihydropyridines (**185**, **186** and **187**) (1,4-DHPs) from 2-aminopyridine (**188**) catalyzed pseudo three-component reaction of nitroketene-*N*, S-acetals (**183**) and aldehydes (**184**).

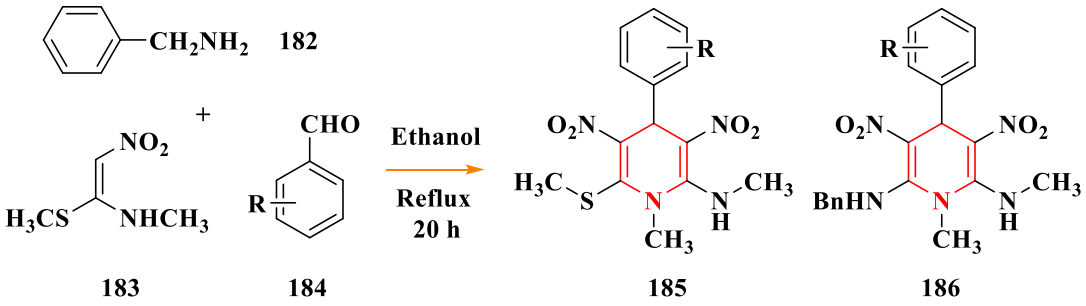

R = 4-F, 4-Br, 4-OH, 4-OCH_3

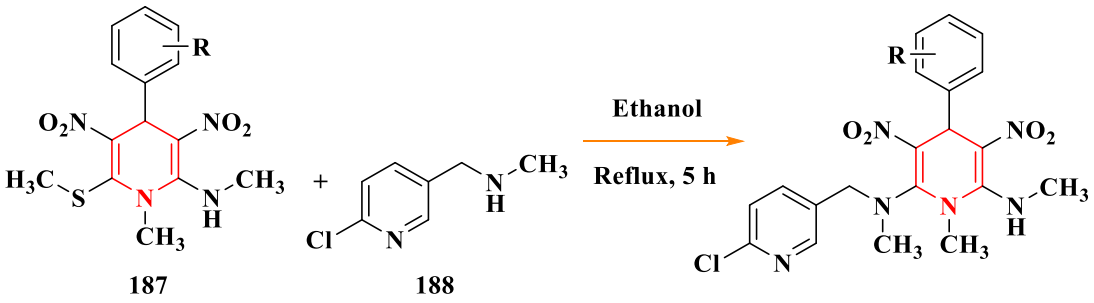

187 188

R = 4-F, 4-Br, 4-OH, 4-OCH$_3$ Neonicotinoid insecticide (189)

Also, an analog of neonicotinoid (**189**), for example, nitenpyram was designed by the treatment of a solution of 1,4-DHPs with the synthesized amines in ethanol under reflux for 5 h.

Chao *et al*., 2014 reported a Hantzsch type four-component synthesis of spiro-oxindole derivatives (**194**) bearing dihydropyridines. This one-pot reaction was successfully achieved by malononitrile (**30**), aromatic amines (**191**), *N*-pyrrolidine-2,4-dione (**190**), and isatin (**192**) where 4-dimethylamino pyridine (4-DMAP) was used as a catalyst in ethanol: the recorded yield was 80-95 %.

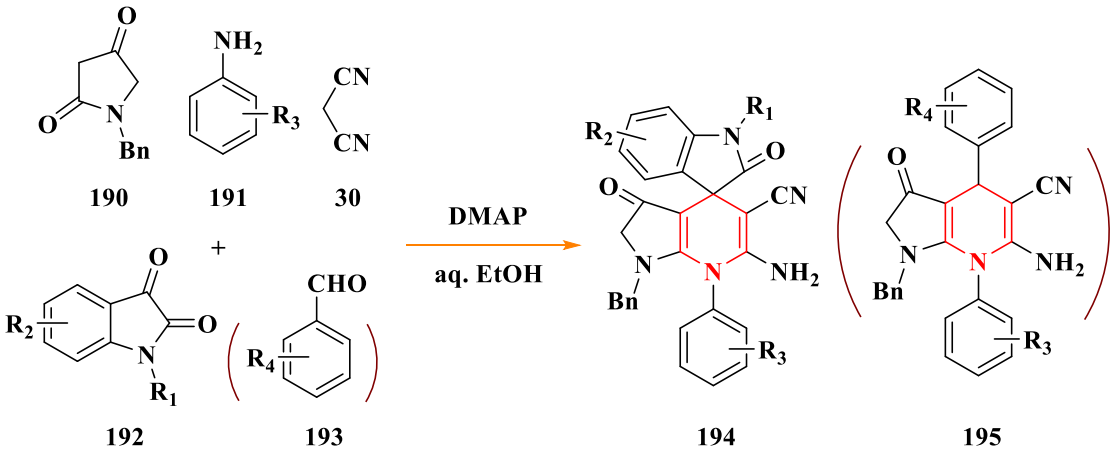

190 191 30 192 193 194 195

R$_1$ = H & CH$_3$; R$_2$ = H, 5-NO$_2$, 5-CH$_3$; R$_3$ = 3-Br, 4-CH$_3$, 4-F, 4-Cl; R$_4$ = H, 4-CH$_3$, 4-Cl.

Recently, Habibi *et al*., 2017 presented a three-component efficient synthesis of 4*H*-pyrans (**198**) from aromatic aldehydes (**196**), malononitrile (**30**) and β-keto esters (**197**) by using hexamethylenetetramine (HMTA) as a catalyst. These molecular building blocks are well known for their biological activity and were synthesized by using 25 mol % of HMTA and water: 81-95 % yield was obtained.

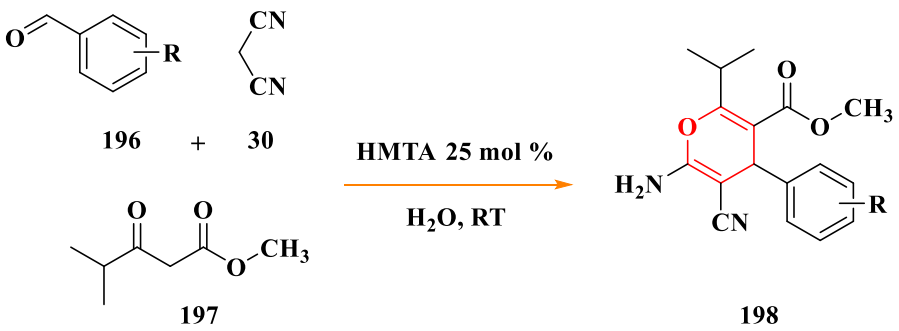

R = 3-NO_2, 4-Cl, 3-OCH_3, 4-NO_2, 4-OCH_3, 2-Cl

Magar *et al.*, 2013 reported a three-component condensation of the 2-aminochromene derivative (**204**) by a one-pot fashion from aromatic aldehydes (**203**), phenol (**202**) and active methylene compounds (**30**), in the presence of silica gel supported polyamine heterogeneous catalyst (**201**). IR, SEM and TGA studies were used for the catalyst characterization. A maximum of 95 % yield was afforded after 2 to 5.30 h under reflux conditions.

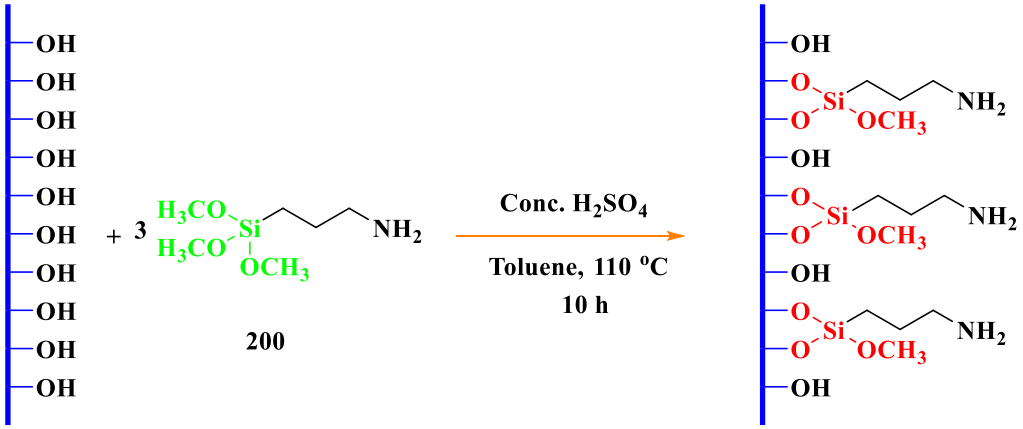

199 Synthesis of solid supported amino functionalized catalyst GN3 201

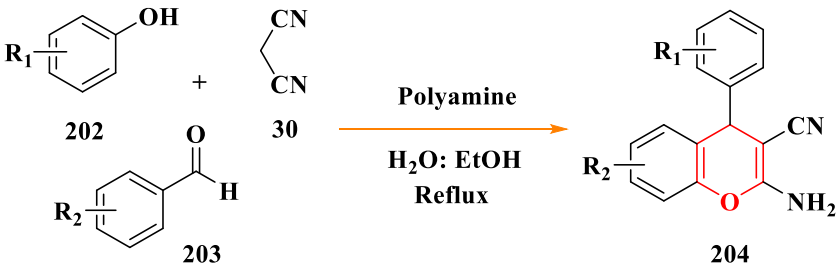

R_1 = H & 4-Cl; R_2 = H, 4-Cl, 4-NO_2, 3-NO_2, 4-CH_3, 4-OH

Recently, Romdhane and Jannet, 2013 reported a one-pot three-component condensation reaction of aldehydes (**205**), malononitrile (**30**) with methyl acetoacetate (**180**) and 8-hydroxyquinoline (**207**), separately. The reaction was carried out by using sodium carbonate as a catalyst in ethanol for 3 h: maximum yield of 81% was obtained.

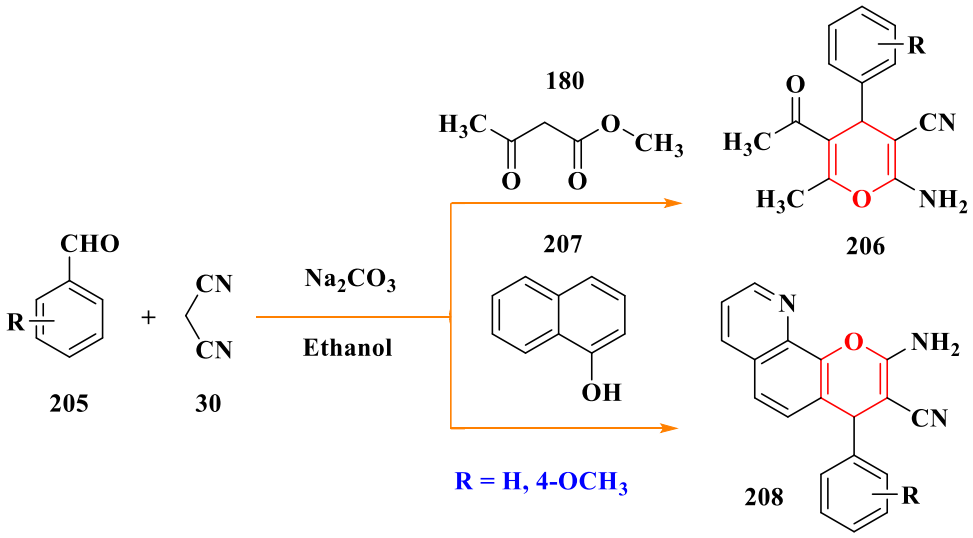

El-Agrody and Al-Ghamdi, 2011 published the synthesis of 4*H*-pyrano[3,2-*h*]quinoline-3-carbonitrile derivatives (**211**) from 8-hydroxy-2-methylquinoline (**209**) with α-cyano-*p*-chloro/bromocinnamonitriles (**210**). A maximum of 91 % yield was reported when piperidine in ethanol was used as a catalyst under refluxing condition for 60 minutes.

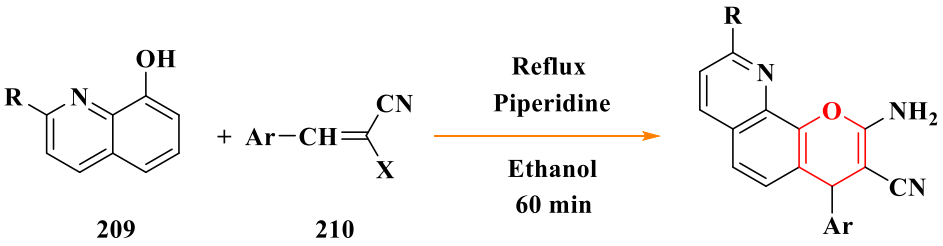

These classical methods for the synthesis of biologically active scaffold molecules such as peptides, α-aminophosphonates, 1,4-dihydropyridines, 4*H*-chromenes and 4*H*-pyrans have several drawbacks such as long reaction time, lower product yields and harsh refluxing conditions. Thus, it is evident that the development of more flexible and effective protocols, such as ultrasonication and microwave irradiation are required.

2.3. Ultrasonic and Microwave irradiations

Ultrasound in chemistry, also referred to as sonochemistry, offers a method of chemical activation which has broad applications. It uses equipment which is relatively inexpensive. The driving force for sonochemistry is cavitation therefore the general requirement is that at least one of the phases should be a liquid. The use of ultrasound has wide applicability but presents a significant scientific challenge in understating its underlying physical phenomenon i.e. acoustic cavitation. The use of sonochemistry fits into the theme of sustainable chemistry because it aims to use less/non-hazardous chemicals and solvents, reduce energy consumption, and increase product selectivity (Mason, 2003).

Recently, Guo and Yuan, 2010 reported a *L*-proline catalyzed efficient multi-component Hantzsch reaction, in ethanol, at 60℃ under ultrasound irradiation to afford the corresponding 1,4-dihydropyridine (**214**) derivatives in high yields. A maximum of 92 % yield was obtained within 30 minutes whilst the classical synthesis was completed in 6-8 h.

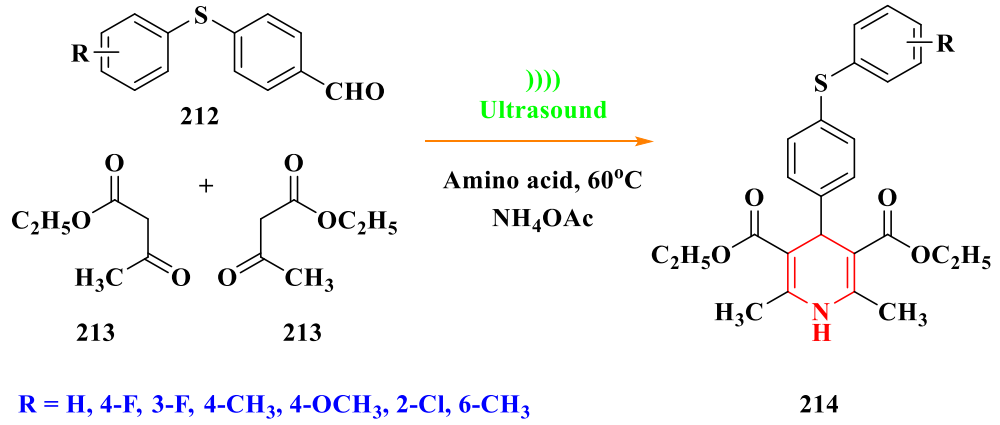

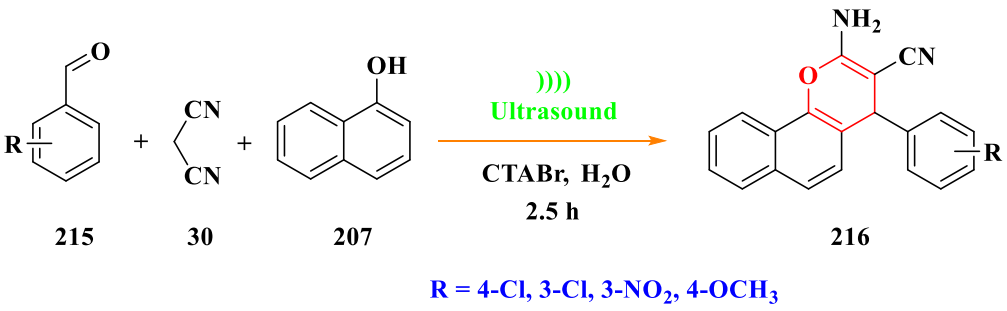

Multi-component synthesis of 4*H*-benzo[*h*]pyrans (**216**) was achieved by Jin *et al*., 2004 by reacting aromatic aldehydes (**215**), malononitrile (**30**) and naphthols (**207**), in one-

pot, using cetyl trimethyl ammonium bromide (CTABr) as a catalyst under ultrasonic irradiation. The reaction was carried out at room temperature for 2.5 h to afford 95 % yield.

Due to the ability of solids and liquids being able to transform electromagnetic energy into heat, microwave (MW) radiation has been widely employed as an energy source. Microwave irradiation has several advantages over conventional heating and these include homogeneous, rapid heating (deep internal heating), acceleration in reactions as a result of the heating rate (which cannot be reproduced by classical heating) and selective heating.

Recently, Lei Zhang *et al*., 2013 reported a novel and efficient methodology for the synthesis of three distinct sets of indole-based heterocyclic compounds from 1*H*-indole-2-carbaldehyde (**217**) via the Ugi condensation reaction. Cesium carbonate (Cs_2CO_3) was used as a base catalyst and the reaction was carried out using DMSO as a solvent at 80℃ under MW for 40 min.

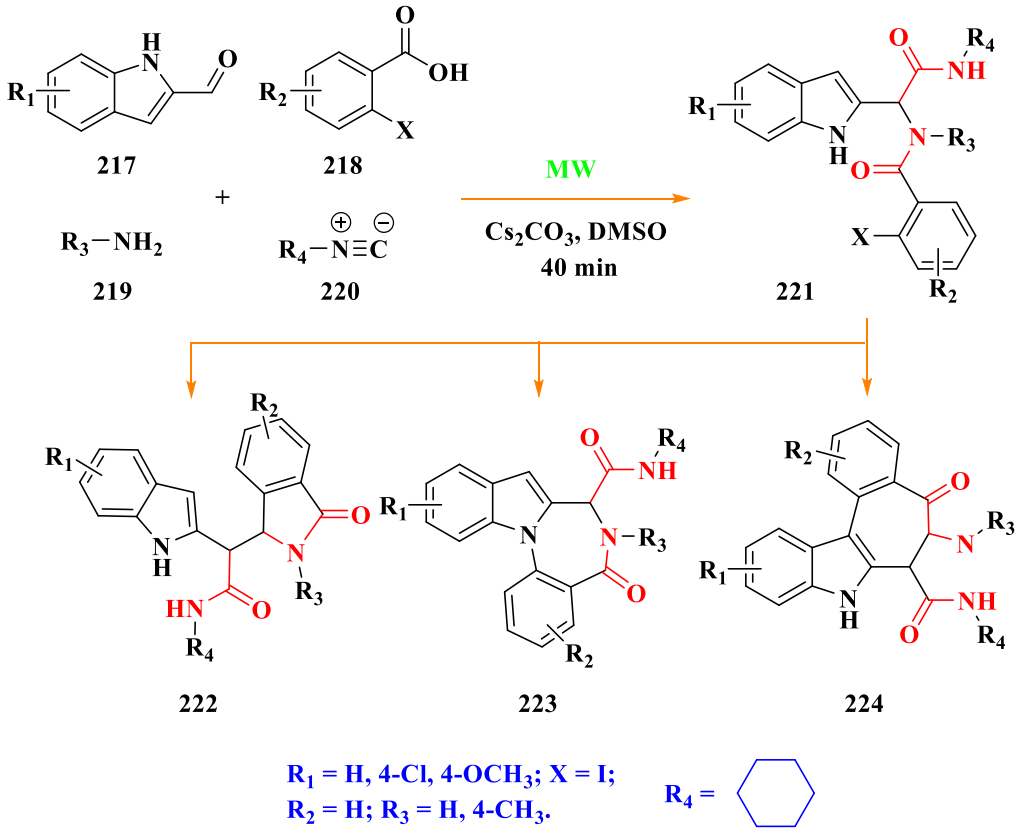

Keglevich *et al*., 2011 described an efficient MW synthesis of α-hydroxyphosphonates (**226**) via Kabachnik-Fields reaction. Sodium carbonate was used as a catalyst under MW condition for 20 minutes.

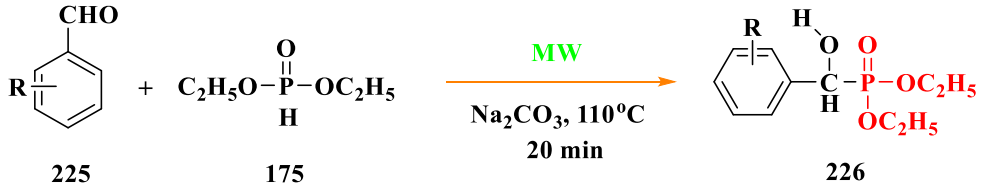

225 175 226

R = H, 4-OCH_3, 4-OEt etc

Al-Awadi *et al*., 2012 presented a Hantzsch-type pseudo four-component reaction for the synthesis of 2-unsubstituted dihydropyridines (**230**) from enaminones (**228**). The reaction offered 84-95 % yield under MW irradiation. Moderated yields were obtained under conventional route.

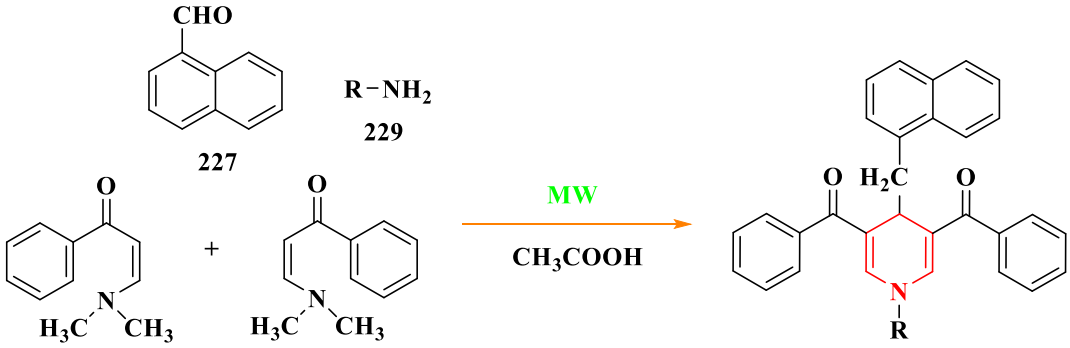

228 228 230

R=H, C_6H_5, p-HOC_6H_4, p-$CH_3OC_6H_4$

These investigations indicate that ultrasonic and MW-assisted organic reactions produce high yields of the target compound whilst lower quantities of side products are obtained. Hence the purification of the products via column chromatography is easier and faster. Indeed, new reactions and conditions that cannot be achieved by conventional heating can be performed using these techniques.

2.4. Heterogeneous catalysis

A heterogeneous catalyst is a material that continually creates active sites with its reactants under optimal reaction conditions. These active sites change the rates of the chemical reactions of the reactants localized on them without changing the thermodynamic equilibrium between the materials. In catalysis, a catalyst support plays

an important role and these materials are usually solid with high surface area. The activity of heterogeneous catalysts occurs at the surface area atoms. Consequently, great effort is made to maximize the surface area of a catalyst by distributing it over the support. The most frequently used catalyst supports are silica, graphene, zeolites and alumina (Ma and Zaera, 2006).

Due to its remarkable properties, boron nitride (BN) has shown promise as a novel support in catalysis and as a replacement for traditional oxide supports in different processes (Sun *et al.*, 2016). Hexagonal BN has not been studied extensively as a support; there are recent reports in the literature about the good performance of BN based catalysts in some catalytic processes. Several studies describe the use of BN supported noble metals for the deep oxidation of volatile organic compounds. Yabe *et al.*, 2012 reported a novel palladium-supported-on-BN catalyst (Pd/BN) (**233**) which is applicable for the partial-hydrogenation of mono and disubstituted alkynes to furnish the corresponding alkenes in the presence of diethylenetriamine (DETA), which exhibited an unprecedented acceleration effect for hydrogenation.

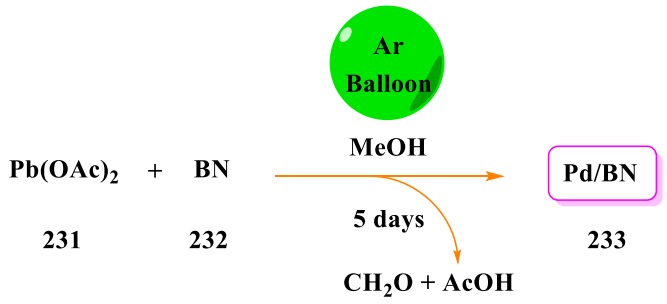

Preparation of Pd/BN catalyst

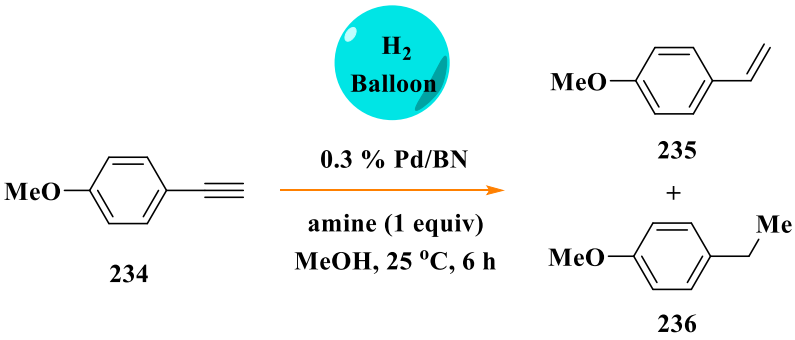

Wu *et al.*, 2001 have shown that a Pt/BN catalyst can remain active for 80 h at 185℃, while the activity of traditional Pt/γ-Al_2O_3 at the same temperature was found to decrease continuously with time. Lin *et al.*, 2002 and Wu *et al.*, 2003 have studied Pt/BN as a

catalyst for the deep oxidation of methanol and benzene. Jacobsen, 2001 studied a Ba-Ru/BN catalyst for ammonia synthesis and found that the activity of this catalyst is significantly higher than that of traditional catalysts. The selective hydrogenation of α,β-unsaturated aldehydes into unsaturated alcohols was achieved by BN supported Pt-Sn catalysts (Wu and Chen, 2005).

Boron nitride can be considered as a good candidate support. The choice of BN as the support was also directed by the search for new hydrophobic supports with high thermal conductivity, adapted to high-energy oxidation reactions under severe conditions. BN is one of the most interesting non-oxide ceramic materials because of its low density, excellent resistance to chemical attacks, high melting point, good thermal conductivity and high stability with respect to oxidation (Postole *et al*., 2005; Perdigón-Melón *et al*., 2002). Prior to the discovery of BN, materials traditionally used as supports of active phases were γ-Al_2O_3 and SiO_2. These materials possess low thermal conductivity and many acidic and basic sites, which causes sintering of the supported metal on hot spots and coverage of the catalyst by water (Yao *et al*., 1979; Trimm and Önsan, 2001). Moreover, the metal support interaction present in most oxide-supported metal catalysts has a negative influence on the catalytic activity (Carstens *et al*., 1998).

Ionic liquids (ILs) are gaining considerable attention as catalysts and support for multi-phasic catalysis because they can be tuned for specific applications. In comparison with the traditional catalysts, a main advantage of ILs is their structural diversity, which allows tuning of their properties. The tunable structures of the ILs by a combination of different cations with anions make them highly promising candidates for tailored catalysts (Rogers, 2007). ILs based imidazolium cations have been extensively studied with a variety of structural modifications leading to differences in the physical and chemical properties of the liquid. The use of ILs has broadened its scope to its role as a catalyst and reagent.

Recently, Siddiqui *et al*., 2014 reported a novel three-component one-pot methodology for rapid access to pyrido[1,2-*c*][1,3,5]thiadiazin-4-ones (**239**). A task-specific ionic liquid [bmim]SCN was used which could be recycled. The usage of water and easy recyclability of the ionic liquid were the green chemistry aspects of the study which was further explained.

Shaterian and Kangani, 2013 reported the synthesis of pyrazolo[1,2-a][1,2,4]triazole-1,3-dione derivatives (**242**) via a three-component reaction of aryl aldehydes (**240**), 4-phenylurazole (**241**) and malononitrile (**30**) in the presence of catalytic amount of 2-hydroxyethyl ammonium formate and 2-hydroxyethyl ammonium acetate as effective mild basic ILs at room temperature.

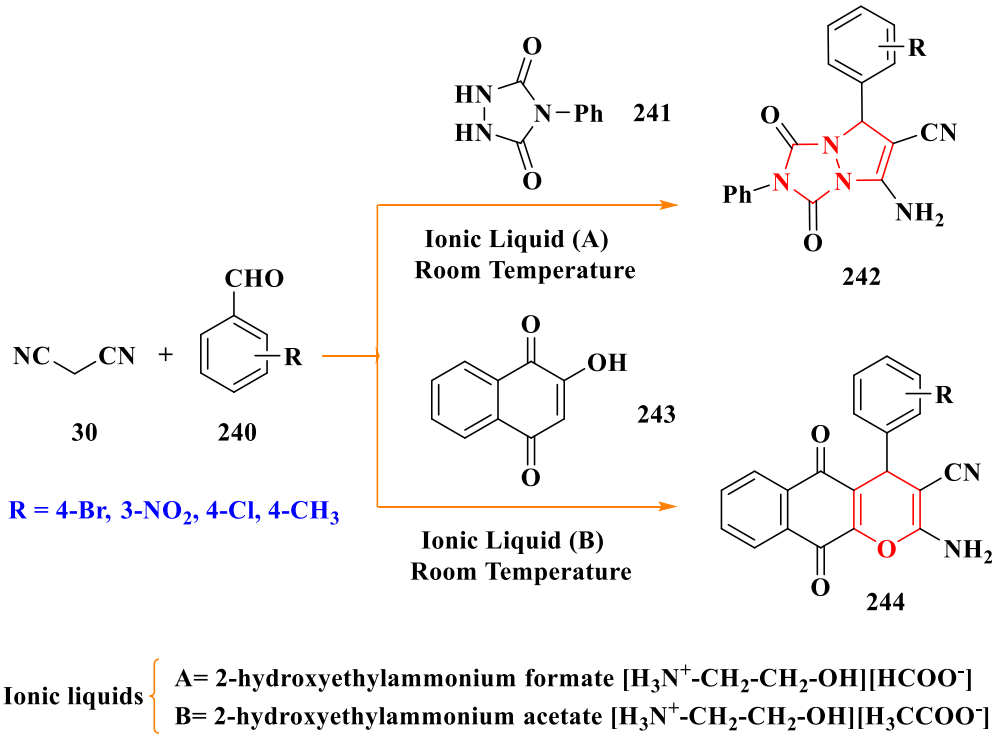

2.5. Biological applications

2.5.1. Antibacterial and antifungal activity against human diseases

Antibiotics are one of the most important weapons in fighting against bacterial infections and have greatly benefited the health-related quality of human life since their introduction. Over the past few decades, these health benefits are under threat as many commonly used antibiotics have become less effective against certain illnesses due to the bacteria developing resistance to antibiotics. Thus, it is essential to investigate alternate

drugs with reduced resistance. Novel drugs which are synthesized are playing a significant role in the prevention and treatment of human diseases.

The discovery and development of antimicrobial agents that have met with enormous success over the past 50 years provided many classes of natural products and semi-synthetic or synthetic compounds (marketing of over 100 antibacterial agents). Among them, quinoline and its derivatives, oxygen, nitrogen and sulfur-based molecules are still an important class of therapeutically useful antibacterial drugs (Hafez *et al*., 2015). The control of deadly infectious diseases including tuberculosis, caused by *Mycobacterium tuberculosis* is seriously threatened as multi-drug resistance is emerging and dissemination of resistant pathogenic microbes is the major concern. Additionally, patients with HIV/AIDS are immuno-compromised and very susceptible to opportunistic microbial infections including tuberculosis which necessitate continuous research into novel classes of antimicrobial agents. This requires active investigation with the goal of overcoming the phenomenon of multiple drug resistance (MDR). It is well-known that the quinoline nucleus and its derivatives, oxygen and sulfur-based moieties play a vital role in the search for a wide antibacterial activity spectrum. Structure-activity relationship (SAR) studies revealed that the antimicrobial activity of these heterocyclic molecules depends on the nature of the peripheral substituents and their spatial relationship within the nitrogen, oxygen and sulfur ring skeleton. Thus, these are promising new chemical targets for bacteria and fungi as well as host-based, immunological approaches and as evolving strategies for antimicrobial therapy.

2.5.1.1. Antibacterial activity against *Staphylococcus aureus*

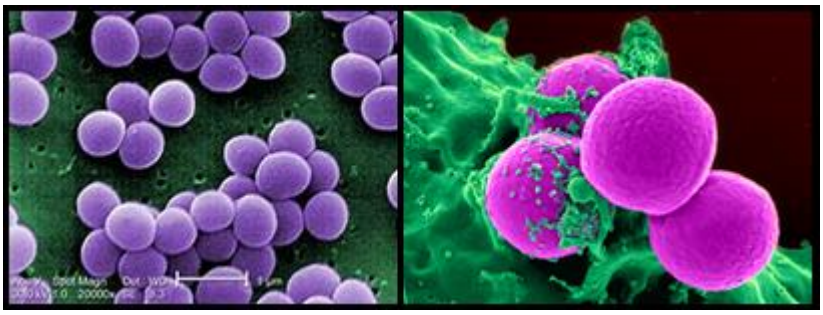

Fig. 11. SEM images of *Staphylococcus aureus* (Hess *et al*., 2012)

***Staphylococcus aureus* (*S. aureus*) (Fig. 11)** is a Gram-positive and a major human pathogen that causes a wide range of infections after injury or surgery. It affects

approximately 500,000 patients in hospitals annually (Awasthi, 2009). In animals and humans that are immune compromised or immune deficient, the bacteria may be life-threatening. Approximately 30% of individuals carry *S. aureus* in their nose, pharynx or back of the throat and on their skin. *S. aureus* causes numerous infections at various sites of the body (Hess *et al*., 2012). Some of these include, skin infections (causes boils, furuncles, styles, impetigo and other superficial skin infections in humans), infections of surgical and trauma wounds, urinary tract infections, food poisoning and gastro-intestinal tract infections, infections of organs including pneumonia (lung), osteomyelitis (bone), endocarditis (heart), phlebitis (veins and blood vessels), mastitis (breast and formation of abscesses) and meningitis (brain) (Tong *et al*., 2015).

2.5.1.2 Antibacterial activity against *Bacillus cereus*

Fig. 12. SEM images of *Bacillus cereus* (Nishimura *et al*., 2003)

***Bacillus cereus* (*B. cereus*) (Fig. 12)** is a Gram-positive bacteria, rod-shaped, aerobic, motile, a betahemolytic bacterium that produces toxins. These toxins can cause diarrhea, abdominal cramps, nausea and vomiting. The bacteria are present in foods and can multiply quickly at room temperature. Some strains are harmful to humans and can cause foodborne illness. *B. cereus* is also known to cause difficult-to-eradicate chronic skin infections, though less aggressive than necrotizing fasciitis, it can cause keratitis (Pinna *et al*., 2001).

2.5.1.3 Antibacterial activity against *Enterococcus faecalis*

Enterococcus faecalis (*E. faecalis*) **(Fig. 13)** normally a gut commensal, is a Gram-positive and a frequent cause of many serious human infections, including urinary tract infections, endocarditis, bacteraemia, and wound infections (Pinheiro and Mayer, 2014).

Among the diseases that *E. faecalis* causes, urinary tract infections are the most common, responsible for approximately 110,000 cases yearly, many of which are nosocomial.

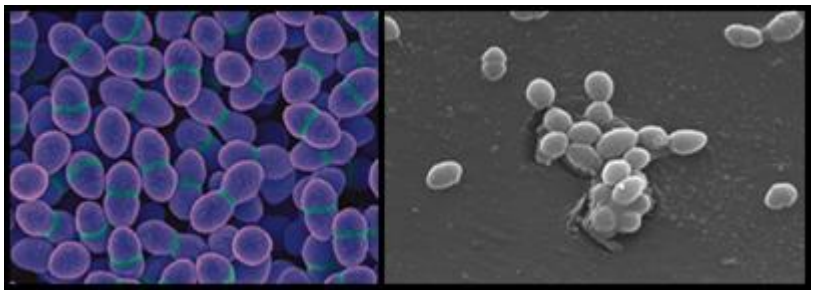

Fig. 13. SEM images *Enterococcus faecalis* (Bulacio *et al*., 2015)

Infections with *E. faecalis* can be difficult to treat because of their frequent resistance to multiple antibiotics, including vancomycin (Zhanel *et al*., 2001), a drug of last resort for many Gram-positive infections.

2.5.1.4 Antibacterial activity against *Escherichia coli*

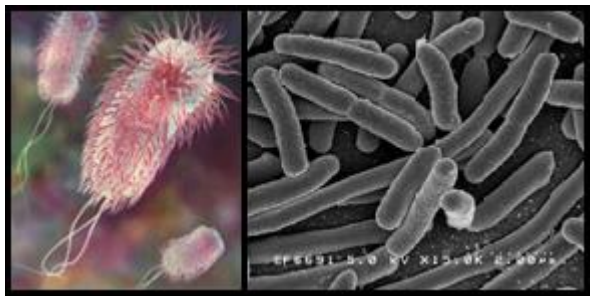

Fig. 14. *Escherichia coli* (Leung *et al*., 2016)

***Escherichia coli* (*E. coli*) (Fig. 14)** is a Gram-negative bacterium that lives in the digestive tracts of humans and animals. There are many types of *E. coli* and some can cause bloody diarrhea. Various strains of *E. coli* such as strain O157: H7, may also cause severe anaemia or kidney failure, which can lead to death. Other strains of *E. coli* can cause urinary tract infections amongst other infections (Vincent *et al*., 2010). Normally, *E. coli* infection occurs by coming into contact with faeces of humans or animals. This can happen when you drink water or eat food that has been contaminated by faeces.

2.5.1.5. Antibacterial activity against *Pseudomonas aeruginosa*

Pseudomonas aeruginosa (P. aeruginosa) is Gram-negative and an important pathogen which causes 10 % to 20 % of infections in most hospitals. *P. aeruginosa* infection is

especially prevalent among patients with burn wounds, cystic fibrosis, acute leukemia, organ transplants and intravenous-drug addiction.

Fig. 15. *Pseudomonas aeruginosa* (Tsang *et al*., 2003)

P. aeruginosa **(Fig. 15)** is a common nosocomial contaminant and epidemics have been traced to many items in the hospital environment. Patients who are hospitalized for extended periods are frequently colonized by this organism and are at increased risk of developing infection. The most serious infections include malignant external otitis, endophthalmitis, endocarditis, meningitis, pneumonia and septicaemia (Young and Amstrong, 1972).

2.5.1.6 Antifungal activity against *Candida albicans*

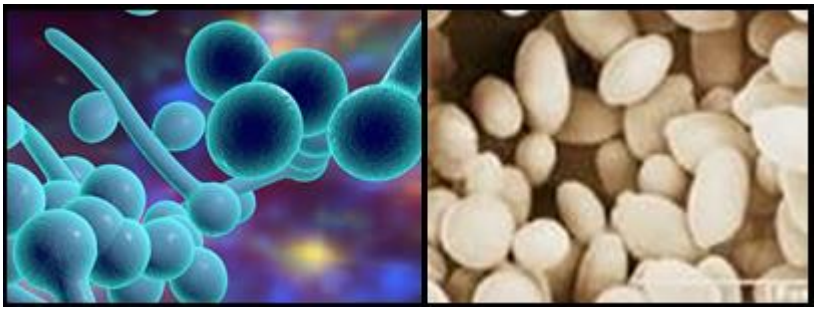

Fig. 16. *Candida albicans* (Staniszewska *et al*., 2013)

***Candida albicans* (*C. albicans*) (Fig. 16)** is a fungus that is normally present on the skin and in mucous membranes such as the vagina, mouth or rectum (Mayer *et al*., 2013). The fungus can also travel through the blood stream and affect the throat, intestines and heart valves. An infection in the bloodstream can detrimental affect the kidneys, heart, lungs, eyes or organs causing high fever, chills, anaemia, rash or shock. To infect host tissue, the usual unicellular yeast-like form of *C. albicans* reacts to environmental cues and switches into an invasive, multicellular filamentous form, called dimorphism (Ryan and Ray, 2004). In addition, an overgrowth infection is considered a superinfection, usually

applied when an infection becomes opportunistic and very resistant to antifungals. Antibiotics were used to suppress or cure its effectiveness.

2.5.1.7 Antifungal activity against *Candida utilis*

Fig. 17. *Candida utilis* (Waghmare *et al*., 2015)

Candida utilis **(Fig. 17)** is common yeast causing urinary tract infections (UTIs). The systematic disease caused by the organism is usually associated with the patients who are receiving fluconazole as an antifungal therapy, but this species was a common etiologic agent prior to the fluconazole era. The detection of these organisms in urinary tract specimens, especially clean catch or catheterized (in and out) urine samples, is vital. In the absence of uropathogen or uropathogen predominance signs, in the diagnosis of UTI, the patient may not be administered any antimicrobial therapy (Hazen *et al*., 1999).

2.5.2. Antioxidant activities

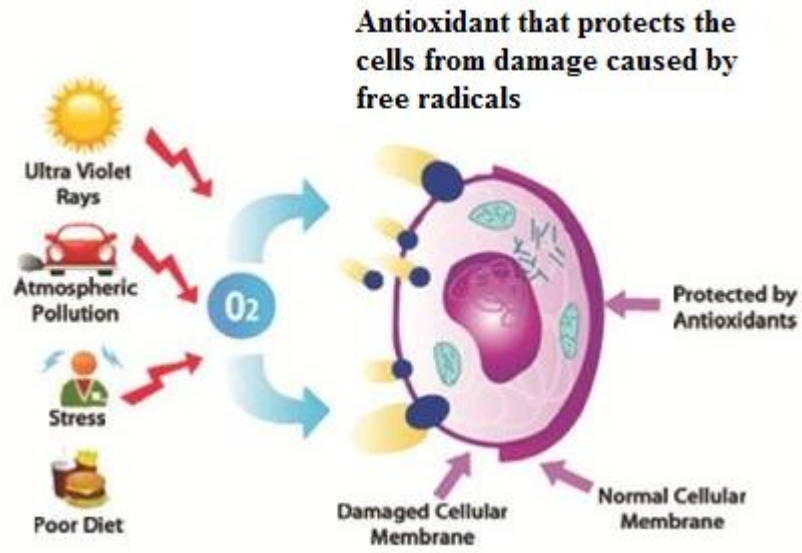

Fig. 18. The effect of antioxidants (Lobo *et al*., 2010)

Free radicals are highly reactive and have the potential to damage cells (Lobo *et al*., 2010). Free radicals are formed naturally in the body and play an important role in many normal cellular homeostatic processes. At high concentrations, however, free radicals can be hazardous to the body and can damage all major components of cells, including DNA, proteins, and cell membranes. The damage to cells caused by free radicals, especially the damage to DNA, may play a role in the development of cancer and other health conditions. Moreover, some environmental toxins, cigarette smoke, metals, and high-oxygen atmospheres, may contain large amounts of free radicals or stimulate the body's cells to produce more free radicals **(Fig. 18)**.

Antioxidants interact with and neutralize free radicals, thus preventing them from causing damage (Lu *et al*., 2013). Antioxidants are also known as "free radical scavengers". The body makes some of the antioxidants it uses to neutralize free radicals. These antioxidants are called endogenous antioxidants such as superoxide dismutase (SOD), catalase (CAT), glutathione peroxidase (GPx) and glutathione (GSH). However, the body relies on external (exogenous) sources primarily from the diet to obtain the rest of the antioxidants it requires (Rahal *et al*., 2014). In laboratory and animal studies, the presence of increased levels of exogenous antioxidants has been shown to prevent free radical damage that has been associated with carcinogenesis. Therefore, investigations into dietary antioxidant supplementation to help lower the risk of developing or dying from cancer have been conducted. Thus, it is relevant that prior to introducing antioxidant therapy into mainstream medicine, significant advances in basic cell biology, pharmacology and clinical bioanalysis will be required.

Notably, α-diphenyl-β-picrylhydrazyl hydrate (DPPH) free radical scavenging assay offers an approach for evaluating the antioxidant potential of compounds. It is a rapid, simple, inexpensive and widely used method to measure the ability of compounds to act as free radical scavengers or hydrogen donors, and to evaluate antioxidant activity of foods. It can also be used to quantify antioxidants in complex biological systems for solid or liquid samples. The DPPH method is unique in carrying out the reaction of the sample with DPPH in methanol/water, which facilitates the extraction of antioxidant compounds from the sample. Antioxidant analysis by other methods may be limited to those compounds soluble in the selected solvents. The advantage of this method is that DPPH is allowed to react with the whole sample with sufficient time to allow DPPH to react

slowly even with weak antioxidants (Kedare and Singh, 2011). This method may be utilized in aqueous and nonpolar organic solvents and can be used to examine both hydrophilic and lipophilic antioxidants (Prior *et al*., 2005).

2.5.3. Toxicity assessment

Toxicity testing is paramount in the screening of newly developed drugs before it can be used in humans (Parasuraman, 2011). The essence of toxicity testing is not just to determine how safe a substance/drug is, but to characterize the possible toxic effects it can produce. The guiding principles of toxicity testing are to determine the effect of the test substances/drug on laboratory animals and assess the potential hazard on a human that is exposed to a lower dose. Toxicity testing is employed in a wide range of different animal species with long-term administration of drug, regular monitoring of physiological, biochemical abnormalities and detailed post-mortem examination at the end of the trial to detect gross or histological abnormalities. The use of animals in toxicity testing is most likely to continue because of the benefits they offer in examining a substance/drug in a whole functioning organism. The toxicity test enables a dose-response curve to be determined which ensures the safety of new chemicals for use as pesticides, drugs, or food additives before they are registered for general use in industry or clinical use (Woolley and Woolley, 2008).

Fig. 19. *Artemia salina* (Brine shrimp) (Hentschel and Tata, 1976)

The cytotoxicity assays are often tedious, expensive and lack simple and rapid screening procedures. Nowadays, brine shrimp lethality assays are extensively used in research and applied toxicology (Costa-Lotufo *et al*., 2005). There is a tendency to use *Artemia salina* in toxicological tests that screen a large number of drugs and plants (Manjili *et al*., 2012;

Ramazani *et al*., 2010; Ramazani *et al*., 2010; Sangian *et al*., 2013). *Artemia salina,* brine shrimp larvae **(Fig. 19)**, is one of the most valuable test organisms available for toxicity testing, and research suggests that there are several applications in toxicology and ecotoxicology therefore it will continue to be used widely (Nunes *et al*., 2006).

2.5.4. Molecular Docking

The development of new drugs is one of the most challenging tasks in science today. Combined efforts of the pharmaceutical industry, academic researchers and biotech companies have not only improved the process of drug design but also contributed to the advances. Computational modeling and stimulations have become integral procedures in introducing new drugs to the market and it is safe to assume that the role of theoretical computations in this field will increase in the future (Alonso *et al*., 2006). Protein activity in organisms involves interactions with biomolecules, which makes them perfect targets for rationally designed drugs.

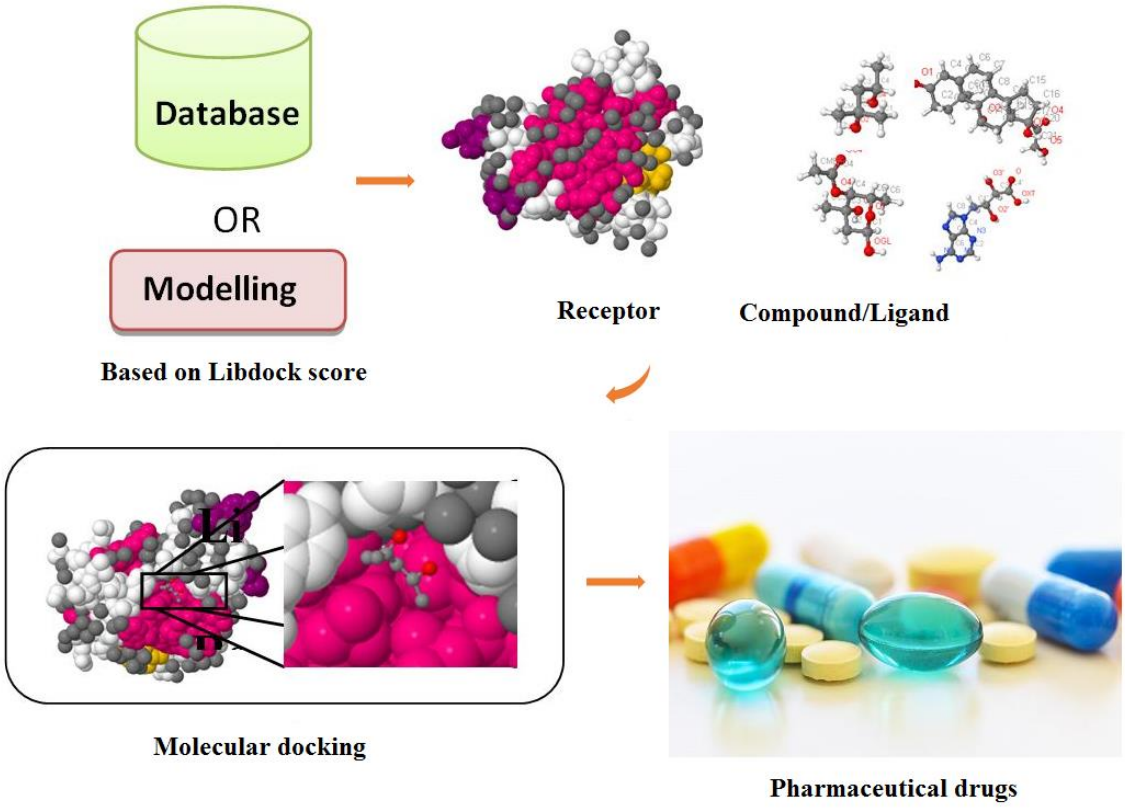

Fig. 20. Structure-based drug design (Molecular docking)

After the Human Genome Project (Burley *et al*., 1999) was completed, it soon became evident that a protein's crystallographic structure alone, in general, is insufficient to

understand its function (Albert *et al*., 2002). In fact, a complete description of the structure and dynamics of the protein along with its interacting partners is required. Such a demand from pharmaceutical industry has recently forced transition in the development of theoretical methods for protein examination; from protein structure prediction to the modeling of whole protein complexes.

Molecular docking is a technique used for predicting the structure of a molecular complex, given the structures of its individual components and these methods play an important role in drug design. Molecular docking is a method which predicts the orientation of one macromolecule of protein to the ligand when bound to each other thus forming a stable complex at the atomic level (Meng *et al*., 2011). The drug discovery program is oriented towards the search for lead structures and thus the virtual screening/molecular docking program constitutes a great tool which further undergoes limited optimization to identify the promising lead molecule **(Fig. 20)**. DNA is specifically a molecular target for many of the clinically available drugs. It was reported that small drug molecules which contain planar polyaromatic systems bind to double-stranded DNA and exhibit more than one binding mode i.e., the intercalation and covalent binding. It has been oriental as a target for many antitumor agents as well as antibiotic drugs. Hence further interaction of the drug with DNA and the rational designing of selective targets in pharmacology are important to study (Kedare and Singh, 2011; Rescifina *et al*., 2014).

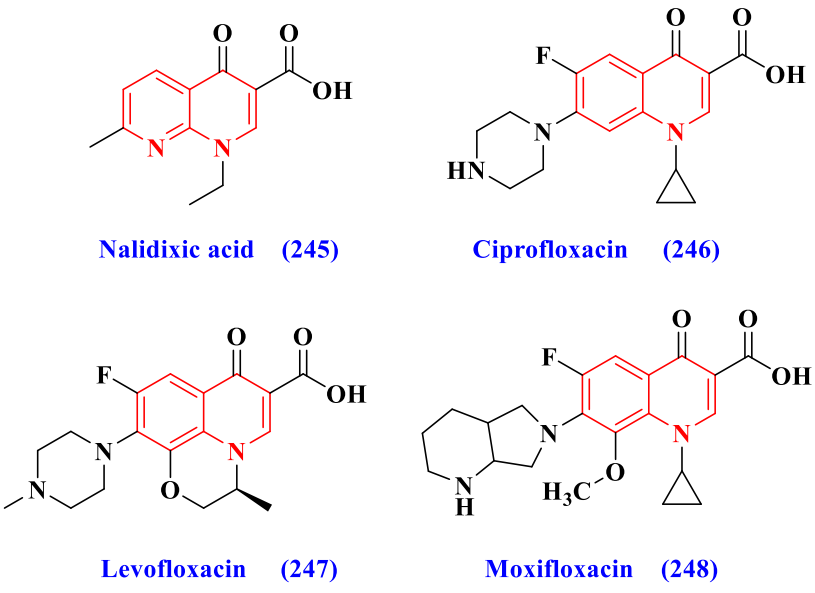

Fig. 21. Examples of more potent fluoroquinolone drugs

Fluoroquinolones **(Fig. 21)** are an important class of broad-spectrum antibacterial agents, whose spectra of activity has been parallel to modifications in the structure of the first quinolone, nalidixic acid. Nalidixic acid (**245**) was initially administered to treat Gram-negative urinary tract infections in humans and animals (Fraunfelder, 1996). Fluoroquinolone drugs are active against a wide range of Gram-negative and Gram-positive pathogens and show improved oral absorption and systematic distribution. Thus, the clinical applications of these compounds have been extended to the treatment of lower respiratory tract infections, skin and soft tissue infections, sexually transmitted diseases and urinary tract infections (Chen *et al*., 2012).

Quinolone and quinoline antibiotics inhibit DNA synthesis by targeting two essential type II topoisomerases, DNA gyrase and topoisomerase IV. The mechanism of quinolone inhibition occurs via the formation of a ternary cleavage complex with the topoisomerase enzyme and DNA (Hiasa and Shea, 2000). It is accepted that for quinolones and quinolines to inhibit DNA gyrase activity, they must form a stable interaction with the DNA gyrase-DNA complex. To overcome the lack of crystallographic data for the ternary complex, computational tools, such as molecular docking are useful for predicting the structures of protein-ligand complexes and providing information on the modes of interaction between ligands and receptors.

References

[1] McMurry, J. 1999. Organic Chemistry, US.

[2] Patwardhan, B., Warude, D., Pushpangadan, P., Bhatt, N. 2005. Ayurveda and traditional Chinese medicine: A comparative overview. Evidence-Based Complementary and Alternative Medicine, (2) 465-473.

[3] Chan, N., Li, S., Perez, E. 2016. Interactions between Chinese nutraceuticals and Western medicines. Nutraceuticals, 875-882.

[4] Da Cheng, H., Xiao-Jie, G., Pei, G. X. 2015. Phytochemical and biological research of Papaver pharmaceutical resources. Medicinal Plants: Chemistry Biology and Omics, 217-251.

[5] Harvey, A. L. 2008. Natural products in drug discovery. Drug discovery today, (13) 894-901.

[6] Nicolaou, K. C. 2014. Organic synthesis: The art and science of replicating the molecules of living nature and creating others like them in the laboratory. Proceedings of the Royal Society A, (470) 20130690.

[7] Hendrickson, J. B. 1975. Systematic synthesis design. IV. Numerical codification of construction reactions. Journal of the American Chemical Society, (97) 5784-5800.

[8] Newhouse, T., Baran, P. S., Hoffmann, R. W. 2009. The economies of synthesis. Chemical Society Reviews, (38) 3010-3021.

[9] Cabrele, C., Reiser, O. 2016. The modern face of synthetic heterocyclic chemistry. The Journal of organic chemistry, (81) 10109-10125.

[10] Franzén, R. G. 2000. Recent advances in the preparation of heterocycles on solid support: A review of the literature. Journal of combinatorial chemistry, (2) 195-214.

[11] Lindsley, C. W. 2015. 2014 prescription medications in the United States: tremendous growth, specialty/orphan drug expansion, and dispensed prescriptions continue to increase. ACS Chemical Neuroscience, (6) 811-812.

[12] Xu, P., Yu, B., Li, F. L., Cai, X. F., Ma, C. Q. 2006. Microbial degradation of sulfur, nitrogen and oxygen heterocycles. Trends in Microbiology, (14) 398-405.

[13] Anderson, J. L., Prystowsky, E. N. 1999. Sotalol: An important new antiarrhythmic. American Heart Journal, (137) 388-409.

[14] Chan R. S. 1974. Introduction to Chemical Nomenclature. Heterocyclic Chemistry. Butterworth's, London.

[15] Willenbring, D., Tantillo, D. J. 2008. Mechanistic possibilities for oxetane formation in the biosynthesis of Taxol's D ring. Russian Journal of General Chemistry, (78) 723-731.

[16] Koehn, F. E., Carter, G. T. 2005. The evolving role of natural products in drug discovery. Nature reviews Drug discovery, (4) 206-220.

[17] (a) Raj, T., Bhatia, R. K., Sharma, M., Saxena, A. K. Ishar, M. P. S. 2010. Cytotoxic activity of 3-(5-phenyl-3H-[1, 2, 4] dithiazol-3-yl) chromen-4-ones and 4-oxo-4H-chromene-3-carbothioic acid N-phenylamides. European Journal of Medicinal Chemistry, (45) 790-794. (b) Saundane, A. R., Vijaykumar, K., Vaijinath, A. V. 2013. Synthesis of novel 2-amino-4-(5′-substituted 2′-phenyl-1H-indol-3′-yl)-6-aryl-4H-pyran-3-carbonitrile derivatives as antimicrobial and antioxidant agents. Bioorganic & Medicinal Chemistry Letters, (23) 1978-1984. (c) Paliwal, P. K., Jetti, S. R., Jain, S. 2013. Green approach towards the facile synthesis of dihydropyrano (c) chromene and pyrano [2, 3-d] pyrimidine derivatives and their biological evaluation. Medicinal Chemistry Research, (22) 2984-2990. (d) Venkatesham, A., Rao, R. S., Nagaiah, K., Yadav, J. S., RoopaJones, G., Basha, S. J., Sridhar, B., Addlagatta, A. 2012. Synthesis of new chromeno-annulated cis-fused pyrano [3, 4-c] pyran derivatives via domino Knoevenagel–hetero-Diels–Alder reactions and their biological evaluation towards antiproliferative activity. MedChemComm, (3) 652-658. (e) Makawana, J. A., Patel, M. P., Patel, R. G. 2012. Synthesis and antimicrobial evaluation of new pyrano [4, 3-b] pyran and pyrano [3, 2-c] chromene derivatives bearing a 2-thiophenoxyquinoline nucleus. Archiv der Pharmazie, (345) 314-322. (f) Patil, A. D., Freyer, A. J., Eggleston, D. S., Haltiwanger, R. C., Bean, M. F., Taylor, P. B., Caranfa, M. J., Breen, A. L., Bartus, H. R. 1993. The inophyllums, novel inhibitors of HIV-1 reverse transcriptase isolated from the Malaysian tree, Calophyllum inophyllum Linn. Journal of Medicinal Chemistry, (36) 4131-4138. (g) Smith, C. W., Bailey, J. M., Billingham, M. E., Chandrasekhar, S., Dell, C. P., Harvey, A. K., Hicks, C. A., Kingston, A. E., Wishart, G. N. 1995. The anti-rheumatic potential of a series of 2, 4-di-substituted-4H-naphtho [1, 2-b] pyran-3-carbonitriles. Bioorganic & Medicinal Chemistry Letters, (5) 2783-2788. (h) Patil, S. A., Wang, J., Li, X. S., Chen, J., Jones, T. S., Hosni-Ahmed, A., Patil,

R., Seibel, W. L., Li, W., Miller, D. D. 2012. New substituted 4H-chromenes as anticancer agents. Bioorganic & Medicinal Chemistry Letters, (22) 4458-4461.

[18] (a) Bonsignore, L., Loy, G., Secci, D., Calignano, A. 1993. Synthesis and pharmacological activity of 2-oxo-(2H) 1-benzopyran-3-carboxamide derivatives. European Journal of Medicinal Chemistry, (28) 517-520. (b) Konkoy, C. S., Fick, D. B., Cai, S. X., Lan, N. C., Keana, J. F. W. 2001. PCT Int. Appl. WO 0075123. Chem. Abstracts, (134) 29313a.

[19] (a) Schweizer, E. E., Meeder-Nycz, O. 1977. Chromenes, chromanes, chromones. Elis, GP Wiley Interscience, New York. (b) Abd El-Rahman, N. M., El-Kateb, A. A., Mady, M. F. 2007. Simplified approach to the uncatalyzed Knoevenagel condensation and Michael addition reactions in water using microwave irradiation. Synthetic Communications, (37) 3961-3970. (c) Darbarwar, M., Sundaramurthy, V. 1982. Synthesis of coumarins with 3: 4-fused ring systems and their physiological activity. Synthesis, (05) 337-388.

[20] (a) Sofan, M. A., El-Taweel, F. M., Elagamey, A. G. A., Elnagdi, M. H. 1989. Studies on cinnamonitriles: The reaction of cinnamonitriles with cyclopentanone. Liebigs Annalen der Chemie, (9) 935-936. (b) Abdel-Galil, F. M., Riad, B. Y., Sherif, S. M., Elnagdi, M. H. 1982. Activated nitriles in heterocyclic synthesis: a novel synthesis of 4-azoloyl-2-aminoquinolines. Chemistry Letters, (11) 1123-1126.

[21] (a) Ellis, G. P. 1977. In the chemistry of heterocyclic compounds. chromenes, chromanes and chromones, A. Weissberger and EC Taylor. (b) Armesto, D., Horspool, W. M., Martin, N., Ramos, A., Seoane, C. 1989. Synthesis of cyclobutenes by the novel photochemical ring contraction of 4-substituted 2-amino-3, 5-dicyano-6-phenyl-4H-pyrans. The Journal of Organic Chemistry, (54) 3069-3072.

[22] Han, Y. F., Xia, M. 2010. Multicomponent synthesis of cyclic frameworks on Knoevenagel-initiated domino reactions. Current Organic Chemistry, (14) 379-413.

[23] Shestopalov, A. M., Litvinov, Y .M., Rodinovskaya, L. A., Malyshev, O. R., Semenova, M. N., Semenov, V. V. 2012. Polyalkoxy substituted 4h-chromenes: Synthesis by domino reaction and anticancer activity. ACS combinatorial science, (14) 484-490.

[24] Tsyganov, D. V., Khrustalev, V. N., Konyushkin, L. D., Raihstat, M. M., Firgang, S. I., Semenov, R. V., Kiselyov, A. S., Semenova, M. N., Semenov, V. V. 2014. 3-(5-)-Amino-o-diarylisoxazoles: Regioselective synthesis and antitubulin activity. European Journal of Medicinal Chemistry, (73) 112-125.

[25] Mahmoodi, M., Aliabadi, A., Emami, S., Safavi, M., Rajabalian, S., Mohagheghi, M. A., Khoshzaban, A., Samzadeh-Kermani, A., Lamei, N., Shafiee, A., Foroumadi, A. 2010. Synthesis and in-vitro cytotoxicity of poly-functionalized 4-(2-arylthiazol-4-yl)-4h-chromenes. Archiv der Pharmazie, (343) 411-416.

[26] Lee, S. H., Jaganath, I. B., Wang, S. M., Sekaran, S. D. 2011. Antimetastatic effects of Phyllanthus on human lung (A549) and breast (MCF-7) cancer cell lines. PLoS One, (6) 20994.

[27] Salama, S. K., Darweesh, A. F., Abdelhamid, I. A., Elwahy, A. H. 2017. Microwave assisted green multicomponent synthesis of novel bis (2-amino-tetrahydro-4h-chromene-3-carbonitrile) derivatives using chitosan as eco-friendly basic catalyst. Journal of Heterocyclic Chemistry, (54) 305-312.

[28] Gong, K., Wang, H. L., Luo, J., Liu, Z. L. 2009. One-pot synthesis of polyfunctionalized pyrans catalyzed by basic ionic liquid in aqueous media. Journal of Heterocyclic Chemistry, (46) 1145-1150.

[29] Pandit, K. S., Chavan, P. V., Desai, U. V., Kulkarni, M. A., Wadgaonkar, P. P. 2015. Tris-hydroxymethylaminomethane (THAM): A novel organocatalyst for a environmentally benign synthesis of medicinally important tetrahydrobenzo [b] pyrans and pyran-annulated heterocycles. New Journal of Chemistry, (39) 4452-4463.

[30] Joule, J. A. 2016. Natural products containing nitrogen heterocycles-some highlights 1990-2015. In Advances in Heterocyclic Chemistry, (119) 81-106.

[31] Joule, J. A., Mills, K. 2010. Heterocyclic Chemistry, Wiley.

[32] Anton, A., Baird, B. R. 2006. Kirk-Othmer Encyclopaedia of Chemical Technology, Wiley.

[33] Baxter, P. N., Dali-Youcef, R. 2005. Nitrogen heterocyclic carbon-rich materials: synthesis and spectroscopic properties of dehydropyridoannulene macrocycles. The Journal of organic chemistry, (70) 4935-4953.

[34] Hab, D., Mlostoń, G. 2017. Materials Chemistry. Chemistry of Heterocyclic Compounds, (53) 1.

[35] (a) Li, J. J., Gribble, G. 2000. Palladium in heterocyclic chemistry: A Guide for the synthetic chemist, Pergamon Press, New York. (b) Husson, H. P., Royer, J. 2009. Asymmetric synthesis of nitrogen heterocycles. Wiley-VCH, Verlag, Weinheim. (c) Orru, R. V., Ruijter, E. 2010. Synthesis of heterocycles via multicomponent reactions II (Vol. 2). Springer Science & Business Media, Berlin, Heidelberg. (d) Eicher, T., Hauptmann, S., Speicher, A. 2013. The chemistry of heterocycles: Structures, reactions, synthesis, and applications. John Wiley & Sons, Somerset. NJ. (e) Wolfe, J. P. 2013. Synthesis of heterocycles via metal-catalyzed reactions that generate one or more carbon-heteroatom bonds (Vol. 32). Springer, Berlin, Heidelberg.

[36] (a) Vo, C. V. T., Bode, J. W. 2014. Synthesis of saturated N-heterocycles. The Journal of organic chemistry, (79) 2809-2815. (b) Allais, C., Grassot, J. M., Rodriguez, J., Constantieux, T. 2014. Metal-free multicomponent syntheses of pyridines. Chemical reviews, (114) 10829-10868. (c) Yamamoto, Y. 2014. Synthesis of heterocycles via transition-metal-catalyzed hydroarylation of alkynes. Chemical Society Reviews, (43) 1575-1600.

[37] Orhan P., M., Tekiner, B., Suzen, S. 2013. Recent studies of antioxidant quinoline derivatives. Mini Reviews in Medicinal Chemistry, (13) 365-372.

[38] Solomon, V. R., Lee, H. 2011. Quinoline as a privileged scaffold in cancer drug discovery. Current Medicinal Chemistry, (18) 1488-1508.

[39] Lavrado, J., Moreira, R., Paulo, A. 2010. Indolo quinolines as scaffolds for drug discovery. Current Medicinal Chemistry, (17) 2348-2370.

[40] Kumar, S., Bawa, S., Gupta, H. 2009. Biological activities of quinoline derivatives. Mini Reviews in Medicinal Chemistry, (9) 1648-1654.

[41] Michael, J. P. 2002. Quinoline, quinazoline and acridone alkaloids. Natural Product Reports, (19) 742-760.

[42] Michael, J. P. 1999. Quinoline, quinazoline and acridone alkaloids. Natural product reports, (16) 697-709.

[43] Kharwar, R. N., Mishra, A., Gond, S. K., Stierle, A., Stierle, D. 2011. Anticancer compounds derived from fungal endophytes: Their importance and future challenges. Natural product reports, (28) 1208-1228.

[44] Singh, I. P., Bodiwala, H. S. 2010. Recent advances in anti-HIV natural products. Natural product reports, (27) 1781-1800.

[45] Williams, P., Sorribas, A., Howes, M. J. R. 2011. Natural products as a source of Alzheimer's drug leads. Natural product reports, (28) 48-77.

[46] Chauhan, P. M. S., Srivastava, S. K. 2001. Present trends and future strategy in chemotherapy of malaria. Current Medicinal Chemistry, (8) 1535-1542.

[47] Chen, Y. L., Fang, K. C., Sheu, J. Y., Hsu, S. L., Tzeng, C. C. 2001. Synthesis and antibacterial evaluation of certain quinolone derivatives. Journal of Medicinal Chemistry, (44) 2374-2377.

[48] Roma, G., Di Braccio, M., Grossi, G., Mattioli, F., Ghia, M. 2000. 1,8-Naphthyridines IV. 9-Substituted N, N-dialkyl-5-(alkylamino or cycloalkylamino)[1, 2, 4] triazolo [4, 3-a][1, 8] naphthyridine-6-carboxamides, new compounds with anti-aggressive and potent anti-inflammatory activities. European Journal of Medicinal Chemistry, (35) 1021-1035.

[49] Bawa, S., Kumar, S., Drabu, S., Kumar, R. 2010. Structural modifications of quinoline-based antimalarial agents: Recent developments. Journal of Pharmacy and Bioallied Sciences, (2) 64-71.

[50] Gryzlo, B., Kulig, K. 2014. Quinoline-a promising fragment in the search for new antimalarials. Mini Reviews in Medicinal Chemistry, (14) 332-344.

[51] Kaur, K., Jain, M., Reddy, R. P., Jain, R. 2010. Quinolines and structurally related heterocycles as antimalarials. European Journal of Medicinal Chemistry, (45) 3245-3264.

[52] Gorka, A. P., de Dios, A., Roepe, P. D. 2013. Quinoline drug–heme interactions and implications for antimalarial cytostatic versus cytocidal activities. Journal of Medicinal Chemistry, (56) 5231-5246.

[53] Bongarzone, S., Bolognesi, M. L. 2011. The concept of privileged structures in rational drug design: focus on acridine and quinoline scaffolds in neurodegenerative and protozoan diseases. Expert Opinion on Drug Discovery, (6) 251-268.

[54] Reynolds, K. A., Loughlin, W. A., Young, D. J. 2013. Quinolines as chemotherapeutic agents for leishmaniasis. Mini Reviews in Medicinal Chemistry, (13) 730-743.

[55] Keri, R. S., Patil, S. A. 2014. Quinoline: A promising antitubercular target. Biomedicine & Pharmacotherapy, (68) 1161-1175.

[56] Singh, S., Kaur, G., Mangla, V., Gupta, M. K. 2015. Quinoline and quinolones: Promising scaffolds for future antimycobacterial agents. Journal of Enzyme Inhibition and Medicinal Chemistry, (30) 492-504.

[57] Afzal, O., Kumar, S., Haider, M. R., Ali, M. R., Kumar, R., Jaggi, M., Bawa, S. 2015. A review on anticancer potential of bioactive heterocycle quinoline. European Journal of Medicinal Chemistry, (97) 871-910.

[58] Vlahopoulos, S., Critselis, E., Voutsas, I. F., Perez, S. A., Moschovi, M., Baxevanis, C. N., Chrousos, G. P. 2014. New use for old drugs? Prospective targets of chloroquines in cancer therapy. Current Drug Targets, (15) 843-851.

[59] Zajdel, P., Partyka, A., Marciniec, K., Bojarski, A. J., Pawlowski, M., Wesolowska, A. 2014. Quinoline-and isoquinoline-sulfonamide analogs of aripiprazole: Novel antipsychotic agents. Neurology and Therapy, (6) 57-75.

[60] Mukherjee, S., Pal, M. 2013. Quinolines: A new hope against inflammation. Drug Discovery Today, (18) 389-398.

[61] Mukherjee, S., Pal, M. 2013. Medicinal chemistry of quinolines as emerging anti-inflammatory agents: An overview. Current Medicinal Chemistry, (20) 4386-4410.

[62] Musiol, R. 2013. Quinoline-based HIV integrase inhibitors. Current Pharmaceutical Design, (19) 1835-1849.

[63] Musiol, R., Serda, M., Hensel-Bielowka, S., Polanski, J. 2010. Quinoline-based antifungals. Current Medicinal Chemistry, (17) 1960-1973.

[64] Mahamoud, A., Chevalier, J., Davin-Regli, A., Barbe, J. 2006. Quinoline derivatives as promising inhibitors of antibiotic efflux pump in multidrug resistant Enterobacter aerogenes isolates. Current drug targets, (7) 843-847.

[65] Costedoat-Chalumeau, N., Dunogué, B., Morel, N., Le Guern, V., Guettrot-Imbert, G. 2014. Hydroxychloroquine: A multifaceted treatment in lupus. La Presse Medicale, (43) e167-e180.

[66] Mahajan, R. 2013. Bedaquiline: First FDA-approved tuberculosis drug in 40 years. International Journal of Applied and Basic Medical Research, (3) 1.

[67] Chou, L. C., Chen, C. T., Lee, J. C., Way, T. D., Huang, C. H., Huang, S. M., Teng, C. M., Yamori, T., Wu, T. S., Sun, C. M., Chien, D. S. 2010. Synthesis and preclinical evaluations of 2-(2-fluorophenyl)-6, 7-methylenedioxyquinolin-4-one monosodium phosphate (CHM-1− P-Na) as a potent antitumor agent. Journal of Medicinal Chemistry, (53) 1616-1626.

[68] Chou, L. C., Tsai, M. T., Hsu, M. H., Wang, S. H., Way, T. D., Huang, C. H., Lin, H. Y., Qian, K., Dong, Y., Lee, K. H., Huang, L. J. 2010. Design, synthesis, and preclinical evaluation of new 5, 6-(or 6, 7-) disubstituted-2-(fluorophenyl) quinolin-4-one derivatives as potent antitumor agents. Journal of Medicinal Chemistry, (53) 8047-8058.

[69] Solomon, V. R., Lee, H. 2011. Quinoline as a privileged scaffold in cancer drug discovery. Current Medicinal Chemistry, (18) 1488-1508.

[70] Gasparotto, V., Castagliuolo, I., Chiarelotto, G., Pezzi, V., Montanaro, D., Brun, P., Palù, G., Viola, G., Ferlin, M. G. 2006. Synthesis and biological activity of 7-phenyl-6, 9-dihydro-3 H-pyrrolo [3, 2-f] quinolin-9-ones: A new class of antimitotic agents devoid of aromatase activity. Journal of Medicinal Chemistry, (49) 1910-1915.

[71] Wall, M. E., Wani, M. C., Cook, C. E., Palmer, K. H., McPhail, A. A., Sim, G. A. 1966. Plant antitumor agents. I. The isolation and structure of camptothecin, a novel alkaloidal leukemia and tumor inhibitor from camptotheca acuminata1, 2. Journal of the American Chemical Society, (88) 3888-3890.

[72] Buta, J. G., Novak, M. J. 1978. Isolation of camptothecin and 10-methoxycamptothecin from Camptotheca acuminata by gel permeation chromatography. Industrial & Engineering Chemistry Product Research and Development, (17) 160-161.

[73] Aravinda, T., Naik, H. B., Naik, H. P. 2009. 1, 2, 3-triazole fused quinoline-peptidomimetics: Studies on synthesis, DNA binding and photonuclease activity. International Journal of Peptide Research and Therapeutics, (15) 273-279.

[74] Ghandi, M., Rahimi, S., Zarezadeh, N. 2017. Synthesis of novel tetrazole containing quinoline and 2,3,4,9-tetrahydro-1h-β-carboline derivatives. Journal of Heterocyclic Chemistry, (54) 102-109.

[75] El-Gamal, K. M. 2016. Synthesis and antimicrobial evaluation of polyfunctionally heterocyclic compounds bearing quinoline moiety. Organic Chemistry: Current Research, (5) 100-168.

[76] Murphy, M. B., Scriven, A. J., Dollery, C. T. 1983. Role of nifedipine in treatment of hypertension. British Medical Journal (Clinical Research Ed.), (287) 257-259.

[77] Masotti, G., Morettini, A., Galanti, G., Paoli, G., Poggesi, L. 1985. Antihypertensive action of nifedipine: Effects on arteries and veins. The Journal of Clinical Pharmacology, (25) 27-35.

[78] Janis, R. A., Triggle, D. J. 1983. New developments in calcium ion channel antagonists. Journal of Medicinal Chemistry, (26) 775-785.

[79] Morad, M. G. Y. E., Goldman, Y. E., Trentham, D. R. 1983. Rapid photochemical inactivation of Ca2+-antagonists shows that Ca^{2+} entry directly activates contraction in frog heart. Nature, (304) 635-638.

[80] Loev, B., Goodman, M. M., Snader, K. M., Tedeschi, R., Macko, E. 1974. Hantzsch-type dihydropyridine hypotensive agents. Journal of Medicinal Chemistry, (17) 956-965.

[81] Pajouhesh, H., Feng, Z. P., Ding, Y., Zhang, L., Pajouhesh, H., Morrison, J. L., Belardetti, F., Tringham, E., Simonson, E., Vanderah, T. W., Porreca, F. 2010. Structure-activity relationships of diphenylpiperazine N-type calcium channel inhibitors. Bioorganic & Medicinal Chemistry Letters, (20) 1378-1383.

[82] Yamamoto, T., Takahara, A. 2009. Recent updates of N-type calcium channel blockers with therapeutic potential for neuropathic pain and stroke. Current Topics in Medicinal Chemistry, (9) 377-395.

[83] Oike, M., Inoue, Y., Kitamura, K., Kuriyama, H. 1990. Dual action of FRC8653, a novel dihydropyridine derivative, on the Ba2+ current recorded from the rabbit basilar artery. Circulation Research, (67) 993-1006.

[84] Takahara, A., Fujita, S. I., Moki, K., Ono, Y., Koganei, H., Iwayama, S., Yamamoto, H. 2003. Neuronal Ca2+ channel blocking action of an antihypertensive drug, cilnidipine, in IMR-32 human neuroblastoma cells. Hypertension Research, (26) 743-747.

[85] Nobili, S., Landini, I., Giglioni, B., Mini, E. 2006. Pharmacological strategies for overcoming multidrug resistance. Current Drug Targets, (7) 861-879.

[86] Sorkin, E. M., Clissold, S. P. 1987. Nicardipine. Drugs, (33) 296-345.

[87] Lavilla, R. 2002. Recent developments in the chemistry of dihydropyridines. J. Chem. Society, Perkin Transactions 1, (9) 1141-1156.

[88] Varache-Lembège, M., Nuhrich, A., Zemb, V., Devaux, G., Vacher, P., Vacher, A. M., Dufy, B. 1996. Synthesis and activities of a thienyl dihydropyridine series on intracellular calcium in a rat pituitary cell line (GH3/B6). European Journal of Medicinal Chemistry, (31) 547-556.

[89] Janis, R. A., Silver, P. J., Triggle, D. J. 1987. Drug action and cellular calcium regulation. Advances in Drug Research, (16) 309-591.

[90] Edraki, N., Mehdipour, A. R., Khoshneviszadeh, M., Miri, R. 2009. Dihydropyridines: Evaluation of their current and future pharmacological applications. Drug Discovery Today, (14) 1058-1066.

[91] Safak, C., Simsek, R. 2006. Fused 1,4-dihydropyridines as potential calcium modulatory compounds. Mini Reviews in Medicinal Chemistry, (6) 747-755.

[92] Shan, R., Velazquez, C., Knaus, E. E. 2004. Syntheses, calcium channel Agonist-Antagonist modulation activities, and nitric oxide release studies of Nitrooxyalkyl 1,4-Dihydro-2, 6-dimethyl-3-nitro-4-(2,1,3-benzoxadiazol-4-yl) pyridine-5-carboxylate racemates, enantiomers, and diastereomers. Journal of Medicinal Chemistry, (47) 254-261.

[93] Velázquez, C., Knaus, E. E. 2004. Synthesis and biological evaluation of 1,4-dihydropyridine calcium channel modulators having a diazen-1-ium-1, 2-diolate nitric oxide donor moiety for the potential treatment of congestive heart failure. Bioorganic & Medicinal Chemistry, (12) 3831-3840.

[94] Gaudio, A. C., Korolkovas, A., Takahata, Y. 1994. Quantitative structure-activity relationships for 1,4-dihydropyridine calcium channel antagonists (nifedipine analogues): A quantum chemical/classical approach. Journal of Pharmaceutical Sciences, (83) 1110-1115.

[95] Goldmann, S., Stoltefuss, J. 1991. 1,4-Dihydropyridines: Effects of chirality and conformation on the calcium antagonist and calcium agonist activities. Angewandte Chemie International Edition in English, (30) 1559-1578.

[96] Triggle, D. J., Langs, D. A., Janis, R. A. 1989. Ca2+ channel ligands: Structure-function relationships of the 1,4-dihydropyridines. Medicinal research reviews, (9) 123-180.

[97] Bossert, F., Vater, W. 1989. 1,4-Dihydropyridines-a basis for developing new drugs. Medicinal Research Reviews, (9) 291-324.

[98] Bossert, F., Meyer, H., Wehinger, E. 1981. 4-Aryldihydropyridines, a new class of highly active calcium antagonists. Angewandte Chemie International Edition in English, (20) 762-769.

[99] Janis, R. A., Triggle, D. J. 1984. 1, 4-Dihydropyridine Ca2+ channel antagonists and activators: A comparison of binding characteristics with pharmacology. Drug Development Research, (4) 257-274.

[100] Briede, J., Stivrina, M., Vigante, B., Stoldere, D., Duburs, G. 2008. Acute effect of antidiabetic 1,4-dihydropyridine compound cerebrocrast on cardiac function

and glucose metabolism in the isolated, perfused normal rat heart. Cell Biochemistry and Function, (26) 238-245.

[101] Kharkar, P. S., Desai, B., Gaveria, H., Varu, B., Loriya, R., Naliapara, Y., Shah, A., Kulkarni, V. M. 2002. Three-dimensional quantitative structure-activity relationship of 1,4-dihydropyridines as antitubercular agents. Journal of Medicinal Chemistry, (45) 4858-4867.

[102] Abbas, H. A. S., El Sayed, W. A., Fathy, N. M. 2010. Synthesis and antitumor activity of new dihydropyridine thio glycosides and their corresponding dehydrogenated forms. European Journal of Medicinal Chemistry, (45) 973-982.

[103] Swarnalatha, G., Prasanthi, G., Sirisha, N., Chetty, C. M., 2011. 1,4-dihydropyridines: a multtifunctional molecule-a review. International Journal of ChemTech Research, (3) 75-89.

[104] Sriram, D., Yogeeswari, P., Dinakaran, M., Banerjee, D., Bhat, P., Gadhwal, S. 2010. Discovery of novel antitubercular 2, 10-dihydro-4aH-chromeno [3, 2-c] pyridin-3-yl derivatives. European Journal of Medicinal Chemistry, (45) 120-123.

[105] Nayyar, A., Malde, A., Jain, R., Coutinho, E. 2006. 3D-QSAR study of ring-substituted quinoline class of anti-tuberculosis agents. Bioorganic & Medicinal Chemistry, (14) 847-856.

[106] Ivanov, E. V., Ponomarjova, T. V., Merkusev, G. N., Dubur, G. Y., Bisenieks, E. A., Dauvorte, A. Z., Pilscik, E. M. 1990. Experimental studies on Diethon: A new radioprotective substance of the skin. Radiobiologia Radiotherapia, (31) 69-78.

[107] Klimaviciusa, L., Klusa, V., Duburs, G., Kaasik, A., Kalda, A., Zharkovsky, A. 2007. Distinct effects of atypical 1,4-dihydropyridines on 1-methyl-4-phenylpyridinium-induced toxicity. Cell Biochemistry and Function, (25) 15-21.

[108] Klusa, V. 1995. Cerebrocrast. Neuroprotectant, cognition enhancer. Drugs of the Future, (20) 135-138.

[109] Suresh, T., Swamy, S. K., Reddy, V. M. 2007. Synthesis and bronchodilatory activity of new 4-aryl-3, 5-bis (2-chlorophenyl)-carbamoyl-2, 6-dimethyl-1,4-dihydropyridines & their 1-substituted analogues. Indian Journal of Chemistry, (46B) 115.

[110] Khadilkar, B., Borkar, S. 1998. Silica gel supported ferric nitrate: A convenient oxidizing reagent. Synthetic communications, (28) 207-212.

[111] Priego, J. G., Ortega, M. P., Sunkel, C. E., Casa-Juana, M. F. D. 1992. Trombodipine platelet aggregation inhibitor, antithrombotic PCA-4230. Drugs Future, (17) 465-468.

[112] Cooper, K., Fray, M. J., Parry, M. J., Richardson, K., Steele, J. 1992. 1,4-Dihydropyridines as antagonists of platelet activating factor. 1. Synthesis and structure-activity relationships of 2-(4-heterocyclyl) phenyl derivatives. Journal of Medicinal Chemistry, (35) 3115-3129.

[113] Trivedi, A., Dodiya, D., Dholariya, B., Kataria, V., Bhuva, V., Shah, V. 2011. Synthesis and biological evaluation of some novel 1, 4-dihydropyridines as potential antitubercular agents. Chemical Biology & Drug Design, (78) 881-886.

[114] Hilgeroth, A. 2002. Dimeric 4-Aryl-1, 4-dihydropyridines: Development of a third class of nonpeptidic HIV-1 protease inhibitors. Mini Reviews in Medicinal Chemistry, (2) 235-245.

[115] Vijesh, A. M., Isloor, A. M., Peethambar, S. K., Shivananda, K. N., Arulmoli, T., Isloor, N. A. 2011. Hantzsch reaction: Synthesis and characterization of some new 1,4-dihydropyridine derivatives as potent antimicrobial and antioxidant agents. European Journal of Medicinal Chemistry, (46) 5591-5597.

[116] Mai, A., Valente, S., Meade, S., Carafa, V., Tardugno, M., Nebbioso, A., Galmozzi, A., Mitro, N., De Fabiani, E., Altucci, L., Kazantsev, A. 2009. Study of 1,4-dihydropyridine structural scaffold: Discovery of novel sirtuin activators and inhibitors. Journal of Medicinal Chemistry, (52) 5496-5504.

[117] Hilgeroth, A. 2002. Dimeric 4-aryl-1, 4-dihydropyridines: Development of a third class of nonpeptidic HIV-1 protease inhibitors. Mini Reviews in Medicinal Chemistry, (2) 235-245.

[118] Kawase, M., Shah, A., Gaveriya, H., Motohashi, N., Sakagami, H., Varga, A., Molnár, J. 2002. 3, 5-Dibenzoyl-1,4-dihydropyridines: Synthesis and MDR reversal in tumor cells. Bioorganic & Medicinal Chemistry, (10) 1051-1055.

[119] Gullapalli, S., Ramarao, P. 2002. L-type Ca2+ channel modulation by dihydropyridines potentiates κ-opioid receptor agonist induced acute analgesia and inhibits development of tolerance in rats. Neuropharmacology, (42) 467-475.

[120] Tasaka, S., Ohmori, H., Gomi, N., Iino, M., Machida, T., Kiue, A., Naito, S., Kuwano, M. 2001. Synthesis and structure-activity analysis of novel dihydropyridine derivatives to overcome multidrug resistance. Bioorganic & Medicinal Chemistry Letters, (11) 275-277.

[121] Zhu, X. Q., Wang, H. Y., Wang, J. S., Liu, Y. C. 2001. Application of NAD (P) H model Hantzsch 1, 4-dihydropyridine as a mild reducing agent in preparation of cyclo compounds. The Journal of Organic Chemistry, (66) 344-347.

[122] Zhao, B. J., Cheng, J. P. 2000. Mechanisms of the oxidations of NAD (P) H model Hantzsch 1, 4-dihydropyridines by nitric oxide and its donor N-methyl-N-nitrosotoluene-p-sulfonamide. The Journal of Organic Chemistry, (65) 8158-8163.

[123] Hulubei, V., Meikrantz, S. B., Quincy, D. A., Houle, T., McKenna, J. I., Rogers, M. E., Steiger, S., Natale, N. R. 2012. 4-Isoxazolyl-1, 4-dihydropyridines exhibit binding at the multidrug-resistance transporter. Bioorganic & Medicinal Chemistry, (20) 6613-6620.

[124] Sashidhara, K. V., Kumar, M., Khedgikar, V., Kushwaha, P., Modukuri, R. K., Kumar, A., Gautam, J., Singh, D., Sridhar, B., Trivedi, R. 2012. Discovery of coumarin-dihydropyridine hybrids as bone anabolic agents. Journal of Medicinal Chemistry, (56) 109-122.

[125] Trivedi, A. R., Dodiya, D. K., Dholariya, B. H., Kataria, V. B., Bhuva, V. R., Shah, V. H. 2011. Synthesis and biological evaluation of some novel N-aryl-1, 4-dihydropyridines as potential antitubercular agents. Bioorganic & Medicinal Chemistry Letters, (21) 5181-5183.

[126] Niraj, K. L., Divyesh, C. M., Manish, P. P., Ranjan, G. P. 2011. Microwave assisted synthesis of novel Hantzsch 1,4-dihydropyridines, acridine-1,8-diones and polyhydroquinolines bearing the tetrazolo[1,5-a]quinoline moiety and their antimicrobial activity assess. Chinese Chemical Letters, (22) 1407-1410.

[127] Ghandi, M., Zarezadeh, N. 2015. A one pot four component reaction providing quinoline based 1,4 dihydropyridines. Journal of the Iranian Chemical Society, (12) 1313-1324.

[128] Kathrotiya, H. G., Patel, M. P. 2013. Synthesis and identification of β-aryloxyquinoline based diversely fluorine substituted N-aryl quinolone derivatives as a new class of antimicrobial, antituberculosis and antioxidant agents. European Journal of Medicinal Chemistry, (63) 675-684.

[129] (a) Metzner, P., Thuillier, A. 1994. Sulfur reagents in organic synthesis. Academic Press, New York. (b) Nagao, Y. 1977. Tumor inhibitors having potential for interaction with mercapto enzymes and/or coenzymes: A review. Bioorganic Chemistry, (6) 287-309. (c) Nudelman, A. 1984. The chemistry of

optically active sulfur compounds. Gordon and Breach, New York. (d) Chatgilialoglu, C., Asmus, K. D. 2013. Sulfur-centered reactive intermediates in chemistry and biology. Springer, New York.

[130] Koval, I. V. 2007. Reactions of thiols. Russian Journal of Organic Chemistry, (43) 319-346.

[131] (a) Wuts, P. G., Greene, T. W. 2006. Greene's protective groups in organic synthesis. John Wiley & Sons, New York. (b) Koval, I. V. E. 1994. Sulfides in organic synthesis: Application of sulfides. Russian Chemical Reviews, (63) 147-168. (c) Mukaiyama, T., Araki, M., Takei, H. 1973. Reaction of S-(2-pyridyl) thioates with Grignard reagents. Convenient method for the preparation of ketones. Journal of the American Chemical Society, (95) 4763-4765. (d) McGarvey, G. J., Williams, J. M., Hiner, R. N., Matsubara, Y., Oh, T. 1986. L-Aspartic acid in acyclic stereoselective synthesis. Synthetic studies on amphotericin B. Journal of the American Chemical Society, (108) 4943-4952. (e) Conrow, R., Portoghese, P. S. 1986. Efficient preparation of polyfunctional. Alpha-diketones from carboxylic acids. The Journal of Organic Chemistry, (51) 938-940.

[132] Glauser, T. A., Nelson, A. N., Zembower, D. E., Lipsky, J. J., Weinshilboum, R. M. 1993. Diethyldithiocarbamate S-methylation: evidence for catalysis by human liver thiol methyltransferase and thiopurine methyltransferase. Journal of Pharmacology and Experimental Therapeutics, (266) 23-32.

[133] Xiao, M. Y., Gustafsson, B., Niu, Y. P. 2006. Metabotropic glutamate receptors in the trafficking of ionotropic glutamate and GABAA receptors at central synapses. Current Neuropharmacology, (4) 77-86.

[134] Syniugin, A. R., Ostrynska, O. V., Chekanov, M. O., Volynets, G. P., Starosyla, S. A., Bdzhola, V. G., Yarmoluk, S. M. 2016. Design, synthesis and evaluation of 3-quinoline carboxylic acids as new inhibitors of protein kinase CK2. Journal of enzyme inhibition and medicinal chemistry, (31) 160-169.

[135] Wu, L., Wang, Y., Song, H., Tang, L., Zhou, Z., Tang, C. 2013. Enantioselective organocatalytic domino Michael/aldol reactions: an efficient procedure for the stereo controlled construction of 2h-thiopyrano [2, 3-b] quinoline scaffolds. Chemistry-An Asian Journal, (8) 2204-2210.

[136] Hagrs, M., Bayoumi, A. H., El-Gamal, K. M., Mayhoub, A. S., Abulkhair, H. S. 2015. Synthesis and preliminary antimicrobial evaluation of some new 6-

methoxyquinoline-3-carbonitrile derivatives. Beni-Suef University Journal of Basic and Applied Sciences, (4) 338-345.

[137] Biewenga, G. P., Haenen, G. R., Bast, A. 1997. The pharmacology of the antioxidant lipoic acid. General Pharmacology: The Vascular System, (29) 315-331.

[138] Packer, L. 1998. α- Lipoic acid: A metabolic antioxidant which regulates NF-κB signal transduction and protects against oxidative injury. Drug Metabolism Reviews, (30) 245-275.

[139] Packer, L., Witt, E. H., Tritschler, H. J. 1995. Alpha-lipoic acid as a biological antioxidant. Free Radical Biology and Medicine, (19) 227-250.

[140] Tirosh, O., Sen, C. K., Roy, S., Kobayashi, M. S., Packer, L. 1999. Neuroprotective effects of α-lipoic acid and its positively charged amide analogue. Free Radical Biology and Medicine, (26) 1418-1426.

[141] Harnett, J. J., Auguet, M., Viossat, I., Dolo, C., Bigg, D., Chabrier, P. E. 2002. Novel lipoic acid analogues that inhibit nitric oxide synthase. Bioorganic & Medicinal Chemistry Letters, (12) 1439-1442.

[142] Boldyrev, A., Bulygina, E., Leinsoo, T., Petrushanko, I., Tsubone, S., Abe, H. 2004. Protection of neuronal cells against reactive oxygen species by carnosine and related compounds. Comparative Biochemistry and Physiology Part B: Biochemistry and Molecular Biology, (137) 81-88.

[143] Roghani, M., Behzadi, G., 2001. Neuroprotective effect of vitamin E on the early model of Parkinson's disease in rat: behavioral and histochemical evidence. Brain Research, (892) 211-217.

[144] Stamford, J. A., Isaac, D., Hicks, C. A., Ward, M. A., Osborne, D. J., O'Neill, M. J. 1999. Ascorbic acid is neuroprotective against global ischaemia in striatum but not hippocampus: histological and voltammetric data. Brain Research, (835) 229-240.

[145] Rosini, M., Andrisano, V., Bartolini, M., Bolognesi, M. L., Hrelia, P., Minarini, A., Tarozzi, A., Melchiorre, C. 2005. Rational approach to discover multipotent anti-Alzheimer drugs. Journal of Medicinal Chemistry, (48) 360-363.

[146] Benchekroun, M., Alejandro, R., Javier, E., Rafael, L., Patrycja, M., Izaskun, B., María L. J., Daniel, J., Jana, J., Vendula, S., Ondrej, S., Oscar, M., Bautista, A., Bernard, R., Olivier, O., Josemarco, C., Lhassane, I. 2016. The antioxidant additive approach for Alzheimer's disease therapy: New ferulic (lipoic) acid plus

melatonin modified tacrines as cholinesterases inhibitors, direct antioxidants, and nuclear factor (erythroid-derived 2)-like 2 activators. Journal of Medicinal Chemistry, (59) 9967-9973.

[147] Roy, S., Packer, L. 1998. Redox regulation of cell functions by α-lipoate: Biochemical and molecular aspects. Biofactors, (7) 263-267.

[148] (a) Domling, A., Wang, W., Wang, K. 2012. Chemistry and biology of multicomponent reactions. Chemical Reviews, (112) 3083-3135. (b) Akritopoulou-Zanze, I. 2008. Isocyanide-based multicomponent reactions in drug discovery. Current Opinion in Chemical Biology, (12) 324-331. (c) Weber, L. 2002. The application of multi-component reactions in drug discovery. Current Medicinal Chemistry, (9) 2085-2093. (d) Hulme, C., Gore, V. 2003. Multi-component Reactions: Emerging Chemistry in Drug Discovery, 'From Xylocain to Crixivan. Current Medicinal Chemistry, (10) 51-80.

[149] Dömling, A. 2006. Recent developments in isocyanide based multicomponent reactions in applied chemistry. Chemical Reviews, (106) 17-89.

[150] (a) Simon, C., Constantieux, T., Rodriguez, J. 2004. Utilisation of 1,3-dicarbonyl derivatives in multicomponent reactions. European Journal of Organic Chemistry, (24) 4957-4980. (b) Ugi, I. 1962. Neuere methoden der präparativen organischen chemie iv mit sekundär-reaktionen gekoppelte α-additionen von immonium-ionen und anionen an isonitrile. Angewandte Chemie, (74) 9-22. (c) Ugi, I. 1982. From isocyanides via four-component condensations to antibiotic syntheses. Angewandte Chemie International Edition in English, (21) 810-819.

[151] Armstrong, R. W., Combs, A. P., Tempest, P. A., Brown, S. D., Keating, T. A. 1996. Multiple-component condensation strategies for combinatorial library synthesis. Accounts of Chemical Research, (29) 123-131.

[152] Montgomery, J. 2000. Nickel-catalyzed cyclizations, couplings, and cycloadditions involving three reactive components. Accounts of Chemical Research, (33) 467-473.

[153] Dömling, A., Ugi, I. 2000. Multicomponent reactions with isocyanides. Angewandte Chemie International Edition, (39) 3168-3210.

[154] Ulaczyk-Lesanko, A., Hall, D. G. 2005. Wanted: New multicomponent reactions for generating libraries of polycyclic natural products. Current Opinion in Chemical Biology, (9) 266-276.

[155] Mironov, M. A. 2006. Design of multi-component reactions: from libraries of compounds to libraries of reactions. QSAR & Combinatorial Science, (25) 423-431.

[156] Tempest, P. A. 2005. Recent advances in heterocycle generation using the efficient Ugi multiple-component condensation reaction. Current Opinion in Drug Discovery & Development, (8) 776-788.

[157] Ramón, D. J., Yus, M. 2005. Asymmetric multicomponent reactions (AMCRs): The new frontier. Angewandte Chemie International Edition, (44) 1602-1634.

[158] Kappe, C. O. 2003. The generation of dihydropyrimidine libraries utilizing Biginelli multicomponent chemistry. QSAR & Combinatorial Science, (22) 630-645.

[159] Orru, R. V., de Greef, M. 2003. Recent advances in solution-phase multicomponent methodology for the synthesis of heterocyclic compounds. Synthesis, (10) 1471-1499.

[160] Ugi, I., Werner, B., Dömling, A. 2003. The chemistry of isocyanides, their multicomponent reactions and their libraries. Molecules, (8) 53-66.

[161] Balme, G., Bossharth, E., Monteiro, N. 2003. Pd-assisted multicomponent synthesis of heterocycles. European Journal of Organic Chemistry, (21) 4101-4111.

[162] Zhu, J. 2003. Recent developments in the isonitrile-based multicomponent synthesis of heterocycles. European Journal of Organic Chemistry, (7) 1133-1144.

[163] Hulme, C., Gore, V. 2003. Multi-component reactions: emerging chemistry in drug discovery, from xylocain to crixivan. Current Medicinal Chemistry, (10) 51-80.

[164] Masciadri, R., Kamer, M., Nock, N. 2003. Regioselective Friedel-Crafts alkylation of anilines and amino-substituted heteroarenes with hexafluoroacetone sesquihydrate. European Journal of Organic Chemistry, (21) 4286-4291.

[165] Dömling, A. 2002. Recent advances in isocyanide-based multicomponent chemistry. Current Opinion in Chemical Biology, (6) 306-313.

[166] Lockhoff, O., Frappa, I. 2002. Glyco conjugate libraries accessed by multicomponent reactions. Combinatorial Chemistry & High Throughput Screening, (5) 361-372.

[167] Orru, R. V., Ruijter, E. 2010. Synthesis of heterocycles via multicomponent reactions II. Springer, Heidelberg.

[168] Toure, B. B., Hall, D. G. 2009. Natural product synthesis using multicomponent reaction strategies. Chemical Reviews, (109) 4439-4486.

[169] Kalinski, C., Umkehrer, M., Weber, L., Kolb, J., Burdack, C., Ross, G. 2010. On the industrial applications of MCRs: molecular diversity in drug discovery and generic drug synthesis. Molecular Diversity, (14) 513-522.

[170] Zhu, J., Bienayme, H. 2005. Multicomponent reactions. Wiley, Weinheim.

[171] Ugi, I., Meyr, R., Fetzer, U., Steinbrückner, C. 1959. DE-B 1, 103, 337. Angewandte Chemie International Edition, (71) 386.

[172] Passerini, M. 1921. Isonitriles. II. Compounds with aldehydes or with ketones and monobasic organic acids. Gazzetta Chimica Italiana, (51) 181-189.

[173] Van Leusen, A. M., Jurjen W., Otto, H. O. 1977. Chemistry of sulfonylmethyl isocyanides. 12. Base-induced cycloaddition of sulfonylmethyl isocyanides to carbon, nitrogen double bonds. Synthesis of 1, 5-disubstituted and 1, 4, 5-trisubstituted imidazoles from aldimines and imidoyl chlorides. The Journal of Organic Chemistry, (42) 1153-1159.

[174] Strecker, A. 1854. About a new body resulting from aldehyde-ammonia and hydrocyanic acid. Justus Liebig's Annalen der Chemie, (91) 349-351.

[175] Hantzsch, A. 1881. Condensation products of aldehyde ammonia and ketone-type compounds. European Journal of Inorganic Chemistry, (14) 1637-1638.

[176] (a) Biginelli, P. 1891. About aldehyduramide of acetoacetic ether. European Journal of Inorganic Chemistry, (24) 1317-1319. (b) Biginelli, P. 1891. About aldehyduramide of acetoacetic ether. II. European Journal of Inorganic Chemistry, (24) 2962-2967. (c) Kappe, C. O. 1993. 100 years of the Biginelli dihydropyrimidine synthesis. Tetrahedron, (49) 6937-6963.

[177] (a) Ugi, I., Fetzer, U., Eholzer, U., Knupfer, H., Offermann, K. 1965. Isonitrile syntheses. Angewandte Chemie International Edition, (4) 472-484. (b) Ugi, I., Steinbrückner, C. 1960. About a new condensation principle. Angewandte Chemie International Edition, (72) 267-268.

[178] Keating, T. A., Armstrong, R. W. 1996. Post condensation modifications of Ugi four-component condensation products: 1-Isocyanocyclohexene as a convertible isocyanide. Mechanism of conversion, synthesis of diverse structures, and

demonstration of resin capture. Journal of the American Chemical Society, (118) 2574-2583.

[179] Szardenings, A. K., Burkoth, T. S., Lu, H. H., Tien, D. W., Campbell, D. A. 1997. A simple procedure for the solid phase synthesis of diketopiperazine and diketomorpholine derivatives. Tetrahedron, (53) 6573-6593.

[180] Hulme, C., Ma, L., Cherrier, M. P., Romano, J. J., Morton, G., Duquenne, C., Salvino, J., Labaudiniere, R. 2000. Novel applications of convertible isonitriles for the synthesis of mono and bicyclic γ-lactams via a UDC strategy. Tetrahedron Letters, (41) 1883-1887.

[181] Hulme, C., Ma, L., Romano, J., Morrissette, M. 1999. Remarkable three-step-one-pot solution phase preparation of novel imidazolines utilizing a UDC (Ugi/de-Boc/cyclize) strategy. Tetrahedron Letters, (40) 7925-7928.

[182] Golebiowski, A., Klopfenstein, S. R., Shao, X., Chen, J. J., Colson, A. O., Grieb, A. L., Russell, A. F. 2000. Solid-supported synthesis of a peptide β-turn mimetic. Organic Letters, (2) 2615-2617.

[183] Tempest, P., Ma, V., Thomas, S., Hua, Z., Kelly, M. G., Hulme, C. 2001. Two-step solution-phase synthesis of novel benzimidazoles utilizing a UDC (Ugi/de-Boc/cyclize) strategy. Tetrahedron Letters, (42) 4959-4962.

[184] Nixey, T., Tempest, P., Hulme, C. 2002. Two-step solution-phase synthesis of novel quinoxalinones utilizing a UDC (Ugi/de-Boc/cyclize) strategy. Tetrahedron Letters, (43) 1637-1639.

[185] Faggi, C., Marcaccini, S., Pepino, R., Pozo, M. C. 2002. Studies on isocyanides and related compounds; Synthesis of 1,4-benzodiazepine-2, 5-diones via Ugi four-component condensation. Synthesis, (18) 2756-2760.

[186] Zhang, W., Tempest, P. 2004. Highly efficient microwave-assisted fluorous Ugi and post-condensation reactions for benzimidazoles and quinoxalinones. Tetrahedron Letters, (45) 6757-6760.

[187] Hulme, C., Dietrich, J. 2009. Emerging molecular diversity from the intra-molecular Ugi reaction: Iterative efficiency in medicinal chemistry. Molecular Diversity, (13) 195-207.

[188] Tejedor, D., Garcia-Tellado, F. 2007. Chemo-differentiating ABB′ multicomponent reactions. Privileged building blocks. Chemical Society Reviews, (36) 484-491.

[189] Isambert, N., Lavilla, R. 2008. Heterocycles as key substrates in multicomponent reactions: The fast lane towards molecular complexity. Chemistry-A European Journal, (14) 8444-8454.

[190] Willy, B., Mueller, T. J. 2008. Consecutive multi-component syntheses of heterocycles via palladium-copper catalyzed generation of alkynones. Arkivoc, (1) 195-208.

[191] Simon, C., Constantieux, T., Rodriguez, J. 2004. Utilisation of 1,3-dicarbonyl derivatives in multicomponent reactions. European Journal of Organic Chemistry, (24) 4957-4980.

[192] Chandgude, A. L., Dömling, A. 2017. N-hydroxyimide Ugi reaction toward α-hydrazino amides. Organic Letters, (19) 1228-1231.

[193] Venkata Prasad, J., Krishnamurthy, S., Moriguchi, T., Tsuge, A. 2017. Efficient synthesis of novel pyrrolo [2, 3-c] pyridone derivatives using the Ugi four-component reaction followed by condensation reaction. New Journal of Chemistry, (41) 97-107.

[194] Kabachnik, M. I., Medved, T. Y. 1952. New synthesis of aminophosphonic acids. Doklady Akademii Nauk, (83) 689-692.

[195] (a) Atherton, F. R., Hassall, C. H., Lambert, R. W. 1986. Synthesis and structure-activity relationships of antibacterial phosphono peptides incorporating (1-aminoethyl) phosphonic acid and (aminomethyl) phosphonic acid. Journal of Medicinal Chemistry, (29) 29-40. (b) Paige, L. A., Zheng, G. Q., DeFrees, S. A., Cassady, J. M., Geahlen, R. L. 1989. S-(2-oxopentadecyl)-CoA, a nonhydrolyzable analog of myristoyl-CoA, is a potent inhibitor of myristoyl-CoA: Protein N-myristoyltransferase. Journal of Medicinal Chemistry, (32) 1665-1667. (c) Peyman, A., Stahl, W., Wagner, K., Ruppert, D., Budt, K. H. 1994. Non-peptide-based inhibitors of human immunodeficiency virus-1 protease. Bioorganic & Medicinal Chemistry Letters, (4) 2601-2604. (d) Jin, L., Song, B., Zhang, G., Xu, R., Zhang, S., Gao, X., Hu, D., Yang, S. 2006. Synthesis, X-ray crystallographic analysis, and antitumor activity of N-(benzothiazole-2-yl)-1-(fluorophenyl)-O, O-dialkyl-α-aminophosphonates. Bioorganic & Medicinal Chemistry Letters, (16) 1537-1543.

[196] Sampath, C., Chandrakala, P., Suresh, M., Vijaya, B. R., Anjaneyulu, E., Venkateswarlu, C. 2013. Synthesis, spectral characterization and antimicrobial evaluation of novel α- Aminophosphonates. Der Pharma Chemica, (5) 327-333.

[197] Amulrao U. B., Nilesh L. P., Mahesh N. P., Raghao S. M. 2012. Synthetic utility of Kabachnik-Fields reaction: A convenient one-pot three-component synthesis of N-phenyl isoquinolone-1-phosphonates. Tetrahedron Letters, (53) 6940-6942.

[198] Badadhe, P. V., Chavan, N. M., Ghotekar, D. S., Mandhane, P. G., Joshi, R. S., Gill C. H. 2011. Synthesis, characterization and biological screening of some novel thiazolidin-4-one and aminophosphonate derivatives. Phosphorus, Sulfur, and Silicon and the Related Elements, (186) 2021-2032.

[199] (a) Khadilkar, B. M., Chitnavis, A. A. 1995. Rate enhancement in the synthesis of some 4-aryl-1, 4-dihydropyridines using methyl 3-aminocrotonate under microwave irradiation. ChemInform, (26) 652. (b) Khadilkar, B. M., Gaikar, V. G., Chitnavis, A. A. 1995. Aqueous hydrotrope solution as a safer medium for microwave enhanced hantzsch dihydropyridine ester synthesis. Tetrahedron Letters, (36) 8083-8086.

[200] Rao, H. S. P., Parthiban, A. 2014. One-pot pseudo three-component reaction of nitroketene-N, S-acetals and aldehydes for synthesis of highly functionalized hexa-substituted 1,4-dihydropyridines. Organic & Biomolecular Chemistry, (12) 6223-6238.

[201] Chao, H., Wei, M., Hao, L., Yanping, L., Jingchao, T. 2014. DMAP-catalyzed four-component one-pot synthesis of highly functionalized spirooxindole-1,4-dihydropyridines derivatives in aqueous ethanol. Tetrahedron, (70) 8768-8774.

[202] Habibi, M., Habibi, A., Hakimi Nasab, S., Dolati, H., Mahdavi, S. M. 2017. Effective and green one-pot multicomponent synthesis of novel derivatives of 4H-pyrans in the presence of hexamethylenetetramine as catalyst in water medium. Journal of Heterocyclic Chemistry, (54) 1598-1603.

[203] Magar, R. L., Thorat, P. B., Jadhav, V. B., Tekale, S. U., Dakea, S. A., Patil, B. R., Pawar, R. P. 2013. Silica gel supported polyamine: A versatile catalyst for one-pot synthesis of 2-amino-4H-chromene derivatives, Journal of Molecular Catalysis A: Chemical, (374) 118-124.

[204] Romdhane, A., Jannet, H. B. 2013. Synthesis of new pyran and pyranoquinoline derivatives. Arabian Journal of Chemistry, (10) S3128-S3134.

[205] El-Agrody, A. M., Al-Ghamdi, A. M. 2011. Synthesis of certain novel 4H-pyrano [3, 2-h] quinoline derivatives. Arkivoc, (xi) 134-146.

[206] (a) Mason, T. J. 2003. Sonochemistry and sonoprocessing: the link, the trends and (probably) the future. Ultrasonics Sonochemistry, (10) 175-179. (b) Mason,

T. J., Cintas, P. 2002. Handbook of green chemistry and technology. Ed, J. Clark and D. Macquarrie, Blackwell Science, Oxford.

[207] Guo, S., Yuan, Y. 2010. One-pot synthesis of 1, 4-dihydropyridine and polyhydro-quinoline derivatives via l-proline catalyzed Hantzsch multicomponent reaction under ultrasound irradiation. Chinese Journal of Chemistry, (28) 811-817.

[208] Jin, T. S., Xiao, J. C., Wang, S. J., Li, T. S. 2004. Ultrasound-assisted synthesis of 2-amino-2-chromenes with cetyltrimethylammonium bromide in aqueous media. Ultrasonics Sonochemistry, (11) 393-397.

[209] Zhang, L., Zhao, F., Zheng, M., Zhai, Y., Liu, H. 2013. Rapid and selective access to three distinct sets of indole-based heterocycles from a single set of Ugi-adducts under microwave heating. Chemical Communications, (49) 2894-2896.

[210] Keglevich, G., Róza Tóth, V., Drahos, L. 2011. Microwave-assisted synthesis of α-hydroxy-benzylphosphonates and-benzylphosphine oxides. Heteroatom Chemistry, (22) 15-17.

[211] Al-Awadi, N. A., Ibrahim, M. R., Elnagdi, M. H., John, E., Ibrahim, Y. A. 2012. Enaminones in a multicomponent synthesis of 4-aryldihydropyridines for potential applications in photoinduced intramolecular electron-transfer systems. Beilstein Journal of Organic Chemistry, (8) 441.

[212] Ma, Z., Zaera, F. 2006. Heterogeneous catalysis by metals. Encyclopaedia of Inorganic and Bioinorganic Chemistry, John Wiley.

[213] Sun, W., Meng, Y., Fu, Q., Wang, F., Wang, G., Gao, W., Huang, X., Lu, F. 2016. High-yield production of boron nitride nanosheets and its uses as a catalyst support for hydrogenation of nitroaromatics. ACS Applied Materials & Interfaces, (8) 9881-9888.

[214] Yabe, Y., Yamada, T., Nagata, S., Sawama, Y., Monguchi, Y., Sajiki, H. 2012. Development of a palladium on boron nitride catalyst and its application to the semihydrogenation of alkynes. Advanced Synthesis & Catalysis, (354) 1264-1268.

[215] Wu, J. C. S., Lin, Z. A., Pan, J. W., Rei, M. H. 2001. A novel boron nitride supported Pt catalyst for VOC incineration. Applied Catalysis A: General, (219) 117-124.

[216] Lin, C. A., Wu, J. C., Pan, J. W., Yeh, C. T. 2002. Characterization of boron-nitride-supported Pt catalysts for the deep oxidation of benzene. Journal of Catalysis, (210) 39-45.

[217] Wu, J. C., Fan, Y. C., Lin, C. A. 2003. Deep oxidation of methanol using a novel Pt/boron nitride catalyst. Industrial & Engineering Chemistry Research, (42) 3225-3229.

[218] Jacobsen, C. J. 2001. Boron nitride: A novel support for ruthenium-based ammonia synthesis catalysts. Journal of Catalysis, (200) 1-3.

[219] Wu, J. C., Chen, W. C. 2005. A novel BN supported bi-metal catalyst for selective hydrogenation of crotonaldehyde. Applied Catalysis A: General, (289) 179-185.

[220] Postole, G., Caldararu, M., Ionescu, N. I., Bonnetot, B., Auroux, A., Guimon, C. 2005. Boron nitride: A high potential support for combustion catalysts. Thermochimica Acta, (434) 150-157.

[221] Perdigón-Melón, J. A., Auroux, A., Guil, J. M., Bonnetot, B. 2002. Preparation of BN catalyst supports from molecular precursors. Influence of the precursor on the properties of the BN ceramic. Studies in Surface Science and Catalysis, (143) 227-237.

[222] Yao, H. C., Sieg, M., Plummer, H. K. 1979. Surface interactions in the Pt/γ-Al2O3 system. Journal of Catalysis, (59) 365-374.

[223] Trimm, D. L, Önsan, Z. I. 2001. On board fuel conversion for hydrogen-fuel-cell-driven vehicles. Catalysis Reviews, (43) 31-84.

[224] Carstens, J. N., Su, S. C., Bell, A. T. 1998. Factors affecting the catalytic activity of Pd/ZrO2 for the combustion of methane. Journal of Catalysis, (176) 136-142.

[225] Rogers, R. D. 2007. Materials science: Reflections on ionic liquids. Nature, (447) 917-918.

[226] Siddiqui, I. R., Srivastava, A., Srivastava, A., Shamim, S., Waseem, M. A. 2014. Ionic liquid promoted one-pot approach for the synthesis of pyrido [1, 2-c][1, 3, 5] thiadiazin-4-ones and thiazolo [3, 2-c][1, 3, 5] thiadiazin-4-ones in water. Arabian Journal of Chemistry. (11) 256-264.

[227] Shaterian, H. R., Kangani, M. 2013. Mild Brønsted basic ionic liquids catalyzed three component synthesis of pyrazolo [1, 2-a][1, 2, 4] triazole-1, 3-dione and 2-amino-3-cyano-5, 10-dioxo-4-phenyl-5, 10-dihydro-4H-benzo [g] chromene derivatives. Scientia Iranica, (20) 571-579.

[228] Hafez, H. N., Alshammari, A. G., El-Gazzar, A. R. 2015. Facile heterocyclic synthesis and antimicrobial activity of polysubstituted and condensed pyrazolopyranopyrimidine and pyrazolopyranotriazine derivatives. Acta Pharmaceutica, (65) 399-412.

[229] Hess, D. J., Henry-Stanley, M. J., Barnes, A. M., Dunny, G. M., Wells, C. L. 2012. Ultrastructure of a novel bacterial form located in Staphylococcus aureus in vitro and in vivo catheter-associated biofilms. Journal of Histochemistry & Cytochemistry, (60) 770-776.

[230] Awasthi, S. 2009. Taking aim at novel vaccines market. Human Vaccines, (5) 654-657.

[231] Tong, S. Y., Davis, J. S., Eichenberger, E., Holland, T. L., Fowler, V. G. 2015. Staphylococcus aureus infections: Epidemiology, pathophysiology, clinical manifestations, and management. Clinical Microbiology Reviews, (28) 603-661.

[232] Nishimura, M., Wada, M., Akiba, T., Yamada, M. 2003. Scanning electron microscopy of food-poisoning bacterium Bacillus cereus using a variable-pressure SEM. Journal of Electron Microscopy, (52) 153-159.

[233] Pinna, A., Sechi, L. A., Zanetti, S., Usai, D., Delogu, G., Cappuccinelli, P., Carta, F. 2001. Bacillus cereus keratitis associated with contact lens wear. Ophthalmology, (108) 1830-1834.

[234] Bulacio, M. D. L. Á., Galván, L. R., Gaudioso, C., Cangemi, R., Erimbaue, M. I. 2015. Enterococcus faecalis biofilm: Formation and development in vitro observed by scanning electron microscopy. Acta Odontológica Latinoamericana, (28) 210-214.

[235] Pinheiro, E. T., Mayer, M. P. A. 2014. Enterococcus faecalis in Oral Infections. JBR Journal of Interdisciplinary Medicine and Dental Science, (3) 160.

[236] Zhanel, G. G., Hoban, D. J., Karlowsky, J. A. 2001. Nitrofurantoin is active against vancomycin-resistant enterococci. Antimicrobial Agents and Chemotherapy, (45) 324-326.

[237] Leung, Y. H., Xu, X., Ma, A. P., Liu, F., Ng, A. M., Shen, Z., Gethings, L. A., Guo, M. Y., Djurišić, A. B., Lee, P. K., Lee, H. K. 2016. Toxicity of ZnO and TiO2 to Escherichia coli cells. Scientific Reports, (6) 35243.

[238] Vincent, C., Boerlin, P., Daignault, D., Dozois, C. M., Dutil, L., Galanakis, C., Reid-Smith, R. J., Tellier, P. P., Tellis, P. A., Ziebell, K., Manges, A. R. 2010.

Food reservoir for Escherichia coli causing urinary tract infections. Emerging Infectious Diseases, (16) 88.

[239] Tsang, K. W., Shum, D. K., Chan, S., Ng, P., Mak, J., Leung, R., Shum, I. H., Ooi, G. C., Tipoe, G. L., Lam, W. K. 2003. Pseudomonas aeruginosa adherence to human basement membrane collagen in vitro. European Respiratory Journal, (21) 932-938.

[240] Young, L. S., Amstrong, D. 1972. Pseudomonas aeruginosa infections. CRC Critical Reviews in Clinical Laboratory Sciences, (3) 291-347.

[241] Staniszewska, M., Bondaryk, M., Swoboda-Kopec, E., Siennicka, K., Sygitowicz, G., Kurzatkowski, W. 2013. Candida albicans morphologies revealed by scanning electron microscopy analysis. Brazilian Journal of Microbiology, (44) 813-821.

[242] Mayer, F. L., Wilson, D., Hube, B. 2013. Candida albicans pathogenicity mechanisms. Virulence, (4) 119-128.

[243] Ryan, K. J., Ray, C. G. 2004. Medical microbiology, McGraw Hill.

[244] Waghmare, S. R., Mulla, M. N., Marathe, S. R., Sonawane, K. D. 2015. Ecofriendly production of silver nanoparticles using Candida utilis and its mechanistic action against pathogenic microorganisms. 3 Biotech, (5) 33-38.

[245] Hazen, K. C., Theisz, G. W., Howell, S. A. 1999. Chronic urinary tract infection due to Candida utilis. Journal of Clinical Microbiology, (37) 824-827.

[246] Lobo, V., Patil, A., Phatak, A., Chandra, N. 2010. Free radicals, antioxidants and functional foods: Impact on human health. Pharmacognosy Reviews, (4) 118.

[247] Lu, L. Y., Ou, N., Lu, Q. B. 2013. Antioxidant induces DNA damage, cell death and mutagenicity in human lung and skin normal cells. Scientific Reports, (3) 3169.

[248] Rahal, A., Kumar, A., Singh, V., Yadav, B., Tiwari, R., Chakraborty, S., Dhama, K. 2014. Oxidative stress, prooxidants, and antioxidants: The interplay. Biomed Research International, (2014) 19.

[249] Kedare, S. B., Singh, R. P. 2011. Genesis and development of DPPH method of antioxidant assay. Journal of Food Science and Technology, (48) 412-422.

[250] Prior, R. L., Wu, X., Schaich, K. 2005. Standardized methods for the determination of antioxidant capacity and phenolics in foods and dietary supplements. Journal of Agricultural and Food Chemistry, (53) 4290-4302.

[251] Parasuraman, S. 2011. Toxicological screening. Journal of Pharmacology and Pharmacotherapeutics, (2) 74.

[252] Woolley, D., Woolley, A. 2008. A guide to practical toxicology: Evaluation, prediction, and risk. CRC Press, New York.

[253] Hentschel, C. C., Tata, J. R. 1976. The molecular embryology of the brine shrimp. Trends in Biochemical Sciences, (1) 97-100.

[254] Costa-Lotufo, L. V., Khan, M. T. H., Ather, A., Wilke, D. V., Jimenez, P. C., Pessoa, C., de Moraes, M. E. A., de Moraes, M. O. 2005. Studies of the anticancer potential of plants used in Bangladeshi folk medicine. Journal of Ethnopharmacology, (99) 21-30.

[255] Manjili, H. K., Jafari, H., Ramazani, A., Davoudi, N. 2012. Anti-leishmanial and toxicity activities of some selected Iranian medicinal plants. Parasitology Research, (111) 2115-2121.

[256] Ramazani, A., Sardari, S., Zakeri, S., Vaziri, B. 2010. In vitro antiplasmodial and phytochemical study of five Artemisia species from Iran and in vivo activity of two species. Parasitology Research, (107) 593-599.

[257] Ramazani, A., Zakeri, S., Sardari, S., Khodakarim, N., Djadidt, N. D. 2010. In vitro and in vivo anti-malarial activity of Boerhavia elegans and Solanum surattense. Malaria Journal, (9) 124.

[258] Sangian, H., Faramarzi, H., Yazdinezhad, A., Mousavi, S. J., Zamani, Z., Noubarani, M., Ramazani, A. 2013. Antiplasmodial activity of ethanolic extracts of some selected medicinal plants from the northwest of Iran. Parasitology Research, (112) 3697-3701.

[259] Nunes, B. S., Carvalho, F. D., Guilhermino, L. M., Van Stappen, G. 2006. Use of the genus Artemia in ecotoxicity testing. Environmental Pollution, (144) 453-462.

[260] Alonso, H., Bliznyuk, A. A., Gready, J. E. 2006. Combining docking and molecular dynamic simulations in drug design. Medicinal Research Reviews, (26) 531-568.

[261] Burley, S. K., Almo, S. C., Bonanno, J. B., Capel, M., Chance, M. R., Gaasterland, T., Lin, D., Šali, A., Studier, F. W., Swaminathan, S. 1999. Structural genomics: Beyond the human genome project. Nature Genetics, (23) 151-157.

[262] Albert, B., Johnson, A., Alexander, J. 2002. Molecular Biology of the Cell, Garland Science, New York.

[263] Meng, X. Y., Zhang, H. X., Mezei, M., Cui, M. 2011. Molecular docking: A powerful approach for structure-based drug discovery. Current Computer-Aided Drug Design, (7) 146-157.

[264] Kedare, S. B., Singh, R. P. 2011. Genesis and development of DPPH method of antioxidant assay. Journal of Food Science and Technology, (48) 412-422.

[265] Rescifina, A., Zagni, C., Varrica, M. G., Pistarà, V., Corsaro, A. 2014. Recent advances in small organic molecules as DNA intercalating agents: Synthesis, activity, and modeling. European Journal of Medicinal Chemistry, (74) 95-115.

[266] Fraunfelder, F. T. 1996. Drug-induced ocular side effects. Folia Ophthalmologica Japonica, (47) 770-773.

[267] Chen, Y. H., Ko, W. C., Hsueh, P. R. 2012. The role of fluoroquinolones in the management of urinary tract infections in areas with high rates of fluoroquinolone-resistant uropathogens. European Journal of Clinical Microbiology & Infectious Diseases, (31) 1699-1704.

[268] Hiasa, H., Shea, M. E. 2000. DNA gyrase-mediated wrapping of the DNA strand is required for the replication fork arrest by the DNA gyrase-quinolone-DNA ternary complex. Journal of Biological Chemistry, (275) 34780-34786.

Chapter-III

Synthesis of quinolinyl and quinolonyl-lipoyl peptides under microwave irradiation and antimicrobial, antioxidant, toxicity and molecular docking studies

Chapter Three

Synthesis of quinolinyl and quinolonyl-lipoyl peptides under microwave irradiation and antimicrobial, antioxidant, toxicity and molecular docking studies

3.1. Abstract

An efficient one-pot Ugi four-component condensation reaction was implemented for the synthesis of 13 new quinolinyl-lipoyl peptides (QLPs) and one quinolonyl-lipoyl peptide (QOLP) by microwave irradiation. The new *N*-(2-(cyclohexylamino)-1-(2-methoxyquinolin-3-yl)-2-oxoethyl)-5-((*R*)-1,2-dithiolan-3-yl)-*N*-phenylpentanamides were synthesised from substrates lipoic acid, 2-methoxyquinoline-3-carbaldehyde derivatives, aniline derivatives and cyclohexyl isocyanide in methanol. The new *N*-(2-(cyclohexylamino)-2-oxo-1-(2-oxo-1,2-dihydroquinolin-3-yl)ethyl)-5-((R)-1,2-dithiola n-3-yl)-*N*-(2-methoxyphenyl)pentanamide was synthesized from lipoic acid, 2-oxo-1,2-dihydroquinoline-3-carbaldehyde, *o*-anisidine and cyclohexyl isocyanide in methanol. The QLPs and QOLP were characterized by FTIR, ^{1}H-NMR, ^{13}C-NMR and elemental analysis. A total of eight peptides were subjected to antimicrobial, antioxidant and toxicity evaluation. Among them, four peptides showed good antimicrobial activity against *Bacillus cereus*, *Staphylococcus aureus*, *Escherichia coli*, *Enterococcus faecalis*, *Candida albicans* and *Candida utilis* whilst three peptides showed antioxidant potential by the radical scavenging assay. In addition, the brine shrimp assay showed four peptides with mortality rate less than 50 % up to 48 h. Finally, molecular docking studies of the four peptides **41**, **43**, **46** and **47** revealed that the binding affinity of **41** and **43** with DNA gyrase was better than the standard ciprofloxacin: a docking score of 183.24 kcal/mol and 165.01 kcal/mol were recorded for **41** and **43**, respectively, compared to 151.56 kcal/mol for ciprofloxacin. The advantages of this one-pot reaction are its green approach, the use of an inexpensive solvent, short reaction times in the absence of a catalyst and excellent yield of peptides. New biologically active peptides can be synthesized using this facile method.

3.2. Introduction

Recently, the study of peptides has received increased attention due to their anticancer, antihypertensive, antimicrobial, and antioxidant properties (De Mejia *et al*., 2012). A new range of highly selective and non-toxic peptides have been developed and their synthesis has gained attention (Möller *et al*., 2008). Although there are several protocols for the synthesis of new organic compounds, the use of multi-component reactions (MCRs) have grown rapidly because they provide a highly efficient and quick approach for constructing poly-functional molecules from simple materials (Domling *et al*., 2012).

One such example is the Ugi four-component reaction (Ugi-4CR) which is a convenient access to peptides synthesised from substrates such as carboxylic acid, an amine, an aldehyde and an isocyanide. Presently, more feasible substrates are being used to replace traditional substrates viz. diamine (Giovenzana *et al*., 2006), secondary amine (Tron *et al*., 2013) and β-ketoamide (Liéby-Muller *et al*., 2005) which can replace the primary amine whilst phenol (El Kaïm *et al*., 2005) or enol (Castellano *et al*., 2012) can replace the carboxylic acid. Importantly, the selection of appropriate substrates and controlled reaction conditions can promote a cascade operation (Elders *et al*., 2009; Ngouansavanh *et al*., 2007) for synthesizing complicated structures in one-pot (Sinha *et al*., 2013). Isocyanides are being used in the Ugi-4CR for producing peptides with important biological (Pando *et al*., 2011) and chemical activities (Znabet *et al*., 2010; Rivera *et al*., 2009). The combination of various carboxylic acid, aldehyde, amine and isocyanide in the Ugi-4CR is currently being used for the synthesis of new peptides (Khoury *et al*., 2012; Pérez-Labrada *et al*., 2012).

The Ugi-4CR reaction is usually conducted under reflux, in methanol, and the reaction time can take 24 h although catalysts (Zhang *et al*., 2007; Shanbhag *et al*., 2008; Bonnaterre *et al*., 2008; Hügel *et al*., 2009) can be used. The reaction time is usually long whilst product yields are moderate. However recently, researchers have improved on the reaction time and product yields.

Kaur *et al*., 2011 synthesized α-acyl-amino amides (**5**) via Ugi-4CR at room temperature (rt) in the presence of 1-butyl-3-methylimidazolium tetrafluoroborate ([bmim]BF_4). The methodology afforded 55-97 % of yield within 8-16 h.

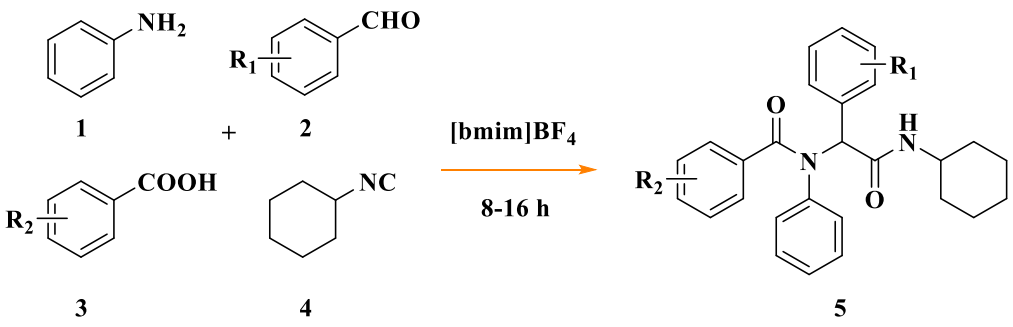

R_1 and R_2 = H, 4-OCH_3

Also, Kanizsai *et al*., 2007 reported the synthesis of a Ugi four-centre three-component reaction in water as medium to construct β-lactam (**9**) libraries. Substrates such as β-amino acids (**6**), aromatic aldehydes (**7**) and cyclohexyl or *tert*-butyl isocyanide (**8**) were used. The observed yield was 45-91 % in 24 h.

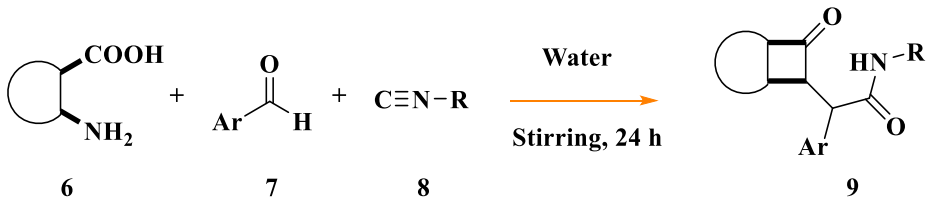

Ar = C_6H_5, $OCH_3C_6H_5$, CH_3CH_2
R = cyclohexyl, *t*-Bu

Recently, Shiri *et al*., 2016 reported the synthesis of peptide derivatives (**14**) containing the 2-chloroquinoline scaffolds by the Ugi-4CR. The substrates used were 2-chloroquinoline-3-carboxaldehydes (**10**), amines (**11**), carboxylic acids (**12**) and isocyanides (**13**). The reaction was carried out in methanol at room temperature for 24 h and the yield was 62-92 %.

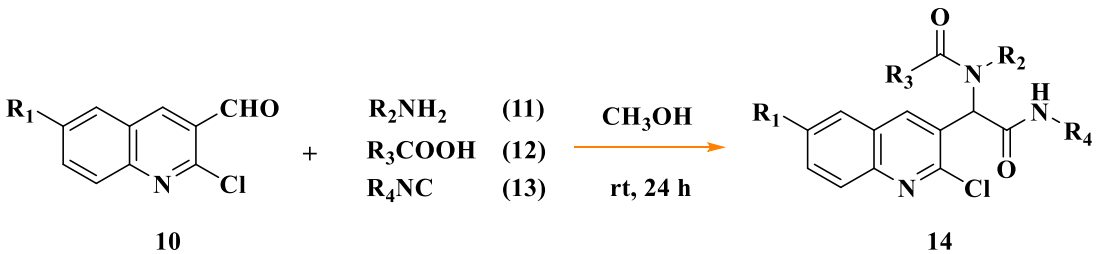

R_1 = H, OCH_3, CH_3
R_2 = C_6H_5, 4-$CH_3C_6H_4$, 4-$OCH_3C_6H_4$, 4-BrC_6H_4

R_3 = CH_3, C_6H_5
R_4 = CycHex, t-Butyl.

Marcaccini *et al.*, 2001 reported the synthesis of *N*-cyclohexyl 2-[*N*-(2-chloroacetyl)-*N*-(4-chlorobenzyl)]amino-2-(4-chlorophenyl) acetamides (**19**) from a mixture of aromatic aldehydes (**15**), amines (**16**), acids (**17**) and isocyanides (**18**). The reaction was conducted in methanol for 30 h at room temperature and the product yield was in the range of 68-86 %.

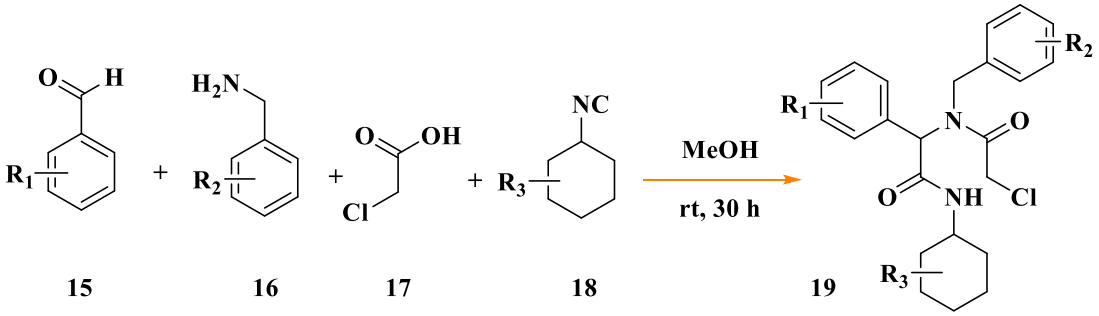

15 16 17 18 19

R_1 = 4-$ClC_6H_4CH_2$, *o*-C_6H_{11}
R_2 = 4-ClC_6H_4, 4-$CH_3OC_6H_4$, 4-BrC_6H_4; R_3= *o*-C_6H_{11}, $C_6H_5CH_2$

El Kaïm *et al.*, 2005 reported the synthesis of a series of peptides: 2-((4-chlorobenzyl)(2-nitrophenyl)amino)-*N*-cyclohexylbutanamides (**24**) from a mixture of nitrophenols (**20**), propanal (**21**), *p*-chlorobenzylamine (**22**) and cyclohexyl isocyanide (**23**). The reaction proceeded at 40℃, in methanol, within 24 h to provide 33-96 % yield.

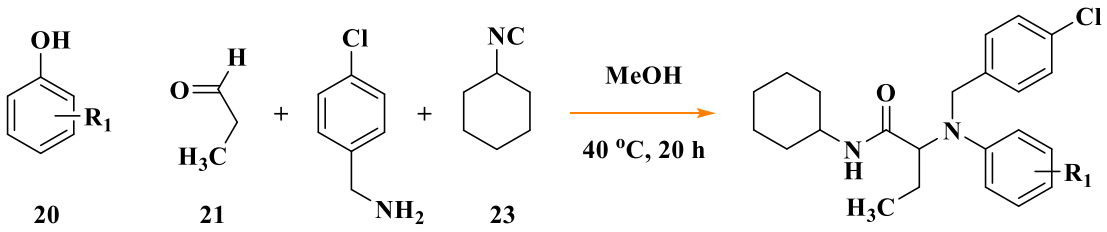

20 21 22 23

R_1= 2-NO_2 & 4-NO_2

24

Váradi *et al.*, 2015 reported the synthesis of bis-amide (**28**) analogues of carfentanil by using aniline (**1**), propanoic acid (**25**), *N*-alkylpiperidones (**26**) and various aliphatic isocyanides (**27**) at 55℃. The reaction was conducted in methanol, for 18 h to give 75-86 % yield.

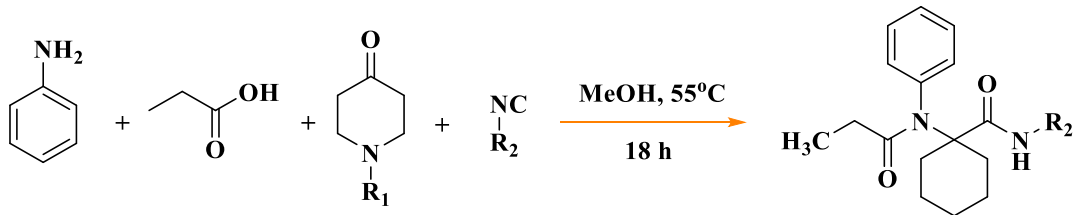

R_1= phenylethyl, cyclopropylmethyl
R_2= cyclopropyl, cyclopentyl, *n*-butyl

Azizi *et al*., 2013 synthesized *N*-(2-(cyclohexylamino)-2-oxo-1-phenylethyl)-*N*-phenylbenzamide (**32**) by the Ugi-4CR. The substrates were isocyanides (**23**), acids (**29** aldehydes (**30**) and amines (**31**). Choline chloride and urea were used in the reaction. The reaction was completed within 2-5 h and the yield was 60-92 %.

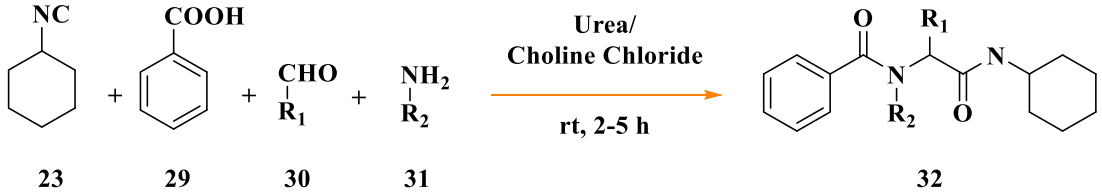

R_1 = C_6H_5, 4-$OCH_3C_6H_5$, 4-ClC_6H_5
R_2 = C_6H_5, 4-$NO_2C_6H_5$, 3-$OCH_3C_6H_5$

As previously discussed in Chapter Two, quinolines are an important class of heterocyclic compounds found in many synthetic and natural products. They possess a wide range of pharmacological activities such as antimalarial, anti-inflammatory, anti-asthmatic, antihypertensive, antibacterial, and as platelet-derived growth factor receptors which are tyrosine kinase inhibiting agents (El Sayed *et al*., 2011). Some examples are Neocryptolepine (**34**), Gatifloxacin (**33**) and Lenvantinib (**35**) **(Fig. 1)** which are effective against Gram-positive and Gram-negative organisms (Lu *et al*., 1999). They inhibit the bacterial enzymes DNA gyrase (Matsui *et al*., 2008) and are multi-kinase inhibitors for various types of cancers (Gatto *et al*., 1999).

The pharmacological activity is due to the compounds intercalating between the base pairs of DNA and interfere with the normal functioning of the enzyme topoisomerase II which is involved in the breaking and releasing of DNA strands (Sigel and Sigel, 2000). The interaction of peptides with DNA has also attracted the attention of biochemists for the development of new DNA reagents for biotechnology and medicine (Grimm *et al*.,

2006). Due to the importance of quinolines, we decided to include a quinoline scaffold into the newly synthesized peptides.

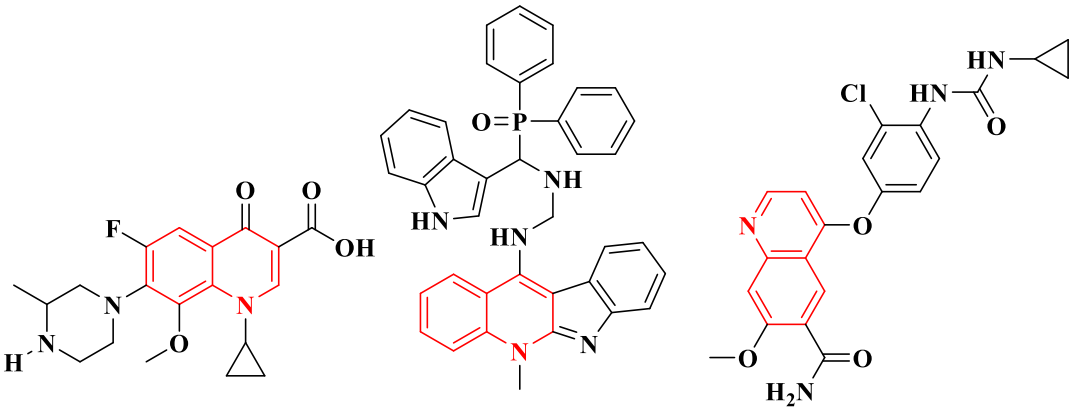

Fig. 1. Examples of biologically active quinolines (Lu *et al*., 1999; Matsui *et al*., 2008; Gatto *et al*., 1999)

In addition to the quinoline scaffold, lipoic acid can be combined with another pharmacophore to improve its biological properties such as the inhibition of acetylcholinesterase (AChE) activity (Biewenga *et al*., 1997). Studies have shown the neuroprotective, anti-Alzheimer and antioxidant activities of lipoic acid (Packer, 1998; Packer *et al*., 1995; Tirosh *et al*., 1999; Rosini *et al*., 2005; Moller *et al*., 2008). Thus, we envisaged that a peptide containing the quinoline ring system and a lipoic acid moiety would display good biological activity. Hence, the synthesis of peptides using Ugi-4CR was conducted.

Traditionally, the Ugi reaction is performed at room temperature or under reflux in methanol with reaction times up to 12–24 h or more using several catalysts (Zhang *et al*., 2007; Shanbhag *et al*., 2008; Bonnaterre *et al*., 2008; Hugel, 2009). However, most of these methods employ long reaction times and moderate yields of products are produced.

Microwave-assisted organic synthesis is a powerful technique that is used to accelerate organic reactions. The notable features of the microwave approach are eco-friendliness, enhanced reaction rates and greater selectivity (Kuang *et al*., 2001). Microwave has been recognized as an important technique for green and sustainable processes and this method advantageous over the traditional thermal method [Strauss *et al*., 1995; Varma, 1999; Bose *et al*., 1997; Nuchter *et al*., 2000; Romanova *et al*., 2000; Perreux and Loupy, 2001;

Deng and Lin, 1997; Elander *et al*., 2000; Caddick, 1995; Lidstrom *et al*., 2001). Due to these advantages, microwave irradiation was selected for this study.

In view of the remarkable importance from a pharmacological, industrial, and synthetic points of view, we report the one-pot synthesis of potentially biological active peptides via the Ugi-4CR under microwave irradiation within the framework of green chemistry protocol under catalyst-free condition. Furthermore, the new peptides were screened for their biological properties such as antimicrobial and antioxidant and their toxicity and binding with DNA gyrase by molecular docking were determined.

3.3. Results and discussion

The starting material, 2-chloroquinoline-3-carbaldehyde (CFQ) was prepared by the Vilsmeier-Haack reaction (Ambika and Singh, 2005). The desired starting material 2-methoxyquinoline-3-carbaldehyde (MQC) (**37**) was obtained from the reaction of K_2CO_3 with CFQ in methanol solution. The quinolone starting material, 2-oxo-1,2-dihydro quinoline-3-carbaldehyde (OQC) (**53**) was prepared from the reaction of glacial CH_3COOH with CFQ.

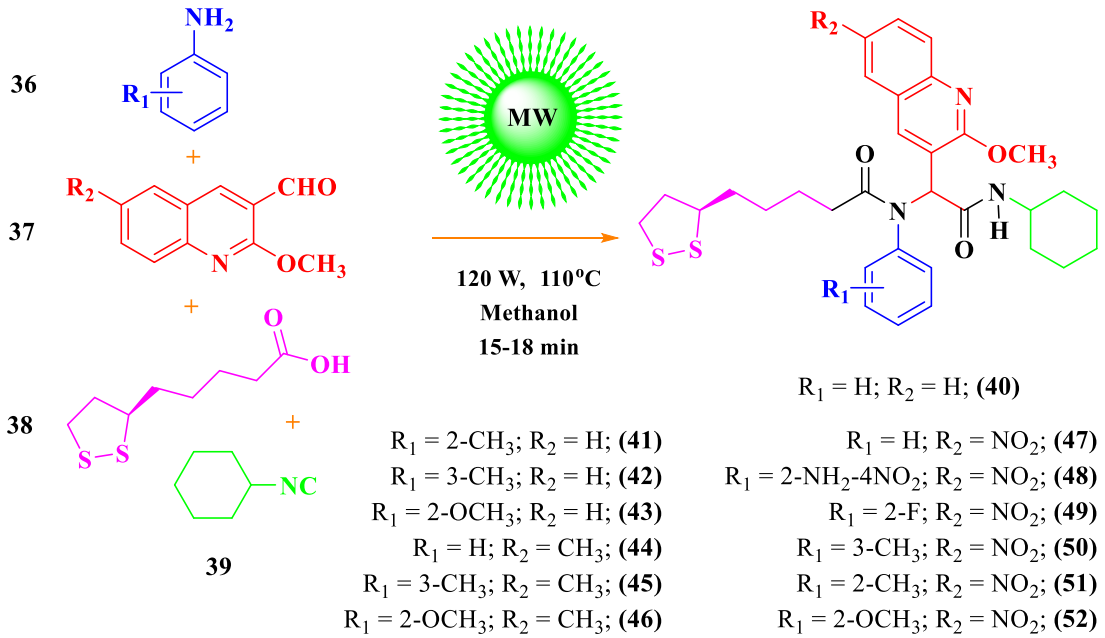

Scheme 1. Synthesis of quinolinyl-lipoyl peptides (**40-52**) via Ugi-4CR under microwave irradiation

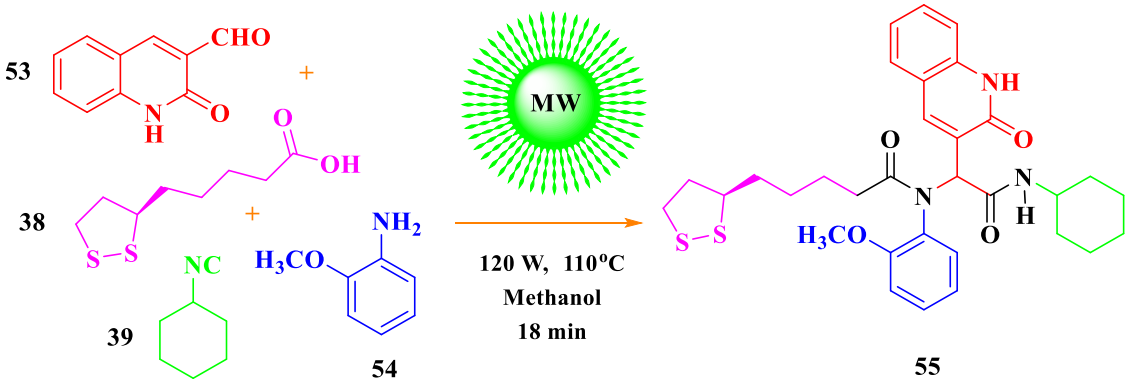

Scheme 2. Synthesis of quinolonyl-lipoyl peptide (**55**) via Ugi-4CR under microwave irradiation

In a preliminary reaction, a mixture of **37** (1 mmol), aniline (1 mmol), lipoic acid (**38**) (1 mmol) and cyclohexyl isocyanide (**39**) (1 mmol) were refluxed in methanol (Ma *et al*., 2006). TLC was used to monitor the progress of the reaction. After 30 h, the product was formed and purified by column chromatography with a mixture of ethyl acetate: petroleum ether (1:3). The yield of the product was 30 %. The reaction was too long and the yield was quite low. Thereafter, **37** (1 mmol), aniline (1 mmol), **38** (1.5 mmol) and **39** (1.5 mmol) in methanol, was used. After 24 h reflux, the product was formed and purified by column chromatography. The yield of the product was 40 %. The same mole ratio of substrates was used and carried out under microwave irradiation at 120 W (110℃) for 15-18 minutes. We were pleased to find that the one-pot reaction proceeded smoothly to deliver the desired product in 90 % yield (**Scheme 1 & 2**). The product was fully characterized by FTIR, ^{1}H-NMR, ^{13}C-NMR, HSQC, COSY, NOESY, HMBC and elemental analysis and was identified as *N*-(2-(cyclohexylamino)-1-(2-methoxyquinolin-3-yl)-2-oxoethyl)-5-((R)-1,2-dithiolan-3-yl)-*N*-phenylpentanamide **(40)**.

The IR spectrum of **40** showed stretching frequencies (cm^{-1}) at 1600 for C=N, 1325 for C-N, 2970 for CH, 1493 for C=C, 2595 for SH, 1625 for C=O, 722 for C-S, 1230 for OCH_3 and 3416 for NH (**Fig. 3.1**, Appendix III). The ^{1}H-NMR spectrum of **40** showed two singlets at δ 7.88 and δ 6.35 for C4-H and C9-H. The NH showed a doublet at δ 5.90 and the coupling constant was found to be 8.4 Hz. Cyclohexyl isocyanide proton CH (C1") showed a multiplet at δ 3.88 (J = 4 Hz) and lipoic acid CH (C19) showed a multiplet at δ 3.52-3.49 (J = 1.72 Hz) (**Fig. 3.2**). The ^{13}C-NMR spectrum (**Fig. 3.3**)

showed the presence of two carbonyl groups at δ 168.72 (C10) and δ 173.67 (C14). The structure was further confirmed by 2D NMR spectral studies. The selected ^{1}H and ^{13}C-NMR chemical shifts are shown in **Fig. 2**.

The ^{13}C, ^{1}H-COSY correlation of carbon signals at δ 140.46, 139.84, 128.91, 127.85, 126.53, 124.27, 119.01, 58.65, 28.72, 25.49 and 24.84 were assigned to C1', C4, C3', C2', C8, C6, C3, C9, C17, C16 and C3", respectively. The carbon signal at δ 139.84 was due to quinolinyl C4-carbon and the spectrum is presented in (**Fig. 3.4**). The ^{1}H, ^{1}H-COSY spectrum of the compound revealed the correlation between doublet of NH at δ 5.90 and CH of cyclohexyl isocyanide at δ 3.88 (**Fig. 3.5**). The ^{1}H, ^{1}H-NOESY spectrum of the compound revealed the doublet of NH at δ 5.90 was coupled with the multiplet of cyclohexyl isocyanide CH (C1") at δ 3.89-3.87 (J = 4 Hz), multiplet of CH_2 (C2") at δ 1.37-1.34 (J = 5.6 Hz) and the multiplet of CH_2 (C6") at δ 1.18-1.15 (J = 3.12 Hz) which was confirmed by the nearby protons of C2" and C6" (**Fig. 3.6**).

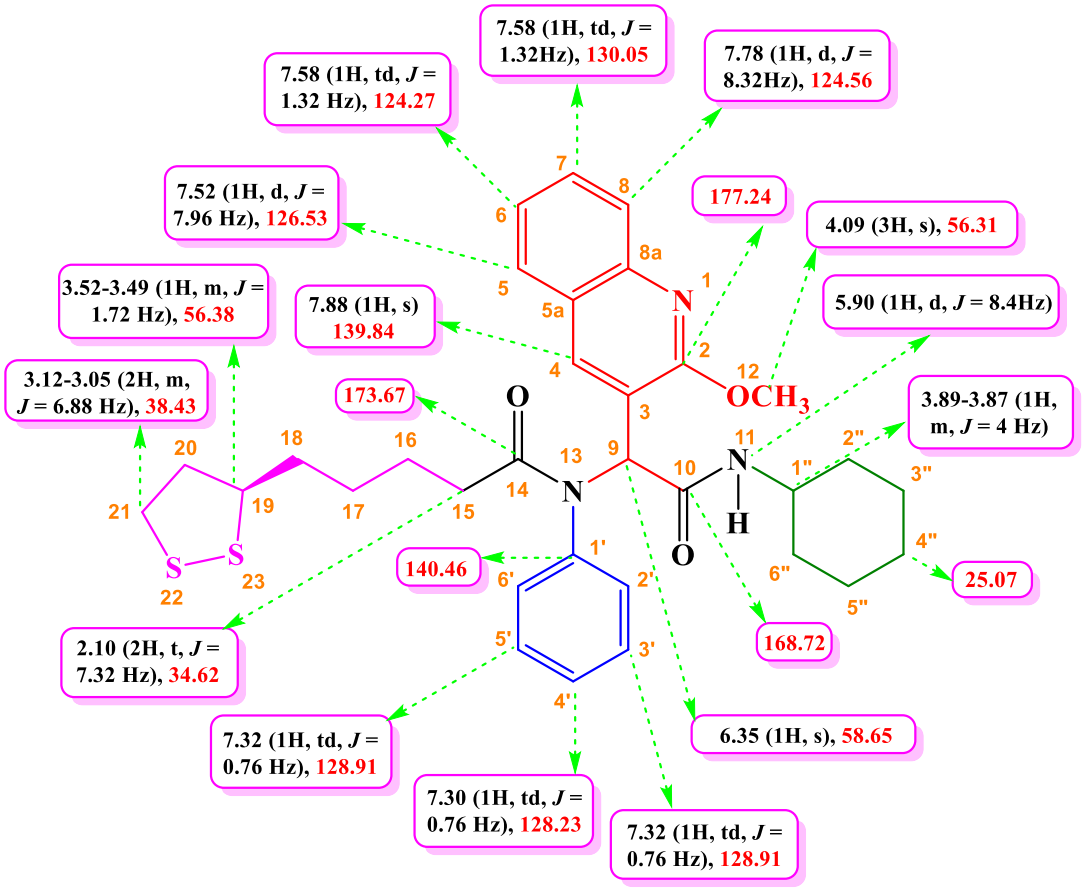

Fig. 2. Selected ^{1}H and ^{13}C-NMR chemical shifts of **40**

The selected (^{1}H and ^{13}C-NMR) HMBC correlation chemical shifts are shown in **Fig. 3**. The HMBC spectrum of **40** (**Fig. 3.7**) showed the long-range correlations as follows: C9-H of **40** coupled with quinolinyl carbon (C4) at δ 139.84, C8a at δ 159.85, carbonyl carbons C10 at δ 168.72 and C14 at δ 173.67 and quaternary carbon C3 at δ 119.01. This correlation of C9-H to the quaternary carbon (C3), carbonyl carbon (C10) of amide group and carbonyl carbon (C14) of lipoic acid indicated that the three groups were attached to C9. Thus it was evident the three different moieties were bonded to a common carbon and hence added valuable information to **40**. The C4-H coupled with α-C of amide group (C9) at δ 58.65 and quinolinyl carbons, (C8a) at δ 159.85, (C1') at δ 140.46, and (C5) at δ 126.53.

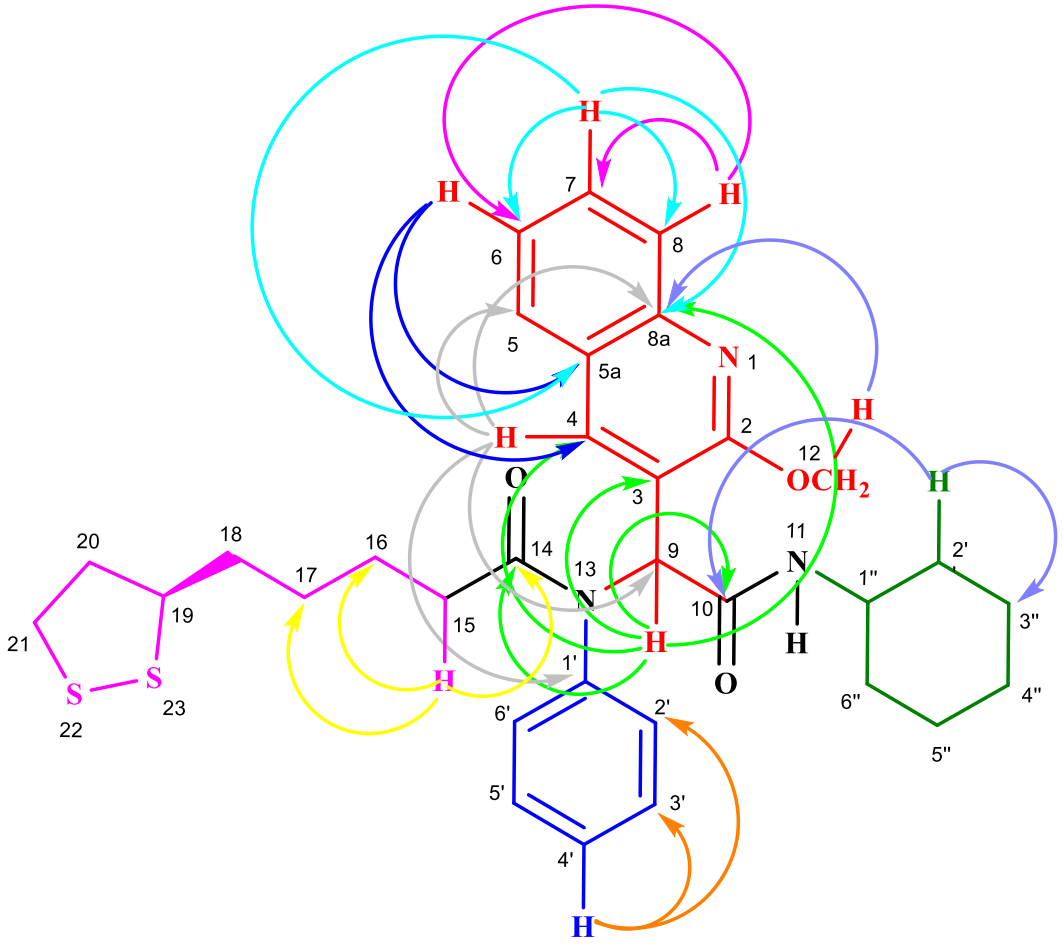

Fig. 3. Selected HMBC correlation chemical shifts of **40**

Table 1. Selected **HMBC** correlations of **40**

Entry	Proton	Correlated Carbons
1	C9-H (s,1H) at δ 6.35	C4 (139.84), C8a (159.85), C10 (168.72), C14 (173.67) and C3 (119.01)
2	C4-H (s, 1H) at δ 7.88	C9 (58.65), C8a (159.85), C1' (140.46), C5 (126.53)
3	C8-H (d, 1H, *J* = 8.32Hz) at δ 7.78	C6 (124.27) and C7 (130.05)
4	C6-H (td, 1H, *J* = 1.08 Hz) at δ 7.59	C4 (139.84) and C5a (145.84)
5	C7-H (td, 1H, J = 1,32 Hz) at δ 7.59	C6 (124.27), C8 (124.56), C4 (139.84) and C5a (145.84)
6	C4'-H (td, 1H, J = 7.16Hz) at δ 7.30	C3' (128.91) and C2' (127.85)
7	C12-H (s, 3H) at δ 4.09	C8a (159.85)
8	C2" (m, *J* = 4 Hz) at δ 3.89-3.87	C3" (24.84) and C10 (168.72)
8	C15-H (m, *J* = 7.32) at δ 2.11-2.08	C16 (25.49), C17 (28.72) and C14 (173.67)

Similarly, C8-H coupled with quinolinyl carbons (C6) at δ 124.27 and (C7) at δ 130.05. The C6-H correlated with quinolinyl carbons (C4) at δ 139.84 and (C5a) at δ 145.84. The C7-H coupled with quinolinyl carbons (C6) at δ 124.27, (C8) at δ 124.56, (C4) at δ 139.84 and (C5a) at δ 145.84. The C4'-H correlated with aromatic carbon of amine (C3') at δ 128.91 and carbon of amine (C2') at δ 127.85. The C12-H correlated with quinolinyl carbon (C8a) at δ 159.85. C2"-H correlated with carbon of cyclohexyl isocyanide (C3") at δ 24.84 and carbonyl carbon of amide group (C10) at δ 168.72. C15-H correlated with carbons of lipoyl moiety (C16) at δ 25.49, (C17) at δ 28.72 and (C14) at δ 173.67. Selected ^{1}H and ^{13}C-NMR and HMBC chemical shifts of **40** are mentioned in **Table 1**.

Based on the above spectral details and mass analysis (TOF-MS, calculated value (*m/z*) 577.80 $[M]^+$, found 600.23 $[M+Na]^+$, **Fig. 3.8**), the structure was confirmed as *N*-(2-(cyclohexylamino)-1-(2-methoxyquinolin-3-yl)-2-oxoethyl)-5-((R)-1,2-dithiolan-3-yl)-*N*-phenylpentanamide (**40**).

The reaction was then optimised by evaluating the effect of solvents and the results are summarized in **Table 2**. The synthesis of **40** was chosen as the model reaction. Various solvents like acetonitrile, dichloromethane, ethanol, water and methanol were used. It

was observed that the reaction in methanol showed the best yield of 90 %. The yield decreased to 40 % when the solvents were changed **(Table 2**, entry 4).

Table 2. Effect of solvent on the synthesis of quinolinyl-lipoyl peptides[a]

Entry	Solvent	Time (min)	Yield (%)[b]
1	Acetonitrile	18	71
2	Dichloromethane	20	70
3	Ethanol	18	75
4	Water	20	40
5	Methanol	15	90

[a] Reaction conditions: **37** (1 mmol), aniline (1 mmol), **38** (1.5 mmol) and **39** (1.5 mmol) were added to methanol as solvent (15 mL) under microwave irradiation (120 W) at 110℃.

[b] Isolated yields.

Conventional heating and the microwave assisted method under various conditions were compared; the results are listed in **Table 3**. Without MW irradiation, **40** was formed at room temperature after 24 h. Also, the reaction at 90℃ and without MW for 24 h, the yield of the obtained **40** was found to be 40-52% **(Table 3**, entries 1 & 2). Moreover, the effect of MW irradiation of different powers was investigated. As shown in **Table 3**, the reaction power was increased to 250 W, the yield of **40** remains unchanged. It was observed that the MW irradiation power of 120 W afforded the best yield of product with 90 % isolated yield within 15 min **(Table 3**, entry 4). Therefore, 120 W was selected as the optimal microwave power for the synthesis.

Table 3. Effect of microwave irradiation on the synthesis of quinolinyl-lipoyl peptides [a]

Entry	**Power (W)**	**Time**	**Yield (%)[b]**
1	Without MW (r.t)	24 h	40
2	Without MW (90 ºC)	24 h	52
3	100	15 min	50
4	120	15 min	90
5	150	15 min	78
6	200	20 min	80
7	250	20 min	80

[a] Reaction conditions: **37** (1 mmol), aniline (1 mmol), **38** (1.5 mmol) and **39** (1.5 mmol) were added to methanol as solvent (15 mL) under microwave irradiation at 110℃.

[b] Isolated yields.

It was found that microwave could raise the rate of reaction and this protocol was used to synthesize the remaining 13 derivatives by selecting the appropriate starting substrate.

Table 4. Synthesis of peptides through Ugi-4CR under microwave irradiation

Entry	Aldehyde	Amine	Product	Time (min)	Yield (%)[b]
1	$C_{11}H_9NO_2$	C_6H_7N	$C_{32}H_{39}N_3O_3S_2$ (**40**)	15	90
2	$C_{11}H_9NO_2$	C_7H_9N	$C_{33}H_{41}N_3O_3S_2$ (**41**)	15	82
3	$C_{11}H_9NO_2$	C_7H_9N	$C_{33}H_{41}N_3O_3S_2$ (**42**)	18	84
4	$C_{11}H_9NO_2$	C_7H_9NO	$C_{33}H_{41}N_3O_4S_2$ (**43**)	15	84
5	$C_{12}H_{11}NO_2$	C_6H_7N	$C_{33}H_{41}N_3O_3S_2$ (**44**)	15	90
6	$C_{12}H_{11}NO_2$	C_7H_9N	$C_{34}H_{43}N_3O_3S_2$ (**45**)	15	89
7	$C_{12}H_{11}NO_2$	C_7H_9NO	$C_{34}H_{43}N_3O_4S_2$ (**46**)	15	86
8	$C_{11}H_8N_2O_4$	C_6H_7N	$C_{32}H_{38}N_4O_5S_2$ (**47**)	15	88
9	$C_{11}H_8N_2O_4$	$C_6H_7N_3O_2$	$C_{32}H_{38}N_6O_7S_2$ (**48**)	15	84
10	$C_{11}H_8N_2O_4$	C_6H_6FN	$C_{32}H_{37}FN_4O_5S_2$ (**49**)	15	80
11	$C_{11}H_8N_2O_4$	C_7H_9N	$C_{33}H_{40}N_4O_5S_2$ (**50**)	18	80
12	$C_{11}H_8N_2O_4$	C_7H_9N	$C_{33}H_{40}N_4O_5S_2$ (**51**)	18	81
13	$C_{11}H_8N_2O_4$	C_7H_9NO	$C_{33}H_{40}N_4O_6S_2$ (**52**)	15	90
14	$C_{10}H_7NO_2$	C_7H_9NO	$C_{32}H_{39}N_3O_4S_2$ (**55**)	18	80

[b] Isolated yield.

The reaction proceeded well with different aldehydes such as 2-methoxy-6-methylquinoline-3-carbaldehyde and 2-methoxy-6-nitroquinoline-3-carbaldehyde with aromatic amines which resulted in a chemical library of fused quinolinyl-lipoyl peptides (**40-52**) and quinolonyl-lipoyl peptide (**55**) **(Table 4)**.

Finally, we observed that the % yield **(Table 4**) of the peptides synthesized with anilines which possessed electron-withdrawing groups was lower than those with electron-donating groups. It was expected when the formation of an imine by nucleophilic addition, the electron withdrawing groups deactivated the aromatic ring by decreasing the electron density on the ring through an inductive effect/ resonance effect and made the formation of imine slower than the substrates containing electron donating groups. The characterization of the peptide **40** was discussed earlier: the derivatives were then easily characterized since the main scaffold was the same with minor alteration due to simple functional groups in the aromatic structure. The FTIR, ^{1}H-NMR, ^{13}C-NMR and elemental analysis for the 14 new peptides are presented in **Appendix-III**.

A plausible mechanism is shown in **Scheme 3**. The initial step was the formation of an imine from the amine **(2)** and aldehyde with loss of one equivalent of water. Proton exchange with lipoic acid activated the iminium ion for nucleophilic addition of cyclohexyl isocyanide with its terminal carbon to nitrilium ion **(3)**.

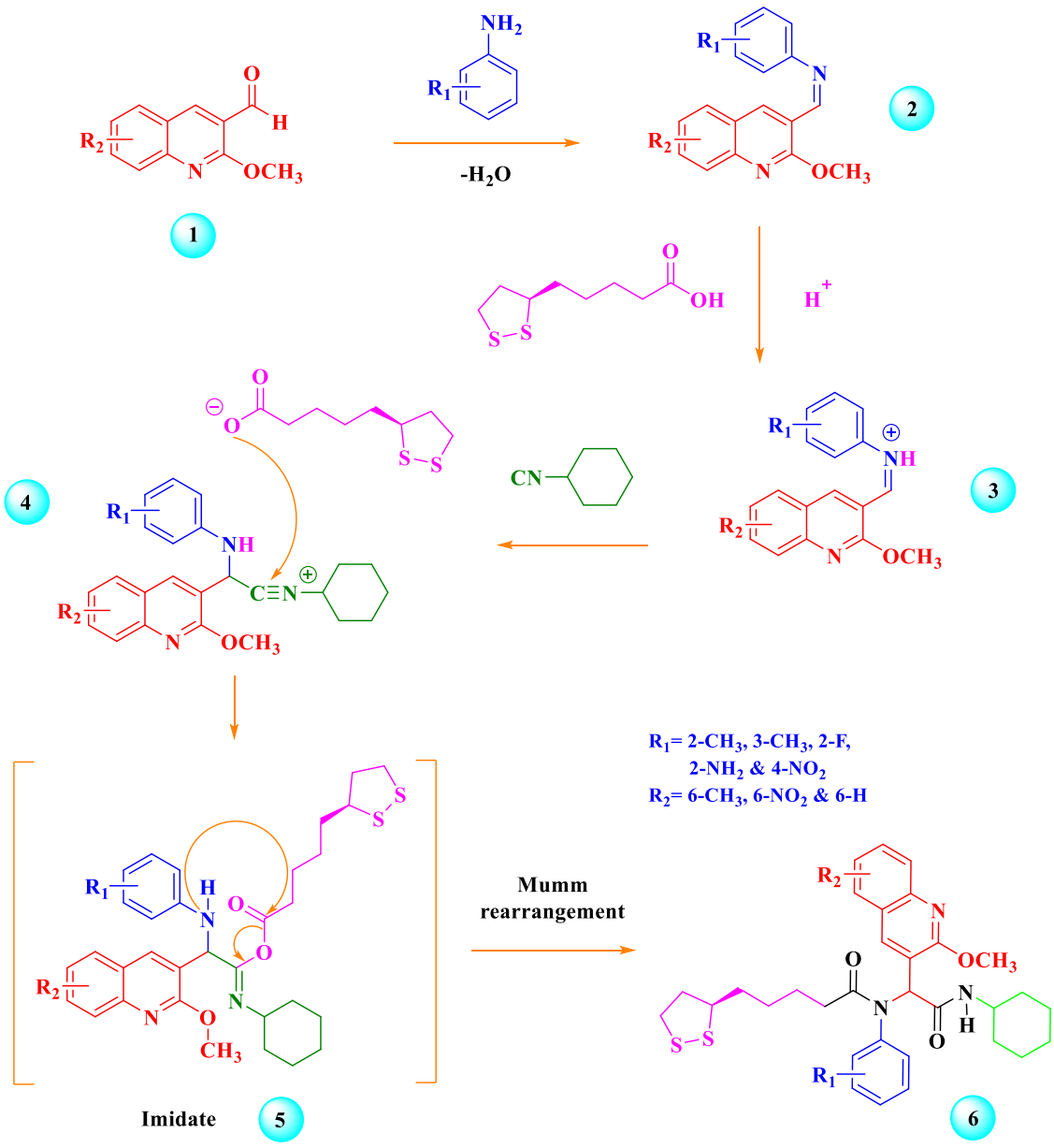

Scheme 3. Plausible mechanism of the synthesis of quinolinyl-lipoyl peptide

A second nucleophilic addition occurred at this intermediate **(4)** with lipoic acid anion. Subsequent reaction of imine with isocyanide and lipoic acid resulted in the intermediate, imidate **(5)**. Some equilibria involving nitrilium trapped by oxygenated anion resulted in the corresponding imidate **(5)**. The last step was thought to be an irreversible arrangement

(i.e. Mumm rearrangement) displacing the whole equilibria by developing a CO double bond (Chéron *et al*., 2012).

The antimicrobial activity of the peptides (**40, 41, 43, 44, 45, 46, 47** and **48**) were assessed against four bacterial strains and two yeast strains using the well diffusion assay method (Balouiri *et al*., 2016). To assess the antimicrobial assay, bacterial cultures were plated on Luria Bertani (LB) Agar and yeast cultures on potato dextrose (PD) agar and kept at 37°C (bacterial cultures for 16 h) and 30°C (yeast cultures for 48 h). Further, bacterial and yeast cultures were grown in LB broth and PD broth at the same condition, respectively.

Table 5. Antimicrobial activity of the novel peptides

Bacteria	**Zone of inhibition by different peptides**								**Ciprofloxacin**
	1	**2**	**3**	**4**	**5**	**6**	**7**	**8**	
Bacillus cereus	0	20 ± 0.3	12 ± 0.2	0	0	0	12 ± 0.4	11 ± 0.3	31 ± 0.2
Staphylococcus aureus	0	0	0	0	0	0	0	0	27 ± 0.4
Escherichia coli	0	0	0	0	0	0	0	0	30 ± 0.6
Enterococcus faecalis	0	0	0	0	0	0	0	0	30 ± 0.5
Yeast									**Geneticin**
Candida albicans	0	0	0	0	0	0	0	0	23 ± 0.6
Candida albicans	0	0	0	0	0	0	0	0	22 ± 0.3

(1= **45**; 2= **47**; 3= **46**; 4= **48**; 5= **40**; 6= **44**; 7= **41**; 8= **43**).

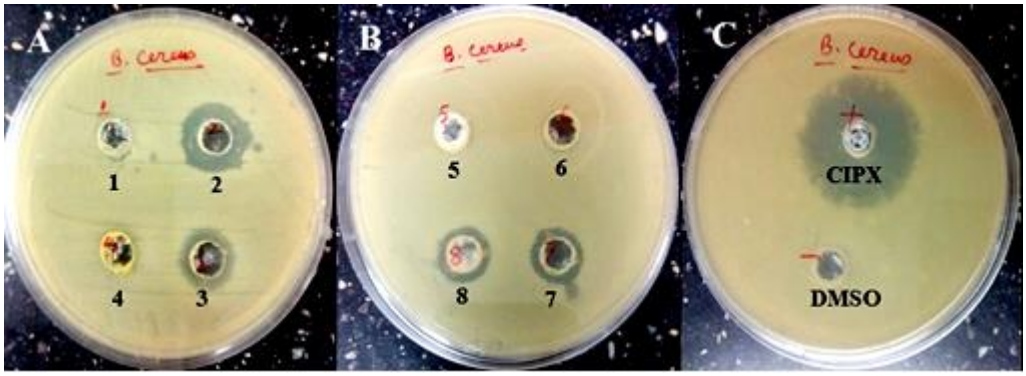

Fig. 4. Antimicrobial screening of different peptides shown by well-diffusion method

(1= **45**; 2= **47**; 3= **46**; 4= **48**; 5= **40**; 6= **44**; 7= **41**; 8= **43**)

The peptides showed antibacterial activity against *Bacillus cereus* (*B. cereus*) **(Table 5)** which was determined by the zone of inhibition **(Fig. 4)**. Amongst all the peptides **41, 43, 46** and **47** showed clear zone inhibition against *B. cereus* **(Fig. 4)**. In addition, the minimum inhibitory concentration (MIC) of all peptides were determined: A clear zone against *B. cereus* by using broth dilution methods were observed (**Table 6**).

The quinolinyl-lipoyl peptides (QLPs) containing methyl group in the ortho position of benzyl moiety (**41**)**,** methoxy group in the ortho position of benzyl ring (**43**), methoxy group in the ortho position of benzyl ring and methyl group in the quinoline moiety (**46**) and nitro group (**47**) showed potential activities towards *B. cereus*. All the other peptides tested, showed no activity against the remaining bacterial and yeast strains.

The antioxidant ability of the peptides were determined by the decolourization of methanol solution of 2,2-diphenyl-1-picrylhydrazyl-hydrate (DPPH). The DPPH radical scavenging assay was used for preliminary screening of the compounds for their antioxidant activity (Shaikh *et al*., 2014).

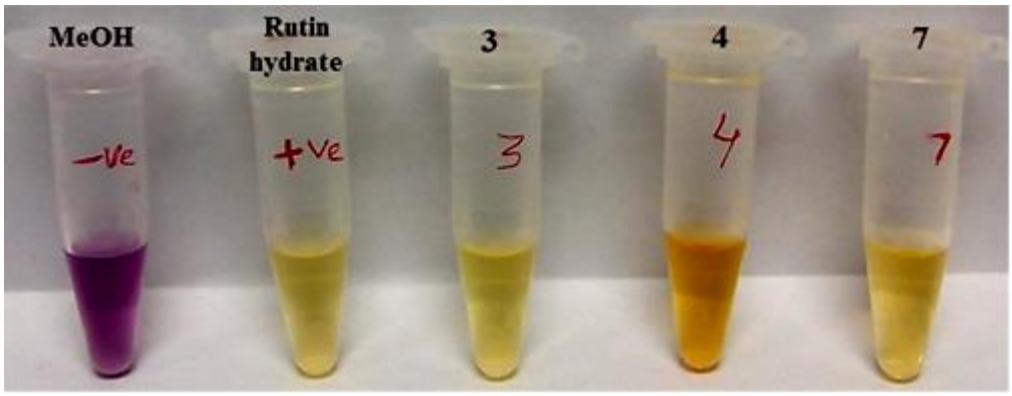

Fig. 5. Qualitative detection of antioxidant properties of different peptides with -ve (methanol) and +ve (Rutin hydrate) control in colour (3= **41**; 4= **46**; 7= **47**).

The results of the antioxidant study revealed that the peptides **41**, **46** and **47** were found to be effective DPPH scavenging agents **(Fig. 5)**.

Furthermore, different concentrations of peptides, which showed positive antioxidant activities, were used with a control (Rutin hydrate) to determine the radical-scavenging inhibitory concentration i.e. IC_{50} (**Table 6**). QLPs containing methyl group in the ortho position of benzyl moiety (**41**), methoxy group in the ortho position of benzyl ring and

methyl group in the quinoline moiety (**46**) and nitro group (**47**) showed significant DPPH scavenging activity.

Table 6. Minimum inhibitory concentration and radical-scavenging inhibitory concentration of different peptides

S.No	Compounds	MIC (µg/mL) (*B. cereus*)	Radical-scavenging IC_{50} (µg/mL)
1	CIPX (control)	0.26 ± 0.11	–
2	RH (control)	–	2.16 ± 1.03
3	**1**	0.67 ± 0.23	6.34 ± 0.89
4	**2**	0.79 ± 0.16	–
5	**3**	–	7.87 ± 1.02
6	**4**	0.43 ± 0.21	–
7	**5**	0.72 ± 0.19	5.23 0.98

(1= **41**; 2= **43**; 3= **46**; 4= **45**; 5= **47**).

The brine shrimp lethality assay was used as a preliminary assessment for toxicity (Carballo *et al*., 2002). The mortality rate (24 and 48 h) of brine shrimp *Artemia salina* treated with different peptides is presented in **Fig. 6**.

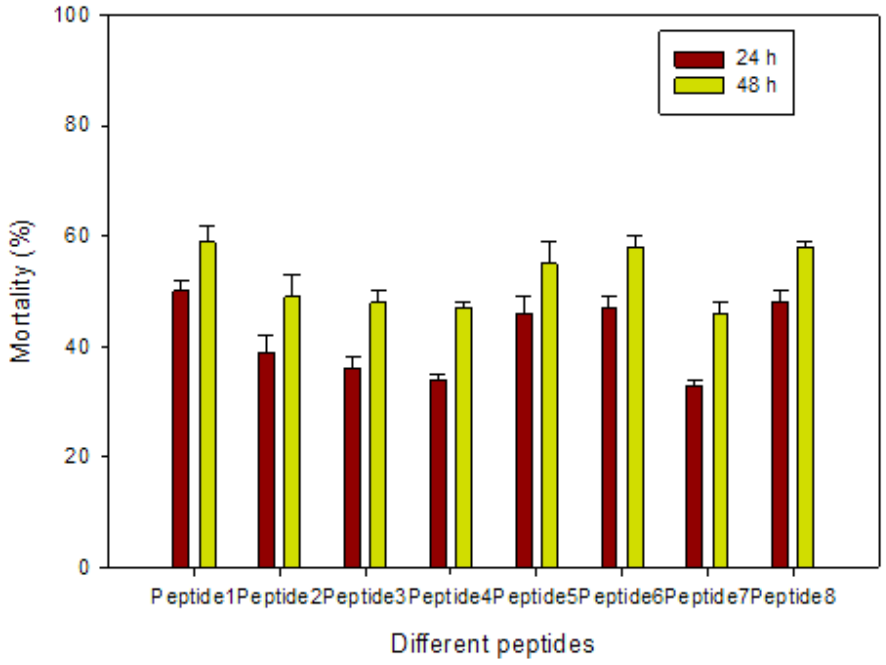

Fig. 6. Mortality rate (24 and 48 h) of brine shrimp *Artemia salina* treated with different peptides

1= **40**; 2= **41**; 3= **43**; 4= **46**; 5= **44**; 6= **45**; 7= **47**; 8= **48**.

The results showed that the mortality rate was below 50 % for QLPs containing methyl group in the ortho position of benzyl moiety (**41**)**,** methoxy group in the ortho position of benzyl ring (**43**), methoxy group in the ortho position of benzyl ring and methyl group in the quinoline moiety (**46**) and nitro group (**47**) when treated with 300 µg of each peptide. This indicated that QLPs are safe to use for biological applications (Meyer *et al*., 1982).

The peptides including **41**, **43**, **46** and **47** showed significant antibacterial activity. To gain more insights into their antibacterial activity, computational studies based on the molecular docking approach were conducted.

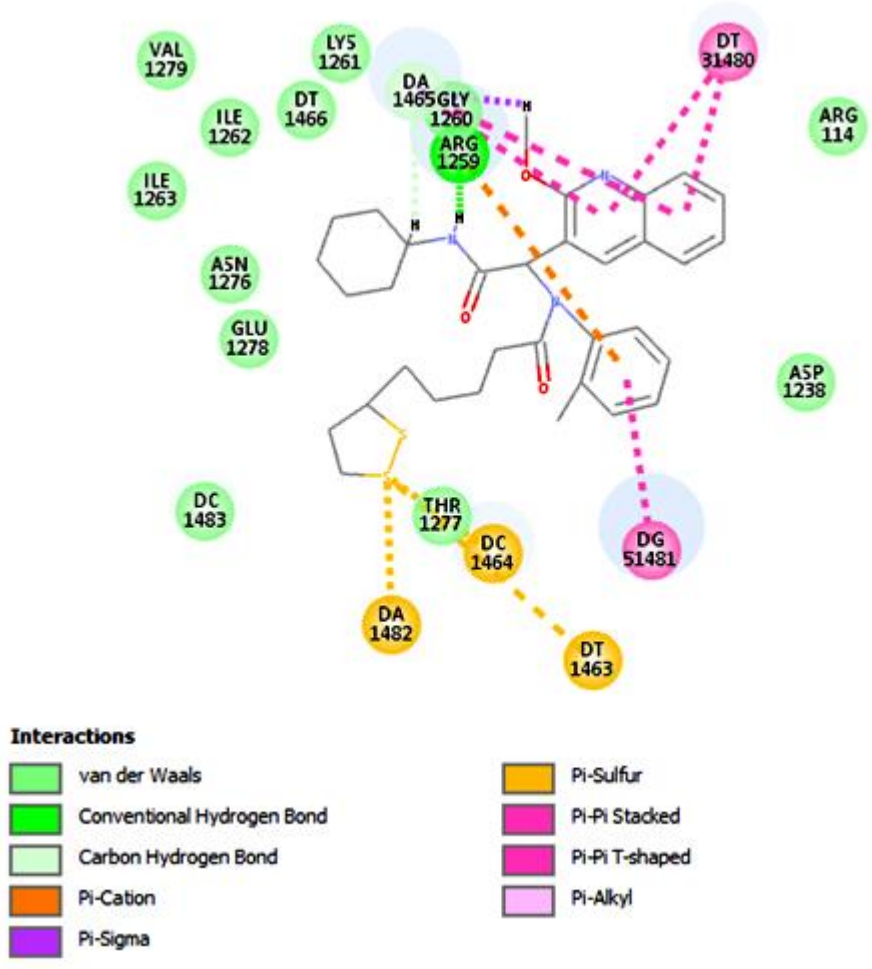

Fig. 7. The binding interactions between QLP (**41**) and DNA-gyrase

Molecular docking was conducted in the Libdock module of Discovery studio. The 3D-models of compounds **41**, **43**, **46** and **47** were constructed in Chembio3D-ultra software and were optimized using the MMFF94 minimization method. The crystal structure of DNA gyrase (PDB ID: 5BS8) (Blower *et al*., 2016) was used as a macromolecular

therapeutic target and the missing atoms were fixed using tLEaP and Chimera software (Kholmurodov *et al*., 2000; Jorgensen *et al*., 1983; Pettersen *et al*., 2004).

The hotspot for ligand docking was constructed around the surrounding of the moxifloxacin (co-crystallized ligand). Ciprofloxacin was used as a reference ligand to assess the antibacterial potency of **41**, **43**, **46** and **47**. The results of molecular docking are presented in **Table 7** based on Libdock score (Rao *et al*., 2007). The ligand binding landscape and their interaction pattern were analysed from the top ranked binding pose.

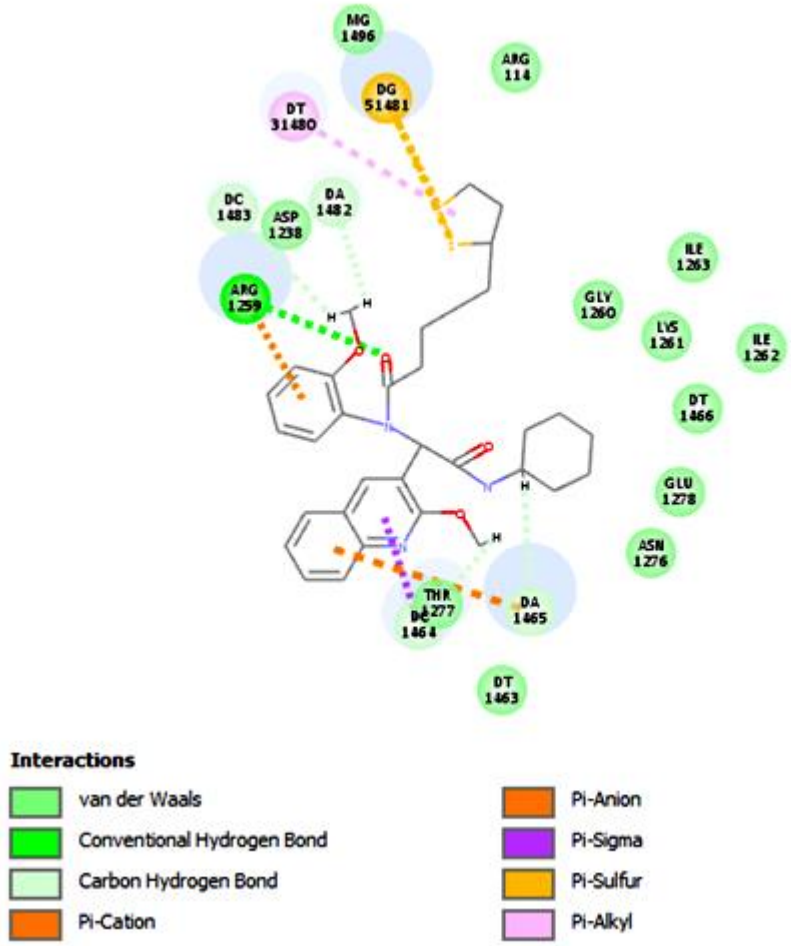

Fig. 8. The binding interactions between QLP (**43**) and DNA-gyrase

Peptides **41** and **43** were docked with a better docking score of 183.24 and 165.01 kcal/mol in comparison to ciprofloxacin (151.56 kcal/mol). The Libdock score of **41** and **43** indicated a higher antibacterial potency over ciprofloxacin **(Table 7)**. The results are in accordance with the preliminary antimicrobial assay. The hydrogen bonding and

hydrophobic forces were found to be the prominent interaction of QLPs with DNA-gyrase **(Fig. 7** and **Fig. 8)**.

Table 7. Libdock scores of active quinoline peptides from molecular docking

S. No	Compounds	Absolute energy	Libdock Score	Antimicrobial activity
1.	**41**	87.5808	183.237	12 ± 0.4
2.	**43**	88.3352	165.014	11 ± 0.3
3.	**46**	-----	-----	20 ± 0.3
4.	**47**	-----	-----	12 ± 0.2
5.	Ciprofloxacin	38.7128	151.561	31 ± 0.2

Molecular docking: Libdock scores for the active molecules of quinoline peptides were obtained from molecular docking protocol of Libdock module of Discovery Studio.

3.4. Conclusion

In conclusion, medicinally active 14 quinoline and quinolone based peptides were synthesised by Ugi four-component reaction under the action of microwave irradiation. All compounds were fully characterized by spectroscopic techniques. A total of eight peptides were evaluated for their antimicrobial and antioxidant activities; compounds **41**, **43**, **46**, **47** showed positive results for antimicrobial activity and **41**, **46**, **47** showed positive results for antioxidant activity. Molecular docking studies of **41** and **43** showed a higher binding affinity towards DNA gyrase than ciprofloxacin based on Libdock score. The advantages for the synthesis of new peptides are the use of inexpensive solvent, eco-friendly and short reaction time. It is envisaged that the peptides will find application in the field of biopharmaceuticals and drug discovery.

3.5. Experimental

General procedure for the microwave synthesis of peptides

A mixture of amine (1 mmol), **37** (1 mmol), **38** (1 mmol) and **39** (1.5 mmol) was dissolved in MeOH (15 mL) and the reaction mixture was transferred to a microwave tube (35 mL). The reaction tube was placed into a CEM microwave discover synthesizer and irradiated at 120 W with the temperature of 110℃ for 15 min. The progress of the reaction was monitored by TLC. After completion, the reaction mixture was allowed to attain room temperature. The solvent was removed under *in vacuo* and the residue was

purified by column chromatography (eluent ethyl acetate: petroleum ether, 1:3) to give the corresponding peptide. The recrystallization of the product was performed with 5:1 EtOAc: MeOH to yield the pure desired product.

Antimicrobial Assay

Approximately, 108 cfu/mL was used to standardize the bacterial and yeast cell concentration. A suspension (100 µL of 108 cfu/mL) of bacteria and yeast was plated on Mueller Hinton Agar plates and PD Agar plates, respectively. A well of 6 mm diameter was made using a sterile cork borer. The peptides (30 µL) were added to each well at concentration of 3 mg/ml and kept at 37°C (bacterial cultures) for 16 h and 30°C (yeast cultures) for 48 h. The assays were carried out in triplicate. Ciprofloxacin (3 mg/ml for bacteria) and Geneticin (50 mg/mL) were used as a positive control while DMSO (100%) as a negative control.

Antioxidant assays

Exactly 200 µL of the compound was added to 3 mL of 0.1 mM DPPH solution, and a colour change was observed at regular intervals. Rutin hydrates were used as a positive control and methanol (95%) as negative control.

Toxicity assessment

The brine shrimp larvae (*Artemia salina*) were hatched in sea water for 24-48 h prior to being used in the test. An aliquot of 5 mL sea water and ten brine shrimp were added to each vial and treated with different peptides having concentration of 300 µg. Brine shrimp death were observed at regular intervals.

References

[1] De Mejia, E. G., Martinez-Villaluenga, C., Fernandez, D., Urado, D., Sato, K. 2012. Bioavailability and safety of food peptides. CRC Press: Boca Raton. FL. 284-312.

[2] Möller, N. P., Scholz-Ahrens, K. E., Roos, N., Schrezenmeir, J. 2008. Bioactive peptides and proteins from foods: Indication for health effects. European Journal of Nutrition, (47) 171-182.

[3] Domling, A., Wang, W., Wang, K. 2012. Chemistry and biology of multicomponent reactions. Chemical Reviews, (112) 3083-3135.

[4] Giovenzana, G. B., Tron, G. C., Di Paola, S., Menegotto, I. G., Pirali, T. 2006. A mimicry of primary amines by bis-secondary diamines as components in the Ugi four-component reaction. Angewandte Chemie International Edition, (118) 1117-1120.

[5] Tron, G. C. 2013. Off the beaten track: The use of secondary amines in the Ugi reaction. European Journal of Organic Chemistry, (10) 1849-1859.

[6] Liéby-Muller, F., Constantieux, T., Rodriguez, J. 2005. Multicomponent domino reaction from β-ketoamides: Highly efficient access to original polyfunctionalized 2, 6-diazabicyclo [2.2.2] octane cores. Journal of the American Chemical Society, (127) 17176-17177.

[7] El Kaïm, L., Grimaud, L., Oble, J. 2005. Phenol Ugi–Smiles systems: Strategies for the multicomponent N-arylation of primary amines with isocyanides, aldehydes, and phenols. Angewandte Chemie International Edition, (117) 8175-8178.

[8] Castellano, T.G., Neo, A.G., Marcaccini, S., Marcos, C.F. 2012. Enols as feasible acid components in the Ugi condensation. Organic Letters, (14) 6218-6221.

[9] Elders, N., Van der Born, D., Hendrickx, L. J., Timmer, B. J., Krause, A., Janssen, E., de Kanter, F. J., Ruijter, E., Orru, R. V. 2009. The efficient one-pot reaction of up to eight Components by the union of multicomponent reactions. Angewandte Chemie International Edition, (48) 5856-5859.

[10] Ngouansavanh, T., Zhu, J. 2007. IBX-mediated oxidative Ugi-type multicomponent reactions: Application to the N and C1 functionalization of tetrahydroisoquinoline. Angewandte Chemie International Edition, (46) 5775-5778.

[11] Sinha, M. K., Khoury, K., Herdtweck, E., Dömling, A. 2013. Tricycles by a new Ugi variation and Pictet–Spengler reaction in one pot. Chemistry-A European Journal, (19) 8048-8052.

[12] Pando, O., Stark, S., Denkert, A., Porzel, A., Preusentanz, R., Wessjohann, L. A. 2011. The multiple multicomponent approach to natural product mimics: Tubugis, N-substituted anticancer peptides with picomolar activity. Journal of the American Chemical Society, (133) 7692-7695.

[13] Znabet, A., Ruijter, E., de Kanter, F.J., Köhler, V., Helliwell, M., Turner, N.J., Orru, R.V. 2010. Highly stereoselective synthesis of substituted prolyl peptides using a combination of biocatalytic desymmetrization and multicomponent reactions. Angewandte Chemie International Edition, (31) 5289-5292.

[14] Rivera, D. G., Wessjohann, L. A. 2009. Architectural chemistry: Synthesis of topologically diverse macromulticycles by sequential multiple multicomponent macrocyclizations. Journal of the American Chemical Society, (131) 3721-3732.

[15] Khoury, K., Sinha, M. K., Nagashima, T., Herdtweck, E., Dömling, A. 2012. Efficient assembly of iminodicarboxamides by a "truly" four-component reaction. Angewandte Chemie International Edition, (51) 10280-10283.

[16] Pérez-Labrada, K., Brouard, I., Méndez, I., Rivera, D. G. 2012. Multicomponent synthesis of Ugi-type ceramide analogues and neoglycolipids from lipidic isocyanides. The Journal of Organic Chemistry, (77) 4660-4670.

[17] Zhang, Y., Donahue, J. P., Li, C. J. 2007. Gold (III)-catalyzed double hydroamination of o-alkynylaniline with terminal alkynes leading to N-vinylindoles. Organic Letters, (9) 627-630.

[18] Shanbhag, G. V., Kumbar, S. M., Halligudi, S. B. 2008. Chemoselective synthesis of β-amino acid derivatives by hydroamination of activated olefins using AlSBA-15 catalyst prepared by post-synthetic treatment. Journal of Molecular Catalysis A: Chemical, (284) 16-23.

[19] Bonnaterre, F., Bois-Choussy, M., Zhu, J. 2008. Synthesis of dihydrophenanthridines by a sequence of Ugi-4CR and palladium-catalyzed intramolecular CH functionalization. Beilstein Journal of Organic Chemistry, (4) 1-11.

[20] Hügel, H. M. 2009. Microwave multicomponent synthesis. Molecules, (14) 4936-4972.

[21] Kaur, S., Singh, V., Kumar, G., Singh, J. 2011. An improved methodology for synthesis of new Ugi adducts and its application in combinatorial synthesis. Arkivoc, (2) 151-160.

[22] Kanizsai, I., Gyónfalvi, S., Szakonyi, Z., Sillanpää, R., Fülöp, F. 2007. Synthesis of bi-and tricyclic β-lactam libraries in aqueous medium. Green Chemistry, (9) 357-360.

[23] Shiri, M., Nejatinejhad-Arani, A. Faghihi, Z., Shintre, S.A., Koorbanally, N. A. 2016. Synthesis and biological evaluation of novel quinoline derivatives as antibacterial and antifungal agents. Organic Chemistry Research, (2) 113-119.

[24] Marcaccini, S., Pepino, R., Pozo, M. C. 2001. A facile synthesis of 2,5-diketopiperazines based on isocyanide chemistry. Tetrahedron Letters, (42) 2727-2728.

[25] El Kaïm, L., Grimaud, L., Oble, J. 2005. Phenol Ugi–Smiles Systems: Strategies for the multicomponent N-arylation of primary amines with isocyanides, aldehydes, and phenols. Angewandte Chemie, (117) 8175-8178.

[26] Váradi, A., Palmer, T.C., Haselton, N., Afonin, D., Subrath, J.J., Le Rouzic, V., Hunkele, A., Pasternak, G.W., Marrone, G.F., Borics, A., Majumdar, S. 2015. Synthesis of carfentanil amide opioids using the Ugi multicomponent reaction. ACS Chemical Neuroscience, (6) 1570-1577.

[27] Azizi, N., Dezfooli, S., Hashemi, M. M. 2013. A sustainable approach to the Ugi reaction in deep eutectic solvent. Comptes Rendus Chimie, (16) 1098-1102.

[28] El Sayed, I., El Kosy, S. M., Hawata, M .A., El Gokha, A. A. A., Tolan, A. Abd, E. S. 2011. Antibacterial activity of α-aminophosphonates bearing neocryptolepine moiety. Journal of American Science, (7) 357-361.

[29] Lu, T., Zhao, X., Drlica, K. 1999. Gatifloxacin activity against quinolone-resistant gyrase: allele-specific enhancement of bacteriostatic and bactericidal activities by the C-8-methoxy group. Antimicrobial Agents and Chemotherapy, (43) 2969-2974.

[30] Matsui, J., Funahashi, Y., Uenaka, T., Watanabe, T., Tsuruoka, A., Asada, M. 2008. Multi-kinase inhibitor E7080 suppresses lymph node and lung metastases of human mammary breast tumor MDA-MB-231 via inhibition of vascular endothelial growth factor-receptor (VEGF-R) 2 and VEGF-R3 kinase. Clinical Cancer Research, (14) 5459-5465.

[31] Gatto, B., Capranico, G., Palumbo, M. 1999. Drugs acting on DNA topoisomerases: Recent advances and future perspectives. Current Pharmaceutical Design, (5) 195-216.

[32] Sigel, H., Sigel, A. 2000. Metal ions in biological systems. Ed., Marcel Dekker, New York.

[33] Grimm, E. L., Brideau, C., Chauret, N., Chan, C.C., Delorme, D., Ducharme, Y., Ethier, D., Falgueyret, J. P., Friesen, R. W., Guay, J., Hamel, P. 2006. Substituted coumarins as potent 5-lipoxygenase inhibitors. Bioorganic & Medicinal Chemistry Letters, (16) 2528-2531.

[34] Biewenga, G. P., Haenen, G. R., Bast, A. 1997. The pharmacology of the antioxidant lipoic acid. General Pharmacology: The Vascular System, (29) 315-331.

[35] Packer, L. 1998. α- Lipoic acid: A metabolic antioxidant which regulates NF-κB signal transduction and protects against oxidative injury. Drug Metabolism Reviews, (30) 245-275.

[36] Packer, L., Witt, E. H., Tritschler, H. J. 1995. Alpha-lipoic acid as a biological antioxidant. Free Radical Biology and Medicine, (19) 227-250.

[37] Tirosh, O., Sen, C. K., Roy, S., Kobayashi, M. S., Packer, L. 1999. Neuroprotective effects of α-lipoic acid and its positively charged amide analogue. Free Radical Biology and Medicine, (26) 1418-1426.

[38] Rosini, M., Andrisano, V., Bartolini, M., Bolognesi, M. L., Hrelia, P., Minarini, A., Tarozzi, A., Melchiorre, C. 2005. Rational approach to discover multipotent anti-Alzheimer drugs. Journal of Medicinal Chemistry, (48) 360-363.

[39] Möller, N. P., Scholz-Ahrens, K. E., Roos, N., Schrezenmeir, J. 2008. Bioactive peptides and proteins from foods: Indication for health effects. European Journal of Nutrition, (47) 171-182.

[40] Zhang, Y., Donahue, J. P., Li, C. J. 2007. Gold (III)-catalyzed double hydroamination of o-alkynylaniline with terminal alkynes leading to N-vinylindoles. Organic Letters, (9) 627-630.

[41] Shanbhag, G. V., Kumbar, S. M., Halligudi, S. B. 2008. Chemoselective synthesis of β-amino acid derivatives by hydroamination of activated olefins using AlSBA-15 catalyst prepared by post-synthetic treatment. Journal of Molecular Catalysis A: Chemical, (284) 16-23.

[42] Bonnaterre, F., Bois-Choussy, M., Zhu, J. 2008. Synthesis of dihydrophenanthridines by a sequence of Ugi-4CR and palladium-catalyzed intramolecular CH functionalization. Beilstein Journal of Organic Chemistry, (4) 1-11.

[43] Hügel, H. M. 2009. Microwave multicomponent synthesis. Molecules, (14) 4936-4972.

[44] Kuang, C., Senboku, H., Tokuda, M. 2001. Convenient and stereoselective synthesis of (Z)-1-bromo-1-alkenes by microwave-induced reaction. Tetrahedron Letters, (42) 3893-3896.

[45] Strauss, C. R., Trainor, R. W. 1995. Developments in microwave-assisted organic chemistry. Australian Journal of Chemistry, (48) 1665-1692.

[46] Varma, R. S. 1999. Solvent-free organic syntheses using supported reagents and microwave irradiation. Green Chemistry, (1) 43-55.

[47] Bose, A. K., Banik, B. K., Lavlinskaia, N., Jayaraman, M., Manhas, M. S. 1997. More chemistry in a microwave. ChemInform, (28) 18-24.

[48] Nüchter, M., Ondruschka, B., Jungnickel, A., Müller, U. 2000. Organic processes initiated by non-classical energy sources. Journal of Physical Organic Chemistry, (13) 579-586.

[49] Romanova, N. N., Kudan, P. V., Gravis, A. G., Bundel', Y. G. 2000. The Use of microwave activation in the chemistry of heterocyclic compounds. Chemistry of Heterocyclic Compounds, (36) 1130-1140.

[50] Perreux, L., Loupy, A. 2001. A tentative rationalization of microwave effects in organic synthesis according to the reaction medium and mechanistic considerations. Tetrahedron, (57) 9199-9223.

[51] Deng, S. G., Lin, Y. S. 1997. Microwave heating synthesis of supported sorbents. Chemical Engineering Science, (52) 1563-1575.

[52] Elander, N., Jones, J. R., Lu, S. Y., Stone-Elander, S. 2000. Microwave-enhanced radiochemistry. Chemical Society Reviews, (29) 239-249.

[53] Caddick, S. 1995. Microwave assisted organic reactions. Tetrahedron, (51) 10403-10432.

[54] Lidström, P., Tierney, J., Wathey, B., Westman, J. 2001. Microwave assisted organic synthesis-a review. Tetrahedron, (57) 9225-9283.

[55] Ambika, S., Singh, R. M. 2005. Vilsmeier-Haack reagent: A facile synthesis of 2-chloro-3-formylquinolines from N-arylacetamides and transformation into different functionalities. Indian Journal of Chemistry, (44B) 1868-1875.

[56] Ma, Z., Xiang, Z., Luo, T., Lu, K., Xu, Z., Chen, J., Yang, Z. 2006. Synthesis of functionalized quinolines via Ugi and Pd-catalyzed intramolecular arylation reactions. Journal of Combinatorial Chemistry, (8) 696-704.

[57] Chéron, N., Ramozzi, R., Kaïm, L.E., Grimaud, L., Fleurat-Lessard, P. 2012. Challenging 50 years of established views on Ugi reaction: A theoretical approach. The Journal of Organic Chemistry, (77) 1361-1366.

[58] Balouiri, M., Sadiki, M., Ibnsouda, S. K. 2016. Methods for in vitro evaluating antimicrobial activity: A review. Journal of Pharmaceutical Analysis, (6) 71-79.

[59] Shaikh, R., Pund, M., Dawane, A., Iliyas, S. 2014. Evaluation of anticancer, antioxidant, and possible anti-inflammatory properties of selected medicinal plants used in Indian traditional medication. J. Traditional and Complementary Medicine, (4) 253-257.

[60] Carballo, J. L., Hernández-Inda, Z. L., Pérez, P., García-Grávalos, M. D. 2002. A comparison between two brine shrimp assays to detect in vitro cytotoxicity in marine natural products. BMC Biotechnology, (2) 17-22.

[61] Meyer, B. N., Ferrigni, N. R., Putnam, J. E., Jacobsen, L. B., Nichols, D. E., McLaughlin, J. L. 1982. Brine shrimp: A convenient general bioassay for active plant constituents. Planta Medica, (45) 31-34.

[62] Blower, T. R., Williamson, B. H., Kerns, R. J., Berger, J. M. 2016. Crystal structure and stability of gyrase-fluoroquinolone cleaved complexes from Mycobacterium tuberculosis. Proceedings of the National Academy of Sciences, (113) 1706-1713.

[63] Kholmurodov, K., Smith, W., Yasuoka, K., Darden, T., Ebisuzaki, T. 2000. A smooth-particle mesh Ewald method for DL_POLY molecular dynamics simulation package on the Fujitsu VPP700. Journal of Computational Chemistry, (21) 1187-1191.

[64] Jorgensen, W. L., Chandrasekhar, J., Madura, J. D., Impey, R. W., Klein, M. L. 1983. Comparison of simple potential functions for simulating liquid water. The Journal of Chemical Physics, (79) 926-935.

[65] Pettersen, E. F., Goddard, T. D., Huang, C. C., Couch, G. S., Greenblatt, D. M., Meng, E. C., Ferrin, T. E. 2004. UCSF Chimera-a visualization system for

exploratory research and analysis. Journal of Computational Chemistry, (25) 1605-1612.

[66] Rao, S. N., Head, M. S., Kulkarni, A., LaLonde, J. M. 2007. Validation studies of the site-directed docking program LibDock. Journal of Chemical Information And Modeling, (47) 2159-2171.

Appendix-III

3.1. *N*-(2-(cyclohexylamino)-1-(2-methoxyquinolin-3-yl)-2-oxoethyl)-5-((R)-1,2-dithiolan-3-yl)-*N*-phenylpentanamide (40)

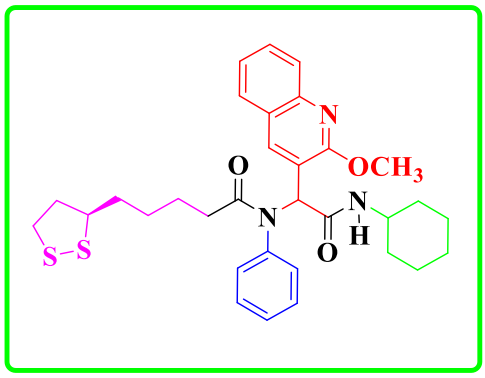

Brown solid, m.p = 123-125℃ ; IR ν_{max} (cm^{-1}): 1600 C=N, 1325 C-N, 2970 CH, 1493 C=C, 1625 C=O, 722 C-S, 685 S-S, 3416 NH. ^{1}H-NMR: (400 MHz, $CDCl_3$) δ (ppm) 7.88 (1H, s, Ar-H), 7.78 (1H, d, *J* = 8.32 Hz, Ar-H), 7.58 (2H, td, *J* = 1.32 Hz, Ar-H), 7.52 (1H, d, *J* = 7.96 Hz, Ar-H), 7.32 (3H, d, *J* = 0.76 Hz, Ar-H), 7.10 (2H, d, *J* = 6.8 Hz, Ar-H), 6.35 (1H, s, CH), 5.90 (1H, d, *J* = 8.4 Hz, N-H), 4.09 (3H, s, OCH_3), 3.89-3.87 (1H, m, *J* = 4 Hz, CH), 3.52-3.51 (1H, m, *J* = 1.72 Hz, CH), 3.12-3.05 (2H, m, *J* = 6.88 Hz, CH_2), 2.40-2.36 (2H, m, *J* = 7.32 Hz, CH_2), 2.10 (3H, t, *J* = 7.32 Hz, 2H(CH_2) and 1H(CH_2)), 2.06 (2H, d, *J* = 2.6 Hz, CH_2), 1.89-1.88 (2H, m, *J* = 4.32 Hz, CH_2) 1.67-1.65 (2H, m, *J* = 7.6 Hz, CH_2), 1.62 (2H, m, *J* = 7.12 Hz, CH_2), 1.60-1.58 (2H, m, *J* = 3.36 Hz, CH_2), 1.37-1.34 (3H, m, *J* = 5.6 Hz, 2H(CH_2) and 1H(CH_2)), 1.18-1.15 (2H, m, *J* = 3.12 Hz, CH_2). ^{13}C-NMR: (100 MHz, $CDCl_3$) δ (ppm) 177.24, 173.67, 168.72, 159.85, 145.84, 140.46, 139.84, 130.05, 128.91, 128.23, 127.85, 126.53, 124.56, 124.27, 119.01, 58.65, 56.38, 53.94, 48.78, 40.17, 38.43, 34.62, 33.60, 32.87, 32.84, 28.72, 25.49, 25.07, 25.01, 24.84, 24.76, 24.49. TOF-MS *m/z*: Calculated: 577.80 $[M]^+$, Found: 600.23 $[M+Na]^+$, 577.25 $[M]^+$. After subtracting the molecular weight of Na, the obtained value was 577.25). Elemental Analysis: Anal. Calc. for $C_{32}H_{39}N_3O_3S_2$: C, 66.52; H, 6.80; N, 7.27; %. Found: C, 66.54; H, 6.81; N, 7.25; %.

3.2. *N*-(2-(cyclohexylamino)-1-(2-methoxyquinolin-3-yl)-2-oxoethyl)-5-((R)-1,2-dithiolan-3-yl)-*N*-(o-tolyl)pentanamide (41)

Dark yellow solid, m.p = 128-130℃; IR ν_{max} (cm^{-1}): 1625 C=N, 1360 C-N, 2949 CH, 1434 C=C, 1683 C=O, 764 C-S, 539 S-S, 3456 NH. ^{1}H-NMR: (400 MHz, CD_3OD-d_4) δ (ppm) 7.96 (1H, s, Ar-H), 7.90 (1H, d, *J*=7.8 Hz, Ar-H), 7.69 (2H, t, *J*=10.4 Hz, Ar-H), 7.53-7.50 (1H, m, *J*=12 Hz, Ar-H), 7.27 (1H, t, *J*=7.32 Hz, Ar-H), 7.11 (1H, t, *J*=7.68 Hz, Ar-H), 6.98 (2H, t, *J*=9.28 Hz, Ar-H), 6.57 (1H, s, NH), 6.14 (1H, s, CH), 4.02 (3H, s, OCH_3), 3.32 (1H, m, *J*=1.52 Hz, CH), 3.12-3.10 (2H, m, *J*=1.64 Hz, CH_2), 3.10-3.07 (2H, m, *J*=1.28 Hz, CH_2), 2.44-2.37 (2H, m, *J*=4.28 Hz, CH_2), 2.32 (1H, t, *J*=7.2 Hz,

CH), 1.98-1.96 (2H, m, *J*=1.82 Hz, CH_2), 1.95 (2H, s, CH_2), 1.87-1.83 (2H, m, *J*=12.27 Hz, CH_2), 1.63-1.62 (2H, m, *J*=4.16 Hz, CH_2), 1.61-1.60 (2H, m, *J*=7.44 Hz, CH_2),1.60-1.58 (2H, m, *J*=2.28 Hz, CH_2), 1.32-1.30 (2H, m, *J*=9.28 Hz, CH_2), 1.29-1.28 (2H, m, *J*=3.96 Hz, CH_2), 1.11-1.09 (3H, m, *J*=9 Hz, CH_3). ^{13}C-NMR: (100 MHz, $CDCl_3$) δ (ppm) 159.32, 159.29, 146.40, 146.40, 146.25, 132.54, 132.08, 129.67, 127.63, 127.60, 123.39, 118.38, 114.18, 114.07, 114.05, 113.94, 77.40, 76.76, 63.90, 63.83, 63.30, 63.23, 56.13, 55.62, 55.22, 54.62, 30.91, 29.69, 16.47, 16.41, 16.41, 16.28, 16.23. TOF-MS *m/z*: Calculated: 591.26 $[M]^+$, Found: 614.35 $[M+Na]^+$, 591.37 $[M]^+$. Elemental Analysis: Anal. Calc. for $C_{33}H_{41}N_3O_3S_2$: C, 66.97; H, 6.98; N, 7.10; %. Found: C, 66.98; H, 6.96; N, 7.12; %.

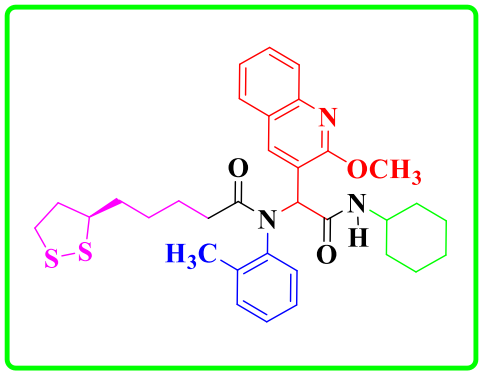

3.3. *N*-(2-(cyclohexylamino)-1-(2-methoxyquinolin-3-yl)-2-oxoethyl)-5-((R)-1,2-dithiolan-3-yl)-*N*-(m-tolyl)pentanamide (42)

Brown solid, m.p = 129-131℃; IR ν_{max} (cm^{-1}): 1616 C=N, 1325 C-N, 2943 CH, 1436 C=C, 1647 C=O, 638 C-S, 538 S-S, 3266 NH. ^{1}H-NMR: (400 MHz, CD_3OD-d_4) δ (ppm) 7.96 (1H, s, Ar-H), 7.70 (2H, d, Ar-H), 7.56 (2H, td, *J*=5.52 Hz, Ar-H), 7.46 (1H, t, *J*=7.48 Hz, Ar-H), 7.37 (1H, t, *J*=7.6 Hz, Ar-H), 6.88 (1H, d, *J*=7.6 Hz, Ar-H), 6.70 (1H, d, *J*=6.6 Hz, Ar-H), 6.37 (1H, s, NH), 4.09 (1H, s, CH), 3.68-3.64 (1H, m, *J*= 5.2, CH), 3.55 (3H, s, OCH_3), 2.97-2.95 (1H, m, *J*=1.96 Hz, CH), 2.83-2.80 (3H, m, *J*=4.68 Hz, CH_3), 2.42 (2H, d, *J*=9.76 Hz, CH_2), 2.34 (2H, d, *J*=1.4 Hz, CH_2), 2.32-2.30 (2H, t, *J*=3.52 Hz, CH_2), 1.95 (2H, d, *J*=8.04 Hz, CH_2), 1.92 (2H, d, *J*=2.64 Hz, CH_2), 1.77 (2H, s, CH_2), 1.75 (2H, t, *J*=4 Hz, CH_2), 1.67-1.65 (2H, m, *J*= 8Hz, CH_2), 1.64-1.63 (2H, m, *J*= 4Hz, CH_2), 1.35 (2H, s, CH_2), 1.31 (2H, d, *J*=7.36 Hz, CH_2). ^{13}C-NMR: (100 MHz, DMSO-d_6) δ (ppm) 169.07, 154.50, 145.52, 140.64, 131.56, 128.06, 127.53, 126.62, 126.60, 113.89, 112.84, 112.61, 107.25, 49.60, 40.46, 40.08, 39.87, 39.67, 39.46, 39.04, 38.83,

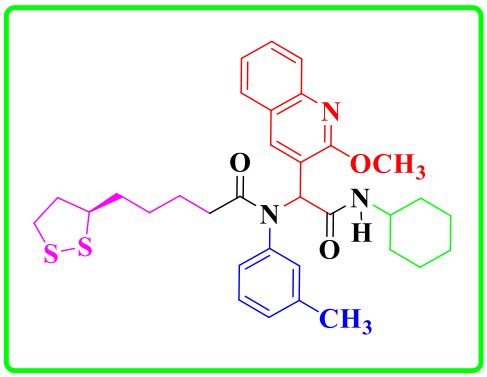

33.26, 31.77, 30.50, 28.99, 27.17, 26.06. Elemental Analysis: Anal. Calc. for $C_{33}H_{41}N_3O_3S_2$: C, 66.97; H, 6.98; N, 7.10; %. Found: C, 66.99; H, 6.97; N, 7.13; %.

3.4. *N*-(2-(cyclohexylamino)-1-(2-methoxyquinolin-3-yl)-2-oxoethyl)-5-((R)-1,2-dithiolan-3-yl)-*N*-(2-methoxyphenyl)pentanamide (43)

Pale brown solid, m.p = 132-134℃; IR ν_{max} (cm^{-1}): 1599 C=N, 1139 C-N, 2970 CH, 1492 C=C, 1625 C=O, 746 C-S, 618 S-S, 3416 NH.

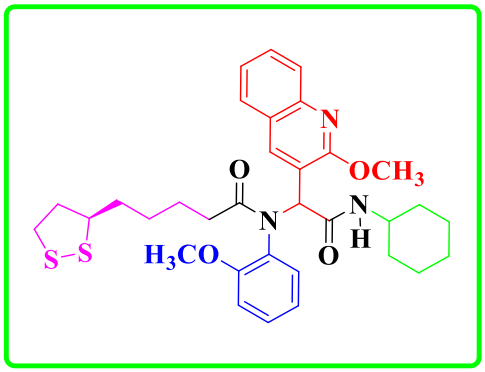

^{1}H-NMR: (400 MHz, CD_3OD-d_4) δ (ppm) 8.00 (1H, s, ArH), 7.91 (1H, s, NH), 7.36 (1H, t, *J*=7.68 Hz, ArH), 7.27 (1H, t, *J*=7.08 Hz, ArH), 7.17-7.10 (1H, m, *J*=9.08 Hz, ArH), 6.99 (1H, d, *J*=8.32 Hz, ArH), 6.89 (2H, t, *J*=7.64 Hz, ArH), 6.60 (1H, d, *J*=8.4 Hz, ArH), 6.46 (1H, s, ArH), 6.17 (1H, s, CH), 4.01 (3H, s, OCH_3), 3.86 (2H, d, *J*=5.16 Hz, CH_2), 3.43 (3H, s, OCH_3), 3.32 (1H, m, *J*=1.52 Hz, CH), 2.12-2.10 (1H, m, *J*=7.12 Hz, CH), 2.01 (2H, s, CH_2), 1.83 (2H, m, *J*=2.0 Hz, CH_2), 1.76 (2H, d, *J*=3.8 Hz, CH_2), 1.62 (2H, m, *J*=1.12 Hz, CH_2), 1.58 (2H, m, *J*=2.4 Hz, CH_2), 1.40 (2H, d, *J*=1.12 Hz, CH_2), 1.38 (2H, m, *J*=2.4 Hz, CH_2), 1.35 (2H, m, *J*=5.32 Hz, CH_2), 1.32 (2H, m, *J*=1.88 Hz, CH_2), 1.24 (2H, s, CH_2). ^{13}C-NMR: (100 MHz, CD_3OD-d_4) δ (ppm) 171.03, 161.79, 161.34, 147.34, 132.44, 129.24, 128.87, 128.73, 127.68, 125.65, 125.27, 121.98, 121.45, 121.10, 120.65, 112.92, 112.29, 79.57, 76.74, 63.97, 62.89, 61.58, 59.82, 59.82, 37.88, 37.23, 37.20, 36.52, 36.46, 36.14, 35.96, 29.99, 28.10, 26.28, 25.90. TOF-MS *m/z*: Calculated: 607.25 $[M]^+$, Found: 630.31 $[M+Na]^+$, 607.33 $[M]^+$. Elemental Analysis: Anal. Calc. for $C_{33}H_{41}N_3O_4S_2$: C, 65.21; H, 6.80; N, 6.91; %. Found: C, 65.20; H, 6.82; N, 6.90; %.

3.5. *N*-(2-(cyclohexylamino)-1-(2-methoxy-6-methylquinolin-3-yl)-2-oxoethyl)-5-((R)-1,2-dithiolan-3-yl)-*N*-phenylpentanamide (44)

Brown solid, m.p = 127-129℃; IR ν_{max} (cm^{-1}): 1738 C=N, 1189 C-N, 2970 CH, 1493 C=C, 1600 C=O, 747 C-S, 655 S-S, 3418 NH. ^{1}H-NMR: (400 MHz, $CDCl_3$) δ (ppm) 8.63 (1H, s, ArH), 8.36 (1H, d, *J*=1.38 Hz, NH), 8.08 (1H, t, *J*=4.52 Hz, ArH), 7.53 (2H, d, *J*=7.88 Hz, ArH), 7.16 (2H, t, *J*=7.4 Hz, ArH), 7.11 (1H, d, *J*=11.12 Hz, ArH), 7.08 (2H, m, *J*=1.88 Hz, ArH), 5.80 (1H, s, CH), 4.03 (3H, s, OCH_3), 3.77-3.73 (2H, m, *J*=3.16 Hz, CH_2), 3.58-3.51 (1H, m, *J*=6.4 Hz, CH), 3.46-3.42 (2H, m, *J*=6.48 Hz, CH_2), 3.14-

3.11 (2H, m, *J*=1.28 Hz, CH_2), 3.09-3.05 (2H, m, *J*=4.0 Hz, CH_2), 2.35-2.33 (2H, m, *J*=7.52 Hz, CH_2), 2.33-2.31 (2H, m, *J*=7.4 Hz, CH_2), 1.88-1.87 (2H, m, *J*=4.44 Hz, CH_2), 1.86-1.85 (2H, m, *J*=7.52 Hz, CH_2), 1.67-1.65 (2H, m, *J*=2.0 Hz, CH_2), 1.53-1.51 (2H, m, *J*=1.52 Hz, CH_2), 1.31 (2H, d, *J*=3.84 Hz, CH_2), 1.30 (2H, d, *J*=4.2 Hz, CH_2), 1.14 (3H, d, *J*=10.32 Hz, CH_3). ^{13}C-NMR: (100 MHz, CD_3OD-d_4) δ (ppm) 177.42, 176.18, 175.06, 161.62, 141.07, 138.96, 132.39, 131.55, 130.78, 130.67, 130.57, 129.96, 125.88, 125.56, 121.05, 119.61, 63.95, 57.47, 48.82, 48.60, 41.31, 41.27, 36.42, 36.32, 36.25, 35.62, 34.76, 33.57, 29.87, 29.78, 26.72, 26.50, 26.02, 25.86, 25.65. TOF-MS *m/z*: Calculated: 591.83 $[M]^+$ Found: 614.24 $[M+Na]^+$, 591.26 $[M]^+$. Elemental Analysis: Anal. Calc. for $C_{33}H_{41}N_3O_3S_2$: C, 66.97; H, 6.98; N, 7.10; %. Found: C, 66.99; H, 6.96; N, 7.12; %.

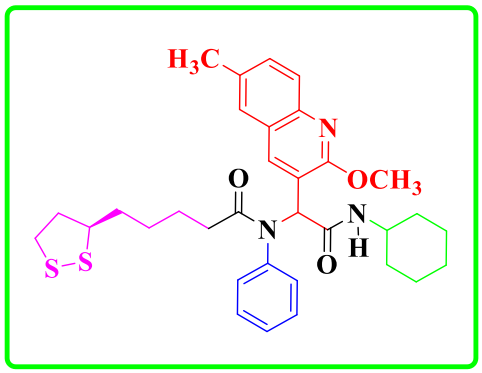

3.6. *N*-(2-(cyclohexylamino)-1-(2-methoxy-6-methylquinolin-3-yl)-2-oxoethyl)-5-((R)-1,2-dithiolan-3-yl)-*N*-(m-tolyl)pentanamide (45)

Brown solid, m.p = 129-131℃; IR ν_{max} (cm^{-1}): 1615 C=N, 1074 C-N, 2970 CH, 1491 C=C, 1645 C=O, 741 C-S, 698 S-S, 3393 NH. ^{1}H-NMR: (400 MHz, $CDCl_3$) δ (ppm) 8.64 (1H, d, *J*=11.28 Hz, ArH), 8.35 (1H, s, ArH), 8.10 (1H, s, NH), 7.63 (1H, d, *J*=8.48 Hz, ArH), 7.42 (1H, s, ArH), 7.07 (2H, d, *J*=12.04 Hz, ArH), 6.99 (2H, d, *J*=7.52 Hz, ArH), 6.24 (1H, s, CH), 4.03 (3H, s, OCH_3), 3.58-3.55 (1H, m, *J*=7.64 Hz, CH), 2.46-2.43 (1H, m, *J*=6.52 Hz, CH), 2.41 (3H, s, CH_3), 2.41 (2H, m, *J*= 5.12 Hz, CH_2), 2.39 (2H, m, *J*=6.68 Hz, CH_2), 2.34 (2H, m, *J*=7.68 Hz, CH_2), 2.33 (2H, m, *J*=3.16 Hz, CH_2), 2.09 (3H, t, *J*=7.36 Hz, CH_3), 1.93-1.91 (2H, m, J=8.56 Hz, CH_2), 1.90-1.88 (2H, m, J=3.44 Hz, CH_2), 1.69 (2H, m, *J*=1.56 Hz, CH_2), 1.68 (2H, m, *J*=1.42 Hz, CH_2), 1.35 (2H, m, *J*=3.2 Hz, CH_2), 1.32 (2H, m, *J*=2.32 Hz, CH_2), 1.25 (2H, s, CH_2). ^{13}C-NMR: (100 MHz, $CDCl_3$) δ (ppm) 160.01, 145.90, 145.75, 139.04, 136.84, 136.78, 129.59, 129.13, 127.76, 126.74, 125.26, 125.23, 124.22, 121.36, 121.34, 119.50, 114.54, 110.55, 77.37, 76.73,

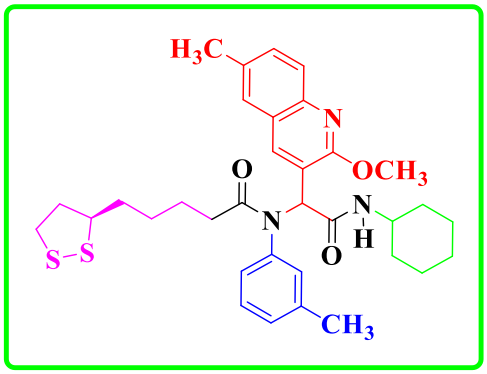

63.55, 63.49, 63.25, 63.18, 53.95, 49.45, 47.93, 21.57, 16.50, 16.44, 16.18, 16.12. TOF-MS *m/z*: Calculated 605.86 $[M]^+$, Found: 605.86 $[M+Na]^+$, 605.28 $[M]^+$. Elemental Analysis: Anal. Calc. for $C_{34}H_{43}N_3O_3S_2$: C, 67.40; H, 7.15; N, 6.94; %. Found: C, 67.42; H, 7.16; N, 6.93; %.

3.7. *N*-(2-(cyclohexylamino)-1-(2-methoxy-6-methylquinolin-3-yl)-2-oxoethyl)-5-((R)-1,2-dithiolan-3-yl)-*N*-(2-methoxyphenyl)pentanamide (46)

Dark brown solid, m.p = 130-132℃; IR ν_{max} (cm^{-1}): 1599 C=N, 1335 C-N, 2970 CH, C=C, 1625 C=O, 722 C-S, 573 S-S, 3416 NH. ^{1}H-NMR: (400 MHz, CD_3OD-d_4) δ (ppm) 7.84 (1H, s, ArH), 7.71 (1H, s, NH), 7.61 (1H, m, *J*=6.6 Hz, ArH), 7.20 (1H, t, *J*=6.96 Hz, ArH), 6.89 (1H, m, *J*=6.32 Hz, ArH), 6.20 (1H, s, CH), 3.70 (3H, s, OCH_3), 3.61 (3H, s, OCH_3), 3.48-3.44 (1H, m, *J*=5.96 Hz, CH), 3.21 (2H, m, *J*=1.72 Hz, CH_2), 3.20 (2H, m, *J*=1.56 Hz, CH_2), 3.06-3.03 (2H, m, *J*=5.36 Hz, CH_2), 3.00-2.95 (2H, m, *J*=6.92 Hz, CH_2), 2.37-2.32 (2H, m, *J*=5.76 Hz, CH_2), 2.21 (2H, d, *J*=7.36 Hz, CH_2), 2.20 (2H, m, *J*=7.24 Hz, CH_2), 1.82-1.79 (1H, m, *J*=6.88 Hz, CH), 1.54-1.52 (2H, m, *J*=7.52 Hz, CH_2), 1.52-1.50 (2H, m, *J*=5.64 Hz, CH_2), 1.38 (2H, m, *J*=5.08 Hz, CH_2), 1.36 (2H, m, *J*=7.04 Hz, CH_2), 1.18 (3H, s, CH_3). ^{13}C-NMR: (100 MHz, CD_3OD-d_4) δ 177.42, 176.18, 175.06, 161.62, 141.07, 138.96, 132.39, 131.55, 130.74, 130.67, 130.57, 129.96, 125.88, 125.56, 121.05, 119.61, 63.95, 57.47, 50.45, 49.66, 49.52, 49.03, 48.82, 41.31, 41.27, 36.32, 36.25, 35.62, 34.76, 33.57, 29.87, 26.72, 26.02, 25.65. TOF-MS *m/z*: Calculated: 621.27 $[M]^+$, Found: 644.29 $[M+Na]^+$, 621.31 $[M]^+$. Elemental Analysis: Anal. Calc. for $C_{34}H_{43}N_3O_4S_2$: C, 65.67; H, 6.97; N, 6.76; %. Found: C, 65.66; H, 6.99; N, 6.78; %.

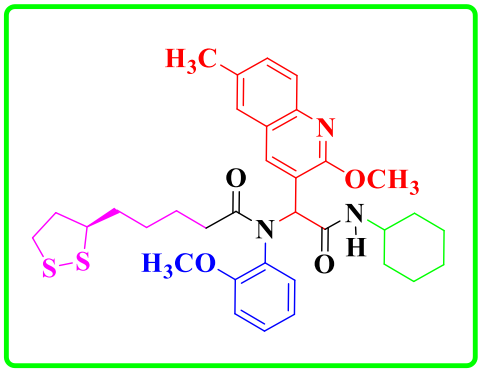

3.8. *N*-(2-(cyclohexylamino)-1-(2-methoxy-6-nitroquinolin-3-yl)-2-oxoethyl)-5-((R)-1,2-dithiolan-3-yl)-*N*-phenylpentanamide (47)

Yellow solid, m.p = 147-149℃; IR ν_{max} (cm^{-1}): 1615 C=N, 1092 C-N, 2852 CH, 1464 C=C, 1721 C=O, 741 C-S, 698 S-S, 3457 NH. ^{1}H-NMR: (400 MHz, CD_3OD-d_4) δ (ppm) 8.25 (1H, s, ArH), 7.99 (2H, t, *J*=2.0 Hz, ArH), 7.98 (2H, t, *J*=2.12 Hz, ArH), 7.57 (1H, d, *J*=7.8 Hz, NH), 6.64 (2H, t, *J*=1.96 Hz, ArH), 6.62 (2H, t, *J*=2.0 Hz, ArH), 6.20 (1H, s, CH), 4.19 (3H, s, OCH_3), 3.33-3.31 (1H, m, *J*=6.56 Hz, CH), 3.18-3.17 (2H, m, *J*=5.4

Hz, CH_2), 2.50-2.43 (1H, m, *J*=5.4 Hz, CH), 2.37 (2H, d, *J*=7.08 Hz, CH_2), 2.35 (2H, m, *J*=7.16 Hz, CH_2), 2.30 (2H, t, *J*=7.28 Hz, CH_2), 1.92-1.87 (2H, m, *J*=6.8 Hz, CH_2), 1.70-1.68 (2H, m, *J*=8.24 Hz, CH_2), 1.68-1.67 (2H, m, *J*=1.48 Hz, CH_2), 1.67-1.66 (2H, m, *J*=3.68 Hz, CH_2), 1.66-1.64 (2H, m, *J*=7.28 Hz, CH_2), 1.51 (2H, m, *J*=1.48 Hz, CH_2), 1.49 (2H, m, *J*=4.16 Hz, CH_2). ^{13}C-NMR: (100 MHz, CD_3OD-d_4) δ (ppm) 177.65, 177.56, 162.80, 161.66, 156.81, 138.93, 138.33, 130.69, 130.09, 129.98, 125.93, 125.60, 121.07, 119.62, 116.89, 113.68, 63.98, 57.58, 41.34, 39.40, 37.79, 36.56, 36.02, 35.80, 35.34, 34.84, 33.70, 32.94, 29.89, 27.84, 26.60, 26.15. TOF-MS *m/z*: Calculated: 622.23 $[M]^+$, Found: 645.28 $[M+Na]^+$, 622.30 $[M]^+$. Elemental Analysis: Anal. Calc. for $C_{32}H_{38}N_4O_5S_2$: C, 61.71; H, 6.15; N, 9.00; %. Found: C, 61.73; H, 6.17; N, 9.02; %.

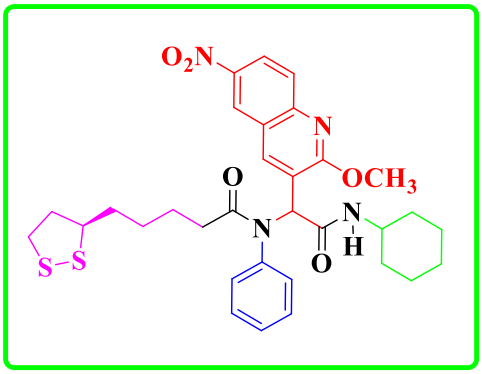

3.9. *N*-(2-amino-4-nitrophenyl)-*N*-(2-(cyclohexylamino)-1-(2-methoxy-6-nitro quinolin-3-yl)-2-oxoethyl)-5-((R)-1,2-dithiolan-3-yl)pentanamide (48)

Reddish brown solid, m.p = 126-128℃; IR ν_{max} (cm^{-1}): 1637 C=N, 1327 C-N, 2970 CH, 1497 C=C, 1738 C=O, 787 C-S, 587 S-S, 3457 NH. ^{1}H-NMR: (400 MHz, CD_3OD-d_4) δ (ppm) 8.45 (1H, s, ArH), 8.23 (1H, d, *J*=2.28 Hz, ArH), 8.20 (1H, d, *J*=2.16 Hz, ArH), 7.60-7.57 (2H, m, *J*=1.2 Hz, ArH), 7.33-7.32 (1H, m, *J*=4.28 Hz, ArH), 6.91 (1H, d, *J*=8.2 Hz, ArH), 6.63-6.60 (2H, m, *J*=2.6 Hz, ArH), 5.12 (1H, s, NH), 4.49 (2H, s, CH_2), 4.33 (1H, s, CH), 4.16 (3H, s, OCH_3), 3.58-3.55 (1H, m, *J*=2.32 Hz, CH), 2.49-2.43 (1H, m, *J*=5.56 Hz, CH), 2.32 (2H, s, CH_2), 2.29 (2H, d, *J*=7.32 Hz, CH_2), 2.17 (2H, s, CH_2), 1.93-1.89 (2H, m, *J*=13.72 Hz, CH_2), 1.88-1.84 (2H, m, *J*=6.8 Hz, CH_2), 1.69-1.68 (2H, m, *J*=2.8 Hz, CH_2), 1.65-1.64 (2H, m, *J*=3.76 Hz, CH_2), 1.63-1.62 (2H, m, *J*=2.68 Hz, CH_2), 1.50-1.48 (2H, m, *J*=3.4 Hz, CH_2), 1.46-1.45 (2H, m, *J*=3.08 Hz, CH_2), 1.28 (2H, s, CH_2). ^{13}C-NMR: (100 MHz, CD_3OD-d_4) δ (ppm) 147.37, 134.67, 131.13, 130.24, 128.56, 126.33, 125.65, 125.32, 125.20, 124.18, 119.41, 117.89, 11.751, 117.47, 113.53, 113.15, 111.54, 109.42, 107.01, 54.34, 54.20, 54.09, 49.74, 44.12, 43.71, 35.10, 33.69, 30.76, 27.80,

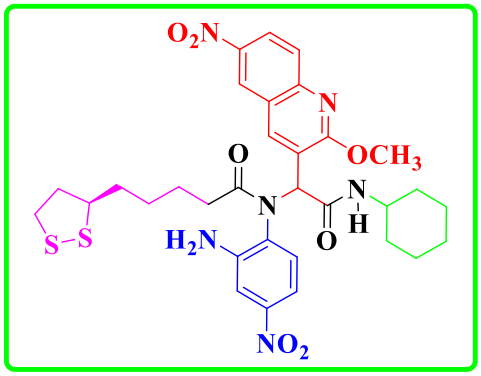

26.58, 26.14, 20.51. TOF-MS *m/z*: Calculated: 682.22 $[M]^+$, Found: 705.24 $[M+Na]^+$, 682.26 $[M]^+$. Elemental Analysis: Anal. Calc. for $C_{32}H_{38}N_6O_7S_2$: C, 56.29; H, 5.61; N, 12.31; %. Found: C, 56.27; H, 5.63; N, 12.33; %.

3.10. *N*-(2-(cyclohexylamino)-1-(2-methoxy-6-nitroquinolin-3-yl)-2-oxoethyl)-5-((R)-1,2-dithiolan-3-yl)-*N*-(2-fluorophenyl)pentanamide (49)

Brown solid, m.p = 127-129℃; IR ν_{max} (cm^{-1}): 1629 C=N, 1351 C-N, 2924 CH, 1499 C=C, 1687 C=O, 788 C-S, 620 S-S, 3447 NH. ^{1}H-NMR: (400 MHz, CD_3OD-d_4) δ (ppm) 8.05 (1H, d, *J*=6.6 Hz, ArH), 7.87 (1H, s, ArH), 7.83 (1H, td, *J*=14.04 Hz, ArH), 7.72 (1H, t, *J*=5.52 Hz, ArH), 7.44 (1H, t, *J*=4.44 Hz, ArH), 7.22 (1H, t, *J*=18.32 Hz, ArH), 6.98-6.95 (1H, m, *J*=9.76 Hz, ArH), 6.41 (1H, s, NH), 6.12 (1H, s, CH), 4.09 (3H, s, OCH_3), 3.69-3.75 (1H, m, *J*=6.2 Hz, CH), 3.33-3.31 (2H, m, *J*=1.64 Hz, CH_2), 3.16-3.11 (2H, m, *J*=2.0 Hz, CH_2), 3.07-3.04 (2H, m, *J*=6.8 Hz, CH_2), 2.45-2.37 (2H, m, *J*=5.6 Hz, CH_2), 2.29 (2H, d, *J*=7.32 Hz, CH_2), 2.26 (1H, d, *J*=4.32 Hz, CH), 1.88-1.86 (2H, m, *J*=2.28 Hz, CH_2), 1.85-1.83 (2H, m, *J*=6.48 Hz, CH_2), 1.76-1.73 (2H, m, *J*=4.24 Hz, CH_2), 1.64-1.60 (2H, m, *J*=7.92 Hz, CH_2), 1.36-1.33 (2H, m, *J*=4.12 Hz, CH_2), 1.29 (2H, t, *J*=7.88, CH_2). ^{13}C-NMR: (100 MHz, $CDCl_3$) δ (ppm) 175.54, 147.10, 146.77, 139.77, 138.44, 137.06, 136.56, 135.34, 133.61, 129.25, 127.63, 127.22, 126.78, 123.97, 111.93, 110.90, 106.56, 54.08, 50.42, 46.19, 45.05, 41.61, 37.07, 33.87, 32.11, 31.90, 31.42, 30.90, 30.30, 30.18, 29.45, 29.39. Elemental Analysis: Anal. Calc. for $C_{32}H_{37}FN_4O_5S_2$: C, 59.98; H, 5.82; N, 8.74; %. Found: C, 59.96; H, 5.84; N, 8.76; %.

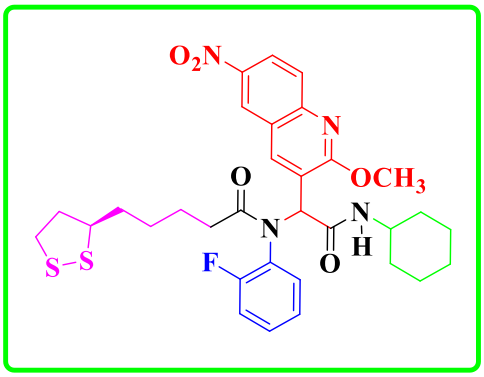

3.11. *N*-(2-(cyclohexylamino)-1-(2-methoxy-6-nitroquinolin-3-yl)-2-oxoethyl)-5-((R)-1,2-dithiolan-3-yl)-*N*-(m-tolyl)pentanamide (50)

Brown solid, m.p = 148-150℃; IR ν_{max} (cm^{-1}): 1599 C=N, 1067 C-N, 2970 CH, 1585 C=C, 1679 C=O, 749 C-S, 688 S-S, 3352 NH. ^{1}H-NMR: (400 MHz, CD_3OD-d_4) δ (ppm) 8.12 (1H, d, *J*=1.68 Hz, ArH), 7.82 (1H, s, ArH), 7.72 (1H, td, *J*=1.48 Hz, ArH), 7.44 (2H, dd, *J*=7.64 Hz, ArH), 7.35 (1H, t, *J*=7.6 Hz, ArH), 7.13 (2H, t, *J*=7.8 Hz, ArH), 6.68 (1H, d, *J*=7.48 Hz, NH), 4.60 (1H, s, CH), 3.90 (3H, s, OCH_3), 3.32 (1H, m, *J*=3.08 Hz, CH), 3.15-3.12 (2H, m, *J*=1.56 Hz, CH_2), 3.10-3.07 (2H, m, *J*=6.96 Hz, CH_2), 2.42 (2H,

t, *J*=1.44 Hz, CH_2), 2.41 (2H, t, *J*=3.28 Hz, CH_2), 2.34 (1H, m, *J*=2.24 Hz, CH), 2.29 (3H, m, *J*=7.16 Hz, CH_3), 2.10 (2H, t, *J*=6.96 Hz, CH_2), 1.94-1.89 (2H, m, *J*=9.12 Hz, CH_2), 1.88-1.86 (2H, m, *J*=6.0 Hz, CH_2), 1.59-1.55 (2H, m, *J*=6.92 Hz, CH_2), 1.33-1.29 (2H, m, *J*=6.28 Hz, CH_2), 0.96 (2H, m, *J*=7.36 Hz, CH_2), 0.92 (2H, m, *J*=7.32 Hz, CH_2). ^{13}C-NMR: (100 MHz, DMSO-d_6) δ (ppm) 155.65, 148.12, 148.01, 128.63, 127.61, 127.36, 126.73, 118.99, 118.04, 115.85, 112.60, 60.31, 59.73, 53.28, 51.91, 40.05, 39.84, 39.63, 39.42, 39.21, 38.80, 31.23, 30.64, 28.95, 28.84, 28.64, 28.50, 22.04, 20.71, 16.73, 16.68, 14.04, 13.90. Elemental Analysis: Anal. Calc. for $C_{33}H_{40}N_4O_5S_2$: C, 62.24; H, 6.33; N, 8.80; %. Found: C, 62.26; H, 6.35; N, 8.81; %.

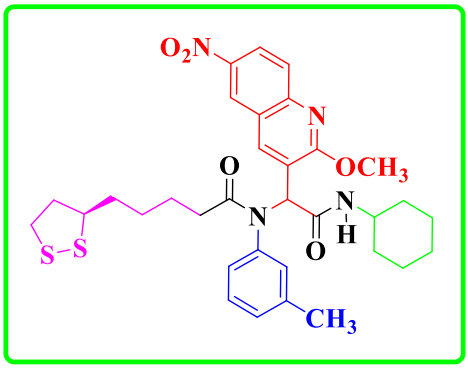

3.12. *N*-(2-(cyclohexylamino)-1-(2-methoxy-6-nitroquinolin-3-yl)-2-oxoethyl)-5-((R)-1,2-dithiolan-3-yl)-*N*-(o-tolyl)pentanamide (51)

Brown solid, m.p = 128-130℃; IR ν_{max} (cm^{-1}): 1612 C=N, 1297 C-N, 2970 CH, 1496 C=C, 1630 C=O, 786 C-S, 639 S-S, 3457 NH. ^{1}H-NMR: (400 MHz, CD_3OD-d_4) δ (ppm) 8.17 (1H, td, *J*=6.52 Hz, ArH), 8.05 (1H, d, *J*=1.56 Hz, NH), 7.96 (1H, s, ArH), 7.73-7.69 (2H, m, *J*=3.28 Hz, ArH), 7.64-7.61 (1H, m, *J*=3.36 Hz, ArH), 7.31 (2H, td, *J*=7.08 Hz, ArH), 4.57 (1H, s, CH), 4.23-4.22 (1H, m, *J*=2.08 Hz, CH), 4.10 (3H, s, OCH_3), 3.59-3.56 (2H, m, *J*=5.96 Hz, CH_2), 3.32 (2H, m, *J*=3.12 Hz, CH_2), 3.31 (2H, m, *J*=3.16 Hz, CH_2), 3.18-3.15 (2H, m, *J*=5.36 Hz, CH_2), 3.13-3.05 (2H, m, *J*=6.76 Hz, CH_2), 2.49-2.44 (1H, m, *J*=5.76 Hz, CH), 2.30 (3H, t, *J*=7.3 Hz, CH_3), 1.92-1.90 (2H, m, *J*=6.76 Hz, CH_2), 1.89-1.87 (2H, m, *J*=6.64 Hz, CH_2), 1.66-1.64 (2H, m, *J*=5.0 Hz, CH_2), 1.63-1.62 (2H, m, *J*=5.4 Hz, CH_2), 1.51-1.49 (2H, m, *J*=8.8 Hz, CH_2), 1.47-1.46 (2H, m, *J*=1.72 Hz, CH_2). ^{13}C-NMR: (100 MHz, $CDCl_3$) δ (ppm) 163.66, 146.17, 146.03, 139.05, 131.76, 129.46, 129.40, 129.38, 129.32, 129.08, 119.56, 115.67, 115.64, 115.45, 115.43, 114.75, 110.77, 77.33, 76.70, 63.40, 63.33, 63.29, 63.22, 56.10, 54.59, 21.54, 16.45, 16.40,

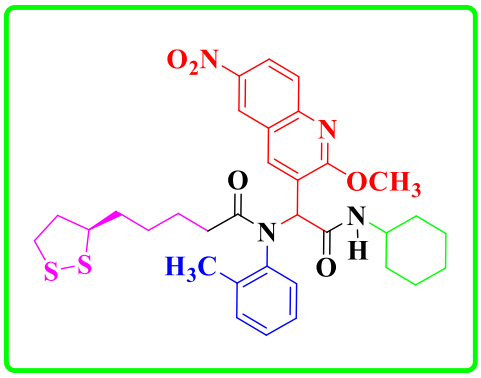

16.26, 16.20. Elemental Analysis: Anal. Calc. for $C_{33}H_{40}N_4O_5S_2$: C, 62.24; H, 6.33; N, 8.80; %. Found: C, 62.26; H, 6.34; N, 8.82; %.

3.13. *N*-(2-(cyclohexylamino)-1-(2-methoxy-6-nitroquinolin-3-yl)-2-oxoethyl)-5-((R)-1,2-dithiolan-3-yl)-*N*-(2-methoxyphenyl)pentanamide (52)

Brown solid, m.p = 140-142℃; IR ν_{max} (cm^{-1}): 1676 C=N, 1366 C-N, 2970 CH, 1495 C=C, 1691 C=O, 734 C-S, 636 S-S, 3457 NH. ^{1}H-NMR: (400 MHz, CD_3OD-d_4) δ (ppm) 8.39 (1H, s, NH), 8.24 (1H, t, *J*=2.84 Hz, ArH), 8.22 (1H, t, *J*=2.76 Hz, ArH), 7.99-7.80 (1H, t, *J*=3.28 Hz, ArH), 7.97 (1H, t, *J*=2.0 Hz, ArH), 7.83 (1H, t, *J*=3.84 Hz, ArH), 7.81 (1H, t, *J*=2.0 Hz, ArH), 6.64 (1H, t, *J*=3.24 Hz, ArH), 6.62 (1H, t, *J*=2.28 Hz, ArH), 6.12 (1H, s, CH), 4.24 (3H, s, OCH_3), 4.11 (3H, s, OCH_3), 3.90 (2H, d, *J*=3.20 Hz, CH_2), 3.59-3.56 (1H, m, *J*=6.0 Hz, CH), 3.33-3.21 (2H, m, *J*=3.16 Hz, CH_2), 3.20-3.18 (2H, m, *J*=5.4 Hz, CH_2), 3.16-3.09 (2H, m, *J*=13.0 Hz, CH_2), 2.49-2.44 (1H, m, *J*=9.0 Hz, CH), 2.38-2.35 (2H, t, *J*=14.52 Hz, CH_2), 2.31 (2H, t, *J*=7.32 Hz, CH_2), 1.94-1.87 (2H, m, *J*=6.88 Hz, CH_2), 1.70-1.68 (2H, m, *J*=7.16 Hz, CH_2), 1.68-1.66 (2H, m, *J*=5.64 Hz, CH_2), 1.66-1.64 (2H, m, *J*=4.56 Hz, CH_2), 1.62 (2H, m, *J*=2.56 Hz, CH_2), 1.29 (2H, d, *J*=1.36 Hz, CH_2). ^{13}C-NMR: (100 MHz, CD_3OD-d_4) δ (ppm) 177.66, 164.27, 161.93, 161.90, 156.82, 150.46, 145.07, 144.91, 138.32, 127.86, 127.34, 126.53, 125.96, 125.91, 122.15, 121.59, 120.98, 120.56, 113.64, 111.76, 57.56, 56.33, 41.31, 37.78, 37.33, 35.79, 34.68, 34.56, 33.69, 30.77, 29.88, 26.14, 25.88. Elemental Analysis: Anal. Calc. for $C_{33}H_{40}N_4O_6S_2$: C, 60.72; H, 6.18; N, 8.58; %. Found: C, 60.74; H, 6.19; N, 8.56; %.

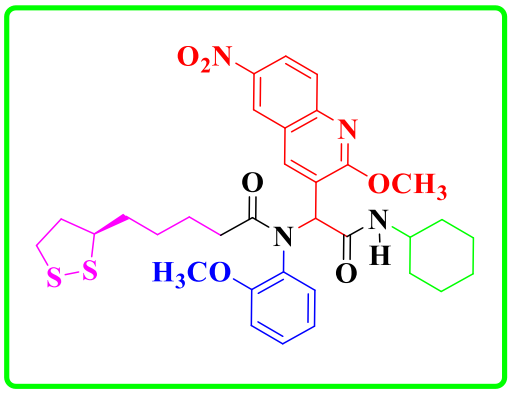

3.14. *N*-(2-(cyclohexylamino)-2-oxo-1-(2-oxo-1,2-dihydroquinolin-3-yl)ethyl)-5-((R)-1,2-dithiolan-3-yl)-*N*-(2-methoxyphenyl)pentanamide (55)

Yellow solid, m.p = 136-138℃; IR ν_{max} (cm^{-1}): 1604 C=N, 1365 C-N, 2970 CH, 1474 C=C, 1625 C=O, 746 C-S, 663 S-S, 3457 NH. ^{1}H-NMR: (400 MHz, CD_3OD-d_4) δ (ppm) 8.10 (1H, s, Ar-H), 8.02 (1H, s, Ar-H), 7.96 (1H, s, NH), 7.69 (2H, dd, *J*= 8Hz, Ar-H), 7.57 (1H, td, *J*=8.4 Hz, Ar-H), 7.38 (1H, d, *J*= 8.24 Hz, Ar-H), 7.28 (1H, td, *J*=7.16 Hz, Ar-H), 6.81 (1H, d, *J*=1.6 Hz, Ar-H), 6.75 (1H, t, *J*= 2.28 Hz, Ar-H), 6.73 (1H, d, *J*=1.52

Hz, Ar-H), 3.75 (3H, s, OCH_3), 3.42 (1H, s, CH), 3.33-3.31 (1H, m, *J*=1.6 Hz, CH), 2.32-2.28 (1H, m, *J*=7.4 Hz, CH), 1.76 (2H, t, *J*=3.64 Hz, CH_2), 1.74-1.72 (2H, m, *J*=2.28 Hz, CH_2), 1.39-1.38 (2H, m, *J*=3.2 Hz, CH_2), 1.37-1.36 (2H, m, *J*=7.56 Hz, CH_2), 1.35 (2H, t, *J*=2.24 Hz, CH_2), 1.32-1.31 (2H, m, *J*=2.76 Hz, CH_2), 1.30-1.28 (2H, m, *J*=12.04 Hz, CH_2), 1.27-1.26 (2H, m, *J*=10.72 Hz, CH_2), 1.25 (2H, d, *J*=1.32 Hz, CH_2), 0.92-0.90 (2H, m, *J*=4.72 Hz, CH_2), 0.89-0.88 (2H, m, *J*=4Hz, CH_2). ^{13}C-NMR: (100 MHz, $CDCl_3$) δ (ppm) 144.12, 143.98, 138.22, 138.18, 136.07, 133.22, 131.41, 131.37, 129.60, 129.57, 127.49, 127.44, 126.83, 116.56, 114.68, 77.35, 7724, 77.03, 76.71, 63.75, 63.68, 63.50, 63.43, 55.98, 54.47, 21.14, 16.40, 16.34, 16.28. Elemental Analysis: Anal. Calc. for $C_{32}H_{39}N_3O_4S_2$: C, 64.73; H, 6.62; N, 7.08; %. Found: C, 64.75; H, 6.64; N, 7.06; %.

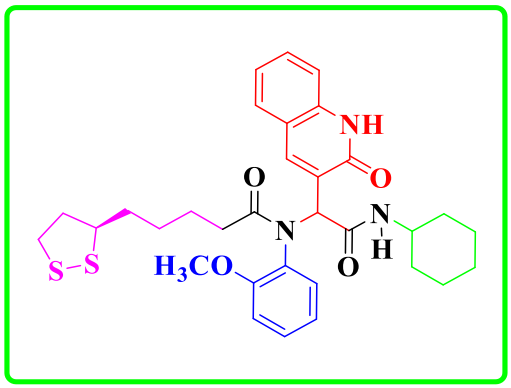

3.1. *N*-(2-(cyclohexylamino)-1-(2-methoxyquinolin-3-yl)-2-oxoethyl)-5-((R)-1,2-dithiolan-3-yl)-*N*-phenylpentanamide (40)

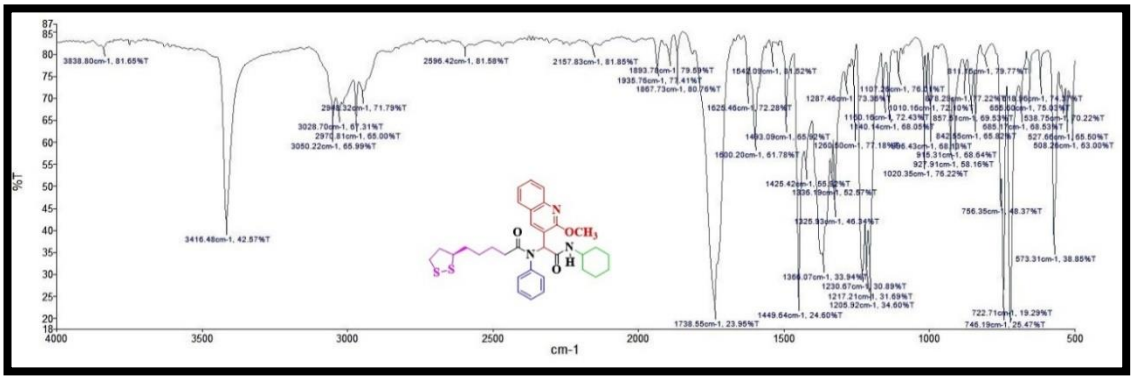

Fig. 3.1. IR spectrum of **40**

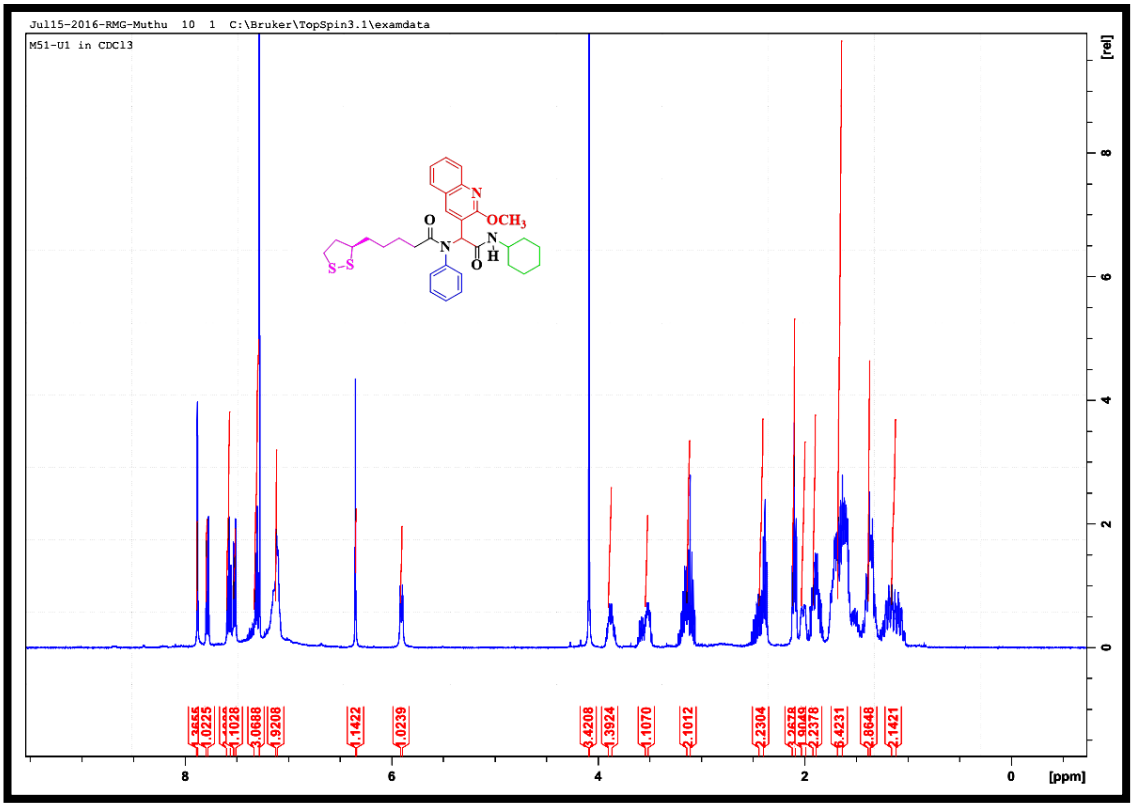

Fig. 3.2. ^{1}H-NMR spectrum for **40**

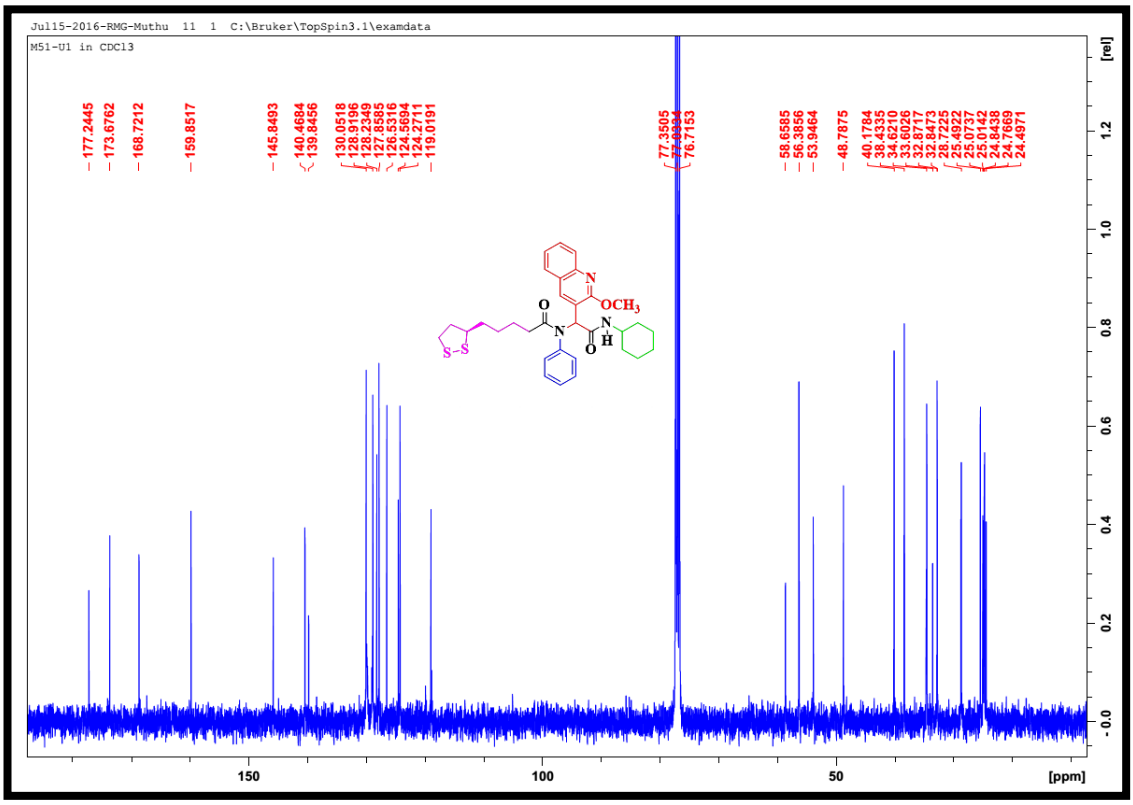

Fig. 3.3. ^{13}C-NMR spectrum for **40**

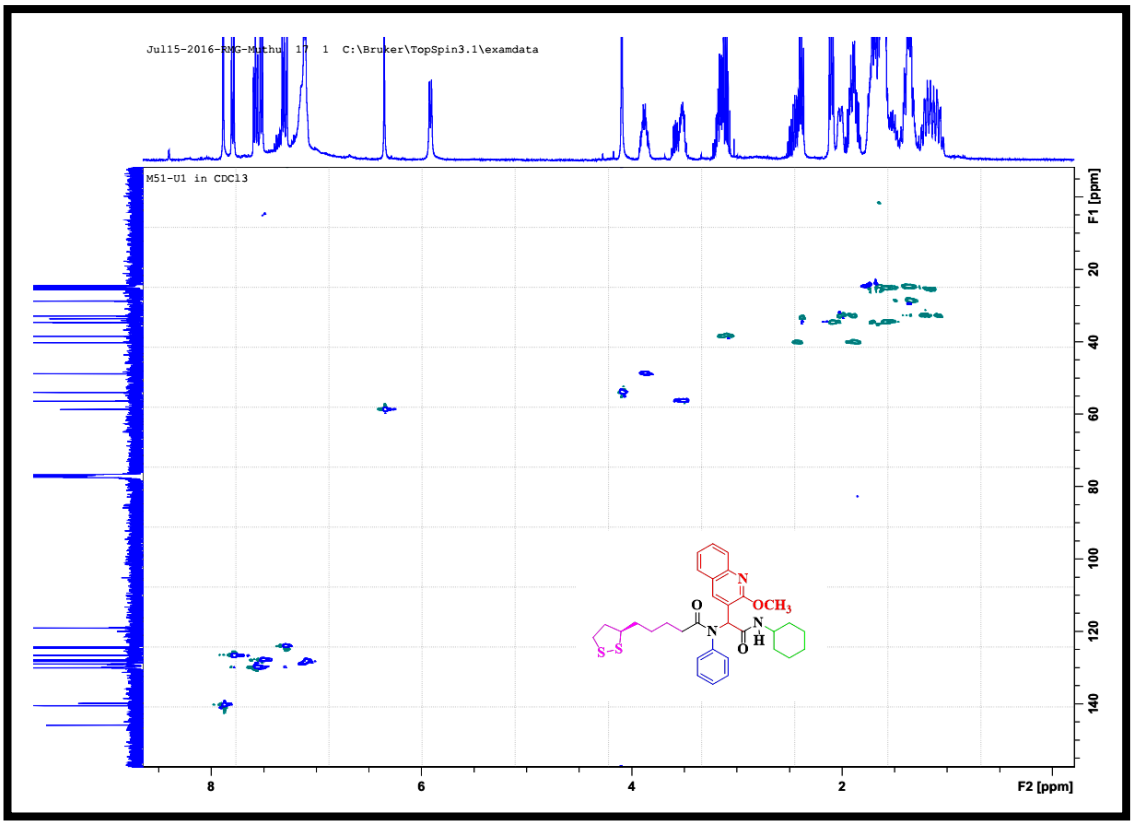

Fig. 3.4. HSQC spectrum for **40**

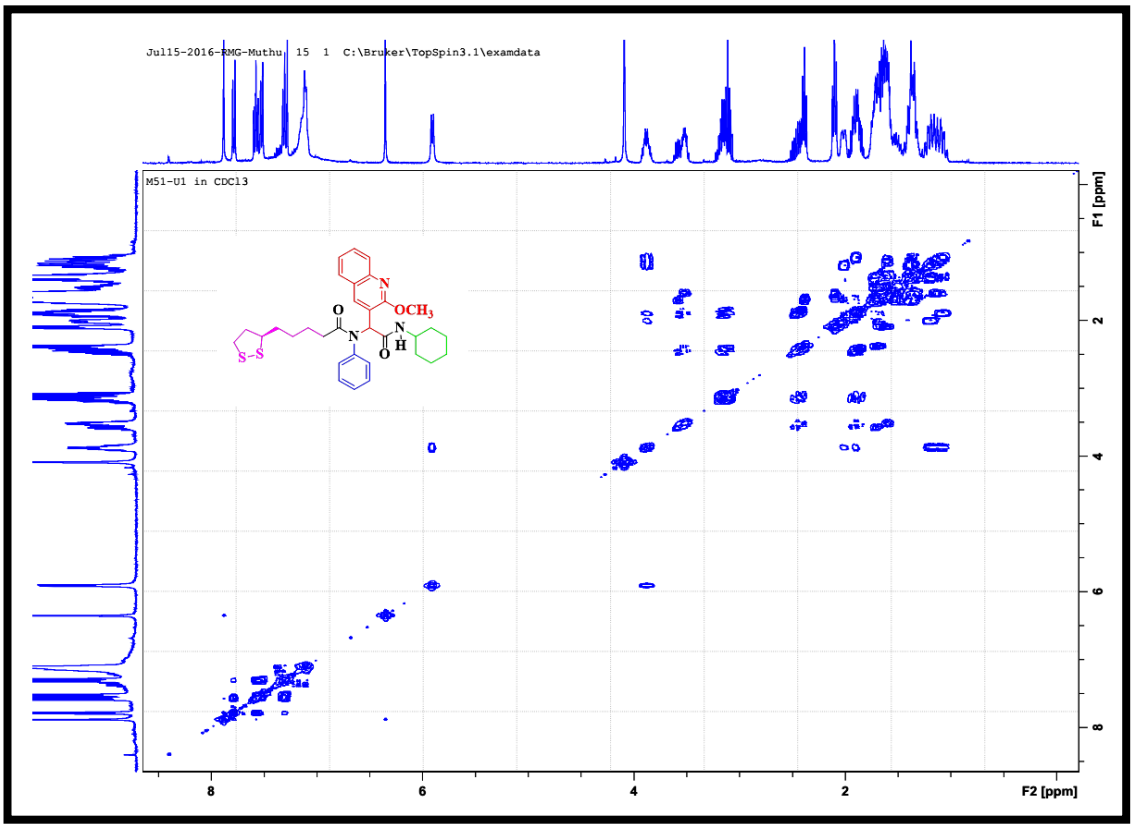

Fig. 3.5. COSY spectrum for **40**

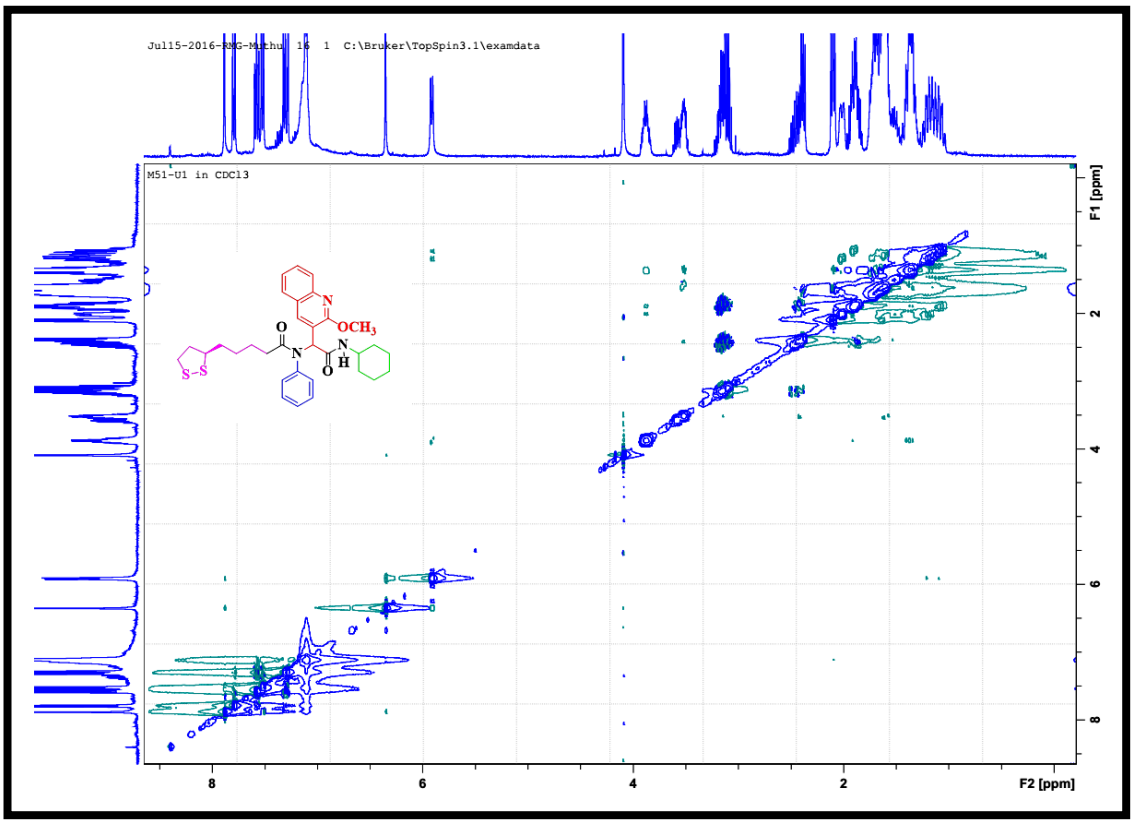

Fig. 3.6. NOESY spectrum for **40**

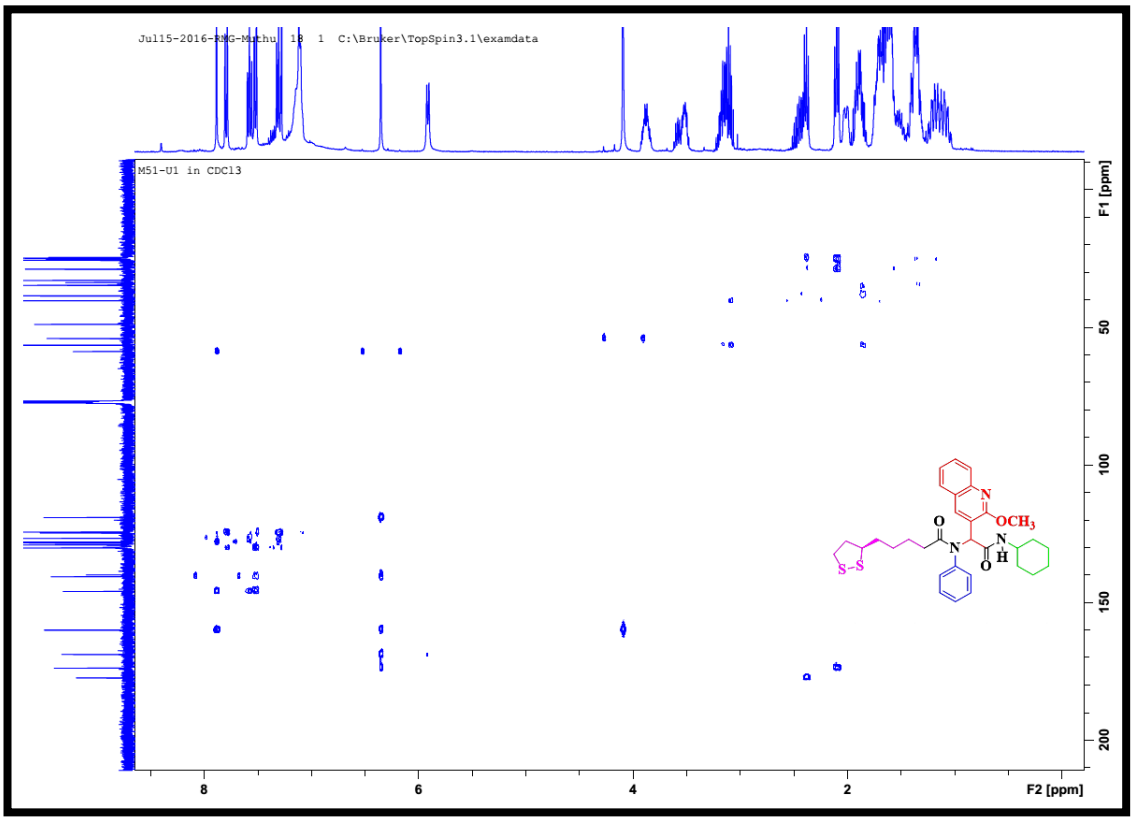

Fig. 3.7. HMBC spectrum for **40**

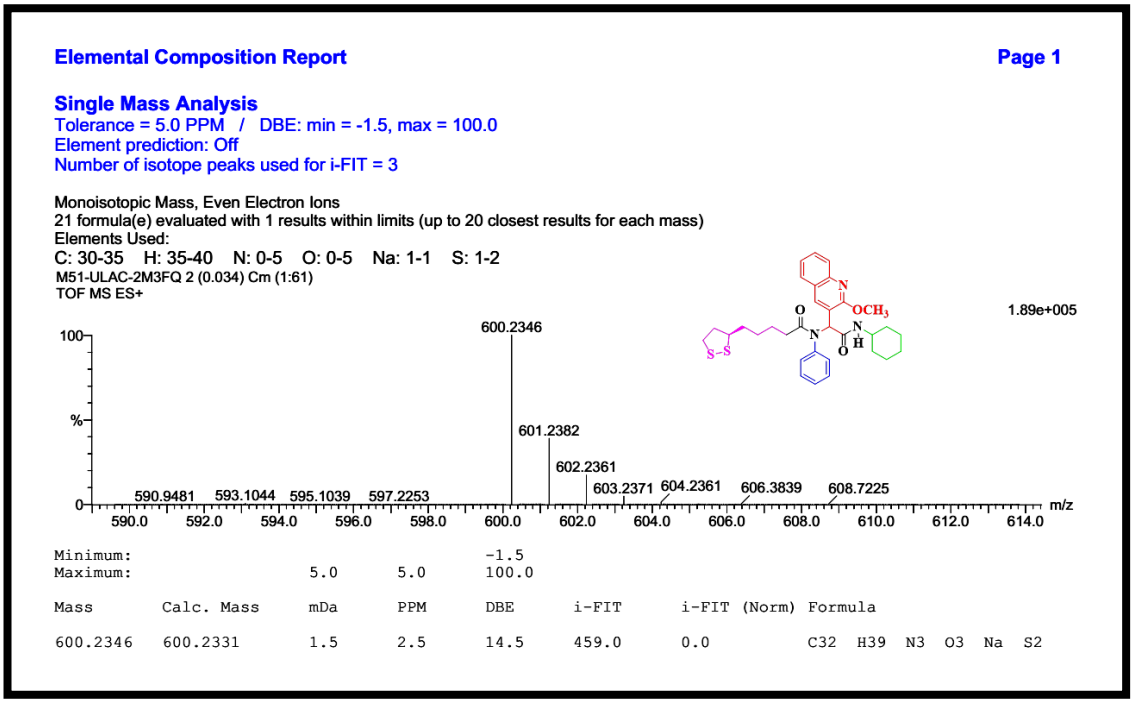

Fig. 3.8. Mass spectrum for **40**

3.2. *N*-(2-(cyclohexylamino)-1-(2-methoxyquinolin-3-yl)-2-oxoethyl)-5-((R)-1,2-dithiolan-3-yl)-*N*-(o-tolyl)pentanamide (41)

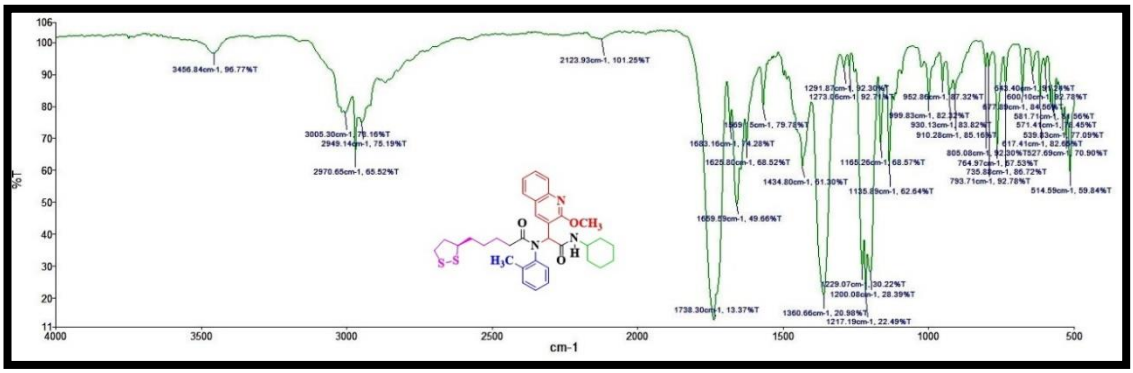

Fig. 3.9. IR spectrum of **41**

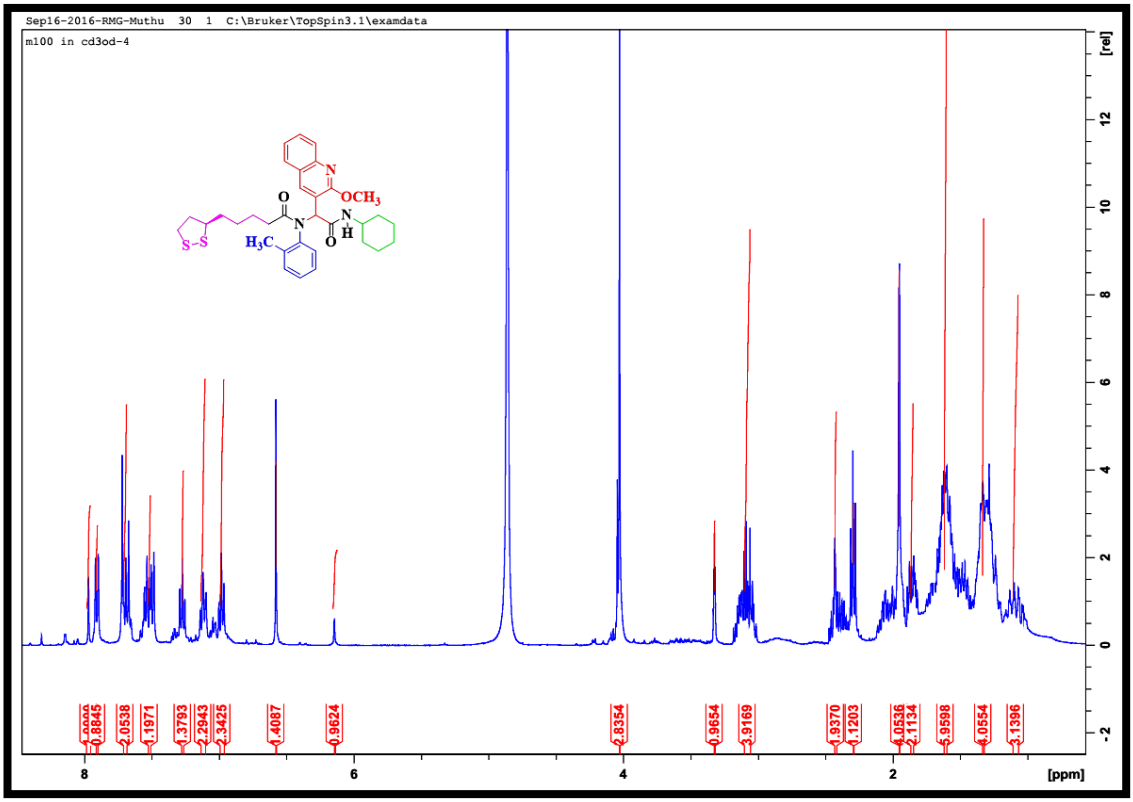

Fig. 3.10. ^{1}H-NMR spectrum for **41**

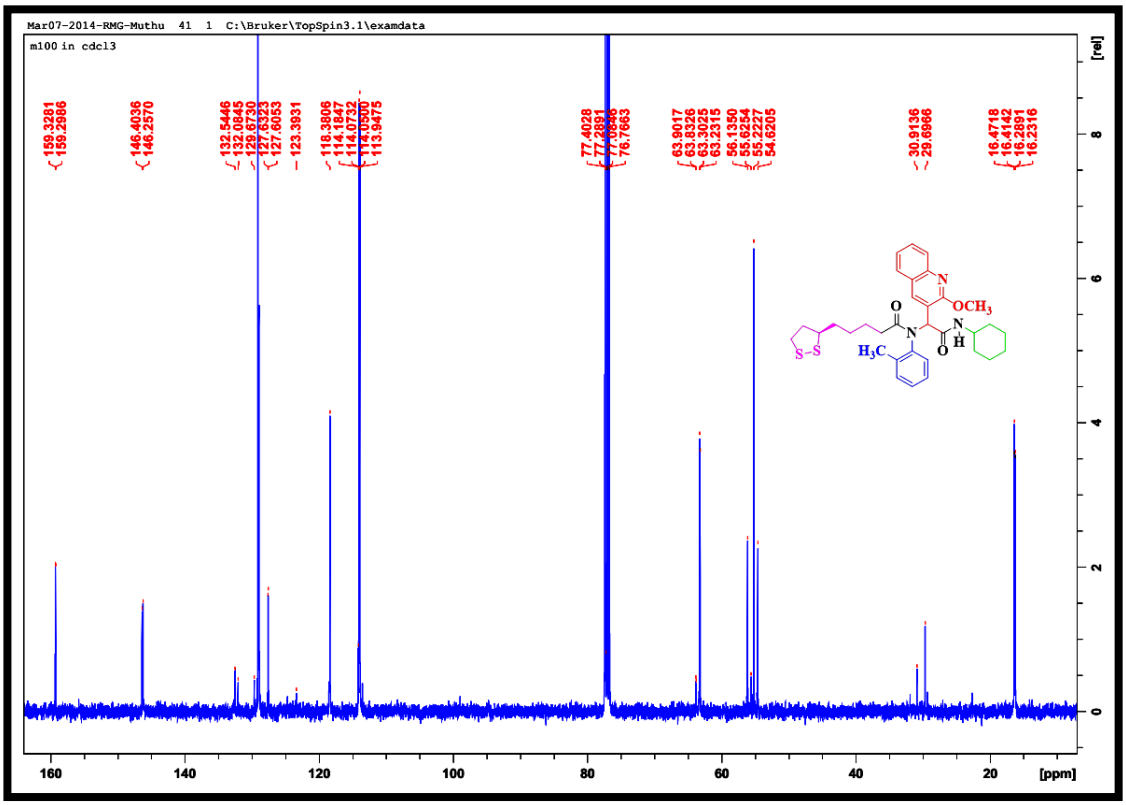

Fig. 3.11. ^{13}C-NMR spectrum for **41**

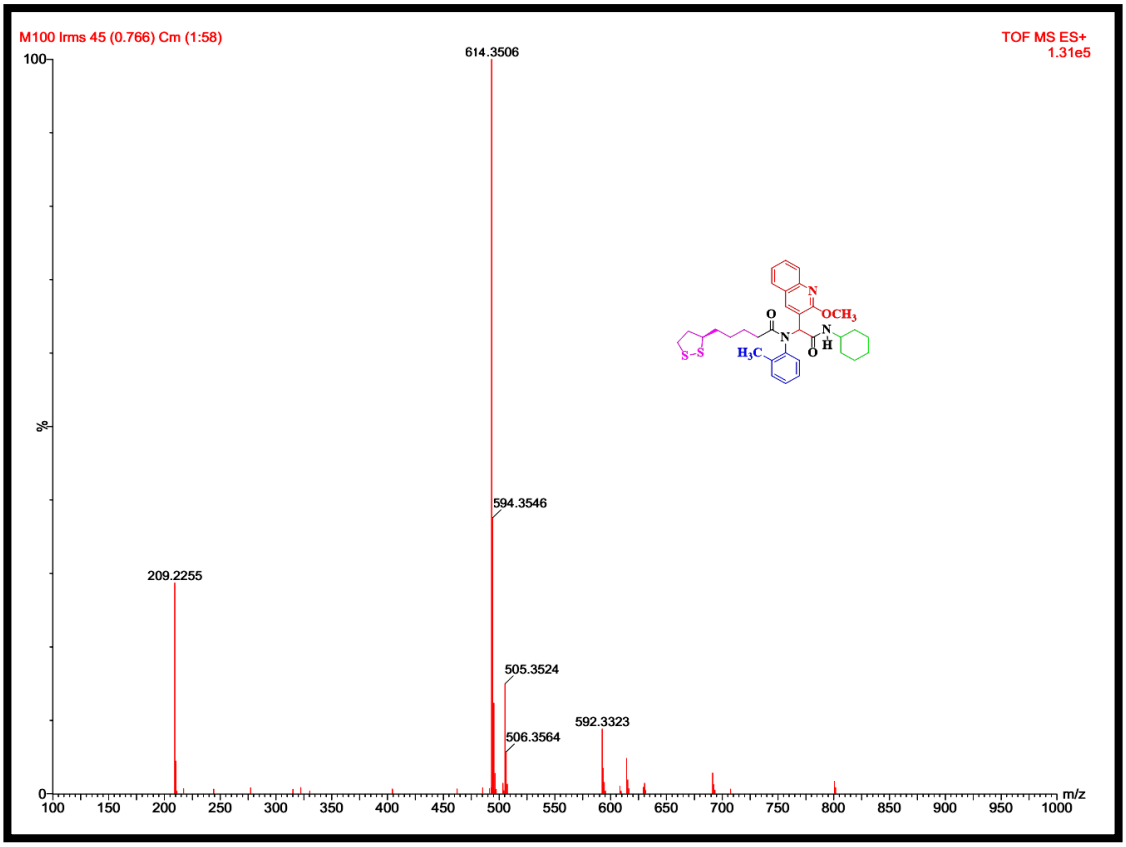

Fig. 3.12. Mass spectrum of **41**

3.3. *N*-(2-(cyclohexylamino)-1-(2-methoxyquinolin-3-yl)-2-oxoethyl)-5-((R)-1,2-dithiolan-3-yl)-*N*-(m-tolyl)pentanamide (42)

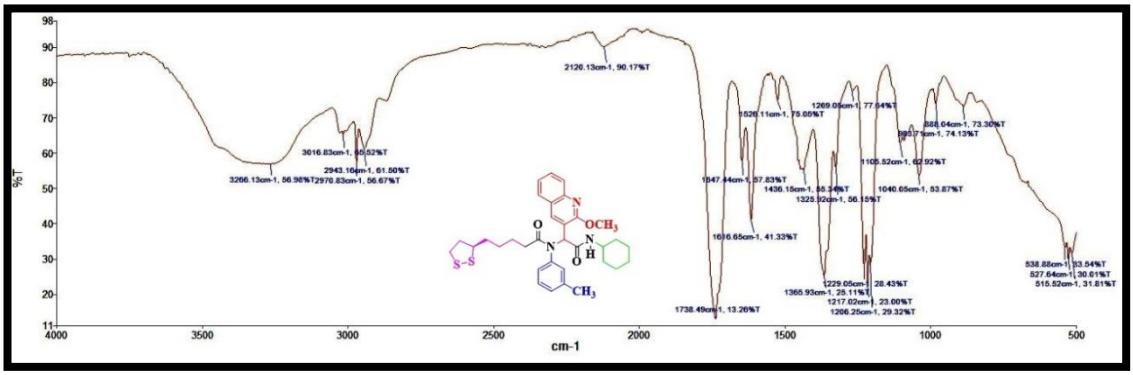

Fig. 3.13. IR spectrum of **42**

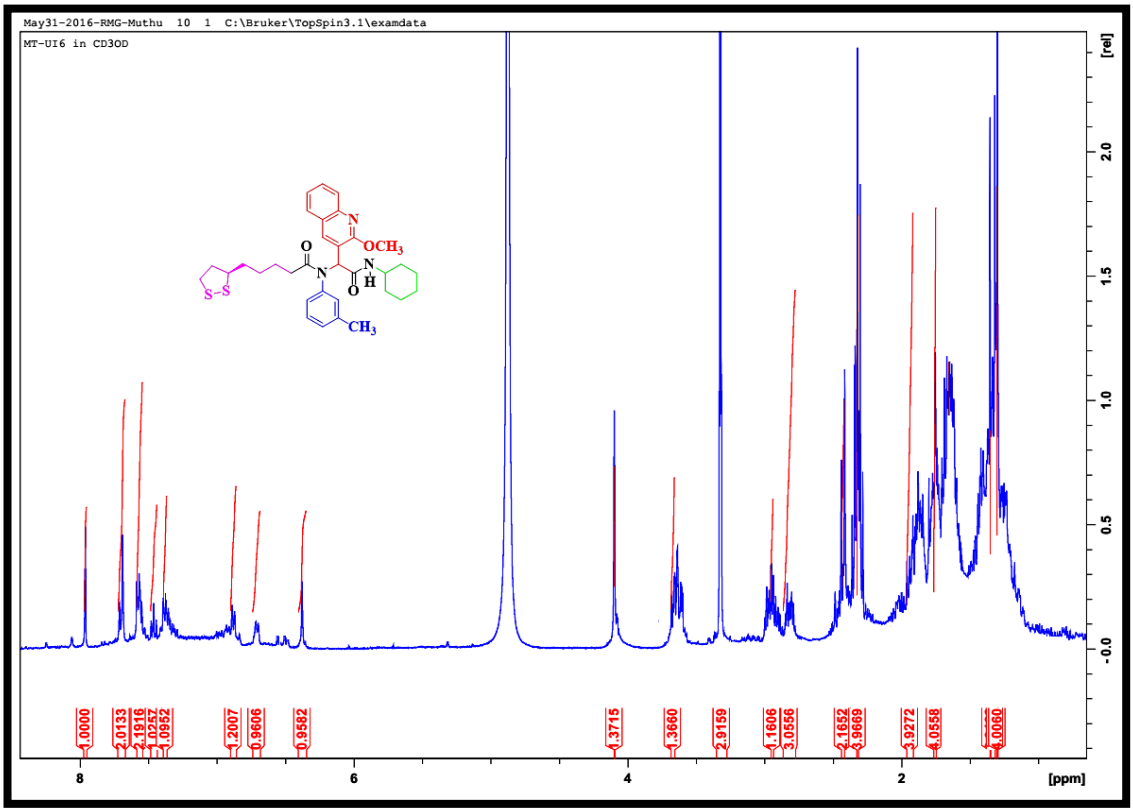

Fig. 3.14. ^{1}H-NMR spectrum for **42**

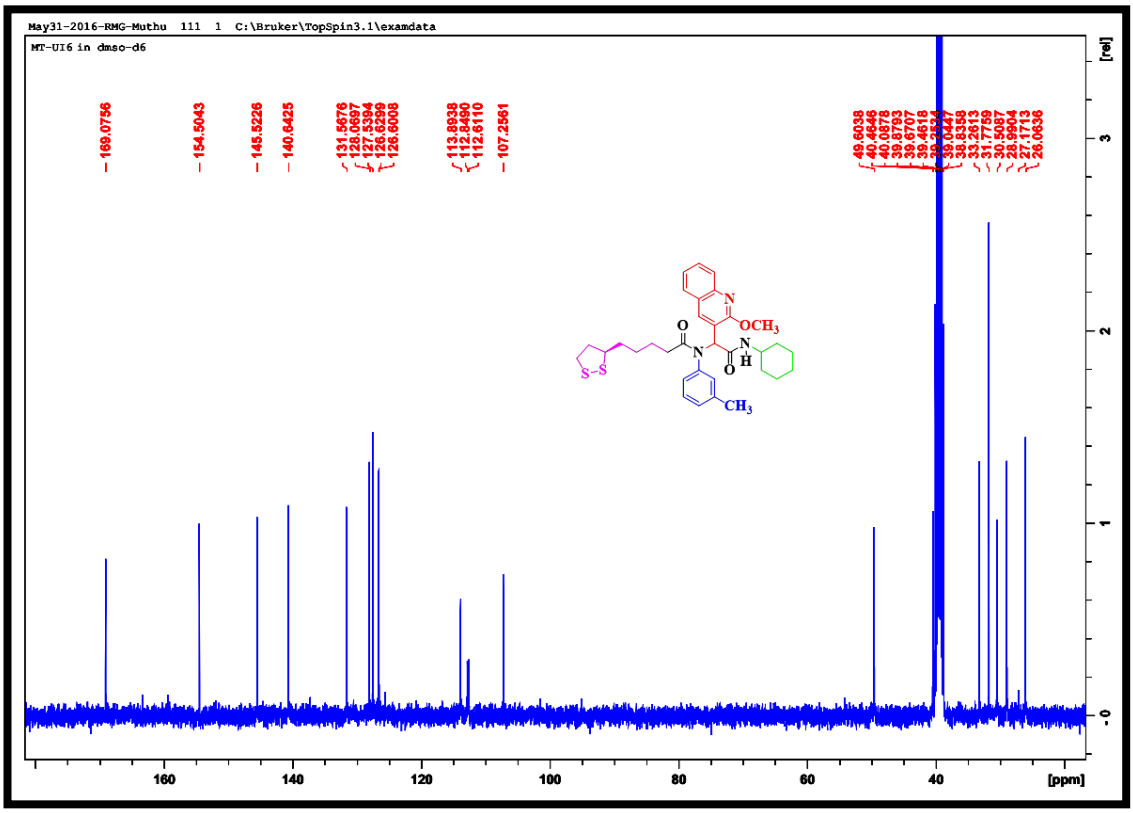

Fig. 3.15. ^{13}C-NMR spectrum for **42**

3.4. *N*-(2-(cyclohexylamino)-1-(2-methoxyquinolin-3-yl)-2-oxoethyl)-5-((R)-1,2-dithiolan-3-yl)-*N*-(2-methoxyphenyl)pentanamide (43)

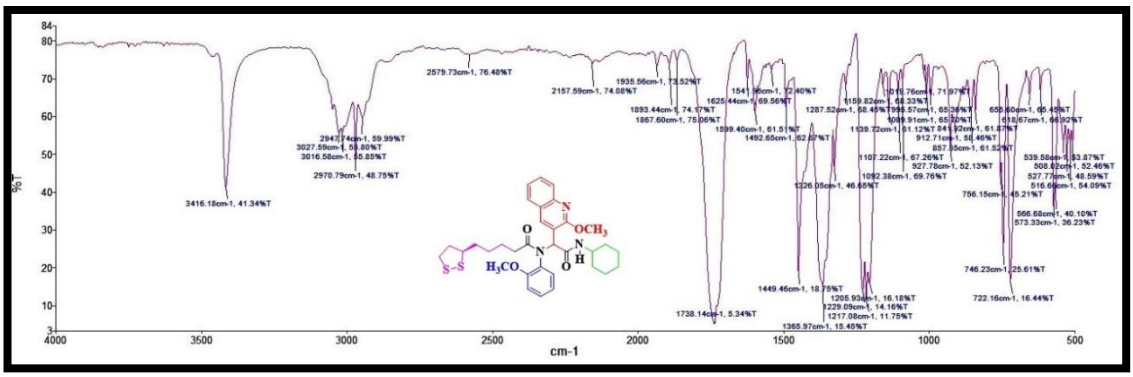

Fig. 3.16. IR spectrum of **43**

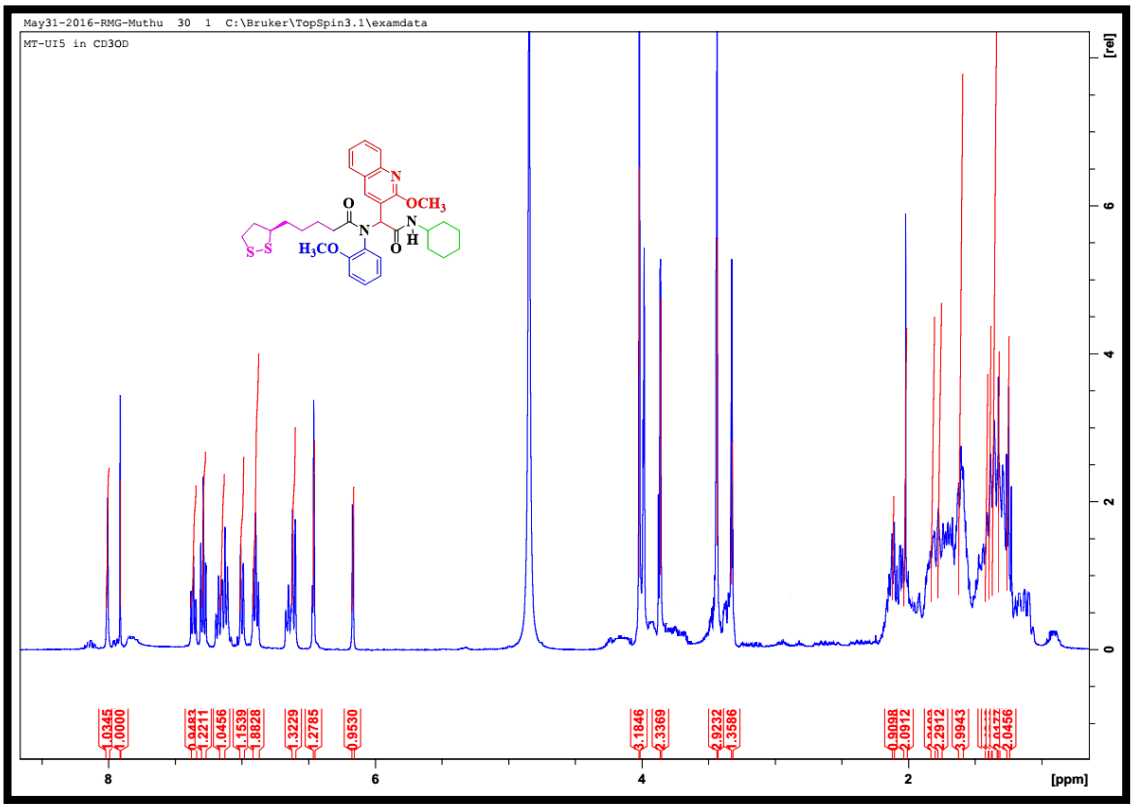

Fig. 3.17. ^{1}H-NMR spectrum for **43**

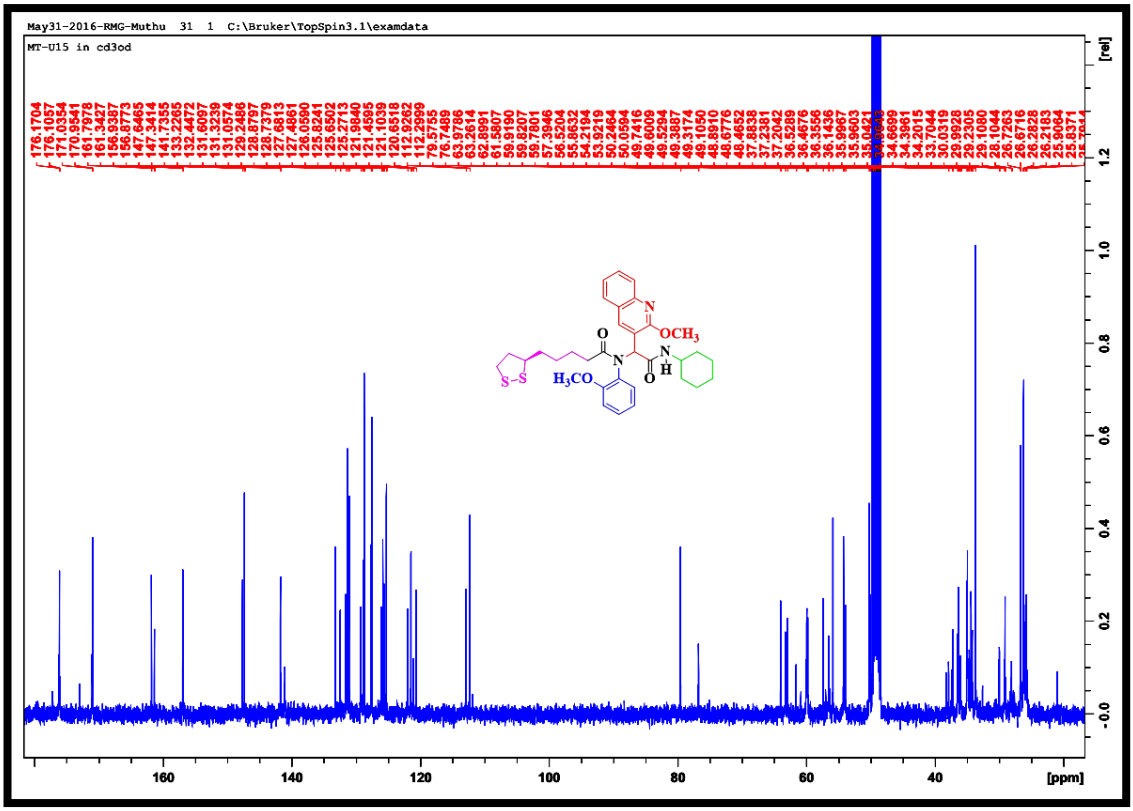

Fig. 3.18. ^{13}C-NMR spectrum for **43**

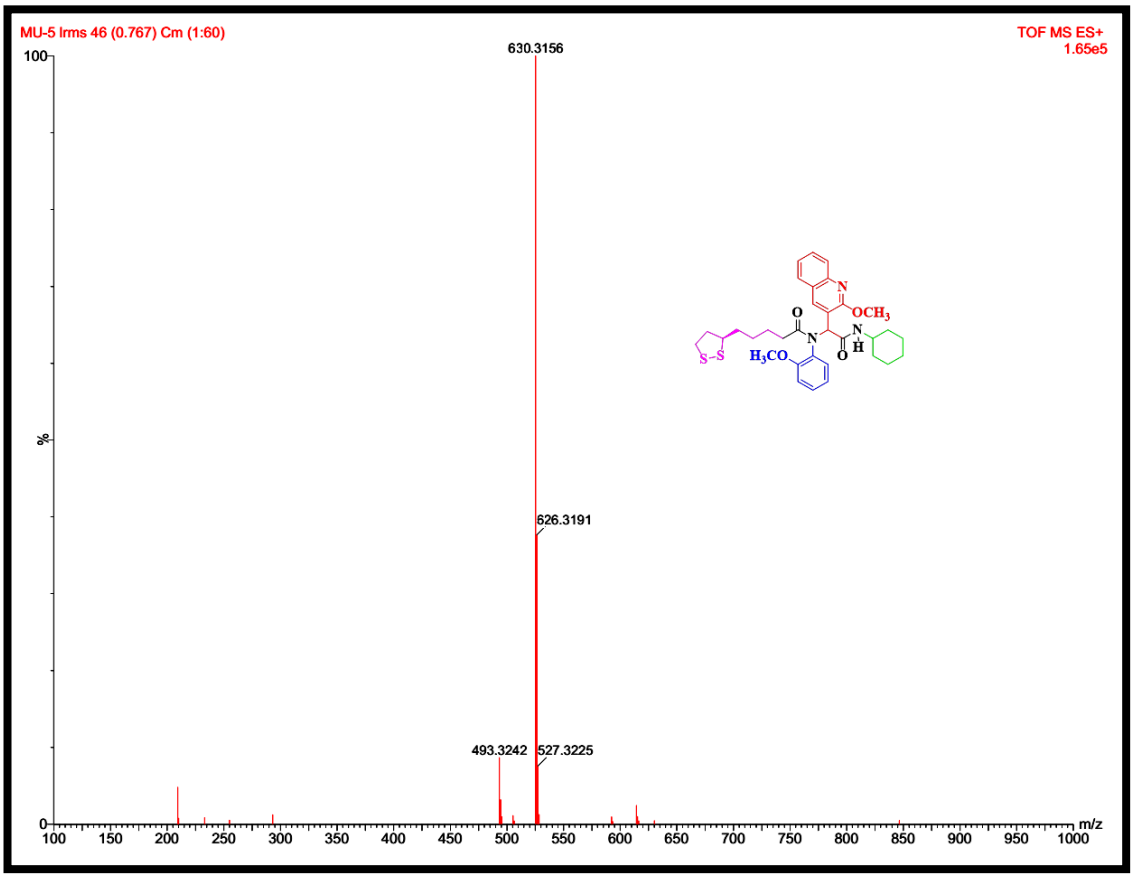

Fig. 3.19. Mass spectrum of **43**

3.5. *N*-(2-(cyclohexylamino)-1-(2-methoxy-6-methylquinolin-3-yl)-2-oxoethyl)-5-((R)-1,2-dithiolan-3-yl)-*N*-phenylpentanamide (44)

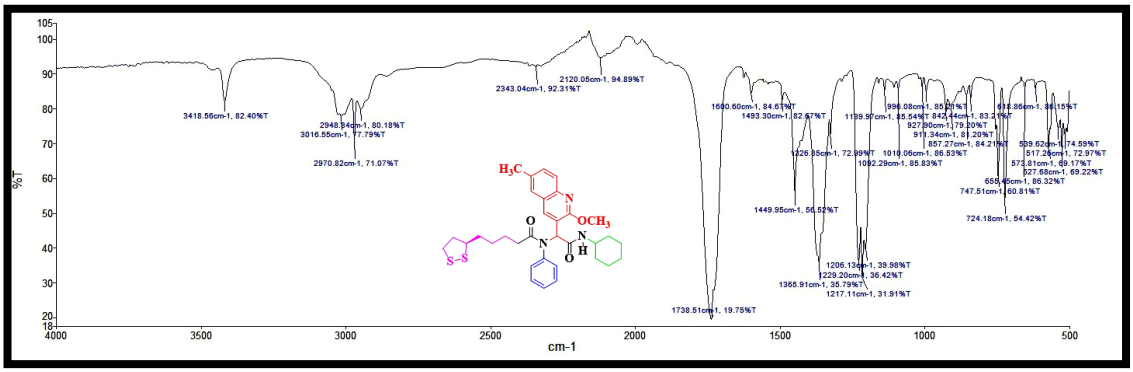

Fig. 3.20. IR spectrum of **44**

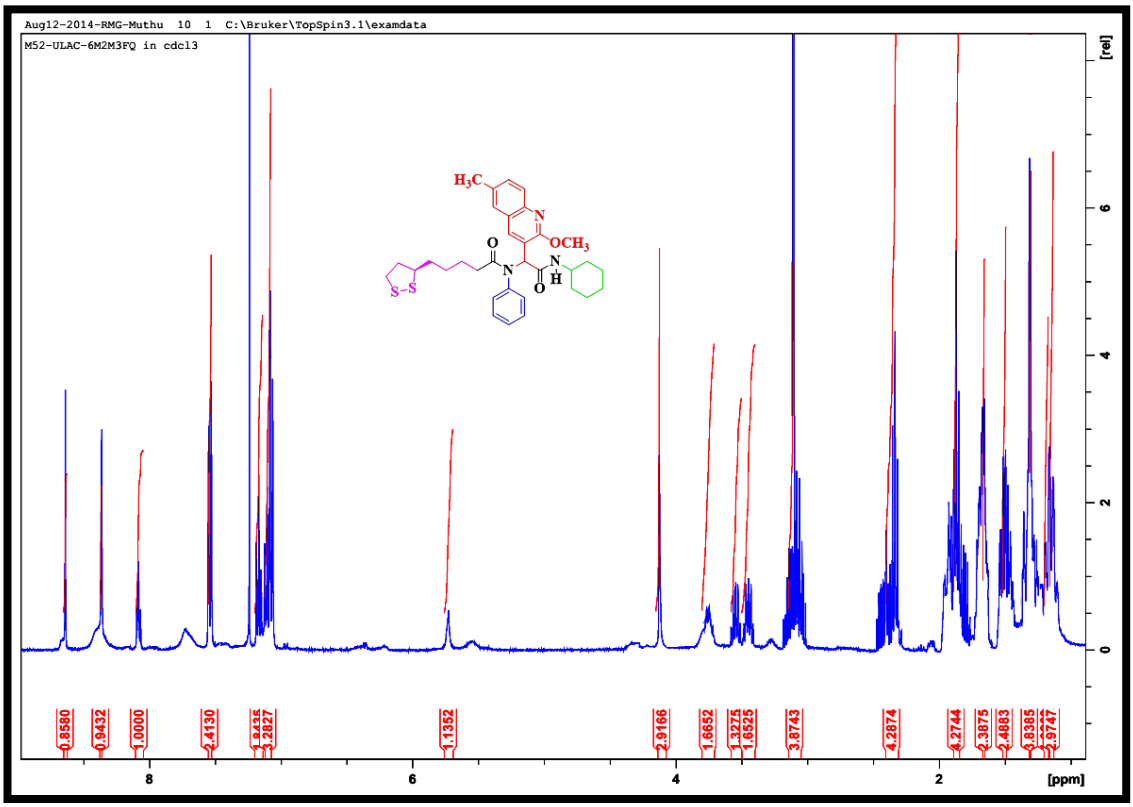

Fig. 3.21. ^{1}H-NMR spectrum for **44**

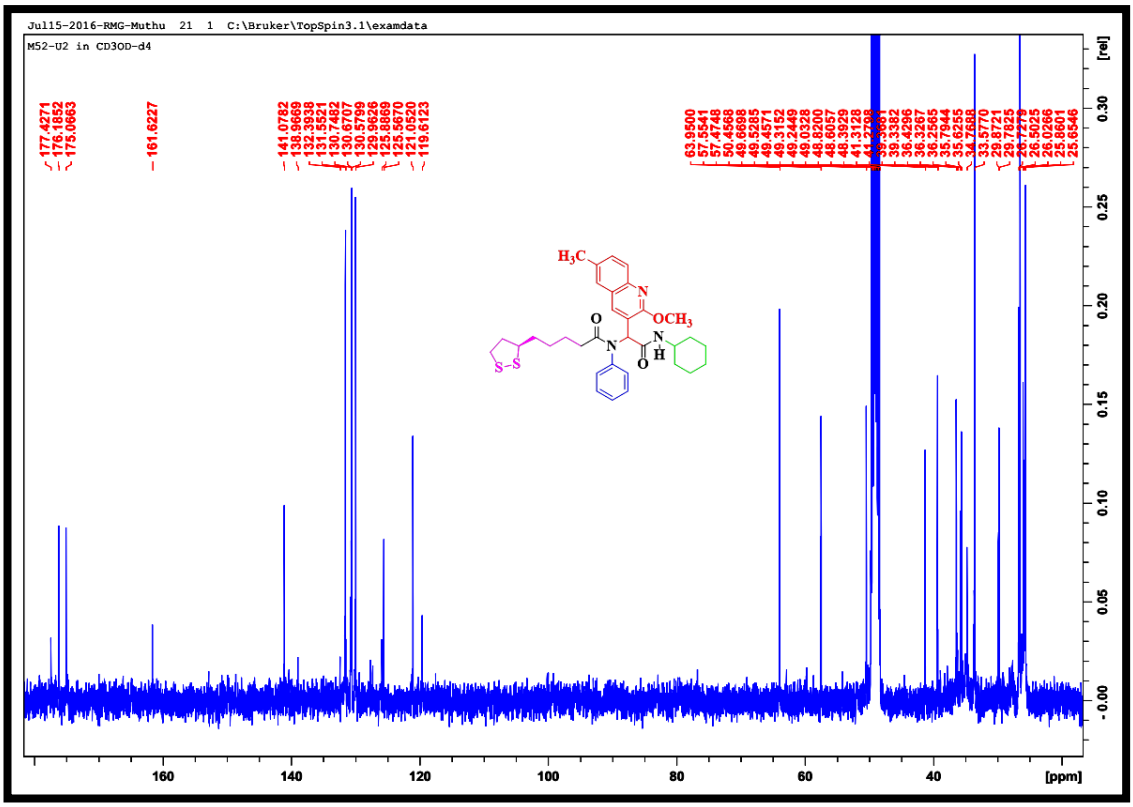

Fig. 3.22. ^{13}C-NMR spectrum for **44**

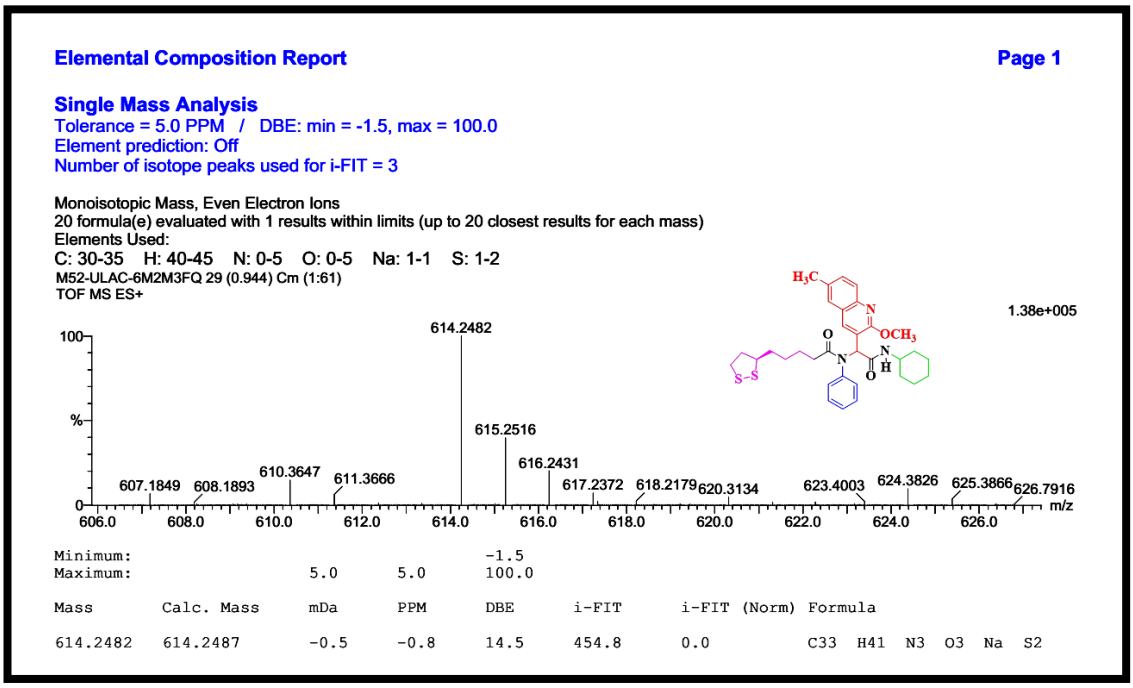

Fig. 3.23. Mass spectrum for **44**

3.6. *N*-(2-(cyclohexylamino)-1-(2-methoxy-6-methylquinolin-3-yl)-2-oxoethyl)-5-((R)-1,2-dithiolan-3-yl)-*N*-(m-tolyl)pentanamide (45)

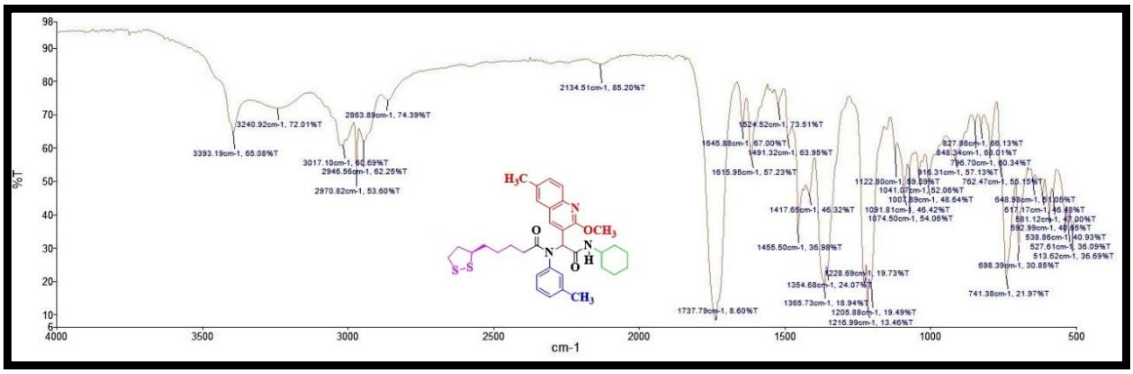

Fig. 3.24. IR spectrum of **45**

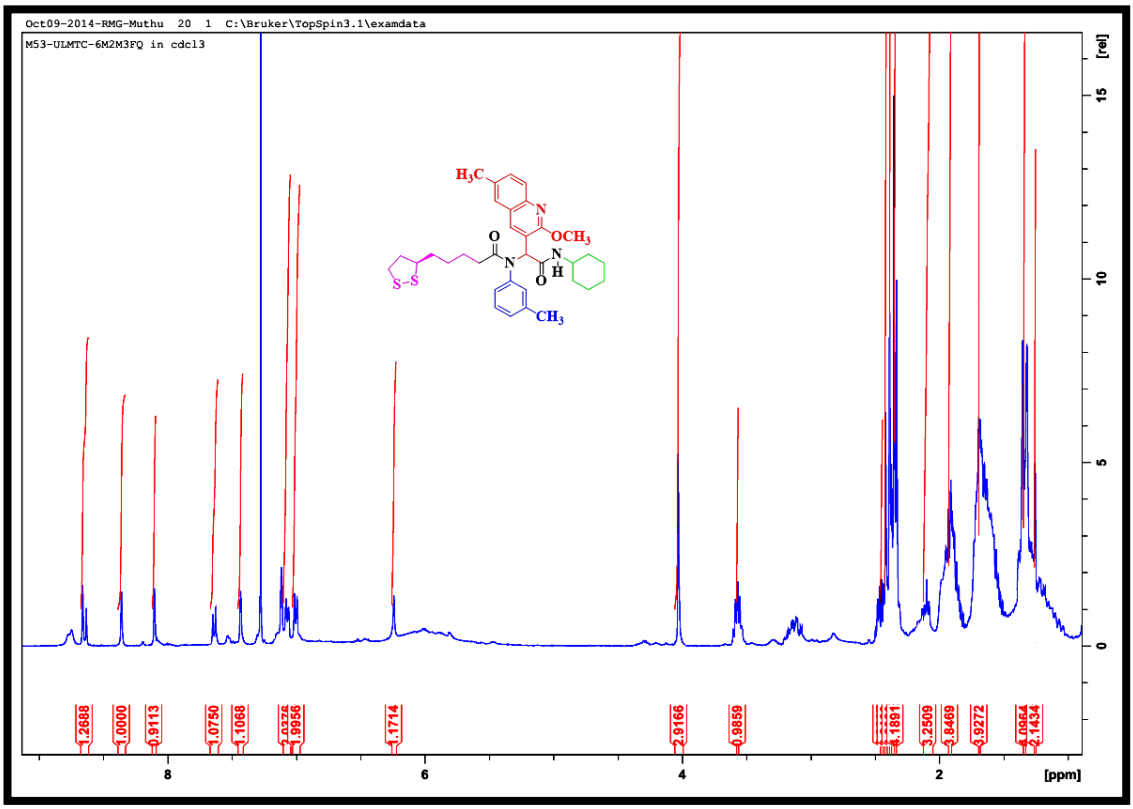

Fig. 3.25. ^{1}H-NMR spectrum for **45**

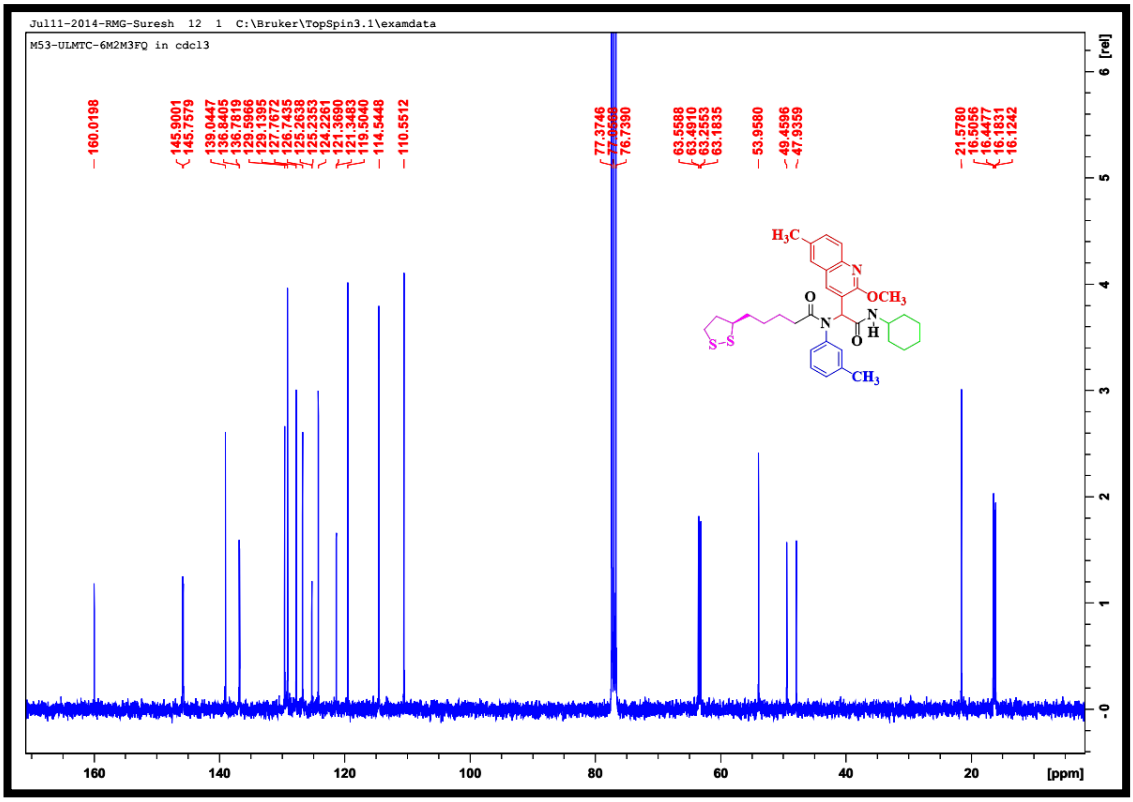

Fig. 3.26. ^{13}C-NMR spectrum for **45**

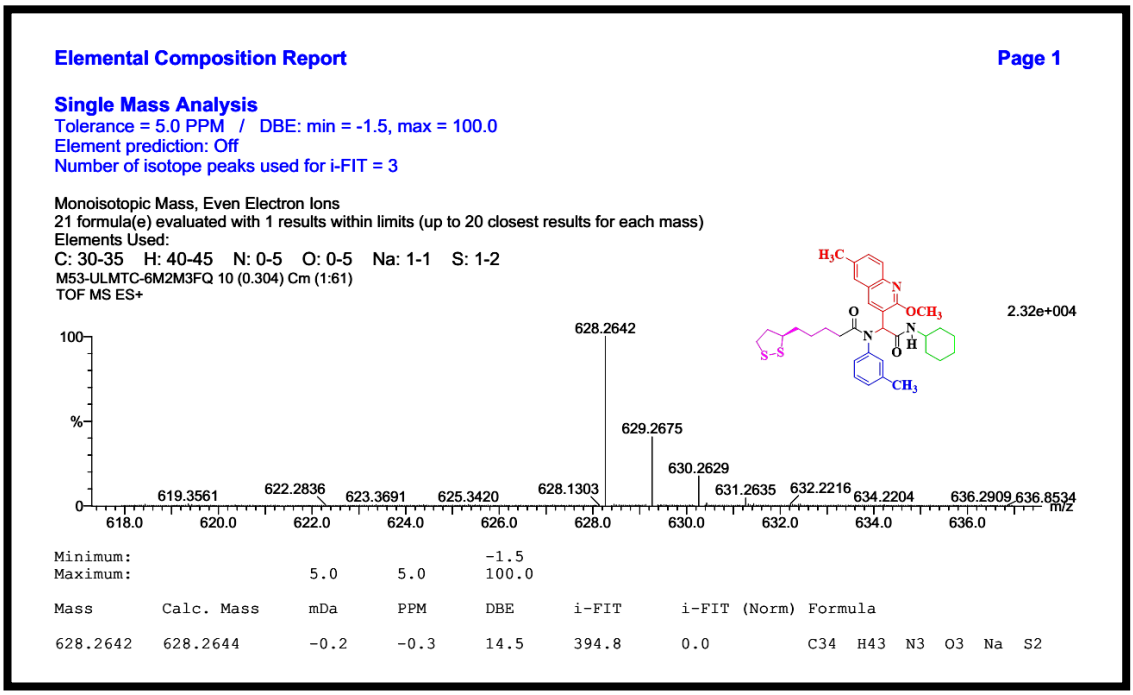

Fig. 3.27. Mass spectrum for **45**

3.7. *N*-(2-(cyclohexylamino)-1-(2-methoxy-6-methylquinolin-3-yl)-2-oxoethyl)-5-((R)-1,2-dithiolan-3-yl)-*N*-(2-methoxyphenyl)pentanamide (46)

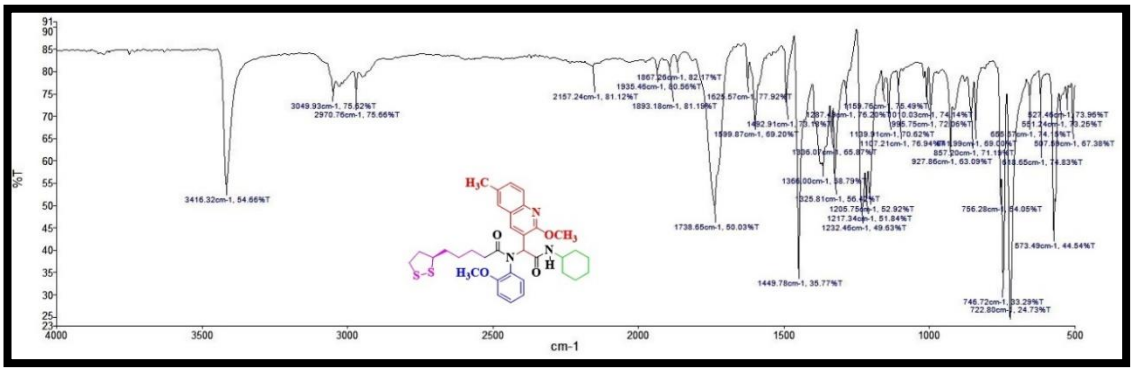

Fig. 3.28. IR spectrum of **46**

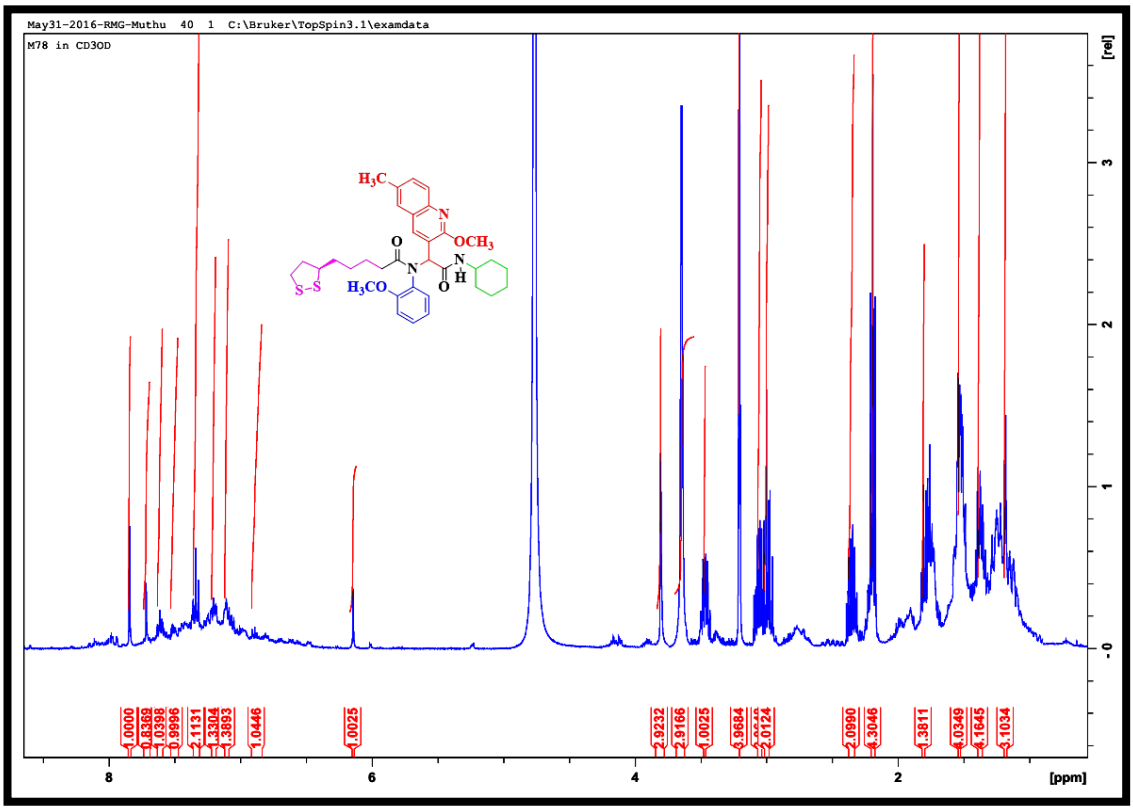

Fig. 3.29. ^{1}H-NMR spectrum for **46**

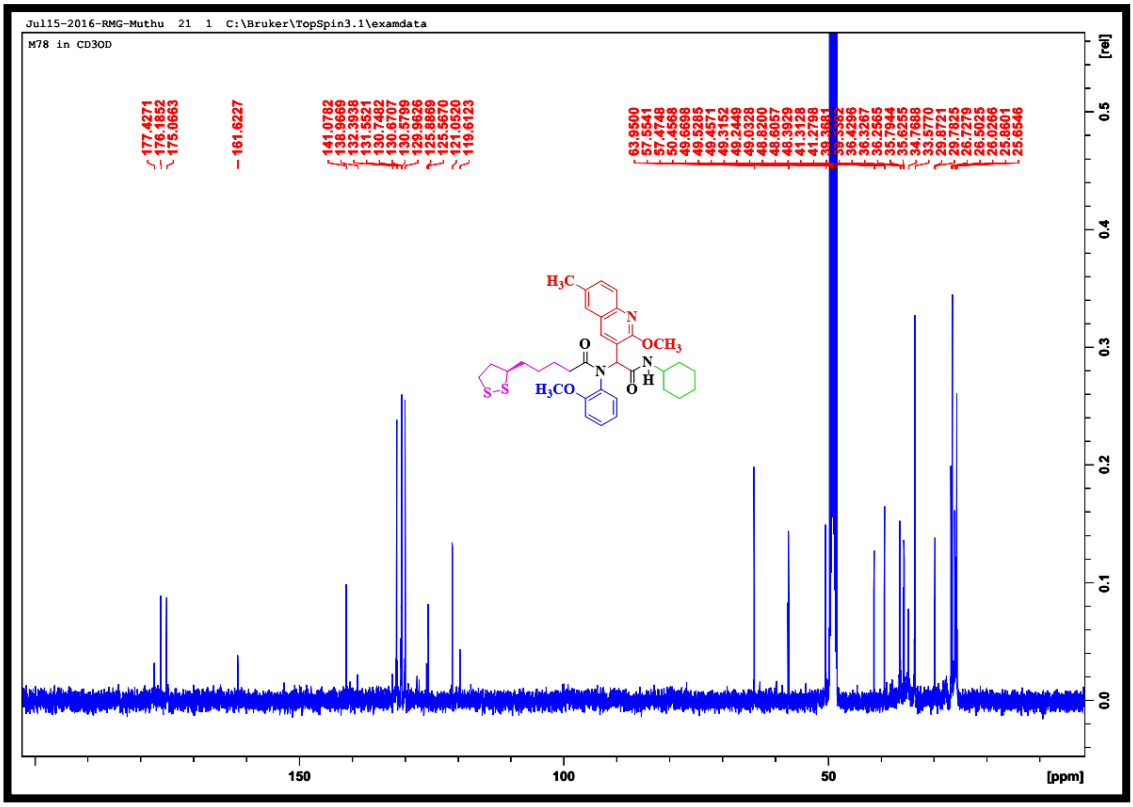

Fig. 3.30. ^{13}C-NMR spectrum for **46**

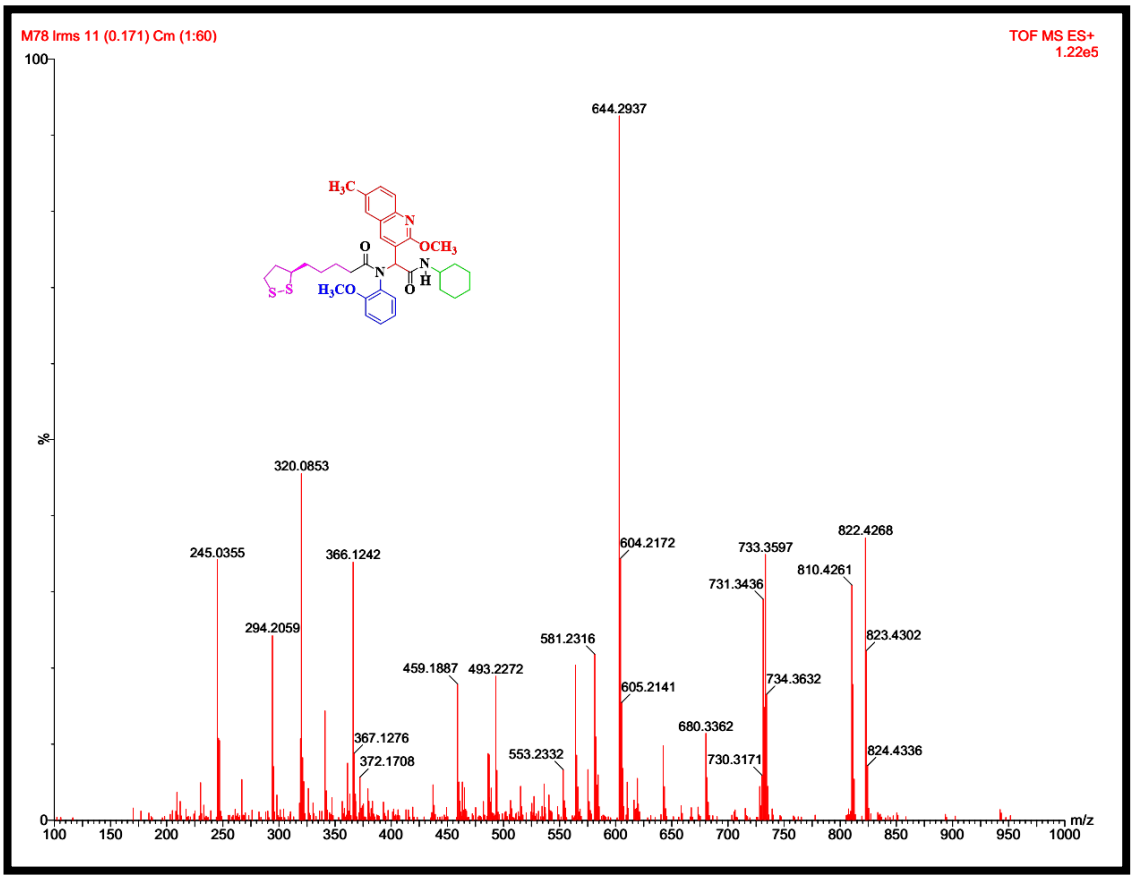

Fig. 3.31. Mass spectrum of **46**

3.8. *N*-(2-(cyclohexylamino)-1-(2-methoxy-6-nitroquinolin-3-yl)-2-oxoethyl)-5-((R)-1,2-dithiolan-3-yl)-*N*-phenylpentanamide (47)

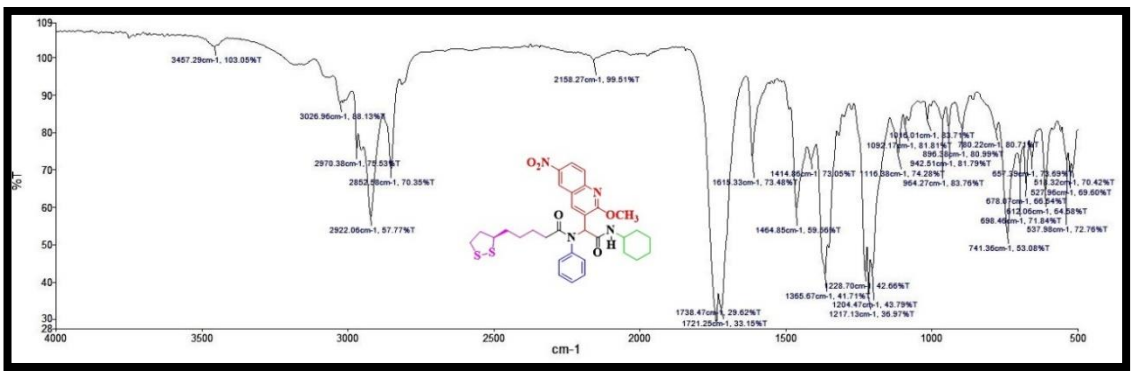

Fig. 3.32. IR spectrum of **47**

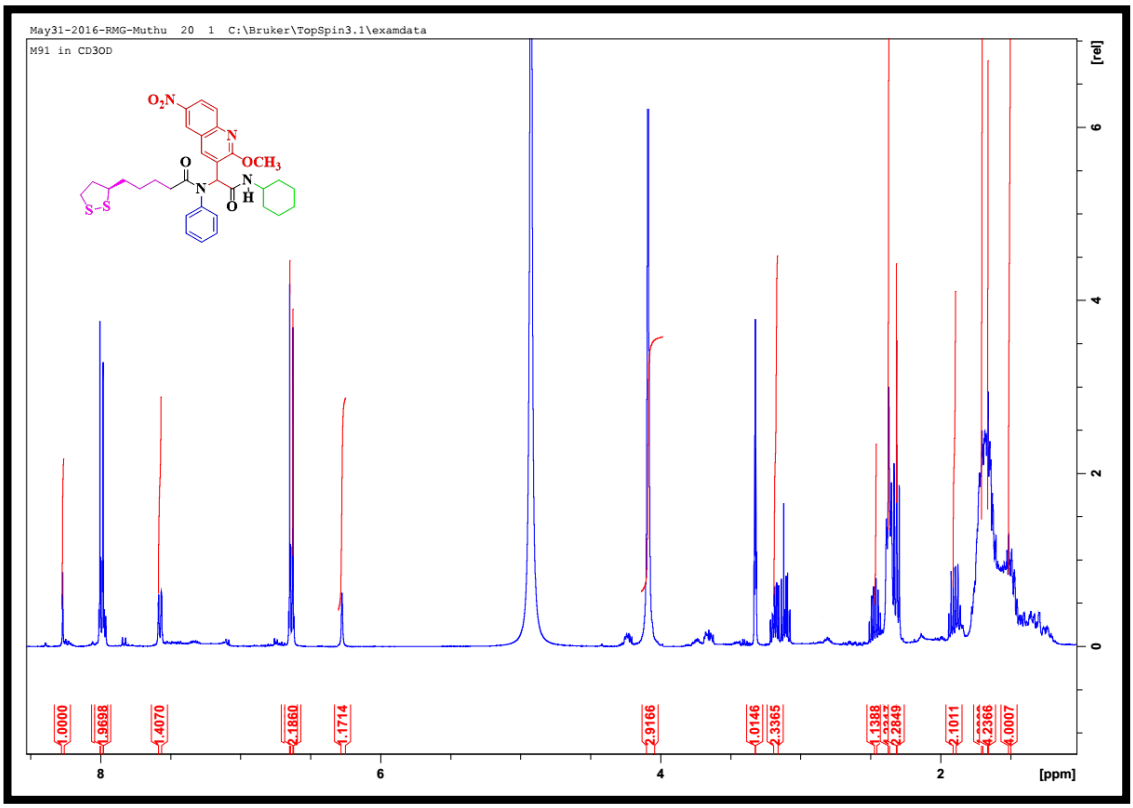

Fig. 3.33. ^{1}H-NMR spectrum for **47**

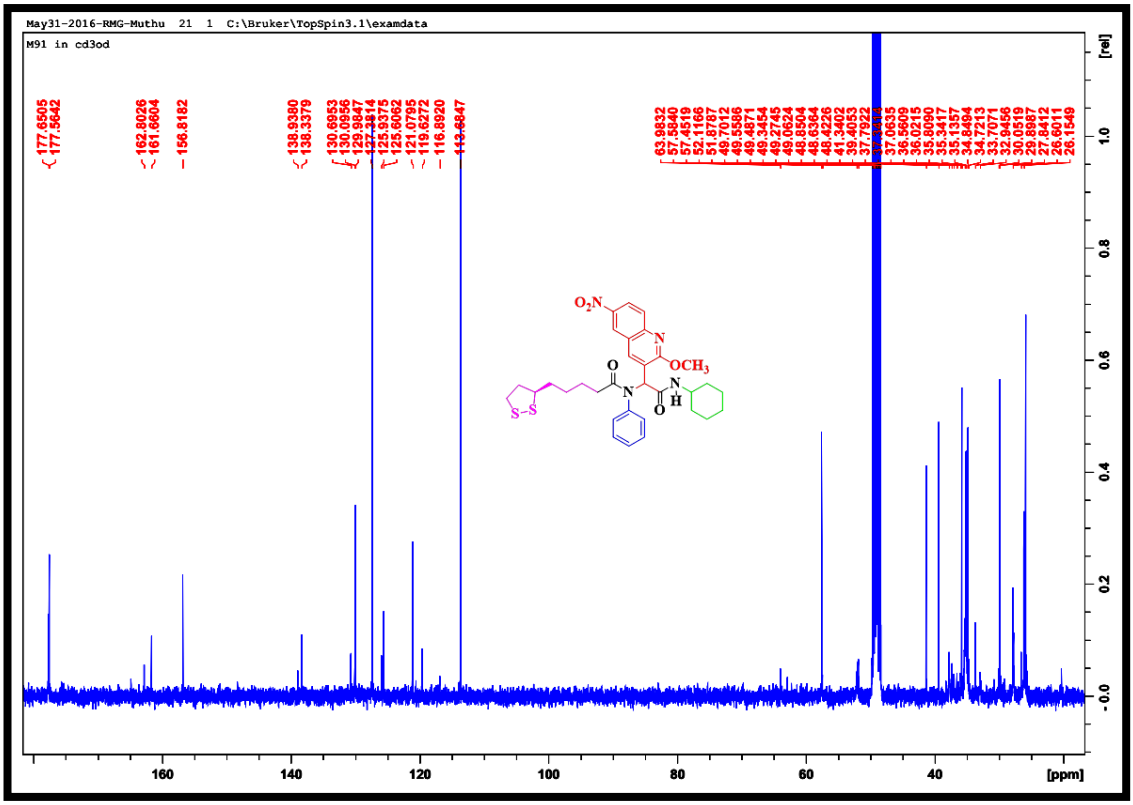

Fig. 3.34. ^{13}C-NMR spectrum for **47**

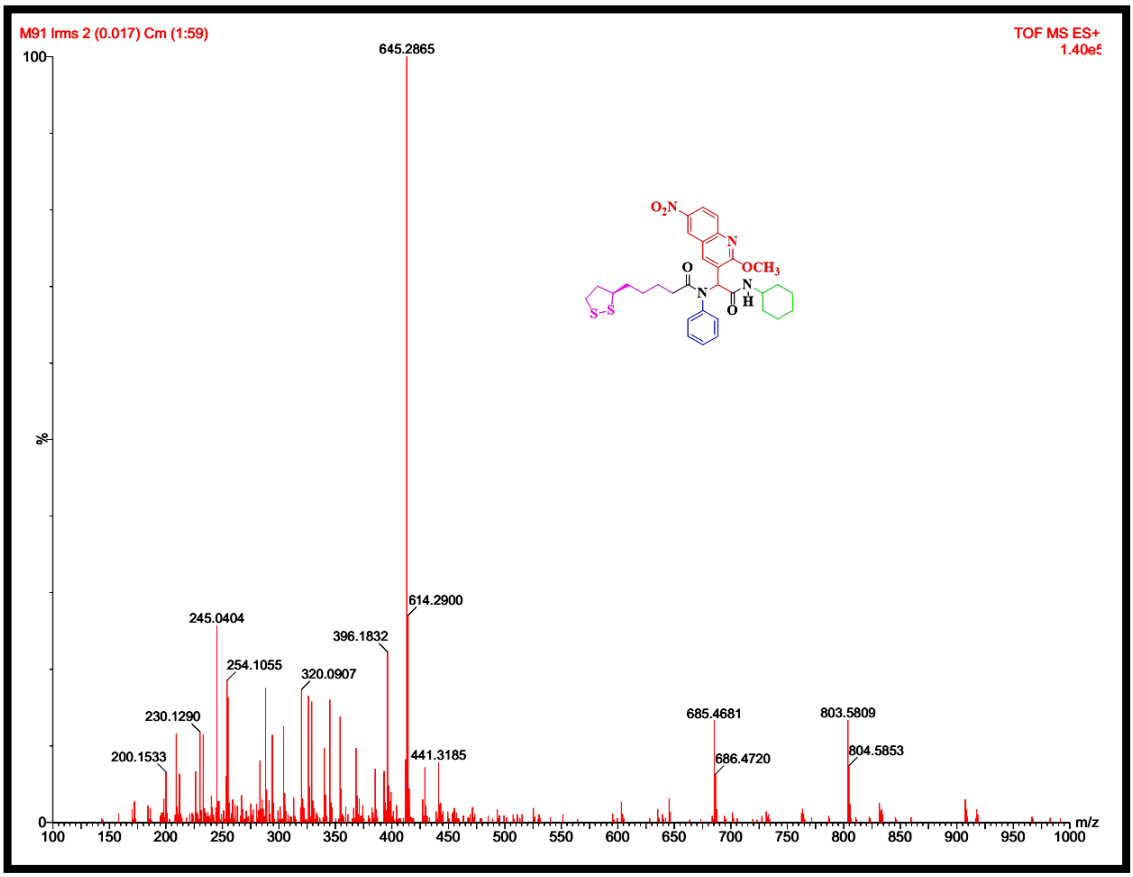

Fig. 3.35. Mass spectrum of **47**

3.9. *N*-(2-amino-4-nitrophenyl)-*N*-(2-(cyclohexylamino)-1-(2-methoxy-6-nitro quinolin-3-yl)-2-oxoethyl)-5-((R)-1,2-dithiolan-3-yl)pentanamide (48)

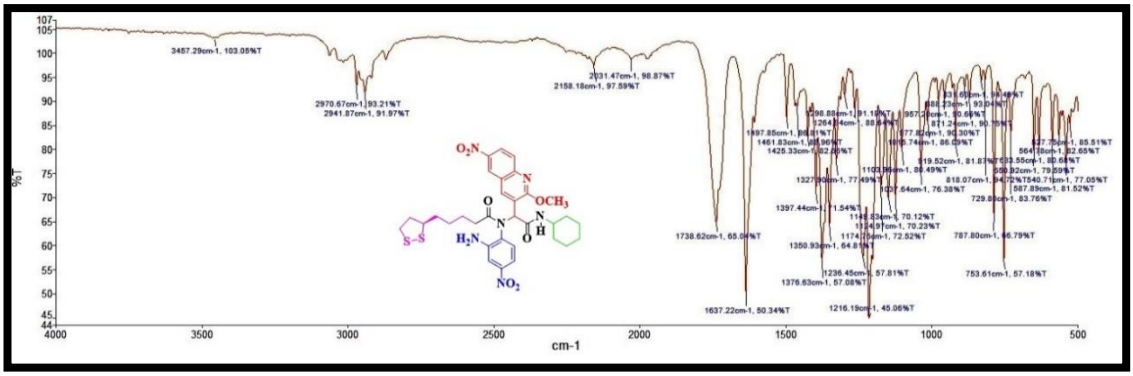

Fig. 3.36. IR spectrum of **48**

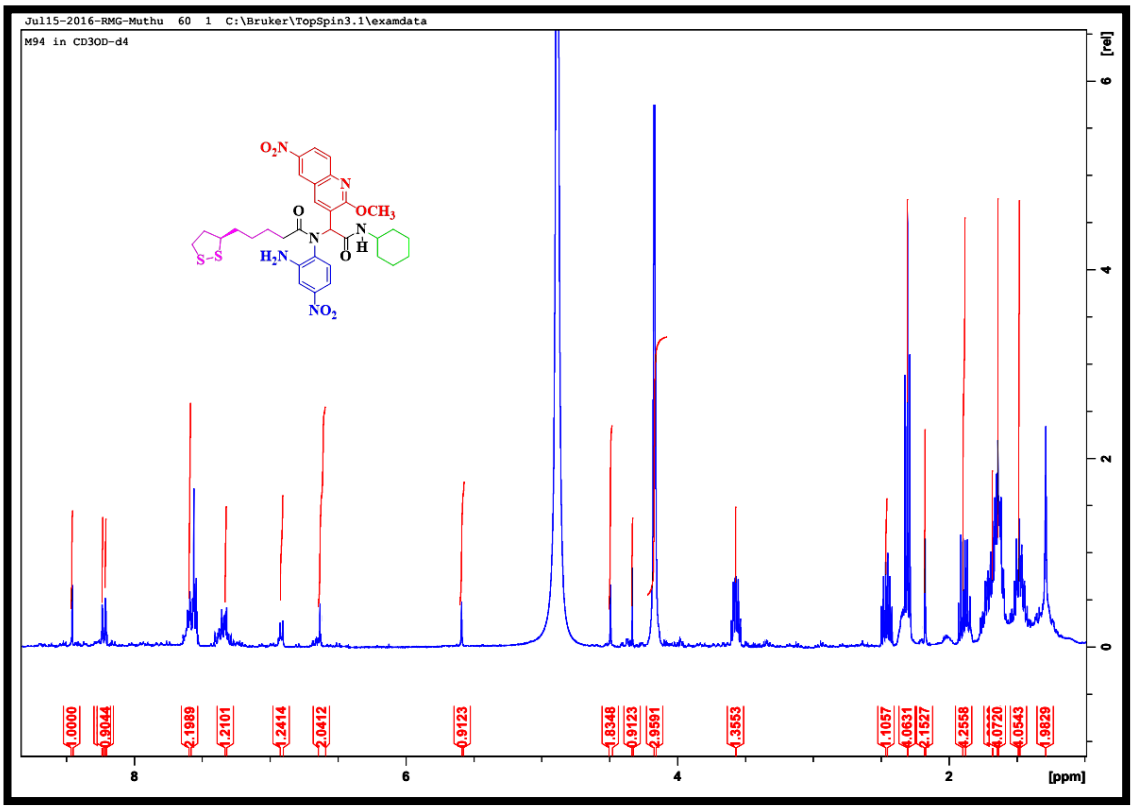

Fig. 3.37. ^{1}H-NMR spectrum for **48**

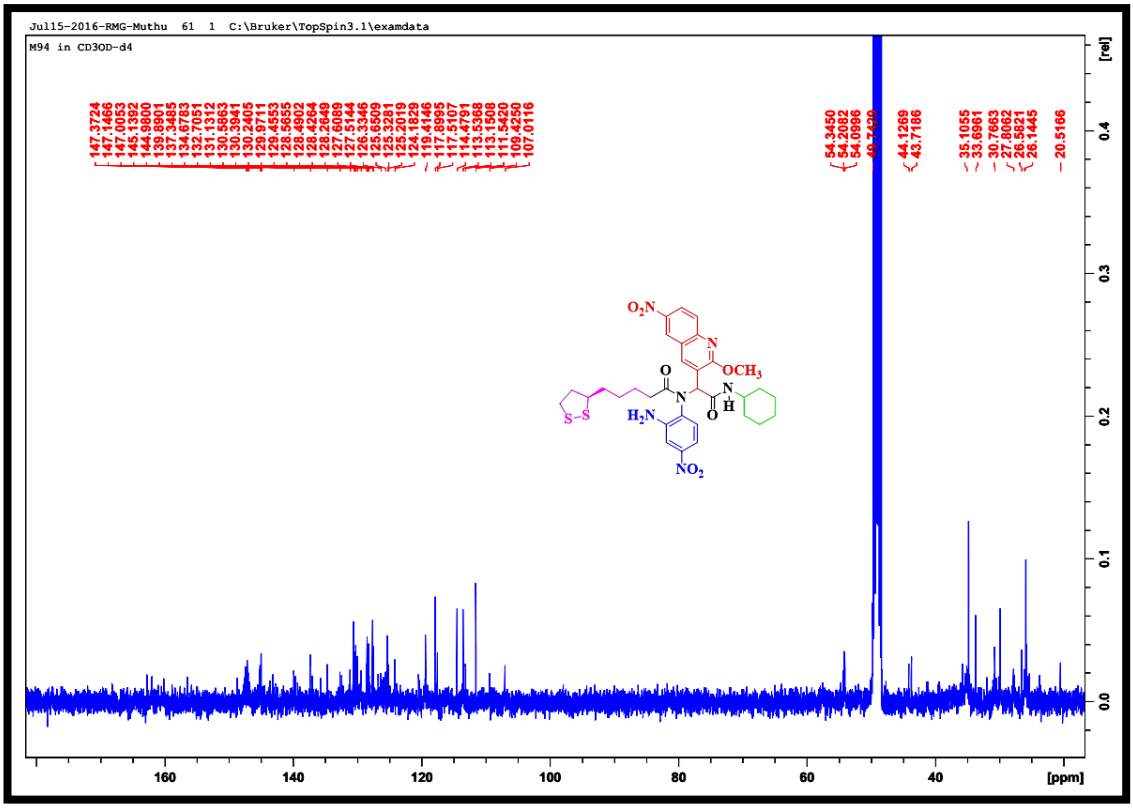

Fig. 3.38. ^{13}C-NMR spectrum for **48**

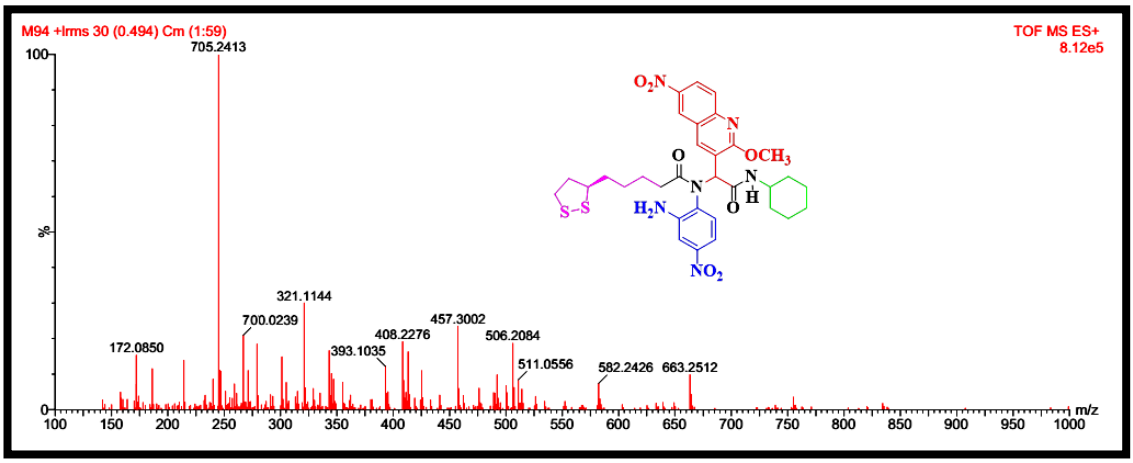

Fig. 3.39. Mass spectrum of **48**

3.10. *N*-(2-(cyclohexylamino)-1-(2-methoxy-6-nitroquinolin-3-yl)-2-oxoethyl)-5-((R)-1,2-dithiolan-3-yl)-*N*-(2-fluorophenyl)pentanamide (49)

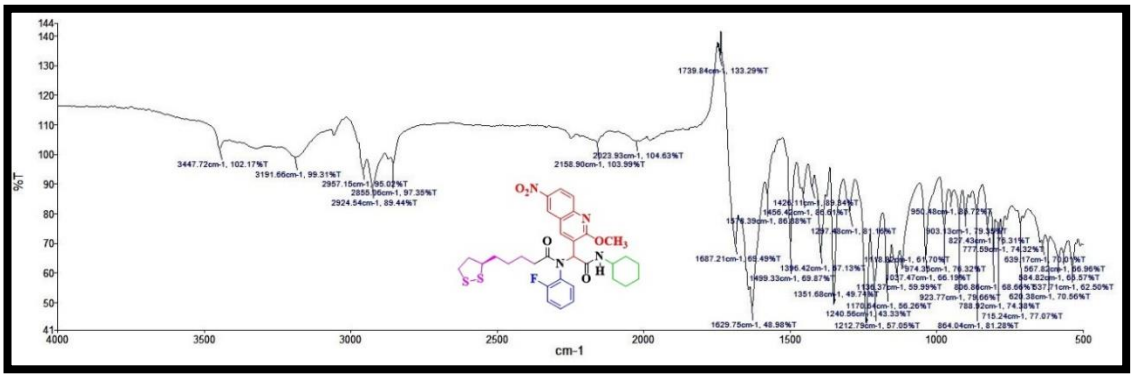

Fig. 3.40. IR spectrum of **49**

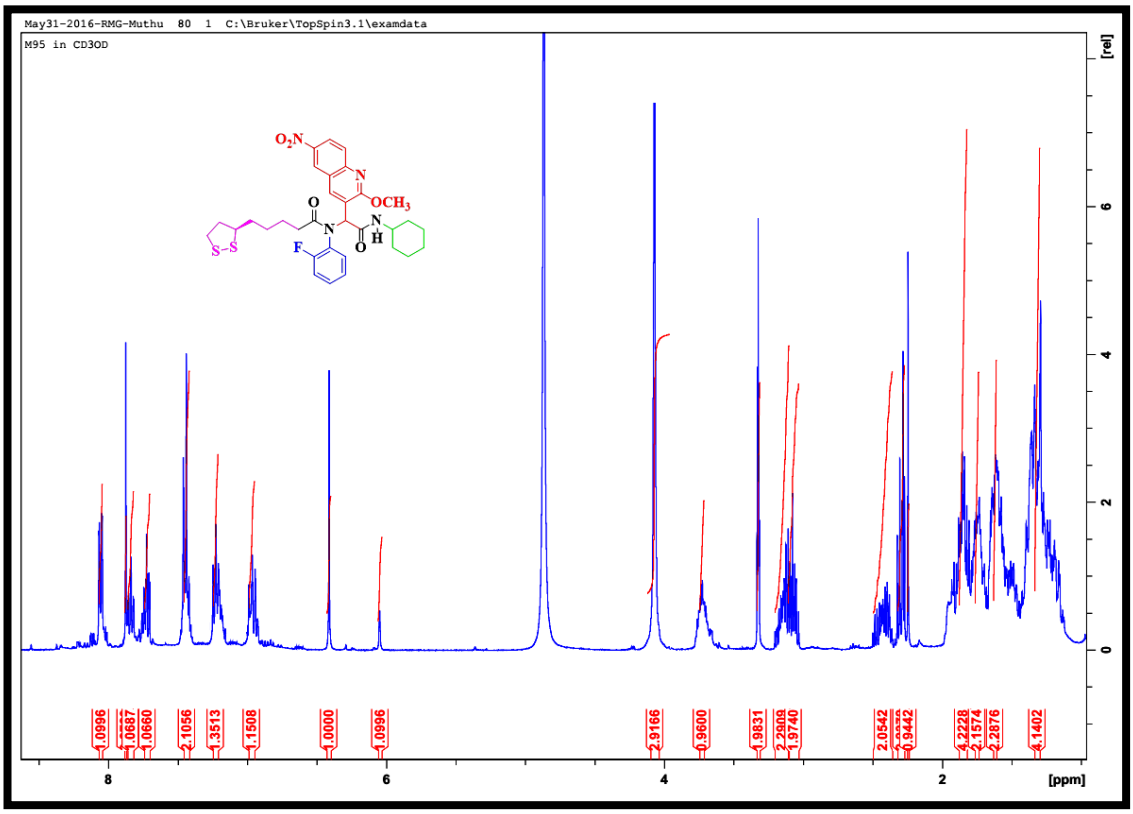

Fig. 3.41. ^{1}H-NMR spectrum for **49**

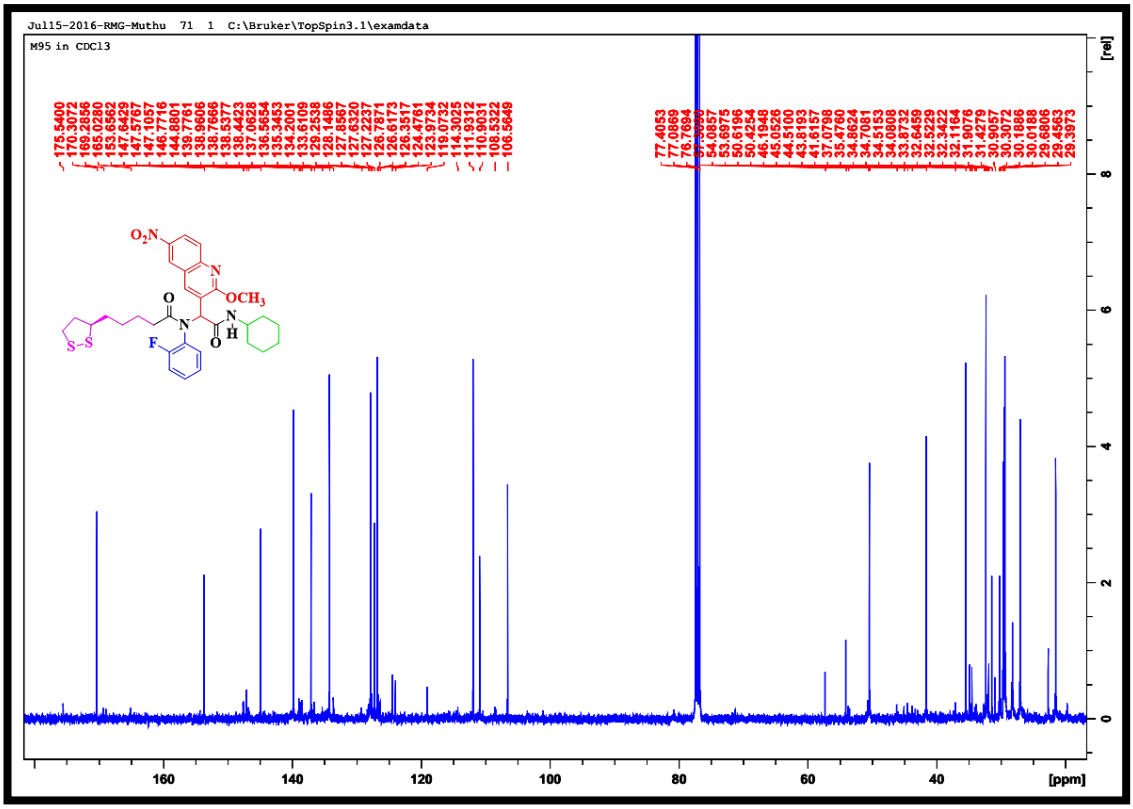

Fig. 3.42. ^{13}C-NMR spectrum for **49**

3.11. *N*-(2-(cyclohexylamino)-1-(2-methoxy-6-nitroquinolin-3-yl)-2-oxoethyl)-5-((R)-1,2-dithiolan-3-yl)-*N*-(m-tolyl)pentanamide (50)

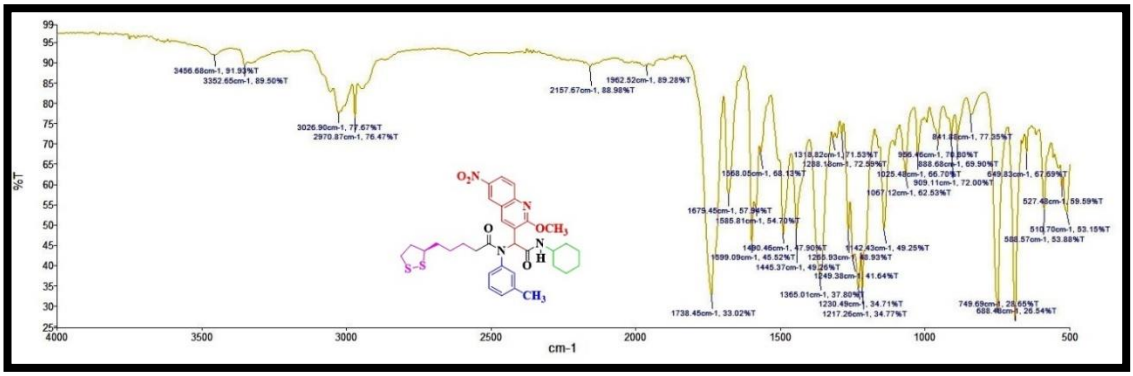

Fig. 3.43. IR spectrum of **50**

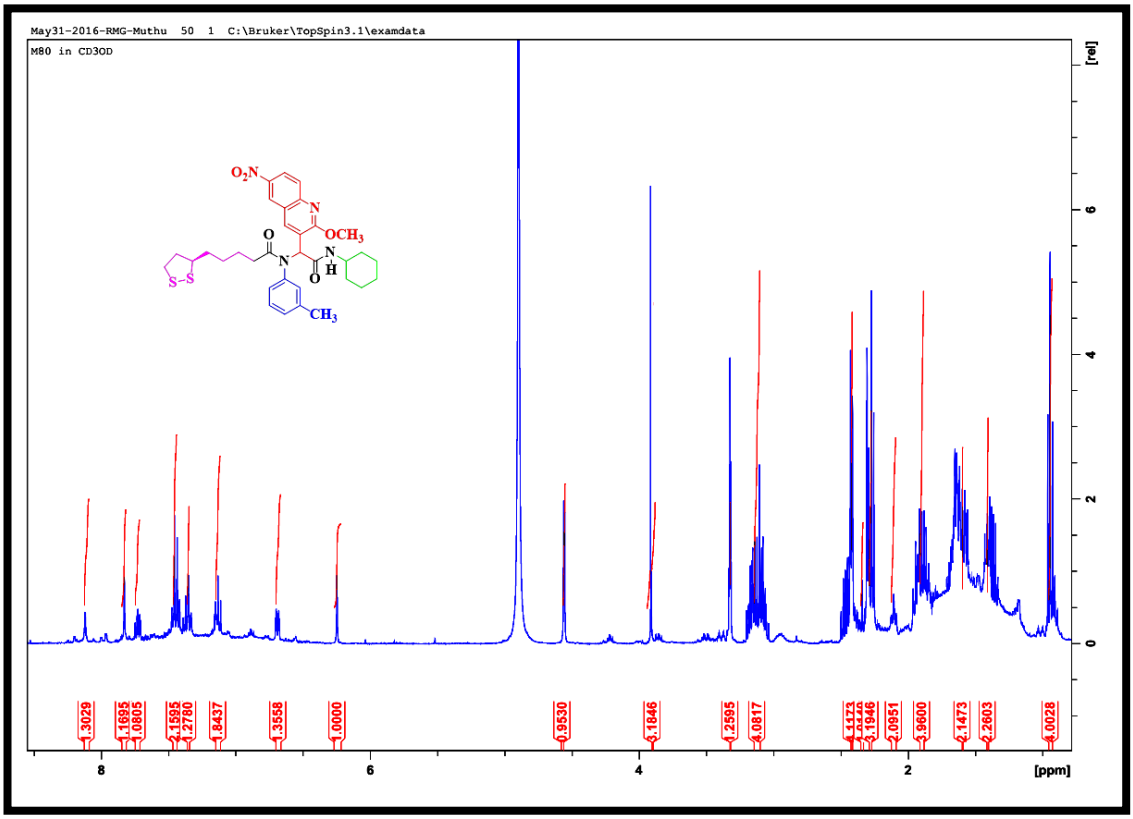

Fig. 3.44. ^{1}H-NMR spectrum for **50**

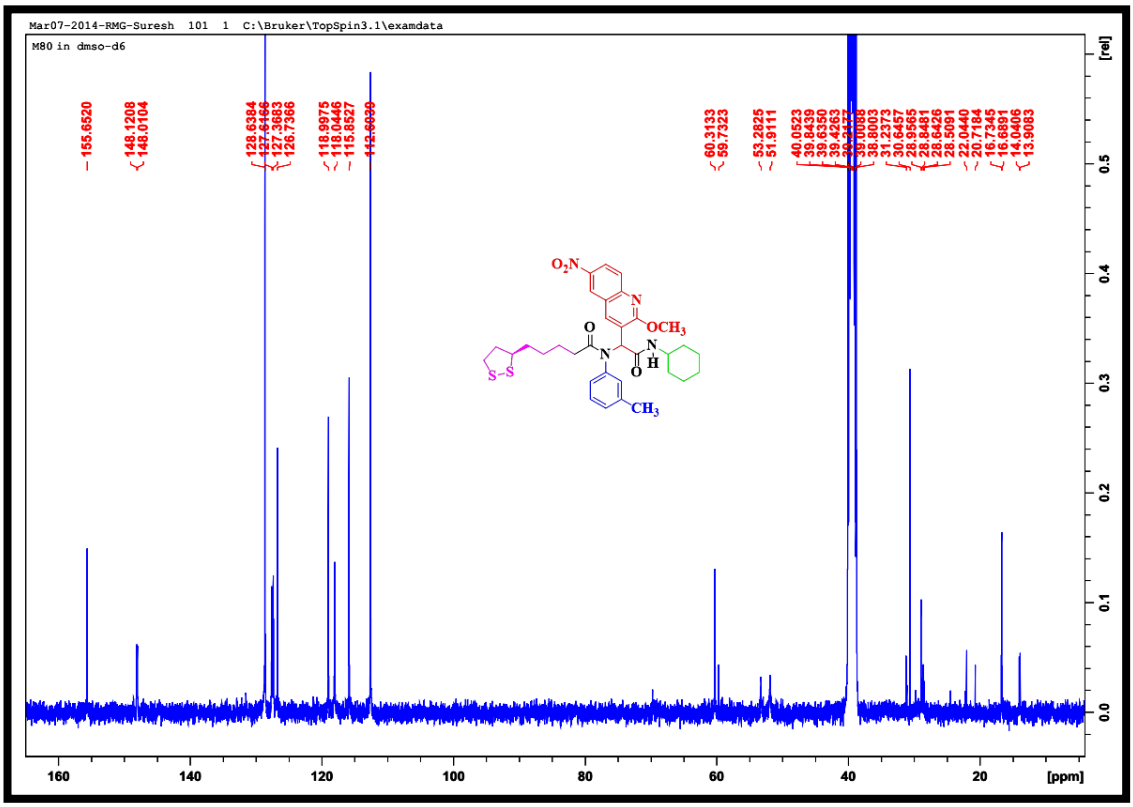

Fig. 3.45. ^{13}C-NMR spectrum for **50**

3.12. *N*-(2-(cyclohexylamino)-1-(2-methoxy-6-nitroquinolin-3-yl)-2-oxoethyl)-5-((R)-1,2-dithiolan-3-yl)-*N*-(o-tolyl)pentanamide (51)

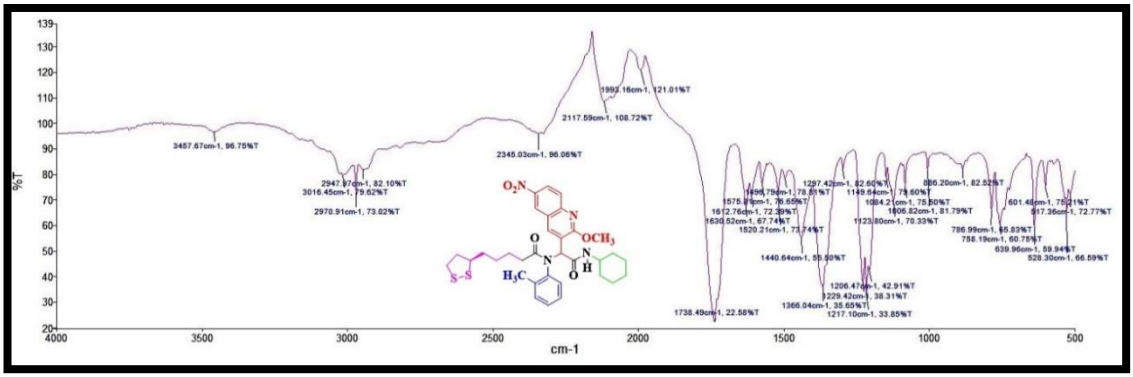

Fig. 3.46. IR spectrum of **51**

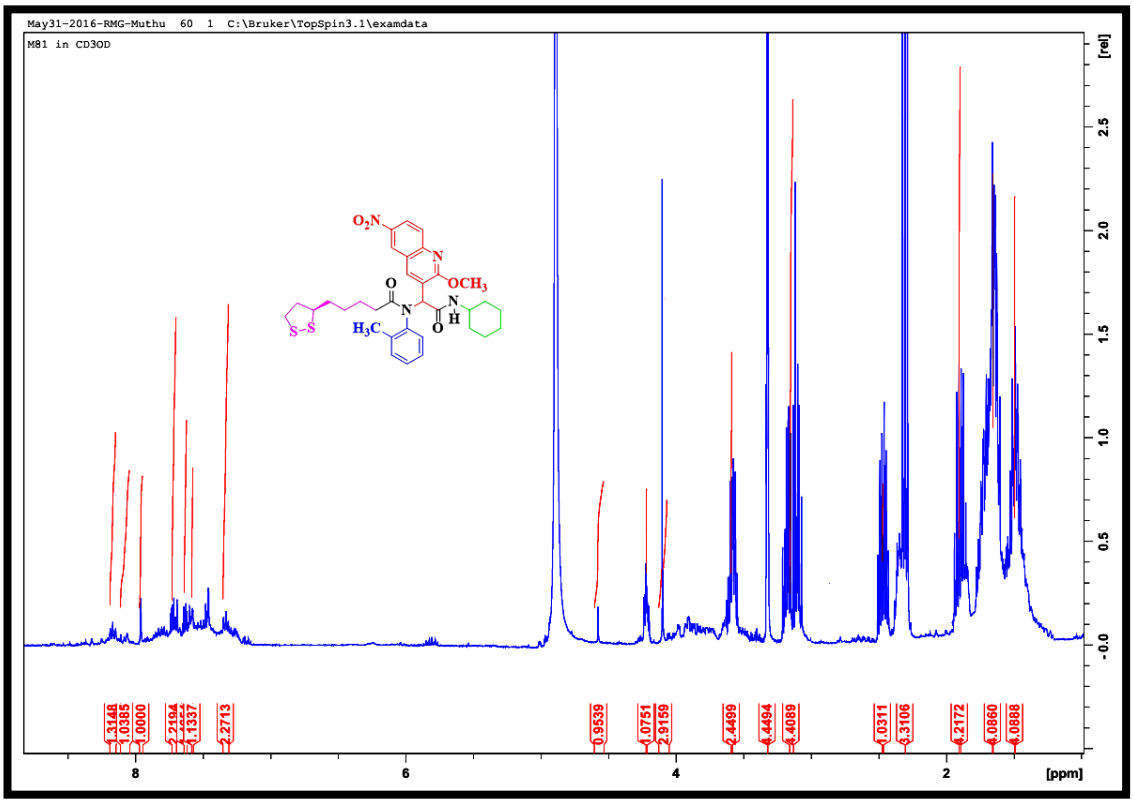

Fig. 3.47. ^{1}H-NMR spectrum for **51**

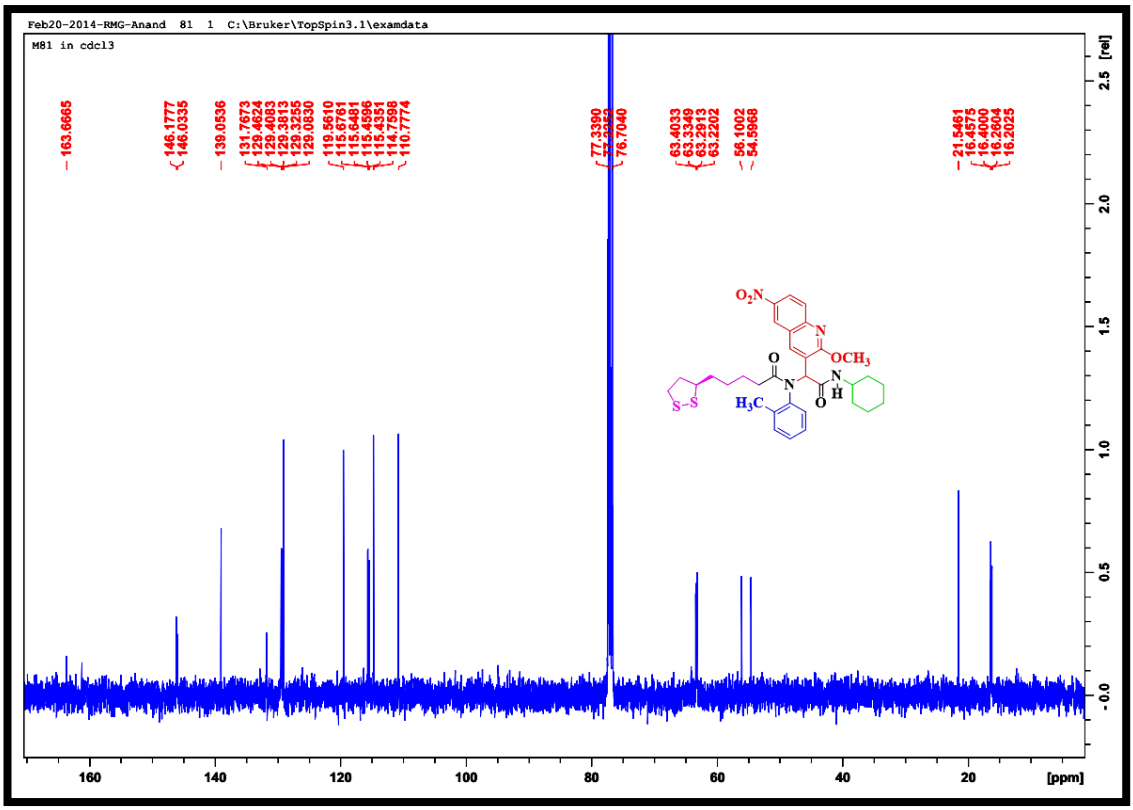

Fig. 3.48. ^{13}C-NMR spectrum for **51**

3.13. *N*-(2-(cyclohexylamino)-1-(2-methoxy-6-nitroquinolin-3-yl)-2-oxoethyl)-5-((R)-1,2-dithiolan-3-yl)-*N*-(2-methoxyphenyl)pentanamide (52)

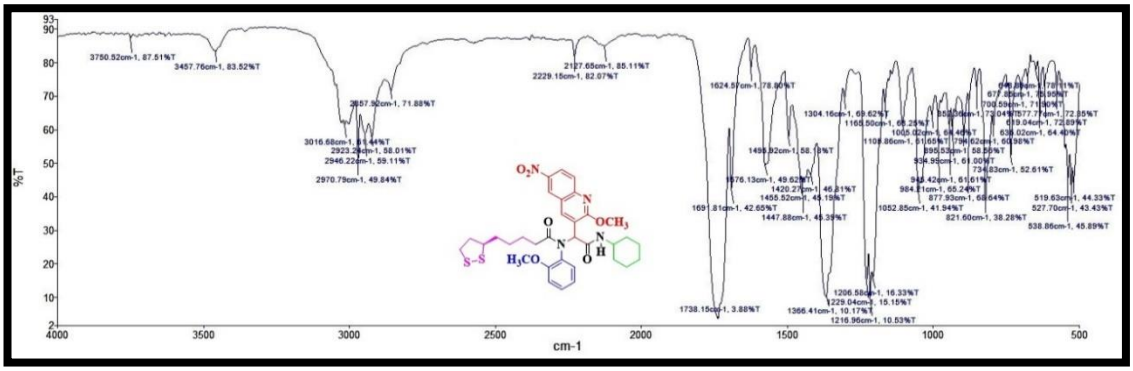

Fig. 3.49. IR spectrum of **52**

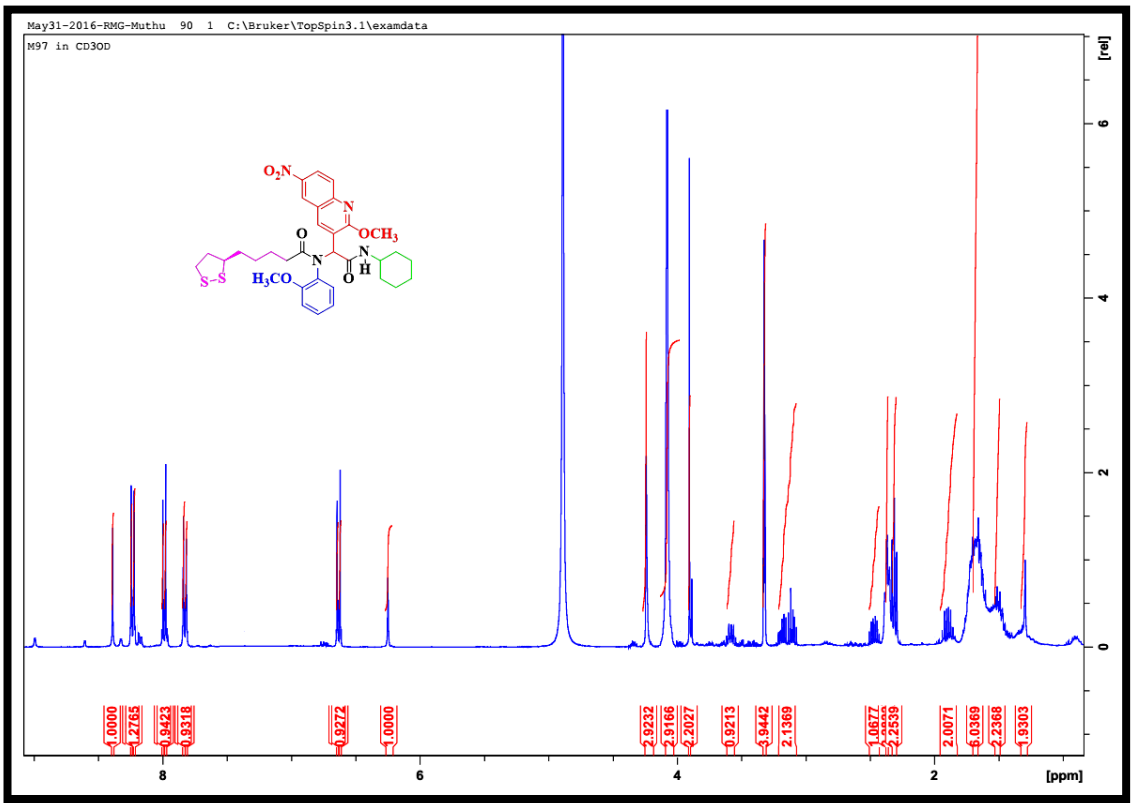

Fig. 3.50. ^{1}H-NMR spectrum for **52**

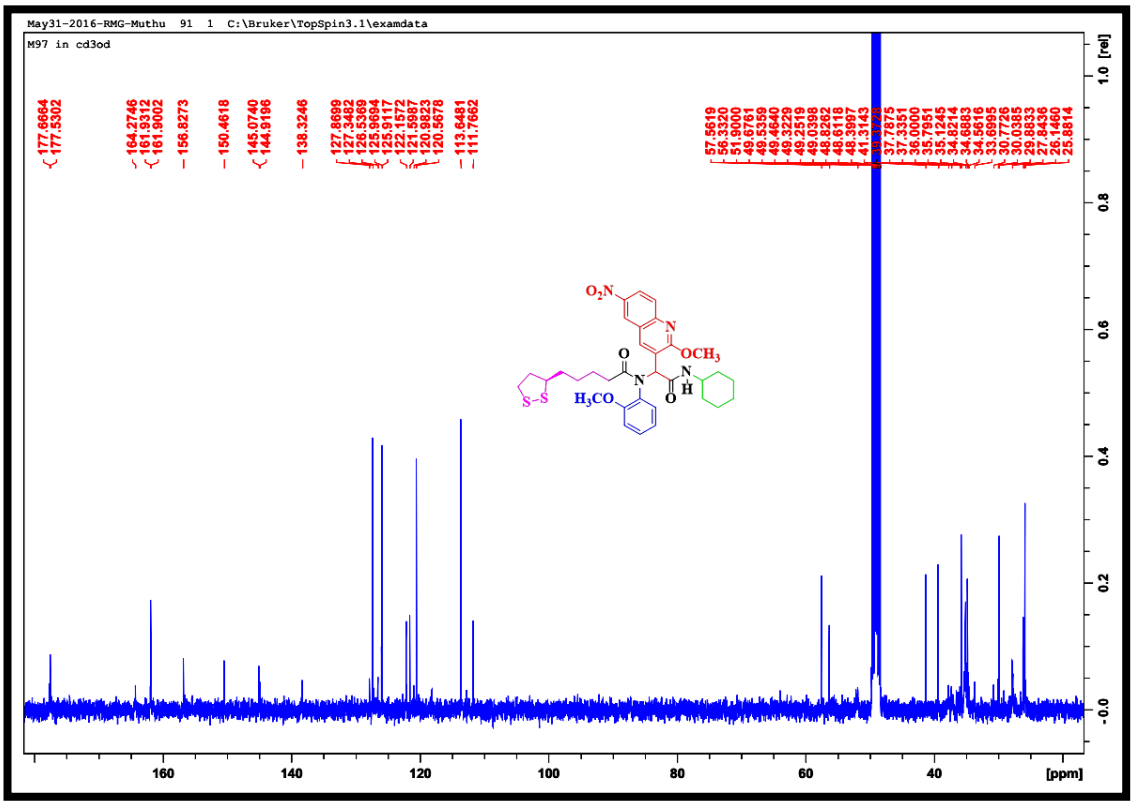

Fig. 3.51. ^{13}C-NMR spectrum for **52**

3.14. *N*-(2-(cyclohexylamino)-2-oxo-1-(2-oxo-1,2-dihydroquinolin-3-yl)ethyl)-5-((R)-1,2-dithiolan-3-yl)-*N*-(2-methoxyphenyl)pentanamide (55)

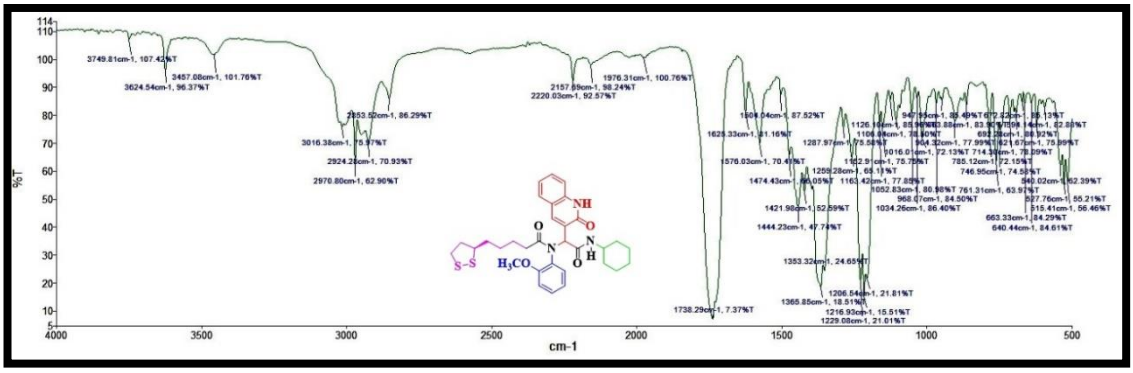

Fig. 3.52. IR spectrum of **55**

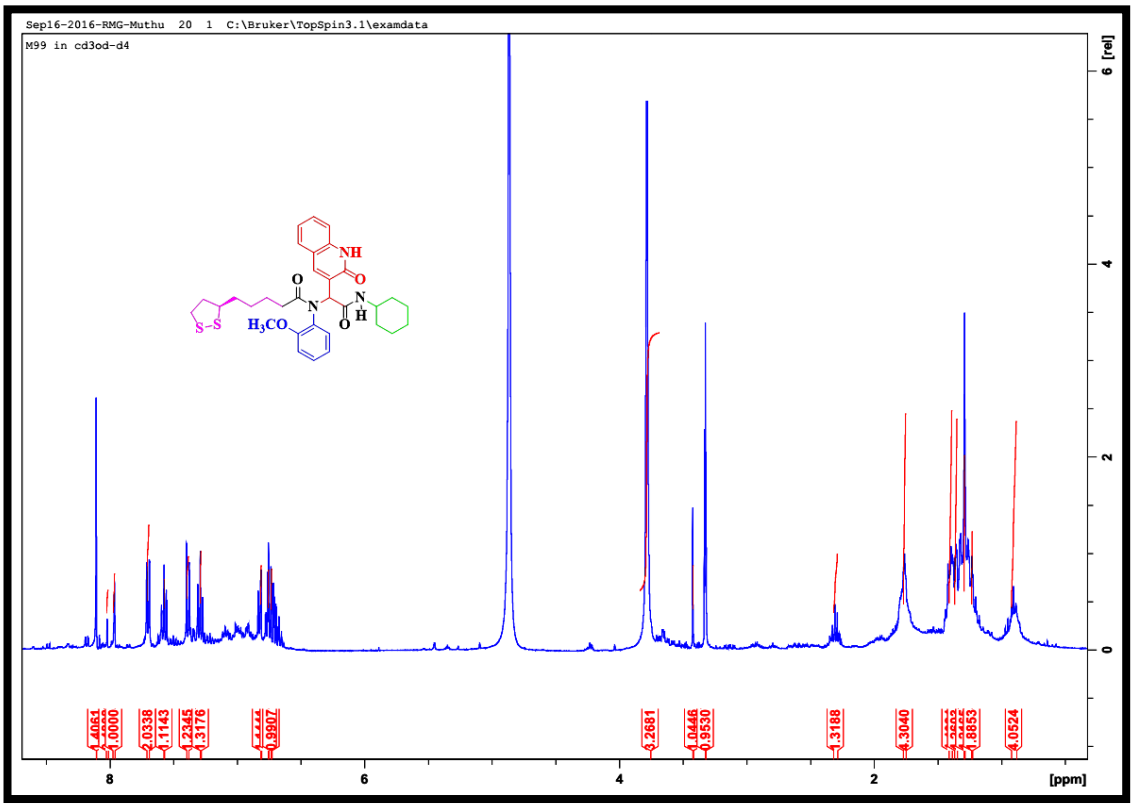

Fig. 3.53. ^{1}H-NMR spectrum for **55**

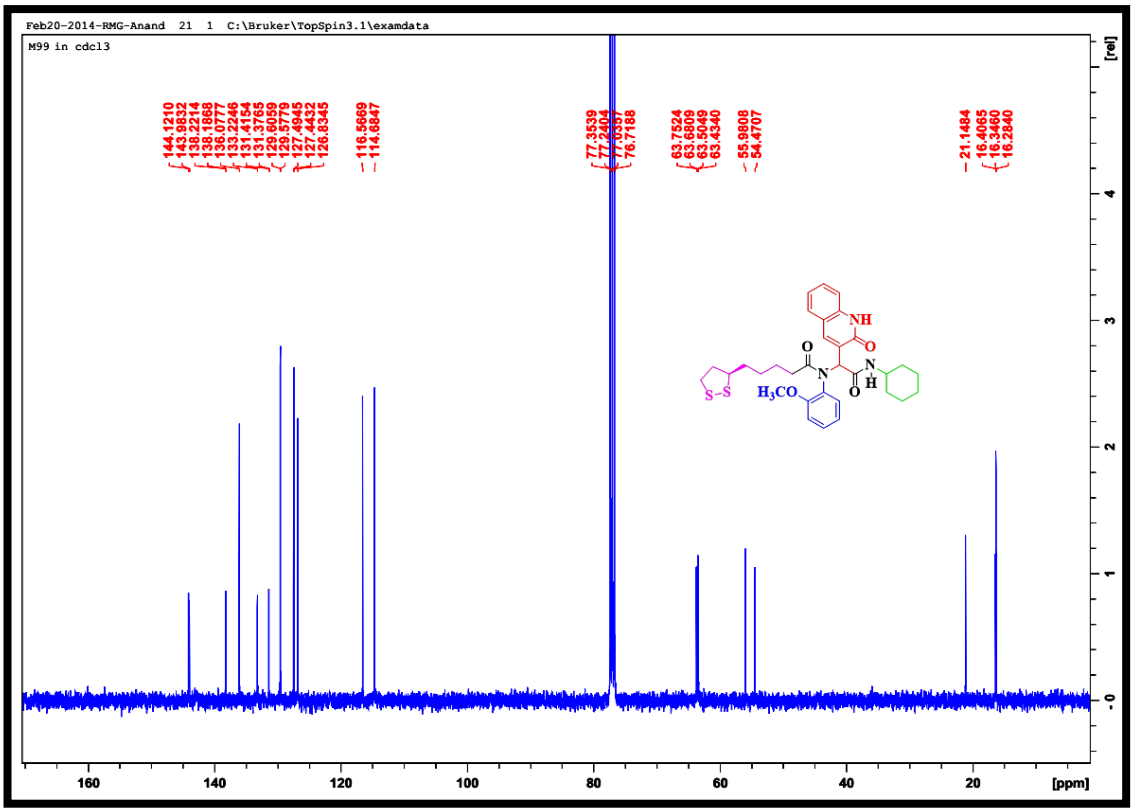

Fig. 3.54. ^{13}C-NMR spectrum for **55**

Chapter-IV

Microwave synthesis of quinolinyl, quinolonyl and indolyl pyrans by humic acid supported ionic liquid catalyst and antimicrobial, antioxidant, toxicity and molecular docking studies

Chapter Four

Microwave synthesis of quinolinyl, quinolonyl and indolyl pyrans by humic acid supported ionic liquid catalyst and antimicrobial, antioxidant, toxicity and molecular docking studies

4.1. Abstract

A series of 12 new quinolinyl-*4H*-pyrans (QPs) were successfully synthesized *via* a three-component reaction of 2-methoxyquinoline-3-carbaldehyde derivatives, malononitrile and 1,3-diketone, using ethanol as the solvent in the presence of a new humic acid supported 1-butyl-3-methylimidazolium thiocyanate ionic liquid catalyst (HASIL) under microwave irradiation. Two quinolonyl-4*H*-pyrans (QOPs) were synthesized from substrates 2-oxo-1,2-dihydroquinoline-3-carbaldehyde derivatives, malononitrile and 1,3-diketone in the presence of HASIL and one indolyl-4*H*-pyran (IP) was synthesized from substrates 4-methylbenzaldehyde, malononitrile and 3-(3*H*-indol-3-yl)-3-oxopropanenitrile in the presence of HASIL in ethanol. HASIL was analysed with various characterization techniques including XRD, SEM with EDX, TEM, TGA, DSC and FTIR. A total of 15 new pyrans were synthesized and characterized by FTIR, ^{1}H-NMR, ^{13}C-NMR and elemental analysis. QPs, QOPs and IP were assessed for antimicrobial and antioxidant activities. Seven QPs and one QOP showed potential antibacterial activities against *Bacillus cereus, Staphylococcus aureus, Escherichia coli* and *Enterococcus faecalis* and whilst nine QPs showed antioxidant activity effectively. QPs, QOPs and IP were then evaluated for toxicity using the brine shrimp assay and five QPs showed mortality rate less than 50 % until 48 h. Molecular docking studies were performed: one QP (**42**) showed higher binding affinity of 96.96 kcal/mol based on LibDock score with Mtb DNA gyrase. The advantages of this synthetic protocol are mild reaction conditions, excellent yields, operational simplicity, the use of an inexpensive and environmentally benign catalyst.

4.2. Introduction

Six-membered heterocyclic compounds containing oxygen is an important class of organic molecules which play a fundamental role in bio-organic chemistry and continue to attract research interest (Abe *et al*., 2005; Sibi *et al*., 2006). The fused pyrans display biological activities which include antimicrobial (Hussein *et al*., 2012), antifungal (Chattapadhyay and Dureja, 2006), antitumor (Wang *et al*., 2011), anti-coagulant, diuretic, spasmolytic and anti-anaphylactic properties (DeSimone *et al*., 2004; Safari *et al*., 2012; Bonsignore *et al*., 1993; Heravi *et al*., 2008; Andreani *et al*., 1960). Furthermore, *4H*-pyrans form the building blocks for important natural products Hatakeyama *et al*., 1988; Singh *et al*., 1996). A number of 2-amino-*4H*-pyrans are used as photoactive materials (Armesto *et al*., 1989), pigments (Maleki *et al*., 1989) and potentially biodegradable agrochemicals (Kumar *et al*., 2009).

The importance of quinoline and its annulated derivatives are recognized by synthetic and biological chemists (Elderfield, 1960; Wright *et al*., 2001; Sahu *et al*., 2002; Bringmann *et al*., 2004; Kouznetsov *et al*., 2005). Compounds possessing this ring system have wide applications as drugs and pharmaceuticals (Peters *et al*., 1984). The pyrano-quinolines are an important class of compounds that contain the basic framework for a number of alkaloids of biological significance (Corral and Orazi, 1967; Sekar and Prasad, 1998; Puricelli *et al*., 2002; Marco and Carreiras, 2003) such as geibalansine, ribalinine and flindersine (**Fig. 1**). Therefore, considerable efforts have been directed towards their preparation (Ghorab *et al*., 2001; Morel and Larghi, 2004) resulting in a number of new compounds possessing diverse biological activities.

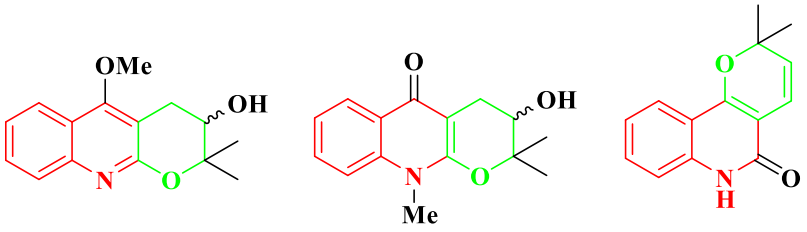

Geibalansine (1) **Ribalinine (2)** **Flindersine (3)**

Fig. 1. Examples of pyrano-quinolines (Corral and Orazi, 1967; Sekar and Prasad, 1998; Puricelli *et al*., 2002; Marco and Carreiras, 2003)

The sulfur-containing molecules also have broad application in medicinal chemistry (Metzner and Thuillier, 1994; Nudelman, 1984; Chatgilialoglu and Asmus, 1991): β-mercapto diketones display pharmacological properties such as diuretic and HIV protease inhibitory activities (Bicking *et al*., 1976; Ding *et al*., 2009; Inomata *et al*., 2005; yamauchi *et al*., 1982).

Recently, growing awareness to environmental issues has led to greener and more sustainable technologies in the chemical industry. Ionic liquids (ILs), which consist of ionic compounds with low melting points and very low vapour pressures, (Wasserscheid and Welton, 2008; Weingärtner, 2008; Wassercheid and Keim, 2000) are in demand. Many different ILs have been synthesized and successfully used as solvents as well as modified catalysts. Homogeneous catalysts containing ILs usually provide the advantages of high catalytic activity and good selectivity, however, drawbacks such as difficulty of product isolation and recovery of catalyst, use of large amounts of expensive ILs and possible toxicological concerns are evident. ILs in heterogeneous form usually overcome these drawbacks especially the supported solid catalysts with ILs. These reflect good stability of the active species, ease of handling, separation and recycling. In this context, ILs are now widely used for immobilization of homogeneous catalysts (Mehnert, 2005; Riisagera *et al*., 2006; Gu and Li, 2009; Van Doorslaer *et al*., 2010).

An easy access to pyran derivatives is highly desirable as they possess unique pharmacological properties (Green *et al*., 1995; Jin *et al*., 2004). The most straight forward synthesis of this heterocyclic system involves a three-component coupling of an aromatic aldehyde, malononitrile and 1, 3-diketones. Recently, several multi-component reactions have been described. Evdokimov *et al*., 2007 reported a one-pot synthesis of heterocyclic privileged medicinal scaffolds by fusing malononitrile with aldehydes and thiols, in ethanol. The reaction was catalyzed by triethylamine.

Ding *et al*., 2013 reported the synthesis of 2-amino-3-phenylsulfonyl-*4H*-pyrans (**7**) by the condensation of aromatic aldehydes (**4**), dimedone (**5**) and phenylsulfonyl acetonitrile (**6**) in the presence of 2-hydroxyethyl ammonium acetate (HEAA) catalyst. The reaction was achieved in water: ethanol (1:1) medium under reflux conditions within 2-12 h and afforded 71-93 % yield.

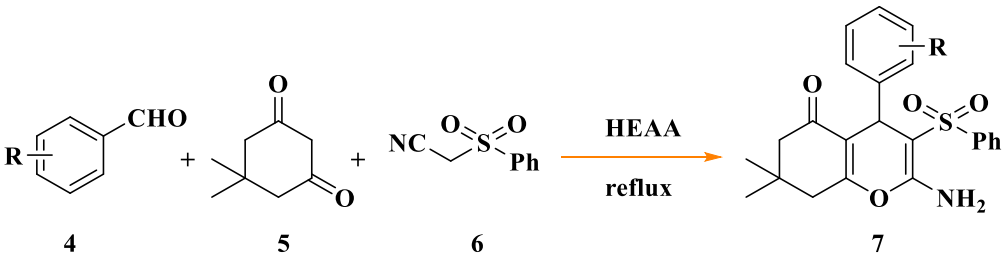

4 5 6 7

R = C_6H_5, 4-$OCH_3C_6H_5$, 2-ClC_6H_5, 2-$NO_2C_6H_5$

Khurana *et al*., 2012 synthesized *4H*-pyrans (**11**) and *4H*-pyrano [2,3-c]pyrazoles (**13**) from aldehydes (**8**), malononitrile (**9**) and ethylacetoacetate (**10**) and pyrazolone (**12**), respectively, in the presence of 1-butyl-3-methyl imidazolium hydroxide ([bmim]OH) catalyst. The protocol was achieved within 30-60 minutes under reflux and a maximum yield of 88-92 % was observed.

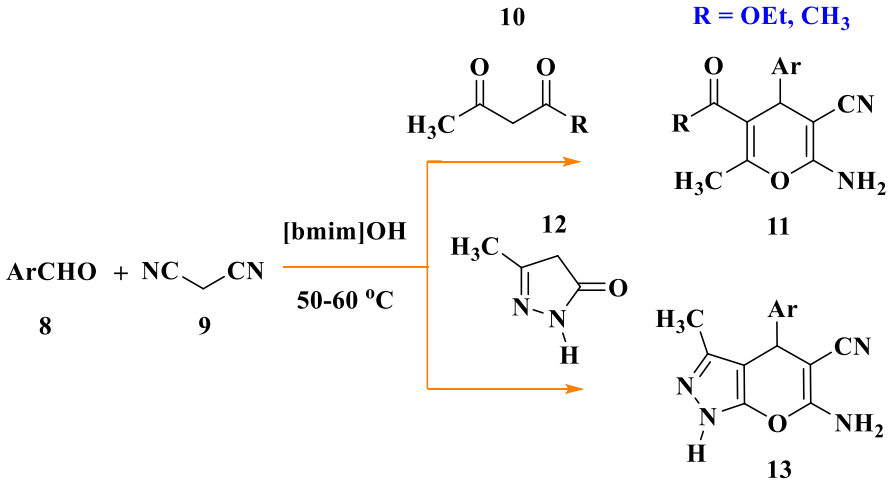

Peng *et al*., 2005 reported the synthesis of *4H*-pyrans (**16**) through one-pot condensation of aromatic aldehydes (**15**), malononitrile (**9**) and 1, 3-diketones (**14**), using tetramethyl guanidine in 1-butyl-3-methylimidazolium tetrafluoroborate ([bmim][BF_4]) ionic liquid as a catalyst. The reaction was achieved within 0.5-1.5 h and the yield was 78-89 %.

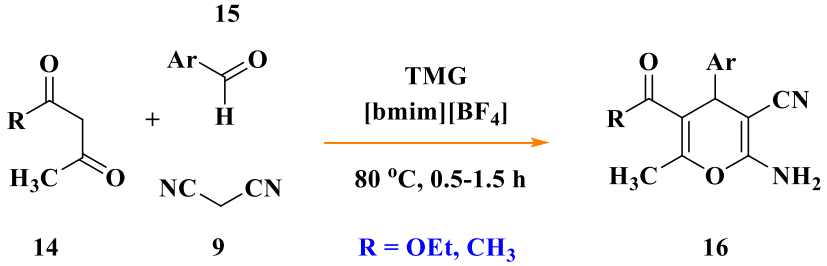

14 9 R = OEt, CH_3 16

Nimbalkar *et al*., 2017 synthesized 6-amino-4-substituted-3-methyl-2,4-dihydro pyrano[2,3-c]pyrazole-5-carbonitriles (**20**) *via* a one-pot condensation reaction from aryl aldehydes (**17**), malononitrile (**9**), hydrazine hydrate (**19**) and ethyl acetoacetate (**18**). A Brønsted acid ionic liquid [BAIL] triethylammonium hydrogen sulphate $[Et_3NH][HSO_4]$ catalyst was used to afford a 85-94 % yield within 15 minutes.

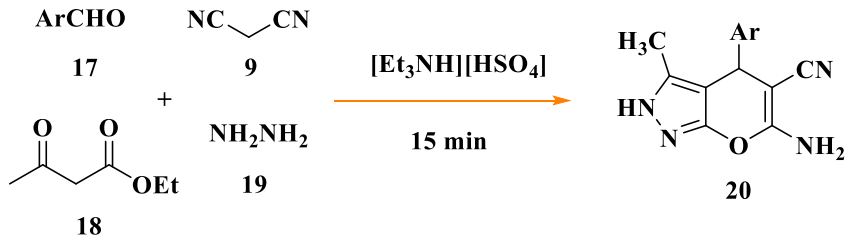

Ar = C_6H_5, 4-ClC_6H_5, 4-FC_6H_5, 4-OHC_6H_5, 2-$NO_2C_6H_5$

Shaabani *et al*., 2005 synthesized 3-cyano-4*H*,5*H*-pyran derivatives (**24**, **26**) in the presence of 1,1,3,3-*N*,*N*,*N*',*N*'-tetramethylguanidinium trifluoroacetate (TMGT) ionic liquid catalyst. The condensation reaction was carried out from a mixture of aldehyde (**21**) and alkyl nitrile (**22**) by heating for 1 h. The yield was 70-82 %.

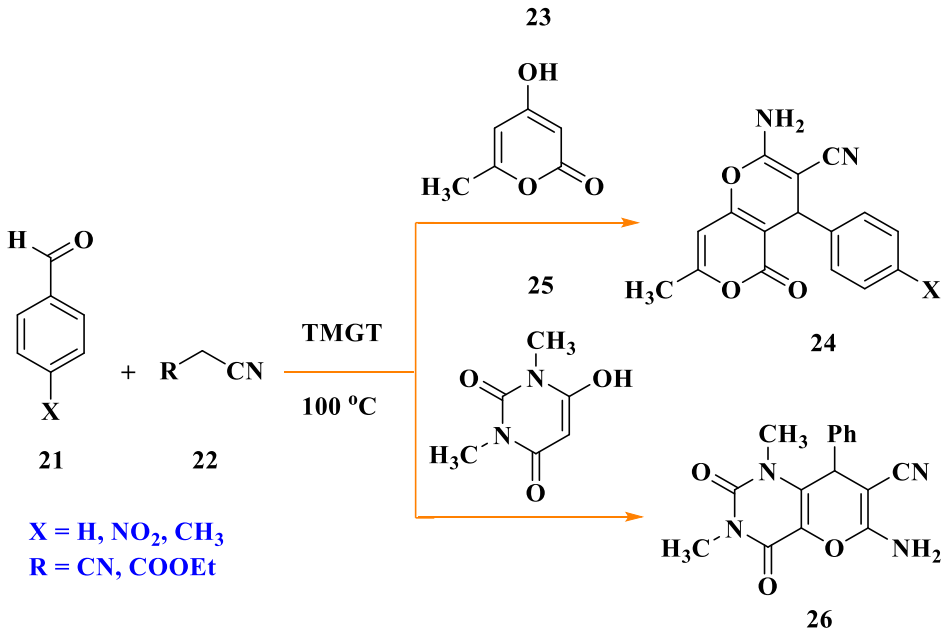

X = H, NO_2, CH_3
R = CN, COOEt

Wang *et al*., 2015 synthesized 3,4-dihydropyrano-[3,2-*c*]chromene derivatives (**29**) from aromatic aldehydes (**28**), malononitrile (**9**) and 4-hydroxycoumarin (**27**) in the presence of poly ethylene glycol grafted *N*,*N*-dimethylaminopyridine functionalized dicationic

ionic liquid ([DMAP-PEG$_{1000}$-DIL][BF$_4$]) and 68-92 % yield was afforded within 60 minutes.

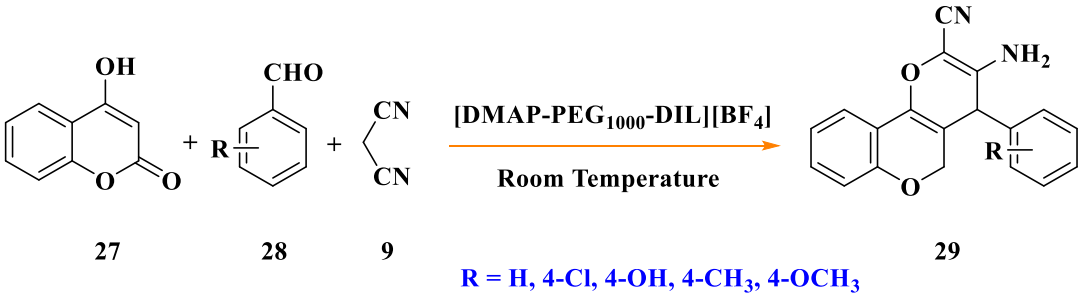

Due to the attractive properties of supported ILs catalysis, we designed a novel catalyst, ie. humic acid supported ionic liquid (HASIL). This was developed by using the homogeneous nature of ILs and a cheap humic acid (HA) as the heterogeneous support to provide large interfacial reaction areas. The supported ILs phase catalysis concept was based on a classical homogeneous catalyst that was dissolved in a thin film of ILs which was further dispersed over the high internal surface area of porous support. In supported ILs phase materials, the dissolved catalyst acts microscopically as a homogeneously dissolved metal complex in its uniform ILs environment while macroscopically in dry solid form that can be recycled easily. HA is known to catalyse many reactions (Klavins *et al*., 2001) and in our study, it was used to enhance the basic nature of the catalyst and provide heterogeneity. Furthermore, HASIL was used to synthesize new quinolinyl-*4H*-pyrans (QPs), quinolonyl-*4H*-pyrans (QOPs) and indolyl-*4H*-pyran (IP) via a three-component reaction of malononitrile, 1,3-diketone and the appropriate aromatic aldehyde. The new compounds were further investigated for antimicrobial, antioxidant and toxicity whilst molecular docking studies were undertaken with Mtb DNA gyrase.

4.3. Results and discussion

The study was initiated by the synthesis of HASIL. Briefly, a solution of 1-butyl-3-methylimidazolium thiocyanate ionic liquid ([bmim]SCN) and HA was stirred for 10 h under an inert atmosphere. The solvent was evaporated *in vacuo* to produce a free flowing powder. It was then reacted with a solution of HA and copper acetate to produce the catalyst, after work-up of the reaction content. A general scheme for the preparation of HASIL is presented in **Fig. 2.**

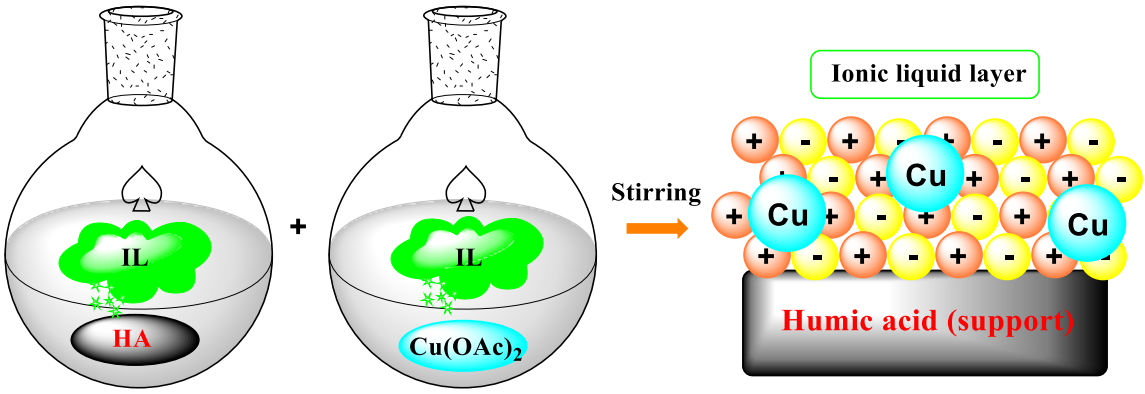

Fig. 2. The synthesis of humic acid supported ionic liquid

The proposed interaction of copper, humic acid and [bmim]SCN (Lu *et al*., 2013; Wilmer *et al*., 2003) is shown in **Fig. 3** below.

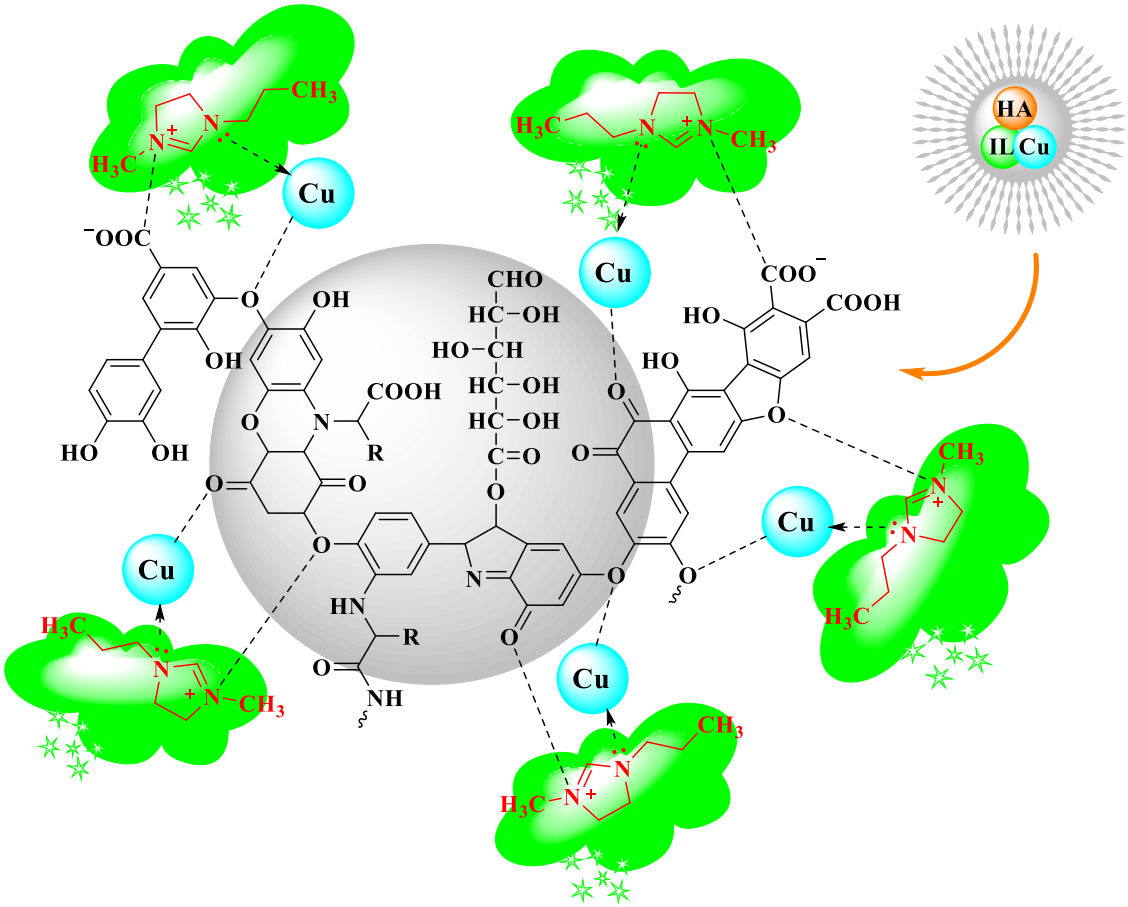

Fig. 3. The possible interaction of humic acid supported ionic liquid (Lu *et al*., 2013; Wilmer *et al*., 2003)

HASIL was then analysed by various characterization techniques including XRD, SEM with EDX, TEM, TGA, DSC and FTIR.

The X-ray diffraction pattern in the 2θ range from 10 to 70^{o} (**Fig. 4**) exhibited small diffuse peaks with a few intense peaks, implying its non-crystalline nature. This was consistent with other HA based catalysts (Chilom and Rice, 2005; Visser and Mendel, 1971). The weak diffraction lines suggested HA particles were coated with ILs. The diffraction observed at 38.5°, 45°, 56° and 62.5° corresponded to (002), (111), (200) and (113) of Bragg's reflection for the cubic structure of copper (Das *et al*., 2014).

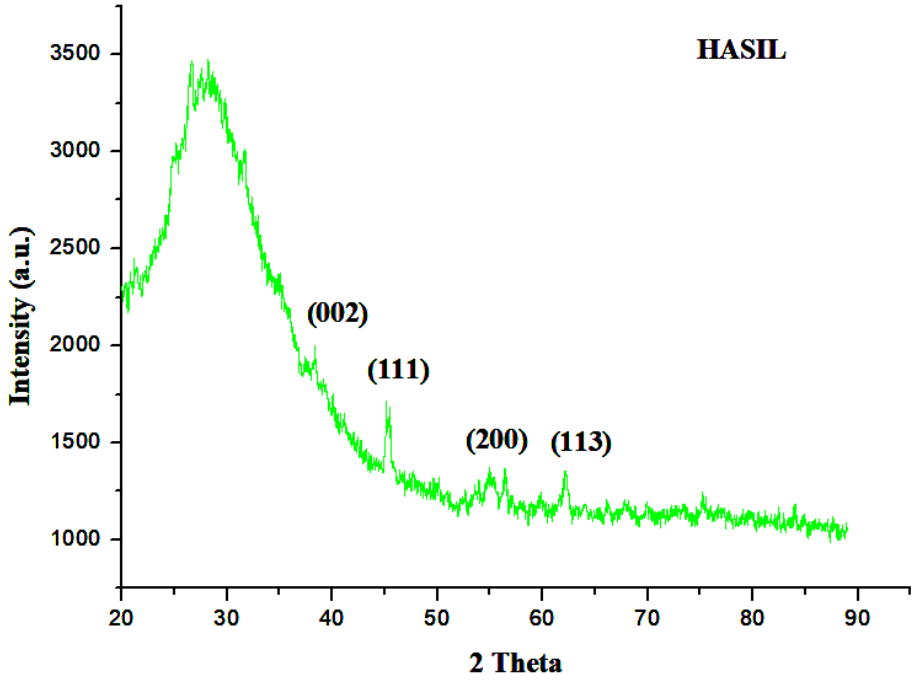

Fig. 4. Powder XRD pattern of humic acid supported ionic liquid

Fig. 5 (**A-D**) provides the SEM images of HASIL where small particles at 20 µm, 10 µm, 2 µm and 1 µm were observed. The small particles suggested that high metal adsorption (Xu *et al*., 2006) was promoted: Cu can form bridges with carboxyl groups of HA, interact by chemisorption with oxidized carbon atoms and form coordination compounds (Pandey *et al*., 2000) with other functional groups such as hydroxyl, phenol, carboxyl and methoxy functional groups. Also, compacted micro-aggregates were formed. The aggregation phenomenon is important for transport of metal ions in natural environments (Chen *et al*., 2007). The humic acid substances in general formed thin thread and net-like

structures that grew into larger rings and sheets with increasing humic and cationic concentrations (Zhang *et al*., 2009).

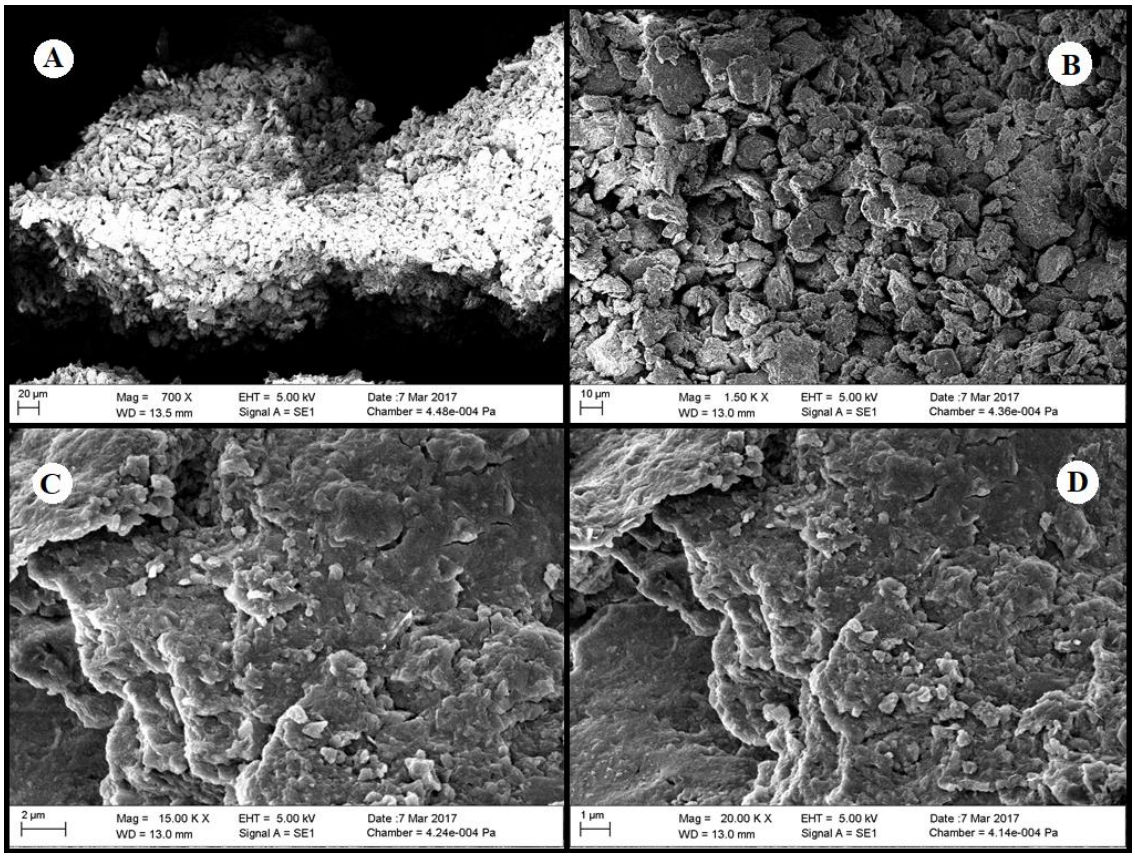

Fig. 5. SEM images of humic acid supported ionic liquid

Fig. 6 (**A**-**B**) showed the EDX pattern and elemental mapping of HASIL. The elements carbon, oxygen, copper and gold (Au) were present. The appearance of Au peaks was due to the coating of sample with conducting material used to reflect electrons by sputter-coating.

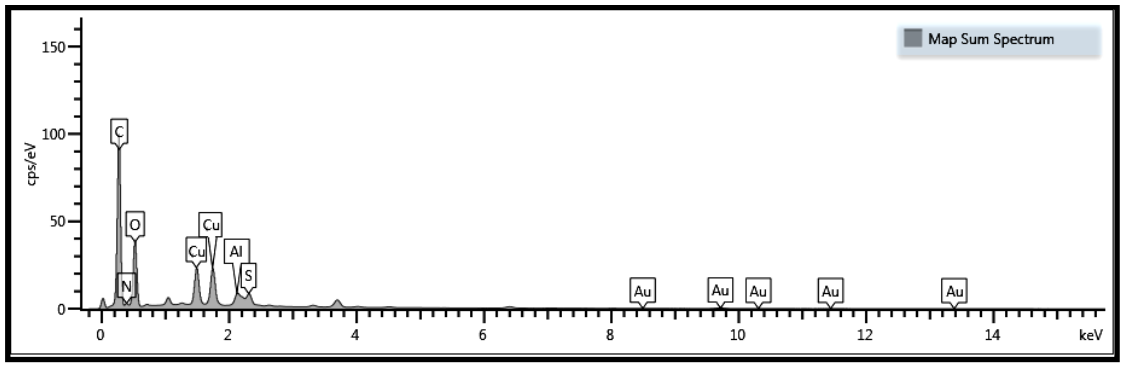

Fig. 6A. EDX spectrum of humic acid supported ionic liquid

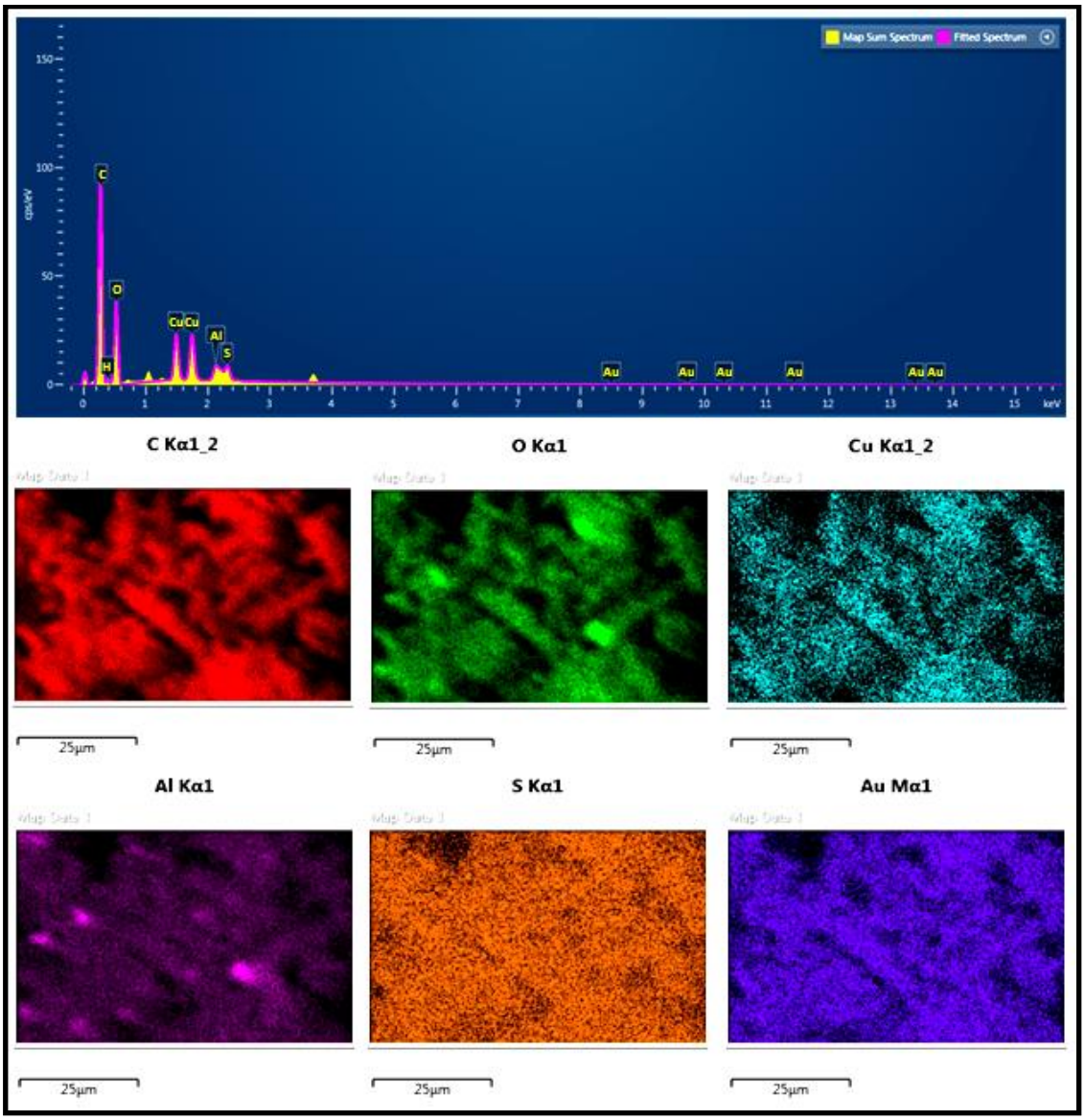

Fig. 6B. Elemental mapping of humic acid supported ionic liquid

The size and morphology of HASIL was obtained by TEM (**Fig. 7**). The images revealed particles with an average size of 166 nm and 250 nm (standard deviation: ± 14 nm calculated by ImageJ, see: particle histogram). The particles formed aggregates with no uniform size and fractal feature, however, few particles were ellipsoidal in shape **(Fig. 7A** and **7C)**. The observed size of the smallest particle was approximately 83 nm **(Fig. 7**: particle histogram).

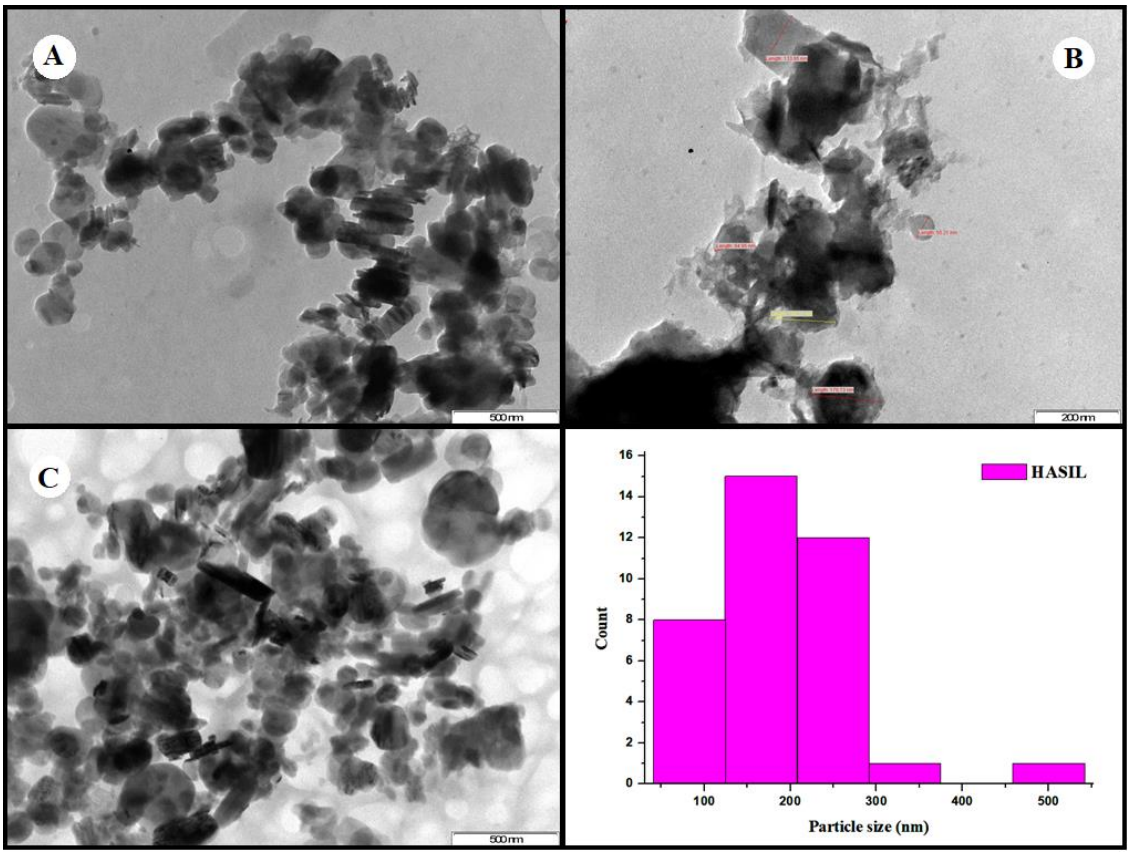

Fig. 7. TEM images of humic acid supported ionic liquid and the particle size

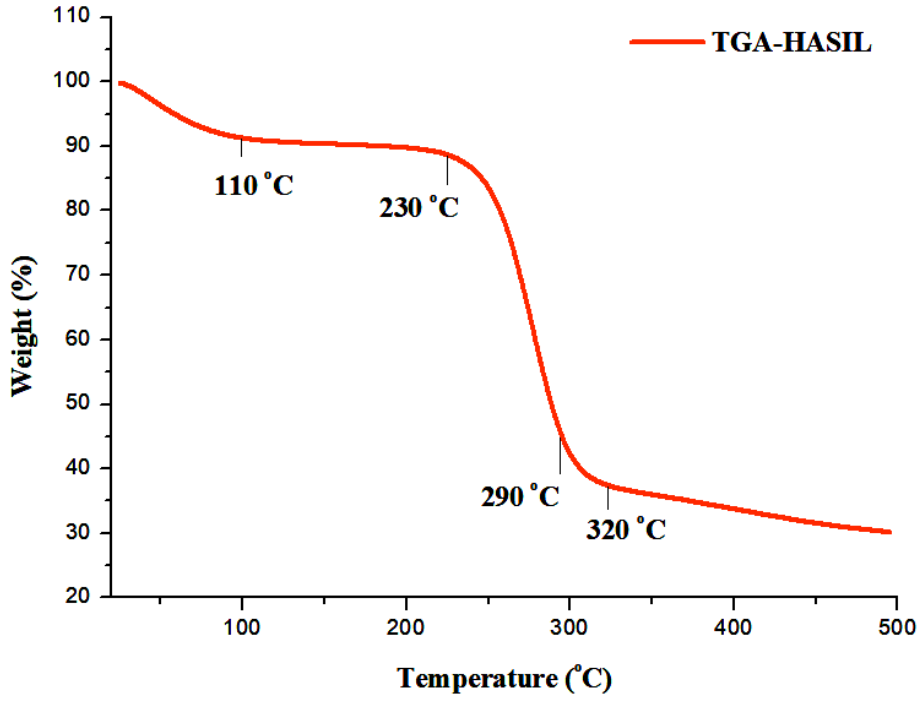

Fig. 8. TGA curve of humic acid supported ionic liquid

The TGA curve (**Fig. 8**) showed that in the temperature range 25-500℃, the mass loss reached about 60 % which suggested possible decomposition of organic components and condensation of hydroxyl groups at high temperatures (Sirbu *et al*., 2010). The mass loss at 110℃ was due to the loss of a water molecule. It was observed that the decomposition process started at nearly 230℃ and ended at 320℃ with a mass loss range of 50-60 %. A temperature range of 244℃ - 390℃ was reported for a [bmim]SCN heterogeneous catalyst thereby suggesting a strong interaction existed between the ILs and HA (Dharaskar *et al*., 2016).

The DSC method is convenient as it is a rapid technique for characteristic curves, whose variation in enthalpy is associated with phase changes in mineral or soil organic matter, reflecting events related to structures and chemical compositions (Kucerík *et al*., 2005; Gibbs *et al*., 2001; Valkova *et al*., 2007).

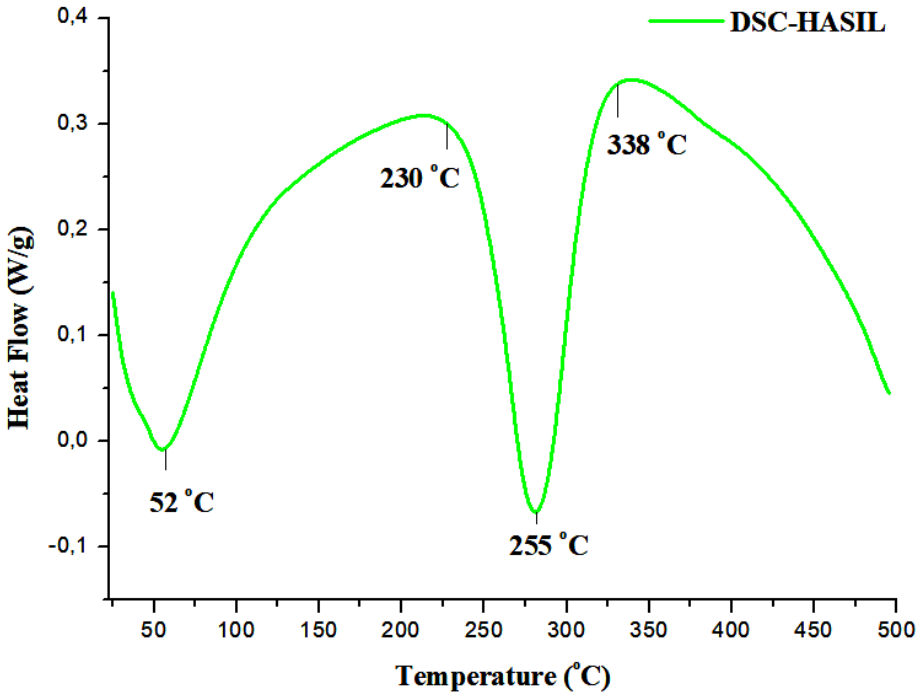

Fig. 9. DSC curve of humic acid supported ionic liquid

The areas under the DSC curves were divided into two groups representing different degrees of resistance to thermal oxidation: a) 230-338℃, which was mostly attributed to labile organic matter, mainly comprising phenolic hydrates and other aliphatic compounds. Nevertheless, decarboxylation and dehydration (removal of OH groups during the formation of the interaction between humic acid and [bmim]SCN) should be

considered and b) 35-175°C, mostly attributable to organic matter, such as polyphenols and polycondensed aromatic substances including HA and black carbon (Dell'Abate *et al*., 2002; Fernandez *et al*., 2011). The temperature of maximum combustion peaks were observed at 230°C and 338°C with two exothermic peaks evident (**Fig. 9)**.

The FTIR spectrum (**Fig. 10**) exhibited a strong stretching band at 3289 cm^{-1} which was assigned to the OH stretch of HA. The other absorption frequencies (cm^{-1}) were observed at 1210 for C-N, 1652 for C=O, 1487 for C=C, 1055 for -C-O and bending frequencies at 1742 for N-H, 1368 for -C-H and 754 for -CH=CH-.

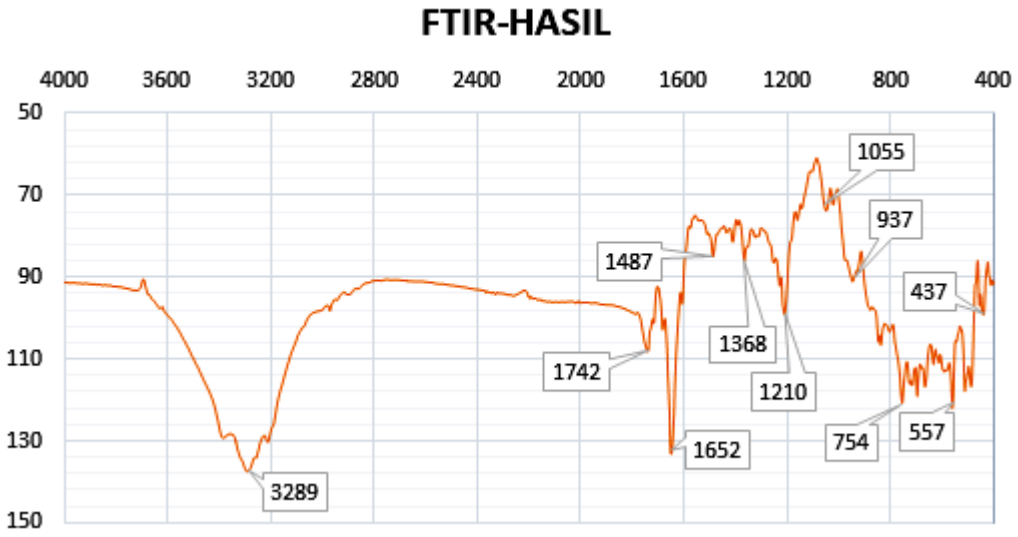

Fig. 10. FTIR spectrum of humic acid supported ionic liquid

The absorption bands (cm^{-1}) were also observed at 557 for Cu-O and 437 for Cu-N. The absorption at 937 cm^{-1} was assigned to –N-O-Cu. This confirmed the formation of –N-O---Cu bond (Sajila *et al*., 2014). These results suggested that Cu was adsorbed on the bulk humic material. It is suggested that the procedure adopted for the preparation of HASIL, where the hydroxyl and carboxylic groups are present in their dissociated form, could create favourable conditions for strong interactions with the positive charges of ionic liquid.

After the successful characterization of HASIL, its catalytic activity was then investigated in a one-pot three-component synthesis of quinolinyl, quinolonyl and indolyl pyran derivatives. The starting materials, 2-chloroquinoline-3-carbaldehyde (CFQ), 2-chloro-6-methylquinoline-3-carbaldehyde (CMFQ) and 2-chloro-7-fluoroquinoline-3-

carbaldehyde (CFFQ) were prepared by the Vilsmeier-Haack reaction (Ambika *et al.*, 2005). The desired starting material, 2-methoxyquinoline-3-carbaldehyde derivatives (MQCs) (**30** and **51**), were synthesized from the reaction of K_2CO_3 with CFQ, CMFQ and CFFQ as discussed in Chapter Three. The quinolone starting materials, 2-oxo-1,2-dihydroquinoline-3-carbaldehyde derivatives were prepared from the reaction of glacial CH_3COOH with corresponding carbaldehyde derivatives. Indole starting material 3-(3*H*-indol-3-yl)-3-oxopropanenitrile (IOPN) was synthesized by the reported literature (Venkatanarayana and Dubey, 2013).

Initially, an equimolar mixture (1 mmol) of the MQC (**30**), malononitrile (**9**) and dimedone (**5**), in ethanol and without catalyst, was investigated. TLC was used to monitor the reaction progress: no products were obtained even up to 24 h. When the same reaction was investigated with a catalytic amount (10 mol %) of HASIL, after 3 h a new product was observed on the TLC plate. The reaction mixture was then subjected to column chromatography for purification. A solvent ratio of 1:3 of ethyl acetate: petroleum ether solvent system resulted in a product of 52 % yield. When the reaction was investigated under microwave irradiation (MW) at 100 W, within 10 minutes the new spot was observed on TLC. Hence MW irradiation became the method of choice for synthesis of new quinolinyl, quinolonyl and indolyl pyrans (**Scheme 1-5**).

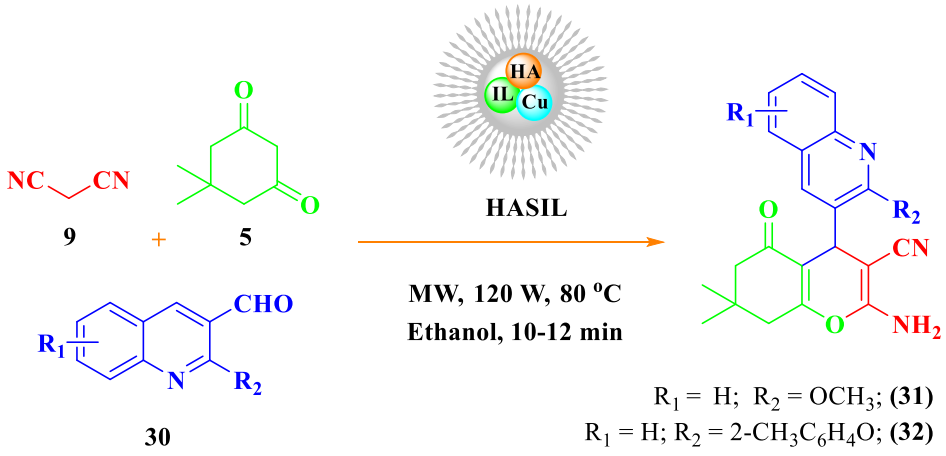

R_1 = H; R_2 = OCH_3; **(31)**
R_1 = H; R_2 = 2-$CH_3C_6H_4O$; **(32)**
R_1 = 7-F; R_2 = OCH_3; **(36)**
R_1 = 6-CH_3; R_2 = Cl; **(41)**
R_1 = 6-CH_3; R_2 = OCH_3; **(42)**

Scheme 1. Synthesis of quinolinyl-*4H*-pyrans (**31**, **32**, **36**, **41** and **42**) in the presence of HASIL under microwave irradiation

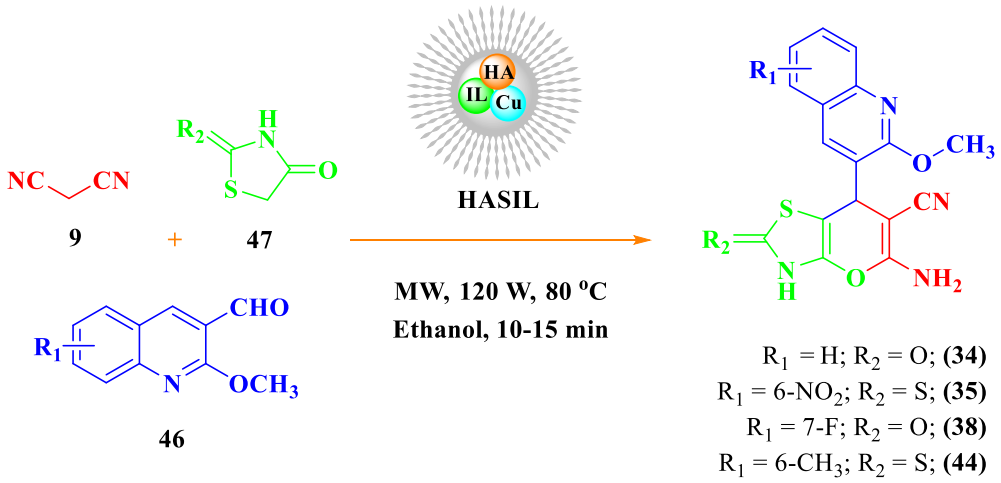

Scheme 2. Synthesis of quinolinyl-*4H*-pyrans (**34**, **38**, **35** and **44**) in the presence of HASIL under microwave irradiation

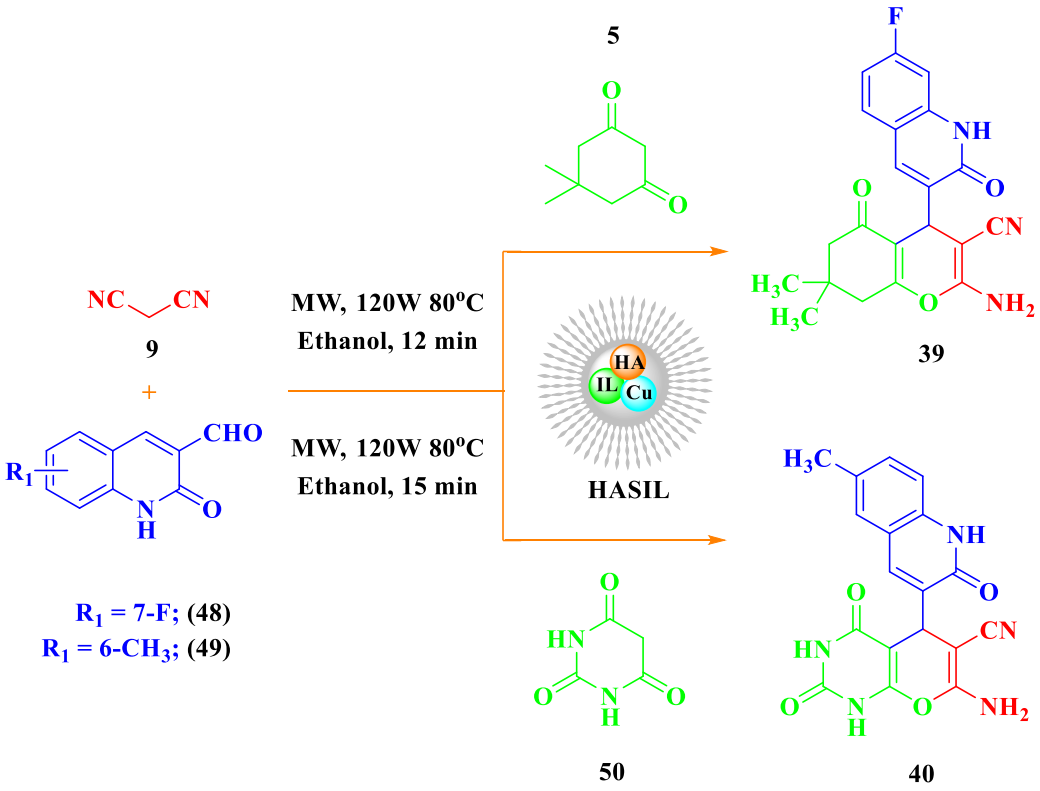

Scheme 3. Synthesis of quinolonyl-*4H*-pyrans (**39** and **40**) in the presence of HASIL under microwave irradiation

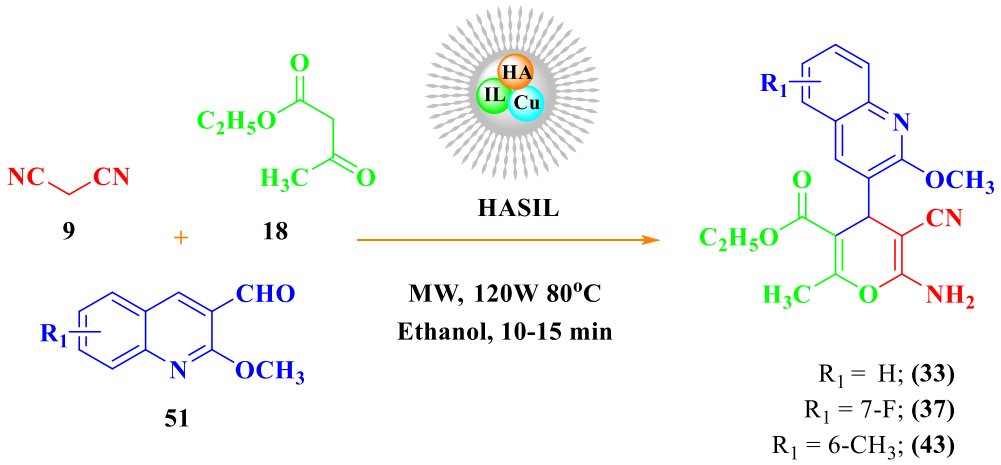

Scheme 4. Synthesis of quinolinyl-*4H*-pyrans (**33**, **37** and **43**) in the presence of HASIL under microwave irradiation

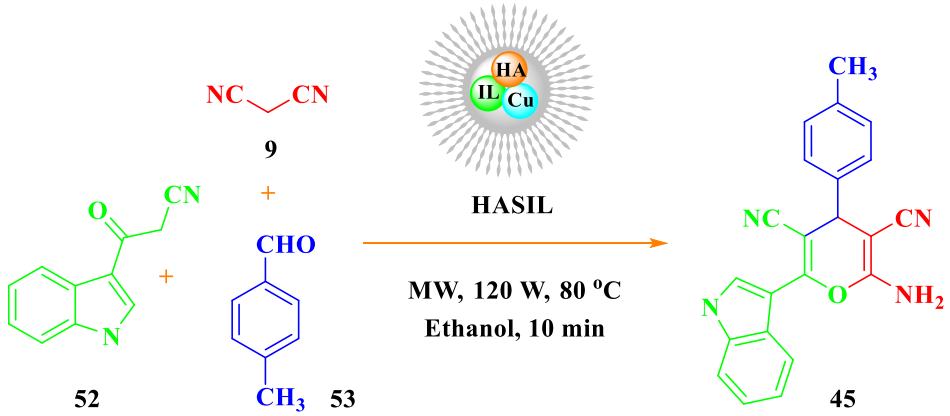

Scheme 5. Synthesis of indolyl-*4H*-pyran (**44**) in the presence of HASIL under microwave irradiation

The structure was confirmed by FTIR, ^{1}H-NMR, ^{13}C-NMR and elemental analysis. As a typical characterization of structures, **31** was then selected.

The FTIR spectrum (**Fig. 4.1**, Appendix IV) of **31** showed stretching frequencies (cm^{-1}) at 2253 for C≡N, 1571 for C=N, 1216 for C-N, 2970 for CH, 1637 for C=C, 1752 for C=O, 2940 for OCH_3 and 3028 for NH. The ^{1}H-NMR spectrum (**Fig. 4.2**) of **31** showed six singlets for C<u>H</u> (C4') at δ 4.68, N<u>H</u>$_2$ (C12') at δ 4.59, methyl proton broad singlet (C<u>H</u>$_3$, C10') at δ 1.44, broad singlet of (C<u>H</u>$_3$, C9') at δ 1.05, broad singlet of OC<u>H</u>$_3$ at δ 4.08 and quinolinyl proton singlet C4, at δ 7.91. The dimedone protons (C<u>H</u>$_2$) showed a

quartets at δ 2.48 and δ 2.22 for C8'-H and C6'-H, respectively. The ^{13}C-NMR spectrum (**Fig. 4.3**) showed the carbonyl group C5' (C=O) at δ 195.94. The methoxy group C9 (OCH_3) was assigned to δ 53.47. The methyl carbon C9' at δ 27.02 and C10' methyl carbon at δ 29.30, was observed. The carbon C6' (CH_2) showed a peak at δ 50.58, C8' showed a peak at δ 40.79. The CH (C4') carbon showed a peak at δ 32.17 and the carbonitrile CN was observed at δ 111.83. The pyran ring carbon atoms C3' at δ 60.83 and in the same pyran ring, C2' at δ 160.15 and C8b' at δ 158.65, were observed. The dimedone carbonyl carbon C7' was identified at δ 32.77. The quinolinyl carbon C3 was observed at δ 125.28 and C=N in the quinolinyl ring showed a peak at δ 162.93 and C4 showed a peak at δ 137.87. The selected ^{1}H-NMR and ^{13}C-NMR chemical shifts of **31** is shown in **Fig. 11**.

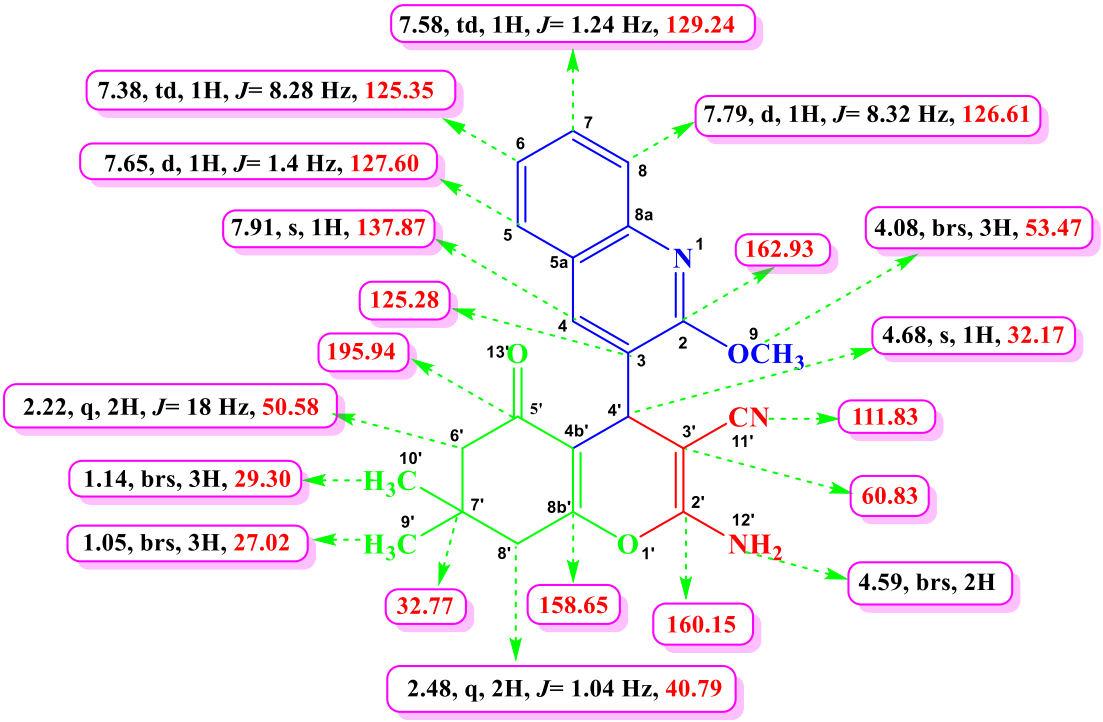

Fig. 11. Selected ^{1}H-NMR and ^{13}C-NMR chemical shifts of **31**

The structure was further confirmed on the basis of 2D NMR spectral studies. The ^{13}C, ^{1}H-COSY correlation of carbon signals at δ 137.87, 129.24, 127.60, 126.61, 125.35, 124.08, 53.47, 50.58, 40.79, 32.17, 29.30 and 27.02 were assigned to C4, C7, C5, C8, C6, C4b', C9, C6', C8', C4', C10' and C9', respectively. The carbon signal at δ 137.87 was due to the quinolinyl carbon (C4) and the spectrum is shown in **Fig. 4.4**.

The ^{1}H, ^{1}H-COSY spectrum (**Fig. 4.5)** revealed the correlation between quartet of C6' (C<u>H</u>$_2$) proton at δ 2.22 and singlet of C<u>H</u>$_3$ (C9') proton δ 1.05. The C9' (C<u>H</u>$_3$) proton at δ 1.05 correlated with quartet of C6' (C<u>H</u>$_2$) proton at δ 2.22.

The ^{1}H, ^{1}H-NOESY spectrum (**Fig. 4.6**) revealed the singlet protons (N<u>H</u>$_2$) at δ 4.59 was coupled with a quartet of C6' (CH_2) at δ 2.22.

The HMBC spectrum **(Fig. 4.7**) showed the long-range correlations as follows: the proton C4'-H, (CH) group was coupled with C3' of pyran ring carbon at δ 60.83 and C11' carbonitrile CN carbon at δ 111.83, quinolinyl carbon C3 at δ 125.28 and dimedone carbons C5' at δ 195.94 and C4b' at δ 124.08.

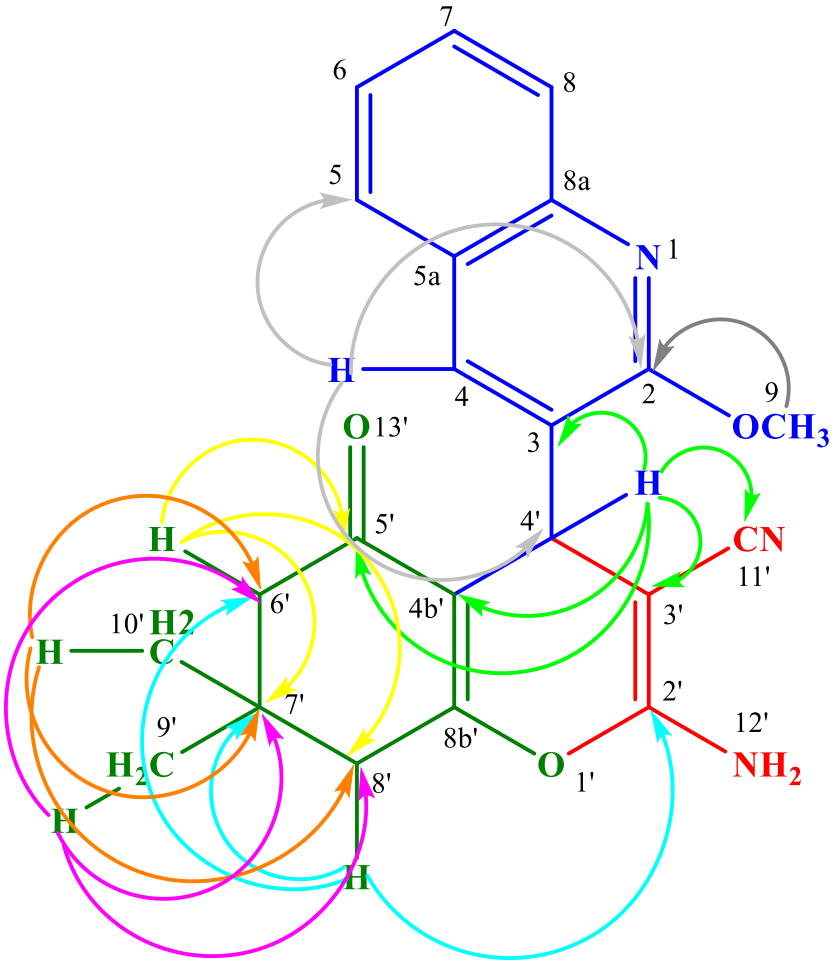

Fig. 12. Selected HMBC correlation spectrum of **31**

This correlation of C4'-<u>H</u> to the pyran ring carbon (C3'), carbonitrile carbon (C11'), quaternary carbon (C3) of quinoline ring and carbons C5' and C4b' of dimedone

indicated that the three groups were attached to C4' (CH). Thus it was evident that three different moieties were bonded to a common carbon (C4') and hence added valuable information to **31**. The selected ^{1}H-NMR, ^{13}C-NMR and HMBC chemical shifts are shown in **Fig. 12**.

The C4-H, quinoline proton was coupled with C4' at δ 32.17, quinolinyl carbons (C5) at δ 127.60 and (C2) at δ 163.92. The C6'-H of dimedone was coupled with C7' at δ 32.77, C8' (40.79) and C5' (195.94). The C8'-H proton was coupled with C7' at δ 32.77, C6' (CH_2) at δ 50.58 and C2' at δ 160.15. The C9'-H (CH_3) was coupled with C2 at δ 162.93. The C10'-H was coupled with C7' at δ 32.77, C8' at δ 40.79 and C6' (CH_2) carbon at δ 50.58. The quinolinyl proton C4-H was coupled with C4' (CH) carbon at δ 32.17, quinolinyl carbons (C5) at δ 127.60 and C2 at δ 162.93. The selected HMBC correlations of **31** is shown in **Table 1.**

Table 1. Selected HMBC correlations of **31**

Entry	Protons	Correlated carbons
1	C4'-H (s, 1H) at δ 4.68 ppm	C3' (60.83), C11' (111.83), C3 (125.28), C5' (195.94) and C4b' (124.08)
2	C4-H (s, 1H) at δ 7.91 ppm	C4' (32.17), C5 (127.60) and C2 (163.92)
3	C6'-H (q, 2H) at δ 2.22 ppm	C7' (32.77), C8' (40.79) and C5' (195.94)
4	C8'-H (q, 2H) at δ 2.48 ppm	C7' (32.77), C6' (50.58) and C2' (160.15)
5	C9'-H (brs, 3H) at δ 1.05 ppm	C2 (162.93)
6	C10'-H (brs, 3H) at δ 1.44 ppm	C7' (32.77), C8' (40.79) and C6' (50.58)
7	C4-H (s, 1H) at δ 7.91 ppm	C4' (32.17), C5 (127.60) and C2 (162.93)

Based on the above spectral details and its elemental analysis (Anal. Calc. for $C_{22}H_{21}N_3O_3$: C, 70.38; H, 5.64; N, 11.19; %. Found: C, 70.36; H, 5.65; N, 11.20; %), the structure was confirmed as 2-amino-4-(2-methoxyquinolin-3-yl)-7,7-dimethyl-5-oxo-5,6,7,8-tetrahydro-*4H*-chromene-3-carbonitrile **(31)**.

To determine the effect of solvents, acetonitrile, dichloromethane, ethanol, water and ethanol-water (1:1) were investigated (**Table 2**). It was found that ethanol gave a high yield of 97 %. The yield decreased to 35 % when other solvents were used. Ethanol is a very polar molecule due to its hydroxyl (OH) group, with the high electronegativity of

oxygen allowing hydrogen bonding to take place with other molecules (Narten and Habenschuss, 1984). This could enable the reaction to occur faster resulting in a maximum yield based on a set time frame.

Table 2. Effect of solvents on the synthesis of quinolinyl-*4H*-pyrans[a]

Entry	Solvent	Time (min)	Yield (%) [b]
1	Acetonitrile	15	73
2	Dichloromethane	15	71
3	Ethanol	10	97
4	Methanol	15	88
5	Water	20	35
6	Ethanol-Water	15	40

[a] Reaction conditions: aldehyde (1 mmol), malononitrile (1 mmol), 1,3-diketone (1 mmol) and HASIL (10 mol%) were added to the ethanol as solvent (15 mL) under microwave irradiation (120 W) at 80℃.

[b] Isolated yields.

When the model reaction was conducted in the presence of 5 mol % of HASIL, the isolated yield of **31** was 71 %. In another attempt, a trace amount of **31** was obtained when HA was used (**Table 3,** entry 1). It was observed that in the presence of 10 mol % of HASIL, the yield of **31** substantially increased to 97 % within 10 minutes (**Table 3,** entry 3). However, on further increasing the amount of the HASIL catalyst to 15 mol % and 20 mol %, no improvements in the yield were observed (**Table 3**, entries 4 and 5). This showed that the best yield of **31** was obtained when 10 mol % of HASIL was used.

Table 3. Optimization of humic acid supported ionic liquid (HASIL) catalyst

Entry	Catalyst	Mol %	Time (min)	Yield (%) [b]
1	HA	25	20	Trace
2	HASIL	5	15	71
3	HASIL	10	10	97
4	HASIL	15	15	90
5	HASIL	20	15	90

[b] Isolated yield

To report the effect of MW irradiation, evaluate and compare normal refluxing with MW assisted method, various conventional and unconventional conditions were screened. The results are listed in **Table 4**. Without microwave, **31** was formed in the presence of

HASIL under stirring at room temperature after 24 h. Also when the reaction was conducted at 90℃ and without microwave irradiation for 3 h the yield of the obtained **31** was found to be 38-52 % (**Table 4,** entries 1 and 2). Moreover, the effect of MW irradiation of different powers was investigated. It was observed that the irradiation power of 120 W at 80℃, afforded the best yield of **31**, with 97 % yield after 10 min (**Table 4,** entry 4).

Table 4. Effect of MW irradiation on the synthesis of quinolinyl-*4H*-pyrans [a]

Entry	Power (W)	Time (min)	Yield (%) [b]
1	Without MW (r.t)	24 h	38
2	Without MW (90 ºC)	3 h	52
3	100	20	75
4	120	10	97
5	150	15	90
6	200	15	90

[a] Reaction conditions: aldehyde (1 mmol), malononitrile (1 mmol), 1,3-diketone (1 mmol) and HASIL (10 mol %) were added to the ethanol as solvent (15 mL) under microwave irradiation (120 W) at 80℃.

[b] Isolated yields.

Following the optimisation of the reaction conditions for the synthesis of **31** with high yield, an investigation on the recyclability of HASIL was conducted.

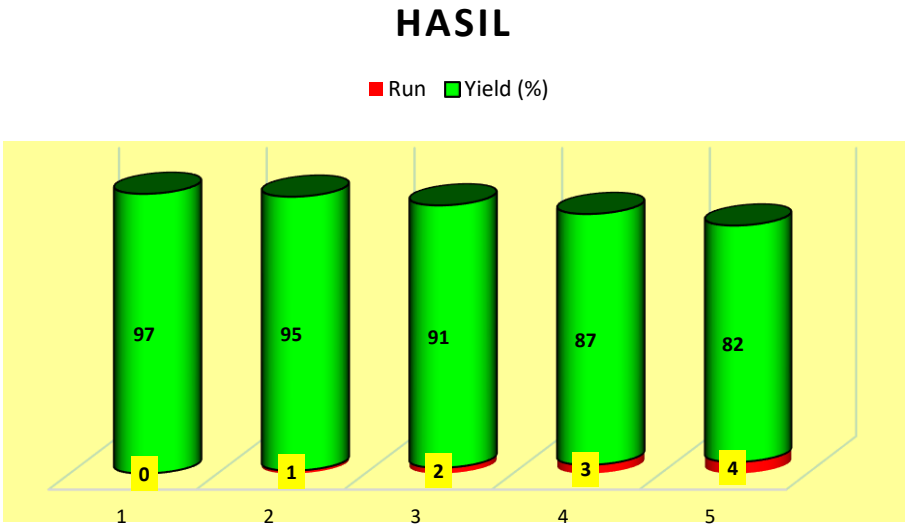

Fig. 13. Recyclability of humic acid supported ionic liquid

Briefly, after synthesis, the reaction mixture was filtered and the solid was washed with MeOH followed by acetone and dried in an oven at 100℃. Five successive cycles of the model reaction were conducted. The activity of HASIL did not show any significant decrease in the yields after five successive runs. It was found that the catalyst displayed good recyclability as there was loss of only 15 % in catalytic activity after five cycles of re-use (**Fig. 13**).

HASIL was further compared with previously reported catalysts (**Table 5,** entries 1-13). The catalysts including montmorillonite K10, $Fe(HSO_4)_3$, TCT, [DMAP-PEG_{1000}-DIL][BF_4], [$PhNMe_2CH_2NMe_2$]Cl^- and DABCO offered more than 90 % yield, however they had drawbacks of long reaction times.

Table 5. Effect of optimization of reported catalysts with HASIL catalyst

Entry	Catalyst	Temp (ºC)	Time	Yield (%)	References
1	Montmorillonite K10	125	30 min	96	Kantevari *et al*., 2007
2	$Fe(HSO_4)_3$	85	25 min	97	Shaterian *et al*., 2008
3	Zwitterionic salt	80	90 min	88	Kundu *et al*., 2010
4	Iodine	125	300 min	87	Das *et al*., 2007
5	TCT	100	40 min	95	Zhang *et al*., 2009
6	*p*-TSA	125	240 min	90	Khodaei *et al*., 2006
7	$K_5CoW_{12}O_{40}.3H_2O$	125	180 min	78	Nagarapu *et al*., 2007
8	[FemSILP]-L-Prolinate	100	300 min	87	Rashikar *et al*., 2010
9	[TEBSA][HSO_4]	120	10 min	89	Hajipour *et al*., 2009
10	[bmim][PF_6]	80	2 hours	90	Rao *et al*., 2012
11	[DMAP-PEG_{1000}-DIL][BF_4]	100	30 min	97	Wang *et al*., 2015
12	[$PhNMe_2CH_2NMe_2$]Cl^-	80	40 min	95	Chen *et al*., 2009
13	DABCO	90	2 hours	97	Tahmassebi *et al*., 2011
14	HASIL	80	10 min	97	Present work

It was found that the protocol used in our study was better suited than that reported with respect to time, temperatures and yields.

Following optimization of the reaction conditions for **31**, the protocol was used to synthesize new quinolinyl pyran derivatives. In summary, 15 novel compounds were synthesized (**Table 6**) and characterized. The FTIR, ^{1}H-NMR, ^{13}C-NMR and elemental analysis for all the synthesized compounds are available in **Appendix IV**. In summary, the one-pot multi-component synthesis by microwave irradiation in the presence of a catalytic amount of a new catalyst HASIL was successfully achieved.

Table 6. Synthesis of quinolinyl-*4H*-pyrans by using **HASIL** under MW conditions

Entry	Aldehydes	1,3-Diketones	Product	Product	Time (min)	Yield (%) [b]
1	$C_{11}H_9NO_2$	$C_8H_{12}O_2$	$C_{22}H_{21}N_3O_3$	**31**	10	97
2	$C_{17}H_{13}NO_2$	$C_8H_{12}O_2$	$C_{28}H_{25}N_3O_3$	**32**	10	96
3	$C_{11}H_9NO_2$	$C_6H_{10}O_3$	$C_{20}H_{19}N_3O_4$	**33**	10	96
4	$C_{11}H_9NO_2$	$C_3H_3NO_2S$	$C_{17}H_{12}N_4O_3S$	**34**	12	90
5	$C_{11}H_8N_2O_4$	$C_3H_3NOS_2$	$C_{17}H_{11}N_5O_4S_2$	**35**	15	88
6	$C_{11}H_8FNO_2$	$C_8H_{12}O_2$	$C_{22}H_{20}FN_3O_3$	**36**	12	89
7	$C_{11}H_8FNO_2$	$C_6H_{10}O_3$	$C_{20}H_{18}FN_3O_4$	**37**	14	92
8	$C_{11}H_8FNO_2$	$C_3H_3NO_2S$	$C_{17}H_{11}FN_4O_3S$	**38**	15	87
9	$C_{10}H_6FNO_2$	$C_8H_{12}O_2$	$C_{21}H_{18}FN_3O_3$	**39**	12	90
10	$C_{11}H_9NO_2$	$C_4H_4N_2O_3$	$C_{18}H_{13}N_5O_4$	**40**	15	85
11	$C_{11}H_8ClNO$	$C_8H_{12}O_2$	$C_{22}H_{20}ClN_3O_2$	**41**	12	89
12	$C_{12}H_{11}NO_2$	$C_8H_{12}O_2$	$C_{23}H_{23}N_3O_3$	**42**	10	93
13	$C_{12}H_{11}NO_2$	$C_6H_{10}O_3$	$C_{21}H_{21}N_3O_4$	**43**	10	95
14	$C_{12}H_{11}NO_2$	$C_3H_3NOS_2$	$C_{18}H_{14}N_4O_2S_2$	**44**	10	93
15	C_8H_8O	$C_{11}H_8N_2O$	$C_{22}H_{16}N_4O$	**45**	10	92

[b] Isolated yields

A suggested mechanism is presented in **Scheme 6**. The active methylene group of malononitrile **(2)** attacked the carbonyl carbon of aldehyde **(1)** and underwent a Knoevenagel condensation to form **3** with loss of water. The methine carbon of the Knoevenagel product **(3)** was activated by HASIL and it reacted with C-H activated compound by a Michael addition to produce intermediate **5**. Thereafter, **5** underwent intramolecular cyclization to form **6** which then underwent tautomerism to produce **7**.

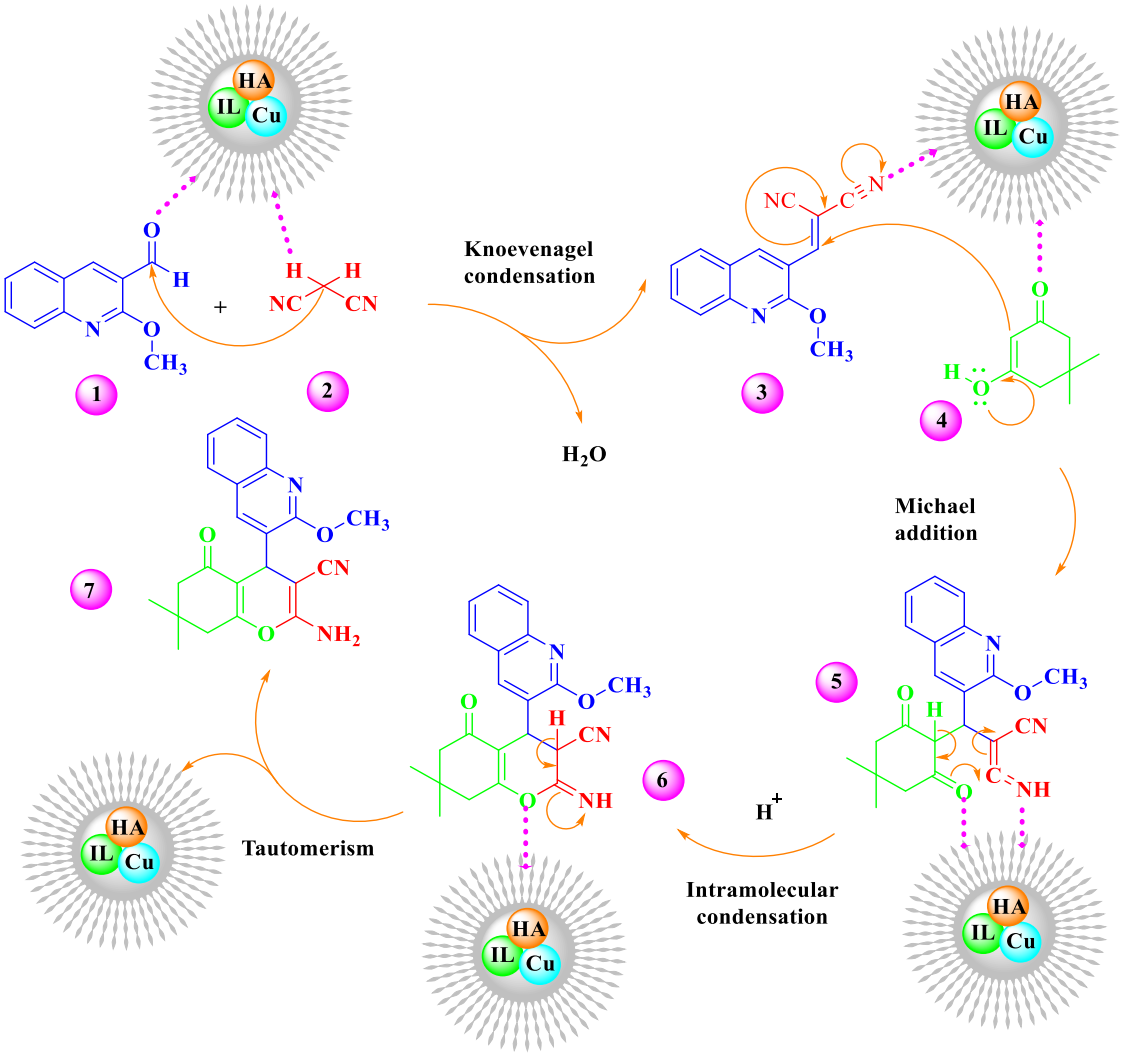

Scheme 6. Suggested mechanism for HASIL promoted synthesis of quinolinyl-*4H*-pyrans

The antibacterial activity was evaluated for QPs by determining the zone of inhibition against a range of Gram-positive (*Bacillus cereus* (*B. cereus*), *Staphylococcus aureus* (*S. aureus*) and *Enterococcus faecalis* (*E. faecalis*)) and Gram-negative (*Escherichia coli* (*E. coli*)) bacteria (**Fig. 14**). It was found that **31**, **34**, **37**, **38** and **43** had preferential activity towards all Gram-positive species tested (**Fig. 14B**).

Moreover, compounds **40** and **44** showed activity towards *S. aureus* only. Interestingly, compound **42** showed its potential antibacterial activity against all species tested. Furthermore, compound **42** was effective against one of Gram-negative (*E. coli*) species (**Table 7**).

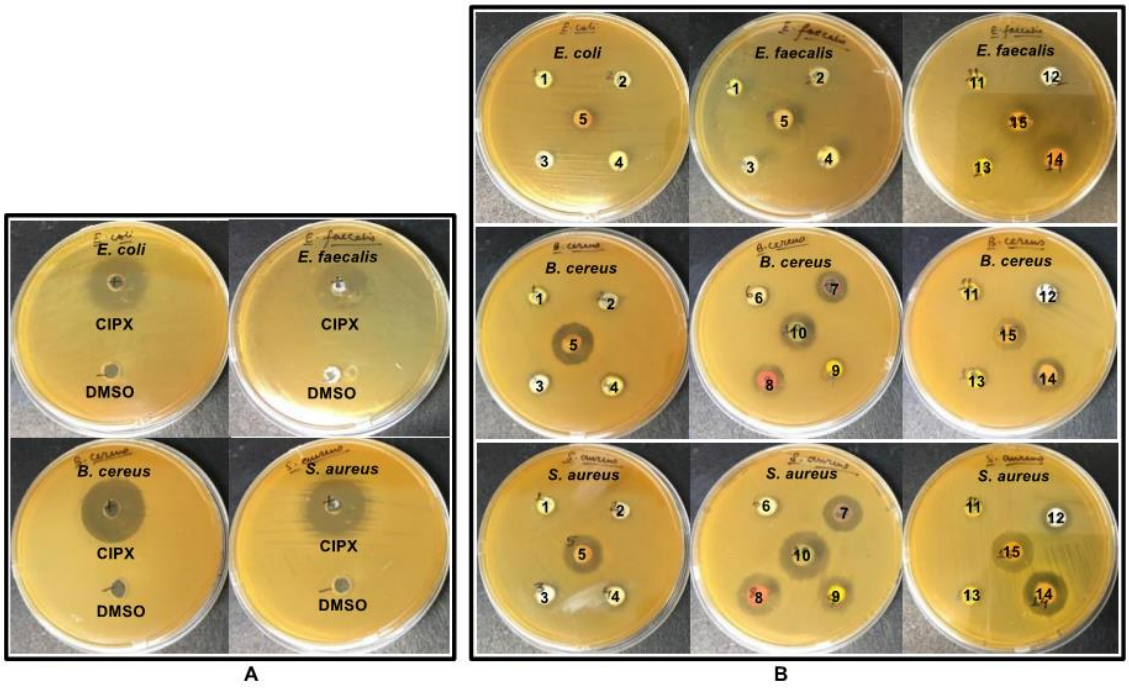

Fig. 14. Growth inhibition of bacterial strains caused by: **(A)** positive (ciprofloxacin) and negative (DMSO) control, **(B)** different derivatives of the (quinolinyl, quinolonyl and indolyl)-*4H*-pyrans

1= **45**; 2= **39**; 3= **32**; 4= **41**; 5= **42**; 6= **33**; 7= **31**; 8= **34**; 9= **44**; 10= **38**; 11= **35**; 12= **40**; 13= **36**; 14= **43**; 15= **37**.

Table 7. Antibacterial screening test of quinolinyl-*4H*-pyrans against Gram-positive and Gram-negative bacterial strains

Bacteria	Zone of inhibition by (quinolinyl, quinolonyl and indolyl)-*4H*-pyran derivatives															Ciprofloxacin (Positive control)
	1	2	3	4	5	6	7	8	9	10	11	12	13	14	15	
Bacillus cereus	0	0	0	0	19 ± 0.2	0	14 ± 0.4	14 ± 0.4	0	16 ± 0.3	0	0	0	13 ± 0.4	12 ± 0.3	25 ± 0.2
Staphylococcus aureus	0	0	0	0	16 ± 0.2	0	17 ± 0.3	16 ± 0.3	15 ± 0.2	21 ± 0.2	0	12 ± 0.4	0	19 ± 0.2	19 ± 0.2	24 ± 0.3
Escherichia coli	0	0	0	0	12 ± 0.3	0	0	0	0	0	0	0	0	0	0	25 ± 0.4
Enterococcus faecalis	0	0	0	0	14 ± 0.4	0	0	0	0	0	0	0	0	17 ± 0.3	13 ± 0.4	20 ± 0.6

1= **45**; 2= **39**; 3= **32**; 4= **41**; 5= **42**; 6= **33**; 7= **31**; 8= **34**; 9= **44**; 10= **38**; 11= **35**; 12= **40**; 13= **36**; 14= **43**; 15= **37**.
Data are means of three replicates (n = 3) ± standard error.

QPs containing methoxy groups (**31, 43** and **44**), sulfur heterocycles (**34** and **38**) fluorinated quinolines (**37** and **38**) and QOP containing quinolonyl ring and methyl group (**40**) showed remarkable antibacterial activity against Gram-positive strains. Interestingly

the QP containing methoxy and methyl groups (**42**) showed potential against both Gram positive and Gram-negative bacteria.

The DPPH radical scavenging assay was used for initial screening of the compounds for their antioxidant activity (Sowndhararajan *et al*., 2013). An antioxidant assay was conducted for all QP derivatives and it was found that compounds **32**, **34**, **35**, **36**, **37**, **38**, **42**, **43** and **44** were effective DPPH scavenging agents. QPs containing a benzyl group (**32**), fused sulfur heterocycles (**34, 35, 38** and **44**), fluorinated quinolines (**36, 37** and **38**) and methyl quinolines (**42** and **43**) showed significant DPPH scavenging activity.

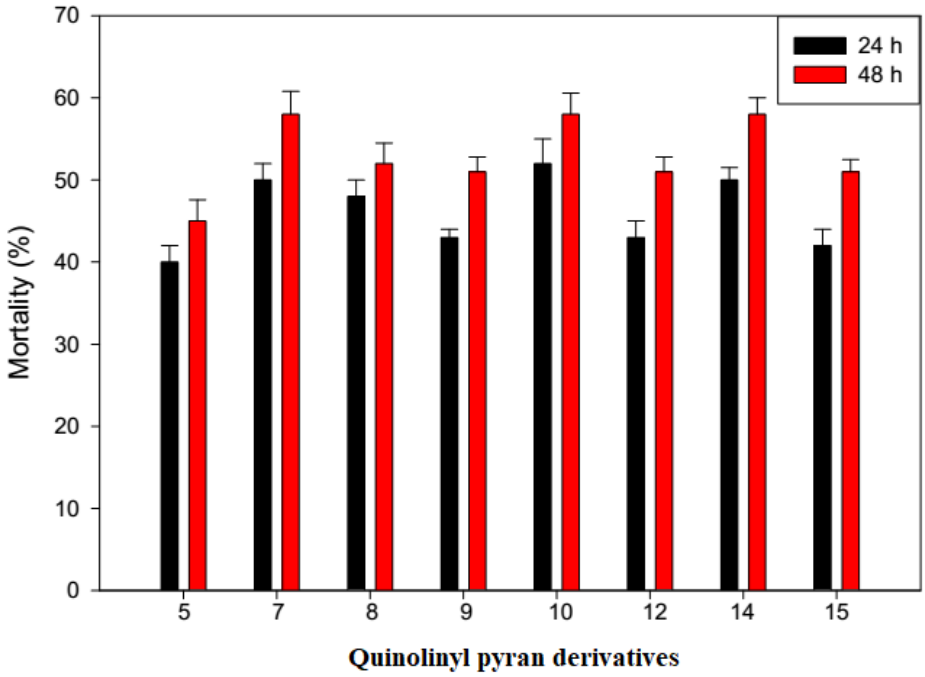

Fig. 15. Toxicity assessment of (quinolinyl, quinolonyl and indolyl)-*4H*-pyrans (**31**, **34**, **37**, **38**, **40**, **42**, **43** and **44**) at different time intervals (24 h and 48 h) in *Artemia salina* (Brine shrimp)

(5= **42**; 7= **31**; 8= **34**; 9= **44**; 10= **38**; 12= **40**; 14= **43**; 15= **37**)

Brine shrimp is one of the most valuable test organisms available for preliminary assessment of toxicity (Rajabi *et al*., 2015). Therefore, the toxicity of all compounds at different intervals (24 h and 48 h), which were active against Gram-positive, Gram-negative or both were evaluated. Amongst all compounds tested, **34**, **37**, **42**, **43** and **44** showed mortality rates below 50% (**Fig. 15**). This suggests that these compounds were less toxic and can be used for further biological and pharmaceutical applications since

less than 50% of brine shrimp mortality rate is considered as safe (Meyer *et al*., 1982). Sulfur-containing QPs (**34** and **44**), fluorinated quinolines (**37**) and methyl quinolines (**43**) showed mortality rates less than 50 %.

The biological importance of quinolinyl pyrans were assessed based on molecular docking. The crystal structure of Mtb gyrase (PDB ID: 4PLB) was used to determine the antibacterial activity of quinolinyl-*4H*-pyran derivatives (Singh *et al*., 2014). The three dimensional structure of Mtb gyrase was prepared in the Chimera software package to carry out molecular docking (Pettersen *et al*., 2004). The ligands (QPs) were built in Chem3D Biodraw and were energetically minized by MM2 method integrated with the same software. Further, ligands were prepared for ionization, conformation and stereoisomers in Discover Studio software packages (Biovia, 2015). Thereafter, molecular docking was conducted using the LibDock module of the Discovery Studio software packages around the bound ligand.

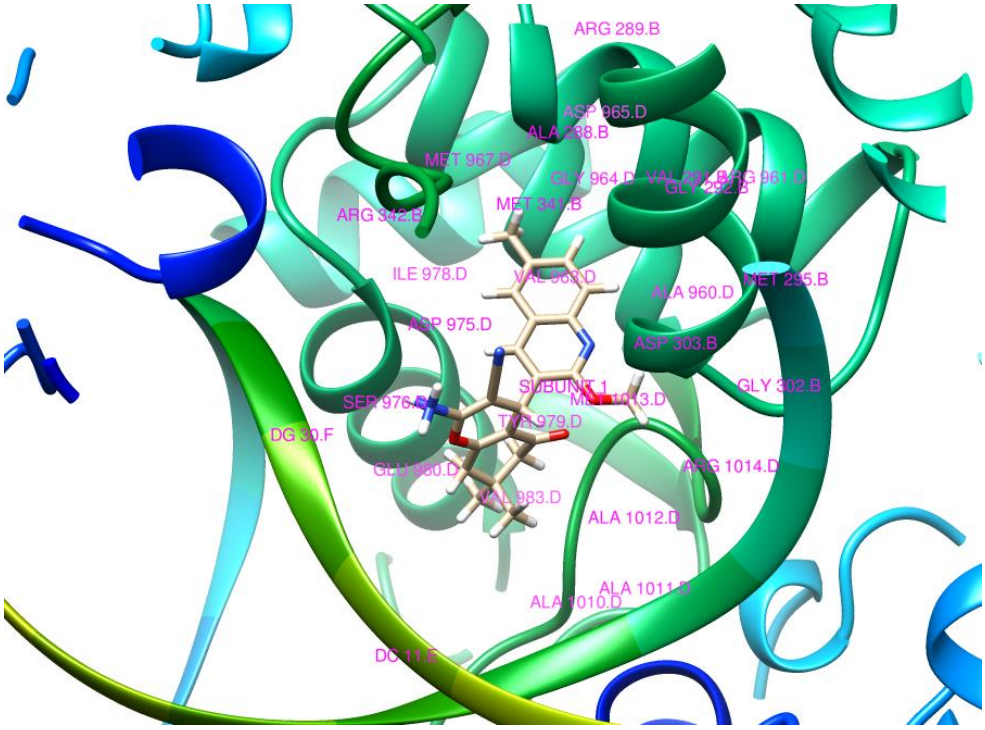

Fig. 16. Ligand binding mode of **42** inside Mtb DNA gyrase

The docking pose of the ligands were ordered based on LibDock score (**Table 8**). The ligands were docked with the scores varying from 74.59 to 96.96 kcal/mol: **31**, **36**, **37, 41** and **42** showed higher binding affinity with the LibDock scores of 96.69, 90.51, 96.30,

92.11 and 96.96, toward Mtb gyrase. **Fig. 16** shows the binding interaction of the ligand (**42**) inside Mtb DNA gyrase.

Table 8. Molecular docking scores of (quinolinyl, quinolonyl and indolyl)-*4H*-pyran derivatives

Entry	Molecule	Absolute Energy	LibDock Score
1	**31**	43.92	96.69
2	**32**	67.44	88.08
3	**33**	59.67	74.59
4	**34**	47.82	91.58
5	**35**	58.46	85.14
6	**36**	43.95	90.51
7	**37**	66.08	96.30
8	**38**	38.40	88.41
9	**39**	61.69	78.97
10	**40**	56.36	79.23
11	**41**	41.66	92.11
12	**42**	49.82	96.96
13	**43**	67.50	82.32
14	**44**	51.36	86.55
15	**45**	---	---
16	**Reference Ligand**	83.08	176.61

4.4. Conclusion

In conclusion, a simple, energy-efficient, convenient, practical method was developed for easy access to a wide range of pharmaceutically functionalized quinolinyl-*4H*-pyrans **(**QPs): QPs were successfully synthesized via a three-component reaction of 2-methoxyquinoline-3-carbaldehydes, malononitrile and 1,3-diketone in the presence of a new humic acid supported 1-butyl-3-methylimidazolium thiocyanate ionic liquid catalyst under microwave irradiation. Seven QPs (**31**, **34**, **37**, **38**, **42**, **43** and **44**) and one QOP (**40**) showed good potential against *B. cereus, S. aureus, E. coli* and *E. faecalis* whilst nine (**32**, **34**, **35**, **36**, **37**, **38**, **42**, **43** and **44**) QPs showed antioxidant activity. The brine shrimp test showed five QPs (**34**, **37**, **42**, **43** and **44**) with mortality rate less than 50 % (48 h). Molecular docking showed higher binding affinity of 96.96 kcal/mol for **42** based on Libdock score with Mtb DNA gyrase. Mild reaction conditions, excellent yields, operational simplicity, clean reaction profiles, energy-efficiency, the use of an

inexpensive and environmentally benign catalyst are the key advantages of the present method of synthesis. Moreover, the reusability of the catalyst is an added advantage.

4.5. Experimental

General synthesis of HASIL

A mixture of [bmim]SCN (5 mmol), in methanol (5 mL), and humic acid (5g) was placed in a round-bottomed flask (100 mL) and stirred at room temperature for 10 h under an inert atmosphere and then dried under reduced pressure until a free flowing powder was obtained. In another 100 mL round-bottomed flask, [bmim]SCN (10 mmol), copper acetate (0.5 mmol) were dissolved in methanol (10 mL) and stirred for 5 minutes. Thereafter, the humic acid pre-treated with ionic liquid was suspended in this solution and the mixture was refluxed for 10 h under an inert atmosphere. The solvent was subsequently evaporated under reduced pressure to produce a free flowing powder which was dried in an oven at 200℃ for 5 h.

Typical procedure for the microwave synthesis of *4H*-pyrans

A catalytic amount (10 mol %) of HASIL was added to a mixture of **30** (1 mmol) and **9** (1 mmol) in ethanol (15 mL) followed by the addition of 1,3-diketone (1 mmol). The reaction tube was placed into a CEM microwave Discover Synthesizer and irradiated at 120 W at a temperature of 80℃ for 10 minutes. The progress of the reaction was monitored by TLC. Following completion, the catalyst was separated by simple filtration. The solvent was evaporated under reduced pressure and the crude product was purified by column chromatography from the eluent (ethyl acetate: petroleum ether, 50 %). The crystallization of *4H*-pyran was performed in ethanol to yield the pure product.

Bacterial strains

The antibacterial activity of each synthesized compound was assessed using four bacterial strains. Two strains of each Gram-positive (*Bacillus cereus, Staphylococcus aureus* and *Enterococcus faecalis*) and Gram-negative (*Escherichia coli*) bacteria were selected. The bacterial strains were provided from the culture collection at Department of Biotechnology and Food Technology, Durban University of Technology, South Africa.

Inoculum preparation

Each bacterial strain was sub-cultured overnight at 37℃ on a Mueller-Hilton agar plate. Further, bacterial cultures were grown in a Mueller-Hilton broth at 37℃, 200 rpm in order to attain the viable count of approximately 10^8 cfu/mL.

Antibacterial activity

The agar well diffusion method was used to evaluate the antibacterial activity. Hundred microliter of ~10^8 cfu/mL bacterial suspension was plated on Mueller-Hinton Agar plates. A well of 6 mm diameter was made using a sterile cork borer and 30 µL of each compound (3 mg/ml) was added in each well and kept at 37 °C for 16 h. The assays were carried out in triplicate. Ciprofloxacin (3 mg/ml) was used as positive control and DMSO (100%) as a negative control.

Antioxidant activity

The antioxidant ability of the quinolinyl-*4H*-pyran derivatives were determined by the decolourization of a methanol solution of 2,2-diphenyl-1-picrylhydrazyl hydrate (DPPH). Hundred microliter of each compound was added separately to 1 mL of 0.1 mM DPPH solution, and a colour change was observed at regular intervals. Rutin hydrate was used as a positive control and methanol (95%) as a negative control.

Toxicity assessment

The brine shrimp larvae (*Artemia salina*) were hatched in sea water for 24-48 h prior to being used. An aliquot of 5 mL sea water containing ten brine shrimp was added to each vial and supplemented with different derivatives of quinolinyl-*4H*-pyran. Derivative concentrations of 300 µg were used in individual vials. Brine shrimp death was observed at regular intervals (24h and 48h) in order to determine the toxic nature of each compound. The data was expressed as % mortality.

References

[1] Abe, I., Oguro, S., Utsumi, Y., Sano, Y., Noguchi, H. 2005. Engineered biosynthesis of plant polyketides: Chain length control in an octaketide-producing plant type III polyketide synthase. Journal of the American Chemical Society, (127) 12709-12716.

[2] Sibi, M. P., Zimmerman, J. 2006. Pyrones to pyrans: Enantioselective radical additions to acyloxy pyrones. Journal of the American Chemical Society, (128) 13346-13347.

[3] Hussein, A. H. M., Gad-Elkareem, M. A., El-Adasy, A. B. A., Khames, A. A., Othman, I. M. 2012. β-Oxoanilides in heterocyclic synthesis: Synthesis and antimicrobial activity of pyridines, pyrans, pyrimidines and azolo, azino pyrimidines incorporating antipyrine moiety. International Journal of Organic Chemistry, (2) 341-351.

[4] Chattapadhyay, T. K., Dureja, P. 2006. Antifungal activity of 4-methyl-6-alkyl-2H-pyran-2-ones. Journal of Agricultural and Food Chemistry, (54) 2129-2133.

[5] Wang, T., Liu, J., Zhong, H., Chen, H., Lv, Z., Zhang, Y., Zhang, M., Geng, D., Niu, C., Li, Y., Li, K. 2011. Synthesis and anti-tumor activity of novel ethyl 3-aryl-4-oxo-3, 3a, 4, 6-tetrahydro-1H-furo [3, 4-c] pyran-3a-carboxylates. Bioorganic & Medicinal Chemistry Letters, (21) 3381-3383.

[6] DeSimone, R. W., Currie, K. S., Mitchell, S. A., Darrow, J. W., Pippin, D. A. 2004. Privileged structures: Applications in drug discovery. Combinatorial Chemistry & High Throughput Screening, (7) 473-493.

[7] Safari, J., Zarnegar, Z., Heydarian, M. 2012. Magnetic Fe_3O_4 nanoparticles as Efficient and Reusable Catalyst for the Green Synthesis of 2-Amino-4 H-chromene in Aqueous Media. Bulletin of the Chemical Society of Japan, (12) 1332-1338.

[8] Bonsignore, L., Loy, G., Secci, D., Calignano, A. 1993. Synthesis and pharmacological activity of 2-oxo-(2H) 1-benzopyran-3-carboxamide derivatives. European Journal of Medicinal Chemistry, (28) 517-520.

[9] Heravi, M. M., Baghernejad, B., Oskooie, H. A. 2008. A novel and efficient catalyst to one-pot synthesis of 2-amino-4H-chromenes by methane sulfonic acid. Journal of the Chinese Chemical Society, (55) 659-662.

[10] Andreani, L.L., Lapi, E. 1960. Aspects and orientations of modern pharmacognosy. Bollettino Chimico Farmaceutico, (99) 583-586.

[11] Hatakeyama, S., Ochi, N., Numata, H., Takano, S. 1988. A new route to substituted 3-methoxycarbonyldihydropyrans; Enantioselective synthesis of (–)-methyl elenolate. Journal of the Chemical Society, Chemical Communications, (17) 1202-1204.

[12] Singh, K., Singh, J., Singh, H. 1996. A synthetic entry into fused pyran derivatives through carbon transfer reactions of 1, 3-oxazinanes and oxazolidines with carbon nucleophiles. Tetrahedron, (52) 14273-14280.

[13] Armesto, D., Horspool, W. M., Martin, N., Ramosand, A., Seoane. C. 1989. Synthesis of cyclobutenes by the novel photochemical ring contraction of 4-substituted 2-amino-3, 5-dicyano-6-phenyl-4H-pyrans. The Journal of Organic Chemistry, (54) 3069-3072.

[14] Maleki, B., Sheikh, S. 1989. One-pot synthesis of 2-amino-2-chromene and 2-amino-3-cyano-4H-pyran derivatives promoted by potassium fluoride. Organic Preparations and Procedures International, (47) 368-378.

[15] Kumar, D., Reddy, V.B., Sharad, S., Dube, U., Kapur, S. 2009. A facile one-pot green synthesis and antibacterial activity of 2-amino-4H-pyrans and 2-amino-5-oxo-5, 6, 7, 8-tetrahydro-4H-chromenes. European Journal of Medicinal Chemistry, (44) 3805-3809.

[16] (a) Elderfield, R. C. 1960. In Heterocyclic Compounds. Ed., John Wiley, New York, London. (b) Wright, C.W., Addae-Kyereme, J., Breen, A. G., Brown, J. E., Cox, M. F., Croft, S. L., Gökçek, Y., Kendrick, H., Phillips, R. M., Pollet, P. L. 2001. Synthesis and evaluation of cryptolepine analogues for their potential as new antimalarial agents. Journal of Medicinal Chemistry, (44) 3187-3194. (c) Sahu, N. P., Pal, C., Mandal, N. B., Banerjee, S., Raha, M., Kundu, A. P., Basu, A., Ghosh, M., Roy, K., Bandyopadhyay, S. 2002. Synthesis of a novel quinoline derivative, 2-(2-methylquinolin-4-ylamino)-N-phenylacetamide-a potential antileishmanial agent. Bioorganic & Medicinal Chemistry, (10) 1687-1693. (d) Bringmann, G., Reichert, Y., Kane, V. V. 2004. The total synthesis of streptonigrin and related antitumor antibiotic natural products. Tetrahedron, (60) 3539-3574. (e) Kouznetsov, V. V., Méndezand, L. Y. V., Gómez, C. M. M. 2005. Recent progress in the synthesis of quinolines. Current Organic Chemistry, (9) 141-161.

[17] Peters, W., Richards, W. H. G. 1984. Antimalarial Drugs II. Ed., Springer Verlag, Berlin Heidelberg, New York, Tokyo.

[18] (a) Corral, R. A., Orazi, O. O. 1967. Isolation, structure and synthesis of (±)-ribalinine. Tetrahedron letters, (8) 583-585. (b) Sekar, M., Prasad, K. R. 1998. Quinoline alkaloids: Synthesis of pyrano [2, 3-b] quinolines, khaplofoline, lunacrine, and demethoxylunacrine. Journal of Natural Products, (61) 294-296. (c) Puricelli, L., Innocenti, G., Monache, G. D., Caniato, R., Filippini, R., Cappelletti, E. M. 2002. In vivo and in vitro production of alkaloids by Haplophyllum patavinum. Natural Product Letters, (16) 95-100. (d) Marco, J. L., Carreiras, M. C. 2003. Recent developments in the synthesis of acetylcholinesterase inhibitors. Mini Reviews in Medicinal Chemistry, (3) 518-524.

[19] (a) Ghorab, M. M., Abdel-Hamide, S. G., Farrag, H. A. 2001. Synthesis of novel quinolines, pyranoquinolines, furoquinolines, thieno-quinoline and their effect on the ultrastructure of some pathogenic microorganisms. Acta Poloniae Pharmaceutica, (58) 175-184. (b) Morel, A. F., Larghi, E. L. 2004. First asymmetric total synthesis of (−)-(R)-and (+)-(S)-geibalansine. Tetrahedron: Asymmetry, (15) 9-10.

[20] (a) Metzner, P., Thuillier, A. 1994. Sulfur Reagents in Organic Synthesis. Academic Press, New York. (b) Nudelman, A. 1984. The chemistry of optically active sulfur compounds. Gordon and Breach, New York. (c) Chatgilialoglu, C., Asmus, K. D. 1991. Sulfur-centered reactive intermediates in chemistry and biology. Springer, New York.

[21] Bicking, J. B., Holtz, W. J., Watson, L. S., Cragoe Jr, E. J. 1976. (Vinylaryloxy) acetic acids. A new class of diuretic agents.1. (Diacylvinylaryloxy) acetic acids. Journal of Medicinal Chemistry, (19) 530-535.

[22] Ding, Y., Prasad, V., Chamakura, V. N. S., Smith, K. L., Chang, E., Hong, J., Yao, N. 2009. Synthesis of Tipranavir Analogues as Non-Peptidic HIV Protease Inhibitors. Letters in Organic Chemistry, (6) 130-133.

[23] Inomata, K., Barragué, M., Paquette, L. A. 2005. Diastereo selectivities realized in the amino acid catalyzed aldol cyclizations of triketo acetonides of differing ring size. The Journal of Organic Chemistry, (70) 533-539.

[24] Yamauchi, M., Katayama, S., Watanabe, T. 1982. 2-Methylthiomethylation of 1,3-dicarbonyl compounds and synthesis of 2-methylene-1, 3-dicarbonyl compounds. Synthesis, (11) 935-937.

[25] Wasserscheid, P., Welton, T. 2008. Ionic liquid in synthesis, Wiley-VCH, Weinheim.

[26] Weingärtner, H. 2008. Understanding ionic liquids at the molecular level: facts, problems, and controversies. Angewandte Chemie International Edition, (47) 654-670.

[27] Wassercheid, P., Keim, W. 2000. Ionic liquids-new "solutions" for transition metal catalysis. Angewandte Chemie International Edition, (39) 3772-3789.

[28] Mehnert, C. P. 2005. Supported ionic liquid catalysis. Chemistry-A European Journal, (11) 50-56.

[29] Riisagera, A., Fehrmanna, R., Haumannb, M., Wasserscheidb, P. 2006. Supported ionic liquids: Versatile reaction and separation media. Topics in Catalysis, (40) 91-102.

[30] Gu, Y., Li, G. 2009. Ionic liquids-based catalysis with solids: State of the art. Advanced Synthesis & Catalysis, (351) 817-847.

[31] Van Doorslaer, C., Wahlen, J., Mertens, P., Binnemans, K., De Vos, D. 2010. Immobilization of molecular catalysts in supported ionic liquid phases. Dalton Transactions, (39) 8377-8390.

[32] a) Green G. R., Evans J. M., Vong A. K. 1995. Comprehensive heterocyclic Chemistry II. Permagon Press, Oxford, UK. b) Jin T. S., Wang A. Q., Wang X., Zhang J. S., Li T. S. 2004. A clean one-pot synthesis of tetrahydrobenzo[b]pyran derivatives catalyzed by hexadecyltrimethyl ammonium bromide in aqueous media. Synlett, (5) 871–873.

[33] Evdokimov, N. M., Kireev, A. S., Yakovenko, A. A., Antipin, M. Y., Magedov, I. V., Kornienko, A. 2007. One-step synthesis of heterocyclic privileged medicinal scaffolds by a multicomponent reaction of malononitrile with aldehydes and thiols. The Journal of Organic Chemistry, (72) 3443-3453.

[34] Ding, M., Zhang, L., Guo, H., Zhong, M. 2013. Basic ionic liquid HEAA catalysed one-pot synthesis of novel 2-amino-3-phenylsulfonyl-4H-pyrans derivatives. Journal of Chemical Research, (37) 780-782.

[35] Khurana, J. M., Chaudhary, A. 2012. Efficient and green synthesis of 4H-pyrans and 4H-pyrano [2, 3-c] pyrazoles catalyzed by task-specific ionic liquid

[bmim]OH under solvent-free conditions. Green Chemistry Letters and Reviews, (5) 633-638.

[36] Peng, Y., Song, G., Huang, F. 2005. Tetramethylguanidine-[bmim][BF_4]. An efficient and recyclable catalytic system for one-pot synthesis of 4H-pyrans. Monatshefte für Chemie/Chemical Monthly, (136) 727-731.

[37] Nimbalkar, U. D., Seijas, J. A., Vazquez-Tato, M. P., Damale, M. G., Sangshetti, J. N., Nikalje, A. P. G. 2017. Ionic liquid-catalyzed green protocol for multi-component synthesis of dihydropyrano [2,3-c] pyrazoles as potential anticancer scaffolds. Molecules, (22) 1628.

[38] Shaabani, A., Samadi, S., Badri, Z., Rahmati, A. 2005. Ionic liquid promoted efficient and rapid one-pot synthesis of pyran annulated heterocyclic systems. Catalysis Letters, (104) 39-43.

[39] Wang, Y., Ye, H., Zuo, G., Luo, J. 2015. Synthesis of a novel poly (ethylene glycol) grafted N, N-dimethyl amino pyridine functionalized dicationic ionic liquid and its application in one-pot synthesis of 3, 4-dihydropyrano [3,2-c] chromene derivatives in water. Journal of Molecular Liquids, (212) 418-422.

[40] Kļaviņš, M., Dipāne, J., Babre, K. 2001. Humic substances as catalysts in condensation reactions. Chemosphere, (44) 737-742.

[41] Lü, R., Qu, Z., Lin, J. 2013. Comparative study of interactions between thiophene\pyridine\benzene\heptane and 1-butyl-3-methylimidazolium trifluoromethanesulfonate by density functional theory. Journal of Molecular Liquids, (180) 207-214.

[42] Wilmer, H., Genger, T., Hinrichsen, O. 2003. The interaction of hydrogen with alumina-supported copper catalysts: a temperature-programmed adsorption/temperature-programmed desorption/isotopic exchange reaction study. Journal of Catalysis, (215) 188-198.

[43] Chilom, G., Rice, J. A. 2005. Glass transition and crystallite melting in natural organic matter. Organic Geochemistry, (36) 1339-1346.

[44] Visser, S.A., Mendel, H. 1971. X-ray diffraction studies on the crystallinity and molecular weight of humic acids. Soil Biology and Biochemistry, (3) 259IN17263-262IN18265.

[45] Das, G., Kalita, R. D., Gogoi, P., Buragohain, A. K., Karak, N. 2014. Antibacterial activities of copper nanoparticle-decorated organically modified montmorillonite/epoxy nanocomposites. Applied Clay Science, (90) 18-26.

[46] Xu, D., Zhu, S., Chen, H., Li, F. 2006. Structural characterization of humic acids isolated from typical soils in China and their adsorption characteristics to phenanthrene. Colloids and Surfaces A: Physicochemical and Engineering Aspects (276) 1-7.

[47] Pandey, A. K., Pandey, S. D., Misra, V. 2000. Stability constants of metal-humic acid complexes and its role in environmental detoxification. Ecotoxicology and Environmental Safety, (47) 195-200.

[48] Chen, C., Wang, X., Jiang, H., Hu, W. 2007. Direct observation of macromolecular structures of humic acid by AFM and SEM. Colloids and Surfaces A: Physicochemical and Engineering Aspects, (302) 121-125.

[49] Zhang, J., Dai, J., Wang, R., Li, F., Wang, W. 2009. Adsorption and desorption of divalent mercury (Hg^{2+}) on humic acids and fulvic acids extracted from typical soils in China. Colloids and Surfaces A: Physicochemical and Engineering Aspects, (335) 194-201.

[50] Sîrbu, C., Cioroianu, T., Rotaru, P. 2010. About the humic acids and thermal behaviour of some humic acids. Physics AUC, (20) 120-126.

[51] Dharaskar, S. A., Wasewar, K. L., Varma, M. N., Shende, D. Z., Yoo, C. 2016. Synthesis, characterization and application of 1-butyl-3-methylimidazolium tetrafluoroborate for extractive desulfurization of liquid fuel. Arabian Journal of Chemistry, (9) 578-587.

[52] Kučerík, J., Kovář, J., Pekař, M., Šimon, P. 2005. Evaluation of oxidation stability of lignite humic substances by DSC induction period measurement. Naturwissenschaften, (92) 336-340.

[53] Gibbs, H. A., O'Garro, L. W., Newton, A.M. 2001. Thermogravimetry: A means of estimating the relative fertility of the mineral soils of Barbados. Thermochimica Acta, (374) 137-143.

[54] Válková, D., Kislinger, J., Pekař, M., Kučerík, J. 2007. The kinetics of thermo-oxidative humic acids degradation studied by isoconversional methods. Journal of Thermal Analysis and Calorimetry, (89) 957-964.

[55] Dell'Abate, M. T., Benedetti, A., Trinchera, A., Dazzi, C. 2002. Humic substances along the profile of two typic haploxerert. Geoderma, (107) 281-296.

[56] Fernández, J. M., Plante, A. F., Leifeld, J., Rasmussen, C. 2011. Methodological considerations for using thermal analysis in the characterization of soil organic matter. Journal of Thermal Analysis and Calorimetry, (104) 389-398.

[57] Sajila, M. 2014. IR spectra, magnetic and thermal studies of copper (II) complex of N-hydroxy–N-(4-chloro) phenyl N'(4-fluoro) phenyl benzamidine hydrochloride. Material Science Research India, (11) 63-65.

[58] Ambika, S., Singh, R. M. 2005. Vilsmeier-Haack reagent: A facile synthesis of 2-chloro-3-formylquinolines from N-arylacetamides and transformation into different functionalities. Indian Journal of Chemistry (44B) 1868-1875.

[59] Venkatanarayana, M., Dubey, P. K. 2013. A facile cyanoacetylation of indoles with cyanocetic acid and propionic anhydride. Indian Journal of Chemistry, (52B) 810-813.

[60] Narten, A. H., Habenschuss, A. 1984. Hydrogen bonding in liquid methanol and ethanol determined by X-ray diffraction. The Journal of Chemical Physics, (80) 3387-3391.

[61] Kantevari, S., Vuppalapati, S. V., Nagarapu, L. 2007. Montmorillonite K10 catalyzed efficient synthesis of amido alkyl naphthols under solvent free conditions. Catalysis Communications, (8) 1857-1862.

[62] Shaterian, H. R., Yarahmadi, H., Ghashang, M. 2008. An efficient, simple and expedition synthesis of 1-amidoalkyl-2-naphthols as 'drug like' molecules for biological screening. Bioorganic & Medicinal Chemistry Letters, (18) 788-792.

[63] Kundu, D., Majee, A., Hajra, A., 2010. Zwitterionic-type molten salt: An efficient mild organocatalyst for synthesis of 2-amidoalkyl and 2-carbamatoalkyl naphthols. Catalysis Communications, (11) 1157-1159.

[64] Das, B., Laxminarayana, K., Ravikanth, B., Rao, B. R. 2007. Iodine catalyzed preparation of amido alkyl naphthols in solution and under solvent-free conditions. Journal of Molecular Catalysis A: Chemical, (261) 180-183.

[65] Zhang, P., Zhang, Z. H. 2009. Preparation of amido alkyl naphthols by a three-component reaction catalyzed by 2,4,6-trichloro-1,3,5-triazine under solvent-free conditions. Monatshefte für Chemie-Chemical Monthly, (140) 199.

[66] Khodaei, M. M., Khosropour, A. R., Moghanian, H. 2006. A simple and efficient procedure for the synthesis of amido alkyl naphthols by p-TSA in solution or under solvent-free conditions. Synlett, (6) 916-920.

[67] Nagarapu, L., Baseeruddin, M., Apuri, S., Kantevari, S. 2007. Potassium dodecatungsto cobaltate trihydrate ($K_5CoW_{12}O_{40}\cdot 3H_2O$): A mild and efficient reusable catalyst for the synthesis of amido alkyl naphthols in solution and under solvent-free conditions. Catalysis Communications, (8) 1729-1734.

[68] Rashinkar, G., Salunkhe, R. 2010. Ferrocene labelled supported ionic liquid phase (SILP) containing organocatalytic anion for multi-component synthesis. Journal of Molecular Catalysis A: Chemical, (316) 146-152.

[69] Hajipour, A. R., Ghayeb, Y., Sheikhan, N., Ruoho, A. E. 2009. Brønsted acidic ionic liquid as an efficient and reusable catalyst for one-pot synthesis of 1-amidoalkyl 2-naphthols under solvent-free conditions. Tetrahedron Letters, (50) 5649-5651.

[70] Rao, M. S., Chhikara, B. S., Tiwari, R., Shirazi, A. N., Parang, K., Kumar, A. 2012. A greener synthesis of 2-aminochromenes in ionic liquid and evaluation of their antiproliferative activities. Chemistry & Biology Interface, (2) 362-372.

[71] Wang, Y., Ye, H., Zuo, G., Luo, J. 2015. Synthesis of a novel poly (ethylene glycol) grafted N, N-dimethylaminopyridine functionalized dicationic ionic liquid and its application in one-pot synthesis of 3, 4-dihydropyrano [3, 2-c] chromene derivatives in water. Journal of Molecular Liquids, (212) 418-422.

[72] Chen, L., Huang, X. J., Li, Y. Q., Zhou, M. Y., Zheng, W. J. 2009. A one-pot multicomponent reaction for the synthesis of 2-amino-2-chromenes promoted by N, N-dimethylamino-functionalized basic ionic liquid catalysis under solvent-free condition. Monatshefte für Chemie-Chemical Monthly, (140) 45-47.

[73] Tahmassebi, D., Bryson, J. A. Binz, S. I. 2011. 1,4-Diazabicyclo [2.2.2] octane as an efficient catalyst for a clean, one-pot synthesis of tetrahydrobenzo [b] pyran derivatives via multicomponent reaction in aqueous media. Synthetic Communications, (41) 2701-2711.

[74] Sowndhararajan, K., Kang, S. C. 2013. Free radical scavenging activity from different extracts of leaves of Bauhinia vahlii wight & Arn. Saudi Journal of Biological Sciences, (20) 319-325.

[75] Rajabi, S., Ramazani, A., Hamidi, M., Naji, T. 2015. Artemia salina as a model organism in toxicity assessment of nanoparticles. DARU Journal of Pharmaceutical Sciences, (23) 20.

[76] Meyer, B. N., Ferrigni, N. R., Putnam, J. E., Jacobsen, L. B., Nichols, D. J., McLaughlin, J. L. 1982. Brine shrimp: A convenient general bioassay for active plant constituents. Planta Medica, (45) 31-34.

[77] Singh, S. B., Kaelin, D. E., Wu, J., Miesel, L., Tan, C. M., Meinke, P. T., Olsen, D., Lagrutta, A., Bradley, P., Lu, J., Patel, S. 2014. Oxabicyclooctane-linked

novel bacterial topoisomerase inhibitors as broad spectrum antibacterial agents. ACS Medicinal Chemistry Letters, (5) 609-614.

[78] Pettersen, E. F., Goddard, T. D., Huang, C. C., Couch, G. S., Greenblatt, D. M., Meng, E. C., Ferrin, T. E. 2004. UCSF Chimera-a visualization system for exploratory research and analysis. Journal of Computational Chemistry, (25) 1605-1612.

[79] Biovia, D. S. 2015. Discovery studio modeling environment. San Diego: Dassault Systemes.

Appendix-IV

4.1. 2-Amino-4-(2-methoxyquinolin-3-yl)-7,7-dimethyl-5-oxo-5,6,7,8-tetrahydro-*4H*-chromene-3-carbonitrile (31)

Pale yellow crystals, m.p = 182-184℃; IR ν_{max} (cm^{-1}): 2253 C≡N, 1571 C=N, 1216 C-N, 2970 CH, 1637 C=C, 1752 C=O, 2940 OCH_3, 3028 NH. ^{1}H-NMR: (400 MHz, $CDCl_3$) δ ppm 7.91 (1H, s, Ar-H), 7.79 (1H, d, *J*= 8.32 Hz, Ar-H), 7.65 (1H, d, *J*= 1.4 Hz, Ar-H), 7.58 (1H, td, *J*= 1.24 Hz, Ar-H), 7.38 (1H, td, *J*= 8.28 Hz, Ar-H), 4.68 (1H, s, CH), 4.59 (2H, brs, NH_2), 4.08 (3H, brs, OCH_3), 2.48 (2H, q, *J*= 1.04 Hz, CH_2), 2.22 (2H, q, *J*= 18 Hz, CH_2), 1.14 (3H, brs, CH_3), 1.05 (3H, brs, CH_3). ^{13}C-NMR: (100 MHz, $CDCl_3$) δ ppm 195.94, 162.93, 160.15, 158.65, 137.87, 129.24, 127.60, 126.61, 126.61, 125.35, 125.28, 124.08, 111.83, 60.83, 53.47, 50.58, 40.79, 32.77, 32.17, 29.30, 27.02. Elemental Analysis: Anal. Calc. for $C_{22}H_{21}N_3O_3$: C, 70.38; H, 5.64; N, 11.19; %. Found: C, 70.36; H, 5.65; N, 11.20; %.

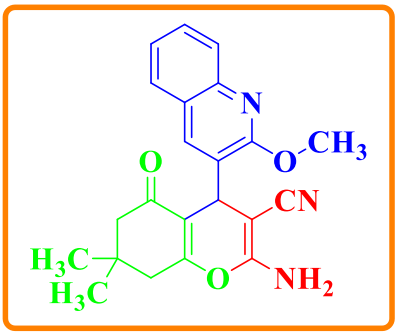

4.2. 2-Amino-7,7-dimethyl-5-oxo-4-(2-(o-tolyloxy)quinolin-3-yl)-5,6,7,8-tetrahydro-*4H*-chromene-3-carbonitrile (32)

Yellow solid, m.p = 209-211℃; IR ν_{max} (cm^{-1}): IR ν_{max} (cm^{-1}): 2246 C≡N, 1577 C=N, 1207 C-N, 2924 CH, 1631 C=C, 1751 C=O, 3327 NH. ^{1}H-NMR: (400 MHz, DMSO-d_6) δ ppm 8.69 (1H, s, Ar-H), 8.05 (2H, d, *J*=7.84 Hz, Ar-H), 7.92 (2H, d, *J*=8.32 Hz, Ar-H), 7.84 (2H, td, *J*=1.36 Hz, Ar-H), 7.63 (2H, td, *J*= 1.04 Hz, Ar-H), 5.21 (1H, s, CH), 4.98 (2H, s, NH_2), 3.01 (3H, brs, CH_3), 2.70 (2H, q, *J*=17.88 Hz, CH_2), 2.41 (2H, q, *J*=16.16 Hz, CH_2), 1.14 (3H, brs, CH_3), 1.12 (3H, brs, CH_3). ^{13}C-NMR: (100 MHz, DMSO-d_6) δ ppm 195.65, 169.07, 154.50, 145.52, 14064, 131.56, 128.06, 127.53, 126.62, 126.60, 113.89, 112.84, 112.61, 107.25, 49.60, 40.46, 40.08, 39.87, 39.67, 39.46, 39.25, 38.83, 33.26, 31.77, 30.50, 28.99, 27.17, 26.06. Elemental Analysis: Anal. Calc. for $C_{28}H_{25}N_3O_3$: C, 74.48; H, 5.58; N, 9.31; %. Found: C, 74.47; H, 5.59; N, 9.33; %.

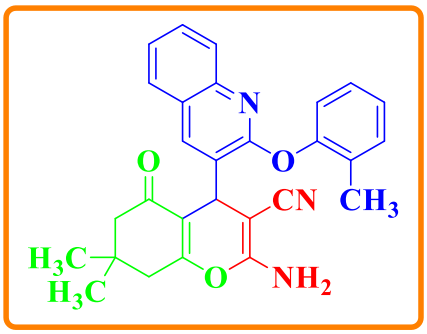

4.3. Ethyl 6-amino-5-cyano-4-(2-methoxyquinolin-3-yl)-2-methyl-*4H*-pyran-3-carboxylate (33)

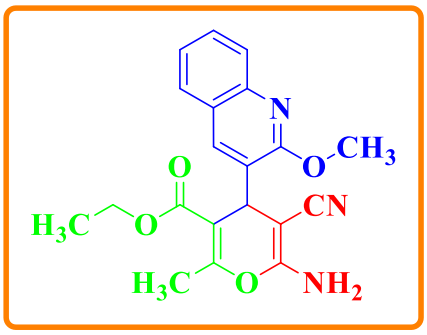

Yellow solid, m.p = 209-211℃; IR ν_{max} (cm^{-1}): 2254 C≡N, 1552 C=N, 1226 C-N, 2970 CH, 1672 C=C, 1722 C=O, 2876 OCH_3, 3361 NH. ^{1}H-NMR: (400 MHz, DMSO-d_6) δ ppm 8.92 (1H, s, Ar-H), 8.21 (1H, d, *J*= 6.40 Hz, Ar-H), 7.78 (1H, dd, *J*=2.52 Hz, Ar-H), 7.52 (1H, dt, *J*=1.12 Hz, Ar-H), 7.30 (1H, t, *J*= 5.56 Hz, Ar-H), 6.98 (2H, brs, NH_2), 4.59 (1H, s, CH), 3.76 (3H, s, OCH_3), 2.59 (2H, q, *J*= 13.52 Hz, CH_2), 1.95 (3H, s, CH_3), 1.23 (3H, s, CH_3). ^{13}C-NMR: (100 MHz, DMSO-d_6) δ ppm 165.40, 158.43, 156.55, 144.83, 128.39, 127.14, 126.77, 119.68, 107.20, 60.10, 57.21, 40.07, 39.86, 39.65, 39.02, 38.82, 38.78, 30.62, 18.07, 13.66. Elemental Analysis: Anal. Calc. for $C_{20}H_{19}N_3O_4$: C, 65.74; H, 5.24; N, 11.50; %. Found: C, 65.76; H, 5.26; N, 11.51; %.

4.4. 5-Amino-7-(2-methoxyquinolin-3-yl)-2-oxo-3,7-dihydro-2H-pyrano[2,3-d]thiazole-6-carbonitrile (34)

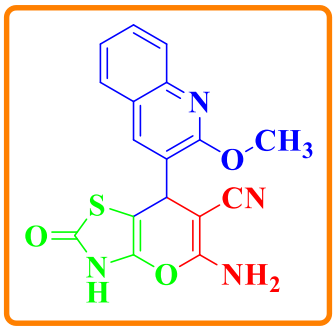

Yellow solid, m.p = 218-220℃; IR ν_{max} (cm^{-1}): 2191 C≡N, 1604 C=N, 1215 C-N, 2970 CH, 1654 C=C, 1751 C=O, 2863 OCH_3, 714 C-S, 2596 S-H, 3393 NH. ^{1}H-NMR: (400 MHz, DMSO-d_6) δ ppm 10.25 (2H, s, NH_2), 8.41 (1H, s, Ar-H), 7.79 (1H, d, *J*=7.44 Hz, Ar-H), 7.56 (1H, t, *J*=7.12 Hz, Ar-H), 7.34 (1H, d, *J*=8.28 Hz, Ar-H), 7.17 (1H, t, *J*=7.24 Hz, Ar-H), 5.13 (1H, s, NH), 4.42 (1H, s, CH), 2.51 (3H, s, OCH_3). ^{13}C-NMR: (100 MHz, $CDCl_3$) δ ppm 159.89, 159.85, 153.12, 150.74, 145.87, 136.85, 136.79, 134.43, 134.29, 134.18, 129.73, 127.76, 126.78, 125.18, 125.16, 124.55, 124.51, 124.33, 120.83, 120.81, 118.20, 118.13, 114.80, 114.62, 113.13, 113.10, 63.63, 63.57, 63.30, 63.23, 54.01, 49.37, 47.84, 16.48, 16.42, 16.20, 16.14. Elemental Analysis: Anal. Calc. for $C_{17}H_{12}N_4O_3S$: C, 57.95; H, 3.43; N, 15.90; %. Found: C, 57.97; H, 3.44; N, 15.92; %.

4.5. 5-Amino-7-(2-methoxy-6-nitroquinolin-3-yl)-2-thioxo-3,7-dihydro-2H-pyrano[2,3-d]thiazole-6-carbonitrile (35)

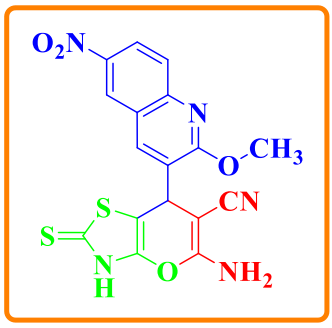

Brown solid, m.p = 249-251℃; IR ν_{max} (cm^{-1}): 2254 C≡N, 1588 C=N, 1047 C-N, 2880 CH, 1608 C=C, 1709 C=O, 2944 OCH_3, 2602 S-H, 1268 C=S, 650 C-S, 3232 NH. ^{1}H-NMR: (400 MHz, DMSO-d_6) δ ppm 8.15 (1H, s, NH), 7.78 (1H, s, Ar-H), 7.65 (2H, d, *J*= 10.24 Hz, Ar-H), 7.55 (1H, d, *J*= 8.44 Hz, Ar-H), 6.80 (2H, brs, NH_2), 4.25 (1H, s, CH), 4.03 (3H, s, OCH_3). ^{13}C-NMR: (100 MHz, $CDCl_3$) δ ppm 150.21, 150.15, 147.07, 146.98, 145.30, 145.16, 139.30, 137.83, 137.78, 130.78, 129.29, 129.12, 129.11, 128.06, 127.90, 127.32, 127.28, 119.92, 114.47, 110.60, 63.99, 63.92, 63.57, 63.49, 52.58, 51.06, 21.55, 16.49, 16.44, 16.14, 16.14, 16.08. Elemental Analysis: Anal. Calc. for $C_{17}H_{11}N_5O_4S_2$: C, 49.39; H, 2.68; N, 16.94; %. Found: C, 49.41; H, 2.70; N, 16.96; %.

4.6. 2-Amino-4-(7-fluoro-2-methoxyquinolin-3-yl)-7,7-dimethyl-5-oxo-5,6,7,8-tetrahydro-*4H*-chromene-3-carbonitrile (36)

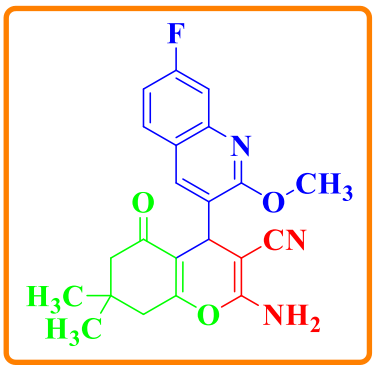

White solid, m.p = 195-197℃; IR ν_{max} (cm^{-1}): 2181 C≡N, 1602 C=N, 1135 C-N, 2970 CH, 1638 C=C, 1678 C=O, 2653 OCH_3, 1007 C-F, 3368 NH. ^{1}H-NMR: (400 MHz, DMSO-d_6) δ ppm 8.03 (1H, s, Ar-H), 7.96 (1H, t, *J*=6.44 Hz, Ar-H), 7.46 (1H, d, *J*=2.52 Hz, Ar-H), 7.33 (1H, t, *J*=6.20 Hz, Ar-H), 7.01 (2H, brs, NH_2), 4.52 (1H, s, CH), 3.96 (3H, s, OCH_3), 2.49 (2H, q, *J*=17.80 Hz, CH_2), 2.24 (2H, q, *J*=16.04 Hz, CH_2), 1.04 (3H, s, CH_3), 0.96 (3H, s, CH_3). ^{13}C-NMR: (100 MHz, $CDCl_3$) δ ppm 155.69, 148.57, 146.43, 146.31, 137.33, 129.20, 129.08, 123.08, 123.04, 122.99, 122.96, 119.70, 118.59, 114.02, 63.67, 63.59, 63.34, 63.27, 58.30, 56.80, 16.43, 16.37, 16.25, 16.19. ^{19}F-NMR: (400 MHz, $CDCl_3$) -107.33. Elemental Analysis: Anal. Calc. for $C_{22}H_{20}FN_3O_3$: C, 67.17; H, 5.12; N, 10.68; %. Found: C, 67.19; H, 5.14; N, 10.70; %.

4.7. Ethyl 6-amino-5-cyano-4-(7-fluoro-2-methoxyquinolin-3-yl)-2-methyl-*4H*-pyran-3-carboxylate (37)

Yellow solid, m.p = 191-193℃; IR ν_{max} (cm^{-1}): 2229 C≡N, 1580 C=N, 1219 C-N, 2919 CH, 1614 C=C, 1708 C=O, 1021 C-F, 3400 NH. ^{1}H-NMR: (400 MHz, DMSO-d_6) δ ppm 8.87 (1H, s, Ar-H), 8.59 (1H, s, Ar-H), 8.02 (1H, d, *J*= 8.04 Hz, Ar-H), 7.83 (2H, s, NH_2), 7.54 (1H, t, *J*=2.88 Hz, Ar-H), 4.43 (1H, s, CH), 4.07 (3H, s, OCH_3), 3.91-3.89 (2H, m, *J*= 16.88 Hz, CH_2), 2.50 (3H, s, CH_3), 2.39 (3H, s, CH_3). ^{13}C-NMR: (100 MHz, $CDCl_3$) δ ppm 176.04, 176.00, 156.24, 155.42, 155.36, 151.51, 151.40, 139.27, 134.26, 126.20, 125.98, 125.80, 123.28, 119.55, 118.32, 112.30, 64.05, 63.98, 63.91, 63.84, 45.62, 44.05, 29.68, 16.45, 16.40, 16.31, 16.26, 14.11. Elemental Analysis: Anal. Calc. for $C_{20}H_{18}FN_3O_4$: C, 62.66; H, 4.73; N, 10.96; %. Found: C, 62.68; H, 4.75; N, 10.95; %.

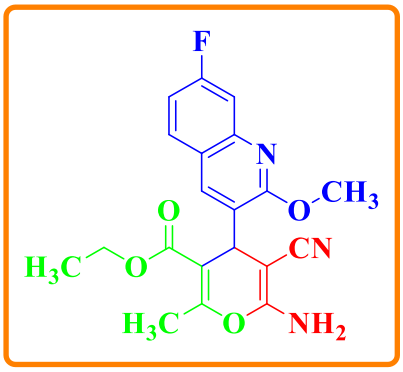

4.8. 5-Amino-7-(7-fluoro-2-methoxyquinolin-3-yl)-2-oxo-3,7-dihydro-2H-pyrano[2,3-d]thiazole-6-carbonitrile (38)

Brown solid, m.p = 205-207℃; IR ν_{max} (cm^{-1}): 2252 C≡N, 1557 C=N, 1292 C-N, 2917 CH, 1621 C=C, 1690 C=O, 2849 OCH_3, 693 C-S, 2606 S-H, 1393 C-F, 3362 NH. ^{1}H-NMR: (400 MHz, $CDCl_3$) δ ppm 8.42 (1H, s, NH), 8.35 (1H, d, *J*= 3.12 Hz, Ar-H), 8.17 (2H, s, NH_2), 7.80 (1H, d, *J* = 5.68 Hz, Ar-H), 7.68 (1H, t, *J*= 7.08 Hz, Ar-H), 7.42 (1H, t, *J*= 7.24 Hz, Ar-H), 4.91 (1H, s, CH), 2.25 (3H, s, OCH_3). ^{13}C-NMR: (100 MHz, $CDCl_3$) δ ppm 206.98, 163.55, 147.90, 147.81, 145.98, 142.30, 137.93, 129.18, 122.84, 121.31, 113.86, 32.97, 32.97, 32.76, 30.92, 22.20, 13.79. Elemental Analysis: Anal. Calc. for $C_{17}H_{11}FN_4O_3S$: C, 55.13; H, 2.99; N, 15.13; %. Found: C, 55.15; H, 2.98; N, 15.15; %.

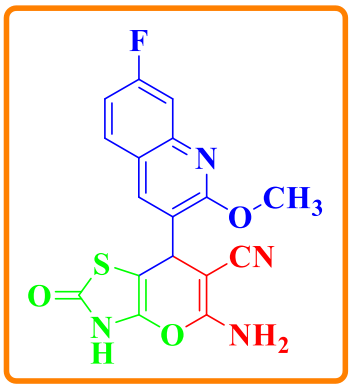

4.9. 2-Amino-4-(7-fluoro-2-oxo-1,2-dihydroquinolin-3-yl)-7,7-dimethyl-5-oxo-5,6,7,8-tetrahydro-*4H*-chromene-3-carbonitrile (39)

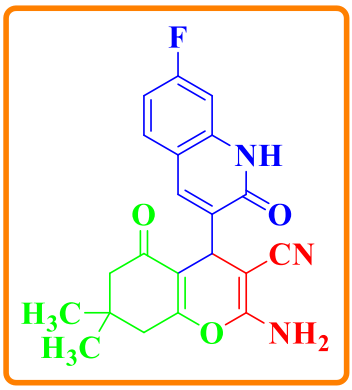

Pale yellow, m.p = 129-131℃; IR ν_{max} (cm^{-1}): 2183 C≡N, 1572 C=N, 1152 C-N, 2979 CH, 1679 C=C, 1722 C=O, 1098 C-F, 3446 NH. ^{1}H-NMR: (400 MHz, DMSO-d_6) δ ppm 8.69 (1H, s, NH), 8.40 (1H, s, Ar-H), 8.10-8.04 (1H, m, *J*= 6.24 Hz, Ar-H), 7.73 (2H, s, NH_2), 7.50 (1H, t, *J*=5.84 Hz, Ar-H), 7.42 (1H, s, Ar-H), 4.09 (1H, s, CH), 2.70-2.57 (2H, m, *J*=17.92 Hz, CH_2), 2.40-2.28 (2H, m, *J*=16.20 Hz, CH_2), 1.25 (3H, s, CH_3), 1.05 (3H, s, CH_3). ^{19}F-NMR: (400 MHz, DMSO-d_6) δ ppm -108.37. ^{13}C-NMR: (100 MHz, $CDCl_3$) δ ppm 195.67, 191.20, 161.94, 140.51, 138.18, 130.13, 126.39, 126.18, 123.93, 122.47, 121.00, 120.52, 119.06, 117.65, 109.32, 108.72, 108.59, 96.60, 37.70, 29.08, 24.84, 19.80, 13.82, 13.72. Elemental Analysis: Anal. Calc. for $C_{21}H_{18}FN_3O_3$: C, 66.48; H, 4.78; N, 11.08; %. Found: C, 66.50; H, 4.79; N, 11.10; %.

4.10. 7-Amino-5-(6-methyl-2-oxo-1,2-dihydroquinolin-3-yl)-2,4-dioxo-1,3,4,5-tetrahydro-2H-pyrano[2,3-d]pyrimidine-6-carbonitrile (40)

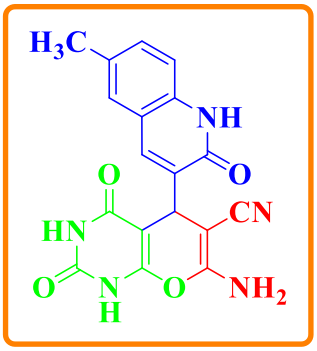

Brown solid, m.p = 237-239℃; IR ν_{max} (cm^{-1}): 2222 C≡N, 1572 C=N, 1217 C-N, 2925 CH, 1651 C=C, 1750 C=O, 3026 NH. ^{1}H-NMR: (400 MHz, DMSO-d_6) δ ppm 12.20 (1H, s, NH), 10.78 (1H, s, NH), 9.42 (1H, s, NH), 8.12 (1H, s, Ar-H), 7.55 (1H, d, *J* = 1.44 Hz, Ar-H), 7.46 (2H, t, *J*=8.44 Hz, Ar-H), 7.29 (2H, s, NH_2), 4.44 (1H, s, CH), 2.36 (3H, brs, CH_3). ^{13}C-NMR: (100 MHz, $CDCl_3$) δ ppm 159.88, 159.84, 145.96, 145.94, 144.53, 144.39, 136.74, 136.68, 129.71, 129.11, 127.70, 126.87, 125.16, 125.13, 124.32, 123.21, 120.66, 120.64, 114.76, 63.60, 63.53, 63.40, 63.32, 53.91, 49.68, 48.15, 16.48, 16.43, 16.16, 16.11. Elemental Analysis: Anal. Calc. for $C_{18}H_{13}N_5O_4$: C, 59.50; H, 3.61; N, 19.28; %. Found: C, 59.52; H, 3.63; N, 19.30; %.

4.11. 2-Amino-4-(2-chloro-6-methylquinolin-3-yl)-7,7-dimethyl-5-oxo-5,6,7,8-tetrahydro-*4H*-chromene-3-carbonitrile (41)

Yellow solid, m.p = 187-189℃; IR ν_{max} (cm^{-1}): 2227 C≡N, 1562 C=N, 1216 C-N, 2923 CH, 1657 C=C, 1751 C=O, 733 C-Cl, 3039 NH. ^{1}H-NMR: (400 MHz, DMSO-d_6) δ ppm 11.38 (2H, s, NH_2), 7.71 (1H, d, *J*= 3.2 Hz, Ar-H), 7.47 (1H, s, Ar-H), 7.35-7.32 (1H, t, *J*=2.52 Hz, Ar-H), 7.30-7.27 (1H, d, *J*=5.56 Hz, Ar-H), 4.51 (1H, s, CH), 2.52 (3H, brs, CH_3), 2.39 (2H, q, *J*= 16.25 Hz, CH_2), 2.25 (2H, q, *J*=12.36 Hz, CH_2), 1.32 (3H, s, CH_3), 0.92 (3H, s, CH_3). ^{13}C-NMR: (100 MHz, $CDCl_3$) δ ppm 176.28, 176.24, 156.26, 155.35, 155.29, 145.21, 145.08, 133.87, 129.37, 125.94, 125.44, 123.41, 120.02, 119.17, 118.28, 114.02, 63.86, 63.79, 63.53, 63.45, 46.20, 44.65, 30.92, 16.44, 16.38, 16.29, 16.24. Elemental Analysis: Anal. Calc. for $C_{22}H_{20}ClN_3O_2$: C, 67.09; H, 5.12; N, 10.67; %. Found: C, 67.10; H, 5.14; N, 10.69; %.

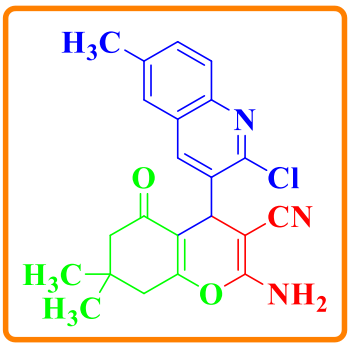

4.12. 2-Amino-4-(2-methoxy-6-methylquinolin-3-yl)-7,7-dimethyl-5-oxo-5,6,7,8-tetrahydro-*4H*-chromene-3-carbonitrile (42)

Yellow solid, m.p = 174-176℃; IR ν_{max} (cm^{-1}): 2223 C≡N, 1579 C=N, 1236 C-N, 2840 CH, 1614 C=C, 1697 C=O, 2970 OCH_3, 3446 NH. ^{1}H-NMR: (400 MHz, $CDCl_3$) δ ppm 7.72 (1H, s, Ar-H), 7.60 (1H, d, *J*= 8.48 Hz, Ar-H), 7.39 (1H, s, Ar-H), 7.32 (1H, dd, *J*= 1.60 Hz, Ar-H), 4.68 (2H, brs, NH_2), 4.54 (1H, s, CH), 3.98 (3H, s, OCH_3), 2.37 (3H, s, CH_3), 2.34 (2H, q, *J*= 12.20 Hz, CH_2), 2.17 (2H, q, *J*= 16.44 Hz, CH_2), 1.02 (3H, s, CH_3), 0.93 (3H, s, CH_3). ^{13}C-NMR: (100 MHz, $CDCl_3$) δ ppm 196.03, 162.96, 159.77, 158.78, 144.09, 137.26, 133.59, 131.22, 126.70, 126.32, 125.37, 125.31, 119.01, 111.86, 60.45, 53.34, 50.57, 40.75, 32.67, 32.12, 29.26, 27.00, 21.26. Elemental Analysis: Anal. Calc. for $C_{23}H_{23}N_3O_3$: C, 70.93; H, 5.95; N, 10.79; %. Found: C, 70.95; H, 5.96; N, 10.81; %.

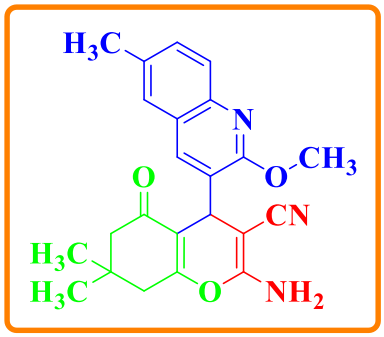

4.13. Ethyl 6-amino-5-cyano-4-(2-methoxy-6-methylquinolin-3-yl)-2-methyl-*4H*-pyran-3-carboxylate (43)

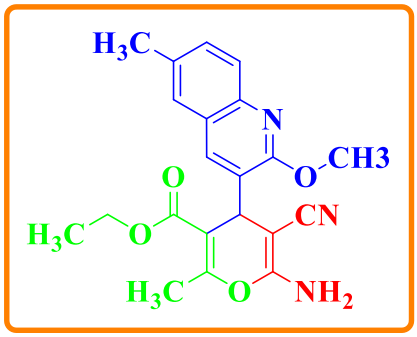

Brown solid, m.p = 188-190℃; IR ν_{max} (cm^{-1}): 2338 C≡N, 1512 C=N, 1240 C-N, 2917 CH, 1627 C=C, 1697 C=O, 2879 OCH_3, 3233 NH. ^{1}H-NMR: (400 MHz, DMSO-d_6) δ ppm 8.30 (1H, s, Ar-H), 7.46 (1H, d, *J*= 3.12 Hz, Ar-H), 7.11 (2H, dt, *J*= 10.20 Hz, Ar-H), 7.05 (2H, brs, NH_2), 4.17 (1H, s, CH), 2.49 (3H, s, OCH_3), 2.06 (2H, q, *J*= 16.04 Hz, CH_2), 1.48 (3H, s, CH_3), 1.02 (3H, s, CH_3), 0.94 (3H, s, CH_3). ^{13}C-NMR: (100 MHz, $CDCl_3$) δ ppm 165.08, 163.08, 160.37, 150.68, 145.77, 142.95, 136.04, 135.32, 130.50, 130.48, 129.90, 129.19, 128.12, 127.44, 126.80, 125.45, 124.02, 120.55, 103.47, 62.02, 61.01, 60.87, 53.58, 33.68, 13.87, 13.47. Elemental Analysis: Anal. Calc. for $C_{21}H_{21}N_3O_4$: C, 66.48; H, 5.58; N, 11.08; %. Found: C, 66.50; H, 5.59; N, 11.10; %.

4.14. 5-Amino-7-(2-methoxy-6-methylquinolin-3-yl)-2-thioxo-3,7-dihydro-2H-pyrano[2,3-d]thiazole-6-carbonitrile (44)

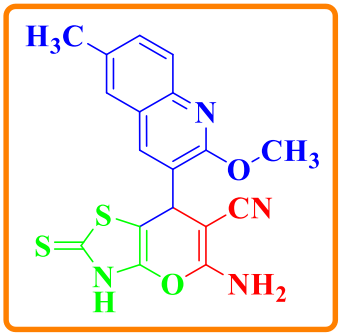

Brown solid, m.p = 198-200℃; IR ν_{max} (cm^{-1}): 2226 C≡N, 1557 C=N, 1229 C-N, 2927 CH, 1688 C=C, 1751 C=O, 2826 OCH_3, 1074 C=S, 615 C-S, 2511 S-H, 3407 NH. ^{1}H-NMR: (400 MHz, DMSO-d_6) δ ppm 12.07 (1H, brs, NH), 8.49 (1H, s, Ar-H), 7.82 (1H, d, *J*=5.88 Hz, Ar-H), 7.74 (2H, dd, *J*=3.96 Hz, Ar-H), 7.46 (2H, brs, NH_2), 4.69 (1H, s, CH), 3.63 (3H, s, OCH_3), 2.39 (3H, s, CH_3). ^{13}C-NMR: (100 MHz, $CDCl_3$) δ ppm 190.41, 189.36, 135.25, 134.93, 128.95, 126.68, 115.73, 77.40, 47.08, 46.45, 40.92, 32.42, 31.42, 29.65, 29.29, 27.40, 20.90. Elemental Analysis: Anal. Calc. for $C_{18}H_{14}N_4O_2S_2$: C, 56.53; H, 3.69; N, 14.65; %. Found: C, 56.55; H, 3.71; N, 14.67; %.

4.15. 2-Amino-6-(2H-indol-3-yl)-4-(p-tolyl)-*4H*-pyran-3,5-dicarbonitrile (45)

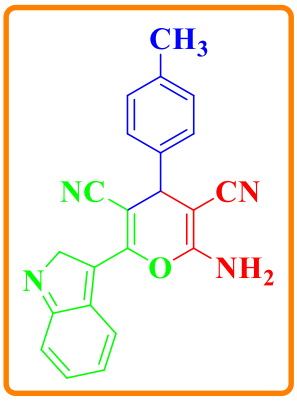

Dark yellow solid, m.p = 201-203℃; IR ν_{max} (cm^{-1}): 2216 C≡N, 1568 C=N, 1289 C-N, 2918 CH, 1614 C=C, 3259 NH. ^{1}H-NMR: (400 MHz, $CDCl_3$) δ ppm 8.72 (2H, brs, NH_2), 8.52 (1H, d, *J*= 3.2 Hz, Ar-H), 8.43 (1H, t, *J*=5.04 Hz, Ar-H), 7.93 (2H, d, *J*=8.12 Hz, Ar-H), 7.44 (1H, t, *J*=4.88 Hz, Ar-H), 7.34-7.29 (3H, dd, *J* = 6.56 Hz, Ar-H), 4.62 (1H, s, CH), 2.43 (2H, s, CH_2), 2.15 (3H, s, CH_3). ^{13}C-NMR: (100 MHz, $CDCl_3$) δ ppm 149.29, 145.99, 145.86, 142.53, 142.50, 129.21, 119.06, 114.10, 110.81, 110.79, 108.90, 108.83, 63.58, 63.51, 63.40, 63.33, 51.12, 49.54, 16.46, 16.41, 16.32, 16.26. Elemental Analysis: Anal. Calc. for $C_{22}H_{16}N_4O$: C, 74.98; H, 4.58; N, 15.90; %. Found: C, 74.99; H, 4.57; N, 15.92; %.

4.1. 2-Amino-4-(2-methoxyquinolin-3-yl)-7,7-dimethyl-5-oxo-5,6,7,8-tetrahydro-*4H*-chromene-3-carbonitrile (31)

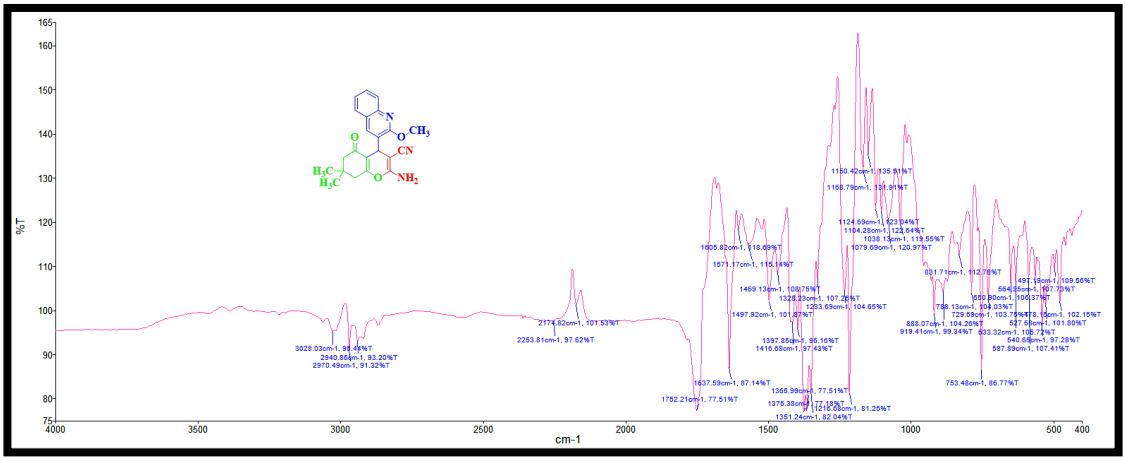

Fig. 4.1. IR spectrum of **31**

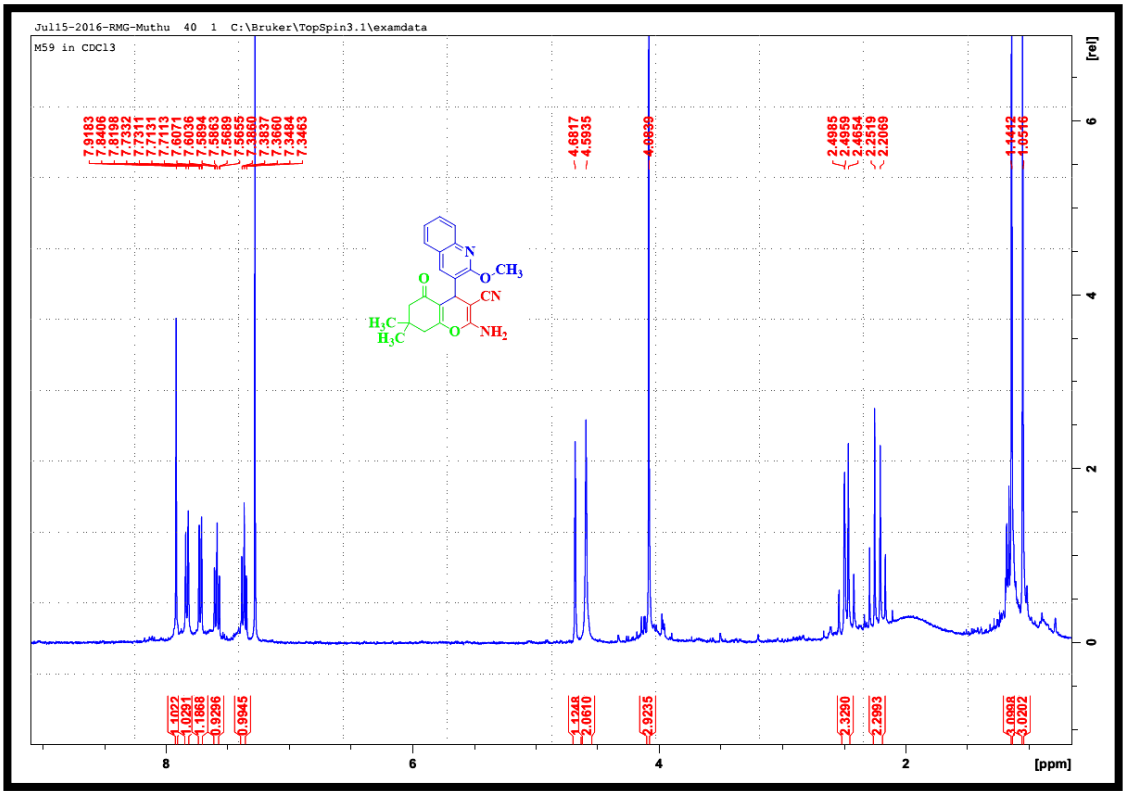

Fig. 4.2. ^{1}H-NMR spectrum of **31**

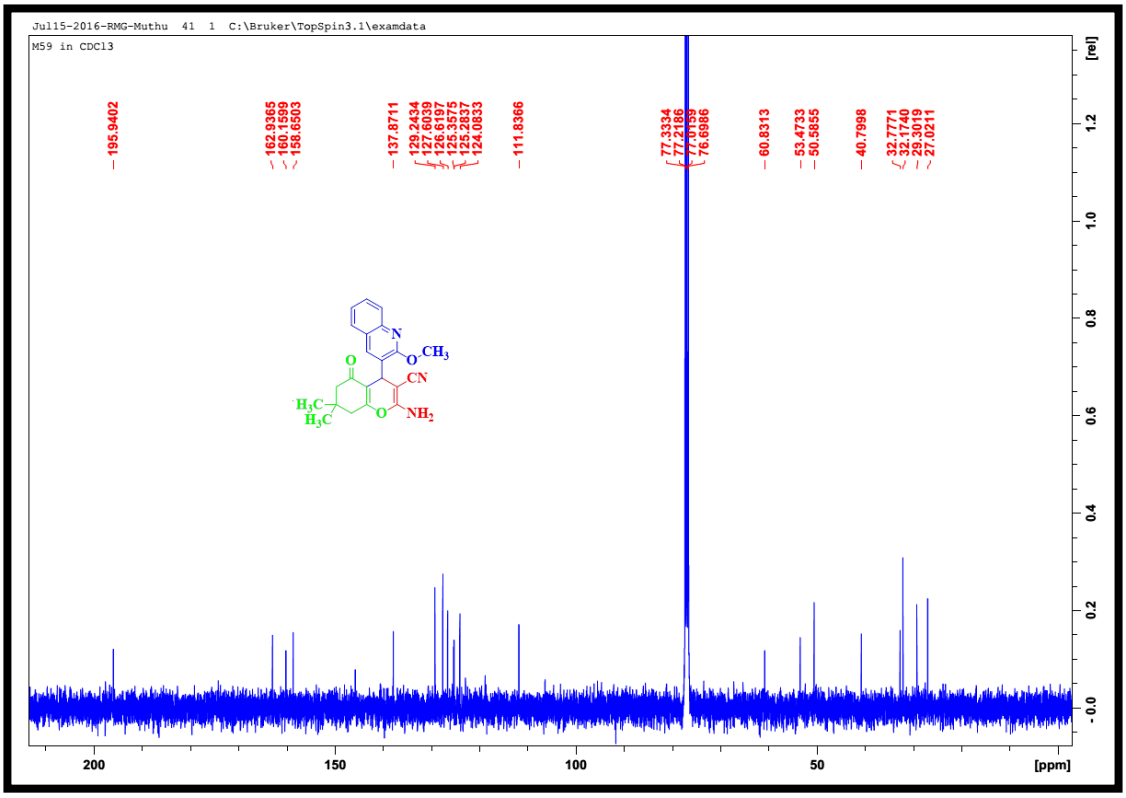

Fig. 4.3. ^{13}C-NMR spectrum of **31**

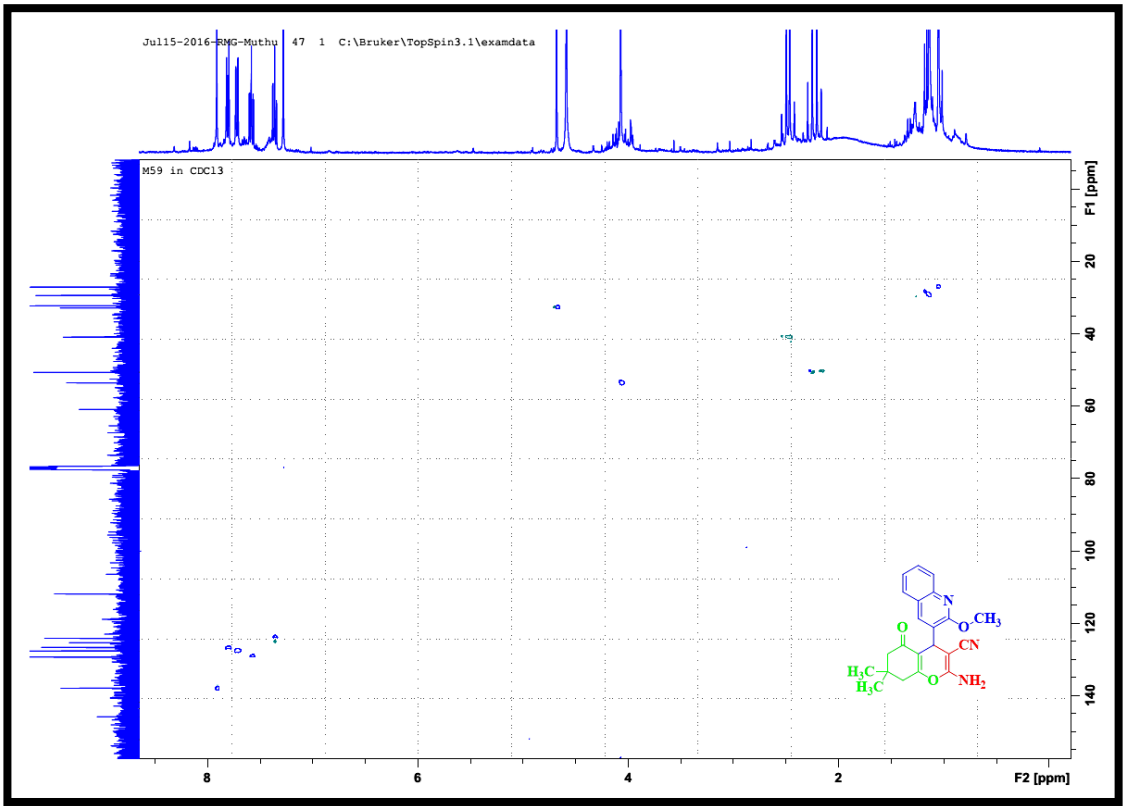

Fig. 4.4. HSQC spectrum of **31**

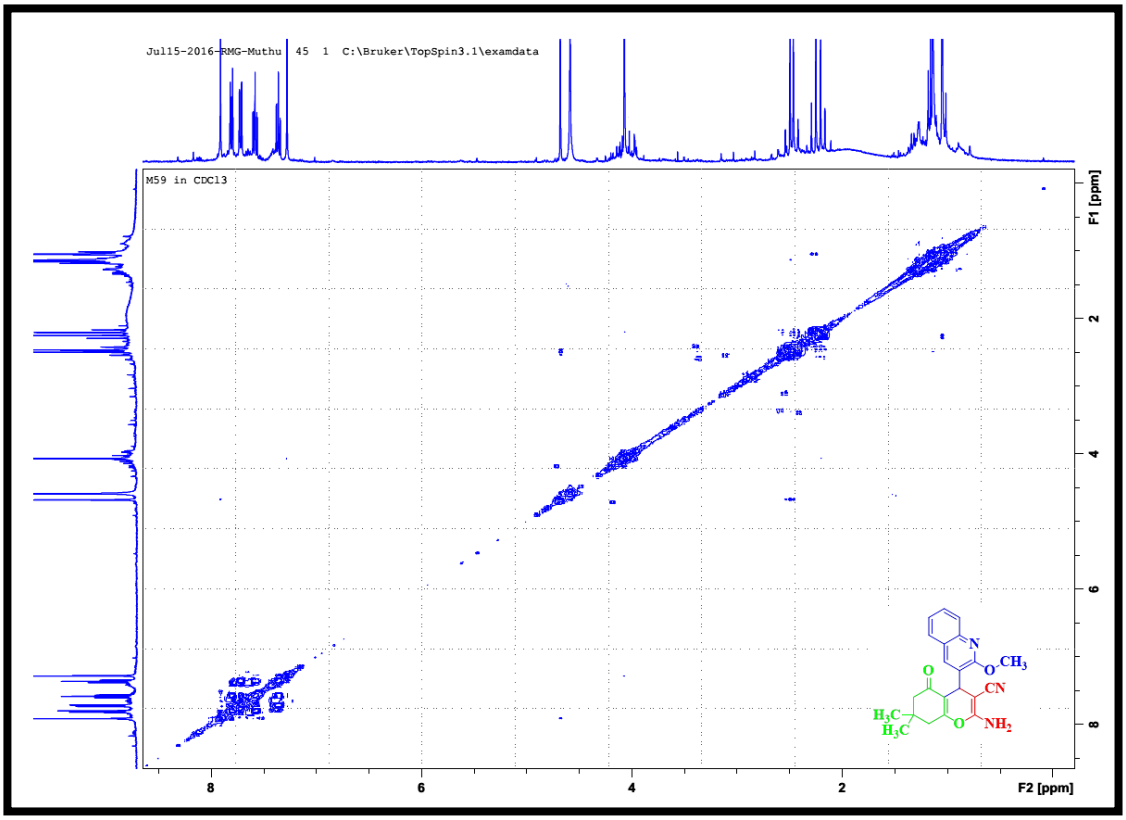

Fig. 4.5. COSY spectrum of **31**

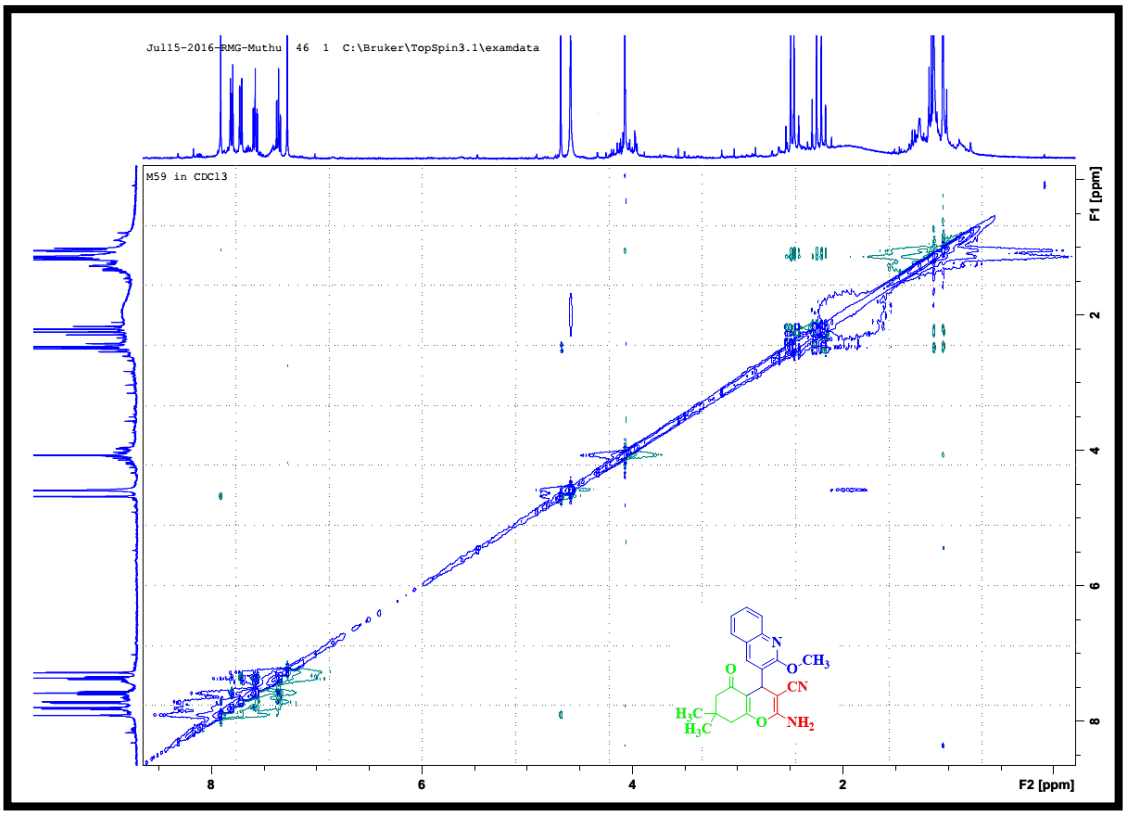

Fig. 4.6. NOESY spectrum of **31**

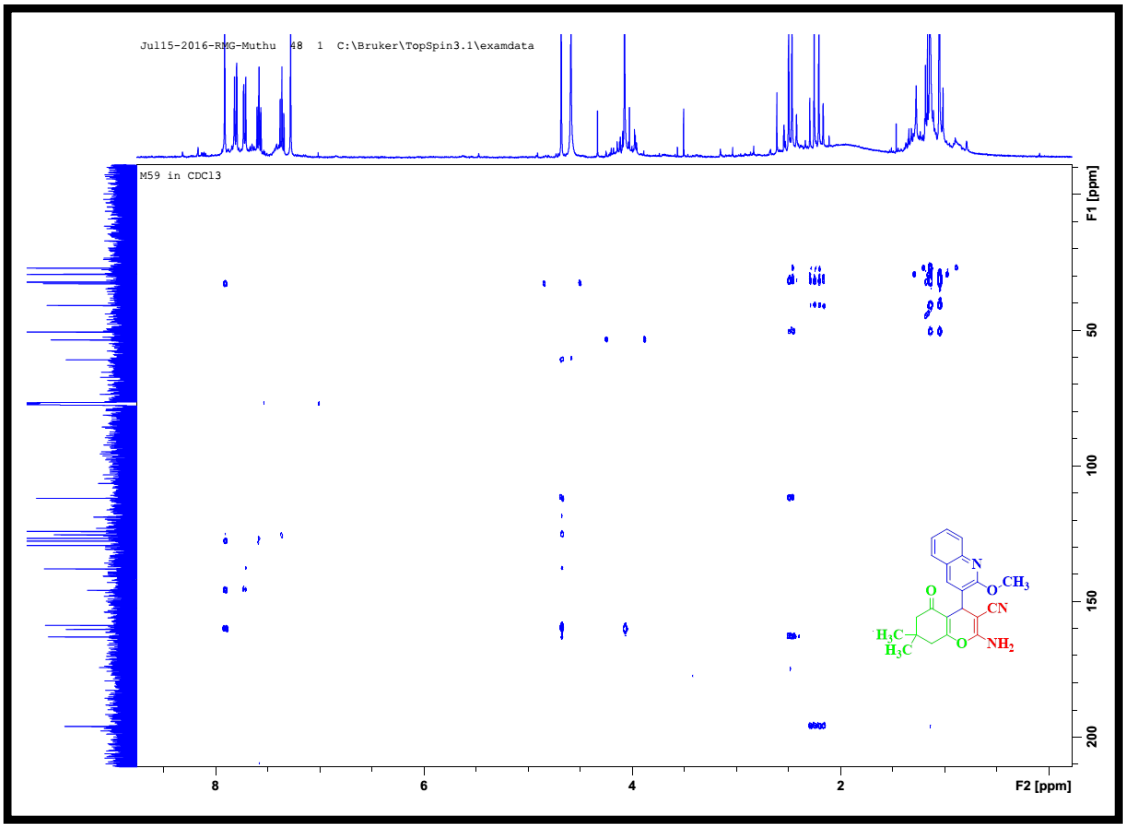

Fig. 4.7. HMBC spectrum of **31**

4.2. 2-Amino-7,7-dimethyl-5-oxo-4-(2-(o-tolyloxy)quinolin-3-yl)-5,6,7,8-tetrahydro-*4H*-chromene-3-carbonitrile (32)

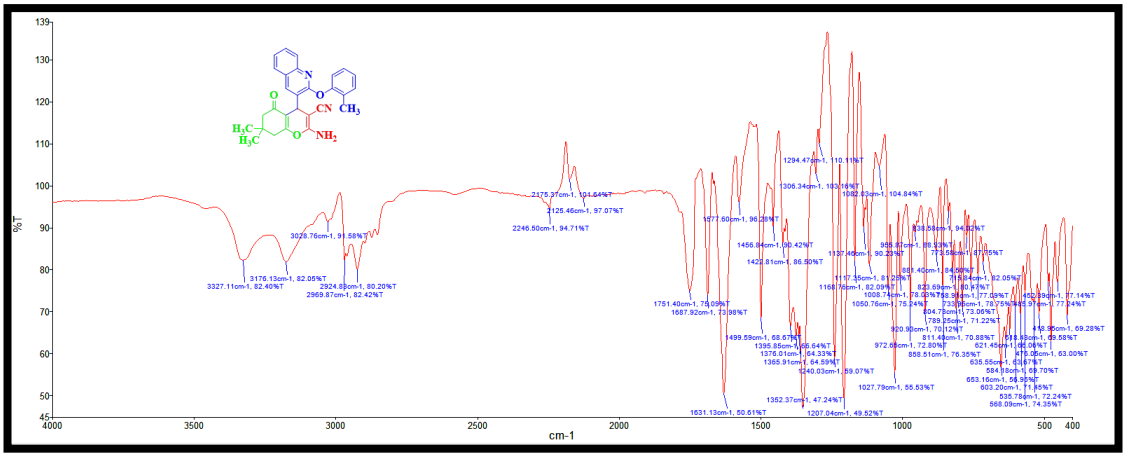

Fig. 4.8. IR spectrum of **32**

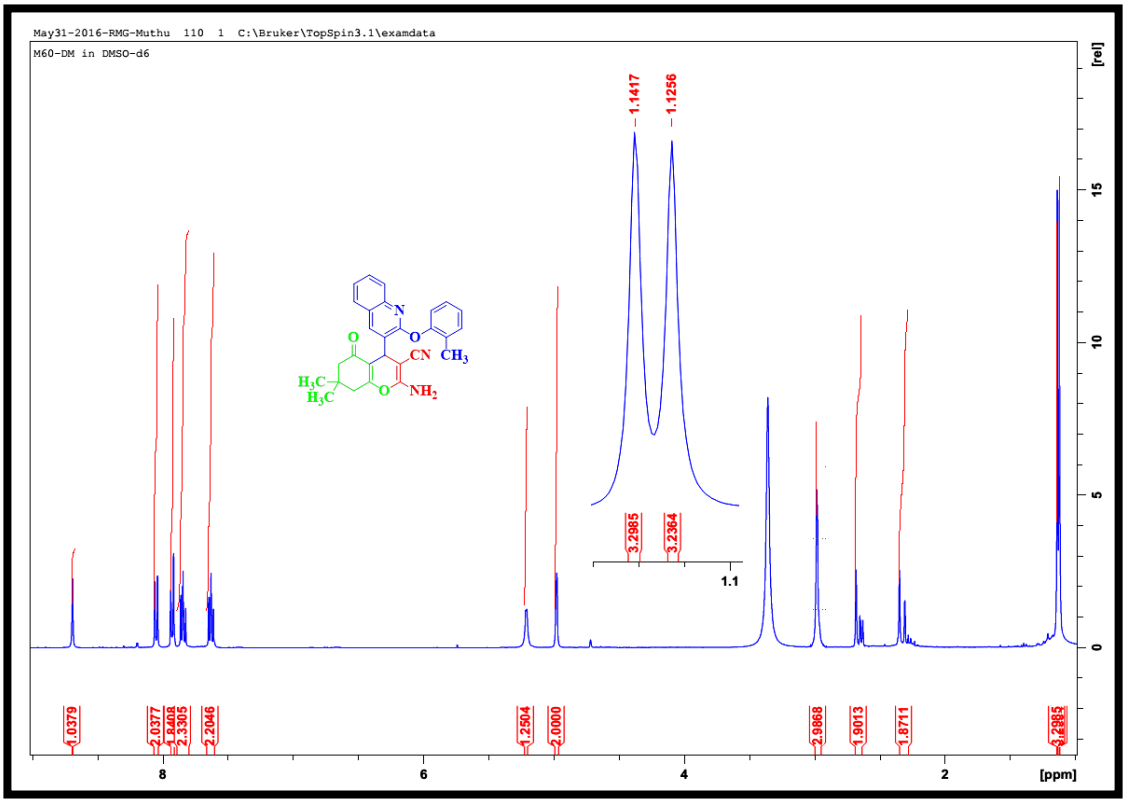

Fig. 4.9. ^{1}H-NMR spectrum of **32**

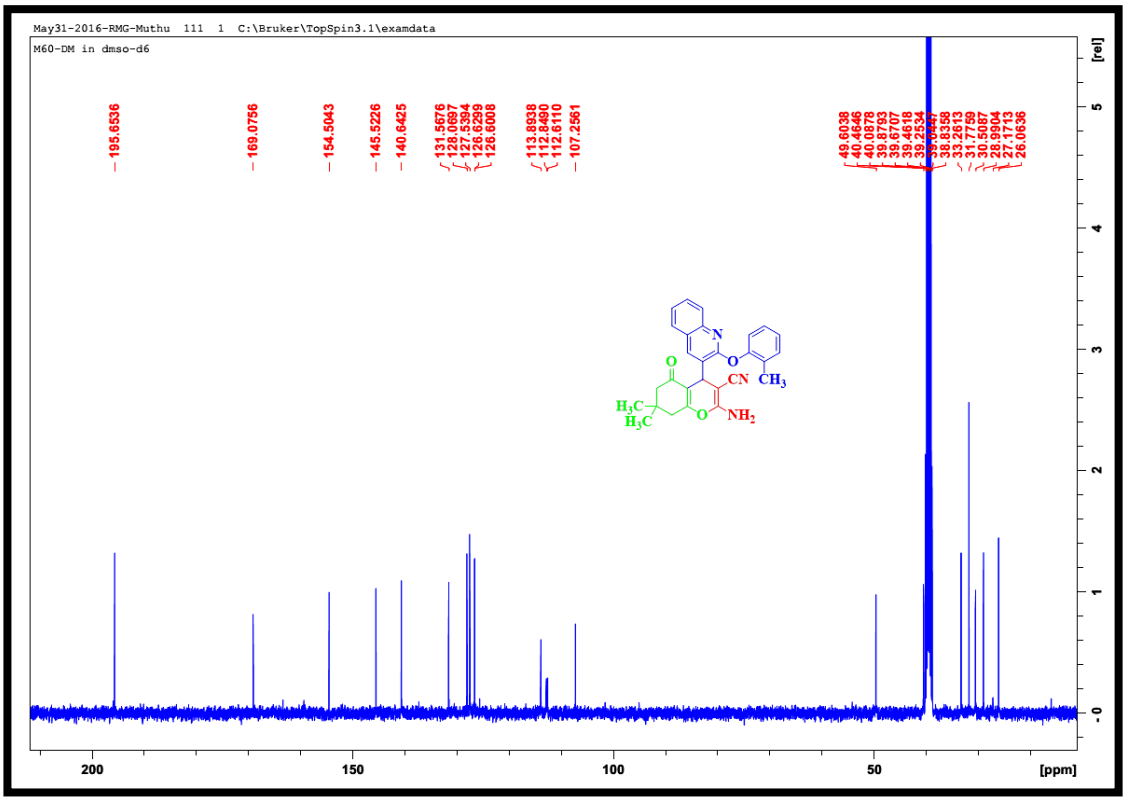

Fig. 4.10. ^{13}C-NMR spectrum of **32**

4.3. Ethyl 6-amino-5-cyano-4-(2-methoxyquinolin-3-yl)-2-methyl-*4H*-pyran-3-carboxylate (33)

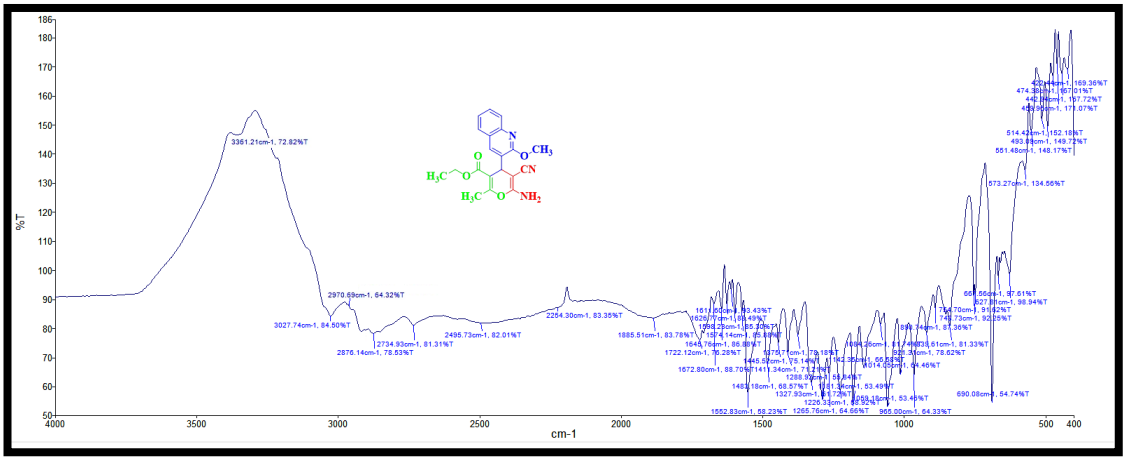

Fig. 4.11. IR spectrum of **33**

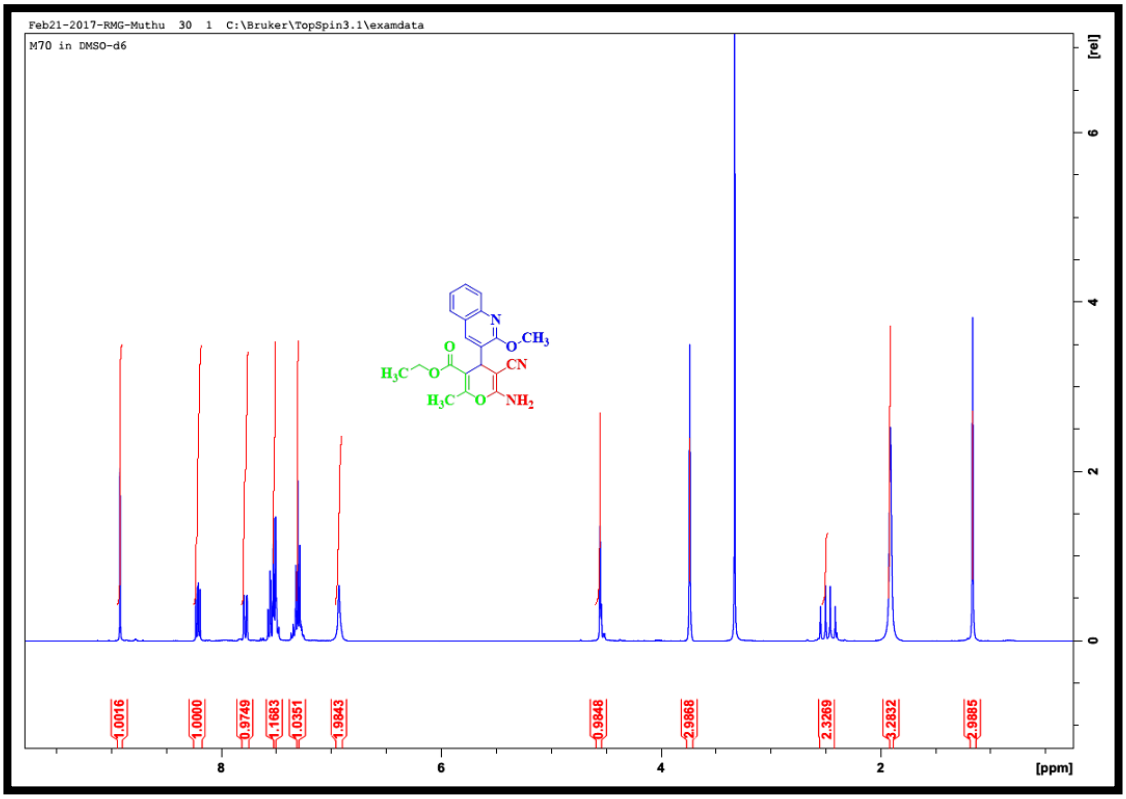

Fig. 4.12. ^{1}H-NMR spectrum of **33**

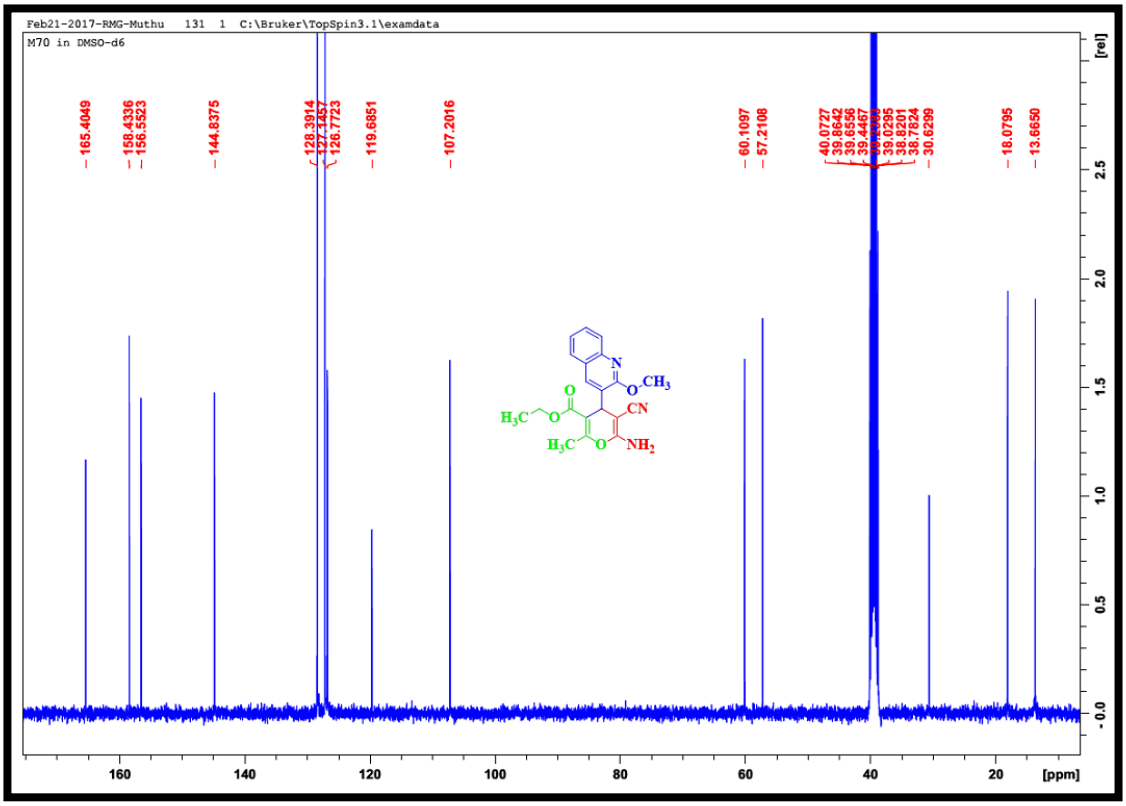

Fig. 4.13. ^{13}C-NMR spectrum of **33**

4.4. 5-Amino-7-(2-methoxyquinolin-3-yl)-2-oxo-3,7-dihydro-2H-pyrano[2,3-d]thiazole-6-carbonitrile (34)

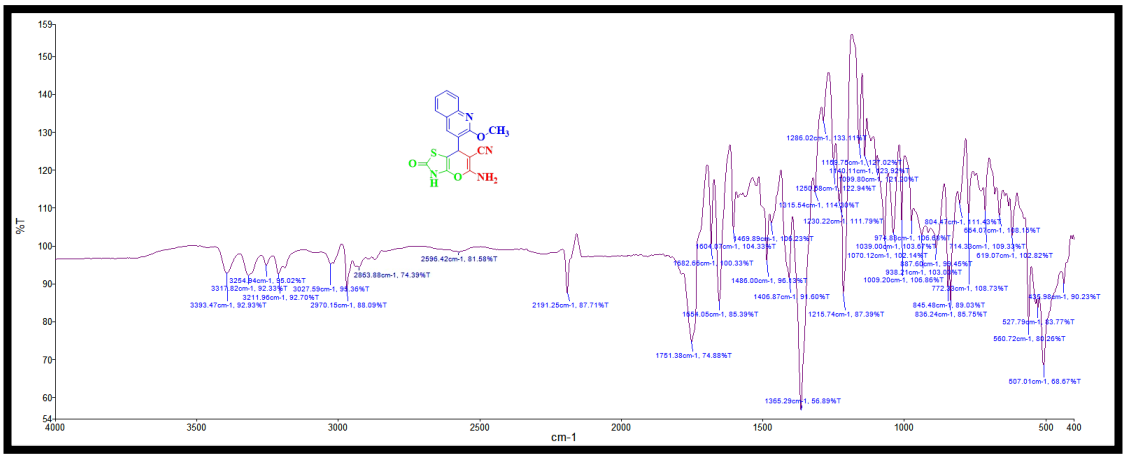

Fig. 4.14. IR spectrum of **34**

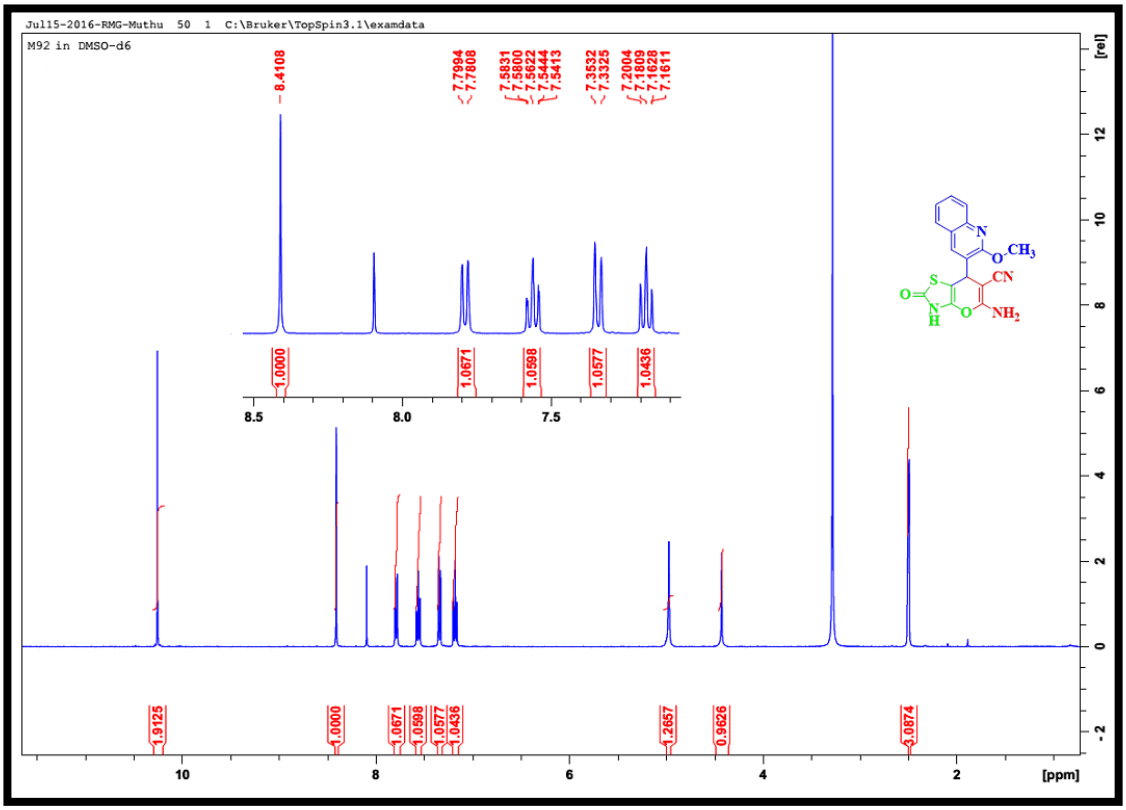

Fig. 4.15. ^{1}H-NMR spectrum of **34**

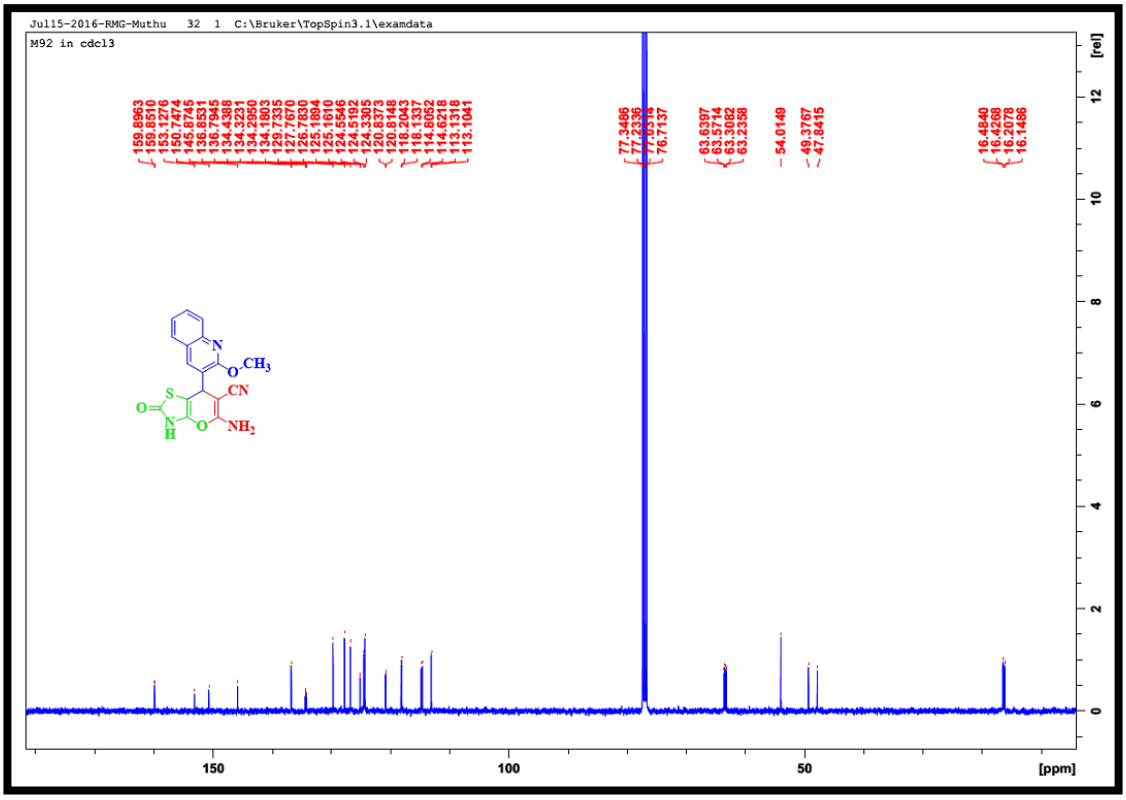

Fig. 4.16. ^{13}C-NMR spectrum of **34**

4.5. 5-Amino-7-(2-methoxy-6-nitroquinolin-3-yl)-2-thioxo-3,7-dihydro-2H-pyrano[2,3-d]thiazole-6-carbonitrile (35)

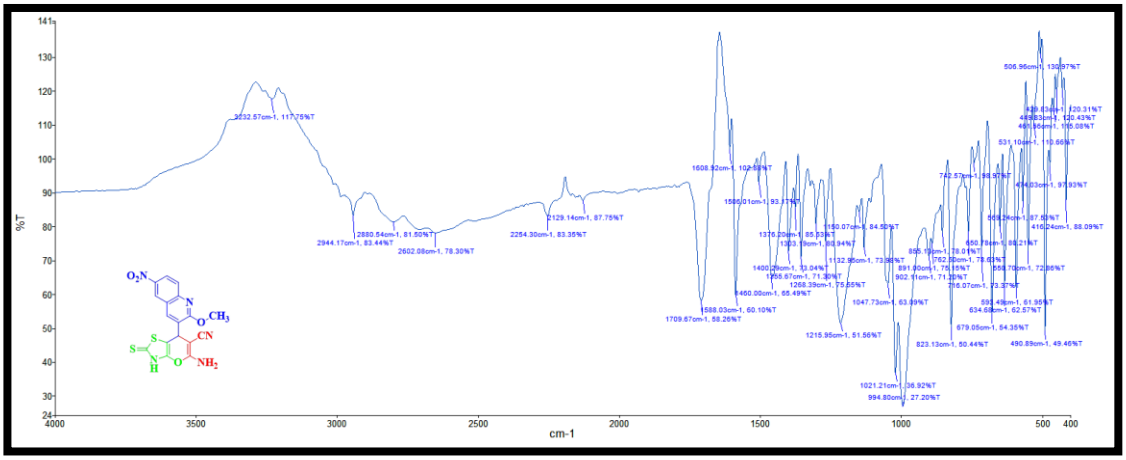

Fig. 4.17. IR spectrum of **35**

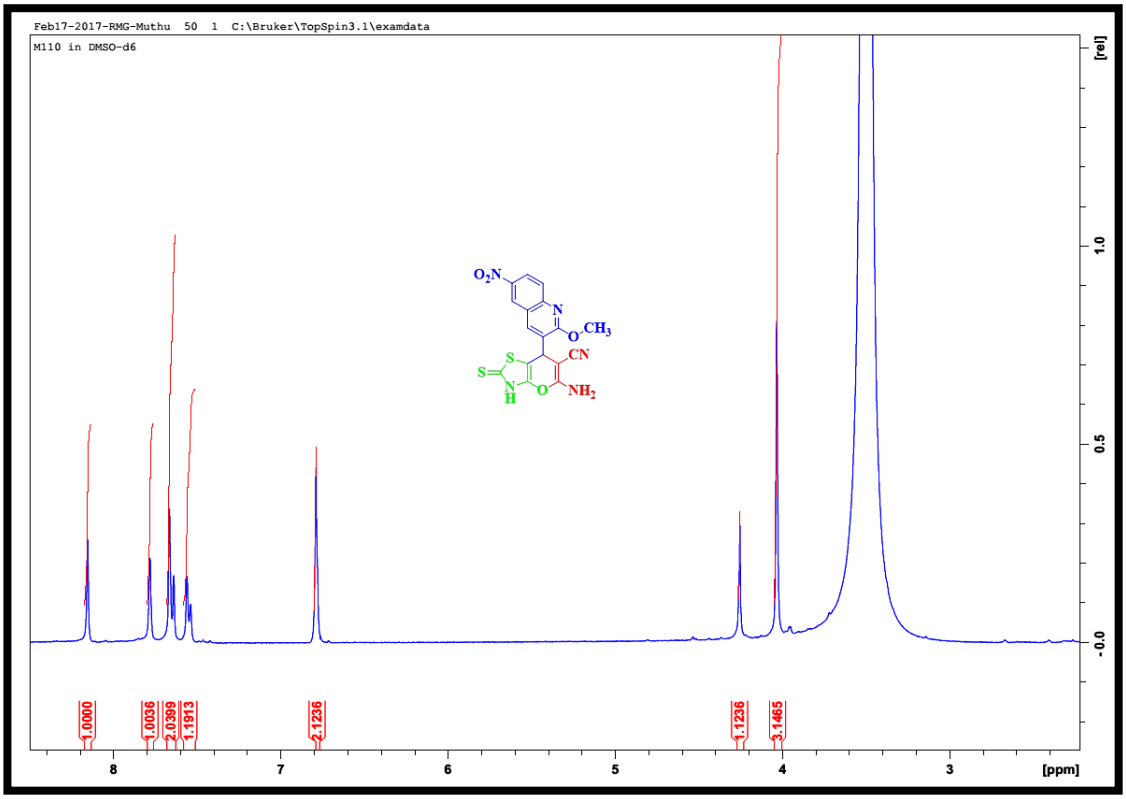

Fig. 4.18. ^{1}H-NMR spectrum of **35**

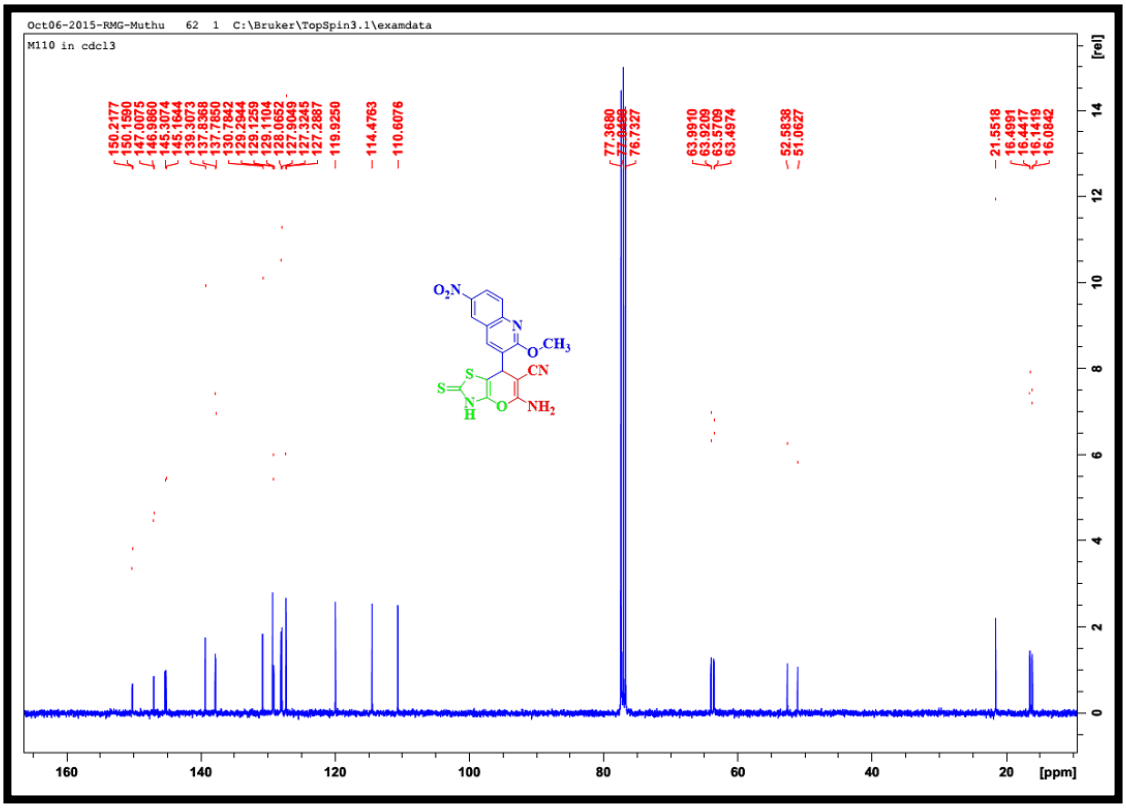

Fig. 4.19. ^{13}C-NMR spectrum of **35**

4.6. 2-Amino-4-(7-fluoro-2-methoxyquinolin-3-yl)-7,7-dimethyl-5-oxo-5,6,7,8-tetrahydro-*4H*-chromene-3-carbonitrile (36)

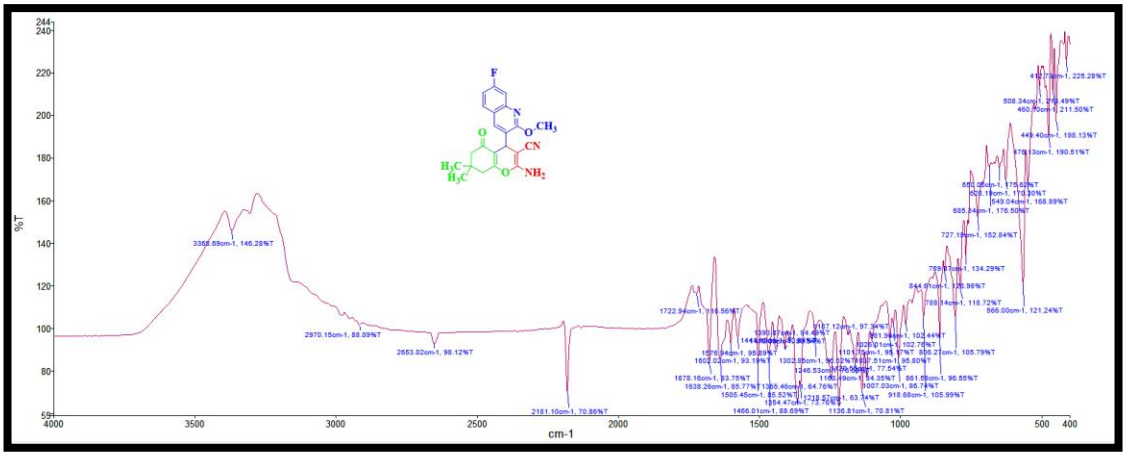

Fig. 4.20. IR spectrum of **36**

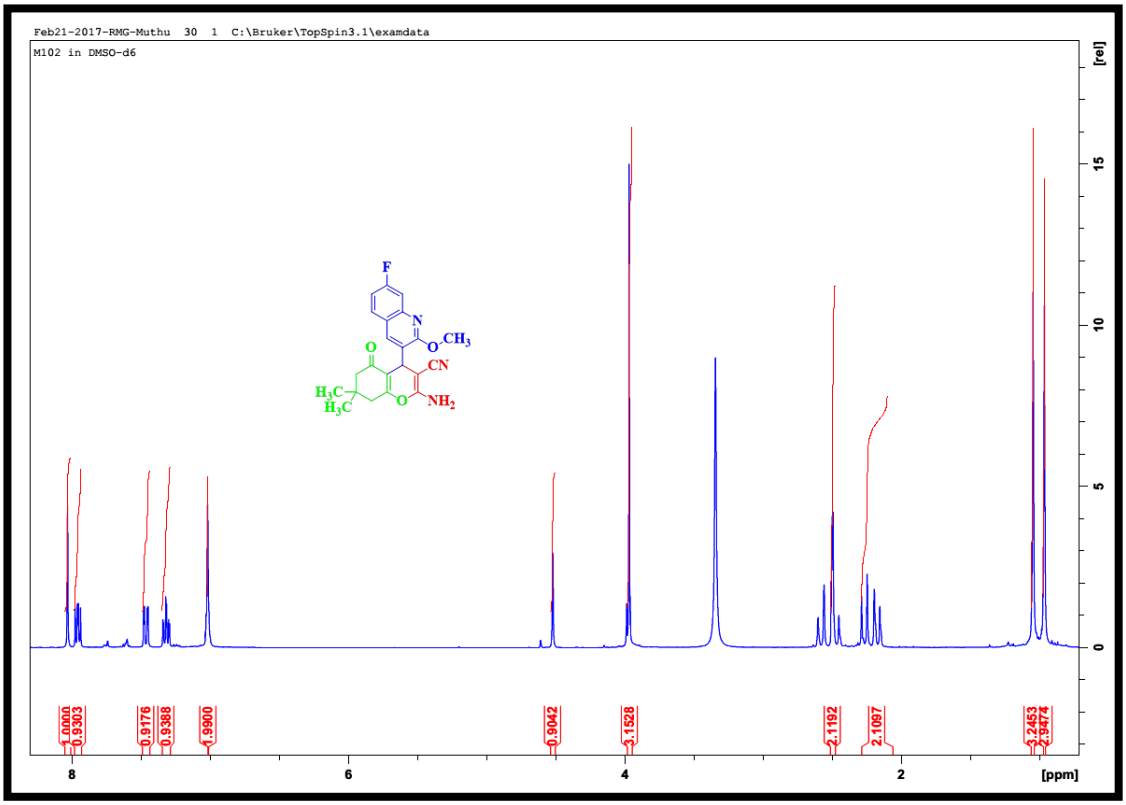

Fig. 4.21. ^{1}H-NMR spectrum of **36**

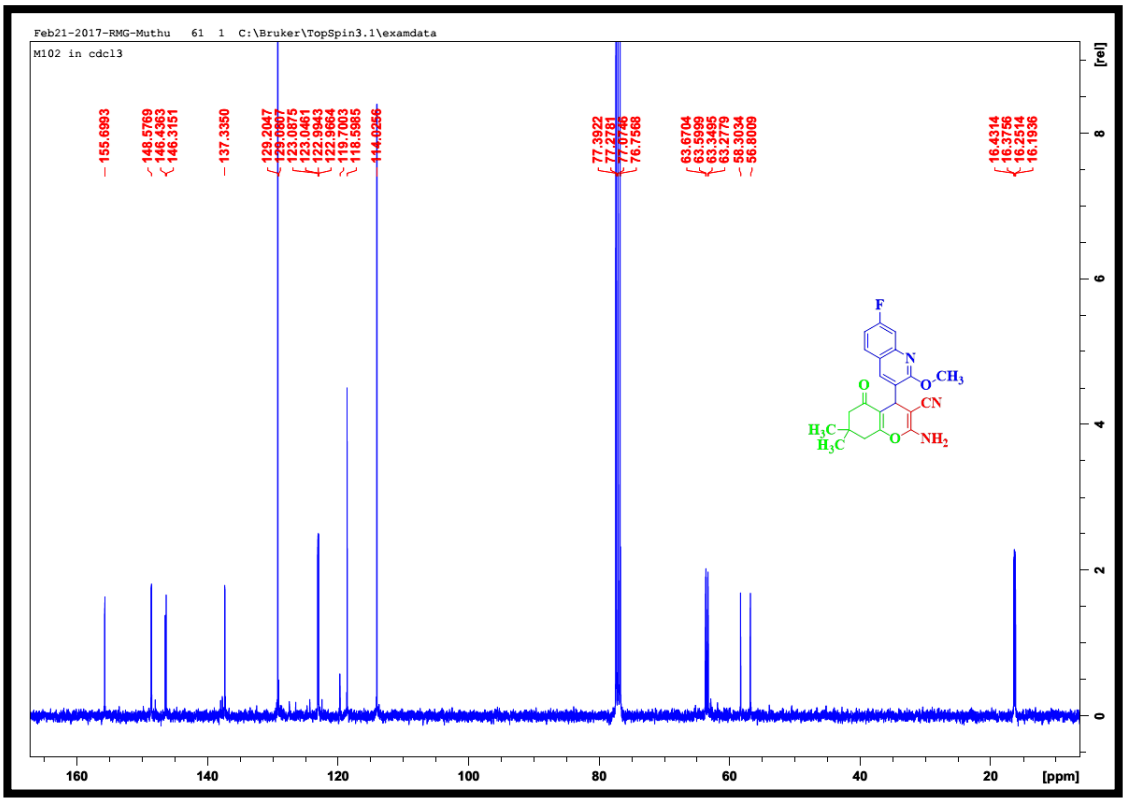

Fig. 4.22. ^{13}C-NMR spectrum of **36**

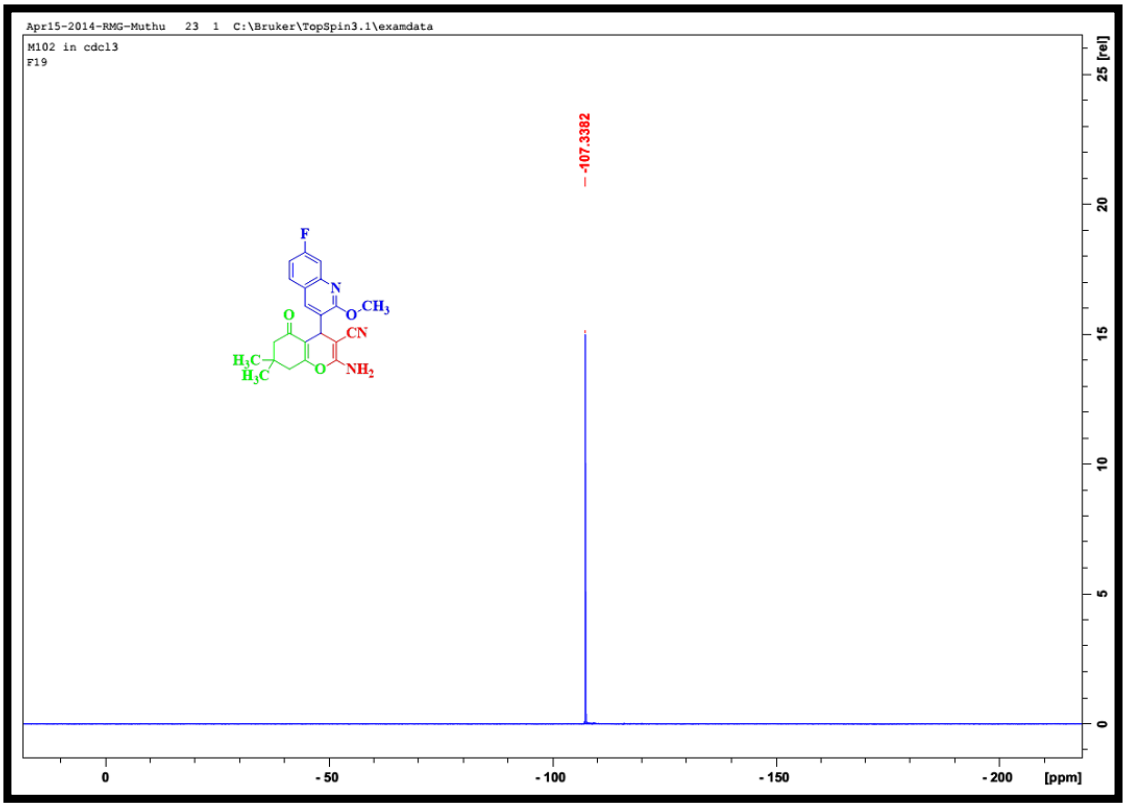

Fig. 4.23. ^{19}F-NMR spectrum of **36**

4.7. Ethyl 6-amino-5-cyano-4-(7-fluoro-2-methoxyquinolin-3-yl)-2-methyl-*4H*-pyran-3-carboxylate (37)

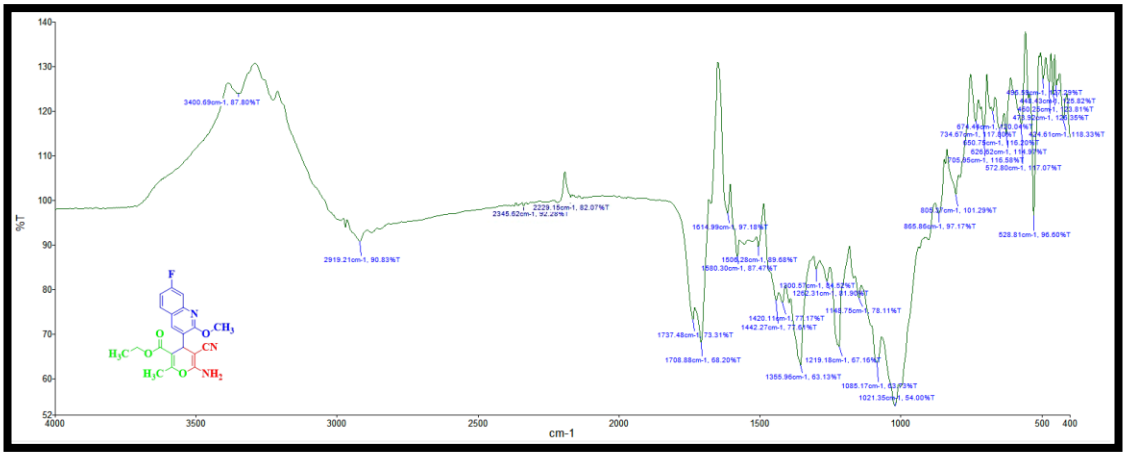

Fig. 4.24. IR spectrum of **37**

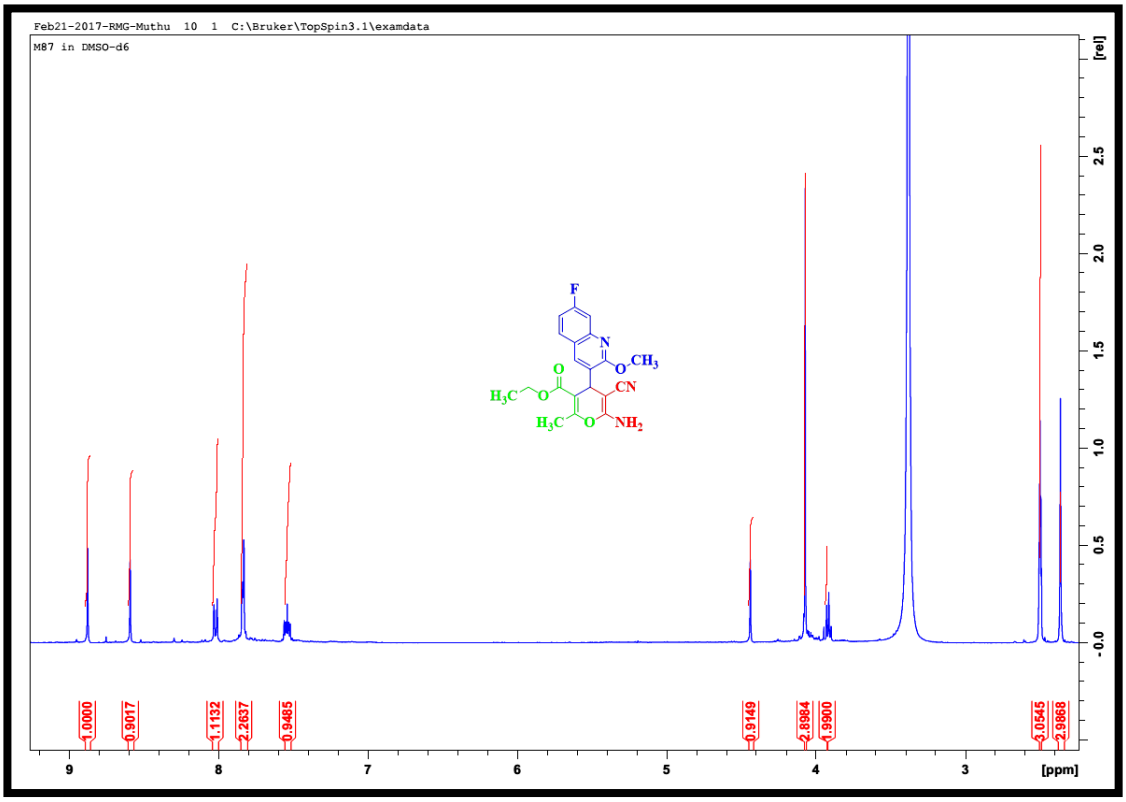

Fig. 4.25. ^{1}H-NMR spectrum of **37**

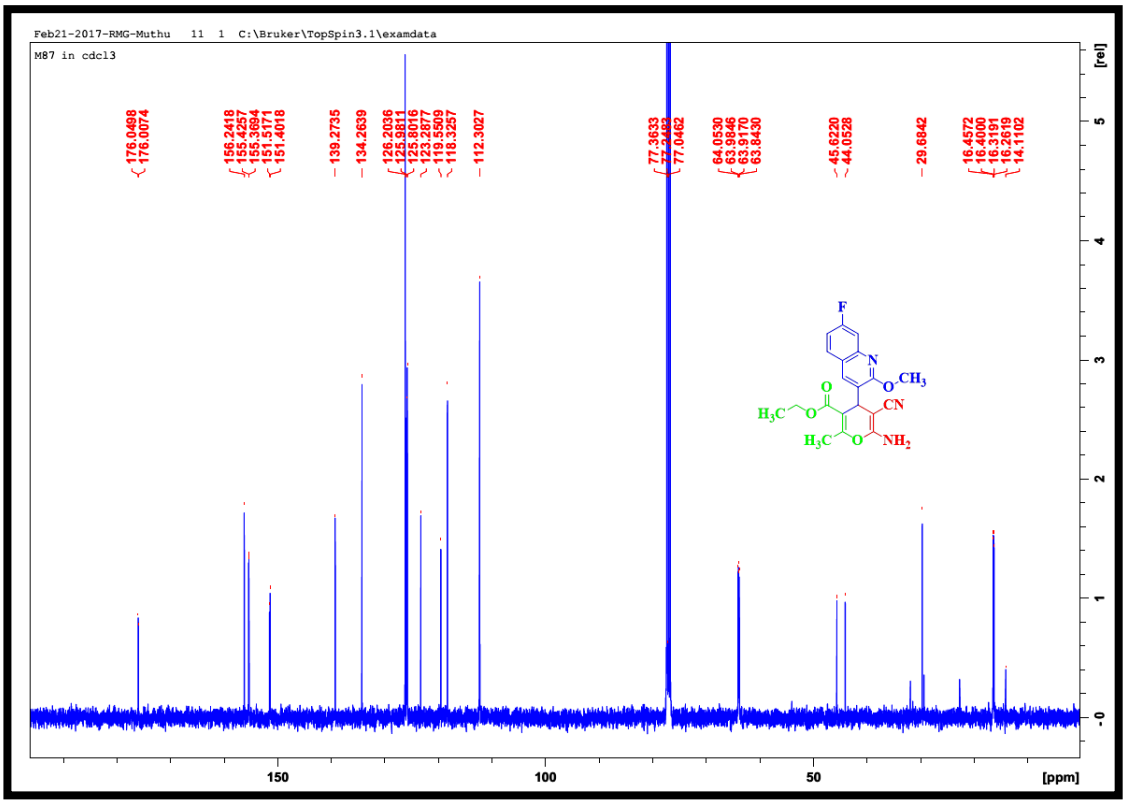

Fig. 4.26. ^{13}C-NMR spectrum of **37**

4.8. 5-Amino-7-(7-fluoro-2-methoxyquinolin-3-yl)-2-oxo-3,7-dihydro-2H-pyrano[2,3-d]thiazole-6-carbonitrile (38)

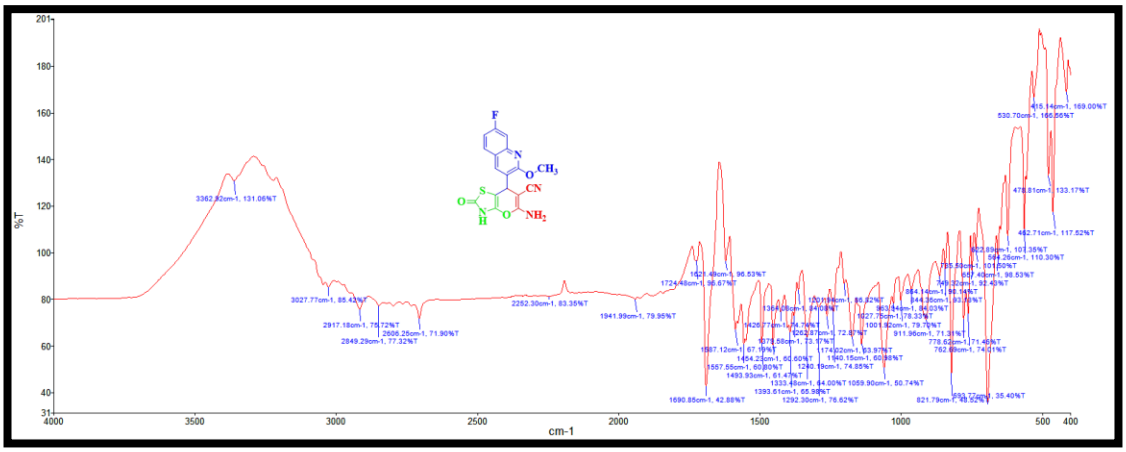

Fig. 4.27. IR spectrum of **38**

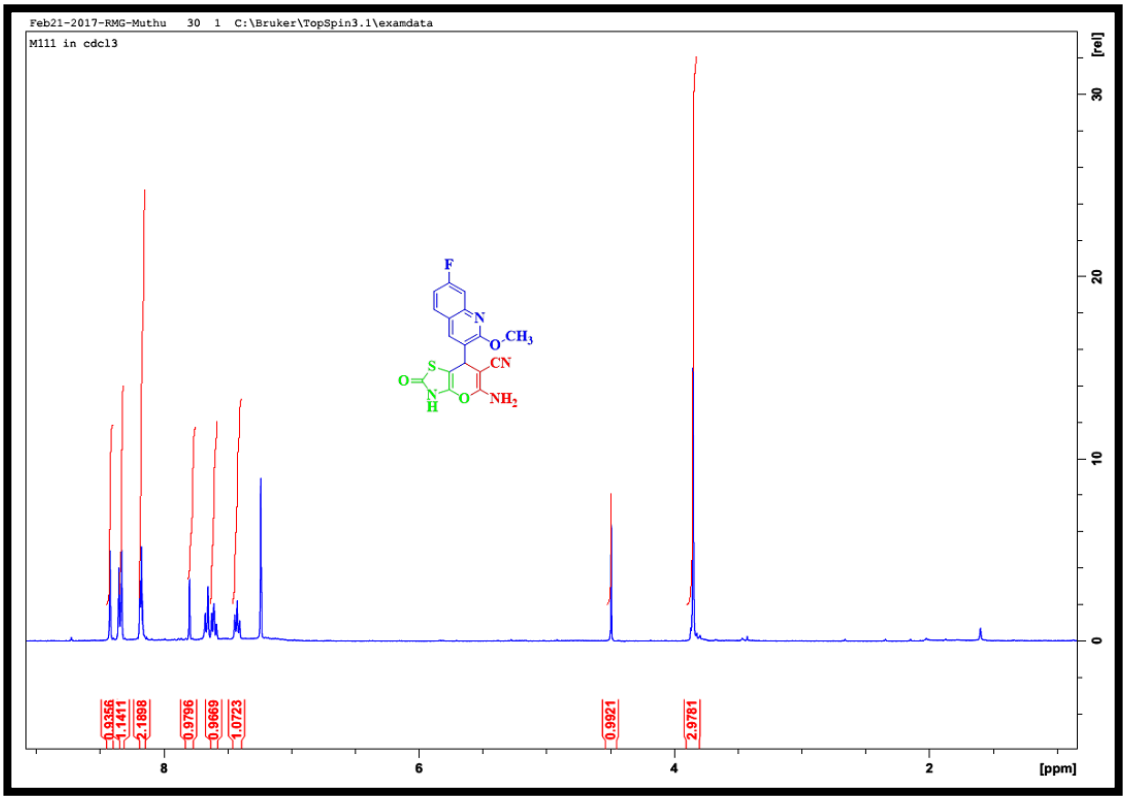

Fig. 4.28. ^{1}H-NMR spectrum of **38**

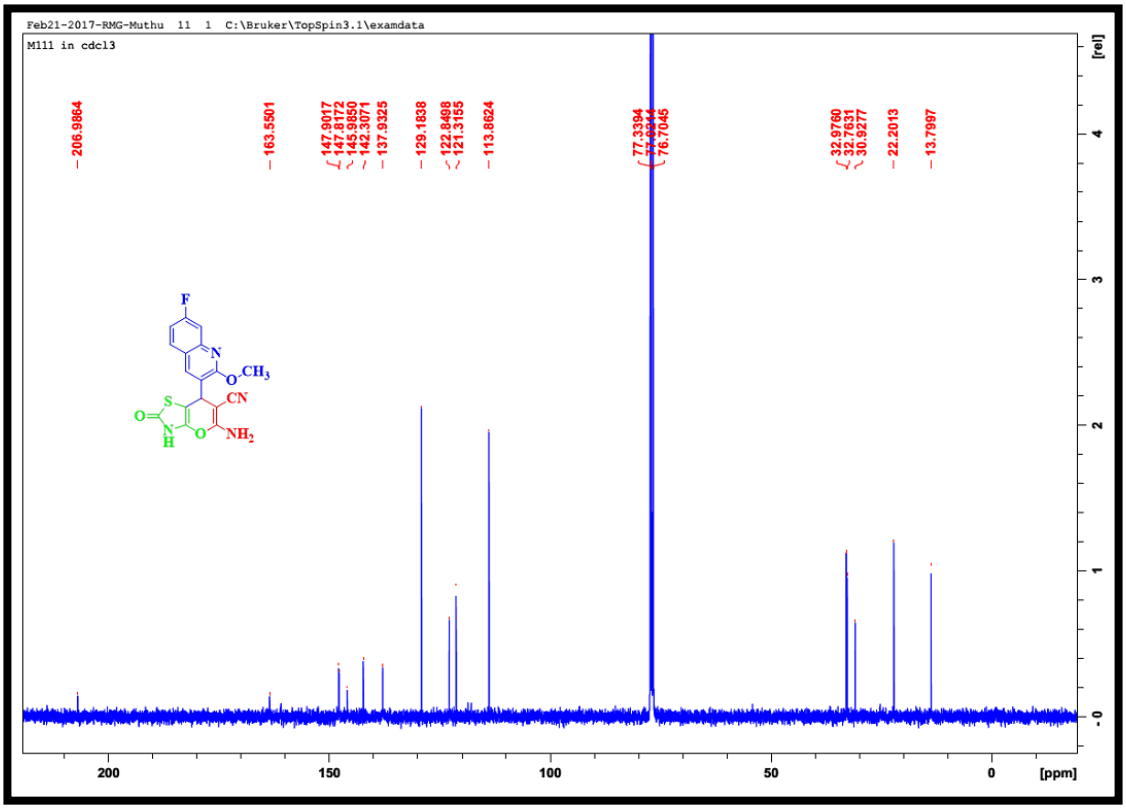

Fig. 4.29. ^{13}C-NMR spectrum of **38**

4.9. 2-Amino-4-(7-fluoro-2-oxo-1,2-dihydroquinolin-3-yl)-7,7-dimethyl-5-oxo-5,6,7,8-tetrahydro-*4H*-chromene-3-carbonitrile (39)

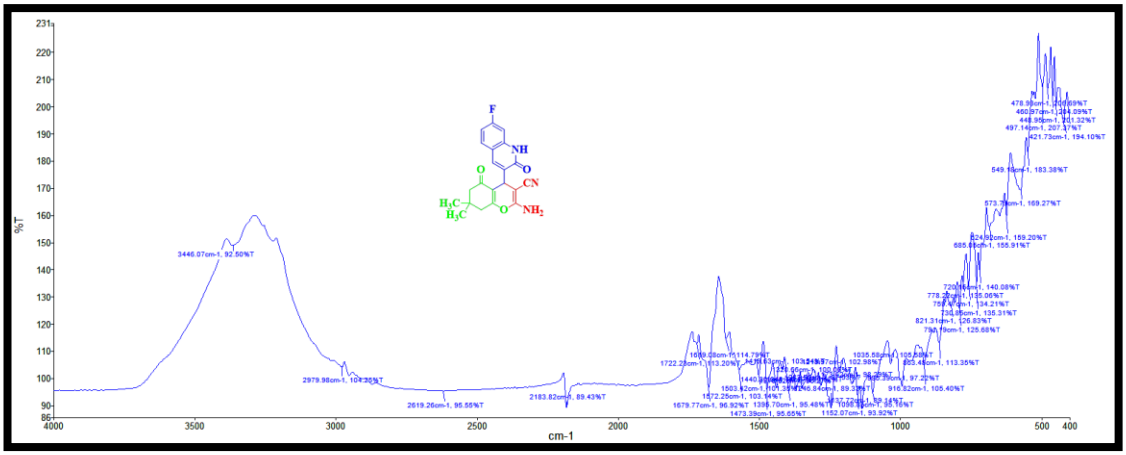

Fig. 4.30. IR spectrum of **39**

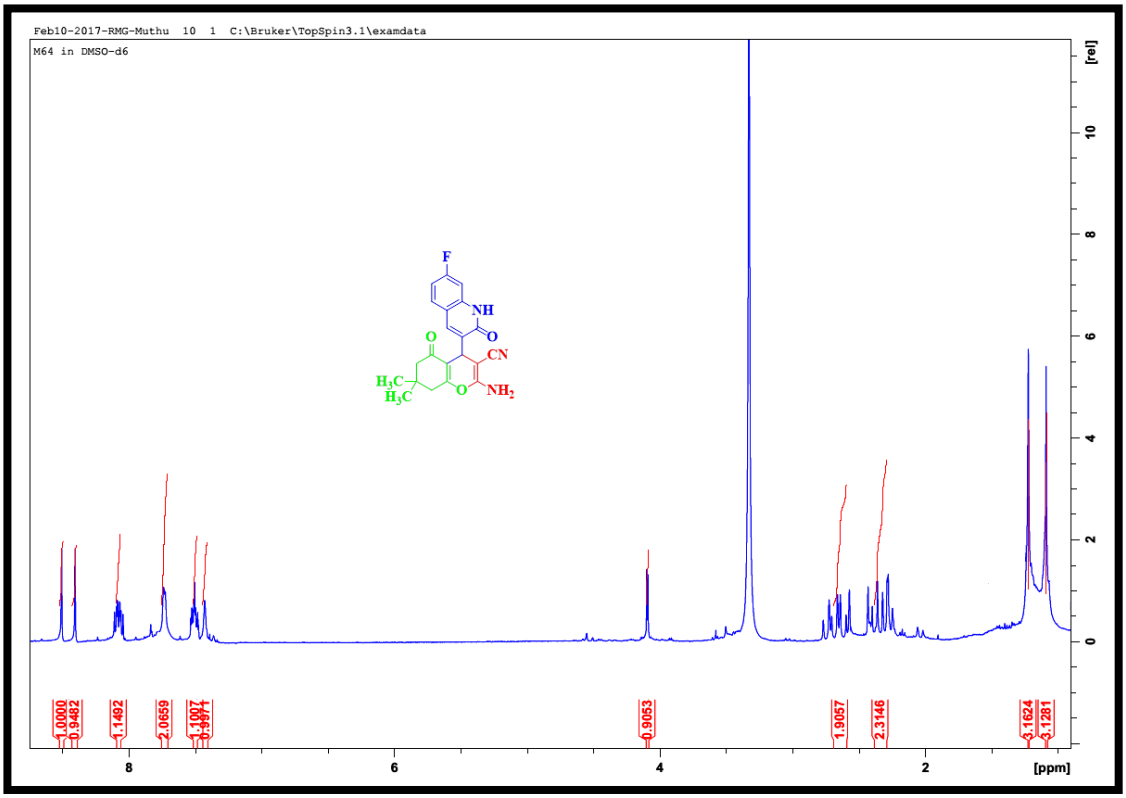

Fig. 4.31. ^{1}H-NMR spectrum of **39**

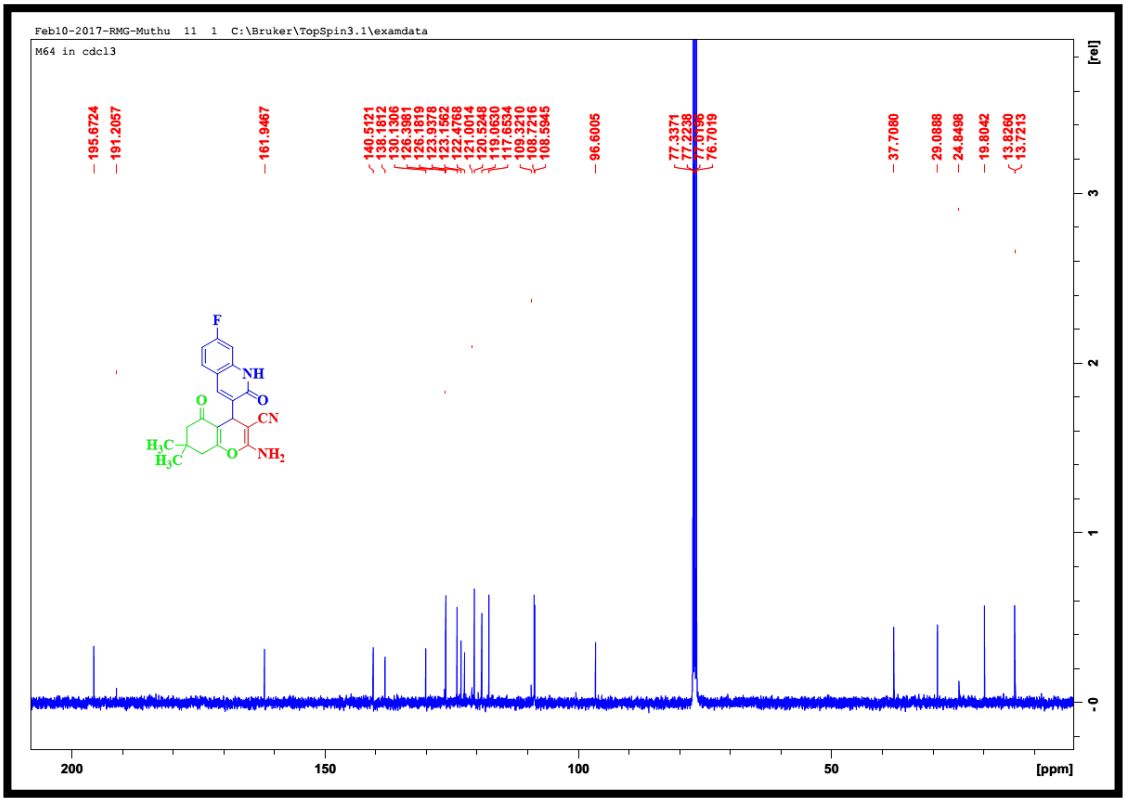

Fig. 4.32. ^{13}C-NMR spectrum of **39**

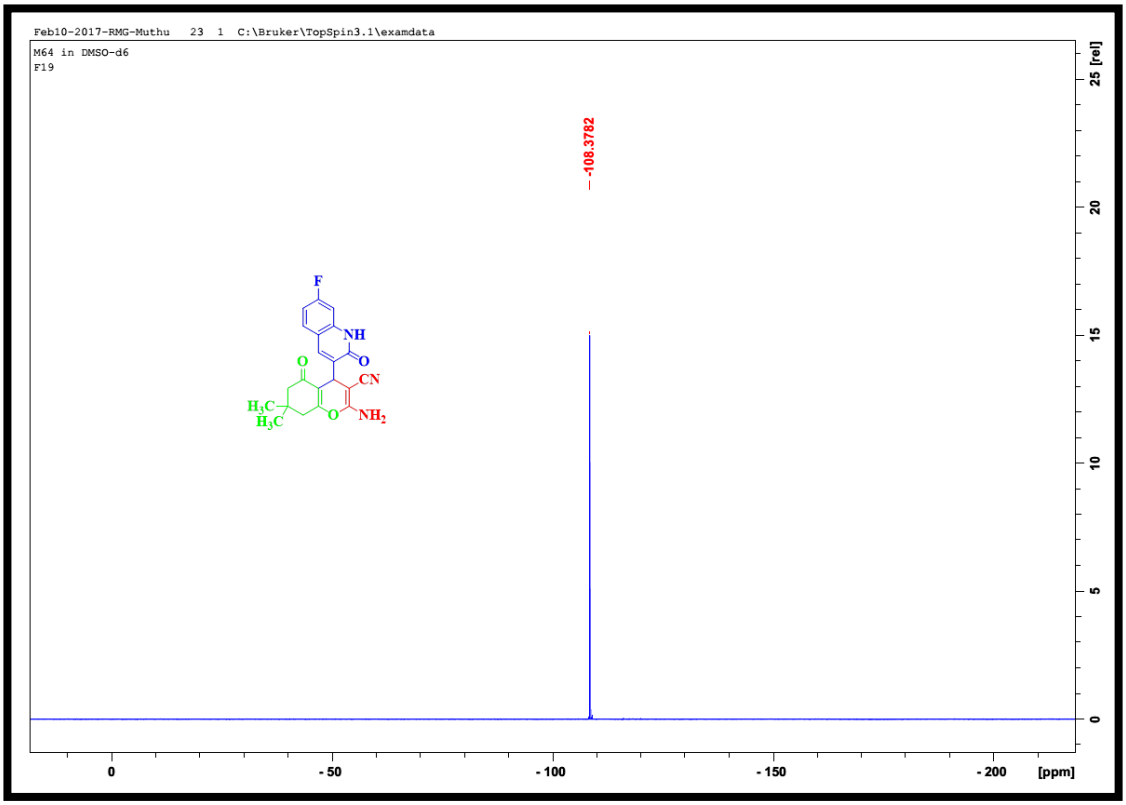

Fig. 4.33. ^{19}F-NMR spectrum of **39**

4.10. 7-Amino-5-(6-methyl-2-oxo-1,2-dihydroquinolin-3-yl)-2,4-dioxo-1,3,4,5-tetrahydro-2H-pyrano[2,3-d]pyrimidine-6-carbonitrile (40)

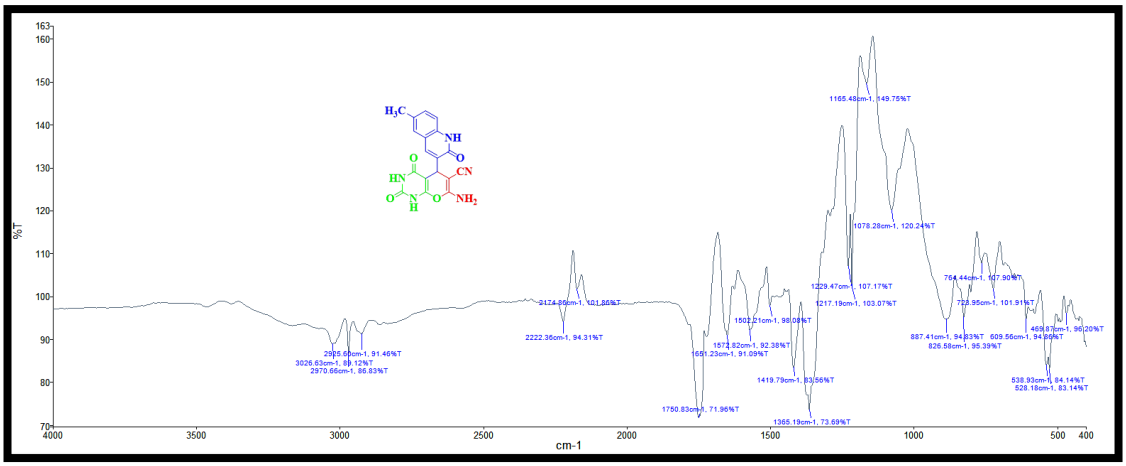

Fig. 4.34. IR spectrum of **40**

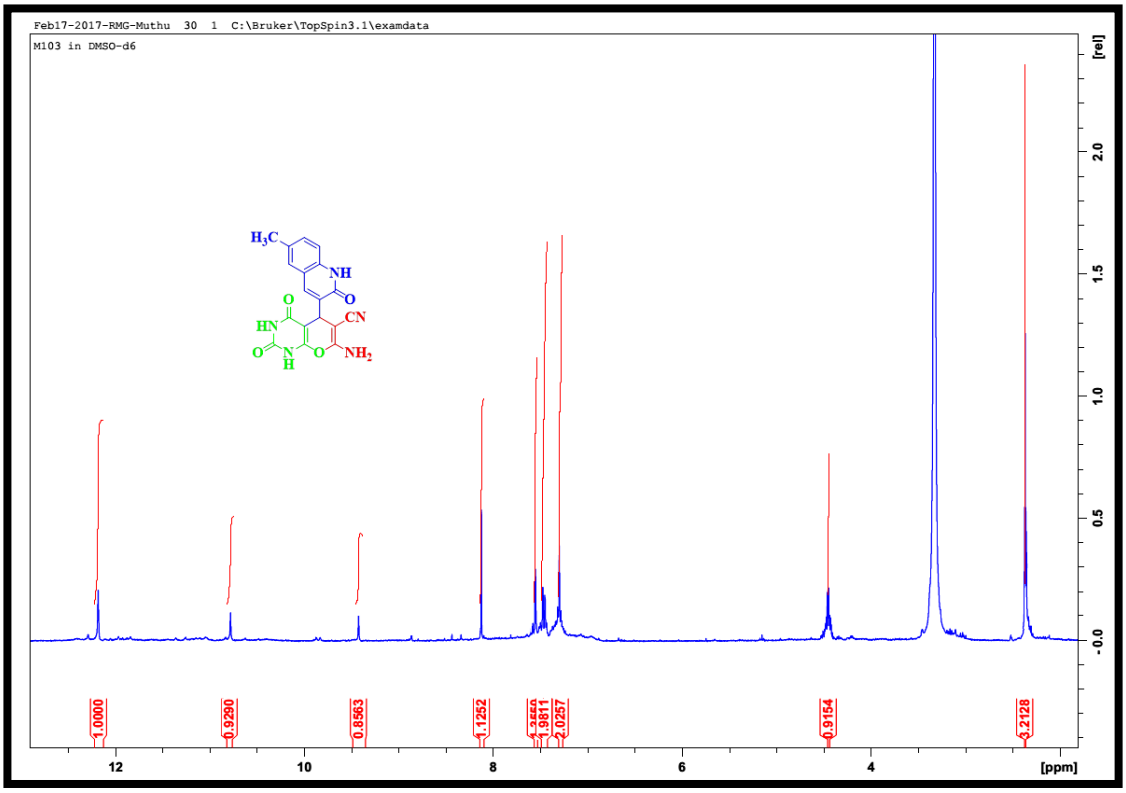

Fig. 4.35. ^{1}H-NMR spectrum of **40**

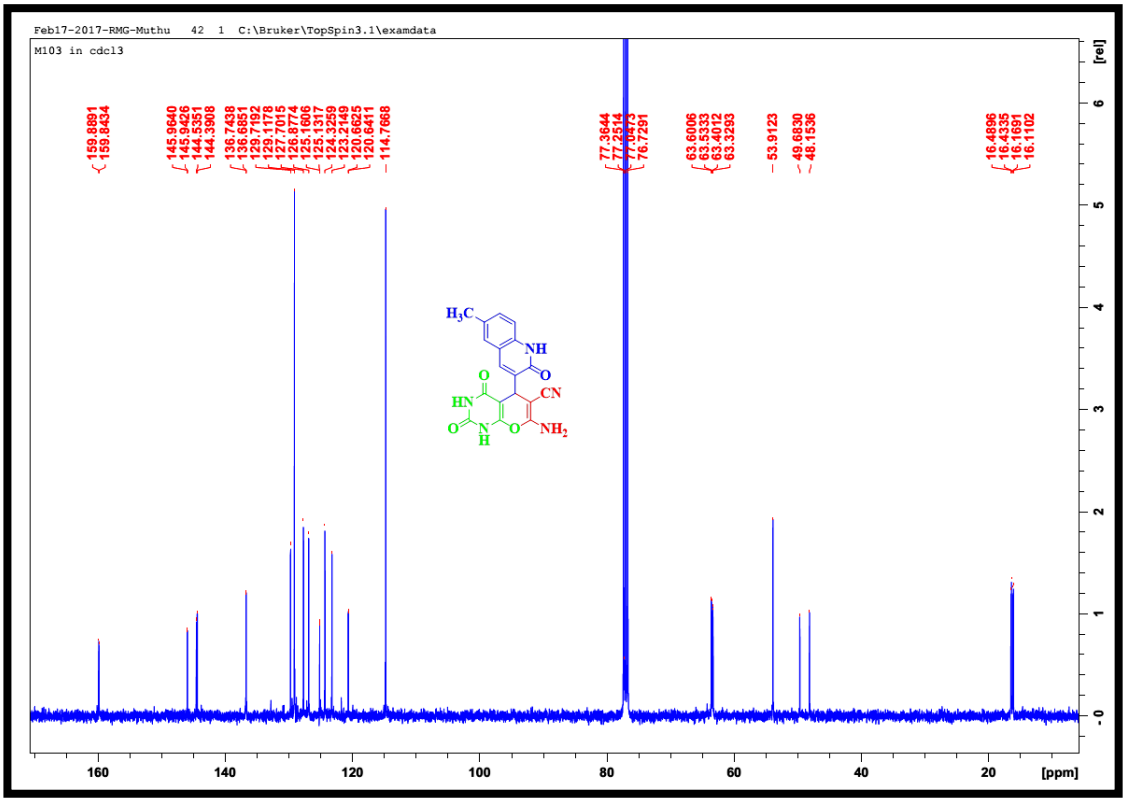

Fig. 4.36. ^{13}C-NMR spectrum of **40**

4.11. 2-Amino-4-(2-chloro-6-methylquinolin-3-yl)-7,7-dimethyl-5-oxo-5,6,7,8-tetrahydro-*4H*-chromene-3-carbonitrile (41)

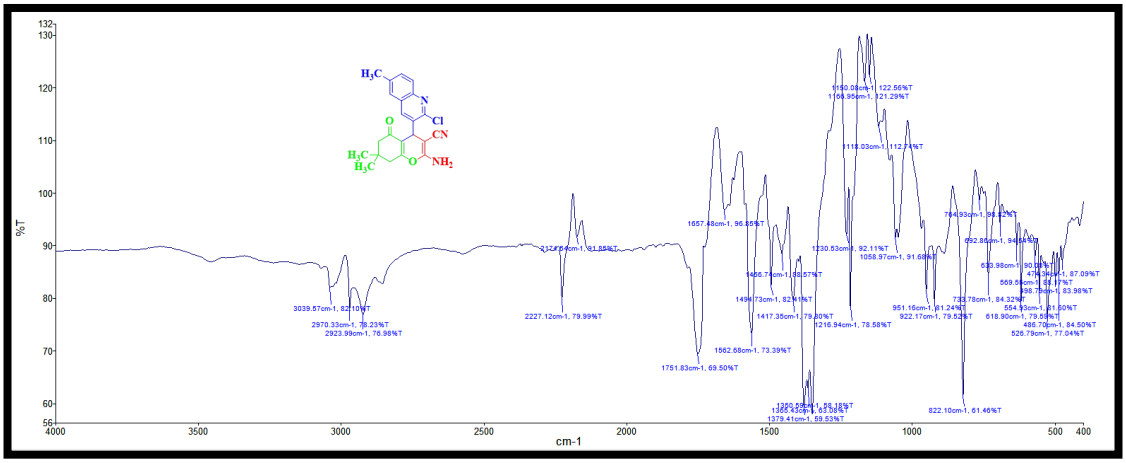

Fig. 4.37. IR spectrum of **41**

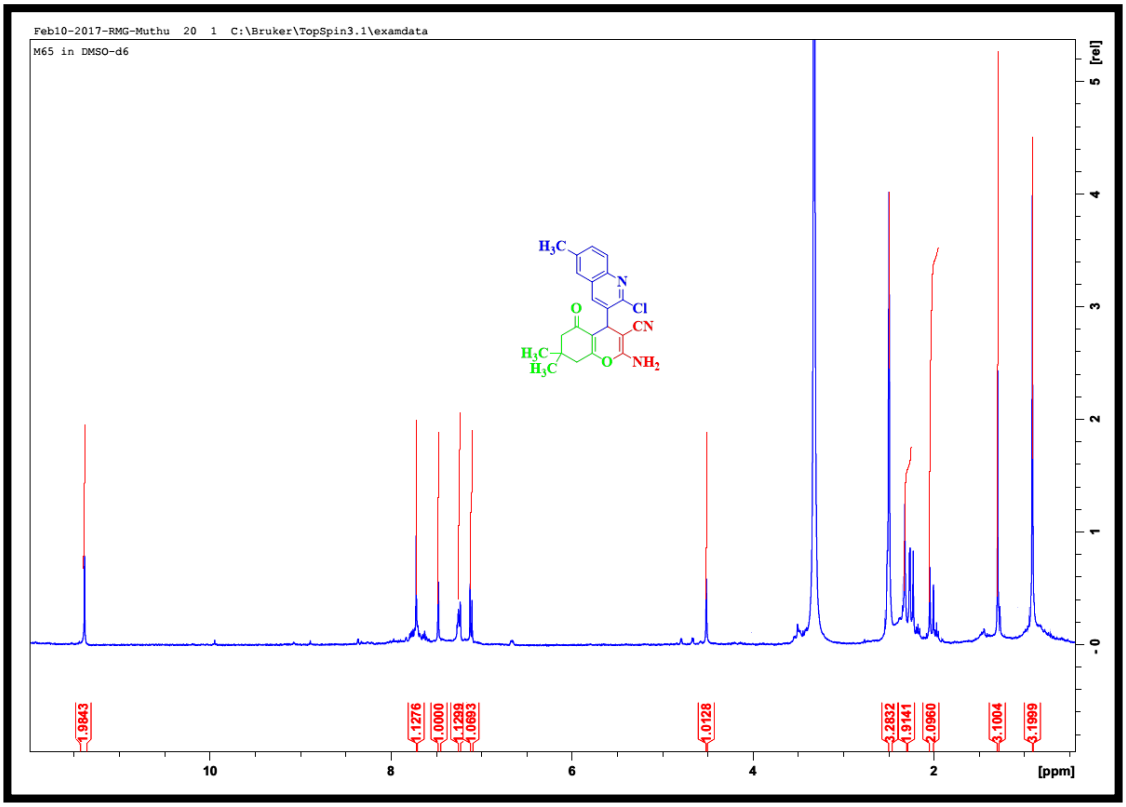

Fig. 4.38. ^{1}H-NMR spectrum of **41**

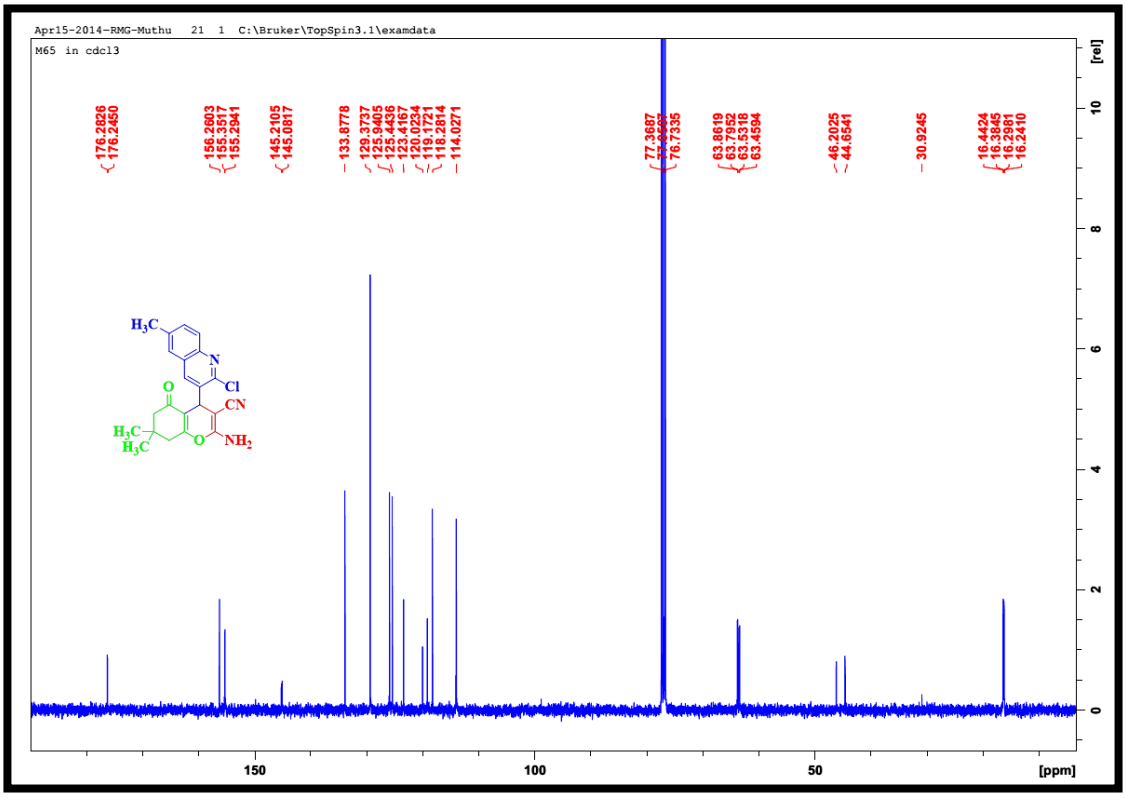

Fig. 4.39. ^{13}C-NMR spectrum of **41**

4.12. 2-Amino-4-(2-methoxy-6-methylquinolin-3-yl)-7,7-dimethyl-5-oxo-5,6,7,8-tetrahydro-*4H*-chromene-3-carbonitrile (42)

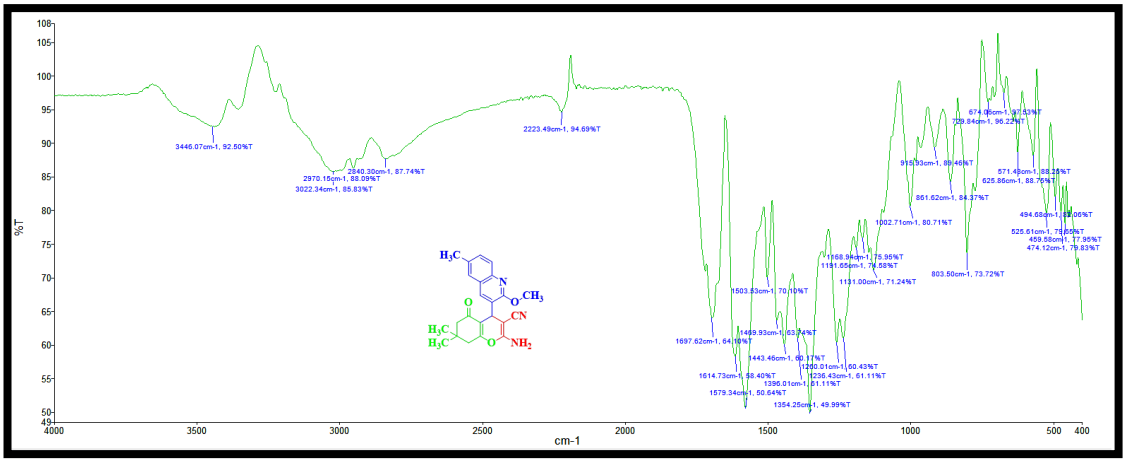

Fig. 4.40. IR spectrum of **42**

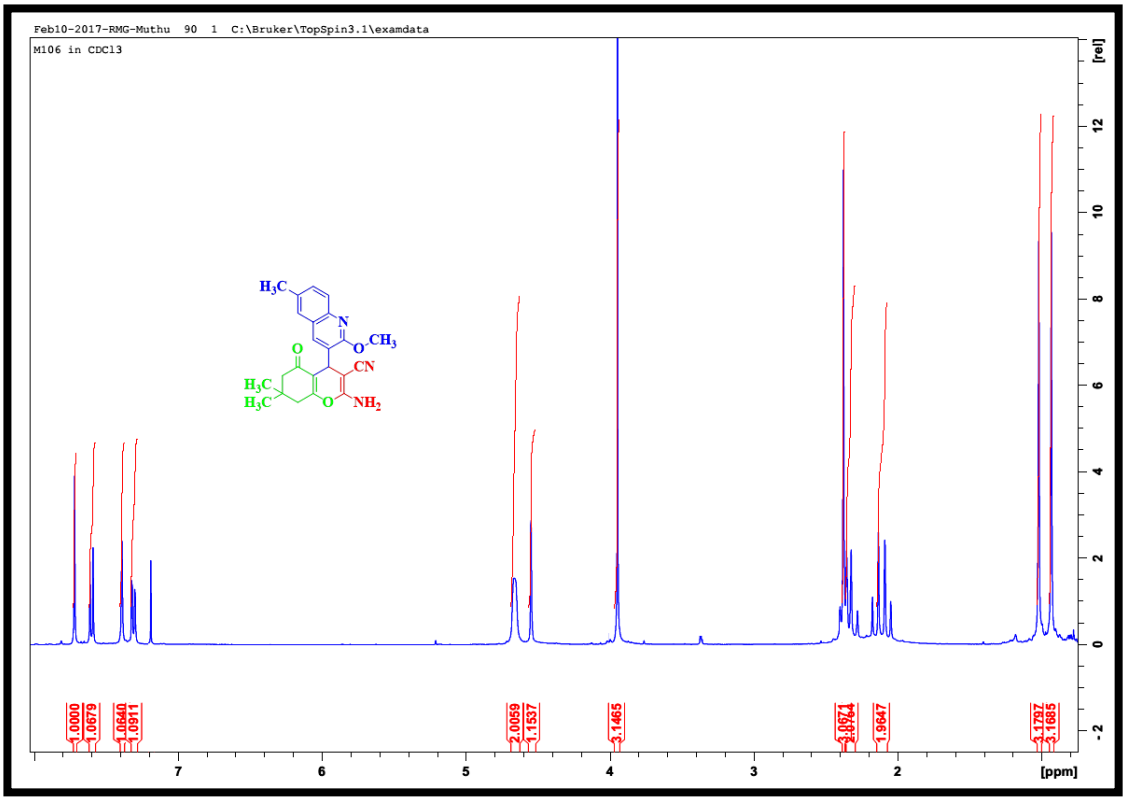

Fig. 4.41. ^{1}H-NMR spectrum of **42**

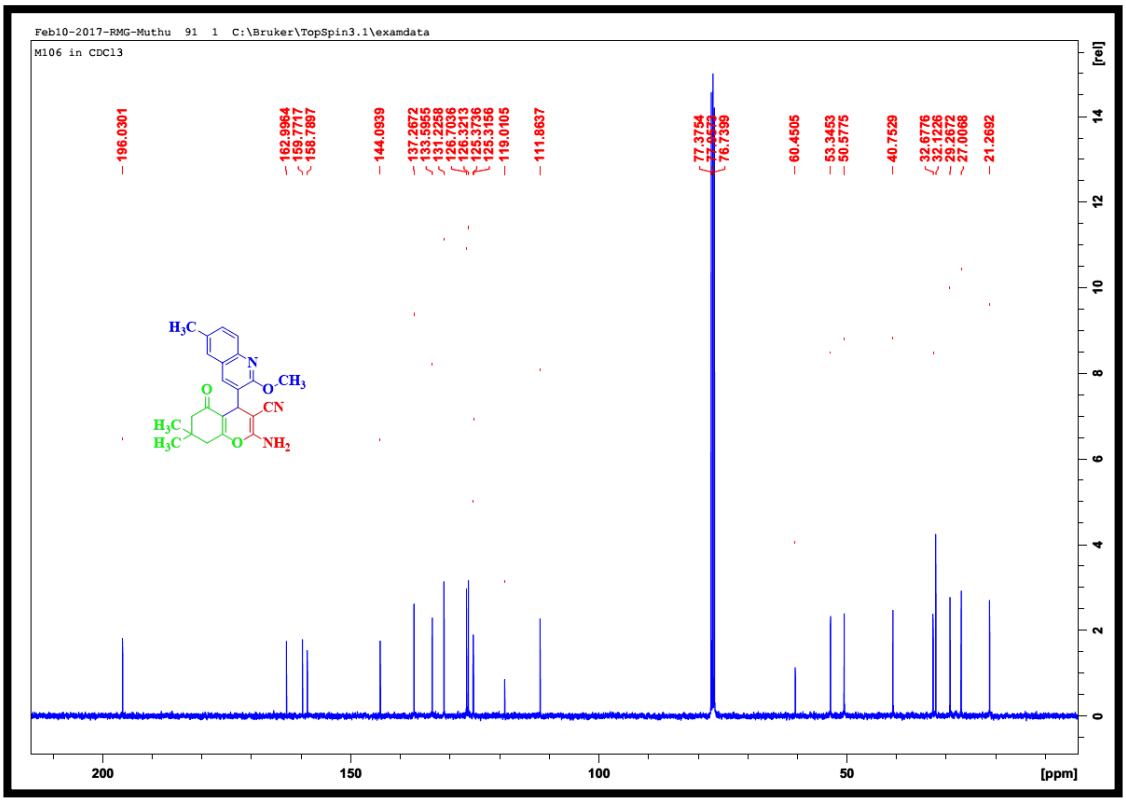

Fig. 4.42. ^{13}C-NMR spectrum of **42**

4.13. Ethyl 6-amino-5-cyano-4-(2-methoxy-6-methylquinolin-3-yl)-2-methyl-*4H*-pyran-3-carboxylate (43)

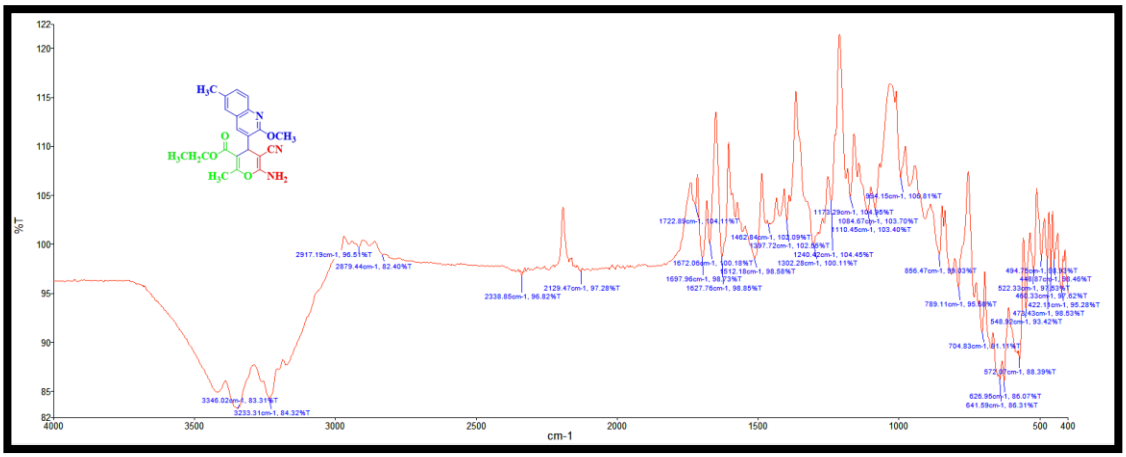

Fig. 4.43. IR spectrum of **43**

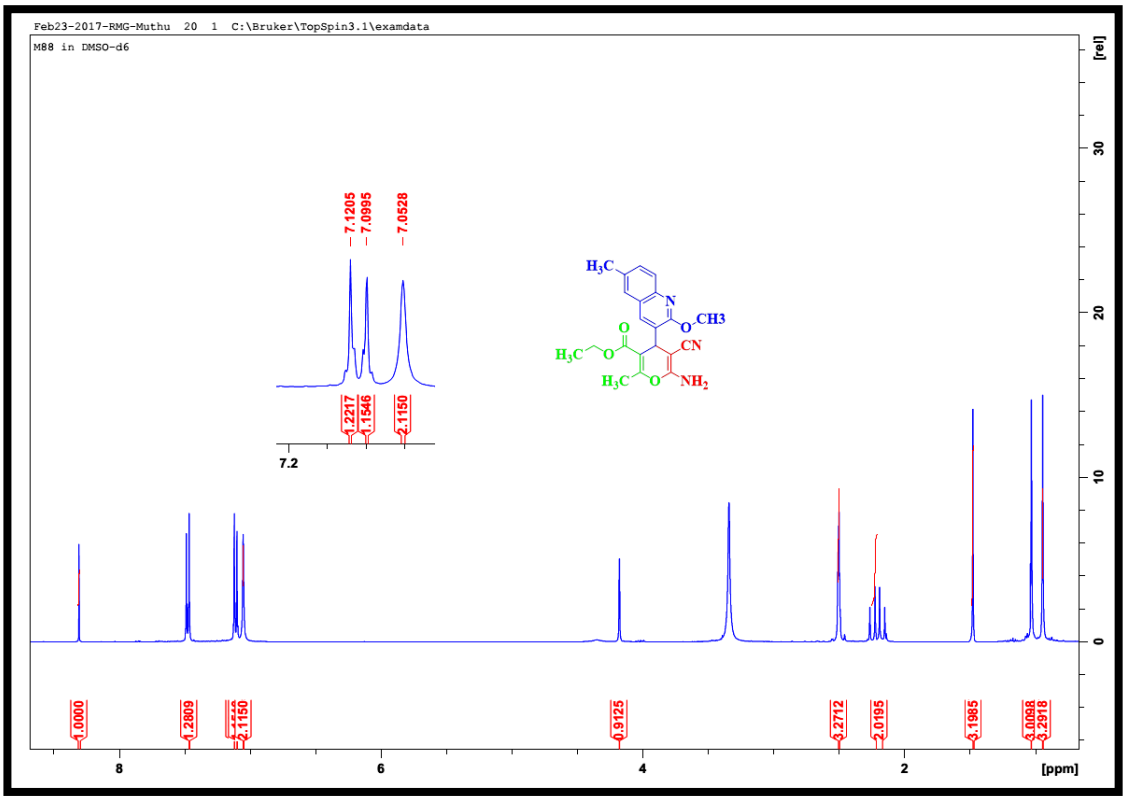

Fig. 4.44. ^{1}H-NMR spectrum of **43**

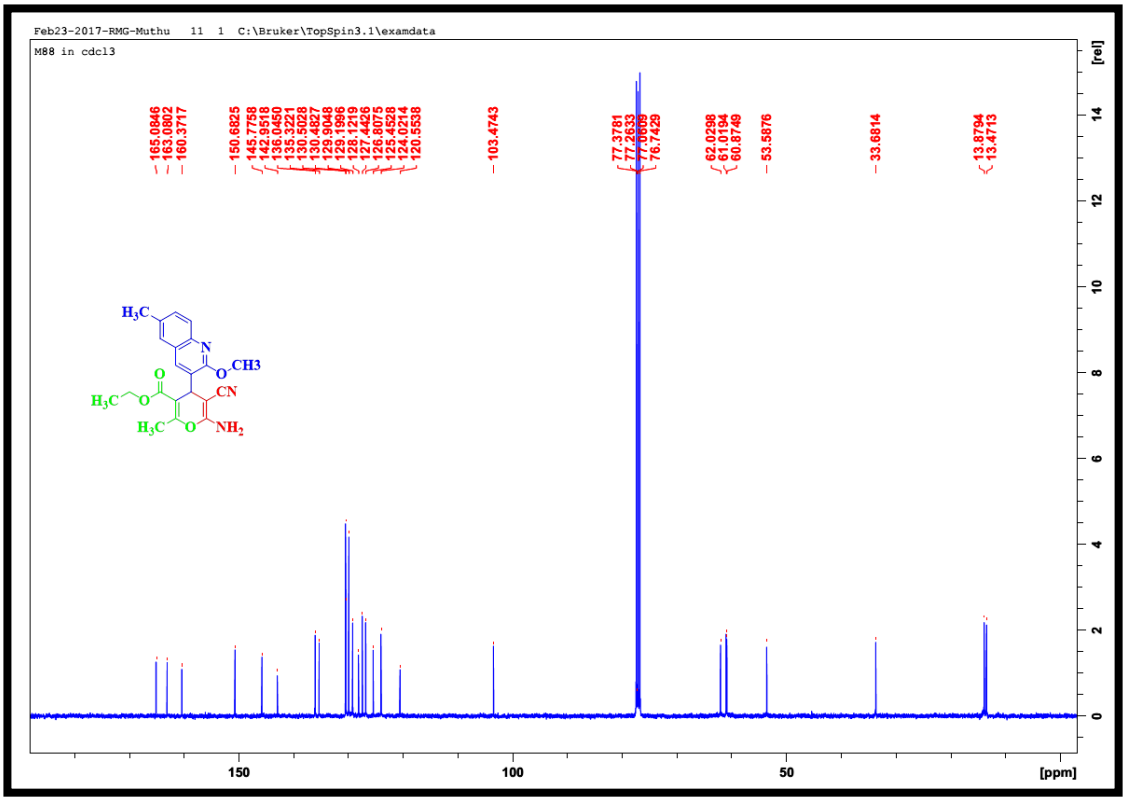

Fig. 4.45. ^{13}C-NMR spectrum of **43**

4.14. 5-Amino-7-(2-methoxy-6-methylquinolin-3-yl)-2-thioxo-3,7-dihydro-2H-pyrano[2,3-d]thiazole-6-carbonitrile (44)

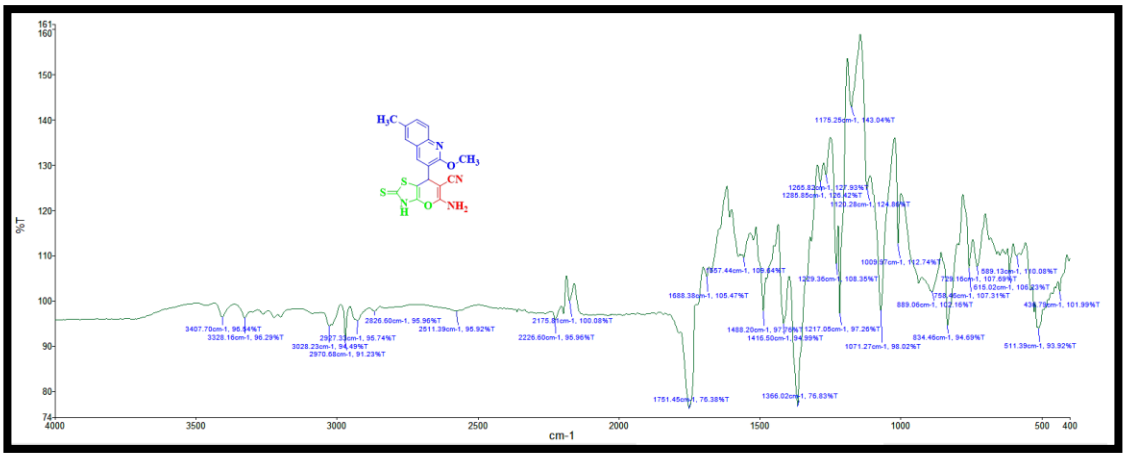

Fig. 4.46. IR spectrum of **44**

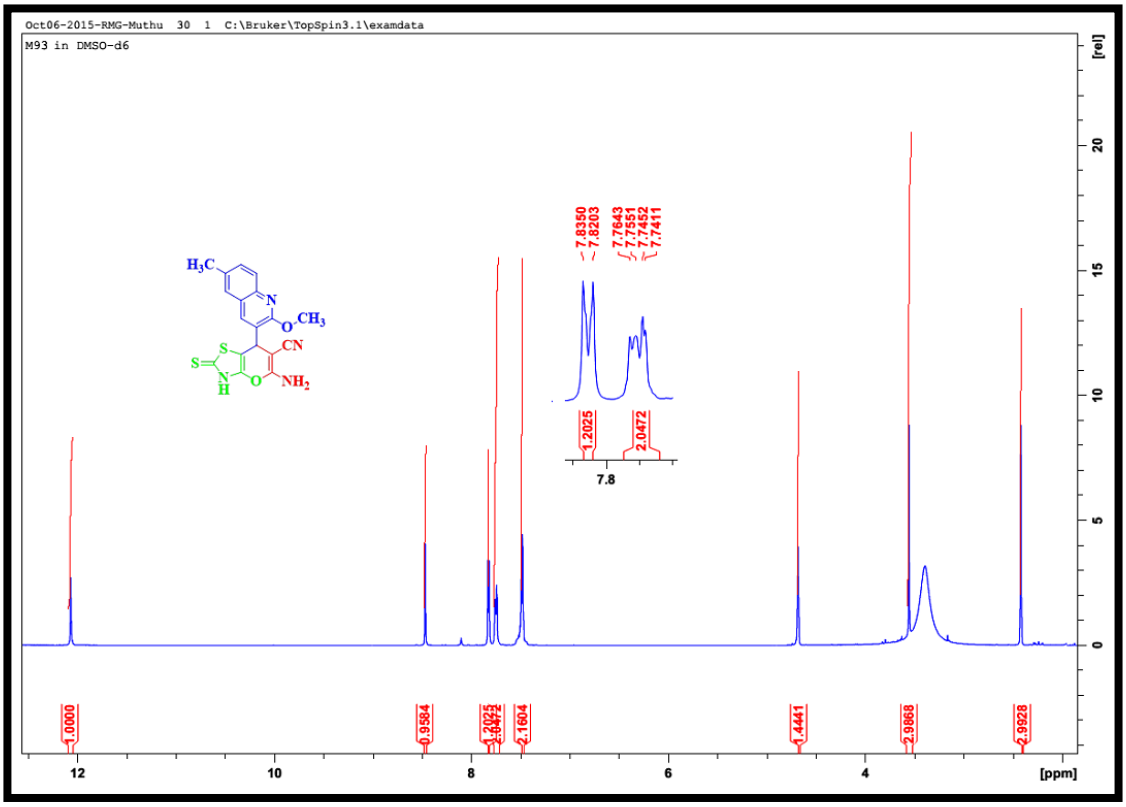

Fig. 4.47. ^{1}H-NMR spectrum of **44**

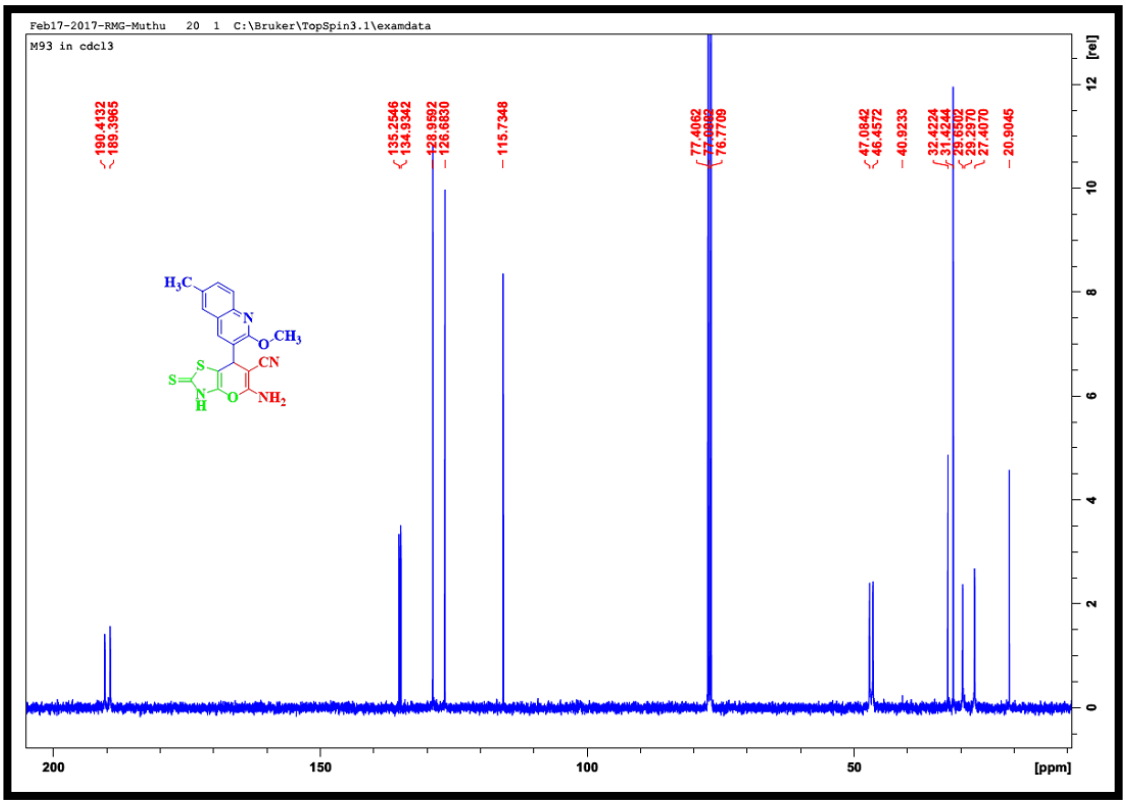

Fig. 4.48. ^{13}C-NMR spectrum of **44**

4.15. 2-Amino-6-(2H-indol-3-yl)-4-(p-tolyl)-*4H*-pyran-3,5-dicarbonitrile (45)

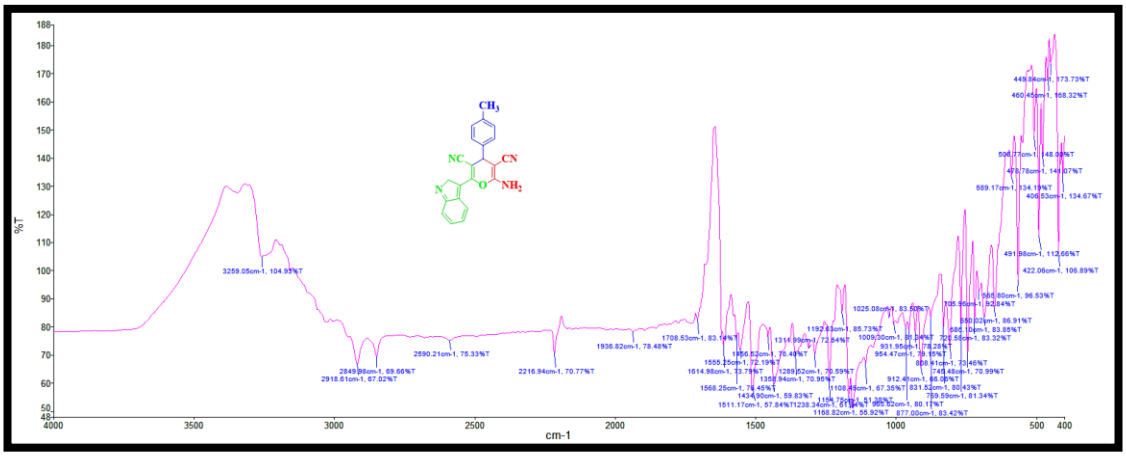

Fig. 4.49. IR spectrum of **45**

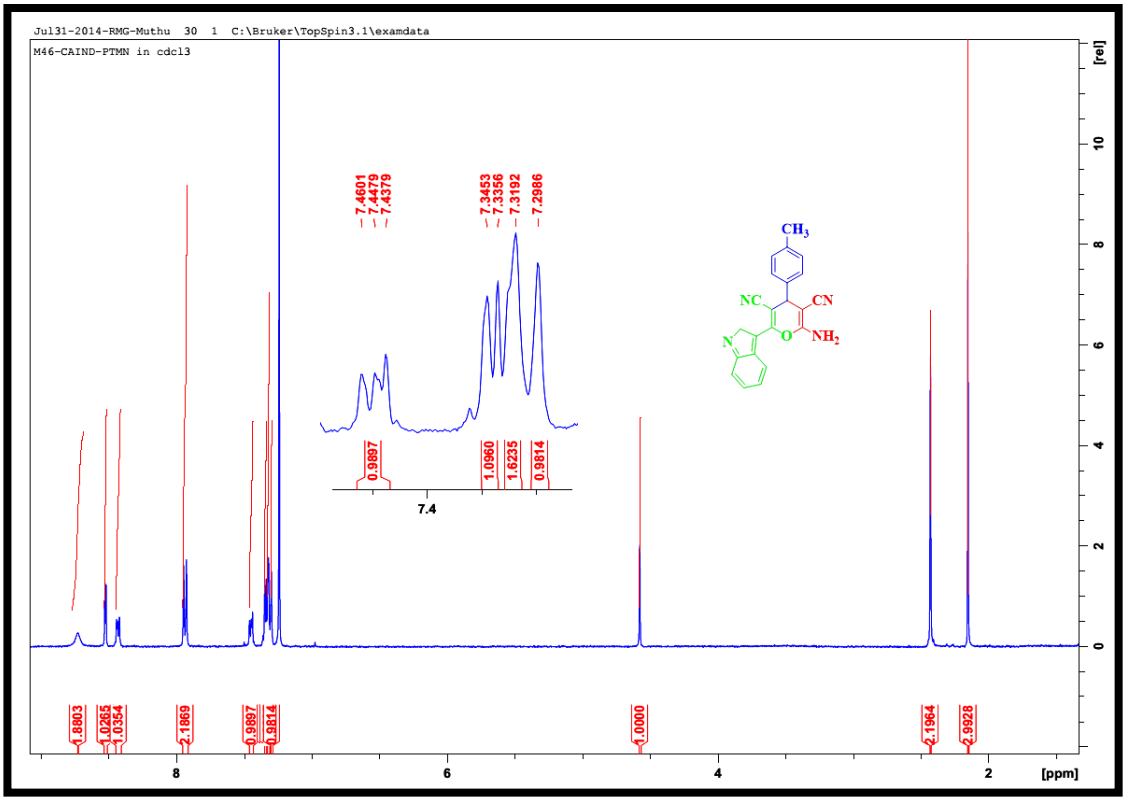

Fig. 4.50. ^{1}H-NMR spectrum of **45**

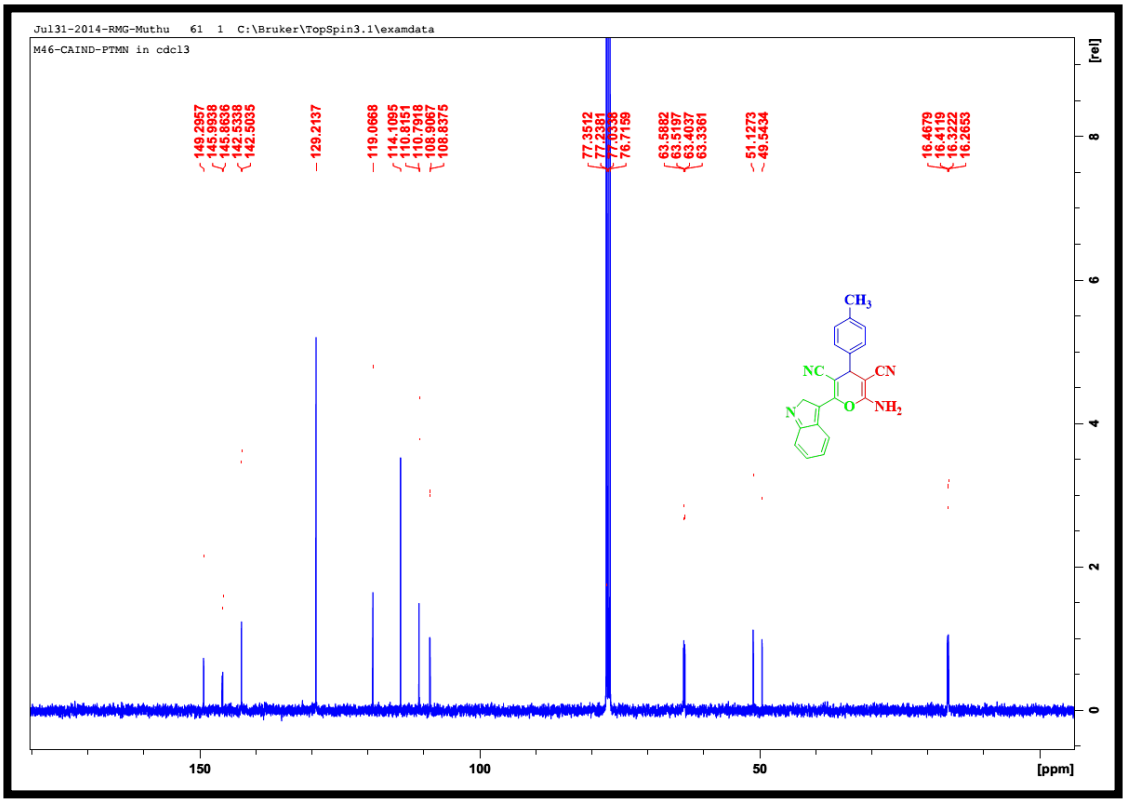

Fig. 4.51. ^{13}C-NMR spectrum of **45**

Chapter-V

Synthesis of α-aminobenzylthioquinolinyl phosphonates catalysed by an iron-loaded boron nitride material and their antimicrobial, antioxidant, toxicity assessment and molecular docking studies

Chapter Five

Synthesis of α-aminobenzylthioquinolinyl phosphonates catalysed by an iron-loaded boron nitride material and their antimicrobial, antioxidant, toxicity assessment and molecular docking studies

5.1. Abstract

A series of novel α-aminobenzylthioquinolinyl phosphonates (BTQPs) were synthesized via the Kabachnik-Fields reaction of 2-(benzylthio)quinoline-3-carbaldehyde derivatives, arylamines and diethylphosphite in the presence of a catalytic amount of iron-loaded boron nitride (Fe/BN) catalyst. The catalyst was prepared by simple stirring of $Fe(OAc)_2$ and boron nitride under a nitrogen atmosphere. Fe/BN was characterized by XRD, SEM with EDX, TEM, TGA, DSC and FTIR. The efficiency of Fe/BN, the effects of solvent and recyclability of the catalyst were optimized. All the synthesized BTQPs were characterized by FTIR, ^{1}H-NMR, ^{13}C-NMR and elemental analysis. A total of 10 BTQPs were subjected to antimicrobial, antioxidant and toxicity assessment studies. Among them, eight BTQPs showed potential antibacterial activities against *Bacillus cereus, Staphylococcus aureus, Escherichia coli and Enterococcus faecalis* whilst six BTQPs showed antioxidant activity effectively. 10 BTQPs were evaluated for toxicity by using brine shrimp and it was observed that eight BTQPs showed mortality rate less than 50 % until 48 h. Molecular docking studies were performed to determine the medicinal application of these molecules based on the Libdock score. Among them, compound **31** showed more potency towards *Staphylococcus aureus* gyrase with Libdock score 149.97 kcal/mol. Eco-friendly methodology, water as solvent, easy work up, mild reaction conditions, shorter reaction time with higher yields, recyclability of the catalyst and non-hazardous solvents are the significant features of the study.

5.2. Introduction

Among the mimics of natural bioactive molecules, α-amino phosphonates (APs) are important due to their vast applications in medicinal chemistry (Moonen *et al*., 2004;

Demmer *et al*., 2011). As a result of continuous efforts in this area, utilization of APs is expanding into many new research areas (Popa *et al*., 2015; Ménard *et al*., 1994). The APs exhibit a wide range of activities including being used as an agent against cancer (Ye *et al*., 2014; Huang *et al*., 2013; Huang *et al*., 2013; Huang *et al*., 2017), tuberculosis (Mulla *et al*., 2014; Subhedar *et al*., 2016), HIV/AIDS (Stowasser *et al*., 1992; Lacbay *et al*., 2014) and bacteria (Ali *et al*., 2012; Sampath *et al*., 2016; Sivala *et al*., 2016). They have been used as mimics of peptides, enzyme inhibitors and also as therapeutic agents for many diseases (De Schutter *et al*., 2014; Ewa *et al*., 2012; Leon *et al*., 2006; Leung *et al*., 2013; Leung *et al*., 2013; Wang *et al*., 2012).

Quinolines are important constituents of pharmacologically active plant extracts and their synthesis has been reported regularly. The quinoline scaffold is also frequently found in the structure of numerous naturally occurring alkaloids and has been associated with a broad spectrum of biological activities. Pharmacological activities such as antituberculosis (Lilienkampf *et al*., 2009), antiproliferation (Sedic *et al*., 2008), anti-inflammatory (Sujatha *et al*., 2017), anticancer (Gakhar *et al*., 2008) and antioxidant (Chung and Woo, 2001) activity have been reported.

The preparation of sulphur-containing compounds is also important in organic synthesis because of their broad application in organic and medicinal chemistry (Metzner and Thuillier, 2013; Nudelman, 1984; Chatgilialoglu and Asmus, 1991). The β-mercapto diketone is a vital sub-class as the compounds display remarkable pharmacological properties such as diuretic and HIV protease inhibitory activities (Bicking *et al*., 1976; Ding *et al*., 2009; Inomata *et al*., 2005; Yamauchi *et al*., 1982). Recently, several MCRs based on sulphur have been described. Evdokimov *et al*., 2007 reported a one-step synthesis of privileged medicinal sulphur based compounds from a mixture of malononitrile, aldehydes and thiols which was catalyzed by triethylamine. Based on the properties of quinolines, phosphonates and sulphur, their fusion into a single heterocycle could lead to new compounds with improved biological activities.

Generally, APs are synthesized by the nucleophilic addition of phosphite to imine in the presence of a Bronsted acid (Petrov *et al*., 1974) or Lewis acids like $ZnCl_2$ (Zawadzki, 1987), BF_3•Et_2O (Laschat and Kunz, 1992) and CdI_2/benzene (Kabachnik *et al*., 2002). The one-pot synthesis of APs have been carried out in organic solvents using lanthanide triflate (Qian and Huang, 1998), $InCl_3$ (Ranu *et al*., 1999), $ZrCl_4$ (Yadav *et al*., 2001),

$In(OTf)_3/MgSO_4$ (Ghosh *et al*., 2004), GaI_3 (Sun *et al*., 2004), $BiCl_3$ (Zhan and Li, 2005), $Cu(OTf)_2$ (Paraskar and Sudalai, 2006), $SbCl_3/Al_2O_3$ (Kumar *et al*., 2008) and an ionic liquid (Yadav *et al*., 2002). The transformations could also be accomplished in the presence of $LiClO_4 \bullet Et_2O$ (Saidi and Azizi, 2002; Azizi and Saidi, 2003), TFA (Akiyama *et al*., 2003), $LiClO_4$ (Azizi *et al*., 2004), metal triflate (Firouzabadi *et al*., 2004), Na_2CaP_2O7 (Elmakssoudi *et al*., 2005), $ZrOCl_2 \bullet 8H_2O$ or $ZrO(ClO_4)_2 \bullet 6H_2O$ (Bhagat and Chakraborti, 2008) and TsCl (Kaboudin and Jafari, 2008). Recently Krishna *et al*., 2010 reported the synthesis of APs (**5**) by condensation of imines (**2**) and dialkyl phosphite (**4**) without a catalyst. The reaction was carried out for six h to afford yields of 66-82 %.

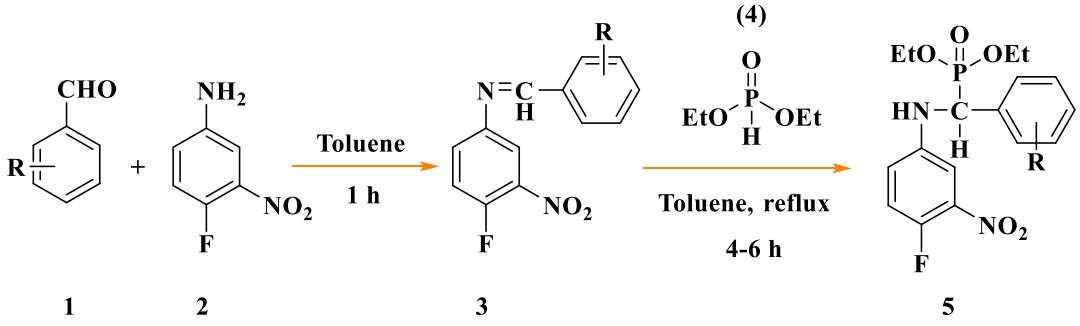

Abdel-Megeed *et al*., 2012 developed a three-component reaction for the synthesis of diphenyl-1-(arylamino)-1-(pyridin-3-yl)ethyl phosphonates (**9**) by using $LiClO_4$, at room temperature. The disadvantage was the long reaction time of 20-30 h to afford the yield of 73-90 %, in the presence of DCM as a solvent.

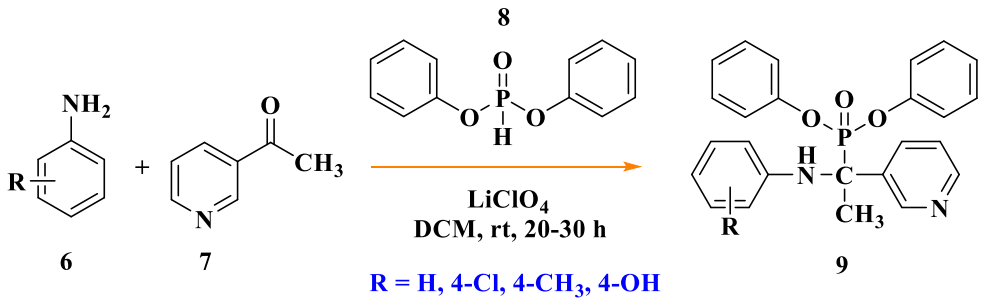

Badadhe *et al*., 2011 showed the synthesis of new functionalized APs (**12**) from various substituted anilines (**11**) and 1-phenyl-3-(pyridin-4-yl)-1H-pyrazole-4-carbaldehyde (**10**) under reflux. The reaction was carried out for 24 h to provide a maximum yield of 58 - 83 %.

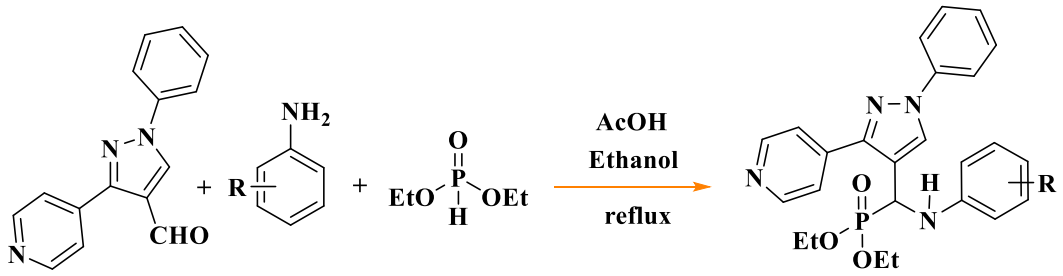

R = 2-Cl, 2-CH_3, 3-F, 4-Cl, 4-CH_3

Chinnam *et al*., 2013 synthesized a series of APs (**16**) by a one-pot three-component reaction of equimolar quantities of 4-amino-N-2-thiazolyl-benzene sulphonamide (**13**), dimethyl phosphite (**15**) and various aldehydes (**14**) under reflux. The reaction was carried out within 5-6 h in absence of a catalyst; the yield was 70-80 %.

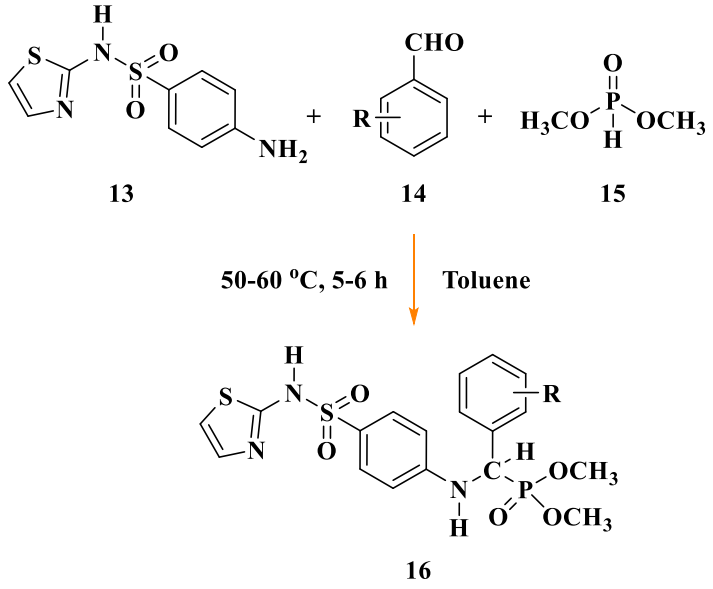

R = 3-NO_2, 3-CN, 4-NO_2, 3-OCH_3, 3-CF_3, 3-Cl

Recently, Ahmed *et al*., 2016 reported the synthesis of aminophenylaminoquinoline analogues (**20**) from phenylenediamine derivatives (**17**) in the presence of a Lewis acid and $LiClO_4$ as a catalyst. The one-pot reaction was carried out within 24-48 h using dry acetonitrile as a solvent with 85-93 % yield.

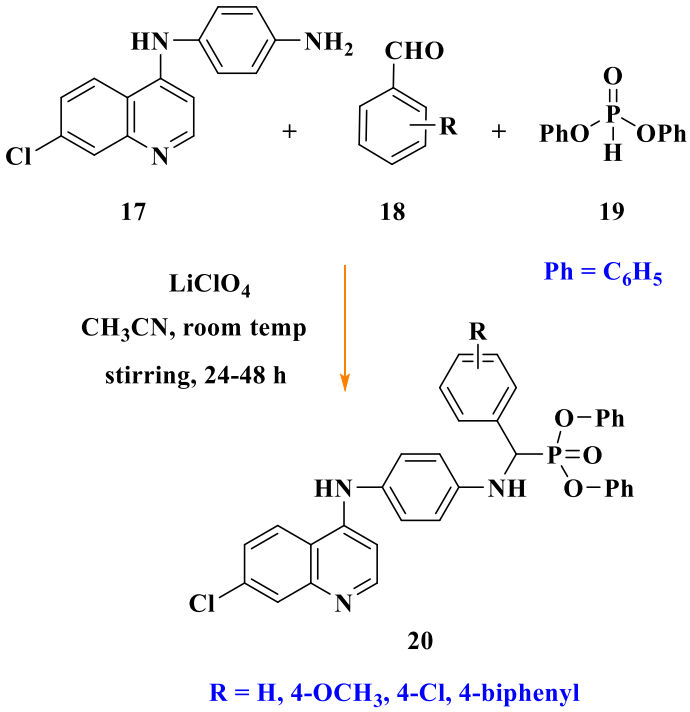

The majority of syntheses had several drawbacks including long reaction times, low product yield, stoichiometric amount of catalyst and costly metal ion catalyst. Therefore, we synthesized new APs with the aid of a new catalyst. Boron nitride was used as a support for iron which resulted in the heterogeneous catalyst.

5.3. Results and discussion

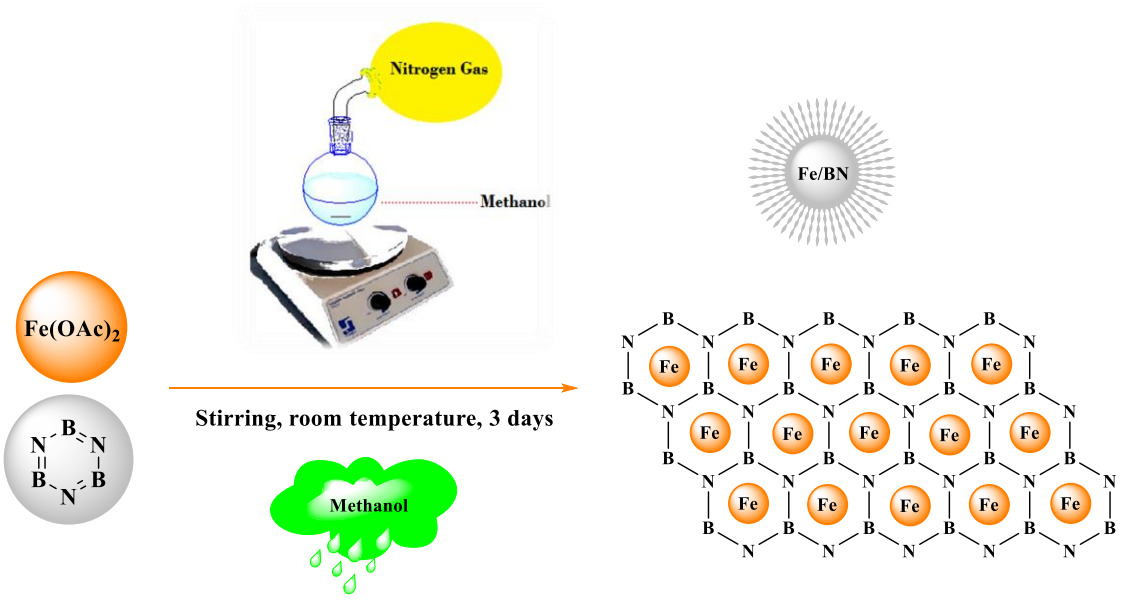

Scheme 1. The preparation of iron loaded boron nitride catalyst

Firstly, the iron-loaded boron nitride catalyst was prepared by simply mixing iron acetate and boron nitride, in methanol, at room temperature for three days. This was performed under a nitrogen atmosphere. A schematic illustration is shown in **Scheme 1**. The novel heterogeneous catalyst was characterized by using techniques including XRD, SEM with EDX, TEM, TGA, DSC and FTIR.

The XRD pattern **(Fig. 1)** showed the diffraction at 33.2°, 42°, 43.7°, 49.3°, 54°, 62.5° and 63.9° which corresponded to the spinel structure of Fe. The average particle size, calculated by using the Debye-Scherrer formula from the main reflection peak (311) at 42° 2θ, was approximately 75 nm. The Bragg's diffraction reflection was observed at approximately 26.5°, 35.2°, 50°, 54.9° and 75.8° which corresponded to the crystalline planes (002), (100), (102), (004) and (220). These peaks confirmed the hexagonal crystal structure of boron nitride (Trivedi *et al*., 2015).

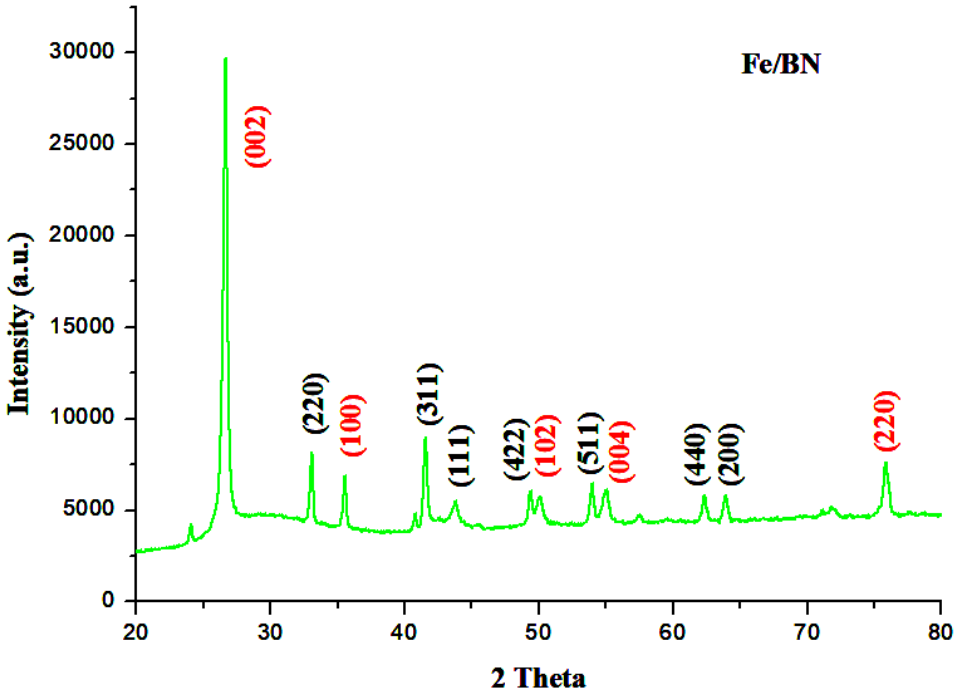

Fig. 1. X-Ray diffraction pattern of iron loaded boron nitride catalyst

The morphologies of Fe/BN is shown in **Fig. 2 (A-D)**. The SEM images showed small uniform pseudo cubic shape particles. The particles were fairly regular. The aggregation of the particles indicated the possible interaction of hexagonal boron nitride (h-BN) with metal. **Fig. 2 (C-D)** shows particles were agglomerated and consisted of irregular rod and plate-like crystals.

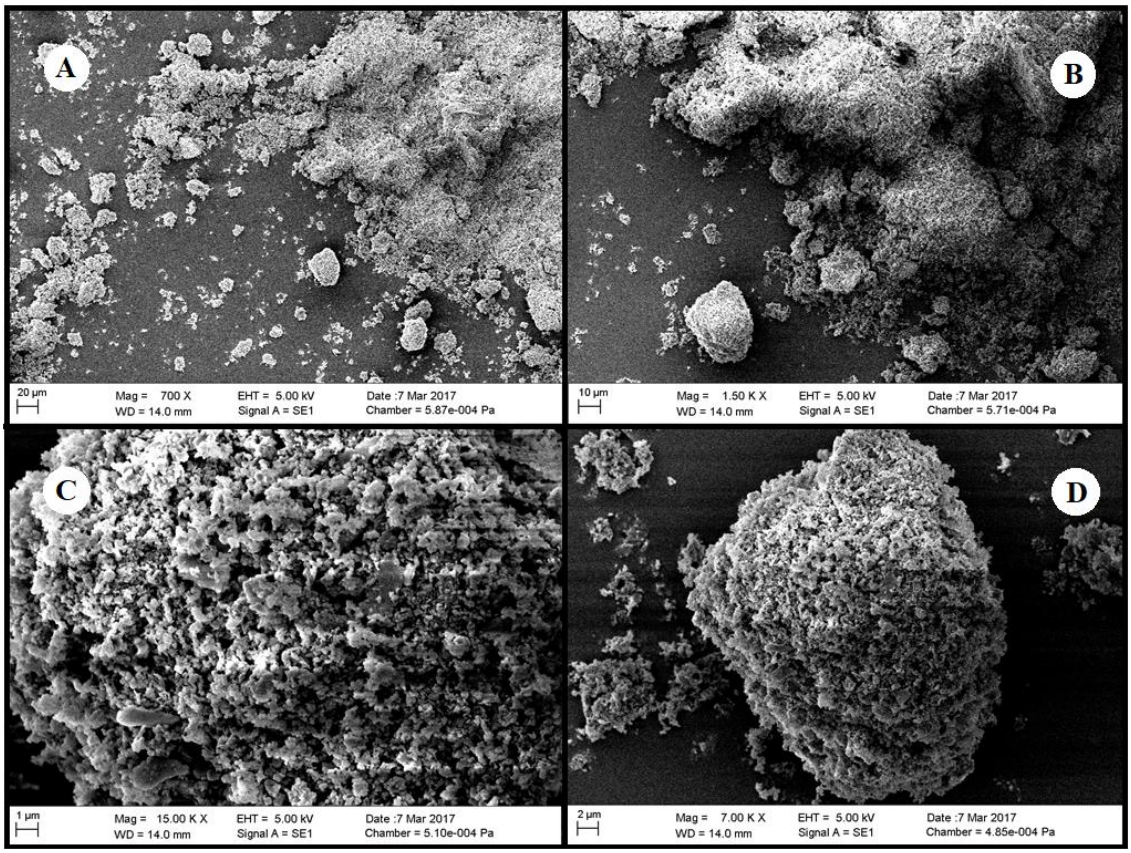

Fig. 2. Scanning electron microscopy images of iron loaded boron nitride catalyst

The dimension of crystals were about 80, 160 nm and 200 nm **(Fig. 4**, see: histogram) and the thickness of sheet was approximately 20~50 nm. The average crystallite size, calculated from Scherrer's formula (Scherrer, 1948), was ~24 nm, thus the observed SEM images suggested that the catalyst consisted of many small crystallites.

Fig. 3 displays the SEM images of Fe/BN showing the elements iron, boron, nitrogen, carbon and gold (Au). The iron peaks were at 0.35, 6.20 and 6.50 keV. The elemental mapping was obtained while running the sample in EDS and is illustrated in **Fig. 3.**

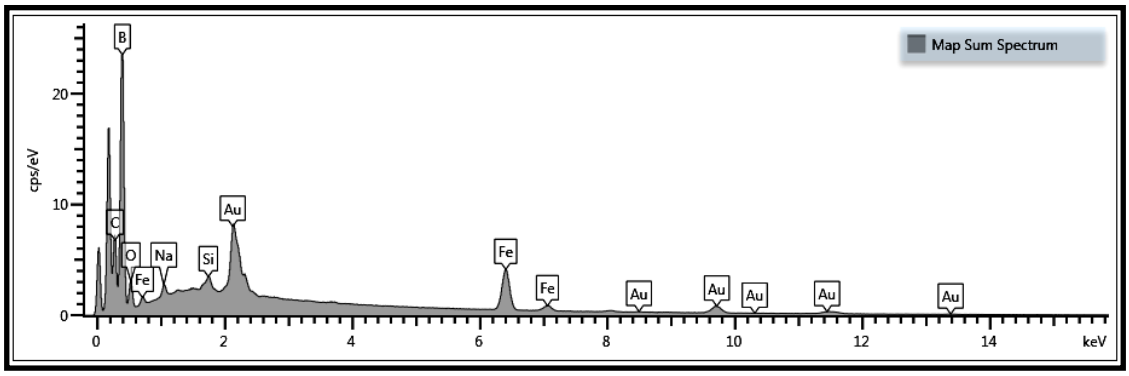

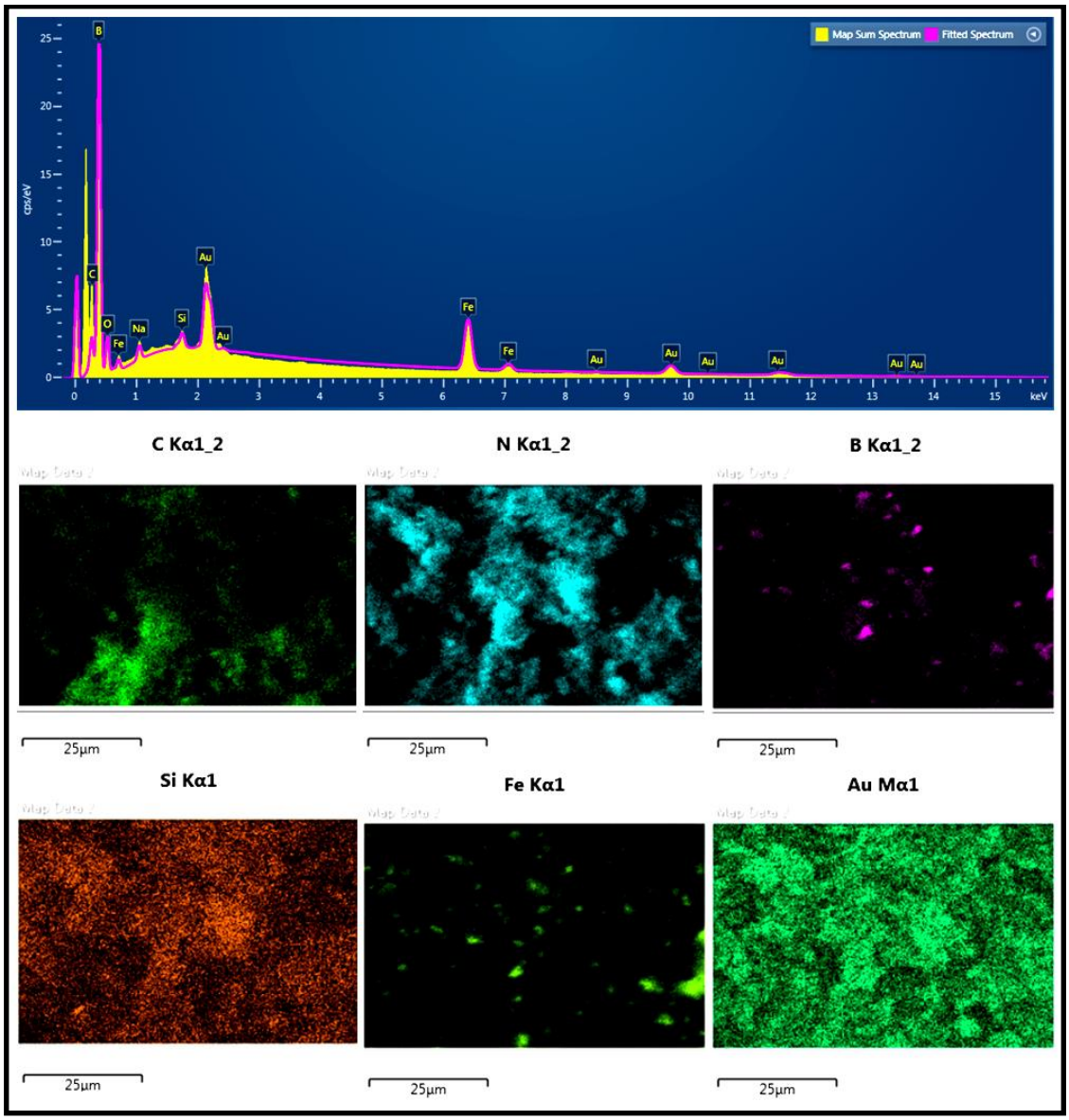

Fig. 3. Energy dispersive X-ray spectrum and elemental mapping of iron loaded boron nitride catalyst

The appearance of Au was due to the coating of the sample with conducting Au material to reflect electrons known as sputter coating.

The particle size and morphology was obtained from TEM analysis and is shown in **Fig. 4 (A-E)**. TEM indicated the presence of two distinct size modes. Particles in the larger size mode were non-agglomerated and displayed a log-normal size distribution.

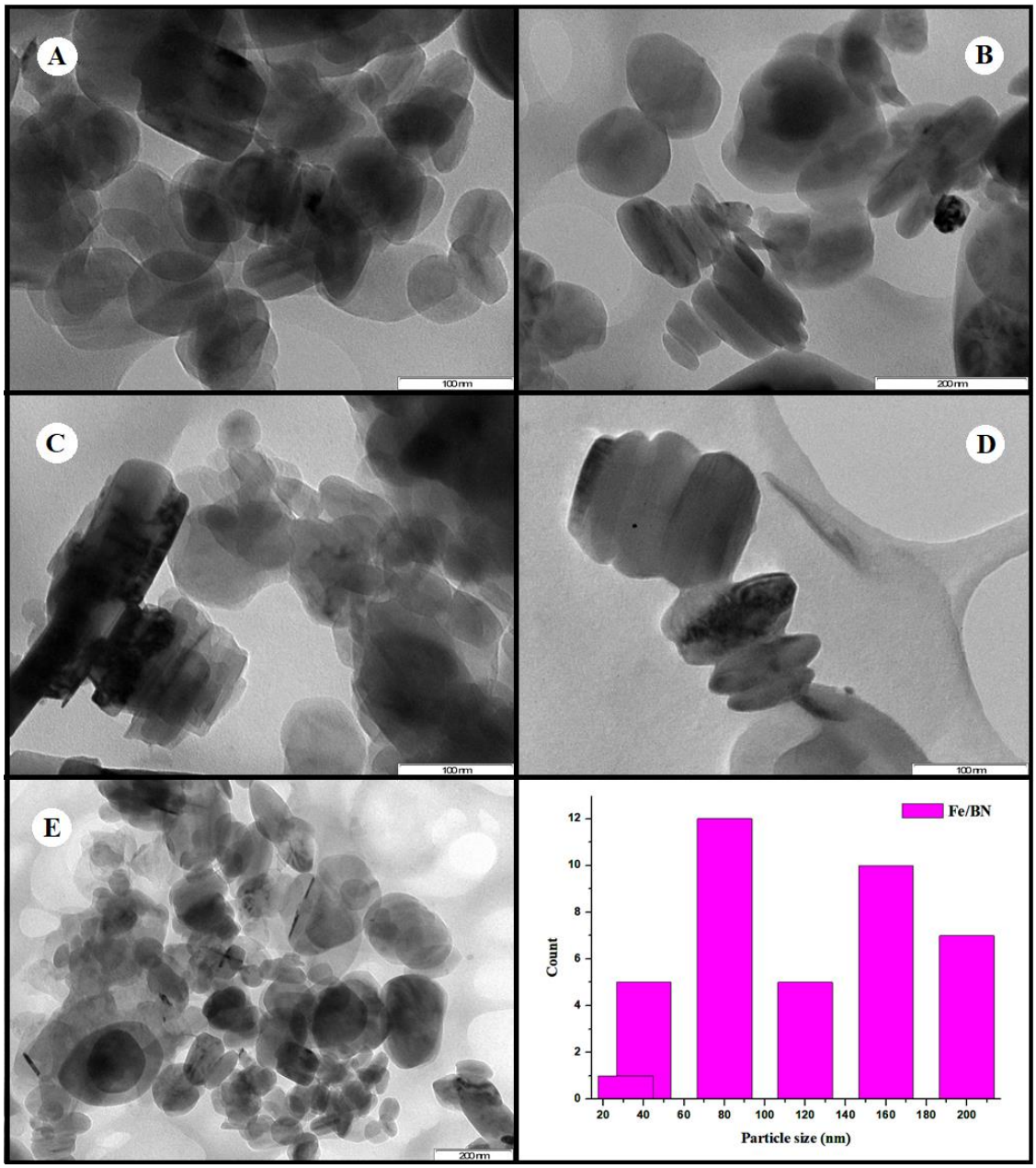

Fig. 4. Transmission electron microscopy images and particle size of iron loaded boron nitride catalyst

The count median diameter of the log-normal size distribution was 160 nm and 200 nm. The average size of the particles was 80 nm (size variation: ± 9 nm by ImageJ, **Fig. 4**: histogram) with an initial process of particle sinterization. The shape of h-BN particles appeared spherical and irregular. The layered appearance of the particles suggested Fe packed within BN. The closely packed aggregated particles and multilayer appearance was possible due to the cavity and movement of atoms towards the interior sphere of h-BN as reported by Chien *et al*., which focused on boron nitride coated Rhodium (Chien

and Van Bokhoven, 2015). Wang *et al*., 2009 also showed the crystallization of boron nitride spheres prepared by vapor phase pyrolysis of ammonia borane.

The degradation of Fe/BN was analysed by thermogravimetric analysis. The TGA curve **(Fig. 5)** indicated that the sample encountered an initial weight loss of ~52 %, when the temperature was increased from room temperature to 130℃, which corresponded to the elimination of adsorbed and bound water molecules. The weight of the sample stabilized in the range of 180℃ - 547℃. The Fe/BN showed further degradation at approximately 725℃ which was ascribed to partial decomposition of metal loaded boron nitride material.

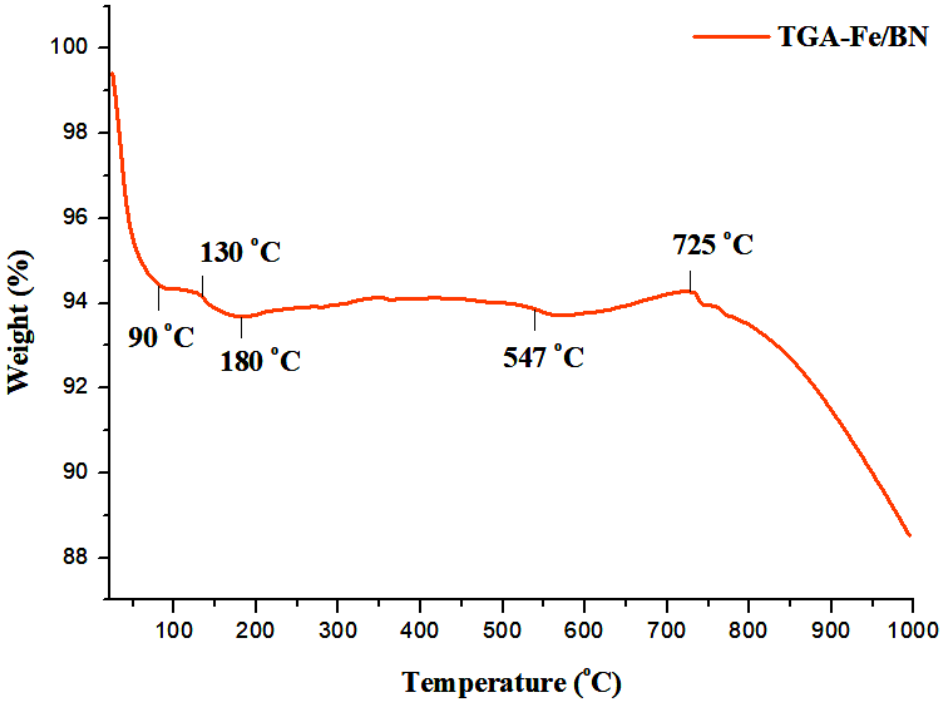

Fig. 5. Thermogravimetric curve of iron loaded boron nitride catalyst

The decomposition and subsequent active oxidation started at temperatures greater than 725℃. This could possibly be attributed to BN oxidation and subsequent formation of boron trioxide (B_2O_3) on its surface. As the powder decomposed, boron reacted with the atmospheric oxygen and produced B_2O_3 while nitrogen gas was released (Oda and Yoshio, 1993). The process can be explained by a chemical reaction below:

$$2BN + 3/2\ O_2 \longrightarrow B_2O_3 + N_2 \uparrow$$

TGA analysis was completed at 1000℃: about 44 % mass loss was observed in the range of 725℃ - 1000℃ (**Fig. 5**).

The DSC curve **(Fig. 6)**, provided information on decomposition and oxidation. A broad endothermic peak occurred between the temperatures of 200℃ - 960℃. This confirmed the crystallization of the Fe phase (Sneha and Sundaram, 2015). The appearance of the peak was directly related to the decomposition of the powder (h-BN) as detected by the thermogravimetric technique (at 725℃) i.e., it absorbed the heat and confirmed the transformation of BN to B_2O_3. Also, a small endothermic peak appeared with a specific band width in temperature range of 95℃ - 200℃. The appearance of the peak could be due to crystallization of the powder and the strong interaction between iron and the support (Sneha and Sundaram, 2015).

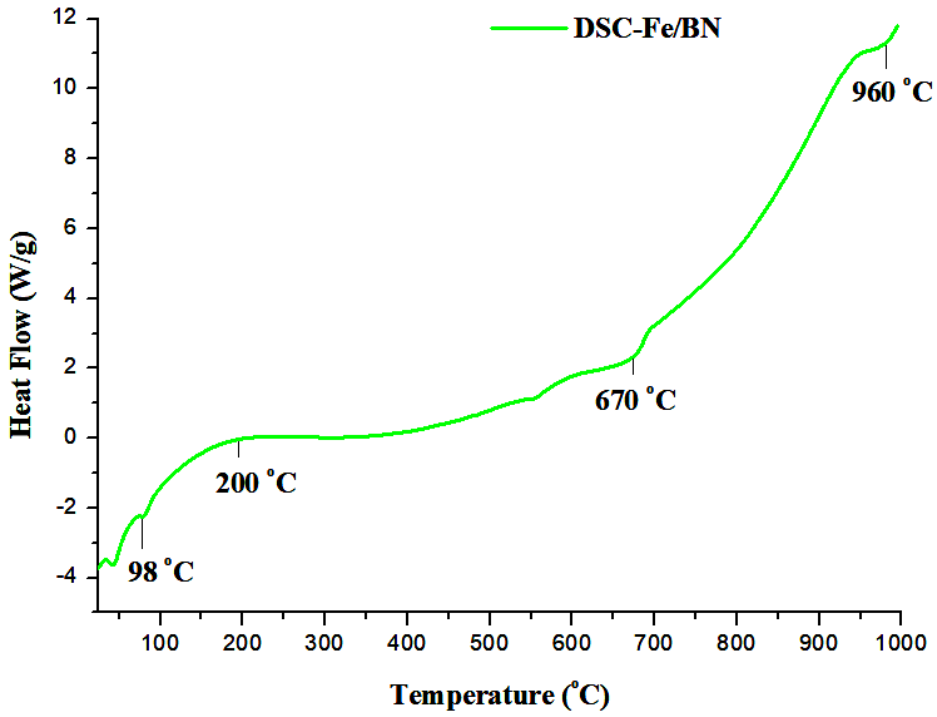

Fig. 6. Differential scanning calorimetry curve of iron loaded boron nitride catalyst

The FTIR spectrum **(Fig. 7)** showed O-H and B-H stretching peaks at 3287 cm^{-1} and 2193 cm^{-1}, respectively. The peaks observed at 1646 cm^{-1} and 828 cm^{-1} were assigned to the stretching frequencies of N-B-N and B-N-B, respectively (Muthu *et al*., 2016). The absorption frequency for Fe-N was observed at 1735 cm^{-1} (Miller and Wilkins, 1952). The O-H absorption was possibly due to moisture.

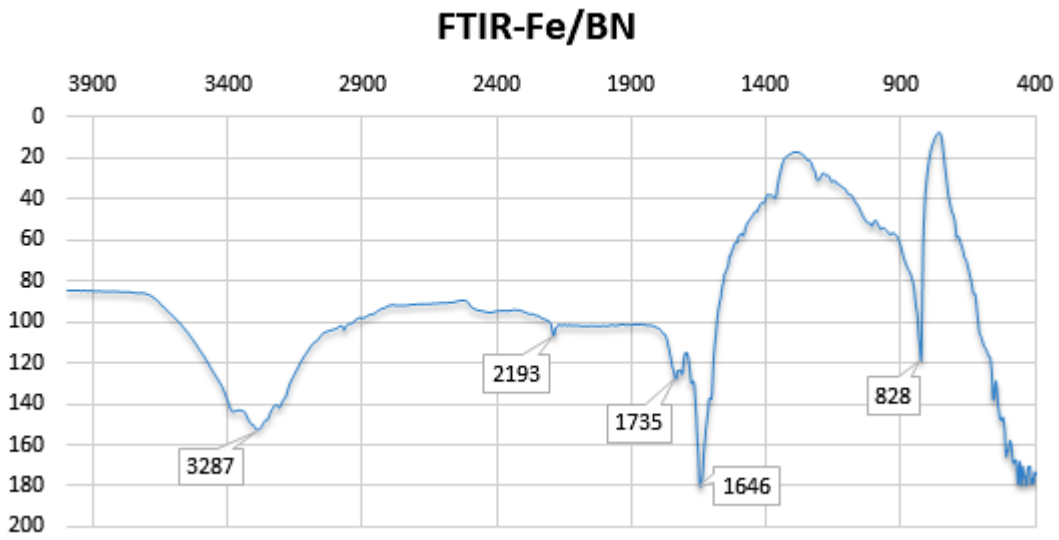

Fig. 7. Fourier transform infrared spectrum of Fe/BN

After the successful characterization of Fe/BN, the heterogeneous catalytic activity was investigated in a one-pot three-component Kabachnik-Fields reaction.

Initially, chloroformylquinoline (CFQ) was synthesized via the Vilsmeier-Haack reaction which is a well-established protocol in our laboratory (Srivastava and Singh, 2005). The starting material, 2-(benzylthio)quinoline-3-carbaldehyde (BTQC), was prepared by heating CFQ with 2-benzyl mercaptan in the presence of NaH at 90℃ for 2-3 h. It was then separated from DCM and water solvent system (1:3) followed by column chromatography. The desired starting material BTQC (**21**) was used for the preparation of APs via the Kabachnik-Fields reaction. At first, a trace amount of APs was obtained when an equivalent mixture of **21** (1 mmol), *m*-toluidine (1 mmol) and diethyl phosphite (**4**) (1 mmol) was used in acetonitrile medium. The reaction was carried out under reflux conditions (90℃) for 3-6 h in the presence of available catalysts: $Mg(ClO_4)_2$, $InCl_3$, CuI, L-proline and $FeCl_3$ according to the reported procedures (Maghsoodlou *et al*., 2009). The reaction was monitored by TLC every 5 minutes. Thereafter, the same mole ratio was used in the presence of Fe/BN (10 mol %) in MeCN medium under reflux condition which resulted in a 60 % yield within 3 h. Microwave irradiation was then used to produce a yield of 65 %. However a maximum yield of 98 % was obtained when water was used as the solvent (**Scheme 2**). The synthesis of **23** which used *m*-toluidine as the variable substrate was the template reaction. The structure of **23** was characterized by FTIR, ^{1}H-NMR, ^{13}C-NMR, HSQC, COSY, NOESY, HMBC and elemental analysis.

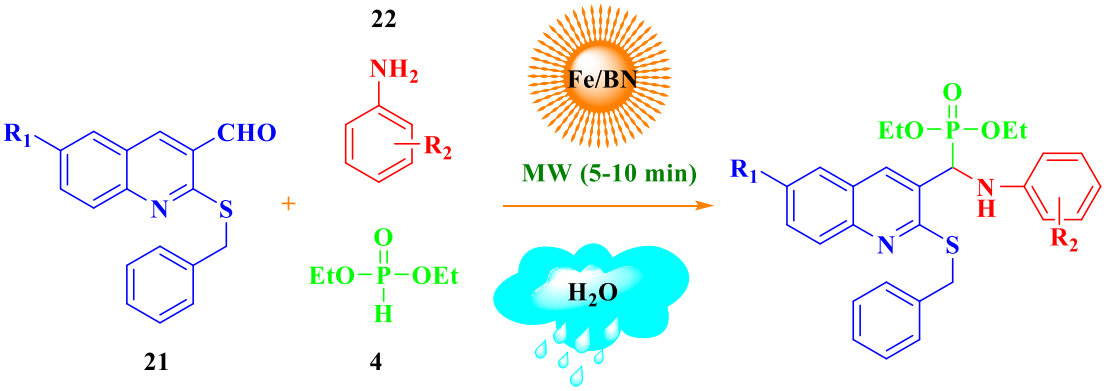

R_1 = H; R_2 = H; **(24)**
R_1 = H; R_2 = 2-OCH_3; **(25)**
R_1 = H; R_2 = 2-CH_3; **(26)**
R_1 = H; R_2 = 3-F; **(27)**
R_1 = H; R_2 = 3-Cl-4-F; **(28)**
R_1 = H; R_2 = 2-NO_2; **(29)**
R_1 = H; R_2 = 2,4-CH_3; **(30)**

R_1 = H; R_2 = 3-CH_3; **(23)**
R_1 = H; R_2 = 4-OCH_3; **(31)**
R_1 = H; Amine = 2-Picolylamine; **(32)**
R_1 = H; R_2 = 4-Br; **(33)**
R_1 = H; R_2 = 4-Cl; **(34)**
R_1 = H; R_2 = 3,4-Cl; **(35)**
R_1 = F; R_2 = 2-OCH_3; **(36)**

Scheme 2. Synthesis of α-aminobenzylthioquinoline phosphonates (**23-36**) by microwave irradiation

The IR spectrum (**Fig. 5.1**, Appendix V) of **23** showed stretching frequencies (cm^{-1}) at 1216 for C-N, 2970 for CH, 1651 for C=C, 1273 for P=O, 1022 for P-O-C, 2585 for S-H, 695 for C-S and 3285 for NH. The ^{1}H-NMR spectrum (**Fig. 5.2**) of **23** showed two singlets: (brs, N<u>H</u> (C1')) at δ 12.46 and methyl group of *m*-toluidine (C<u>H</u>$_3$ (C15)) at δ 2.20. The C9-<u>H</u> proton of (CH) group showed a doublet at δ 5.61. Quinolinyl proton showed a doublet at δ 8.11 with a coupling constant value of *J*=3.72 Hz. The benzylthio group proton of C<u>H</u>$_2$ (C2") showed a multiplet at δ 4.33-4.29 with coupling constant value J=7.32 Hz. The ^{13}C-NMR spectrum (**Fig. 5.3**) of **23** showed a peak at δ 21.55 for methyl group (CH_3) of *m*-toluidine (C15). The methyl carbons (C14) of the phosphoryl group showed a peak at δ 16.50 and C12 was at δ 16.27. The carbons C11 and C13 from ethoxy groups of the phosphoryl group (-OCH_2) showed peaks at δ 63.78 and 63.36. The carbon of the CH_2 (C2") group of benzyl thio group showed a peak at δ 47.29. The quinolinyl carbon C4 showed a peak at δ 130.51 and C9, (CH) group carbon showed a peak at δ 48.82. The quinolinyl carbon (C=N) showed a peak at δ 163.29. The structure was further confirmed on the basis of 2D NMR spectral studies. The selected ^{1}H and ^{13}C-NMR chemical shifts for **23** are shown in **Fig. 8**.

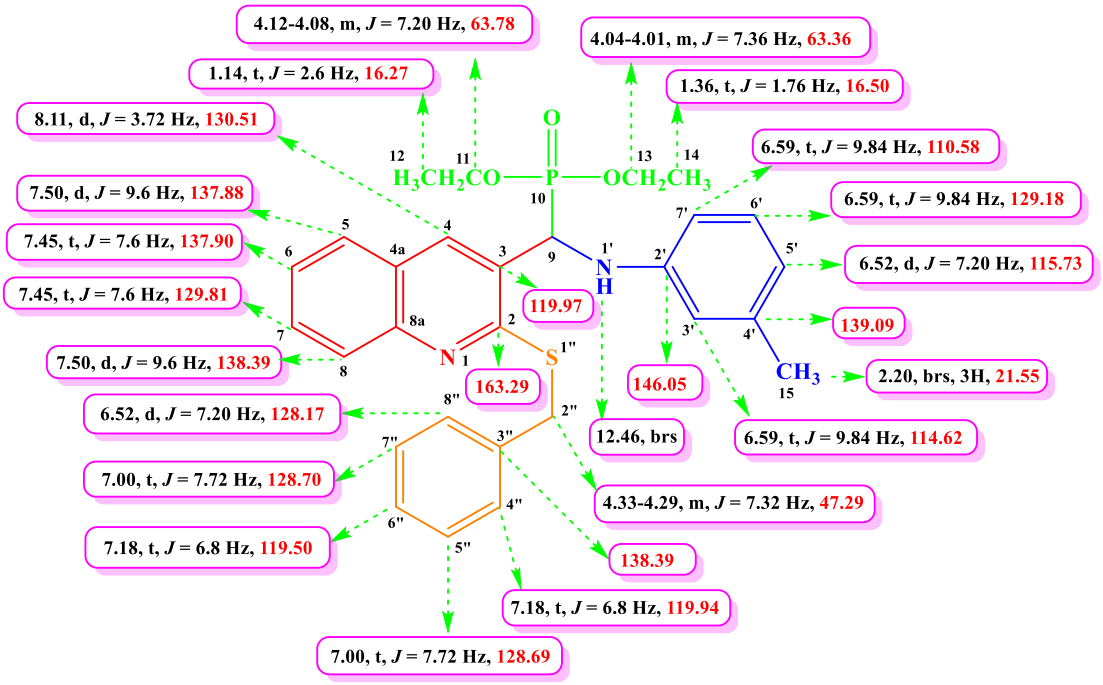

Fig. 8. ^{1}H and ^{13}C-NMR chemical shifts of **23**

The ^{13}C, ^{1}H-COSY correlation of carbon signals at δ 145.91, 139.09, 138.45, 128.70, 128.69, 128.17, 122.71, 119.97, 119.94, 115.73, 114.62, 110.58, 63.78, 63.36, 48.82, 47.29, 21.55, 16.50 and 16.27 were assigned to C8a, C4', C3", C7", C5", C8", C5a, C3, C4", C6", C5', C7', C11, C13, C9, C2", C15, C14 and C12, respectively. The carbon signal at δ 130.51 was due to quinolinyl carbon (C4), is shown in **Fig. 5.5**.

The ^{1}H, ^{1}H-COSY spectrum of **23** (**Fig. 5.6**) showed the correlation between CH (C9) at δ 5.61 with phenyl protons of C3', C6' and C7' at δ 6.59 with coupling constant value J=9.84 Hz was observed. CH_3 (C14) at δ 1.36. The ^{1}H, ^{1}H-NOESY spectrum (**Fig. 5.7**) of **23** showed the singlet of NH at δ 12.46 was coupled with the doublet of C9 (CH) at δ 5.61.

The ^{1}H and ^{13}C-NMR chemical shifts of HMBC correlation is illustrated in **Fig. 9**. The HMBC spectrum of **23 (Fig. 5.8**) showed the long-range correlations as follows: the proton C9-H, (CH) was coupled with *m*-toluidine ring carbons, C6' at δ 129.18, C4' at δ 139.09 and C2' at δ 146.05, quinolinyl carbons C8a at δ 145.91 and C2 at δ 163.29. This correlation of C9-H to the *m*-toluidine ring carbons C6', C4' and C2' and carbons C8a and C2 of quinolinyl moiety indicated that the two groups were attached to C9 (CH).

Thus it was evident that the two different moieties (amine and aldehyde) were bonded to a common carbon and hence added valuable information to **23**.

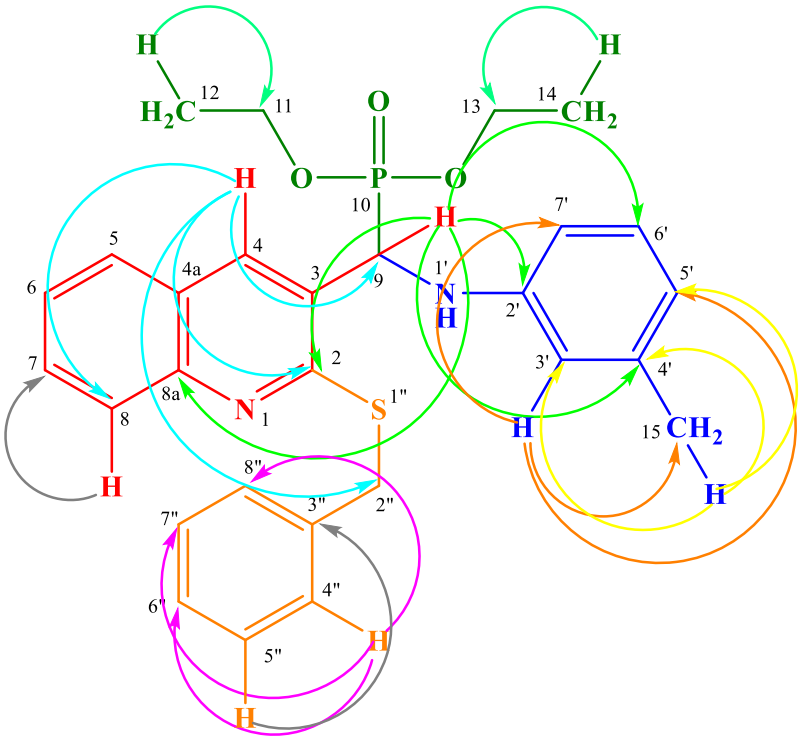

Fig. 9. HMBC correlation of compound **23**

The C4-H proton was coupled with carbons C9 at δ 48.82, C2" at δ 47.29, C8 at δ 138.39 and C2 at δ 163.29. The C4"-H proton was coupled with carbons C6" at δ 119.50, C7" at δ 128.70 and C8" at δ 128.17 of benzyl mercaptan ring. The C3'-H coupled with carbons C15 at δ 21.55, C7' at δ 110.58 and C5' at δ 115.73 of *m*-toluidine ring. The C15-H proton was coupled with *m*-toluidine ring carbons C3' at δ 114.62 and C5' at δ 115.73 and C4' at δ 139.09. The C8-H proton was coupled with quinolinyl carbon C7 at δ 129.18. The C5"-H proton was correlated with C3" at δ 138.45 of benzyl mercaptan ring. The C12-H proton was correlated with carbon C11 at δ 63.78 of phosphoryl group. The C14-H proton was coupled with carbon C13 at δ 63.36. The selected ^{1}H and ^{13}C-NMR HMBC correlated chemical shifts of **23** are shown in **Table 1**.

Table. 1. HMBC correlation and chemical shifts

Entry	Protons	Correlated carbons
1	C9-H (s, 1H, CH) at δ 5.61 ppm	C6' (129.18), C4' (139.09), C8a (145.91), C2' (146.05) and C2 (163.29)
2	C4-H (d, 1H, *J*= 3.72 Hz) at δ 8.11 ppm	C9 (48.82), C2" (47.29), C8 (138.39) and C2 (163.29)
3	C4"-H (t, 1H, CH, *J*= 6.8 Hz) at δ 7.18 ppm	C6" (119.50), C7" (128.70) and C8" (128.17)
4	C3'-H (t, 1H, *J*= 9.84 Hz) at δ 6.59 ppm	C15 (21.55), C7' (110.58) and C5' (115.73)
5	C15-H (s, 3H, CH_3) at δ 2.20 ppm	C3' (114.62), C5' (115.73) and C4' (139.09)
6	C8-H (d, 1H, *J*= 9.6Hz) at δ 7.50 ppm	C7 (129.18)
7	C5"-H (t, 1H, *J*= 7.72 Hz) at δ 7.00 ppm	C3" (138.45)
8	C12-H (t, 3H, *J*= 1.76 Hz) at δ 1.36 ppm	C11 (63.78)
9	C14-H (t, 3H, *J*= 2.6 Hz) at δ 1.14 ppm	C13 (63.36)

Fig. 5.4, showed a sharp peak clearly at δ 22.82 denoting the presence of phosphorous in **23**. Based on the above spectral details and elemental analysis results (Anal. Calc. for $C_{28}H_{31}N_2O_3PS$: C, 66.39; H, 6.17; N, 5.53; %. Found: C, 66.40; H, 6.19; N, 5.55; %), the structure was confirmed as diethyl ((2-(benzylthio)quinolin-3-yl)(m-tolylamino)methyl) phosphonate (**23**).

To determine the effect of the catalyst, the optimum mole ratio of Fe/BN was investigated. The model reaction was carried out with different mole percentages of Fe/BN: 5 mol %, 10 mol %, 15 mol % and 20 mol %, separately. A trace amount of **23** was obtained when 25 mol % of BN was used. Among the various mole percentages, the best yield of **23** was obtained at 10 mol % of Fe/BN, (**Table 2**, entry 3).

Table 2. Catalyst optimization for the synthesis of **23**

Entry	Catalyst	Mol %	Time (min)	Yield (%) [b]
1	BN	25	20	Trace
2	Fe/BN	5	10	75
3	Fe/BN	10	5	98
4	Fe/BN	15	12	91
5	Fe/BN	20	12	91

[b] Isolated yields

Also, the model reaction, in the presence of 10 mol % of Fe/BN, was investigated in different solvents to determine its effect on the reaction yield (**Table 3**). Solvents

including acetonitrile, toluene, ethanol, methanol and water were used. The yield of **23** decreased to 63 % when the solvent was changed and the low yield was due to the presence of some unreacted substances (**Table 3**, entry 2). The best yield of 98 % was obtained when the model reaction was carried out in a water medium (**Table 3**, entry 5).

Water has unique physical and chemical properties such as amphiphilicity, hydrogen bonding capability and can influence the reactivity of chemicals in addition to the selectivity of reactions (Hayashi *et al*., 2008; Lindström, 2002; Head-Gordon and Hura, 2002). The use of hexagonal boron nitride as a catalyst in water solvent requires a basic understanding of the interaction between water and h-BN surface and is important in the understanding of the water-BN interface. Cheng *et al*., 2017 reported the h-BN showed a strong interaction between the O-H bonds of the water molecule at 3420 cm^{-1} in the ligand free C-C coupling reactions using h-BN supported palladium (II) as catalyst and allowed the reactions with high efficiencies and excellent yields when performed in water.

Table 3. Effect of solvents on the synthesis of BTQPs [a]

Entry	Solvent	Time (min)	Yield (%) [b]
1	Acetonitrile	15	65
2	Toluene	12	63
3	Ethanol	10	78
4	Methanol	10	75
5	Water	5	98

[a] Reaction conditions: aldehyde (1 mmol), amine (1 mmol), diethyl phosphite (1 mmol) and Fe/BN (10 mol %) were added to the water as a solvent (15 mL) under microwave irradiation at 90°C.

[b] Isolated yields.

Fe/BN was easily separated by simple filtration from the reaction mixture. After washing with a $CHCl_3$: MeOH (1:1) combination, followed by acetone, the solid was dried in an oven for 1-2 h and subsequently re-used.

The reusability of catalysts is an important aspect of green chemistry which makes them useful for commercial applications. To investigate the catalytic efficacy of the recycled catalyst, five successive cycles were run on the model reaction under the optimal reaction conditions. The yield of **23** decreased in small increments with a total loss of 10 %

activity after five cycles of re-use (**Fig. 10**). This indicated that Fe/BN displays good reusability.

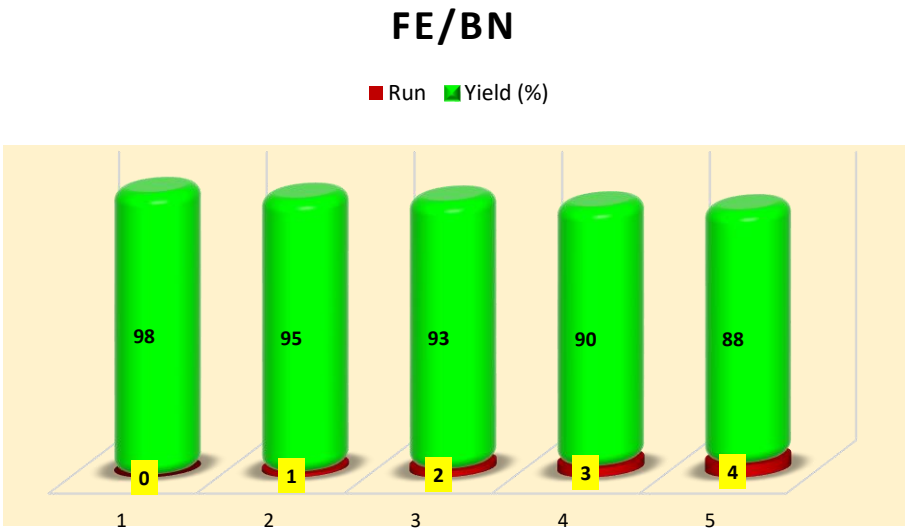

Fig. 10. Reusability of Fe/BN

The next objective was to compare conventional heating with the microwave assisted method: the results are summarized in **Table 4**. Without MW, **23** resulted in 50 % yield in the presence of Fe/BN, under stirring at room temperature and 64 % yield under reflux conditions within 24 h **(Table 4**, entries 1 & 2).

Table 4. Effect of microwave irradiation for the synthesis of **23** [a]

Entry	Power (W)	Time	Yield (%) [b]
1	Without MW (r.t)	24 h	50
2	Without MW (110 °C)	24 h	64
3	100	15 min	71
4	120	5 min	98
5	150	12 min	90
6	200	15 min	90

[a] Reaction conditions: aldehyde (1 mmol), amine (1 mmol), diethyl phosphite (1 mmol) and Fe/BN (10 mol %) were added to the water as a solvent (15 mL) under microwave irradiation at 90℃.

[b] Isolated yields.

In addition, different power of MW irradiation was investigated. It was observed that a maximum percentage (98%) of **23** was obtained at 120 W (with 90℃) power at room

temperature within 5 minutes. The yield of **23** remained unchanged with an increase in the power of MW **(Table 4**, entries 5 & 6). It was found that MW irradiation increased the rate of the reaction leading to more product yield than conventional heating in the same time frame. It might be possible that higher temperatures were obtained by localised heating due to MW irradiation and hence the product yield was increased.

The efficiency of Fe/BN was also compared to previously reported catalysts and these observations are summarised in **Table 5**. It was observed that many catalysts afforded more than 70 % of yield however longer reaction times were noted.

Table 5. Comparison of reported catalysts with Fe/BN catalyst

Entry	Catalyst	Solvent	Temp (°C)	Time	Yield (%)	References
1	$Mg(ClO_4)_2$	EtOH	50	5h/12h	85	Wu *et al*., 2006
2	$Li(Otf)_n$	Free	80	20 m-3.5 h	72-95	Firouzabadi *et al*., 2004
3	GaI_3	CH_2Cl_2	26	3-6 h	74-92	Sun *et al*., 2004
4	$In(Otf)_3$	THF	66	21-35 h	47-85	Ghosh *et al*., 2004
5	$BiNO_3$	Free	26	10 h	93	Bhattacharya *et al*., 2007
6	$BiCl_3$	MeCN	80	6-15 h	80-92	Zhan *et al*., 2005
7	$YbCl_3$	MeCN	26	24 h	63-96	Xu *et al*., 2006
8	SmI_2	MeCN	80	24 h	18-92	Xu *et al*., 2003
9	$(NH)_4Ce(NO_3)_6$	MeCN	26	3 h	86	Ravinder *et al*., 2004
10	$InCl_3$	THF	66	9-12 h	81-93	Ranu *et al*., 1999
11	$Ln(Otf)_3$	$[bmim][PF_6]$	26	27 h	92	Lee *et al*., 2001
12	$TaCl_5$-SiO_2	CH_2Cl_2	RT	22 h	92	Chandrasekhar *et al*., 2001
13	ZnO	Free	RT	9 h	90	Hou *et al*., 2011
14	$CaCl_2$	Free	60	2-4 h	80-96	Kaboudin *et al*., 2008
15	Fe/BN	Water	RT	5 min	98	Present work

The adopted procedure offered a way to compare the effectiveness of Fe/BN with the reported catalysts and 98 % yield was obtained in a relatively shorter reaction time.

Following establishing the optimum reaction conditions for the synthesis of **23** and identifying its correct structure, another 13 derivatives (**24-36**) were synthesised by varying the aniline substrate. **Table 6** summarises the derivatives that were synthesized and the % yield obtained**.** The FTIR, ^{1}H-NMR, ^{13}C-NMR and elemental analysis for all the synthesized compounds are presented in **Appendix V**.

Table 6. Synthesis of α-aminobenzylthioquinoline phosphonates under MW irradiation

Entry	Aldehyde	Amine	Time (min)	Product	Product	Yield (%) [b]
1	$C_{17}H_{13}NOS$	C_7H_9N	5	$C_{28}H_{31}N_2O_3PS$	**23**	98
2	$C_{17}H_{13}NOS$	C_6H_7N	5	$C_{27}H_{29}N_2O_3PS$	**24**	98
3	$C_{17}H_{13}NOS$	C_7H_9NO	5	$C_{28}H_{31}N_2O_4PS$	**25**	97
4	$C_{17}H_{13}NOS$	C_7H_9N	5	$C_{28}H_{31}N_2O_3PS$	**26**	96
5	$C_{17}H_{13}NOS$	C_6H_6FN	6	$C_{27}H_{28}FN_2O_3PS$	**27**	90
6	$C_{17}H_{13}NOS$	C_6H_5ClFN	8	$C_{27}H_{27}ClFN_2O_3PS$	**28**	86
7	$C_{17}H_{13}NOS$	$C_6H_6N_2O_2$	10	$C_{27}H_{28}N_3O_5PS$	**29**	88
8	$C_{17}H_{13}NOS$	$C_8H_{11}N$	5	$C_{29}H_{33}N_2O_3PS$	**30**	90
9	$C_{17}H_{13}NOS$	C_7H_9NO	5	$C_{28}H_{31}N_2O_4PS$	**31**	95
10	$C_{17}H_{13}NOS$	$C_6H_8N_2$	10	$C_{27}H_{30}N_3O_3PS$	**32**	90
11	$C_{17}H_{13}NOS$	C_6H_6BrN	8	$C_{27}H_{28}BrN_2O_3PS$	**33**	88
12	$C_{17}H_{13}NOS$	C_6H_6ClN	8	$C_{27}H_{28}ClN_2O_3PS$	**34**	87
13	$C_{17}H_{13}NOS$	$C_6H_5Cl_2N$	10	$C_{27}H_{27}Cl_2N_2O_3PS$	**35**	86
14	$C_{17}H_{12}FNOS$	C_7H_9NO	6	$C_{28}H_{30}FN_2O_4PS$	**36**	90

b Isolated yields

The presence of electron-donating groups on the amine increased the reaction rate as well as increased the product yield. Those substrates which possessed electron-withdrawing groups had an opposite effect. This electronic effect is common for electrophilic aromatic substitution reactions. However, this particular one-pot reaction is an addition reaction therefore one would generally not expect an electronic effect to play a role in the reaction.

A plausible mechanism is presented in **Scheme 3** for the synthesis of BTQPs. Similar to graphene oxide (Ruifang *et al*., 2016), the isoelectronic nature of BN increased the electrophilicity of the catalyst. The mechanism involved the activation of carbonyl carbon of the aldehyde group **(1)** by Fe/BN followed by the nucleophilic addition of amine **(2)** to produce the imine **(3)** by the removal of water. The subsequent activation of imine **(3)** by Fe/BN facilitated the addition of diethyl phosphite to produce an activated phosphonium intermediate **(4)**, which then resulted in the desired product **(5)**.

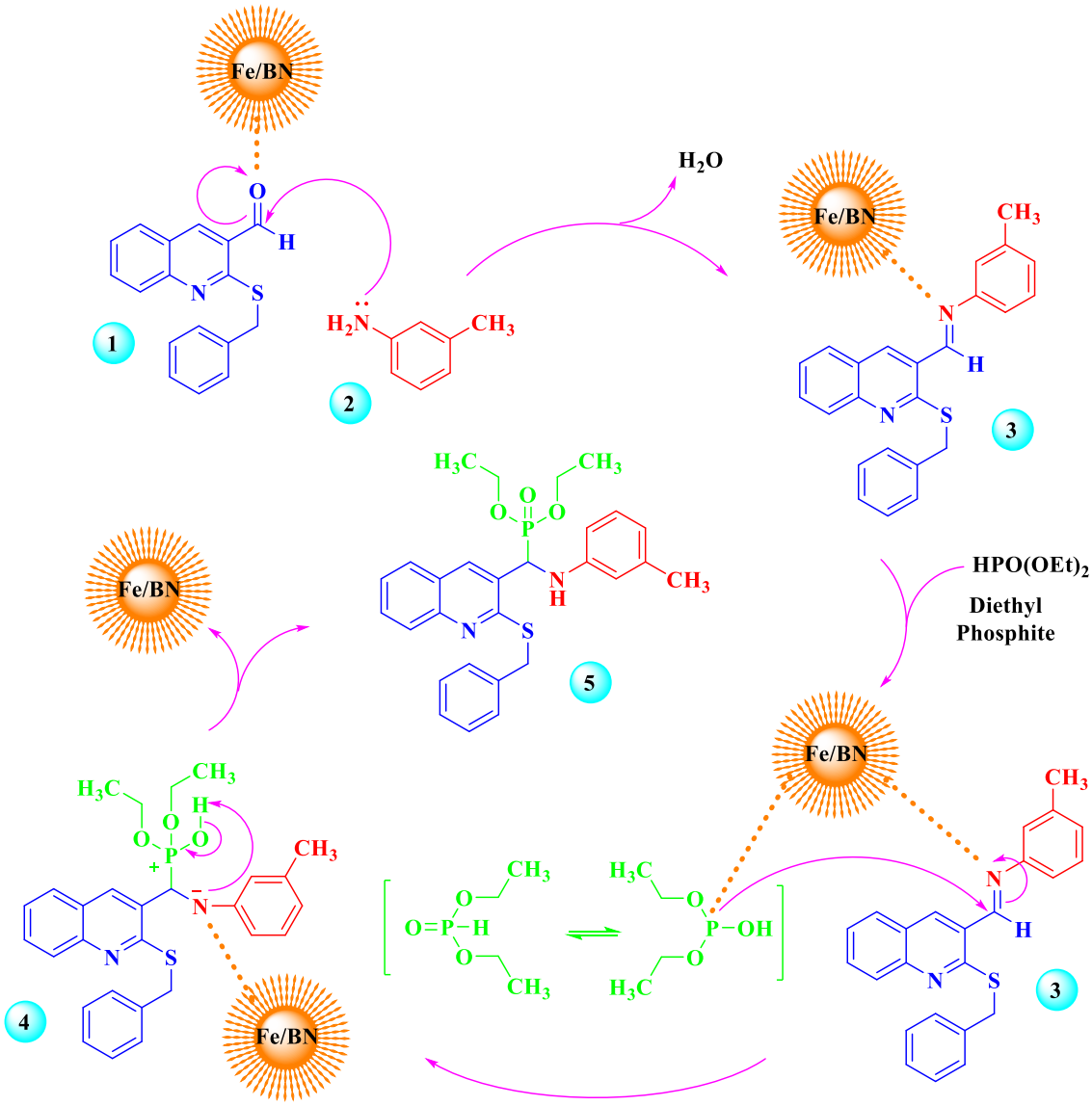

Scheme 3. A plausible mechanism for the synthesis of BTQPs promoted by Fe/BN

The rapid emergence of resistant bacteria is occurring worldwide, endangering the efficacy of antibiotics, which have transformed medicine and saved millions of lives (Golkar *et al.*, 2014; Gould and Bal, 2013). Many decades after the first patients were treated with antibiotics, bacterial infections have again become a threat (Spellberg *et al.*, 2014). In the recent years, some of the α-aminophosphonate derivatives containing heterocycle moieties have been synthesized which have shown biological activities (Luo *et al.*, 2012; Li *et al.*, 2015; Shitre *et al.*, 2014; Gu and Jin, 2012; Wu *et al.*, 2011). It seems that the existence of heterocyclic moieties in the structure of the α-aminophosphonate molecule influenced the biological activity significantly. In this

present study, the aminophosphonates containing a heterocyclic ring: quinoline and sulfur bearing starting material in the synthesis of novel derivatives exhibited significant biological activity.

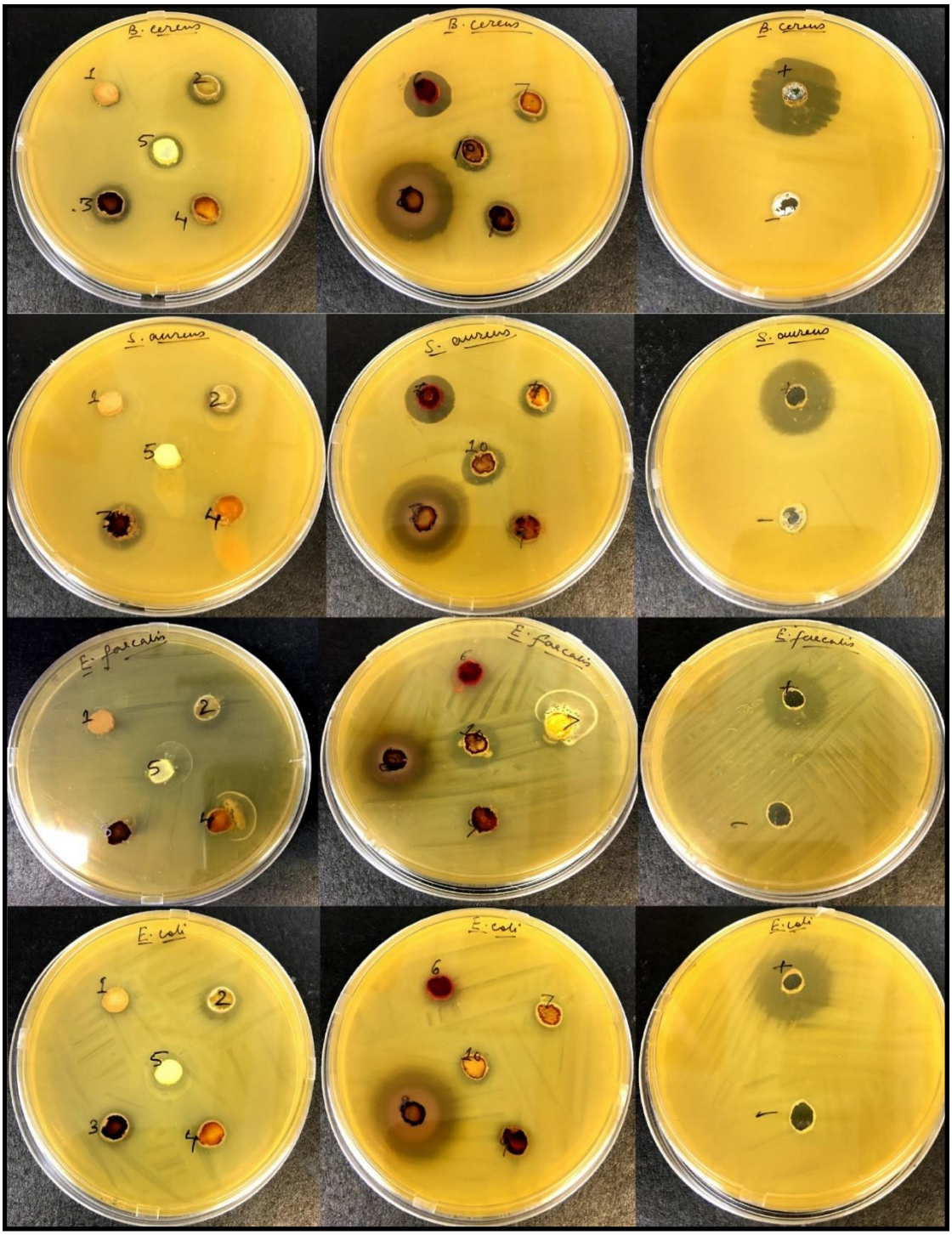

Fig. 11. Antibacterial activity of BTQPs

1= **23**; 2= **24**; 3= **25**; 4= **26**; 5= **27**; 6= **28**; 7= **29**; 8= **31**; 9= **32**; 10=**36**.

Benzylthioquinolinyl phosphonate derivatives were tested for antibacterial efficacy by determining the zone of inhibition against a range of Gram-positive (*Bacillus cereus* (*B. cereus*), *Staphylococcus aureus* (*S. aureus*) and *Enterococcus faecalis* (*E. faecalis*)) and Gram-negative (*Escherichia coli* (*E. coli*) bacteria (**Fig. 11**). The present investigation which focused on three Gram-positive and one Gram-negative bacteria showed that compounds **24**, **25**, **27**, **28**, **29**, **31** and **36** had preferential activity towards all Gram-positive species tested (**Fig. 11**).

Moreover, compound **27** and **32** showed activity against *B. cereus* only. Interestingly, compounds **24**, **31** and **36** showed their potential against all species (both Gram-positive and Gram-negative). Furthermore, compounds **24**, **25**, **31** and **36** were also found to be effective against one of the Gram-negative species (*E. coli*) (**Table 7**).

Table 7. Antibacterial activity of BTQP derivatives

Bacteria	Zone of inhibition by α-aminobenzylthioquinolinyl phosphonate (BTQP) derivatives										Ciprofloxacin (Positive control)
	1	2	3	4	5	6	7	8	9	10	
Bacillus cereus	0	13 ± 0.3	15 ± 0.2	0	13 ± 0.2	15 ± 0.3	10 ± 0.3	27 ± 0.4	10 ± 0.4	12 ± 0.3	27 ± 0.3
Staphylococcus aureus	0	11 ± 0.2	15 ± 0.4	0	0	19 ± 0.4	13 ± 0.4	30 ± 0.3	0	16 ± 0.3	25 ± 0.4
Escherichia coli	0	14 ± 0.4	12 ± 0.3	0	0	0	0	30 ± 0.4	0	10 ± 0.2	25 ± 0.3
Enterococcus faecalis	0	20 ± 0.3	0	0	0	0	0	21 ± 0.4	0	17 ± 0.3	24 ± 0.4

1= **23**; 2= **24**; 3= **25**; 4= **26**; 5= **27**; 6= **28**; 7= **29**; 8= **31**; 9= **32**; 10= **36**.

BTQPs that contained sulfur-based quinoline as core structure with phenyl group (**24**), methoxy group (**25** and **31**), fluorine and chlorine (**28**) and nitro group (**29**) showed antibacterial activity against Gram-positive species. Furthermore, BTQP (**36**) containing methyl group in the quinoline core structure with the sulfur atom of benzyl mercaptan showed preferential activity against Gram-positive bacteria. The potential activity of BTQPs toward *B. cereus* might be due to the presence of fluorine (**27**) and the pyridinyl group with the benzylthioquinoline substrate (**32**). The presence of a phenyl group (**24**), methoxy group (**31**) and methyl-containing benzylthioquinoline substrate with methoxy group (**36**) of BTQP showed potential towards Gram-positive and Gram-negative species. BTQPs that contain the methoxy group in the benzylthioquinoline compound (**25**) showed potential activity against *E.coli*.

Antioxidants are considered important nutraceuticals due to many health benefits (Valko *et al*., 2007). Antioxidant activity was assessed using the 2,2-diphenyl-1-picryl-hydrazyl (DPPH) assay. The scavenging assay was used for initial screening of the compounds for their antioxidant activity. A total of 10 BTQPs were tested. Among them, BTQPs containing sulfur-based quinoline as core structure with methyl groups (**23**) and (**26**), phenyl group (**24**), fluorine (**27**), nitro group (**29**) and methoxy group in the quinoline core structure with sulfur atom of benzyl mercaptan (**36**) showed significant scavenging activities.

Brine shrimp is used for preliminary assessment of toxicity (Rajabi *et al*., 2015). The toxicity was tested for all BTQPs at different intervals (24h and 48h), which displayed activity towards Gram-positive, Gram-negative or both. It was found that among all compounds tested, **23**, **24**, **25**, **26**, **27**, **29**, **31** and **36** have mortality rate below 50% (**Fig. 12**), which suggested that these compounds were safe for further biological applications (Meyer *et al*., 1982).

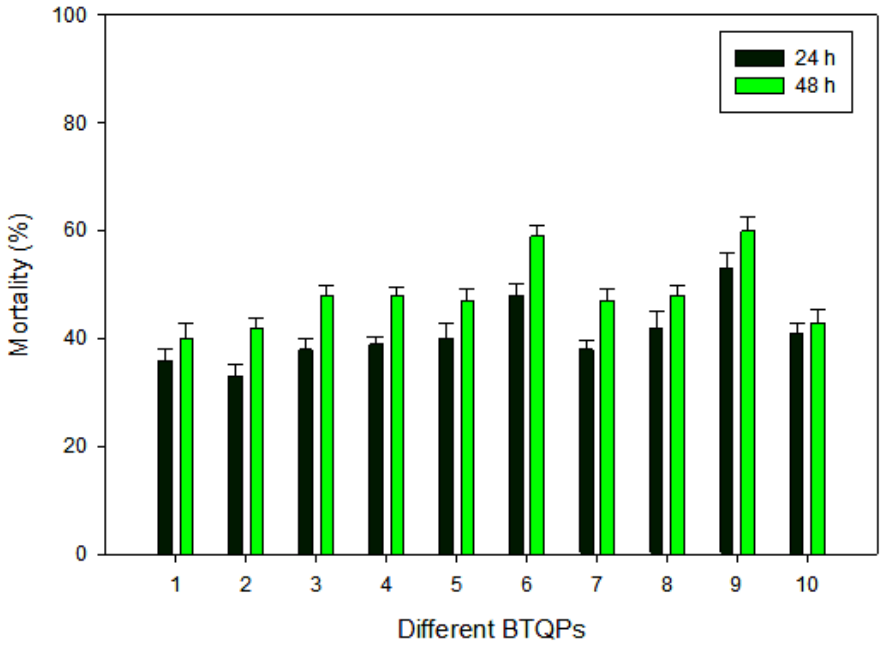

Fig. 12. Toxicity assessment of BTQPs

(1= **23**; 2= **24**; 3= **25**; 4= **26**; 5= **27**; 6= **28**; 7= **29**; 8= **31**; 9= **32**; 10= **36**) at 24 h and 48 h

BTQPs that contained sulfur-based quinoline as core structure with methyl group (**23**), phenyl group (**24**), methoxy group (**25**), methyl group (**26**), fluorine (**27**), nitro group

(**29**), methoxy group (**31**) and methyl group in the quinoline core structure with sulphur atom of benzyl mercaptan (**36**) showed mortality rate below 50 %.

Molecular docking is an *in-silico* approach to estimate the binding free energies in a simplest way. The approach also helps to identify the orientation and conformation of the ligand inside the binding site. In the present study, molecular docking was carried out for α-aminobenzylthioquinoline phosphonates (BTQPs) into the ligand binding domain of *S. aureus* gyrase enzyme. The three-dimensional structure of *S. aureus* gyrase was retrieved from protein data bank (PDB ID: 4PLB) (Singh *et al*., 2014). The ligand series of BTQPs were built in Chem 3D Biodraw and the conformation of all the ligands were optimized by MM2 method. Further, the ligands were prepared in Discovery Studio software (Biovia, 2015) to include the ionization state, conformational analysis and stereoisomers, etc. The three-dimensional structure of *S. aureus* gyrase was also prepared in Chimera software (Pettersen *et al*., 2004). The presence of water molecules was removed and missing hydrogen atoms were added. The LibDock module of the Discovery Studio software was employed to perform molecular docking. All the ligands were docked at the 15Å sphere which was generated around the bound ligand of *S. aureus* gyrase (**Table 8**).

Table 8. Molecular docking scores of α-aminobenzylthioquinoline phosphonates with *Staphylococcus aureus* gyrase

Entry	BTQP	Absolute Energy	LibDock Score
1	**23**	72.56	127.32
2	**24**	69.90	133.27
3	**25**	84.36	126.70
4	**26**	81.65	123.38
5	**27**	73.52	131.36
6	**28**	73.87	130.92
7	**29**	77.80	121.93
8	**30**	73.69	129.34
9	**31**	81.02	149.97
10	**32**	69.68	134.40
11	Reference Ligand	83.08	176.61

The docked molecules showed LibDock scores from 121.93 to 149.97 kcal/mol. The molecule (**31**) showed more potency amongst the series of BTQPs toward *S. aureus* gyrase by forming hydrogen bonding interaction with DC31 (**Fig. 13**).

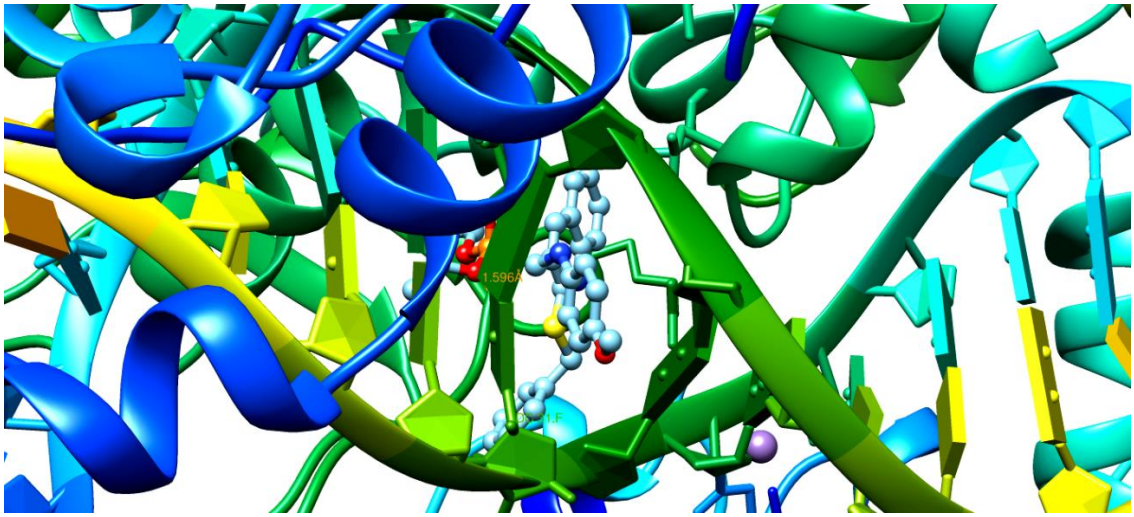

Fig. 13. Hydrogen bonding interaction of **(31)** with *Staphylococcus aureus* gyrase

5.4. Conclusion

In conclusion, a microwave irradiated one-pot three-component synthesis of α-aminobenzylthioquinolinyl phosphonates was developed by using a novel iron-loaded boron nitride catalyst. The catalyst was characterized by XRD, SEM with EDX, TEM, TGA, DSC and FTIR. A total of 14 compounds were synthesized and characterized with FTIR, NMR and elemental analysis. 10 BTQP derivatives were evaluated for antibacterial and antioxidant activities: Compounds **24**, **25**, **27**, **28**, **29**, **31**, **32** and **36** showed positive results for antibacterial activity and **23**, **24**, **26**, **27**, **29** and **36** showed positive results for antioxidant potential, respectively. Since these new BTQPs showed antibacterial, antioxidant and less toxicity, they could be useful for further pharmaceutical applications. Among the synthesized compounds, **31** exhibited potential binding affinity with *S. aureus* gyrase based on *in-silico* molecular docking studies. The study displayed the advantages of green synthesis using water as solvent, shorter reaction times, mild conditions, high yields and reusability of the catalyst.

5.5. Experimental

Preparation of iron loaded boron nitride catalyst

To a solution of anhydrous $Fe(OAc)_2$ (28.1 mg, including 32.2 % (9.02 mg) of Fe metal; 0.5 wt % metal vs BN) in methanol (50 mL), boron nitride (2.66 g, 0.1 mol) was added and the mixture was stirred at room temperature for three days under nitrogen atmosphere. The resulting suspension was filtered and the solid was washed with MeOH, dried under reduced pressure to produce 0.3 % Fe/BN catalyst as a white powder, yield: 2.680 g (99%).

General procedure for the microwave synthesis of α-aminobenzylthioquinolinyl phosphonates

Catalytic amount (10 mol %) of Fe/BN was added to a mixture of aryl amine (1 mmol) and **21** (1 mmol) in water (15 mL) followed by the addition of **4** (1 mmol). The reaction tube was placed in a CEM microwave discover synthesizer and irradiated at 120 W at a temperature of 110℃ for 5 minutes. The reaction was monitored by TLC. Following completion, the catalyst was isolated by simple filtration. The residue was purified by column chromatography from eluent (ethyl acetate: petroleum ether, 25 %) followed by EtOAc: H_2O (1:2) separation. The crystallization of the product was performed in ethanol to yield the pure product.

Bacterial strains

The antibacterial activity of each synthesized compound was assessed using four bacterial strains. Two strains of each Gram-positive (*Bacillus cereus*, *Staphylococcus aureus* and *Enterococcus faecalis*) and Gram-negative (*Escherichia coli*) bacteria were used. The bacterial strains were provided from the culture collection of Department of Biotechnology and Food Technology, Durban University of Technology, South Africa.

Inoculum preparation

Each bacterial strain was sub-cultured overnight at 37℃ on Mueller-Hilton agar plate. Further, bacterial cultures were grown in Mueller-Hilton broth at 37℃, 200 rpm in order to attain the viable count of approximately 10^8 cfu/mL.

Antibacterial activity

The agar well diffusion method was used to evaluate the antibacterial activity. Hundred microliter of~10^8 cfu/mL bacterial suspension was plated on Mueller-Hinton Agar plates. A well of 6 mm diameter was made using a sterile cork borer and 30 µL of each compound (3 mg/ml) was added in each well and kept at 37℃ for 16 h. The assays were carried out in triplicate. Ciprofloxacin (3 mg/ml) was used as positive control and DMSO as the negative control.

Antioxidant assays of BTQP derivatives

The antioxidant ability of the BTQPs were determined by the decolourization of methanol solution of 2,2-diphenyl-1-picrylhydrazyl-hydrate (DPPH). Hundred microliter of each compound was added separately to 1 mL of 0.1 mM DPPH solution, and a colour change was observed at regular intervals. Rutin hydrate was used as the positive control and methanol (95%) as negative control.

Toxicity assessment

The brine shrimp larvae (*Artemia salina*) were hatched in sea water for 24-48 h prior to being used. An aliquot of 5 mL sea water containing ten brine shrimp was added to each vial and supplemented with different derivatives of BTQP. Derivative concentrations of 300 µg were used in individual vial. Brine shrimp death was observed at regular intervals (24 h and 48 h) in order to determine the toxic nature of each compound. The data was expressed as % mortality.

References

[1] Moonen, K., Laureyn, I., Stevens, C. V. 2004. Synthetic methods for azaheterocyclic phosphonates and their biological activity. Chemical Reviews, (104) 6177-6216.

[2] Demmer, C. S., Krogsgaard-Larsen, N., Bunch, L. 2011. Review on modern advances of chemical methods for the introduction of a phosphonic acid group. Chemical Reviews, (111) 7981-8006.

[3] Popa, A., Ene, R., Visinescu, D., Dragan, E.S., Ilia, G., Iliescu, S., Parvulescu, V. 2015. Transitional metals immobilized by coordination on aminophosphonate functionalized copolymers and their catalytic properties. Journal of Molecular Catalysis A: Chemical, (408) 262-270.

[4] Ménard, L., Fontaine, L., Brosse, J. C. 1994. Synthesis and preliminary evaluation of chelating resins containing α-amino alkylphosphonic groups. Reactive Polymers, (23) 201-212.

[5] Ye, M. Y., Yao, G. Y., Pan, Y. M., Liao, Z. X., Zhang, Y. Wang, H. S. 2014. Synthesis and antitumor activities of novel α-aminophosphonate derivatives containing an alizarin moiety. European Journal of Medicinal Chemistry, (83) 116-128.

[6] Huang, X. C., Wang, M., Pan, Y. M., Yao, G. Y., Wang, H. S., Tian, X. Y., Qin, J. K., Zhang, Y. 2013. Synthesis and antitumor activities of novel thiourea α-aminophosphonates from dehydroabietic acid. European Journal of Medicinal Chemistry, (69) 508-520.

[7] Huang, K. B., Chen, Z. F., Liu, Y. C., Li, Z. Q., Wei, J. H., Wang, M., Zhang, G. H., Liang, H. 2013. Platinum (II) complexes with mono-aminophosphonate ester targeting group that induce apoptosis through G1 cell-cycle arrest: Synthesis, crystal structure and antitumour activity. European Journal of Medicinal Chemistry, (63) 76-84.

[8] Huang, X., Huang, R., Gou, S., Wang, Z., Wang, H. 2017. Anticancer platinum (IV) prodrugs containing mono aminophosphonate ester as a targeting group inhibit matrix metalloproteinases and reverse multidrug resistance. Bioconjugate Chemistry, (28) 1305-1323.

[9] Mulla, S. A. R., Pathan, M. Y., Chavan, S. S., Gample, S. P., Sarkar, D. 2014. Highly efficient one-pot multi-component synthesis of α-aminophosphonates and

bis-α-aminophosphonates catalyzed by heterogeneous reusable silica supported dodecatungstophosphoric acid (DTP/SiO_2) at ambient temperature and their antitubercular evaluation against Mycobactrium Tuberculosis. RSC Advances, (15) 7666-7672.

[10] Subhedar, D. D., Shaikh, M. H., Nawale, L., Yeware, A., Sarkar, D., Shingate, B. B. 2016. [Et_3NH][HSO_4] catalyzed efficient synthesis of 5-arylidene-rhodanine conjugates and their antitubercular activity. Research on Chemical Intermediates, (42) 6607-6626.

[11] Stowasser, B., Budt, K. H., Jian-Qi, L., Peyman, A., Ruppert, D. 1992. New hybrid transition state analog inhibitors of HIV protease with peripheric C 2-symmetry. Tetrahedron Letters, (33) 6625-6628.

[12] Lacbay, C. M., Mancuso, J., Lin, Y. S., Bennett, N., Götte, M., Tsantrizos, Y. S. 2014. Modular assembly of purine-like bisphosphonates as inhibitors of HIV-1 reverse transcriptase. Journal of Medicinal Chemistry, (57) 7435-7449.

[13] Ali, N., Ali, S., Zakir, S., Patel, M., Farooqui, M. 2012. Synthesis of new α-aminophosphonate system bearing Indazole moiety and their biological activity. European Journal of Medicinal Chemistry, (50) 39-43.

[14] Sampath, C., Harika, P., Revaprasadu, N. 2016. Design, green synthesis, anti-microbial, and anti-oxidant activities of novel α-aminophosphonates via Kabachnik-Fields reaction. Phosphorus, Sulfur, and Silicon and the Related Elements, (191) 1081-1085.

[15] Sivala, M. R., Devineni, S. R., Golla, M., Medarametla, V., Pothuru, G. K., Chamarthi, N. R. 2016. A heterogeneous catalyst, SiO_2-$ZnBr_2$: An efficient neat access for α-aminophosphonates and antimicrobial activity evaluation. Journal of Chemical Sciences, (128) 1303-1313.

[16] De Schutter, J. W., Park, J., Leung, C. Y., Gormley, P., Lin, Y. S., Hu, Z., Berghuis, A. M., Poirier, J., Tsantrizos, Y. S. 2014. Multistage screening reveals chameleon ligands of the human farnesyl pyrophosphate synthase: Implications to drug discovery for neurodegenerative diseases. Journal of Medicinal Chemistry, (57) 5764-5776.

[17] Ewa, B., Maciej, W., Marcin, S., Grzegorz, D., Michał, Z., Jan, P., Józef, O. 2012. The development of first Staphylococcus aureus SplB protease inhibitors: Phosphonic analogues of glutamine. Bioorganic & Medicinal Chemistry Letters, (22) 5574-5578.

[18] Leon, A., Liu, L., Yang, Y., Hudock, M. P., Hall, P., Yin, F., Studer, D., Puan, K. J., Morita, C. T., Oldfield, E. 2006. Isoprenoid biosynthesis as a drug target: Bisphosphonate inhibition of Escherichia coli K12 growth and synergistic effects of fosmidomycin. Journal of Medicinal Chemistry, (49) 7331-7341.

[19] Leung, C. Y., Park, J., De Schutter, J. W., Sebag, M., Berghuis, A. M., Tsantrizos, Y. S. 2013. Thienopyrimidine bisphosphonate (ThPBP) inhibitors of the human farnesyl pyrophosphate synthase: Optimization and characterization of the mode of inhibition. Journal of Medicinal Chemistry, (56) 7939-7950.

[20] Leung, C. Y., Langille, A. M., Mancuso, J., Tsantrizos, Y. S. 2013. Discovery of thienopyrimidine-based inhibitors of the human farnesyl pyrophosphate synthase-Parallel synthesis of analogs via a trimethylsilyl ylidene intermediate. Bioorganic & Medicinal Chemistry, (21) 2229-2240.

[21] Wang, Q., Zhu, M., Zhu, R., Lu, L., Yuan, C., Xing, S., Fu, X., Mei, Y., Hang, Q. 2012. Exploration of α-aminophosphonate N-derivatives as novel, potent and selective inhibitors of protein tyrosine phosphatases. European Journal of Medicinal Chemistry, (49) 354-364.

[22] Lilienkampf, A., Mao, J., Wan, B., Wang, Y., Franzblau, S. G., Kozikowski, A. P. 2009. Structure-activity relationships for a series of quinoline-based compounds active against replicating and nonreplicating Mycobacterium tuberculosis. Journal of Medicinal Chemistry, (52) 2109-2118.

[23] Sedic, M., Poznic, M., Gehrig, P., Scott, M., Schlapbach, R., Hranjec, M., Karminski-Zamola, G., Pavelic, K., Pavelic, S. K. 2008. Differential antiproliferative mechanisms of novel derivative of benzimidazo [1,2-α] quinoline in colon cancer cells depending on their p53 status. Molecular Cancer Therapeutics, (7) 2121-2132.

[24] Sujatha, B., Mohan, S., Subramanyam, C., Rao, K. P. 2017. Microwave-assisted synthesis and anti-inflammatory activity evaluation of some novel α-aminophosphonates. Phosphorus, Sulfur, and Silicon and the Related Elements, (192) 1110-1113.

[25] Gakhar, G., Ohira, T., Shi, A., Hua, D.H., Nguyen, T. A. 2008. Antitumor effect of substituted quinolines in breast cancer cells. Drug Development Research, (69) 526-534.

[26] Chung, H. S., Woo, W. S. 2001. A quinolone alkaloid with antioxidant activity from the aleurone layer of anthocyanin-pigmented rice. Journal of Natural Products, (64) 1579-1580.

[27] (a) Metzner, P., Thuillier, A. 2013. Sulfur reagents in organic synthesis. Academic Press, New York. (b) Nudelman, A. 1984. The chemistry of optically active sulfur compounds, Gordon and Breach, New York. (c) Chatgilialoglu, C., Asmus, K. D. 1991. Sulfur-centered reactive intermediates in chemistry and biology. Springer Science & Business Media, New York.

[28] Bicking, J. B., Holtz, W. J., Watson, L. S., Cragoe Jr, E. J. 1976. (Vinylaryloxy) acetic acids. A new class of diuretic agents. 1. (Diacylvinylaryloxy) acetic acids. Journal of Medicinal Chemistry, (19) 530-535.

[29] Ding, Y., Prasad, V., Chamakura, V. N. S., Smith, K. L., Chang, E., Hong, J., Yao, N. 2009. Synthesis of tipranavir analogues as non-peptidic hiv protease inhibitors. Letters in Organic Chemistry, (6) 130-133.

[30] Inomata, K., Barragué, M., Paquette, L. A. 2005. Diastereo selectivities realized in the amino acid catalyzed aldol cyclizations of triketo acetonides of differing ring size. The Journal of Organic Chemistry, (70) 533-539.

[31] Yamauchi, M., Katayama, S., Watanabe, T. 1982. 2-Methylthiomethylation of 1,3-dicarbonyl compounds and synthesis of 2-methylene-1,3-dicarbonyl compounds. Synthesis, (11) 935-937.

[32] Evdokimov, N. M., Kireev, A. S., Yakovenko, A. A., Antipin, M. Y., Magedov, I. V. Kornienko, A. 2007. One-step synthesis of heterocyclic privileged medicinal scaffolds by a multicomponent reaction of malononitrile with aldehydes and thiols. The Journal of Organic Chemistry, (72) 3443-3453.

[33] Petrov, K. A., Chauzov, V. A., Erokhina, T. S. 1974. Amino alkyl organophosphorus compounds. Russian Chemical Reviews, (43) 984-1006.

[34] Zawadzki, J. 1987. Infrared studies of SO_2 on carbons-II. The SO_2 species adsorbed on carbon films. Carbon, (25) 495-502.

[35] Laschat, S., Kunz, H. 1992. Carbohydrates as chiral templates: Stereoselective synthesis of (R)-and (S)-α-aminophosphonic acid derivatives. Synthesis, (1) 90-95.

[36] Kabachnik, M. M., Ternovskaya, T. N., Zobnina, E. V., Beletskaya, I. P. 2002. Reactions of hydrophosphoryl compounds with Schiff bases in the presence of CdI_2. Russian Journal of Organic Chemistry, (38) 480-483.

[37] Qian, C., Huang, T. 1998. One-pot synthesis of α-amino phosphonates from aldehydes using lanthanide triflate as a catalyst. The Journal of Organic Chemistry, (63) 4125-4128.

[38] Ranu, B. C., Hajra, A., Jana, U. 1999. General procedure for the synthesis of α-amino phosphonates from aldehydes and ketones using indium (III) chloride as a catalyst. Organic Letters, (1) 1141-1143.

[39] Yadav, J. S., Reddy, B. V. S., Raj, K. S., Reddy, K. B., Prasad, A. R. 2001. Zr^{4+}-catalyzed efficient synthesis of α-aminophosphonates. Synthesis, (15) 2277-2280.

[40] Ghosh, R., Maiti, S., Chakraborty, A., Maiti, D. K., 2004. In $(OTf)_3$ catalysed simple one-pot synthesis of α-amino phosphonates. Journal of Molecular Catalysis A: Chemical, (210) 53-57.

[41] Sun, P., Hu, Z., Huang, Z. 2004. Gallium triiodide catalyzed organic reaction: A convenient synthesis of α-amino phosphonates. Synthetic Communications, (34) 4293-4299.

[42] Zhan, Z. P., Li, J. P. 2005. Bismuth (III) chloride–catalyzed three-component coupling: Synthesis of α-amino phosphonates. Synthetic Communications, (35) 2501-2508.

[43] Paraskar, A. S., Sudalai, A. 2006. A novel $Cu(OTf)_2$ mediated three component high yield synthesis of α-aminophosphonates. Arkivoc, (10) 183-189.

[44] Kumar, S. A, Taneja, S. C., Hundal, M. S., Kapoor, K. K. 2008. One-pot synthesis of α-aminophosphonates catalyzed by antimony trichloride adsorbed on alumina. Tetrahedron Letters, (49) 2208-2212.

[45] Yadav, J. S., Reddy, B. V. S., Sreedhar, P. 2002. An eco-friendly approach for the synthesis of α-aminophosphonates using ionic liquids. Green Chemistry, (4) 436-438.

[46] Saidi, M. R., Azizi, N. 2002. A new protocol for a one-pot synthesis of α-amino phosphonates by reaction of imines prepared in situ with trialkyl phosphites. Synlett, (8) 1347-1349.

[47] Azizi, N., Saidi, M. R. 2003. Synthesis of tertiary α-amino phosphonate by one-pot three-component coupling mediated by LPDE. Tetrahedron, (59) 5329-5332.

[48] Akiyama, T., Sanada, M., Fuchibe, K. 2003. Brønsted acid-mediated synthesis of α-amino phosphonates under solvent-free conditions. Synlett, (10) 1463-1464.

[49] Azizi, N., Rajabi, F. Saidi, M. R. 2004. A mild and highly efficient protocol for the one-pot synthesis of primary α-amino phosphonates under solvent-free conditions. Tetrahedron Letters, (45) 9233-9236.

[50] Firouzabadi, H., Iranpoor, N., Sobhani, S. 2004. Metal triflate-catalyzed one-pot synthesis of α-aminophosphonates from carbonyl compounds in the absence of solvent. Synthesis, (16) 2692-2696.

[51] Elmakssoudi, A., Zahouily, M., Mezdar, A., Rayadh, A., Sebti, S. 2005. $Na_2CaP_2O_7$ a new catalyst for the synthesis of α-amino phosphonates under solvent-free conditions at room temperature. Comptes Rendus Chimie, (8) 1954.

[52] Bhagat, S., Chakraborti, A. K. 2008. Zirconium (IV) compounds as efficient catalysts for synthesis of α-aminophosphonates. The Journal of Organic Chemistry, (73) 6029-6032.

[53] Kaboudin, B., Jafari, E. 2008. Hydro phosphorylation of imines catalyzed by tosyl chloride for the synthesis of α-aminophosphonates. Synlett, (12) 1837-1839.

[54] Krishna, A. B., Reddy, M., Reddy, G., Krishna, B.S., Nayak, S. K., Reddy, C. S. 2010. Synthesis, anti-oxidant and anti-bacterial properties of diethyl (4-flouro-3-nitro phenylamino)(substituted phenyl) methyl phosphonates. International Journal of Applied Biology and Pharmaceutical Technology, (1) 873-882.

[55] Abdel-Megeed M. F., Badr, B. E., Azaam, M. M., El-Hiti, G. A. 2012. Synthesis, antimicrobial and anticancer activities of a novel series of diphenyl 1-(pyridin-3-yl)ethylphosphonates. Bioorganic & Medicinal Chemistry, (20) 2252-2258.

[56] Badadhe, P. V., Chavan, N. M., Ghotekar, D. S., Mandhan, P. G., Joshi, R. S., Gill, C. H. 2011. Synthesis, characterization, and biological screening of some novel thiazolidin-4-one and α-aminophosphonate derivatives. Phosphorus, Sulfur, and Silicon and the Related Elements, (186) 2021–2032.

[57] Chinnam, S., Potturi, C., Maddila, S., Reddy, V. B., Ediga, A., Chinnam, V. 2013. Synthesis, spectral characterization and antimicrobial evaluation of novel α-amino phosphonates, Der Pharma Chemica, (5) 327-333.

[58] Ahmed A. G., Ibrahim M. S. G., Ahmed El, S., Megeed, A., Shaban, E., El-Tantawy, I., El Sayed. 2016. Synthesis and antibacterial activity of novel α-aminophosphonates bearing a quinoline moiety. International Journal of Pharmaceutical Sciences and Research, (7) 181-189.

[59] Trivedi, M. K., Patil, S., Nayak, G., Jana, S., Latiyal, O. 2015. Influence of biofield treatment on physical, structural and spectral properties of boron nitride. Materials Science and Engineering, (4) 4.

[60] Scherrer, P. 1918. Determination of the size and internal structure of colloidal particles using X-rays. Gesellschaft der Wissenschaften zu Göttingen, (2) 98-100.

[61] Chien, A.C., Van Bokhoven, J. A. 2015. Boron nitride coated rhodium black for stable production of syngas. Catalysis Science & Technology, (5) 3518-3524.

[62] Wang, Y., Yamamoto, Y., Kiyono, H., Shimada, S. 2009. Effect of ambient gas and temperature on crystallization of boron nitride spheres prepared by vapor phase pyrolysis of ammonia borane. Journal of the American Ceramic Society, (92) 787-792.

[63] Oda, K., Yoshio, T. O. 1993. Oxidation kinetics of hexagonal boron nitride powder. Journal of Materials Science, (28) 6562-6566.

[64] Sneha, M., Sundaram, N. M. 2015. Preparation and characterization of an iron oxide-hydroxyapatite nanocomposite for potential bone cancer therapy. Int. J. Nano. Medicine, (10) 99-106.

[65] Muthu, T., Anand, K., Sureshkumar, M., Gengan, R. M. 2016. Eco-friendly approach: Graphene like boron nitride modified calcium material for the synthesis of 2-amino-4H-pyran-3-carbonitrile derivatives. Advanced Materials Letters, (7) 790-794.

[66] Miller, F. A., Wilkins, C. H. 1952. Infrared spectra and characteristic frequencies of inorganic ions. Analytical Chemistry, (24) 1253-1294.

[67] Srivastava, A., Singh, R. M. 2005. Vilsmeier-Haack reagent: a facile synthesis of 2-chloro-3-formylquinolines from N-arylacetamides and transformation into different functionalities. Indian Journal of Chemistry, (44B) 1868-1875.

[68] Maghsoodlou, M. T., Khorassani, S. M. H., Hazeri, N., Rostamizadeh, M., Sajadikhah, S. S., Shahkarami, Z., Maleki, N. 2009. An efficient synthesis of α-Amino phosphonates using silica sulfuric acid as a heterogeneous catalyst. Heteroatom Chemistry: An International Journal of Main Group Elements, (20) 316-318.

[69] (a) Hayashi, Y., Itoh, T., Aratake, S., Ishikawa, H. 2008. A diaryl prolinol in an asymmetric, catalytic, and direct crossed-aldol reaction of acetaldehyde. Angewandte Chemie International Edition, (120) 2112-2114. (b) Lindström, U. M. 2002. Stereoselective organic reactions in water. Chemical Reviews, (102)

2751-2772. (c) Head-Gordon, T., Hura, G. 2002. Water structure from scattering experiments and simulation. Chemical Reviews, (102) 2651-2670. d) Bellissent, M. C., Funnel, J. C. 1994. Hydrogen Bond Networks. Kluwer, Academic Publishers, Boston.

[70] Cheng, X., Li, W., Nie, R., Ma, X., Sang, R., Guo, L. Wu, Y. 2017. Ligand-free c-c coupling reactions promoted by hexagonal boron nitride-supported palladium (II) catalyst in water. Advanced Synthesis & Catalysis, (359) 454-466.

[71] Wu, J., Sun, W., Xia, H. G., Sun, X. 2006. A facile and highly efficient route to α-amino phosphonates via three-component reactions catalyzed by $Mg(ClO_4)_2$ or molecular iodine. Organic and Biomolecular Chemistry, (4) 1663-1666.

[72] Firouzabadi, H., Iranpoor, N., Sobhani, S. 2004. Metal triflate-catalyzed one-pot synthesis of α-aminophosphonates from carbonyl compounds in the absence of solvent. Synthesis, (16) 2692–2696.

[73] Sun, P., Hu, Z., Huang, Z. 2004. Gallium triiodide catalyzed organic reaction: a convenient synthesis of α-amino phosphonates. Synthetic Communications, (34) 4293-4299.

[74] Ghosh, R., Maiti, S., Chakraborty, A., Maiti, D. K. 2004. $In(OTf)_3$ catalysed simple one-pot synthesis of α-amino phosphonates. Journal of Molecular Catalysis A: Chemical, (210) 53-57.

[75] Bhattacharya, A. K., Kaur, T. 2007. An efficient one-pot synthesis of alpha-amino phosphonates catalyzed by bismuth nitrate pentahydrate. Synlett, (5) 745-748.

[76] Zhan, Z. P., Li, J. P. 2005. Bismuth(III) chloride-catalyzed three-component coupling: Synthesis of alpha-amino phosphonates. Synthetic Communications, (35) 2501-2508.

[77] Xu, F., Luo, Y., Wu, J., Shen, Q., Chen, H. 2006. Facile one-pot synthesis of α-amino phosphonates using lanthanide chloride as catalyst. Heteroatom Chemistry: An International Journal of Main Group Elements, (5) 389-392.

[78] Xu, F., Luo, Y., Deng, M., Shen, Q. 2003. One-pot synthesis of α-amino phosphonates using samarium diiodide as a catalyst precursor. European Journal of Organic Chemistry, (24) 4728-4730.

[79] Ravinder, K., Vijender, R. A., Krishnaiah, P., Venkataramana, G., Niranjan Reddy, V. L., Venkateswarlu, Y. 2004. CAN catalyzed one-pot synthesis of α-

amino phosphonates from carbonyl compounds. Synthetic Communications, (34) 1677-1683.

[80] Ranu, B. C., Hajra, A., Jana, U. 1999. General procedure for the synthesis of α-amino phosphonates from aldehydes and ketones using indium (III) chloride as a catalyst. Organic Letters, (1) 1141-1143.

[81] Lee, S., Park, J. H., Kang, J., Lee, J. K. 2001. Lanthanide triflate-catalyzed three component synthesis of α-amino phosphonates in ionic liquids. A catalyst reactivity and reusability study. Chemical Communications, (17) 1698-1699.

[82] Chandrasekhar, S., Prakash, S. J., Jagadeshwar, V., Narsihmulu, C. 2001. Three component coupling catalyzed by $TaCl_5$–SiO_2: Synthesis of α-amino phosphonates. Tetrahedron Letters, (42) 5561-5563.

[83] Hou, J. T., Gao, J. W., Zhang, Z. H. 2011. $NbCl_5$: An efficient catalyst for one-pot synthesis of α-aminophosphonates under solvent-free conditions. Applied Organometallic Chemistry, (25) 47-53.

[84] Kaboudin, B., Zahedi, H. 2008. Calcium chloride as an efficient Lewis base catalyst for the one-pot synthesis of α-aminophosphonic esters. Chemistry Letters, (37) 540-541.

[85] Ruifang, N., Rui, S., Xiaojun, M., Yang, Z., Xu, C., Weijian, L., Li, G., Hui, J., Yong, W. 2016. Copper-γ-cyclodextrin complexes immobilized on hexagonal boron nitride as an efficient catalyst in the multicomponent synthesis of 1,2,3-triazoles. Journal of Catalysis, (344) 286-292.

[86] Golkar, Z., Bagazra, O., Pace, D. G. 2014. Bacteriophage therapy: A potential solution for the antibiotic resistance crisis. The Journal of Infection in Developing Countries, (8) 129-136.

[87] Gould, I. M., Bal, A. M. 2013. New antibiotic agents in the pipeline and how they can overcome microbial resistance. Virulence, (4) 185-191.

[88] Spellberg, B., Gilbert, D. N. 2014. The future of antibiotics and resistance: A tribute to a career of leadership by John Bartlett. Clinical Infectious Diseases, (59) S71-S75.

[89] (a) Luo, H., Hu, D., Wu, J., He, M., Jin, L., Yang, S., Song, B. 2012. Rapid synthesis and antiviral activity of (quinazolin-4-ylamino) methyl-phosphonates through microwave irradiation. International Journal of Molecular Sciences, (13) 6730-6746. (b) Li, Y. J., Wang, C. Y., Ye, M. Y., Yao, G. Y., Wang, H. S. 2015. Novel coumarin-containing aminophosphonates as antitumor agent: synthesis,

cytotoxicity, dna-binding and apoptosis evaluation. Molecules, (20) 14791-14809. (c) Shitre, G. V., Bhosale, R. S., Karhale, D. S., Sujitha, P., Kumar, C. G., Krishna, K. R., Bhosale, S. V. 2014. Chemistry & biology interface. Chemistry & Biology, (4) 48-57. (d) Gu, L., Jin, C. 2012. Synthesis and antitumor activity of α-aminophosphonates containing thiazole [5,4-b] pyridine moiety. Organic & Biomolecular Chemistry, (10) 7098-7102. (e) Wu, L., Song, B., Bhadury, P. S., Yang, S., Hu, D., Jin, L. 2011. Synthesis and antiviral activity of novel pyrazole amides containing α-aminophosphonate moiety. Journal of Heterocyclic Chemistry, (48) 389-396.

[90] Valko, M., Leibfritz, D., Moncol, J., Cronin, M. T., Mazur, M., Telser. J. 2007. Free radicals and antioxidants in normal physiological functions and human disease. The International Journal of Biochemistry & Cell Biology, (39) 44-84.

[91] Rajabi, S., Ramazani, A., Hamidi, M., Naji, T. 2015. Artemia salina as a model organism in toxicity assessment of nanoparticles. DARU Journal of Pharmaceutical Sciences, (23) 20.

[92] Meyer, B. N., Ferrigni, N. R., Putnam, J. E., Jacobsen, L. B., Nichols, D. J., McLaughlin, J. L. 1982. Brine shrimp: A convenient general bioassay for active plant constituents. Planta Medica, (45) 31-34.

[93] Singh, S. B., Kaelin, D. E., Wu, J., Miesel, L., Tan, C. M., Meinke, P. T., Olsen, D., Lagrutta, A., Bradley, P., Lu, J., Patel, S. 2014. Oxabicyclooctane-linked novel bacterial topoisomerase inhibitors as broad spectrum antibacterial agents. ACS Medicinal Chemistry Letters, (5) 609-614.

[94] Biovia, D. S. 2015. Discovery studio modeling environment. San Diego: Dassault Systemes.

[95] Pettersen, E. F., Goddard, T. D., Huang, C. C., Couch, G. S., Greenblatt, D. M., Meng, E. C., Ferrin, T.E. 2004. UCSF Chimera-a visualization system for exploratory research and analysis. Journal of Computational Chemistry, (25) 1605-1612.

Appendix-V

5.1. Diethyl ((2-(benzylthio)quinolin-3-yl)(m-tolylamino)methyl)phosphonate (23)

Pale yellow crystals, m.p = 216-218℃; IR ν_{max} (cm^{-1}): 1216 C-N, 2970 CH, 1651 C=C, 1273 P=O, 1022 P-O-C, 2585 S-H, 695 C-S, 3285 NH. ^{1}H-NMR: (400 MHz, $CDCl_3$) δ (ppm) 12.46 (1H, brs, NH), 8.11 (1H, d, *J* = 3.72 Hz, Ar-H), 7.50 (2H, d, *J* = 9.6 Hz, Ar-H), 7.45 (2H, t, *J*= 7.6 Hz, Ar-H), 7.18 (2H, t, *J*= 6.8 Hz, Ar-H), 7.00 (2H, t, *J*= 7.72 Hz, Ar-H), 6.59 (3H, t, *J*= 9.84 Hz, Ar-H), 6.52 (2H, d, *J*= 7.20 Hz, Ar-H), 5.61 (1H, d, *J*= 24.88 Hz, CH),

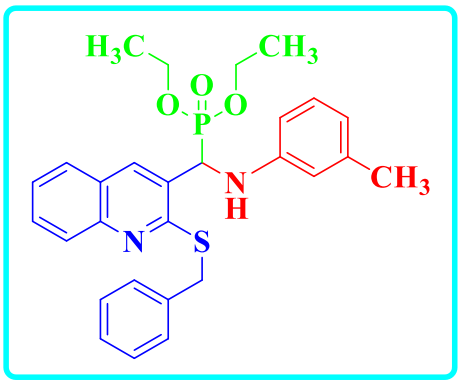

4.33-4.29 (2H, m, *J*= 7.32 Hz, CH_2), 4.12-4.08 (2H, m, *J*= 7.20 Hz, CH_2), 4.04-4.01 (2H, m, *J*= 7.36 Hz, CH_2), 2.20 (3H, brs, CH_3), 1.36 (3H, t, *J*= 1.76 Hz, CH_3), 1.14 (3H, t, *J*= 2.6 Hz, CH_3). ^{13}C-NMR: (100 MHz, $CDCl_3$) δ (ppm) 163.29, 146.05, 145.91, 139.09, 138.45, 138.39, 137.90, 137.88, 130.51, 129.18, 128.70, 128.69, 128.17, 122.71, 119.97, 119.94, 119.50, 115.73, 114.62, 110.58, 63.78, 63.36, 48.82, 47.29, 21.55, 16.50, 16.27. ^{31}P-NMR: (400 MHz, $CDCl_3$) δ (ppm) 22.82. Elemental Analysis: Anal. Calc. for $C_{28}H_{31}N_2O_3PS$: C, 66.39; H, 6.17; N, 5.53; %. Found: C, 66.40; H, 6.19; N, 5.55; %.

5.2. Diethyl ((2-(benzylthio)quinolin-3-yl)(phenylamino)methyl)phosphonate (24)

Brown solid, m.p = 207-209℃; IR ν_{max} (cm^{-1}): 1218 C-N, 2918 CH, 1614 C=C, 1227 P=O, 1081 P-O-C, 2438 S-H, 704 C-S, 3390 NH. ^{1}H-NMR: (400 MHz, DMSO-d_6) δ (ppm) 11.97 (1H, s, NH), 8.50 (1H, s, Ar-H), 8.09 (1H, d, *J*=3.72 Hz, Ar-H), 7.57 (1H, d, *J*= 7.76 Hz, Ar-H), 7.47 (1H, t, *J*= 7.68 Hz, Ar-H), 7.31 (1H, d, *J*= 8.24 Hz, Ar-H), 7.15 (1H, t, *J*= 7.56 Hz, Ar-H), 7.04 (3H, t, *J*= 7.48 Hz, Ar-H), 6.70 (2H, d, *J*= 7.88 Hz, Ar-H), 6.55 (2H, t, *J*= 7.32 Hz, Ar-H), 6.31 (1H, s, Ar-H), 5.96 (1H, s, Ar-H), 5.30 (1H, d, *J*= 10.04 Hz, CH), 4.14-4.07 (2H, m, *J*= 7.08 Hz, CH_2), 4.01-3.95 (2H, m,

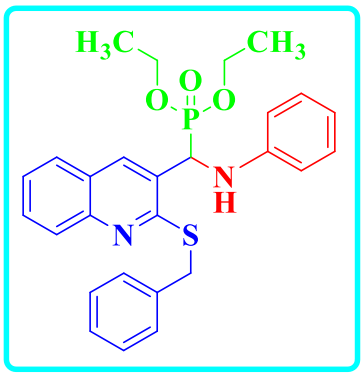

J= 7.36 Hz, CH_2), 3.92-3.85 (2H, m, *J*= 3.04 Hz, CH_2), 1.25 (3H, t, *J*= 3.12 Hz, CH_3), 1.15 (3H, t, *J*= 2.24 Hz, CH_3). ^{13}C-NMR: (100 MHz, DMSO-d_6) δ (ppm) 164.81, 161.50, 161.09, 147.85, 146.95, 146.81, 137.98, 137.97, 137.24, 137.18, 134.15, 130.34, 130.01,

129.49, 128.82, 128.78, 128.21, 127.64, 125.08, 122.08, 118.87, 118.84, 117.25, 116.12, 115.02, 114.22, 113.13, 62.74, 62.68, 62.47, 62.40, 18.97, 16.25, 16.20, 16.07, 16.02. ^{31}P-NMR: (400 MHz, DMSO-d_6) δ (ppm) 22.19. Elemental Analysis: Anal. Calc. for $C_{27}H_{29}N_2O_3PS$: C, 65.84; H, 5.93; N, 5.69; %. Found: C, 65.86; H, 5.95; N, 5.70; %.

5.3. Diethyl ((2-(benzylthio)quinolin-3-yl)((2-methoxyphenyl)amino)methyl) phosphonate (25)

Dark brown solid, m.p = 211-213℃; IR ν_{max} (cm^{-1}): 1217 C-N, 2970 CH, 1672 C=C, 1228 P=O, 1015 P-O-C, 2395 S-H, 708 C-S, 2841 OCH_3, 3395 NH. ^{1}H-NMR: (400 MHz, DMSO-d_6) δ (ppm) 8.24 (1H, s, NH), 7.95 (1H, s, Ar-H), 7.66 (1H, d, *J*= 7.76 Hz, Ar-H), 7.46 (3H, t, *J*= 4.08 Hz, Ar-H), 7.31 (1H, d, *J*= 8.24 Hz, Ar-H), 7.21 (1H, td, *J*= 7.72 Hz, Ar-H), 7.13 (1H, t, *J*= 7.52 Hz, Ar-H), 6.82 (2H, t, *J*= 8.92 Hz, Ar-H), 6.69 (2H, td, *J*= 6.80 Hz, Ar-H), 6.61 (1H, td, *J*= 2.52 Hz, Ar-H), 6.44 (1H, dd, *J*= 6.60 Hz, Ar-H), 5.31 (1H, d, *J*= 16.52 Hz, CH), 4.30 (2H, s, CH_2), 4.14-4.01 (2H, m, *J*= 7.20 Hz, CH_2), 3.99-3.90 (2H, m, *J*= 2.68 Hz, CH_2), 3.88 (3H, s, OCH_3), 1.22 (3H, t, *J*= 7.04 Hz, CH_3), 1.07 (3H, t, *J*= 7.00 Hz, CH_3). ^{13}C-NMR: (100 MHz, DMSO-d_6) δ (ppm) 164.18, 161.16, 161.11, 153.79, 147.02, 146.85, 137.98, 136.72, 136.65, 135.52, 135.48, 135.34, 130.40, 130.16, 128.75, 128.73, 127.89, 127.58, 127.29, 122.04, 121.95, 120.99, 120.91, 120.80, 118.82, 117.72, 117.61, 114.96, 112.90, 110.73, 110.18, 110.12, 62.84, 62.76, 62.76, 62.69, 61.42, 55.64, 55.53, 55.24, 18.50, 16.29, 16.19, 16.13, 16.03, 15.97. ^{31}P-NMR: (400 MHz, DMSO-d_6) δ (ppm) 21.00. Elemental Analysis: Anal. Calc. for $C_{28}H_{31}N_2O_4PS$: C, 64.35; H, 5.98; N, 5.36; %. Found: C, 64.37; H, 5.97; N, 5.38; %.

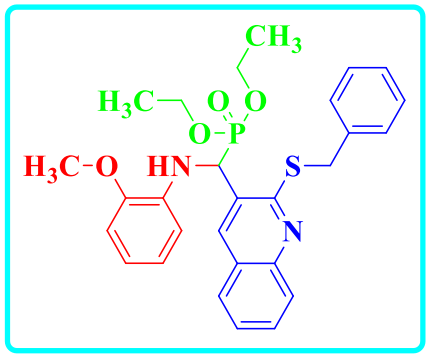

5.4. Diethyl ((2-(benzylthio)quinolin-3-yl)(o-tolylamino)methyl)phosphonate (26)

Brown solid, m.p = 219-221℃; IR ν_{max} (cm^{-1}): 1217 C-N, 2970 CH, 1616 C=C, 1229 P=O, 1040 P-O-C, 2520 S-H, 666 C-S, 3266 NH. ^{1}H-NMR: (400 MHz, $CDCl_3$) δ (ppm) 9.11 (1H, s, NH), 8.46 (1H, s, Ar-H), 7.97 (2H, t, *J*= 7.96 Hz, Ar-H), 7.75 (1H, d, *J*= 8.20 Hz, Ar-H), 7.67 (1H, t, *J*= 7.48 Hz, Ar-H), 7.44 (1H, t, *J*= 7.56 Hz, Ar-H), 7.28 (1H, d,

J= 8.00 Hz, Ar-H), 7.14 (3H, t, *J*= 7.12 Hz, Ar-H), 7.02 (2H, d, *J*= 8.32 Hz, Ar-H), 6.64 (1H, t, *J*= 7.52 Hz, Ar-H), 6.55 (1H, d, *J*= 8.48 Hz, Ar-H), 5.58 (1H, d, *J*= 26.68 Hz, CH), 4.30-4.25 (2H, m, *J*= 3.08 Hz, CH_2), 4.08-4.02 (2H, m, *J*= 7.44 Hz, CH_2), 3.96-3.90 (2H, m, *J*= 9.56 Hz, CH_2), 2.23 (3H, s, CH_3), 1.32 (3H, t, *J*= 7.04 Hz, CH_3), 1.16 (3H, t, *J*= 7.04 Hz, CH_3). ^{13}C-NMR: (100 MHz, $CDCl_3$) δ (ppm) 159.53, 159.42, 146.12, 143.61, 143.48, 136.76, 136.70, 136.30, 133.40, 129.95, 127.74, 126.93, 126.90, 125.14, 125.11, 124.50, 120.03, 119.99, 116.85, 114.36, 63.78, 63.71, 63.59, 63.52, 54.04, 49.44, 47.90, 16.45, 16.40, 16.30, 16.25. ^{31}P-NMR: (400 MHz, $CDCl_3$) δ (ppm) 22.12. Elemental Analysis: Anal. Calc. for $C_{28}H_{31}N_2O_3PS$: C, 66.39; H, 6.17; N, 5.53; %. Found: C, 66.40; H, 6.19; N, 5.55; %.

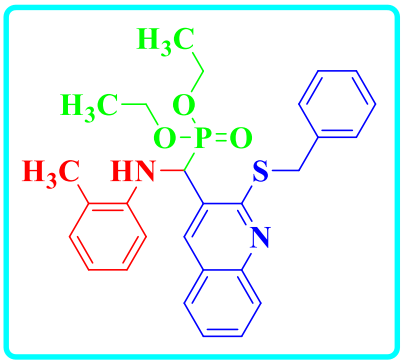

5.5. Diethyl ((2-(benzylthio)quinolin-3-yl)((3-fluorophenyl)amino)methyl) phosphonate (27)

Pale yellow solid, m.p = 229-231℃; IR ν_{max} (cm^{-1}): 1216 C-N, 2970 CH, 1624 C=C, 1304 P=O, 1052 P-O-C, 2570 S-H, 636 C-S, 1366 C-F, 3457 NH. ^{1}H-NMR: (400 MHz, $CDCl_3$) δ (ppm) 8.23 (1H, s, NH), 8.14 (1H, s, Ar-H), 7.91-7.86 (1H, d, *J*= 6.32 Hz, Ar-H), 7.82 (2H, t, *J*= 3.36 Hz, Ar-H), 7.64 (1H, t, *J*= 6.68 Hz, Ar-H), 7.40 (2H, t, *J*= 2.48 Hz, Ar-H), 7.11 (2H, t, *J*= 7.76 Hz, Ar-H), 6.95 (2H, t, *J*= 4.72 Hz, Ar-H), 6.71 (2H, t, *J*= 7.00 Hz, Ar-H), 6.67 (1H, d, *J* = 7.64 Hz, Ar-H), 5.30 (1H, d, *J*= 12.32 Hz, CH), 4.25 (2H, s, CH_2), 4.09-3.98 (2H, m, *J*= 2.72 Hz, CH_2), 3.63-3.51 (2H, m, *J*= 7.12 Hz, CH_2), 1.30 (3H, t, *J*= 7.08 Hz, CH_3), 1.16 (3H, t, *J*= 7.04 Hz, CH_3). ^{13}C-NMR: (100 MHz, $CDCl_3$) δ (ppm) 176.28, 176.24, 156.26, 155.35, 155.29, 145.21, 145.08, 133.87, 129.37, 125.94, 125.44, 123.41, 120.02, 119.17, 118.28, 114.02, 63.86, 63.79, 63.53, 63.45, 46.20, 44.65, 30.92, 16.44, 16.38, 16.29, 16.24. ^{31}P-NMR: (400 MHz, $CDCl_3$) δ (ppm) 22.09. Elemental Analysis: Anal. Calc. for $C_{27}H_{28}FN_2O_3PS$: C, 63.52; H, 5.53; N, 5.49; %. Found: C, 63.54; H, 5.55; N, 5.51; %.

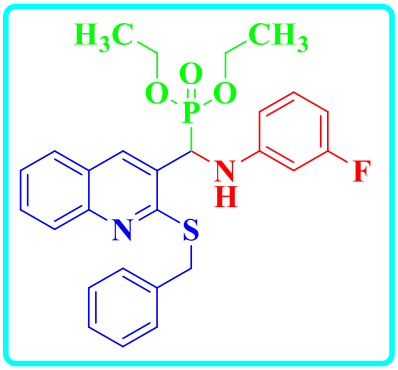

5.6. Diethyl ((2-(benzylthio)quinolin-3-yl)((3-chloro-4-fluorophenyl)amino) methyl)phosphonate (28)

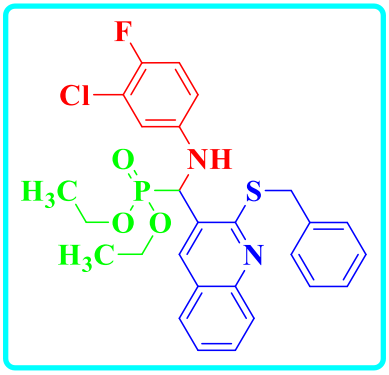

Yellow solid, m.p = 234-236℃; IR ν_{max} (cm^{-1}): 1216 C-N, 2970 CH, 1625 C=C, 1259 P=O, 1034 P-O-C, 2529 S-H, 640 C-S, 1287 C-F, 663 C-Cl, 3457 NH. ^{1}H-NMR: (400 MHz, DMSO-d_6) δ (ppm) 8.81 (1H, s, NH), 8.75 (1H, s, Ar-H), 8.32 (1H, d, *J*= 1.48 Hz, Ar-H), 8.27 (1H, d, *J*= 4.40 Hz, Ar-H), 8.10 (2H, d, *J*= 11.16 Hz, Ar-H), 7.64 (2H, t, *J*= 7.88 Hz, Ar-H), 7.53 (2H, t, *J*= 7.12 Hz, Ar-H), 7.32 (2H, d, *J*= 7.40 Hz, Ar-H), 7.21 (2H, t, *J*= 7.60 Hz, Ar-H), 5.13 (1H, s. CH), 4.27 (2H, s, CH_2), 4.10-3.98 (2H, m, *J*= 7.08 Hz, CH_2), 3.94-3.76 (2H, m, *J*= 8.32 Hz, CH_2), 1.49 (3H, t, *J*= 7.32 Hz, CH_3), 1.37 (3H, t, *J*= 7.12 Hz, CH_3). ^{13}C-NMR: (100 MHz, $CDCl_3$) δ (ppm) 159.89, 159.84, 145.73, 142.96, 142.82, 136.88, 136.82, 132.54, 129.80, 128.48, 127.81, 126.67, 125.14, 124.39, 120.66, 120.63, 119.19, 112.34, 110.51, 63.74, 63.68, 63.38, 63.31, 54.19, 49.93, 48.40, 16.52, 16.46, 16.26, 16.20. ^{31}P-NMR: (400 MHz, DMSO-d_3) δ (ppm) 20.82. Elemental Analysis: Anal. Calc. for $C_{27}H_{27}ClFN_2O_3PS$: C, 59.50; H, 4.99; N, 5.14; %. Found: C, 59.52; H, 4.98; N, 5.16; %.

5.7. Diethyl ((2-(benzylthio)quinolin-3-yl)((2-nitrophenyl)amino)methyl) phosphonate (29)

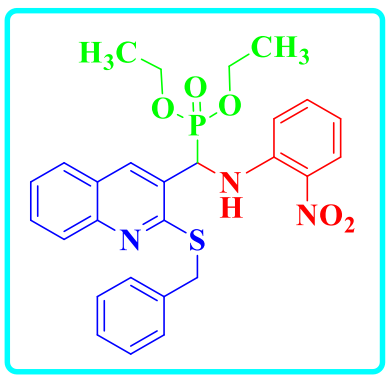

Brown solid, m.p = 226-228℃; IR ν_{max} (cm^{-1}): 1293 C-N, 2970 CH, 1614 C=C, 1137 P=O, 1030 P-O-C, 2451 S-H, 707 C-S, 3381 NH. ^{1}H-NMR: (400 MHz, $CDCl_3$) δ (ppm) 8.39 (1H, s, NH), 8.15 (1H, s, Ar-H), 8.00 (1H, s, Ar-H), 7.82 (1H, d, *J*= 8.36 Hz, Ar-H), 7.65 (1H, d, *J*= 8.00 Hz, Ar-H), 7.55 (1H, t, *J*= 7.40 Hz, Ar-H), 7.30 (1H, t, *J*= 7.52 Hz, Ar-H), 7.02 (2H, t, *J* = 7.32 Hz, Ar-H), 6.98 (2H, t, *J*= 7.12 Hz, Ar-H), 6.74 (3H, t, *J*= 7.48 Hz, Ar-H), 6.44 (1H, d, *J*= 7.60 Hz, Ar-H), 5.37 (1H, d, *J*= 24.76 Hz, CH), 4.19 (2H, s, CH_2), 3.98-3.92 (2H, m, *J*= 7.20 Hz, CH_2), 3.82-3.74 (2H, m, *J*= 4.52 Hz, CH_2), 1.30 (3H, t, *J*= 7.04 Hz, CH_3), 1.06 (3H, t, *J*= 7.00 Hz, CH_3). ^{13}C-

NMR: (100 MHz, $CDCl_3$) δ (ppm) 160.07, 160.02, 147.37, 145.93, 145.91, 136.75, 136.70, 135.82, 135.68, 129.50, 127.76, 126.79, 125.32, 125.29, 124.13, 121.39, 121.37, 121.08, 117.82, 110.83, 109.64, 63.55, 63.49, 63.17, 63.10, 55.50, 53.86, 49.29, 47.76, 16.48, 16.43, 16.21, 16.15. ^{31}P-NMR: (400 MHz, $CDCl_3$) δ (ppm) 21.80. Elemental Analysis: Anal. Calc. for $C_{27}H_{28}N_3O_5PS$: C, 60.33; H, 5.25; N, 7.82; %. Found: C, 60.35; H, 5.27; N, 7.83; %.

5.8. Diethyl ((2-(benzylthio)quinolin-3-yl)((2,4-dimethylphenyl)amino)methyl) phosphonate (30)

Dark yellow crystals, m.p = 222-224℃; IR ν_{max} (cm^{-1}): 1225 C-N, 2971 CH, 1614 C=C, 1318 P=O, 1022 P-O-C, 2384 S-H, 658 C-S, 3971 NH. ^{1}H-NMR: (400 MHz, $CDCl_3$) δ (ppm) 7.99 (1H, s, NH), 7.52 (1H, d, *J*= 8.60 Hz, Ar-H), 7.33 (2H, d, *J*= 2.16 Hz, Ar-H), 7.31 (2H, d, *J*= 2.20 Hz, Ar-H), 7.24 (1H, s, Ar-H), 7.11 (2H, d, *J*= 8.04 Hz, Ar-H), 6.69 (2H, t, *J*= 7.76 Hz, Ar-H), 6.49 (1H, d, *J*= 7.48 Hz, Ar-H), 6.43 (1H, s, Ar-H), 6.36 (1H, dd, *J*= 1.88 Hz, Ar-H), 4.69 (1H, d, *J*= 18.32 Hz, CH), 4.18-4.03 (2H, m, *J*= 7.12 Hz, CH_2), 3.99-3.83 (2H, m, *J*= 6.32 Hz, CH_2), 3.71-3.62 (2H, m, *J*= 9.12 Hz, CH_2), 2.19 (3H, s, CH_3), 1.41 (3H, s, CH_3), 1.27 (3H, t, *J*= 4.16 Hz, CH_3), 1.11 (3H, t, *J*= 7.04 Hz, CH_3). ^{13}C-NMR: (100 MHz, $CDCl_3$) δ (ppm) 165.12, 162.70, 159.87, 159.82, 147.86, 147.75, 147.72, 147.61, 145.99, 145.97, 136.74, 136.68, 130.41, 130.31, 129.70, 127.71, 126.89, 125.71, 125.14, 124.30, 120.75, 120.73, 109.45, 109.42, 105.13, 104.92, 100.61, 100.36, 63.57, 63.50, 63.41, 63.34, 53.92, 49.48, 47.96, 16.48, 16.42, 16.16, 16.10. ^{31}P-NMR: (400 MHz, $CDCl_3$) δ (ppm) 22.18. Elemental Analysis: Anal. Calc. for $C_{29}H_{33}N_2O_3PS$: C, 66.90; H, 6.39; N, 5.38; %. Found: C, 66.92; H, 6.40; N, 5.39; %.

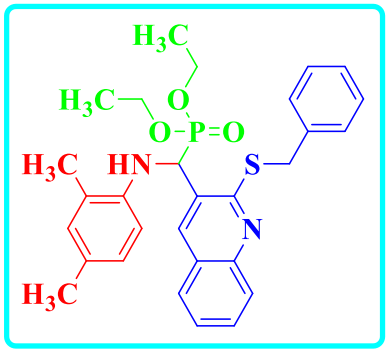

5.9. Diethyl ((2-(benzylthio)quinolin-3-yl)((4-methoxyphenyl)amino)methyl) phosphonate (31)

Dark brown solid, m.p = 239-241℃; IR ν_{max} (cm^{-1}): 1217 C-N, 2970 CH, 1615 C=C, 1230 P=O, 995 P-O-C, 2419 S-H, 700 C-S, 2790 OCH_3, 3390 NH. ^{1}H-NMR: (400 MHz, $CDCl_3$) δ (ppm) 9.01 (1H, s, NH), 8.26 (1H, s, Ar-H), 8.12 (1H, d, *J*= 8.40 Hz, Ar-H),

7.70 (3H, t, *J*= 8.20 Hz, Ar-H), 7.51 (2H, d, *J*= 7.08 Hz, Ar-H), 7.44 (1H, t, *J*= 7.40 Hz, Ar-H), 7.31 (2H, t, *J*= 6.88 Hz, Ar-H), 6.59 (2H, d, *J*= 8.92 Hz, Ar-H), 6.49 (2H, d, *J*= 7.32 Hz, Ar-H), 4.71 (1H, d, *J*= 13.24 Hz, CH), 4.28-4.20 (2H, m, *J*= 7.20 Hz, CH_2), 4.15-4.08 (2H, m, *J*= 7.12 Hz, CH_2), 3.76-3.69 (2H, m, *J*= 7.04 Hz, CH_2), 3.66 (3H, s, OCH_3), 1.34 (3H, t, *J*= 3.24 Hz, CH_3), 1.02 (3H, t, *J*= 7.04 Hz, CH_3). ^{13}C-NMR: (100 MHz, $CDCl_3$) δ (ppm) 149.07, 149.01, 145.76, 145.73, 145.29, 145.14, 137.52, 137.15, 137.10, 133.22, 132.95, 130.76, 128.01, 127.79, 127.22, 127.19, 126.53, 121.46, 115.45, 112.78, 64.08, 64.00, 63.80, 63.72, 52.54, 51.01, 21.48, 16.53, 16.47, 16.16, 16.10. ^{31}P-NMR: (400 MHz, $CDCl_3$) δ (ppm) 21.34. Elemental Analysis: Anal. Calc. for $C_{28}H_{31}N_2O_4PS$: C, 64.35; H, 5.98; N, 5.36; %. Found: C, 64.37; H, 6.00; N, 5.38; %.

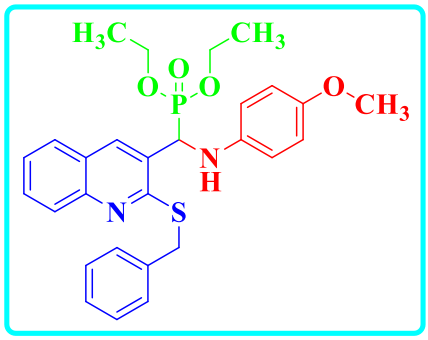

5.10. Diethyl ((2-(benzylthio)quinolin-3-yl)((pyridin-2-ylmethyl)amino)methyl) phosphonate (32)

Brown solid, m.p = 197-199℃; IR ν_{max} (cm^{-1}): 1218 C-N, 2970 CH, 1615 C=C, 1227 P=O, 1050 P-O-C, 2395 S-H, 701 C-S, 3395 NH. ^{1}H-NMR: (400 MHz, $CDCl_3$) δ (ppm) 8.58 (1H, s, Ar-H), 8.06 (1H, s, Ar-H), 7.87 (1H, d, *J*= 4.20 Hz, Ar-H), 7.63 (1H, t, *J*= 6.20 Hz, Ar-H), 7.48 (1H, d, *J*= 6.84 Hz, Ar-H), 7.16 (1H, t, *J*= 4.76 Hz, Ar-H), 7.10 (2H, t, *J*= 7.40 Hz, Ar-H), 6.90 (3H, t, *J*= 7.04 Hz, Ar-H), 6.69 (3H, td, *J*= 7.28 Hz, Ar-H), 5.24 (1H, s, NH), 5.01 (1H, d, *J*= 22.24 Hz, CH), 4.36 (2H, s, CH_2), 4.14-4.08 (2H, m, *J*= 7.32 Hz, CH_2), 4.04-3.98 (2H, m, *J*= 7.28 Hz, CH_2), 3.90-3.83 (2H, m, *J*= 7.08 Hz, CH_2), 1.24 (3H, t, *J*= 7.04 Hz, CH_3), 1.13 (3H, t, *J*= 6.88 Hz, CH_3). ^{13}C-NMR: (100 MHz, $CDCl_3$) δ (ppm) 155.69, 148.57, 146.43, 146.31, 137.33, 129.20, 129.08, 123.08, 123.04, 122.99, 122.96, 119.70, 118.59, 114.02, 77.39, 77.27, 76.75, 63.67, 63.59, 63.34, 63.27, 58.30, 56.80, 16.43, 16.37, 16.25, 16.19. ^{31}P-NMR: (400 MHz, $CDCl_3$) δ (ppm) 21.00. Elemental Analysis: Anal. Calc. for $C_{27}H_{30}N_3O_3PS$: C, 63.89; H, 5.96; N, 8.28; %. Found: C, 63.90; H, 5.98; N, 8.30; %.

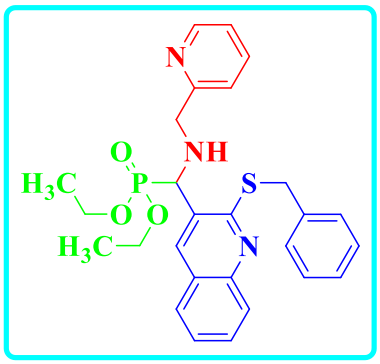

5.11. Diethyl ((2-(benzylthio)quinolin-3-yl)((4-bromophenyl)amino) methyl)phosphonate (33)

Dark yellow solid, m.p = 183-185℃; IR ν_{max} (cm^{-1}): 1217 C-N, 2970 CH, 1614 C=C, 1230 P=O, 995 P-O-C, 705 C-S, 521 C-Br, 3421 NH. ^{1}H-NMR: (400 MHz, $CDCl_3$) δ (ppm) 8.51 (1H, s, NH), 8.20 (1H, s, Ar-H), 8.02 (1H, d, *J*= 8.32 Hz, Ar-H), 7.90 (2H, s, Ar-H), 7.69 (2H, t, *J*= 8.64 Hz, Ar-H), 7.49 (2H, d, *J*= 7.04 Hz, Ar-H), 7.43 (1H, t, *J*= 7.48 Hz, Ar-H), 7.31 (3H, t, *J*= 2.84 Hz, Ar-H), 7.08 (1H, d, *J*= 8.72 Hz, Ar-H), 6.43 (1H, d, *J* = 8.84 Hz, Ar-H), 4.68 (1H, d, *J*= 14.96 Hz, CH), 4.27-4.20 (2H, m, *J*= 7.16 Hz, CH_2), 4.14-4.07 (2H, m, *J*= 7.24 Hz, CH_2), 3.92-3.82 (2H, m, *J*= 7.20 Hz, CH_2), 1.34 (3H, t, *J*= 7.08 Hz, CH_3), 1.00 (3H, t, *J*= 7.04 Hz, CH_3). ^{13}C-NMR: (100 MHz, $CDCl_3$) δ (ppm) 157.48, 144.60, 144.45, 138.37, 134.71, 131.98, 130.19, 129.30, 129.21, 128.50, 127.97, 127.51, 127.23, 125.96, 125.84, 115.31, 110.43, 63.86, 63.80, 51.55, 50.02, 35.17, 16.45, 16.39, 16.12, 16.07. ^{31}P-NMR: (400 MHz, $CDCl_3$) δ (ppm) 19.47. Elemental Analysis: Anal. Calc. for $C_{27}H_{28}BrN_2O_3PS$: C, 56.75; H, 4.94; N, 4.90; %. Found: C, 56.77; H, 4.96; N, 4.91; %.

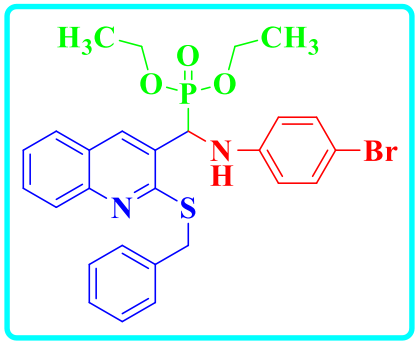

5.12. Diethyl ((2-(benzylthio)quinolin-3-yl)((4-chlorophenyl)amino)methyl) phosphonate (34)

Yellow solid, m.p = 195-197℃; IR ν_{max} (cm^{-1}): 1218 C-N, 2971 CH, 1613 C=C, 1260 P=O, 951 P-O-C, 707 C-S, 752 C-Cl, 3304 NH. ^{1}H-NMR: (400 MHz, $CDCl_3$) δ (ppm) 8.48 (1H, s, NH), 8.10 (1H, s, Ar-H), 7.91 (1H, d, *J*= 8.40 Hz, Ar-H), 7.58 (2H, t, *J*= 8.60 Hz, Ar-H), 7.39 (2H, d, *J*= 7.04 Hz, Ar-H), 7.31 (1H, t, *J*= 7.52 Hz, Ar-H), 7.22 (1H, d, *J*= 6.80 Hz, Ar-H), 7.16 (2H, d, *J*= 5.96 Hz, Ar-H), 6.84 (2H, d, *J*= 8.80 Hz, Ar-H), 6.37 (2H, d, *J*= 8.84 Hz, Ar-H), 4.56 (1H, d, *J*= 6.56 Hz, CH), 4.17-4.10 (2H, m, *J*= 7.20 Hz, CH_2), 3.82-3.72 (2H, m, *J*= 4.44 Hz, CH_2), 3.58-3.51 (2H, m, *J*= 7.08 Hz, CH_2), 1.23 (3H, t, *J*= 7.04 Hz, CH_3), 0.90 (3H, t, *J*= 7.08 Hz, CH_3). ^{13}C-NMR: (100 MHz, $CDCl_3$) δ (ppm) 157.51, 157.45, 147.32, 147.30, 144.20, 144.06, 138.46, 134.67, 134.61, 130.08,

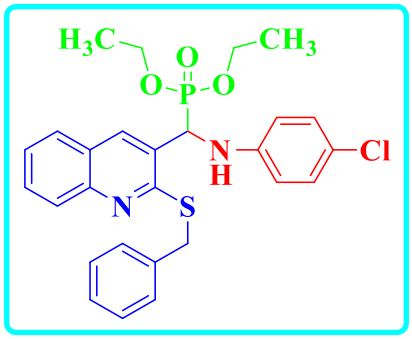

129.42, 129.34, 129.29, 129.21, 129.09, 128.49, 127.97, 127.64, 127.20, 125.98, 125.95, 125.76, 123.26, 115.16, 114.84, 63.83, 63.76, 63.46, 51.65, 50.12, 35.05, 16.47, 16.41, 16.14, 16.08. ^{31}P-NMR: (400 MHz, $CDCl_3$) δ (ppm) 22.39. Elemental Analysis: Anal. Calc. for $C_{27}H_{28}ClN_2O_3PS$: C, 61.53; H, 5.36; N, 5.32; %. Found: C, 61.55; H, 5.38; N, 5.33; %.

5.13. Diethyl ((2-(benzylthio)quinolin-3-yl)((3,4-dichlorophenyl)amino) methyl)phosphonate (35)

Brown solid, m.p = 200-202℃; IR ν_{max} (cm^{-1}): 1225 C-N, 2977 CH, 1673 C=C, 1132 P=O, 1021 P-O-C, 700 C-S, 747 C-Cl, 3307 NH. ^{1}H-NMR: (400 MHz, $CDCl_3$) δ (ppm) 8.49 (1H, s, NH), 8.23 (1H, s, Ar-H), 8.01 (1H, d, *J*= 8.36 Hz, Ar-H), 7.68 (2H, t, *J*= 7.72 Hz, Ar-H), 7.53 (1H, d, *J*= 4.80 Hz, Ar-H), 7.48 (2H, s, Ar-H), 7.32 (2H, t, *J*= 6.96 Hz, Ar-H), 7.27-7.26 (1H, td, *J*= 2.64 Hz, Ar-H), 7.00 (1H, d, *J*= 8.76 Hz, Ar-H), 6.80 (1H, d, *J*= 2.72 Hz, Ar-H), 6.39 (1H, d, *J*= 4.48 Hz, Ar-H), 4.78 (1H, d, *J*= 13.20 Hz, CH), 4.28-4.21 (2H, m, *J*= 7.20 Hz, CH_2), 3.91-3.85 (2H, m, *J*= 4.40 Hz, CH_2), 3.67-3.60 (2H, m, *J*= 2.84 Hz, CH_2), 1.34 (3H, t, *J*= 7.04 Hz, CH_3), 1.01 (3H, t, *J*= 2.40 Hz, CH_3). ^{13}C-NMR: (100 MHz, $CDCl_3$) δ (ppm) 157.48, 157.42, 147.39, 145.29, 145.14, 138.18, 134.64, 134.59, 132.80, 130.66, 130.16, 129.26, 128.50, 128.04, 128.02, 127.93, 127.70, 127.22, 125.90, 125.87, 125.79, 121.24, 115.33, 113.03, 63.95, 63.88, 63.80, 51.44, 49.91, 35.06, 16.46, 16.41, 16.13, 16.08. ^{31}P-NMR: (400 MHz, $CDCl_3$) δ (ppm) 22.57.Elemental Analysis: Anal. Calc. for $C_{27}H_{27}Cl_2N_2O_3PS$: C, 57.76; H, 4.85; N, 4.99; %. Found: C, 57.78; H, 4.87; N, 4.98; %.

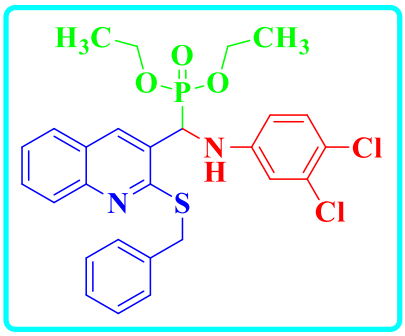

5.14. Diethyl ((2-(benzylthio)-6-fluoroquinolin-3-yl)((2-methoxyphenyl)amino) methyl) phosphonate (36)

Yellow solid, m.p = 201-203℃; IR ν_{max} (cm^{-1}): 1231 C-N, 2918 CH, 1613 C=C, 1148 P=O, 1077 P-O-C, 650 C-S, 2818 OCH_3, 3390 NH. ^{1}H-NMR: (400 MHz, $CDCl_3$) δ (ppm) 8.57 (1H, s, NH), 8.16 (1H, s, Ar-H), 7.85 (2H, t, *J*= 8.44 Hz, Ar-H), 7.59 (1H, t, *J*= 7.76 Hz, Ar-H), 7.34 (3H, td, *J*= 2.96 Hz, Ar-H), 7.15 (2H, t, *J*= 8.16 Hz, Ar-H), 6.69-6.61 (2H, d, *J*= 7.68 Hz, Ar-H), 6.59-6.51 (2H, d, *J*= 8.00 Hz, Ar-H), 5.19 (1H, s, CH), 4.19 (3H, s, OCH_3), 4.03 (2H, s, CH_2), 4.01-3.97 (2H, m, *J*= 3.84 Hz, CH_2), 3.96-3.90

(2H, m, *J*= 3.76 Hz, CH_2), 1.04 (3H, t, *J*= 2.52 Hz, CH_3), 1.01 (3H, t, *J*= 2.60 Hz, CH_3). ^{13}C-NMR: (100 MHz, $CDCl_3$) δ (ppm) 164.96, 163.05, 160.31, 150.51, 145.75, 142.81, 136.06, 132.58, 132.49, 131.23, 129.28, 127.94, 127.41, 126.80, 125.40, 124.09, 120.32, 117.08, 116.85, 103.83, 62.15, 61.52, 60.94, 53.63, 33.70, 13.86, 13.54. ^{31}P-NMR: (400 MHz, $CDCl_3$) δ (ppm) 20.27. ^{19}F-NMR: (400 MHz, $CDCl_3$) δ (ppm) -117.38.

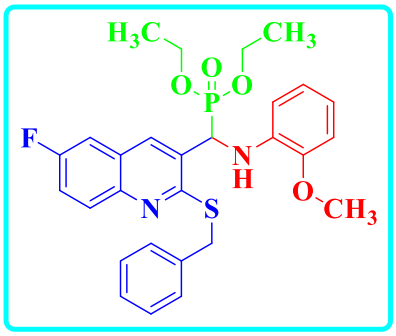

Elemental Analysis: Anal. Calc. for $C_{28}H_{30}FN_2O_4PS$: C, 62.21; H, 5.59; N, 5.18; %. Found: C, 62.23; H, 5.60; N, 5.20; %.

5.1. Diethyl ((2-(benzylthio)quinolin-3-yl)(m-tolylamino)methyl)phosphonate (23)

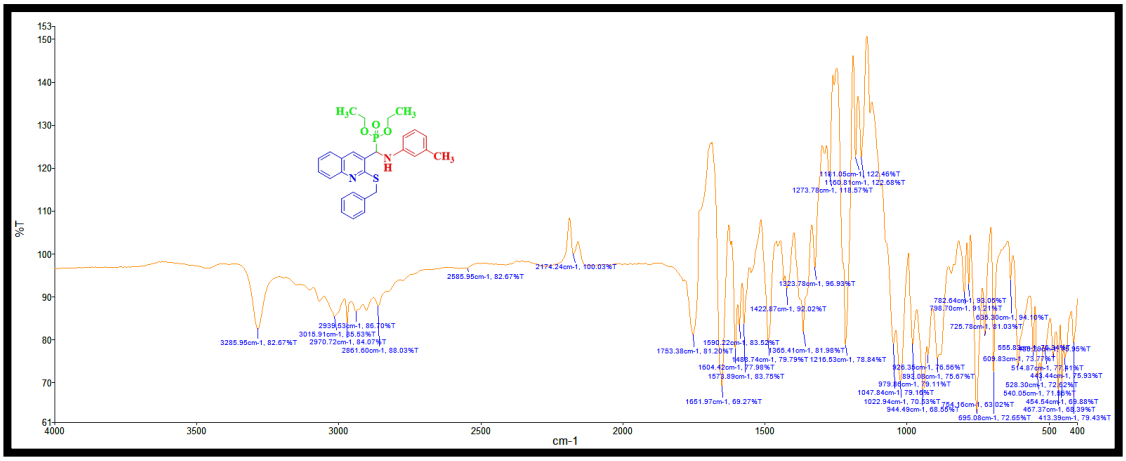

Fig. 5.1. IR spectrum of **23**

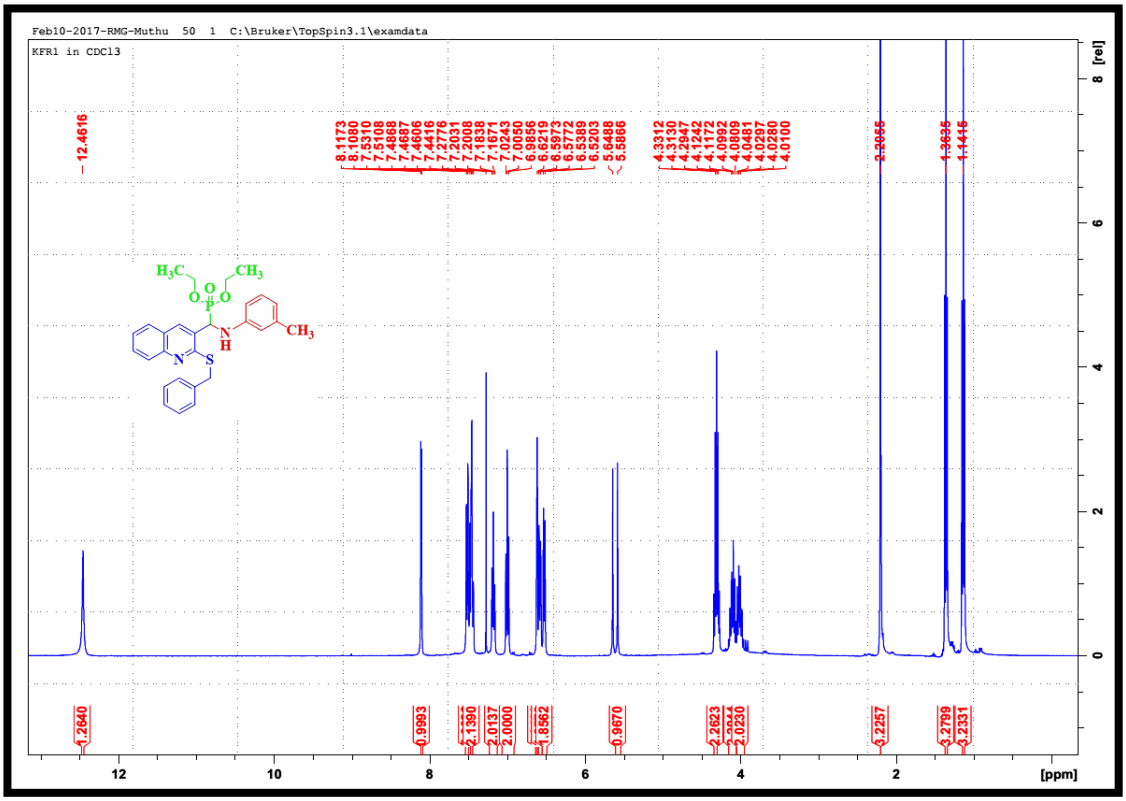

Fig. 5.2. ^{1}H-NMR spectrum of **23**

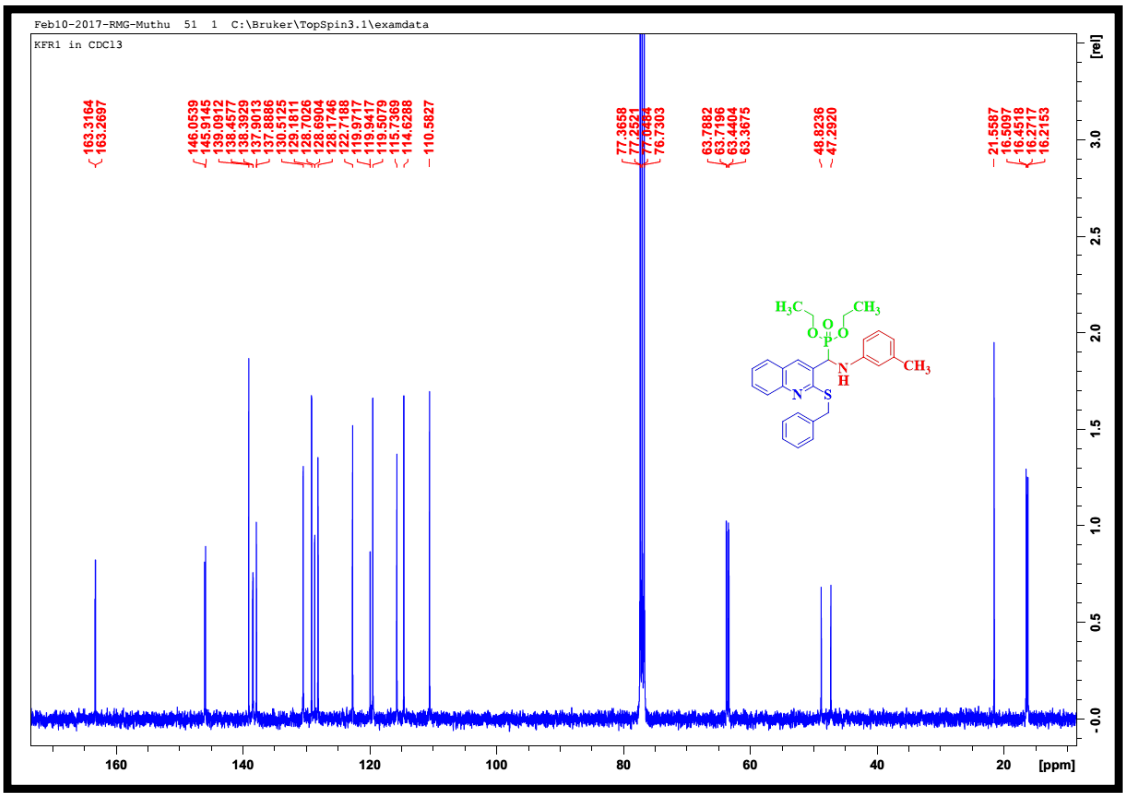

Fig. 5.3. ^{13}C-NMR spectrum of **23**

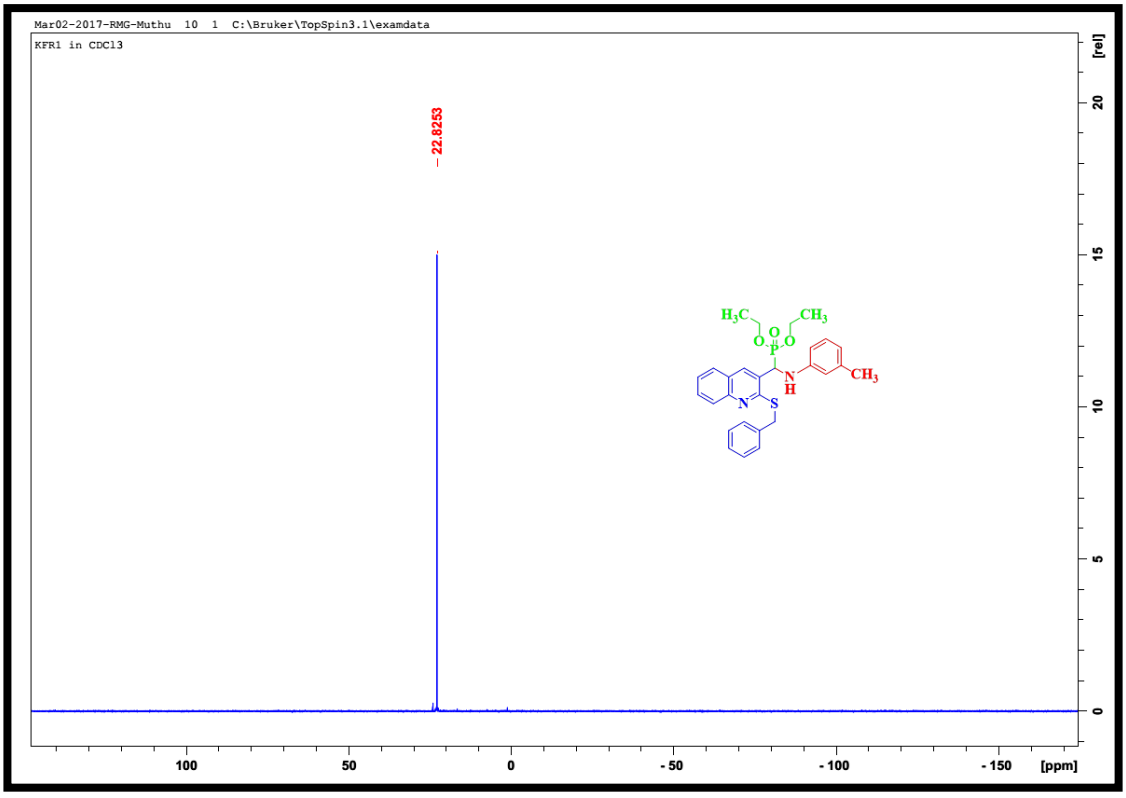

Fig. 5.4. ^{31}P-NMR spectrum of **23**

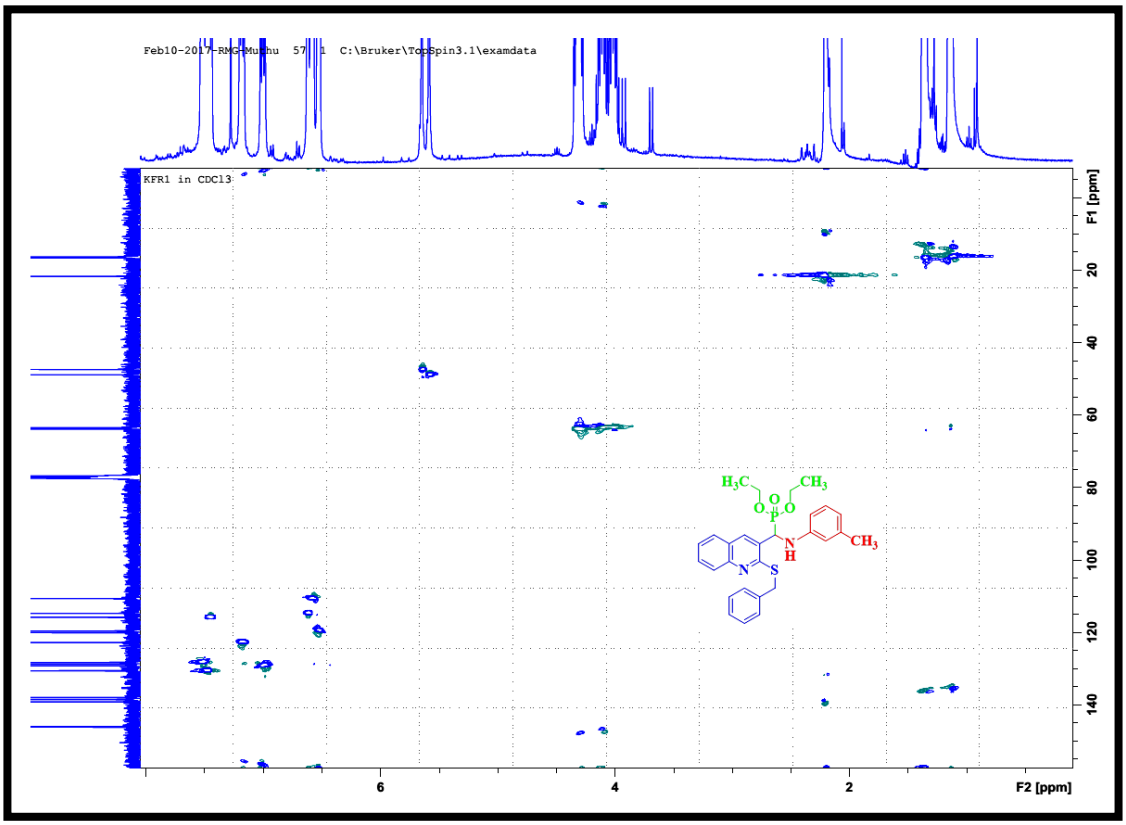

Fig. 5.5. HSQC spectrum of **23**

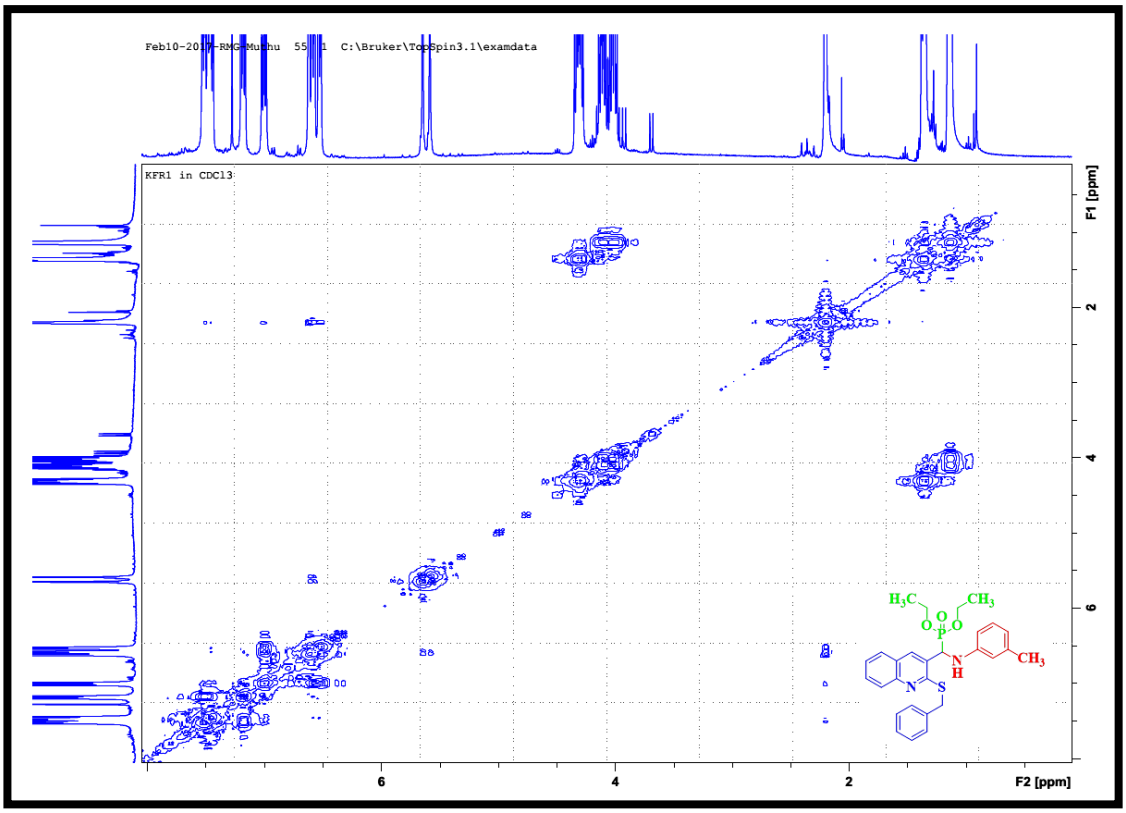

Fig. 5.6. COSY spectrum of **23**

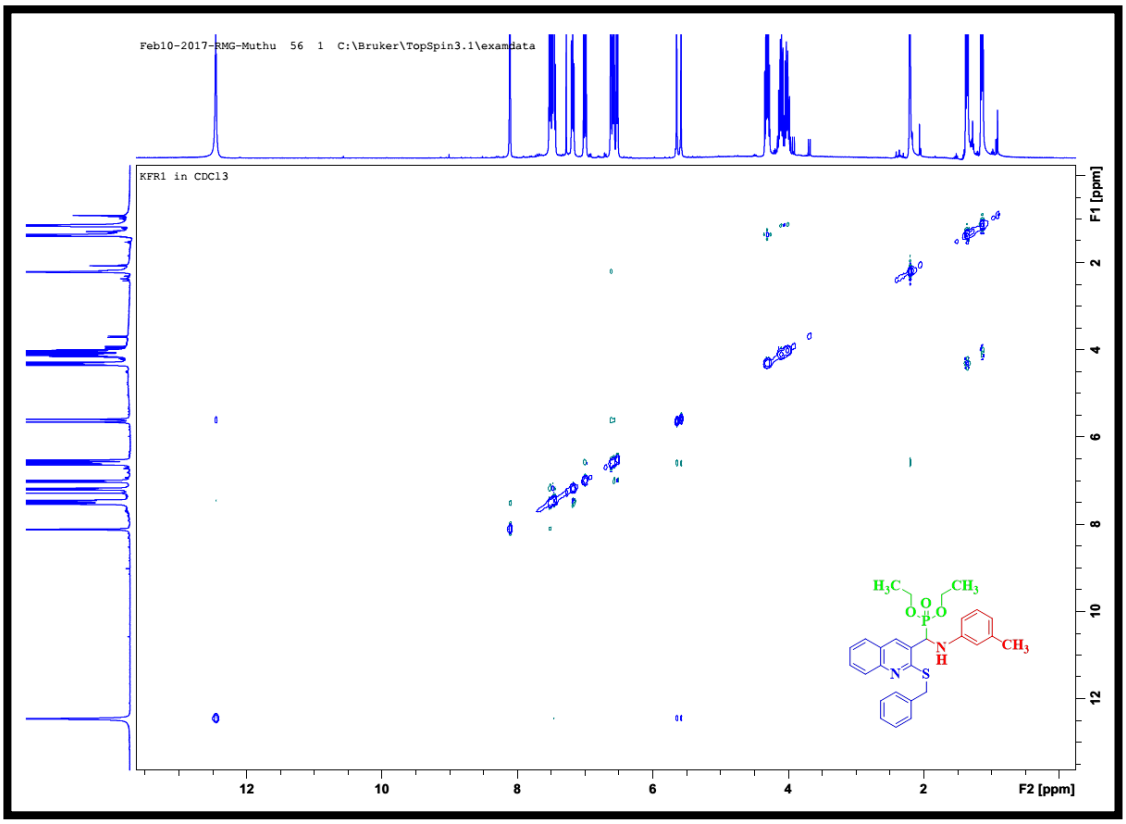

Fig. 5.7. NOESY spectrum of **23**

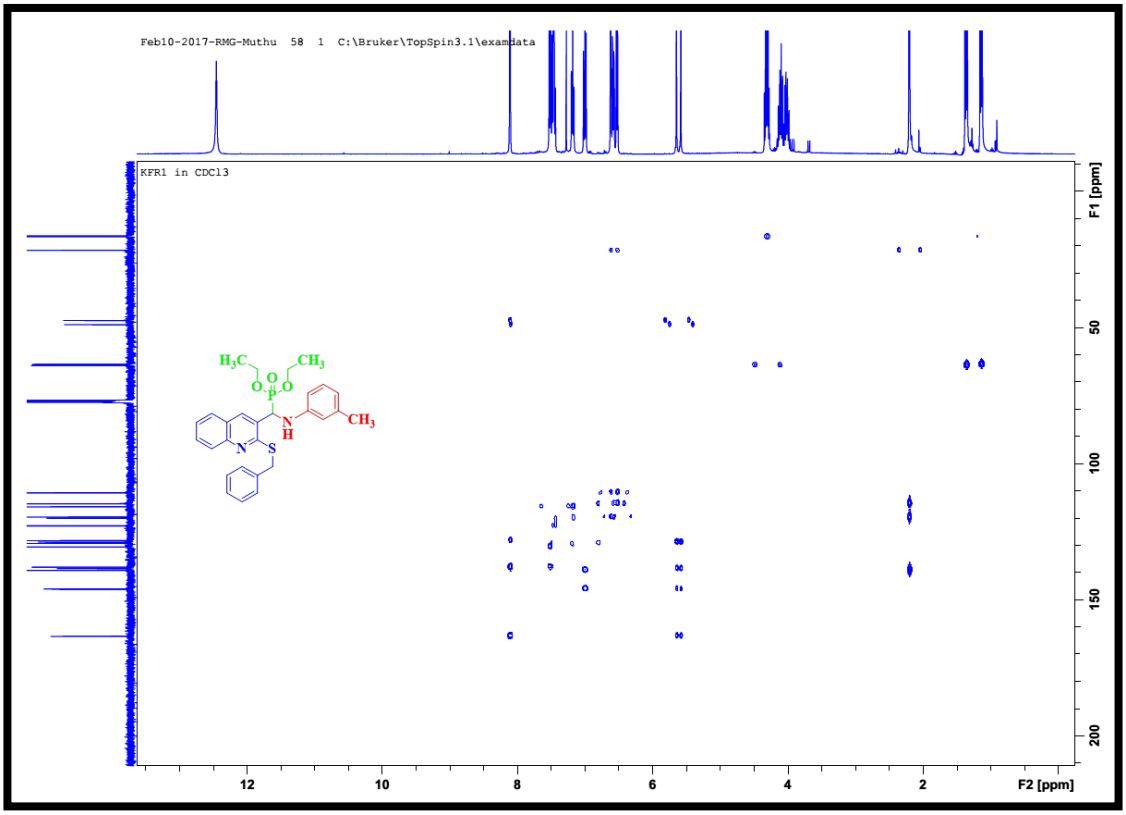

Fig. 5.8. HMBC spectrum of **23**

5.2. Diethyl ((2-(benzylthio)quinolin-3-yl)(phenylamino)methyl)phosphonate (24)

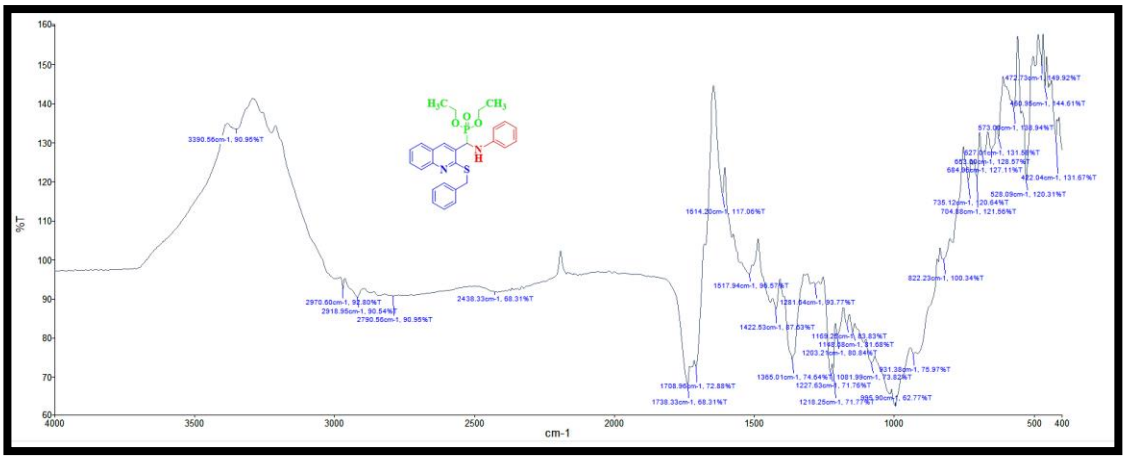

Fig. 5.11. IR spectrum of **24**

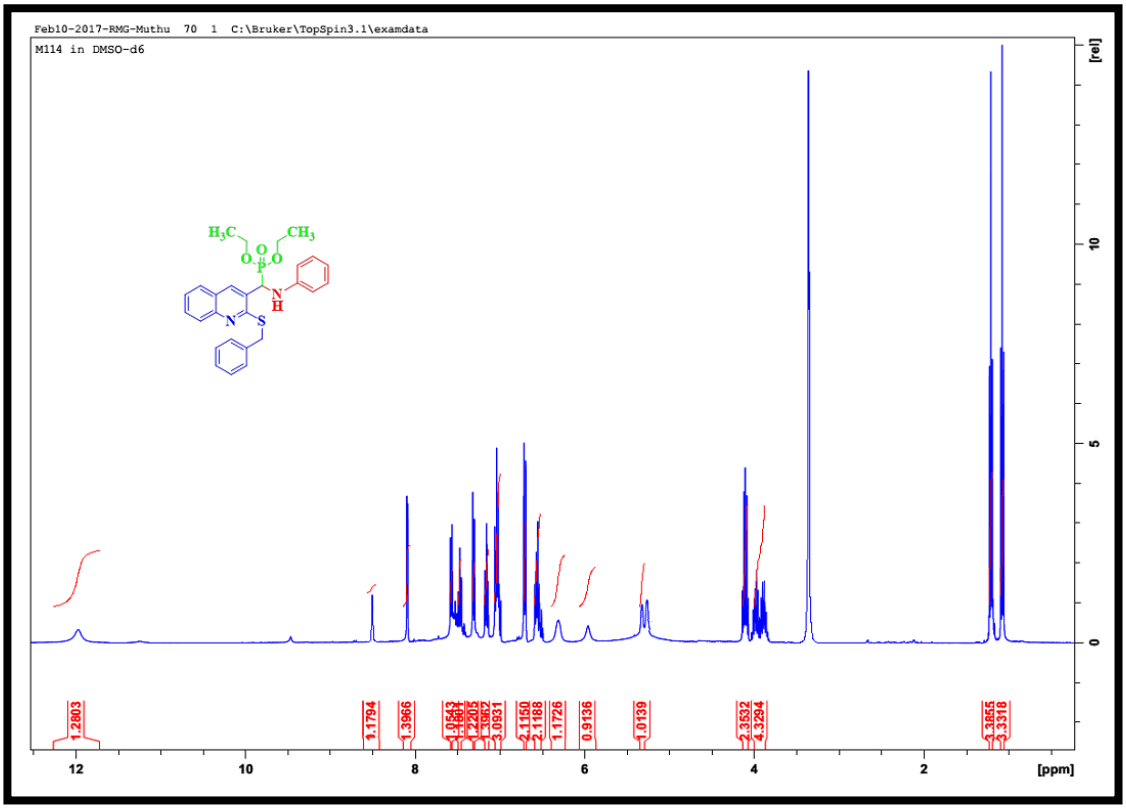

Fig. 5.12. ^{1}H-NMR spectrum of **24**

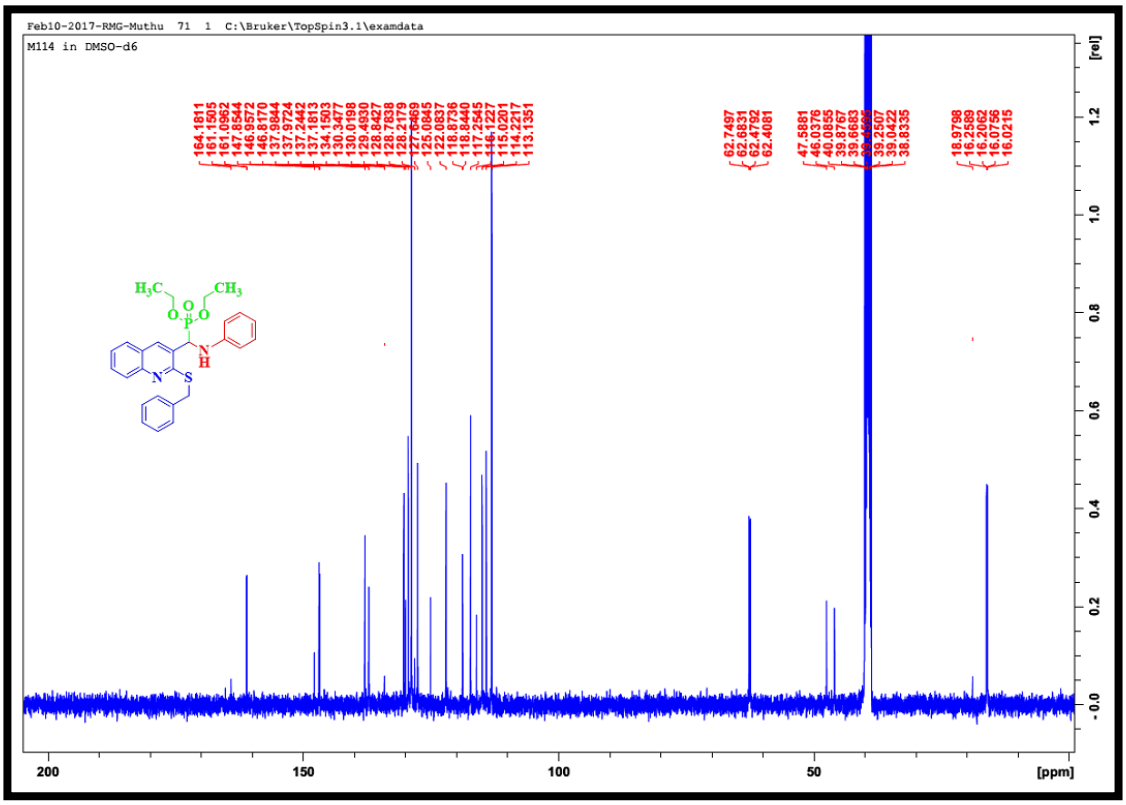

Fig. 5.13. ^{13}C-NMR spectrum of **24**

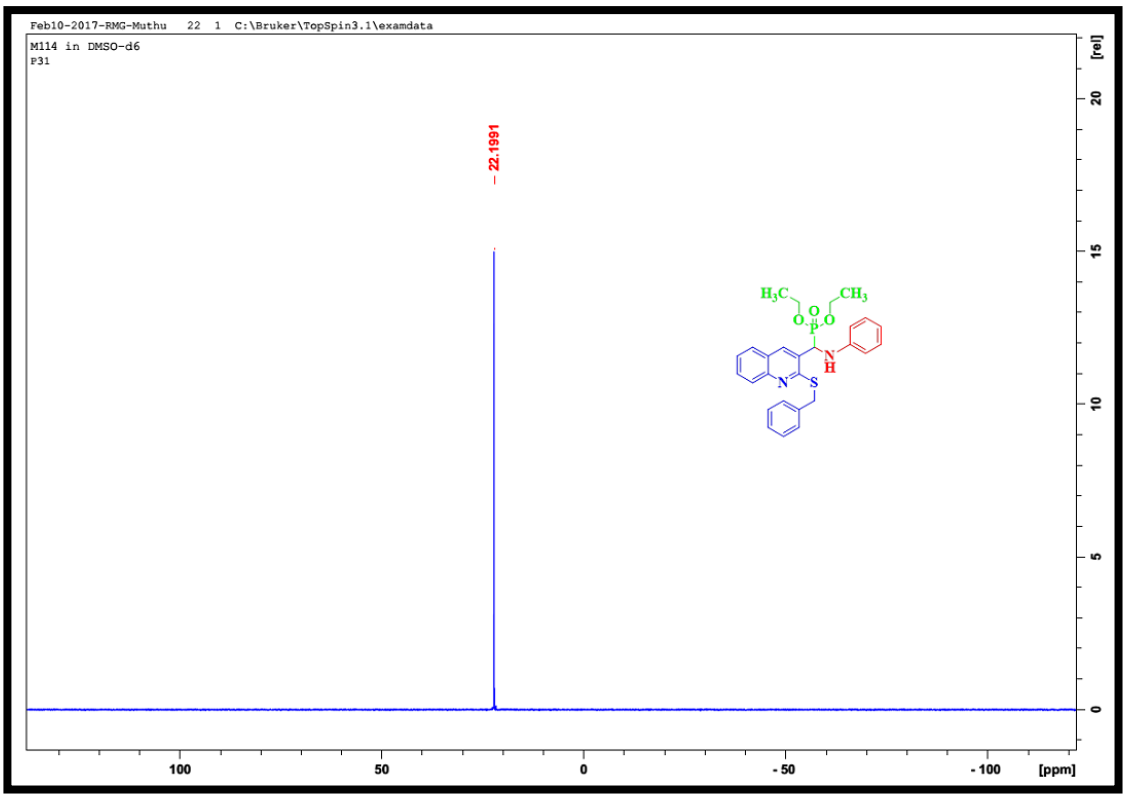

Fig. 5.14. ^{31}P-NMR spectrum of **24**

5.3. Diethyl ((2-(benzylthio)quinolin-3-yl)((2-methoxyphenyl)amino) methyl)phosphonate (25)

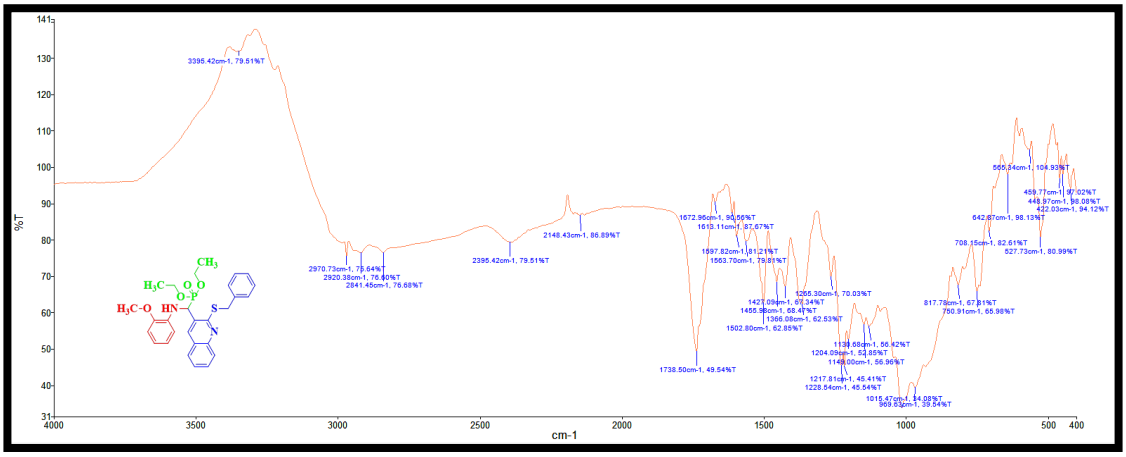

Fig. 5.15. IR spectrum of **25**

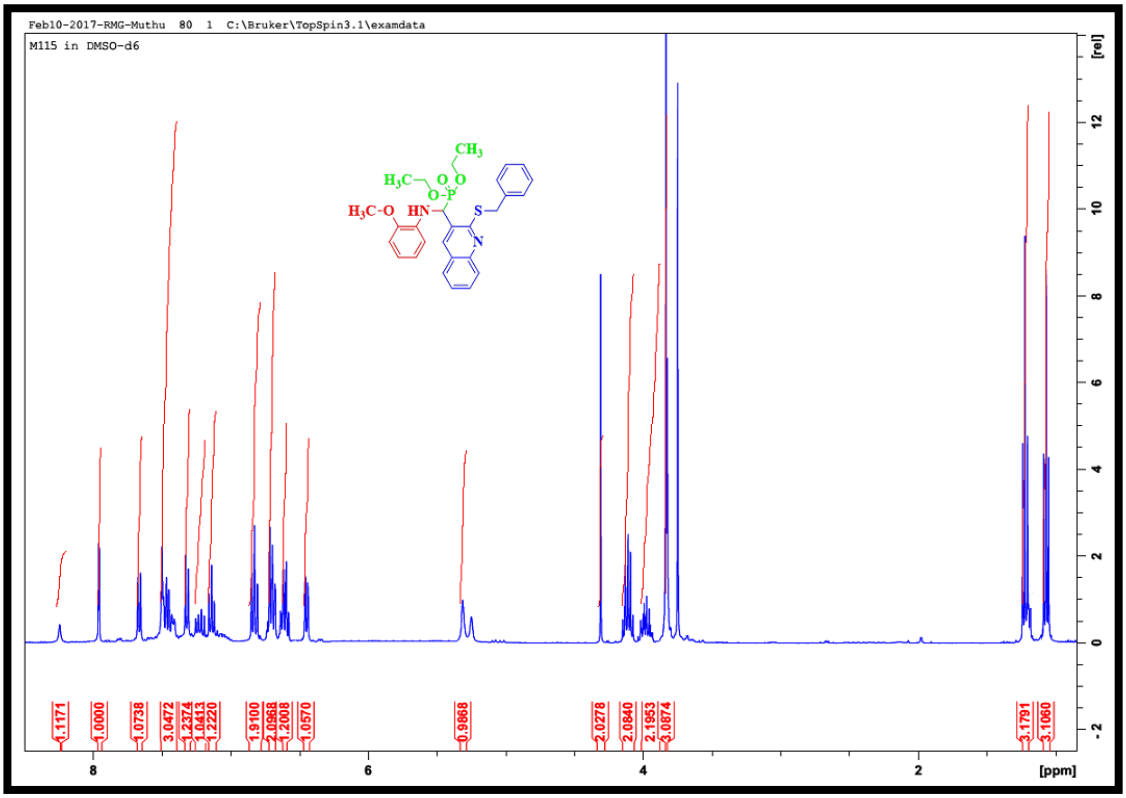

Fig. 5.16. ^{1}H-NMR spectrum of **25**

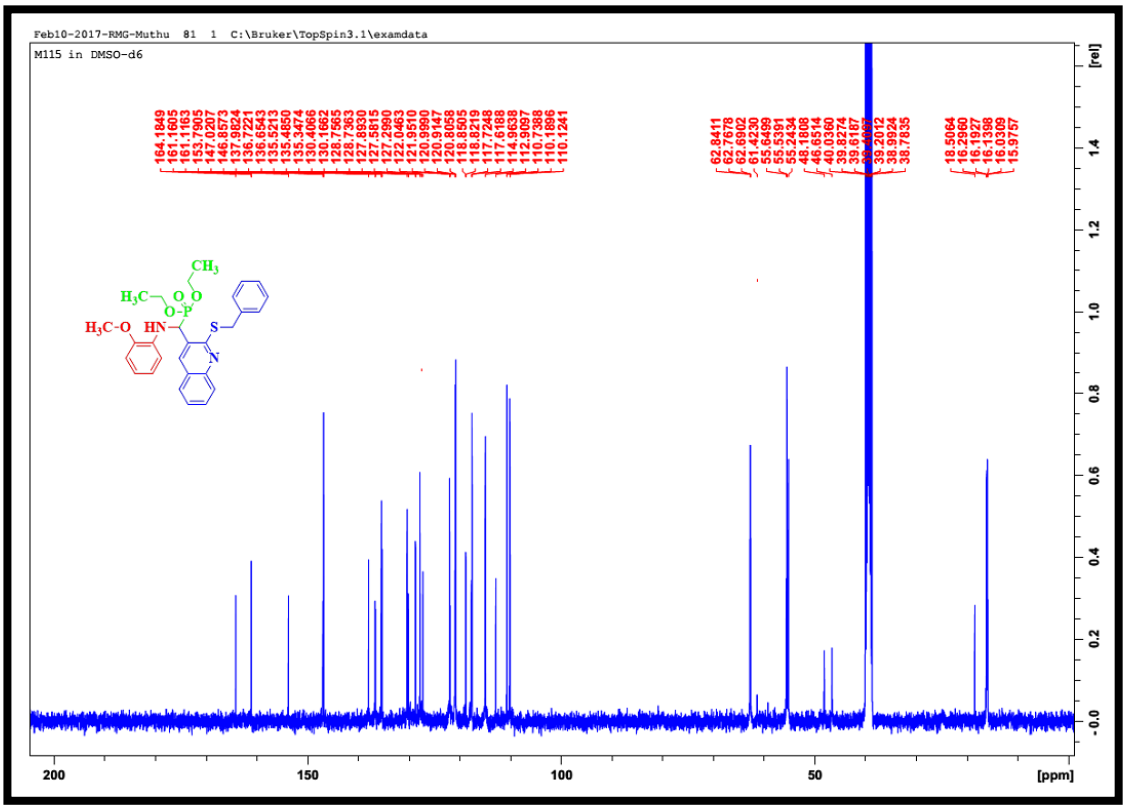

Fig. 5.17. ^{13}C-NMR spectrum of **25**

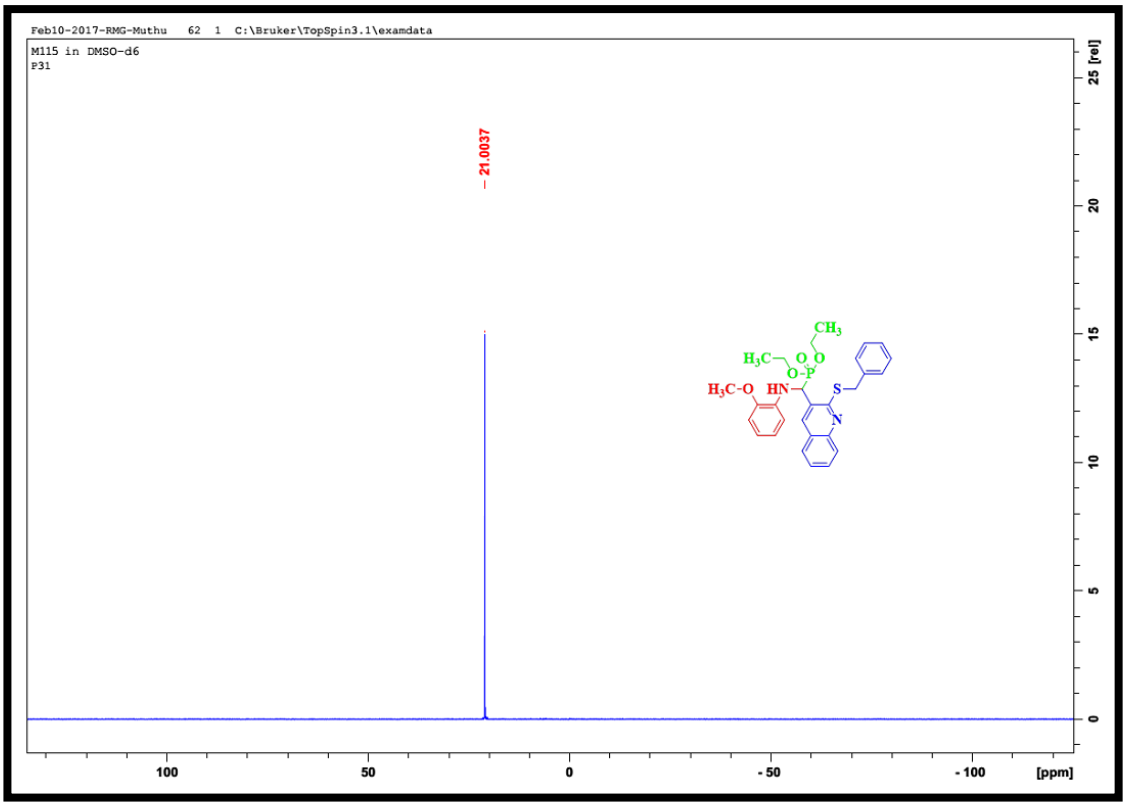

Fig. 5.18. ^{31}P-NMR spectrum of **25**

5.4. Diethyl ((2-(benzylthio)quinolin-3-yl)(o-tolylamino)methyl)phosphonate (26)

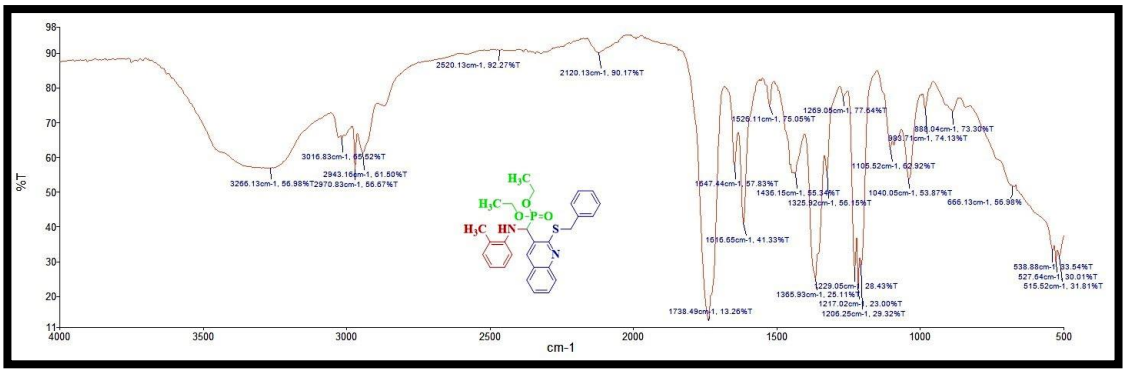

Fig. 5.19. IR spectrum of **26**

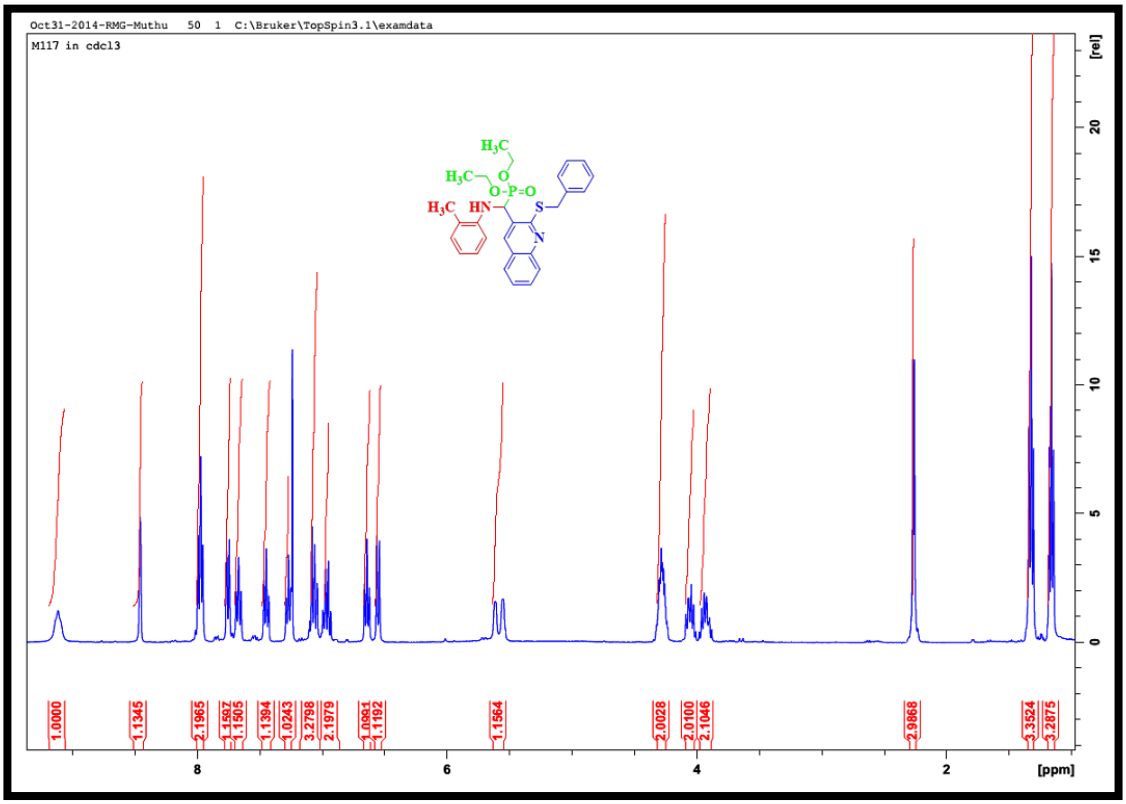

Fig. 5.20. ^{1}H-NMR spectrum of **26**

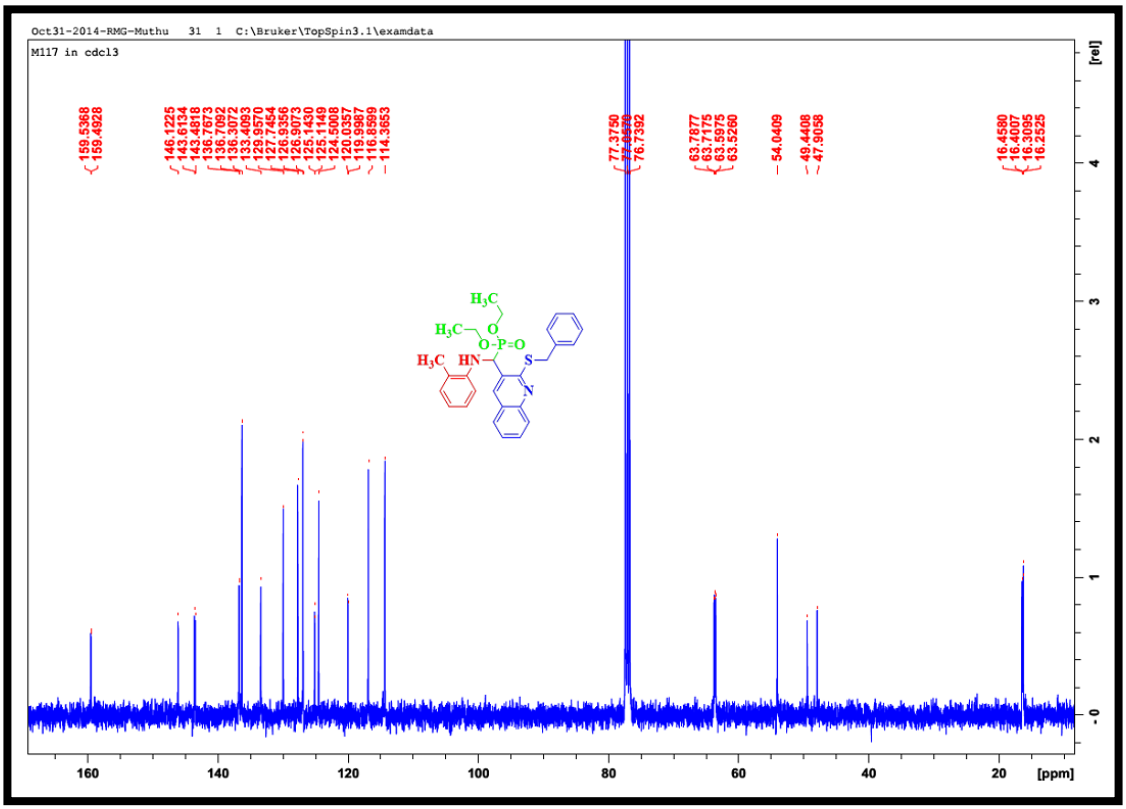

Fig. 5.21. ^{13}C-NMR spectrum of **26**

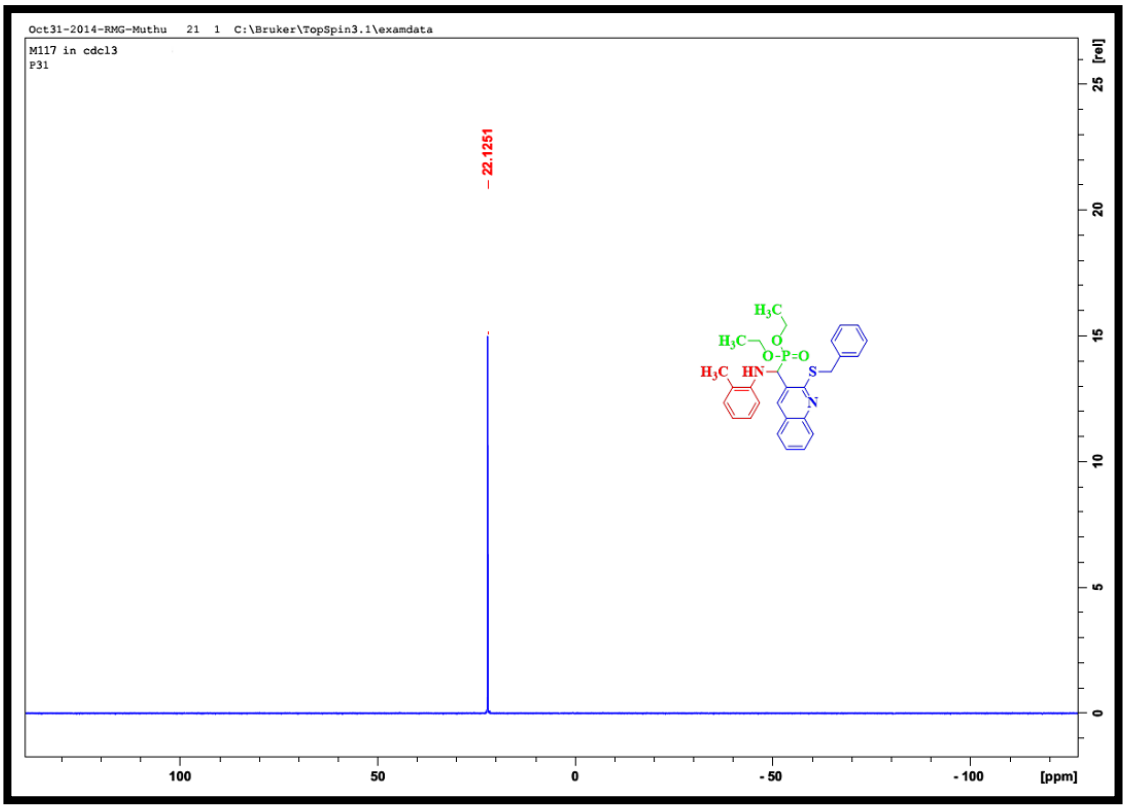

Fig. 5.22. ^{31}P-NMR spectrum of **26**

5.5. Diethyl ((2-(benzylthio)quinolin-3-yl)((3-fluorophenyl)amino)methyl) phosphonate (27)

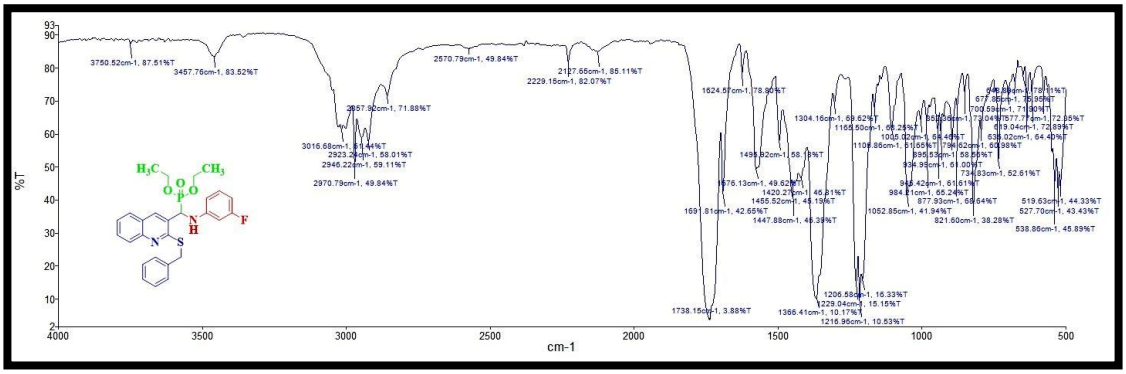

Fig. 5.23. IR spectrum of **27**

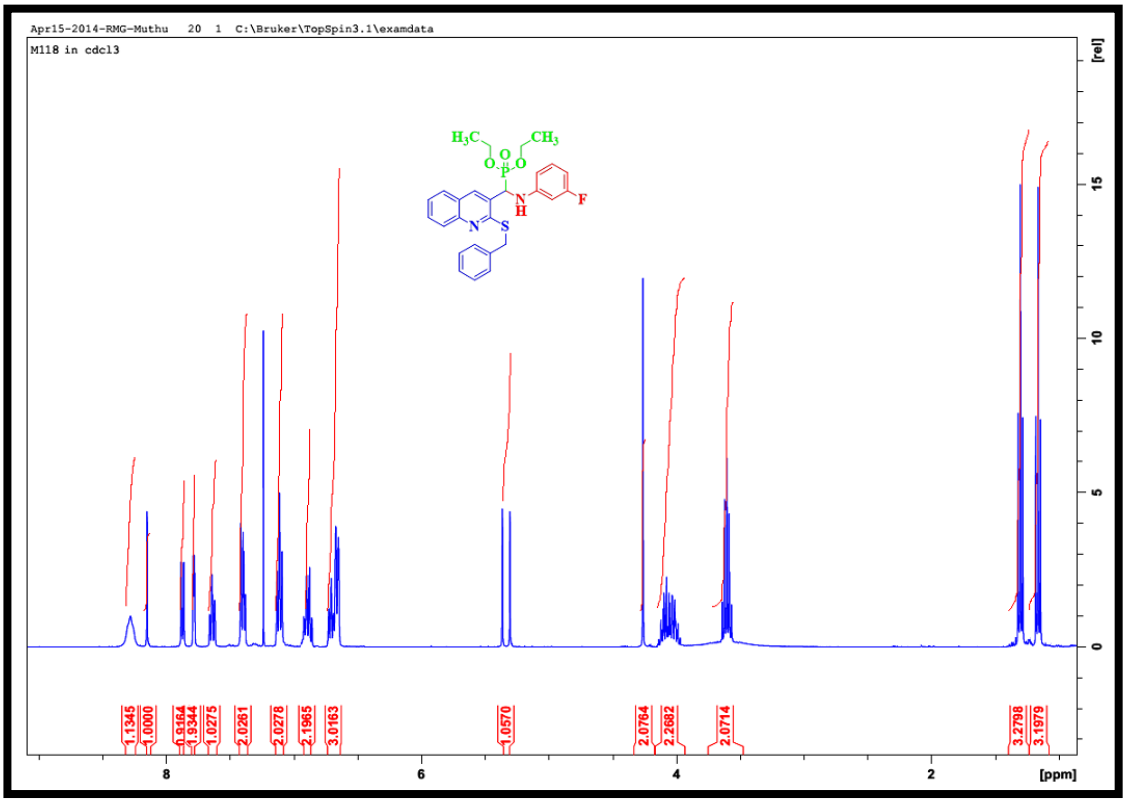

Fig. 5.24. ^{1}H-NMR spectrum of **27**

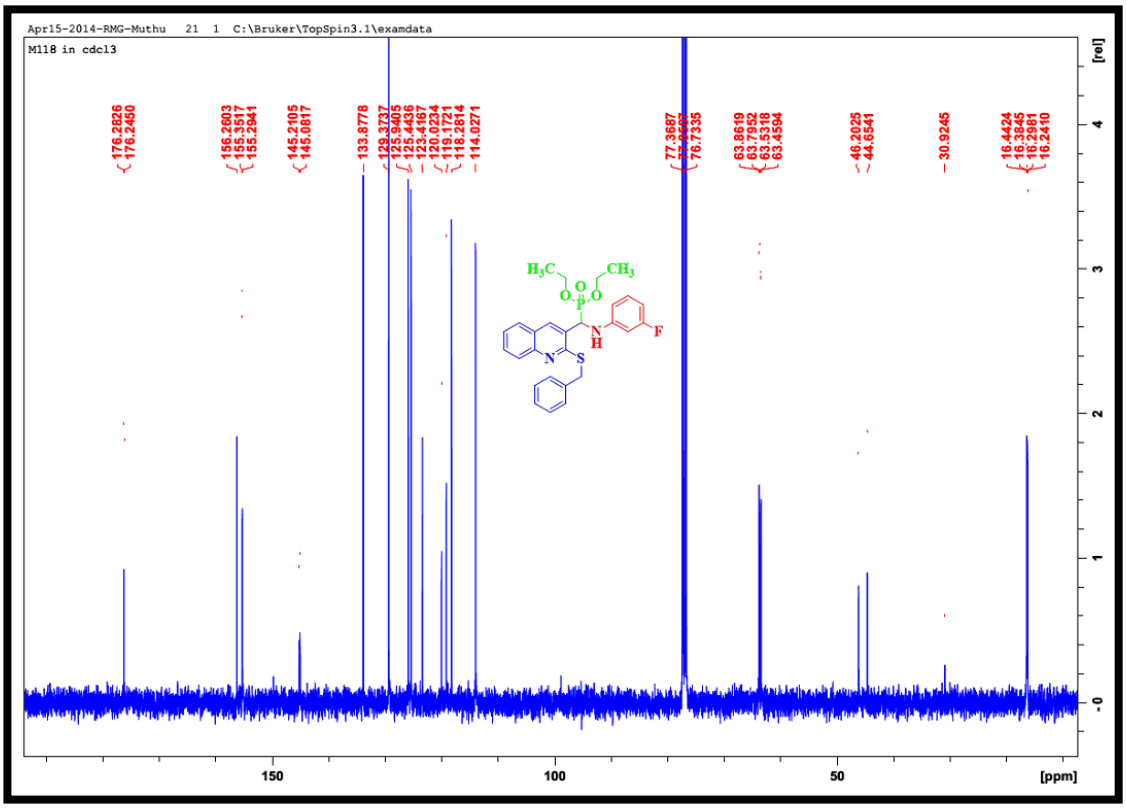

Fig. 5.25. ^{13}C-NMR spectrum of **27**

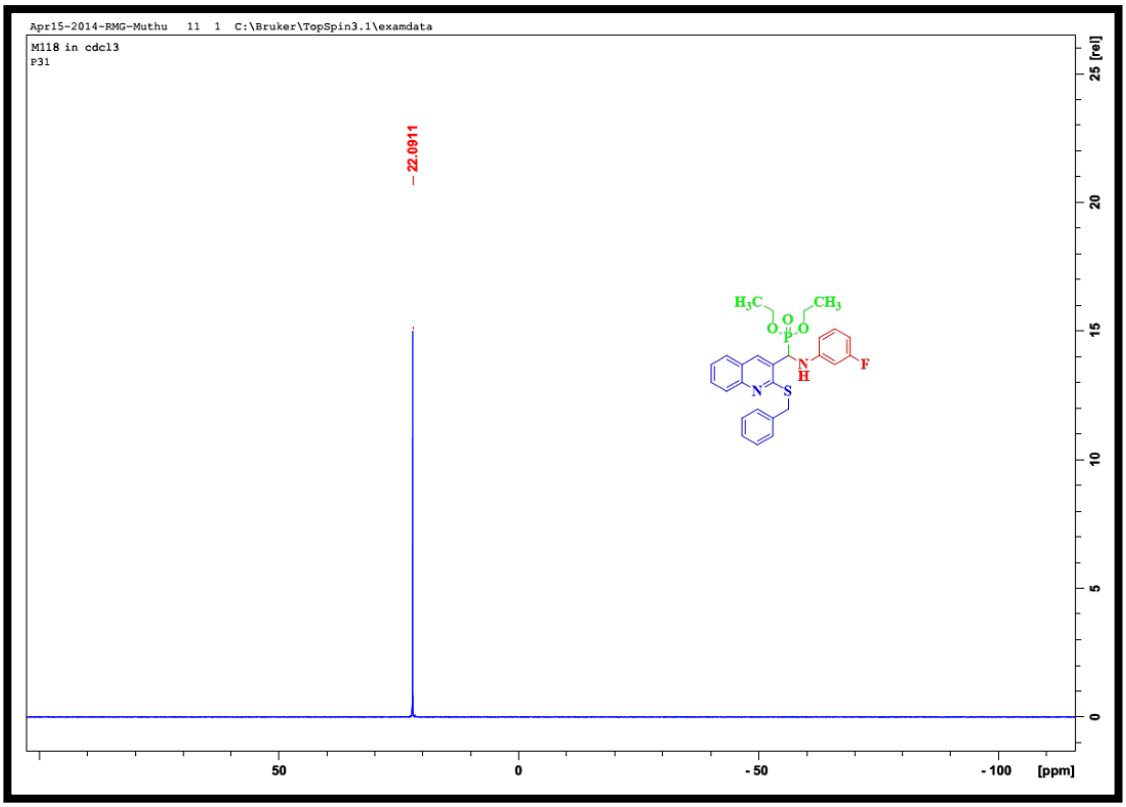

Fig. 5.26. ^{31}P-NMR spectrum of **27**

5.6. Diethyl ((2-(benzylthio)quinolin-3-yl)((3-chloro-4-fluorophenyl)amino) methyl)phosphonate (28)

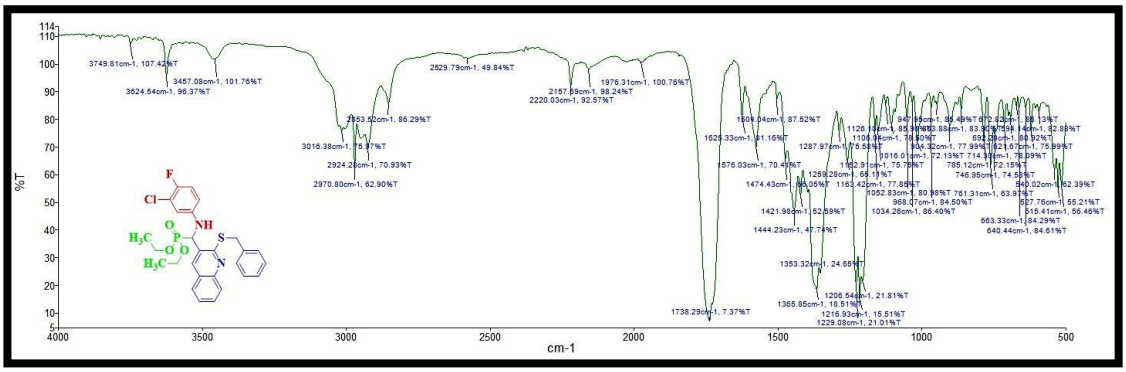

Fig. 5.27. IR spectrum of **28**

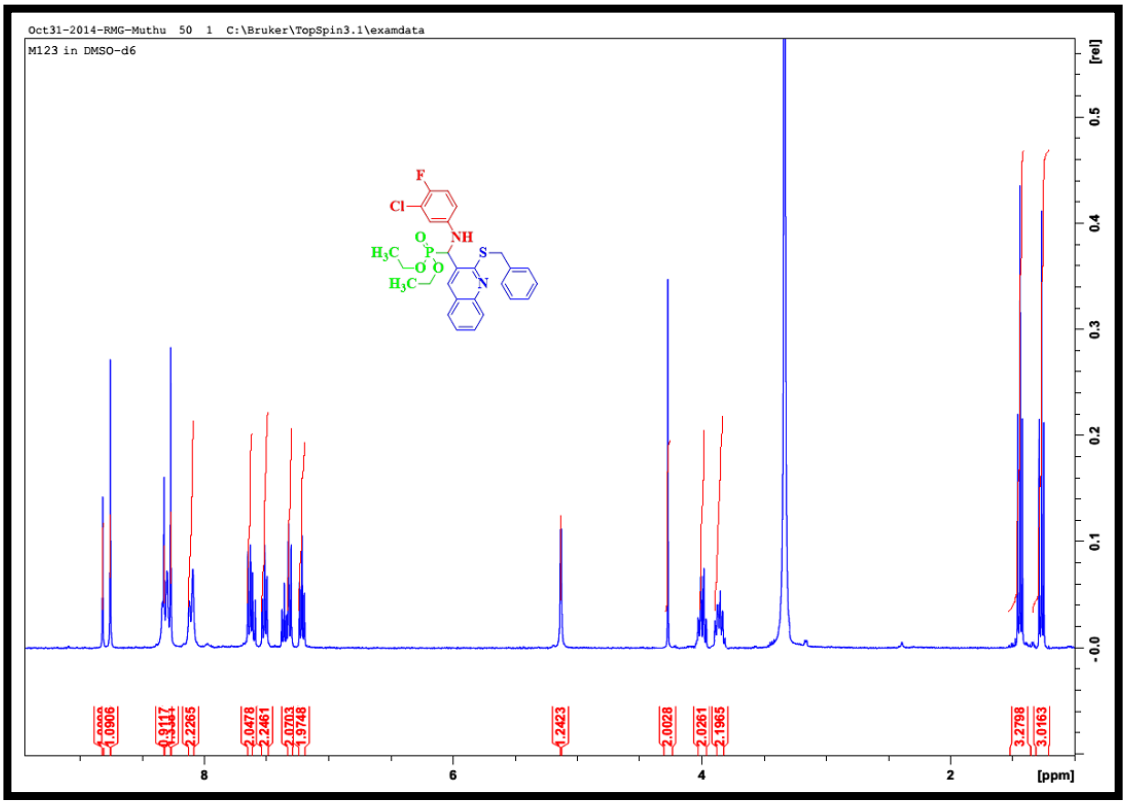

Fig. 5.28. ^{1}H-NMR spectrum of **28**

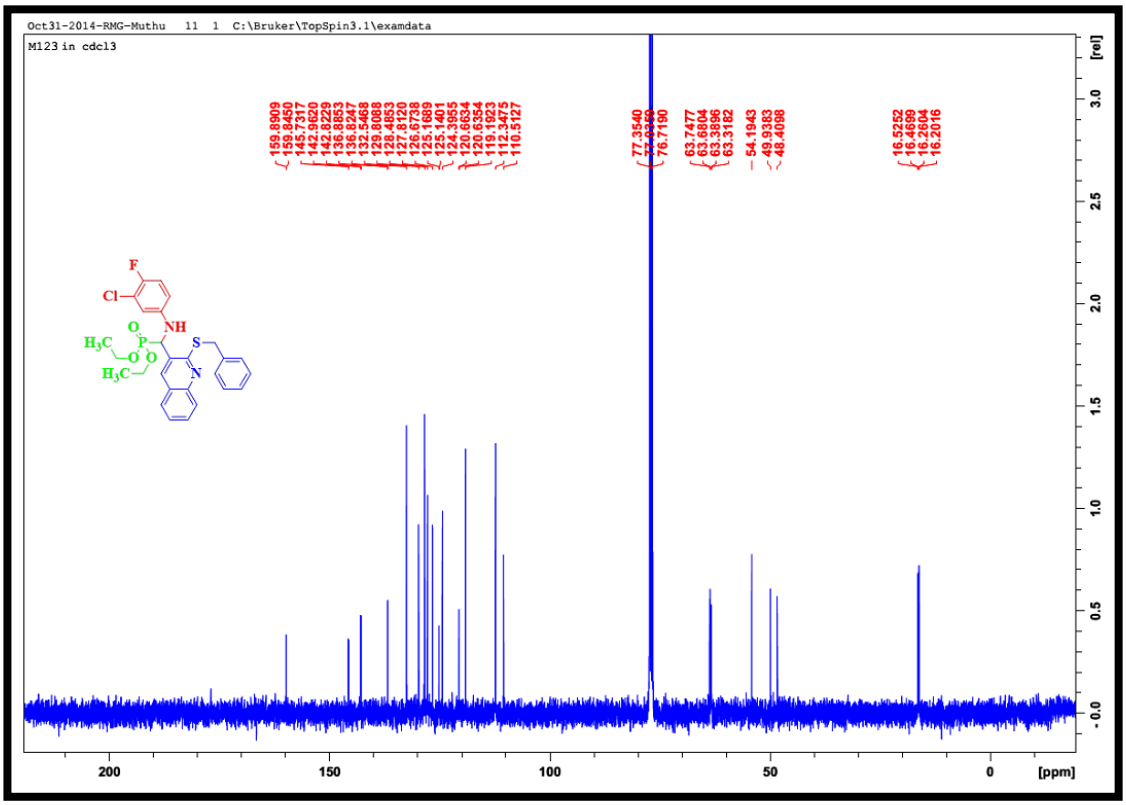

Fig. 5.29. ^{13}C-NMR spectrum of **28**

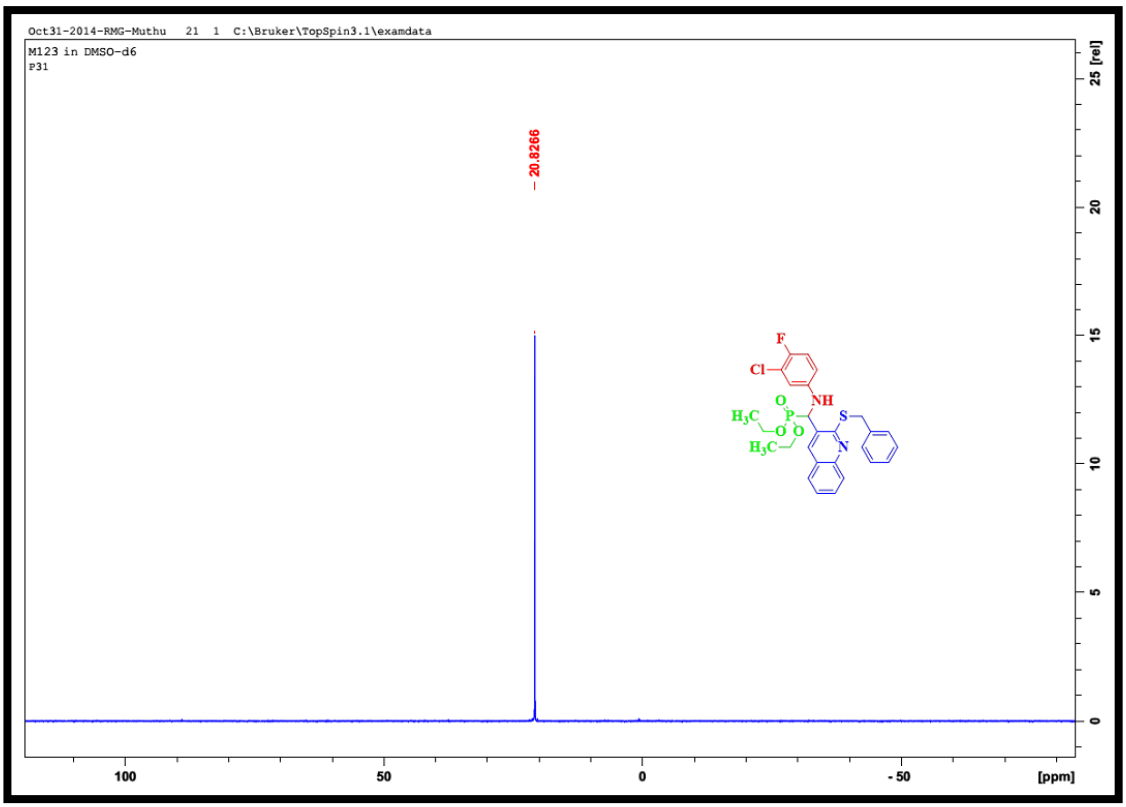

Fig. 5.30. ^{31}P-NMR spectrum of **28**

5.7. Diethyl ((2-(benzylthio)quinolin-3-yl)((2-nitrophenyl)amino)methyl) phosphonate (29)

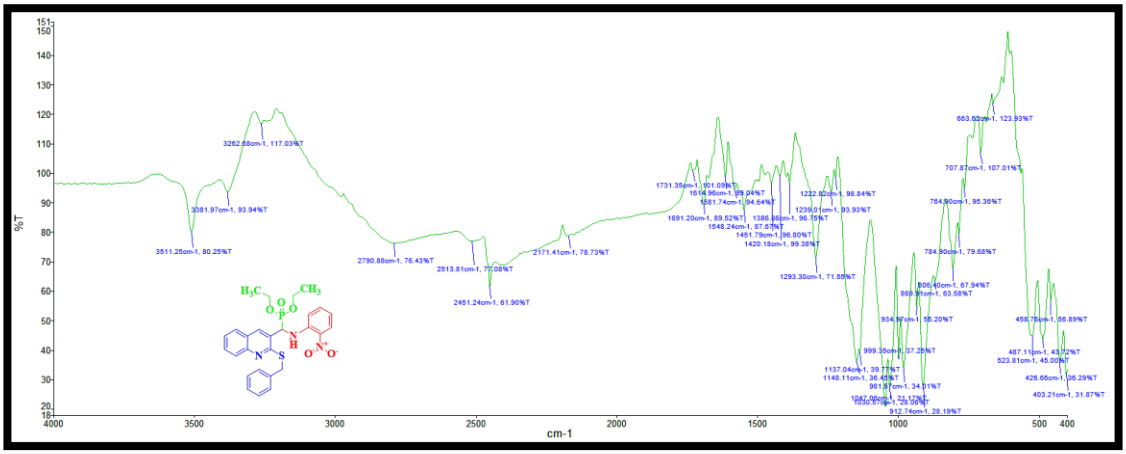

Fig. 5.31. IR spectrum of **29**

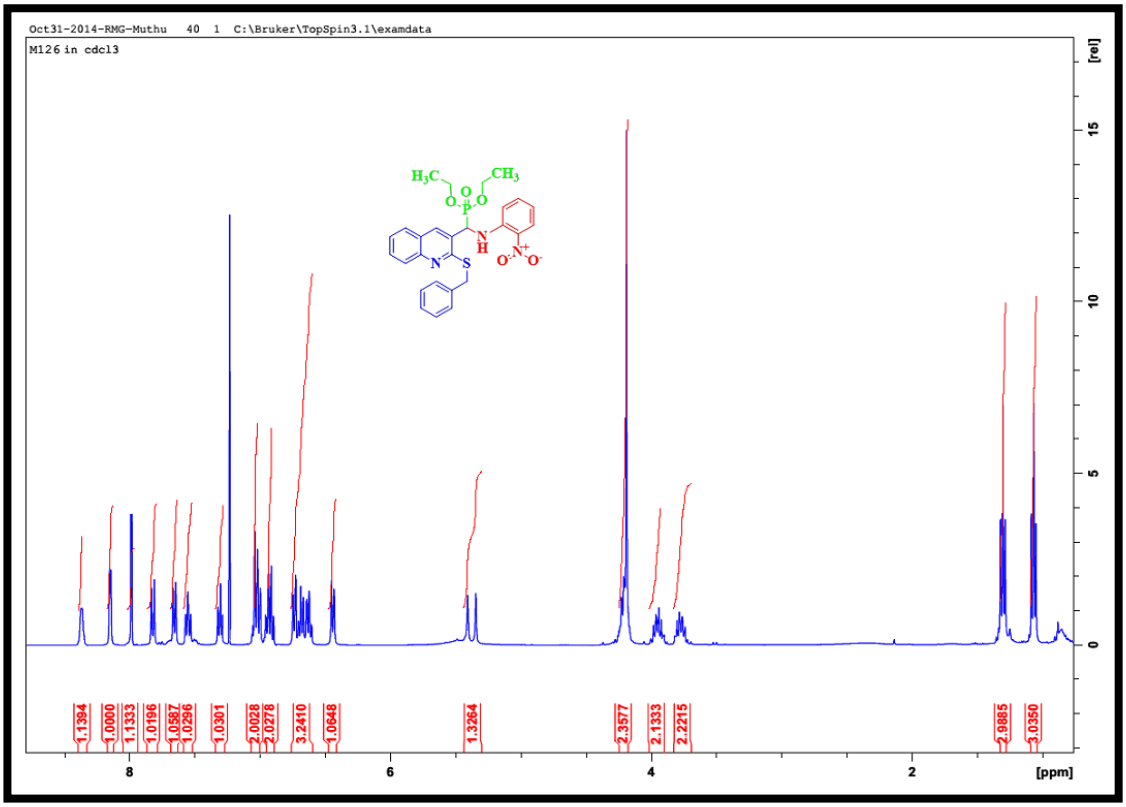

Fig. 5.32. ^{1}H-NMR spectrum of **29**

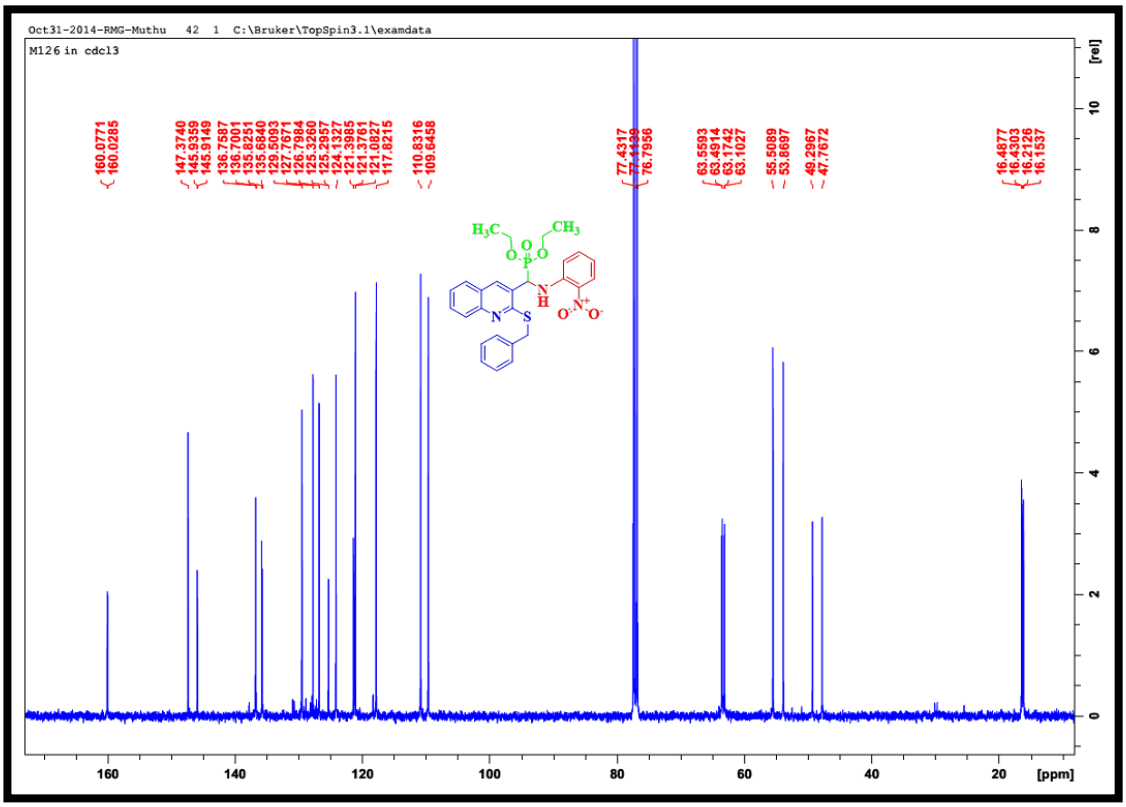

Fig. 5.33. ^{13}C-NMR spectrum of **29**

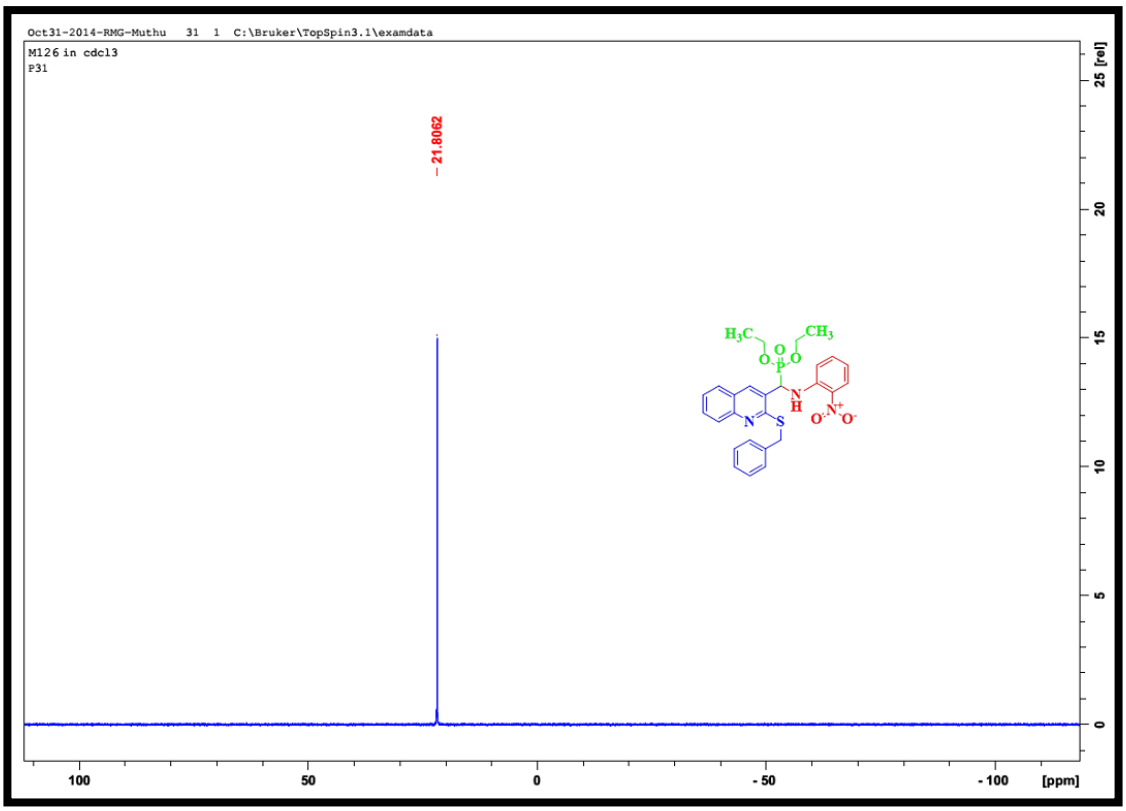

Fig. 5.34. ^{31}P-NMR spectrum of **29**

5.8. Diethyl ((2-(benzylthio)quinolin-3-yl)((2,4-dimethylphenyl)amino)methyl) phosphonate (30)

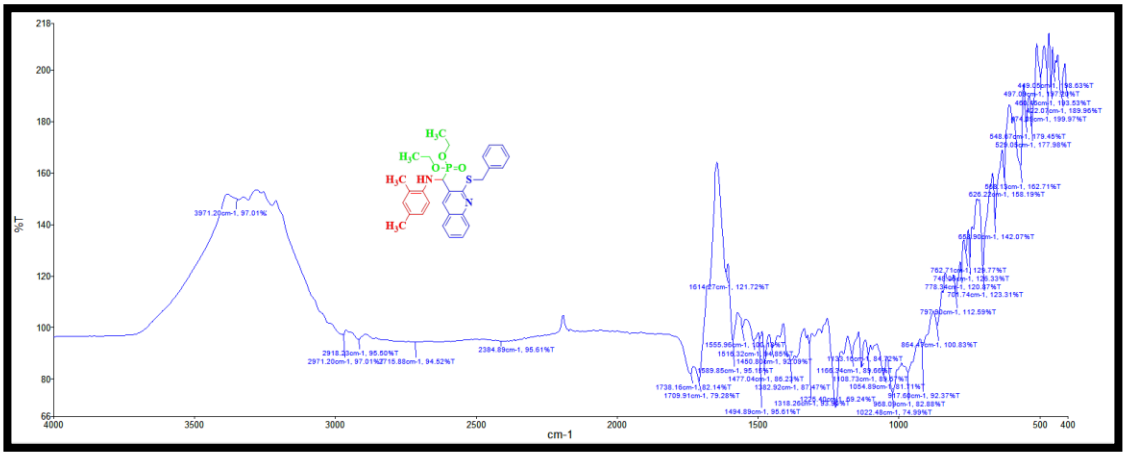

Fig. 5.35. IR spectrum of **30**

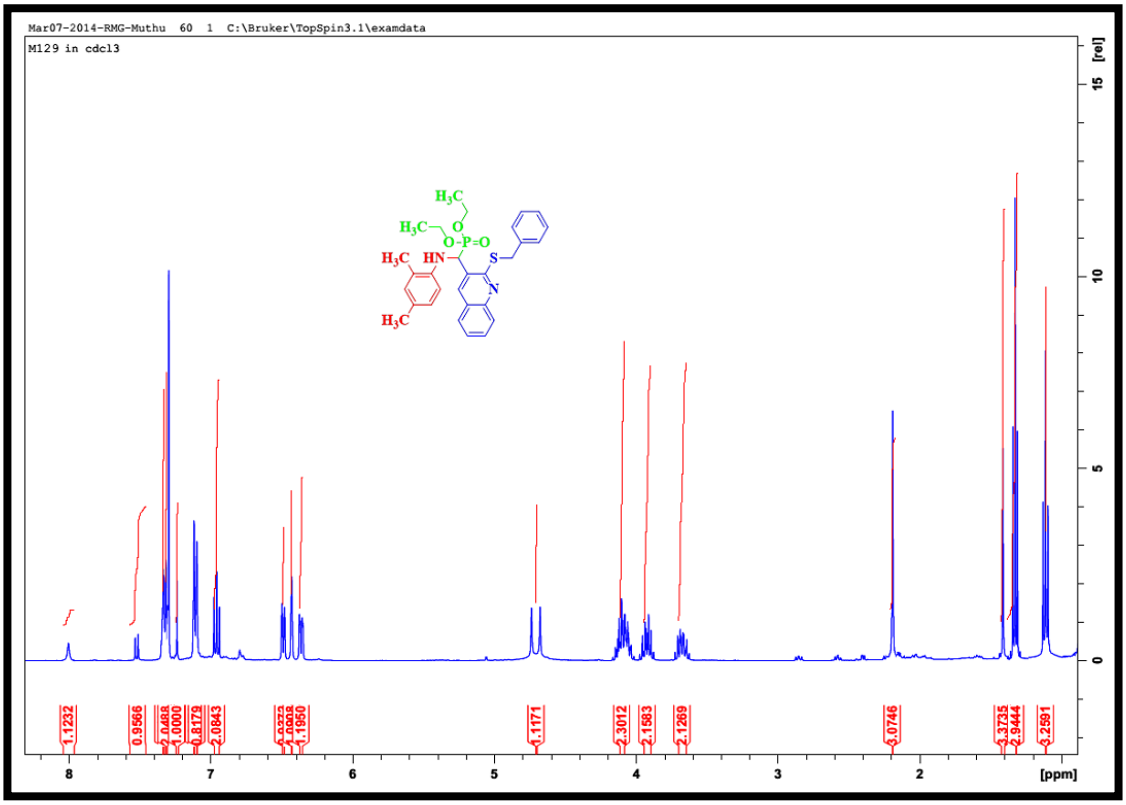

Fig. 5.36. ^{1}H-NMR spectrum of **30**

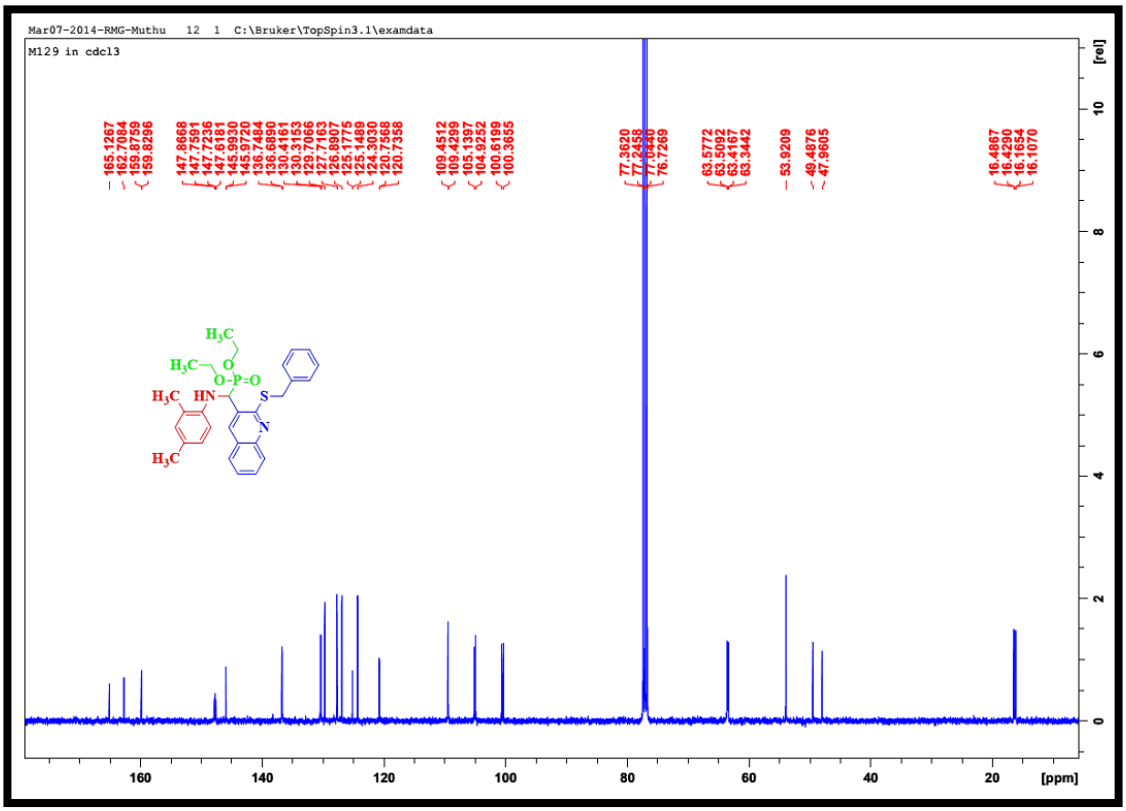

Fig. 5.37. ^{13}C-NMR spectrum of **30**

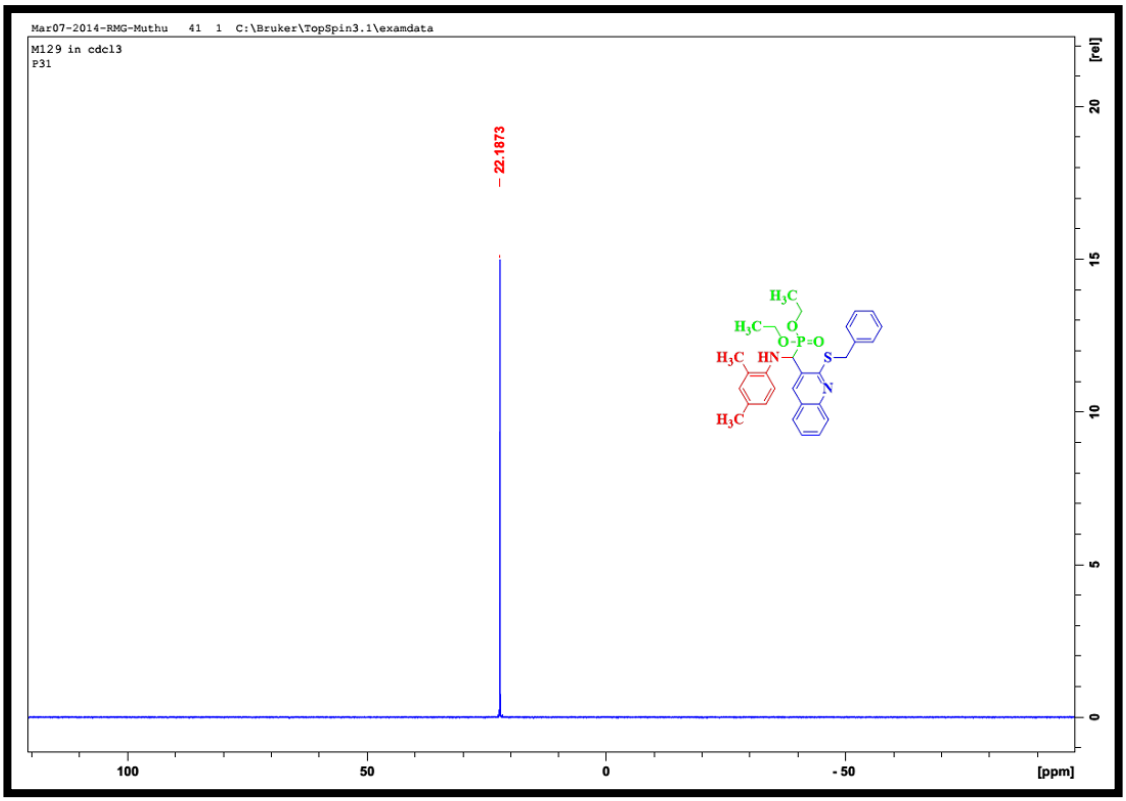

Fig. 5.38. ^{31}P-NMR spectrum of **30**

5.9. Diethyl ((2-(benzylthio)quinolin-3-yl)((4-methoxyphenyl)amino)methyl) phosphonate (31)

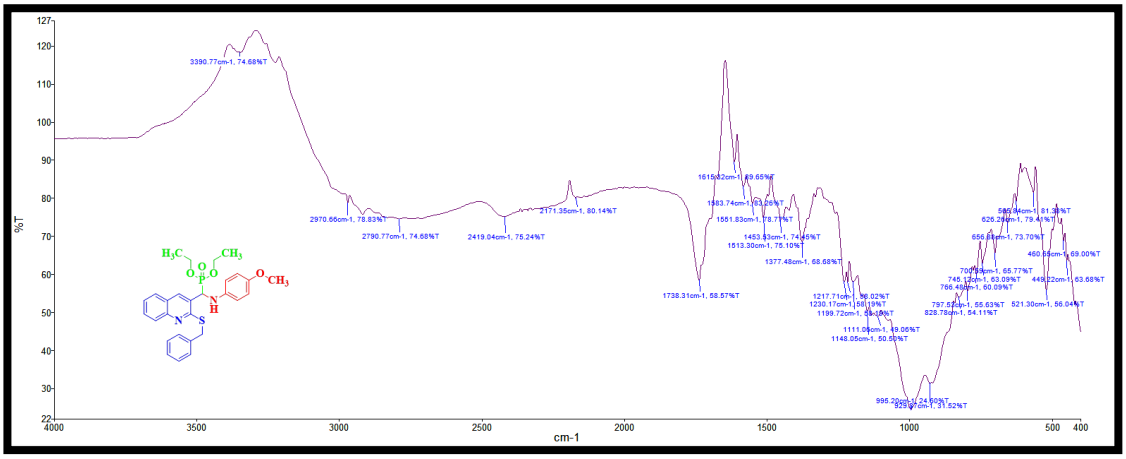

Fig. 5.39. IR spectrum of **31**

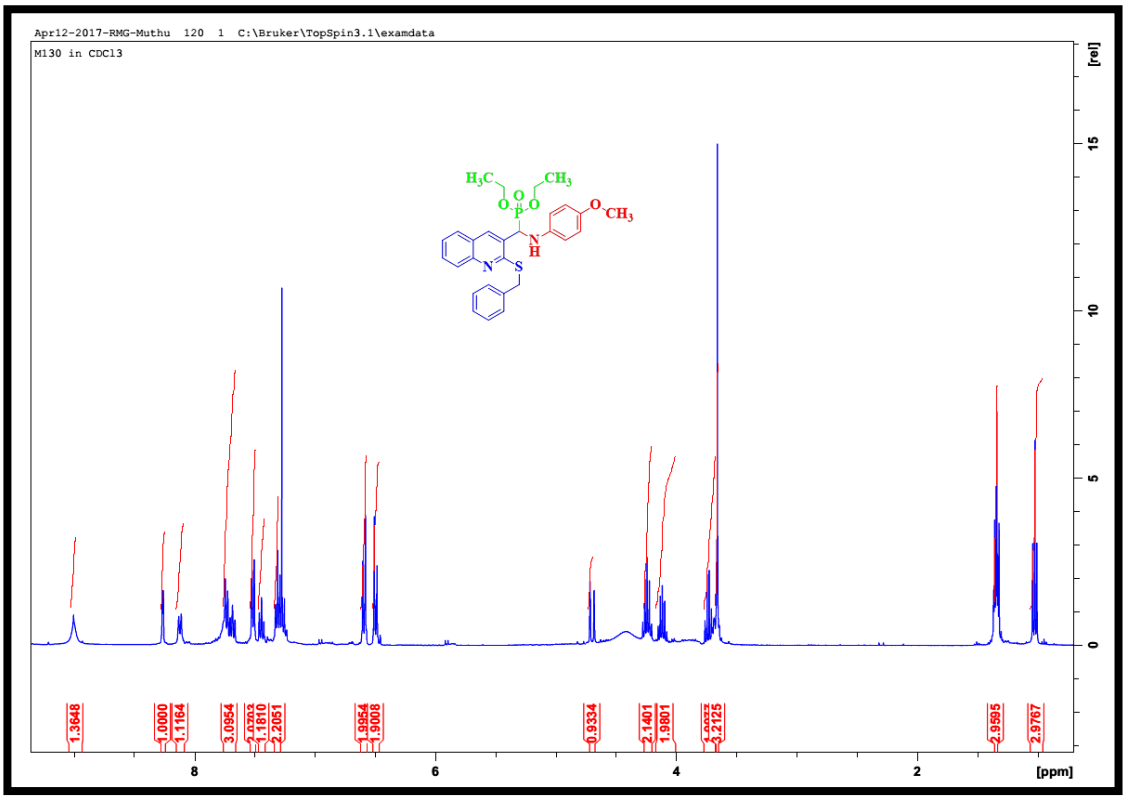

Fig. 5.40. ^{1}H-NMR spectrum of **31**

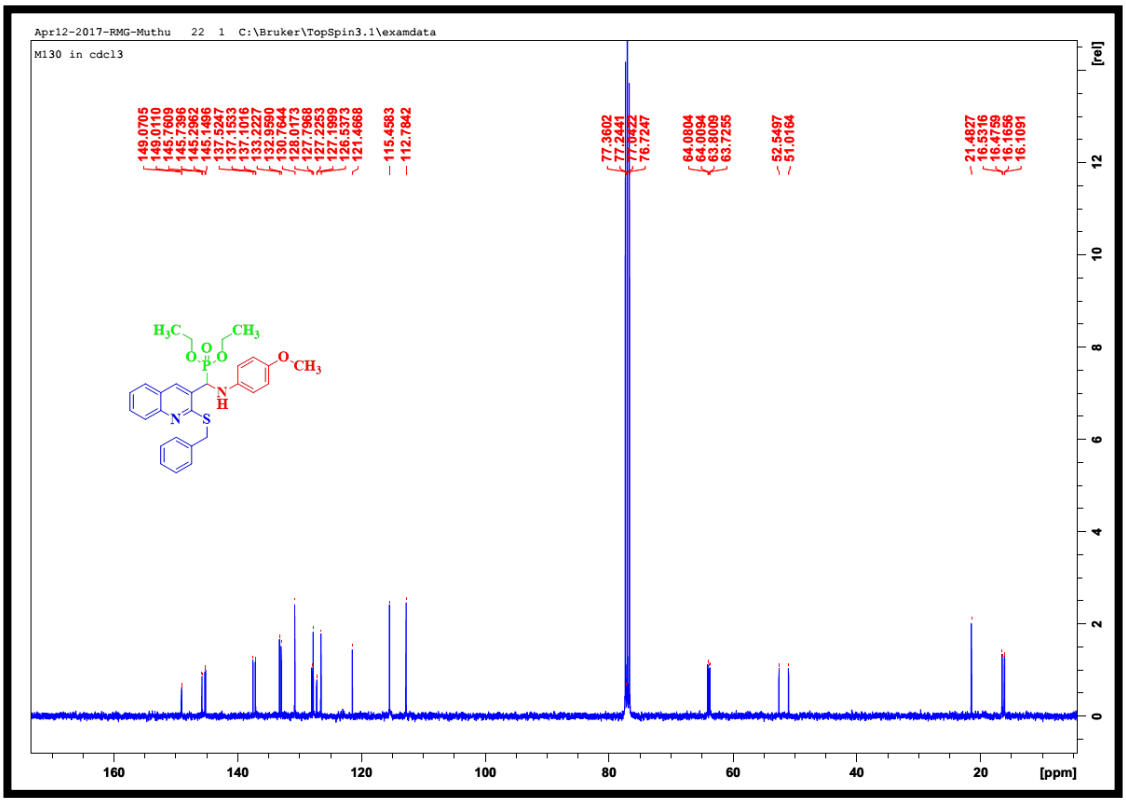

Fig. 5.41. ^{13}C-NMR spectrum of **31**

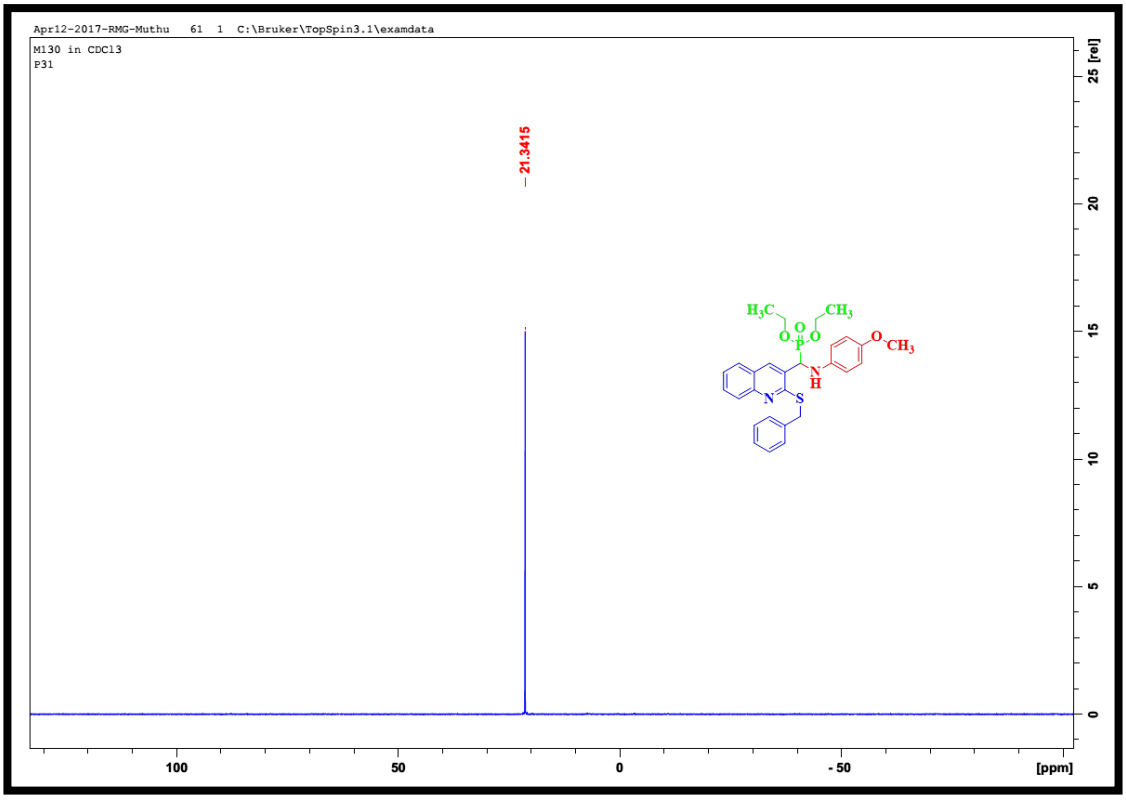

Fig. 5.42. ^{31}P-NMR spectrum of **31**

5.10. Diethyl ((2-(benzylthio)quinolin-3-yl)((pyridin-2-ylmethyl)amino)methyl) phosphonate (32)

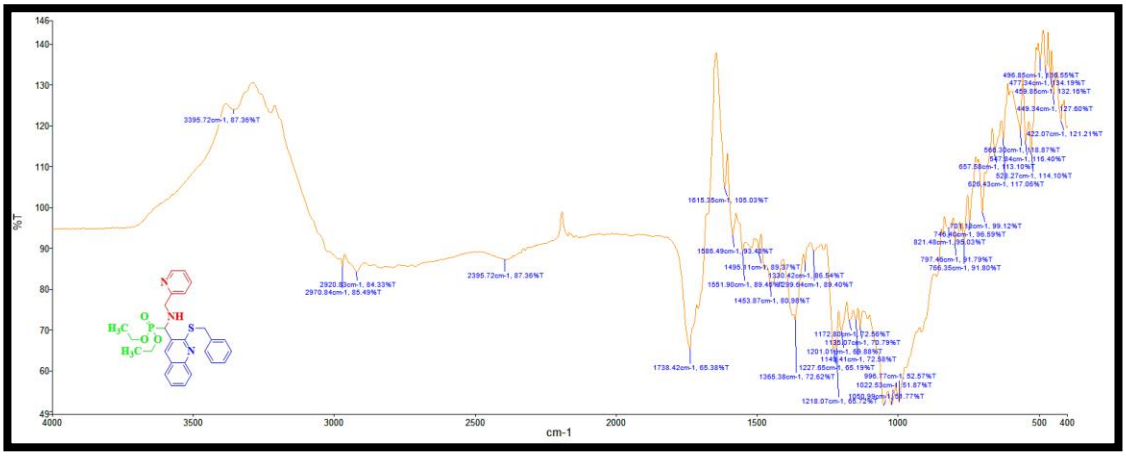

Fig. 5.43. IR spectrum of **32**

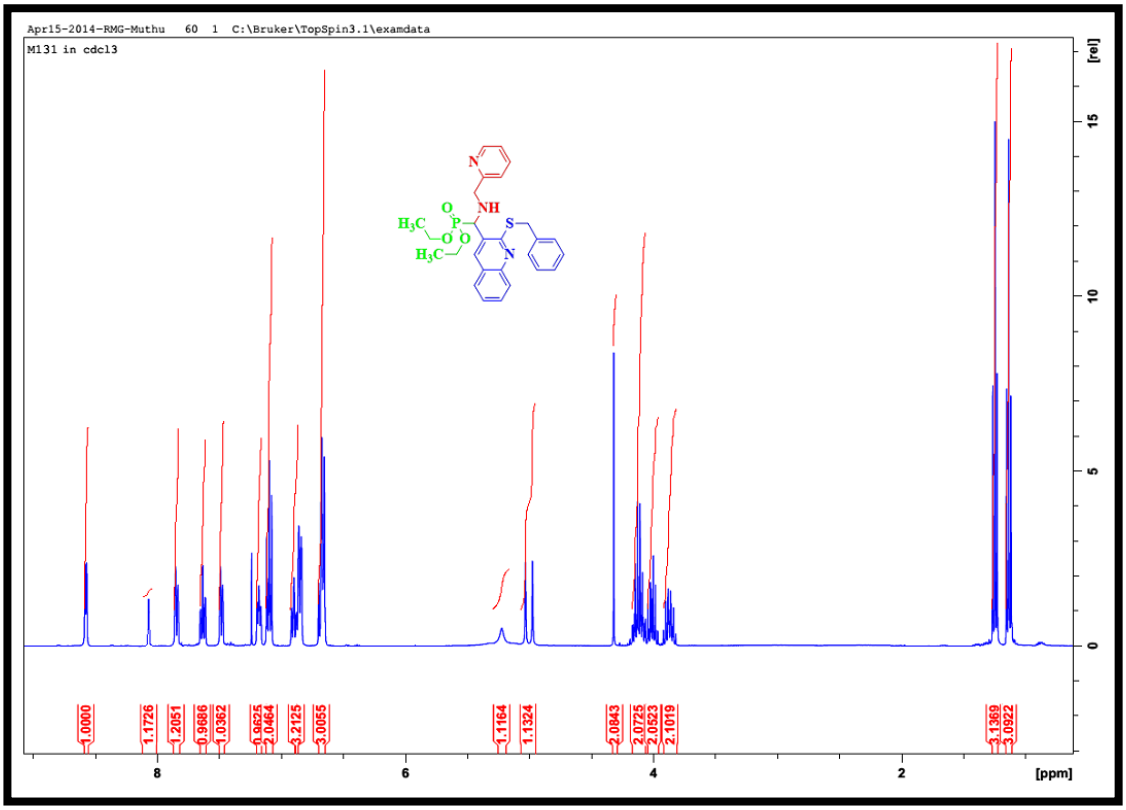

Fig. 5.44. ^{1}H-NMR spectrum of **32**

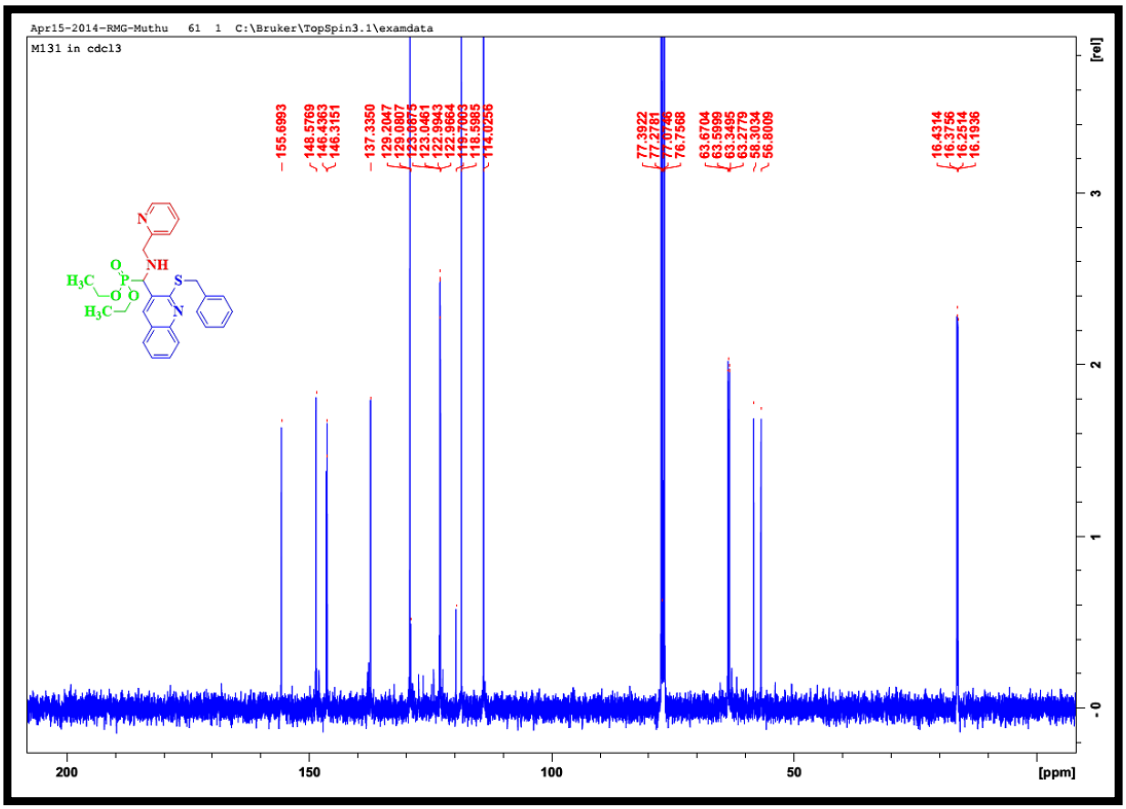

Fig. 5.45. ^{13}C-NMR spectrum of **32**

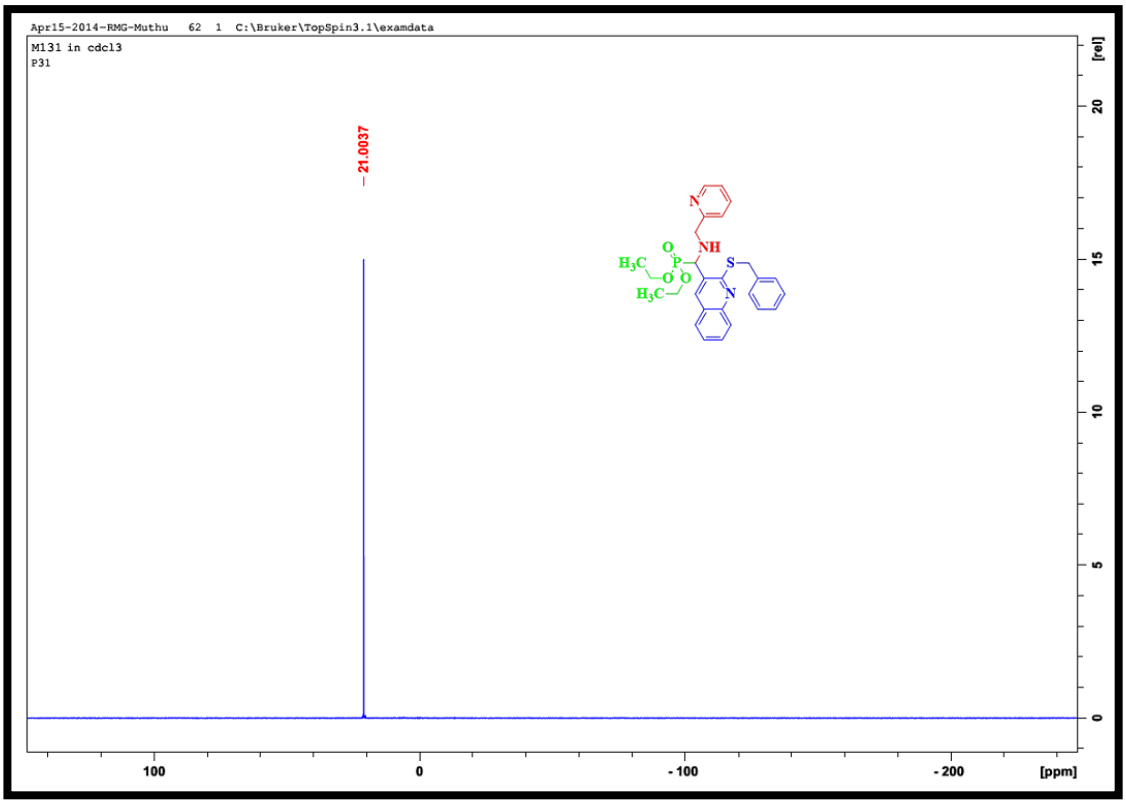

Fig. 5.46. ^{31}P-NMR spectrum of **32**

5.11. Diethyl ((2-(benzylthio)quinolin-3-yl)((4-bromophenyl)amino) methyl)phosphonate (33)

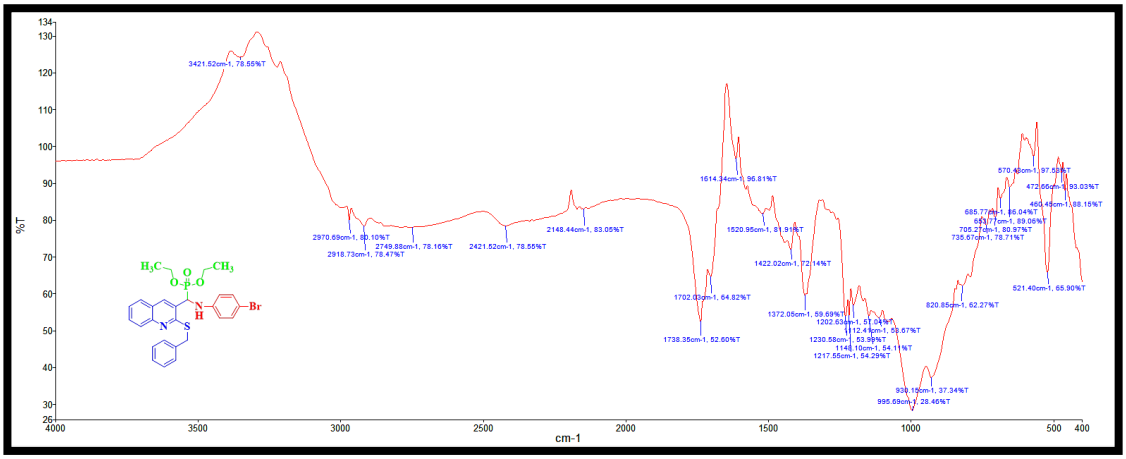

Fig. 5.47. IR spectrum of **33**

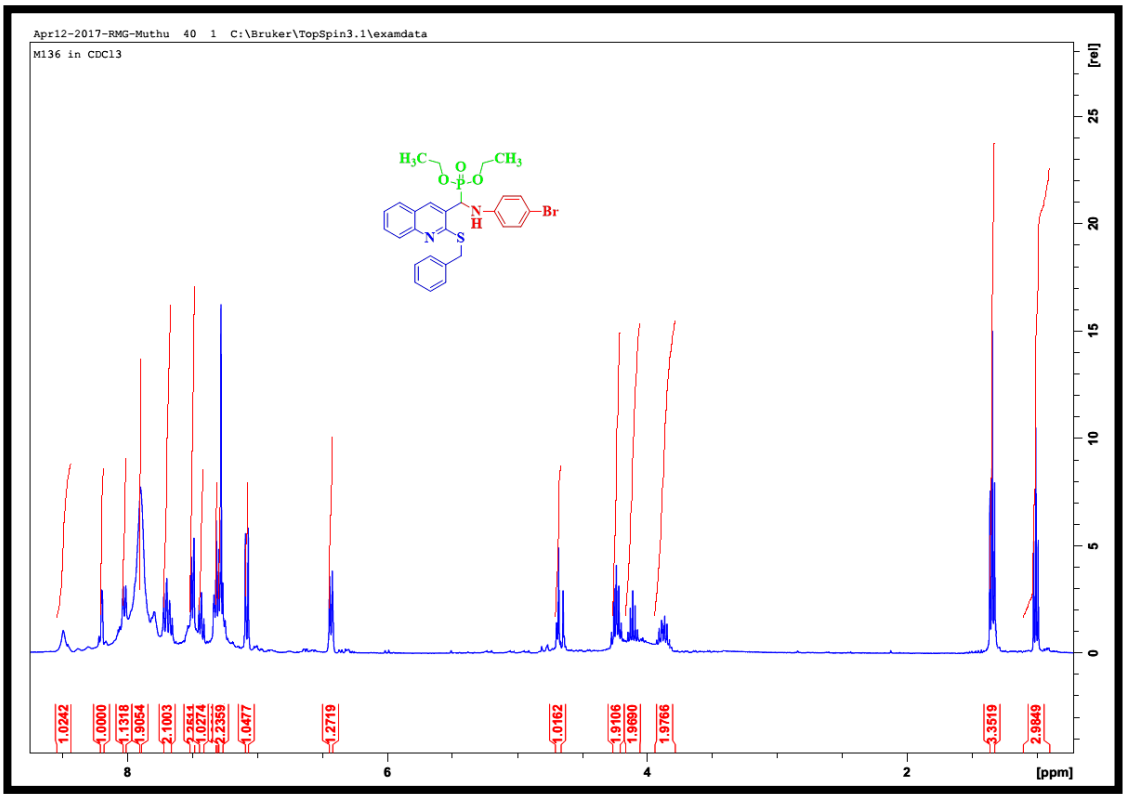

Fig. 5.48. ^{1}H-NMR spectrum of **33**

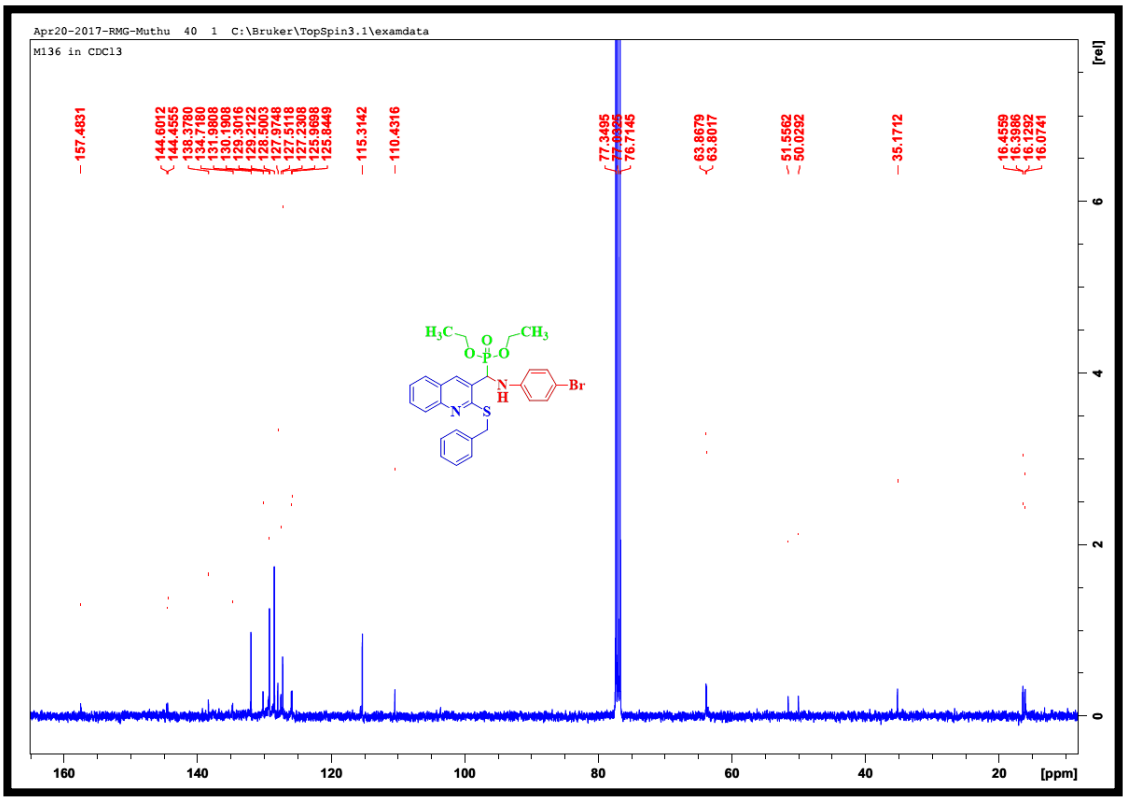

Fig. 5.49. ^{13}C-NMR spectrum of **33**

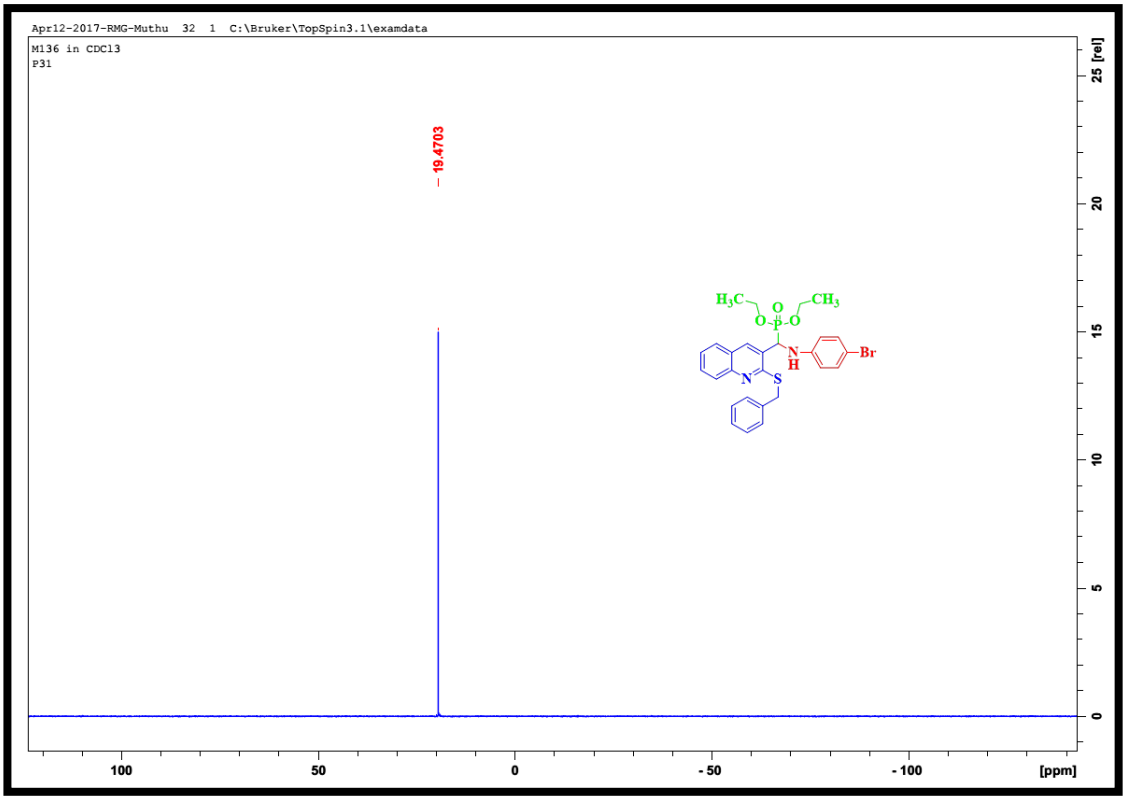

Fig. 5.50. ^{31}P-NMR spectrum of **33**

5.12. Diethyl ((2-(benzylthio)quinolin-3-yl)((4-chlorophenyl)amino)methyl) phosphonate (34)

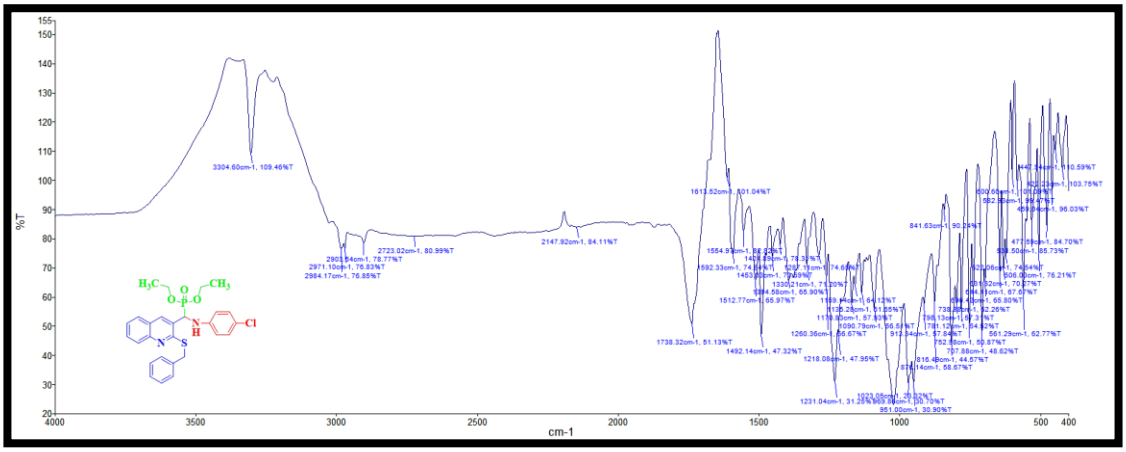

Fig. 5.51. IR spectrum of **34**

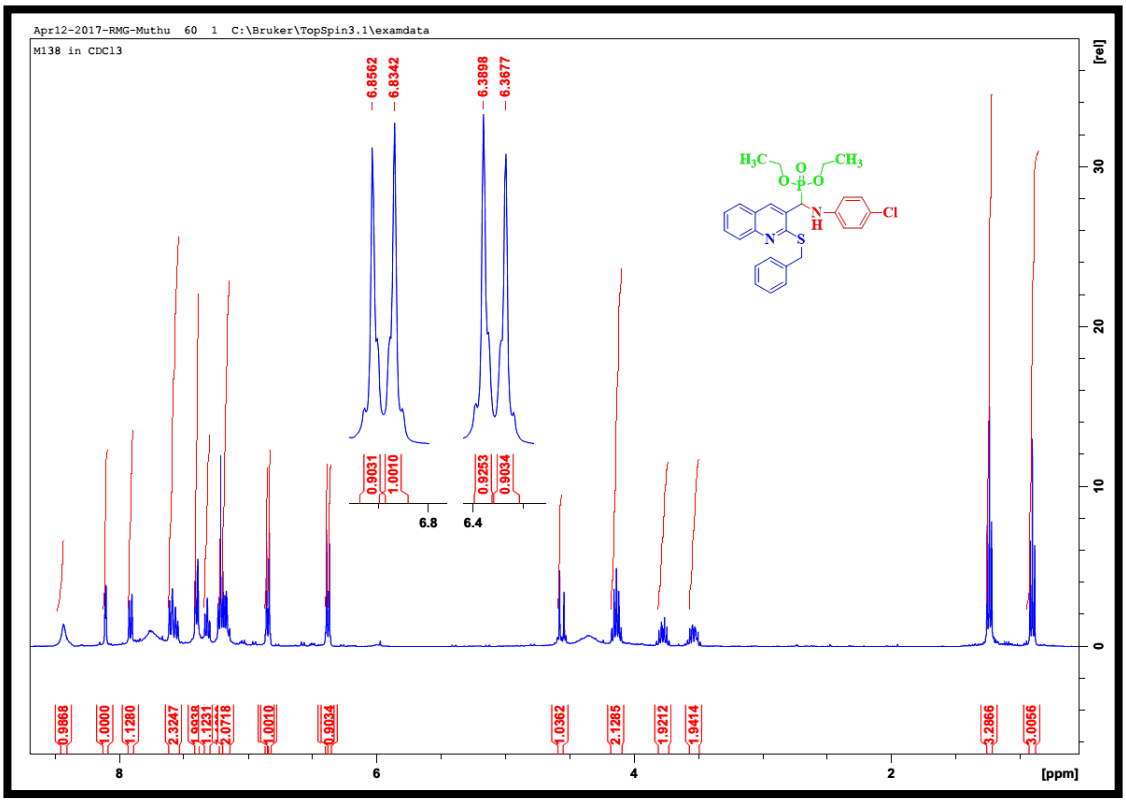

Fig. 5.52. ^{1}H-NMR spectrum of **34**

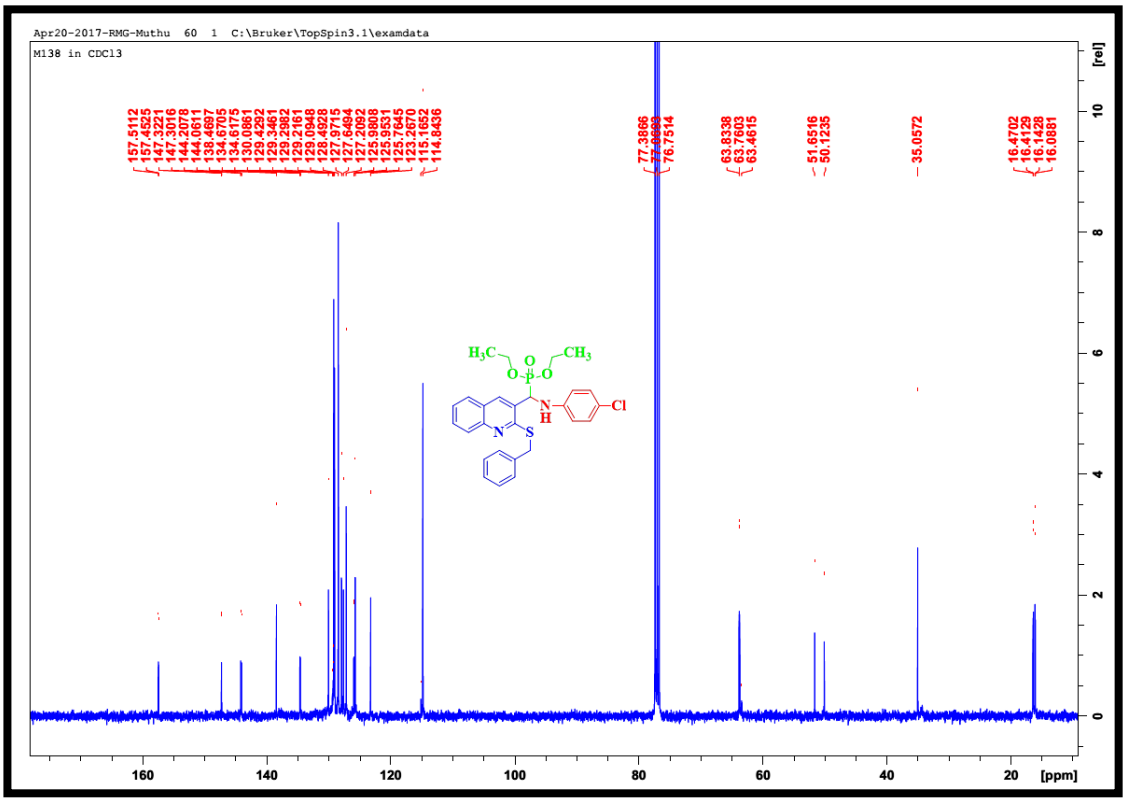

Fig. 5.53. ^{13}C-NMR spectrum of **34**

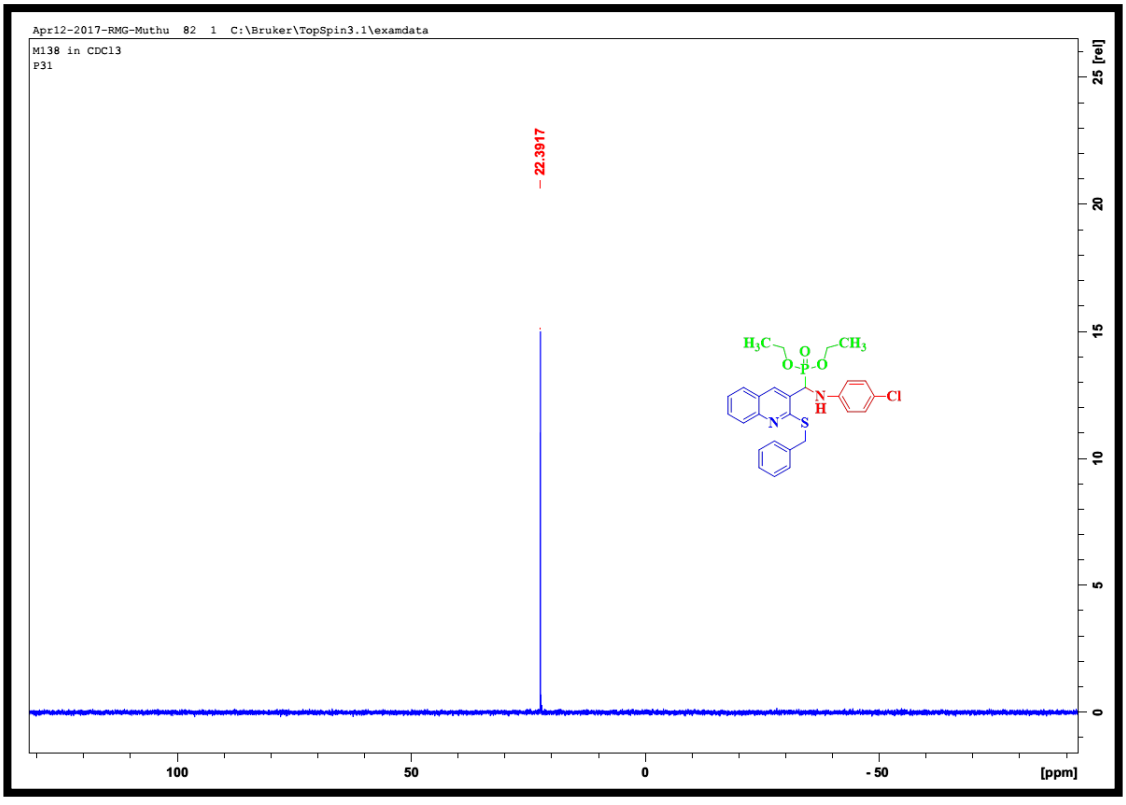

Fig. 5.54. ^{31}P-NMR spectrum of **34**

5.13. Diethyl ((2-(benzylthio)quinolin-3-yl)((3,4-dichlorophenyl)amino) methyl)phosphonate (35)

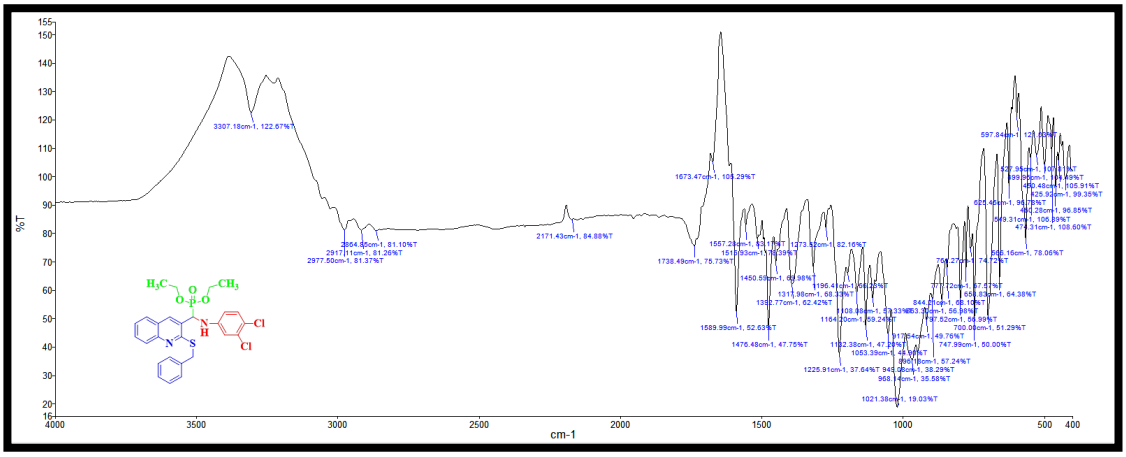

Fig. 5.55. IR spectrum of **35**

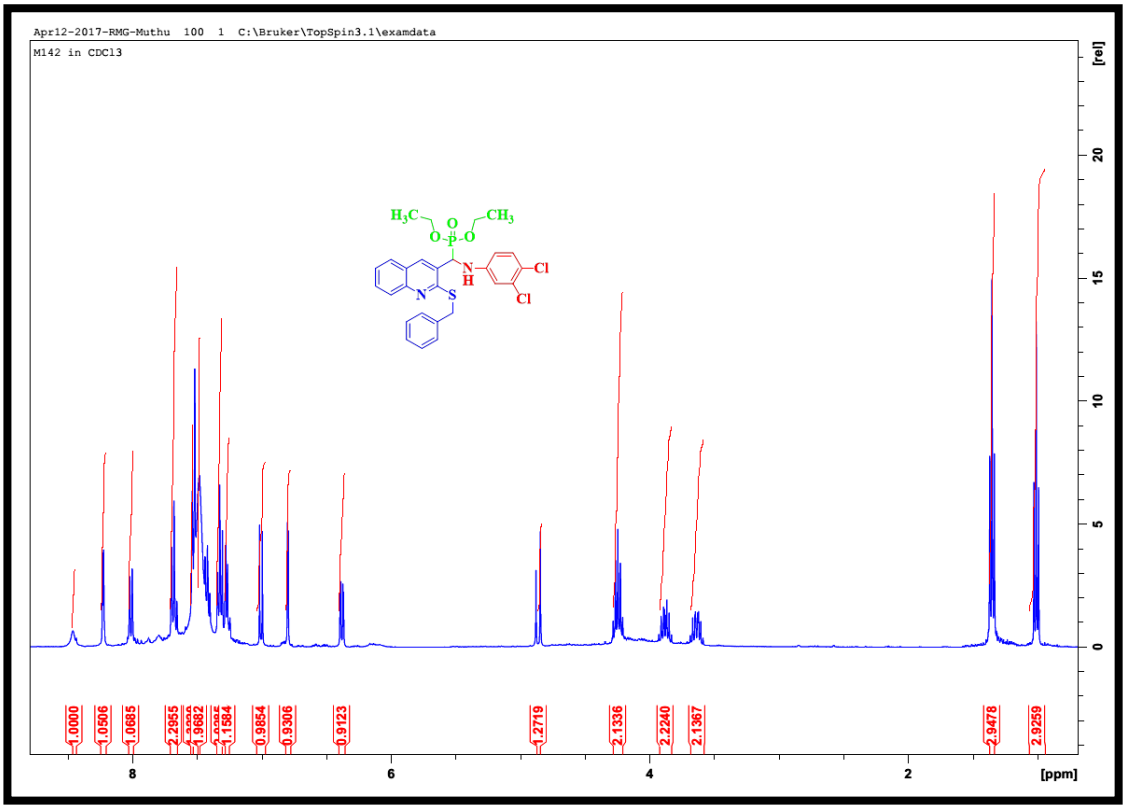

Fig. 5.56. ^{1}H-NMR spectrum of **35**

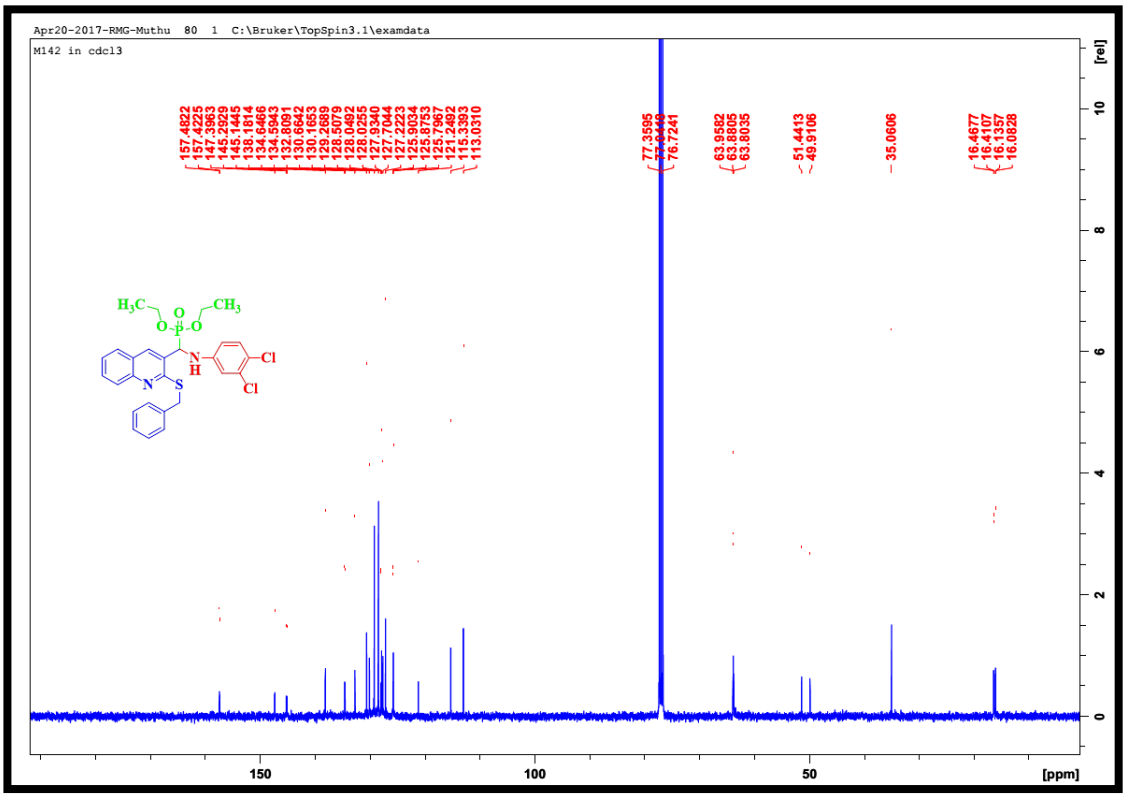

Fig. 5.57. ^{13}C-NMR spectrum of **35**

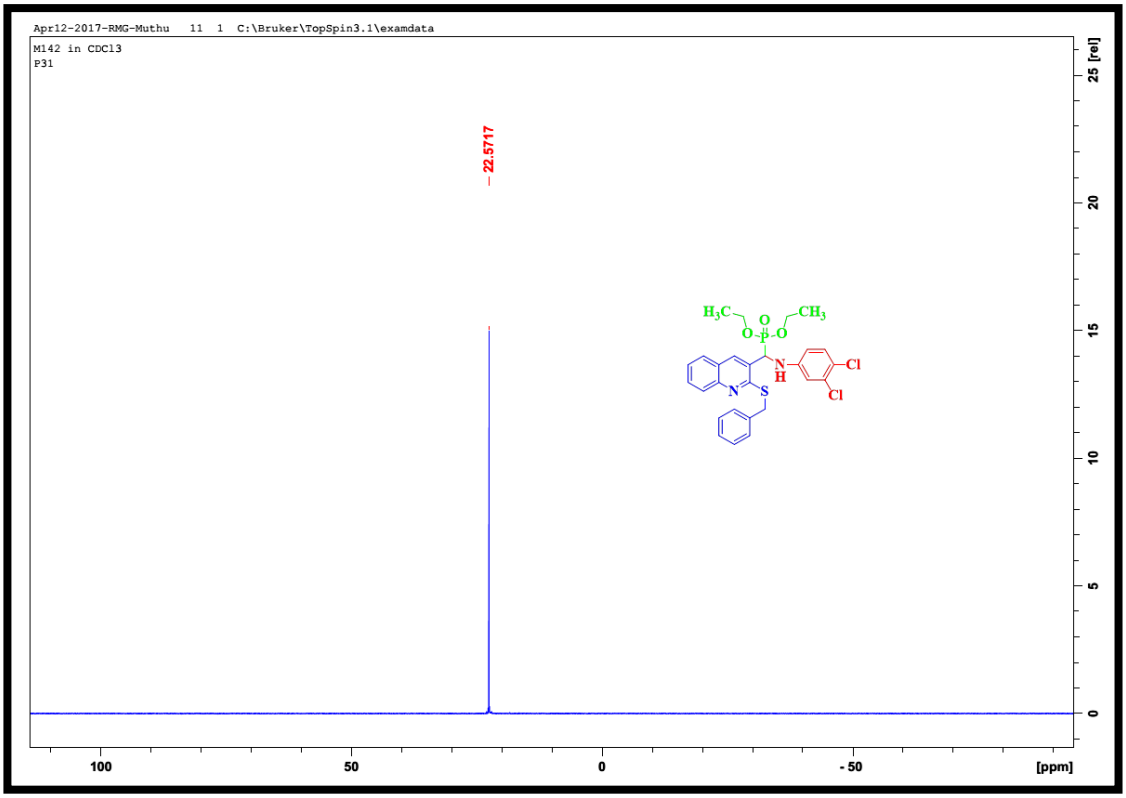

Fig. 5.58. ^{31}P-NMR spectrum of **35**

5.14. Diethyl ((2-(benzylthio)-6-fluoroquinolin-3-yl)((2-methoxyphenyl)amino) methyl) phosphonate (36)

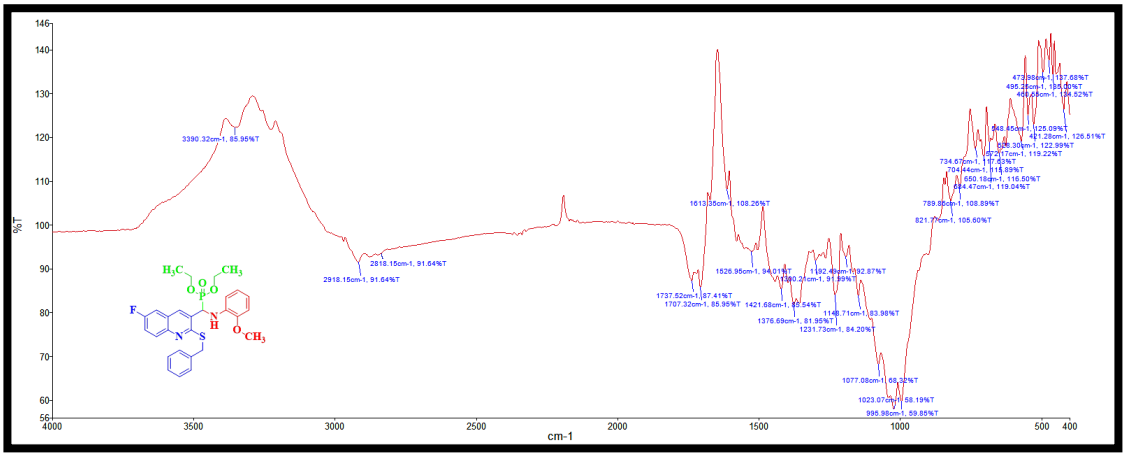

Fig. 5.59. IR spectrum of **36**

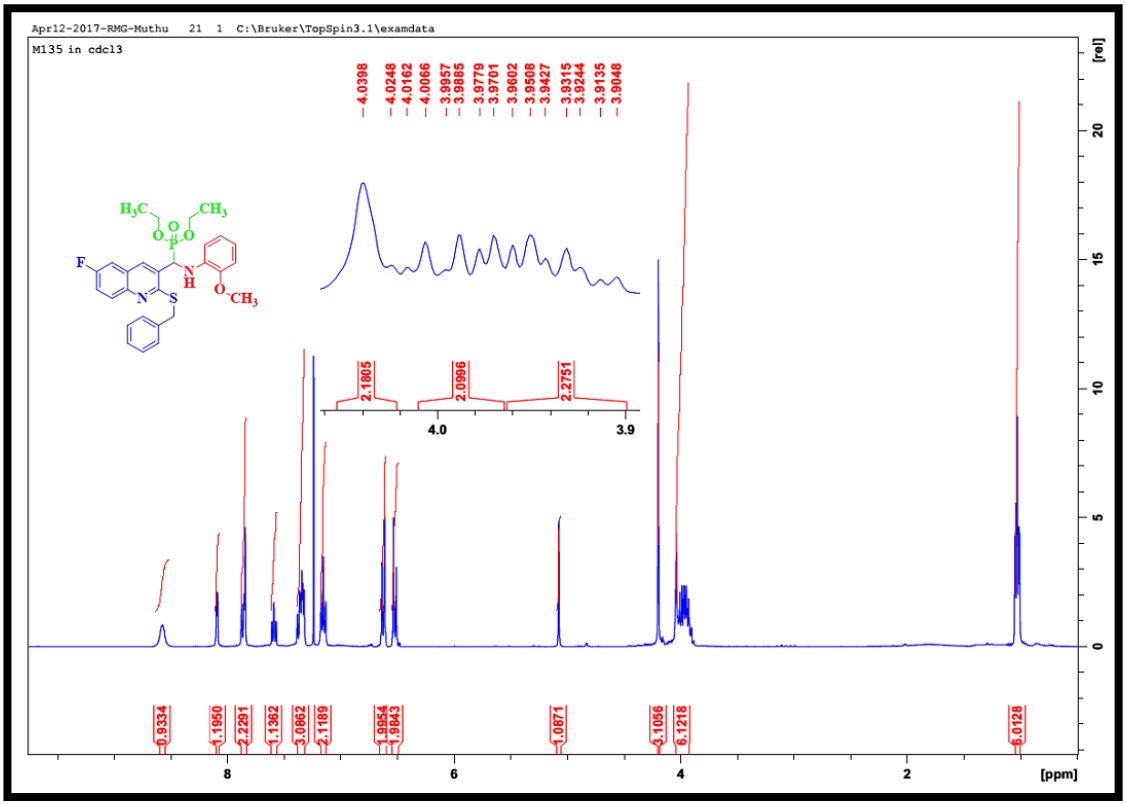

Fig. 5.60. ^{1}H-NMR spectrum of **36**

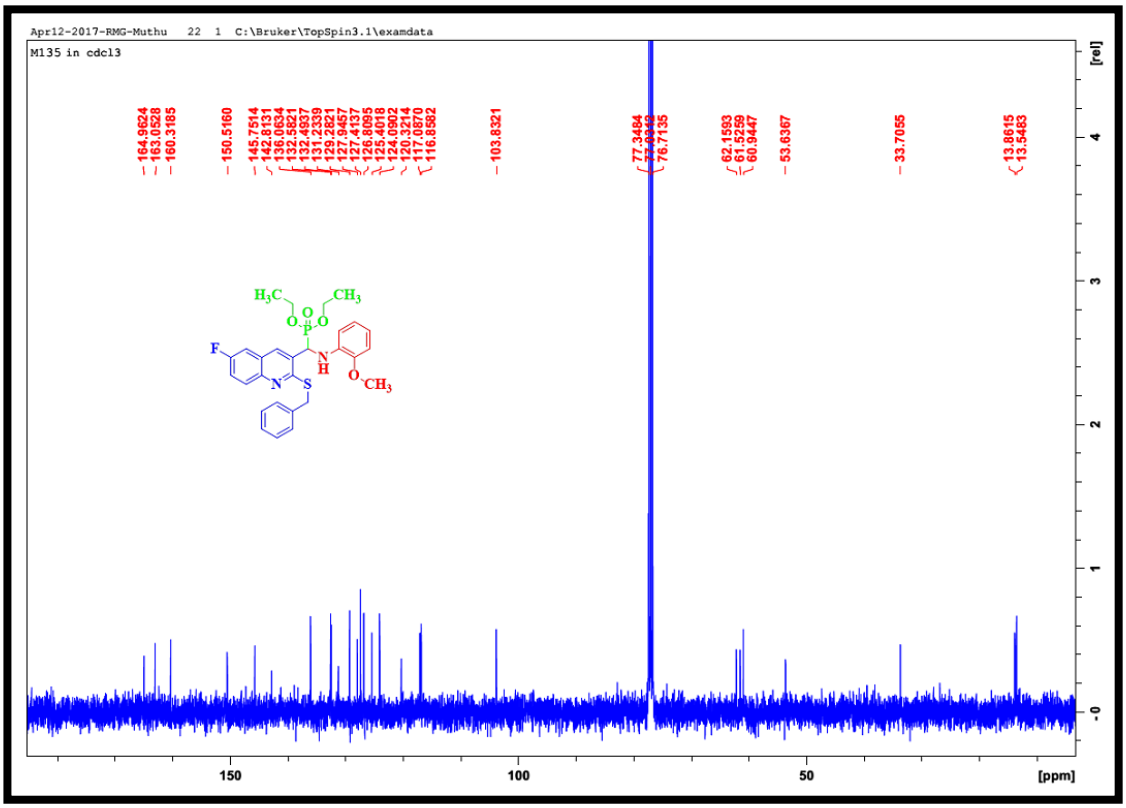

Fig. 5.61. ^{13}C-NMR spectrum of **36**

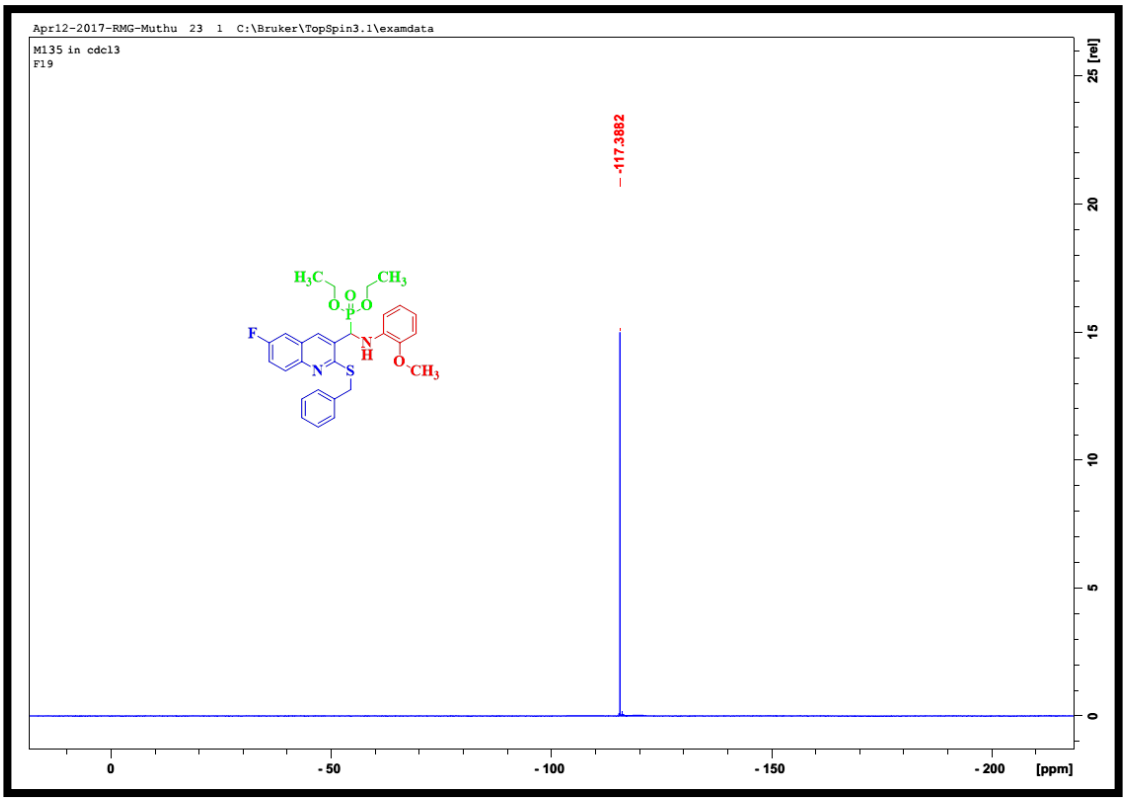

Fig. 5.62. ^{19}F-NMR spectrum of **36**

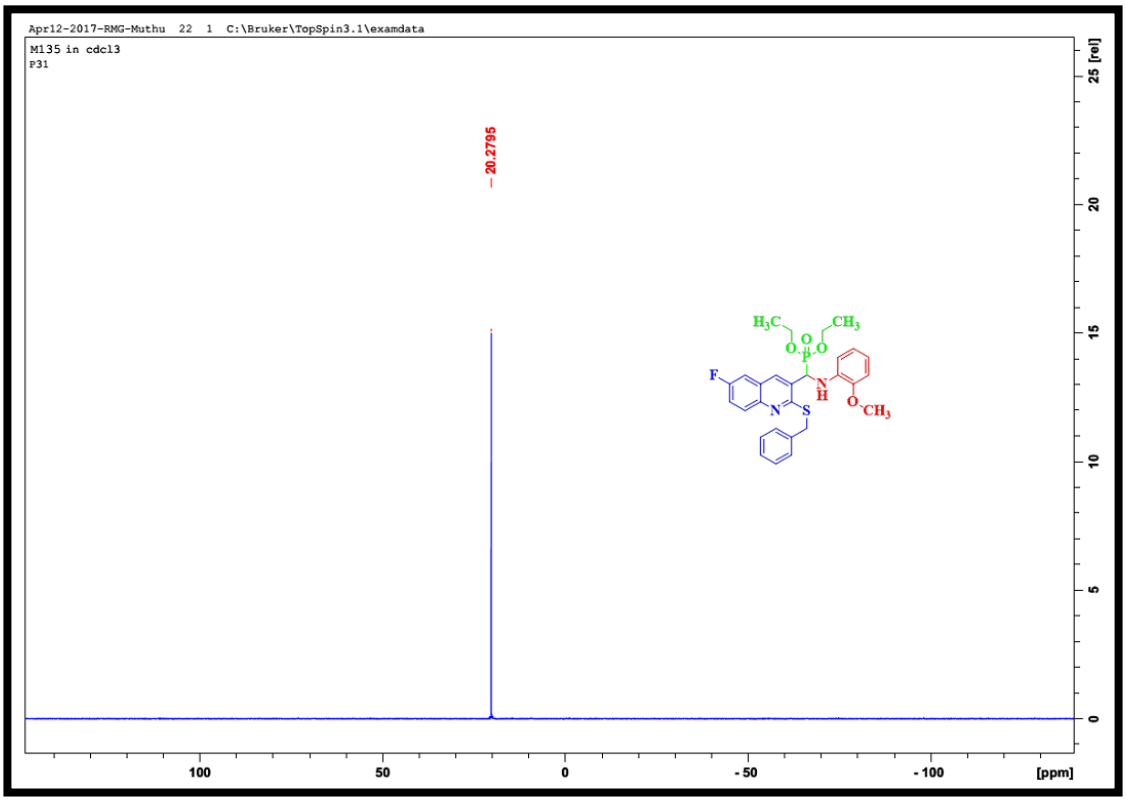

Fig. 5.63. ^{31}P-NMR spectrum of **36**

Chapter-VI

Ultrasonicated synthesis of benzylthioquinolinyl-1,4-dihydropyridines by iodine-loaded boron nitride catalyst and their antimicrobial, antioxidant, toxicity assessment and molecular docking studies

Chapter Six

Ultrasonicated synthesis of benzylthioquinolinyl-1,4-dihydropyridines by iodine-loaded boron nitride catalyst and their antimicrobial, antioxidant, toxicity assessment and molecular docking studies

6.1. Abstract

A series of novel benzylthioquinolinyl-1,4-dihydropyridines (BTQ-DHPs) were synthesized with high yields in short reaction time by a four-component reaction of 2-(benzylthio)quinoline carbaldehyde, malononitrile, arylamines and dimethyl acetylene dicarboxylate in the presence of iodine-loaded boron nitride catalyst (I/BN). A total of 14 novel compounds were synthesized and characterized by FTIR, ^{1}H-NMR, ^{13}C-NMR and elemental analysis. The novel heterogeneous catalyst was synthesised from iodine and boron nitride by simply stirring the mixture for three days. I/BN was analysed by XRD, SEM with EDX, TEM, TGA, DSC and FTIR. A total of 10 BTQ-DHPs were subjected to antibacterial, antioxidant and toxicity studies. Among them, seven BTQ-DHPs showed potential antibacterial activities against *Bacillus cereus*, *Staphylococcus aureus* and *Enterococcus faecalis* whilst four BTQ-DHPs showed antioxidant activity effectively. 10 BTQ-DHPs were evaluated using brine shrimp assay and it was observed that five BTQ-DHPs showed mortality rate less than 50 % (48 h). Furthermore, molecular docking was used to estimate the ligand-protein interactions based on Libdock score. The docked BTQ-DHPs showed Libdock scores ranging from 83.20 to 125.27 kcal/mol. The molecule **24** showed more potency toward *Staphylococcus aureus* gyrase by forming a strong ligand-protein interaction with a Libdock score of 125.27 kcal/mol. The advantages of the protocol used for the synthesis of BTQ-DHPs are the use of water solvent, an inexpensive catalyst with efficient recyclability, mild reaction conditions, and quick reaction time with high yields.

6.2. Introduction

High throughput screening is one of the main strategies used for drug discovery. This requires a good library of lead compounds. To satisfy such requirements, new synthetic

strategies with good efficiency in providing a massive amount of structurally diverse organic products is required. Multi-component reactions (MCRs) which employ three or more reactants to furnish products containing structure or substructure of all starting materials in one-pot is a powerful method for increasing productivity (Dömling, 2006; Dömling and Ugi, 2000; Nair *et al*., 2003; Wan and Liu, 2011). The Hantzsch reaction which provides 1,4-DHPs, is one of the earliest and now a well-known MCR.

The biological activities of 1,4-DHPs include anticonvulsant (Borowicz *et al*., 1997), antihypertensive, antianginal (Love *et al*., 1974; Bossert *et al*., 1981; Breitenbucher *et al*., 2000), antitumor (Boer and Gekeler, 1995), anti-inflammatory (Briukhanov *et al*., 1993), antitubercular (Sushilkumar and Devanand, 2002), analgesic (Gullapalli and Ramarao, 2002), and antithrombolytic (Sunkel *et al*., 1990; Ono and Kimura, 1981). This has increased the interest for the synthesis of 1,4-DHPs as synthetic targets. Interestingly, the combination of 1,4-DHPs and quinoline derivatives are notably an important class of bioactive molecules in the pharmaceutical field (Vijesh *et al*., 2011).

The quinoline scaffold is important in the synthesis of new molecules which provide medical benefits. A number of quinoline derivatives are known to possess antimicrobial, antitumor, antifungal, hypotensive, anti-HIV, analgesic and antiinflammatory properties. Quinoline and its analogues have recently been examined for their mode of action in the inhibition of tyrosine kinases, proteasome, tubulin polymerization, topoisomerase and DNA repair. Substitution of the group in a suitable position of a bioactive molecule is found to exert a profound pharmacological effect (Gasparotto *et al*., 2006). Although the structural core of quinolines can be prepared using various conventional methods, the development of new synthetic methods is important in organic chemistry. For example, quinoline-2-thiones have been investigated as synthetic intermediates (Alhaider *et al*., 1985; Segawa *et al*., 1992; Jinbo *et al*., 1993), as biologically active compounds (Joseph *et al*., 2002), as sulfur-nitrogen mixed donor ligands (Xavier, 1958; Nakano *et al*., 1977; Leeaphon *et al*., 1995) and as the protective group of thiols (Zhang and Matteucci, 1999). However, direct synthetic methods that involve construction of a quinoline scaffold with simultaneous introduction of a thio group are limited (Molina *et al*., 1989). Therefore in the current study, 2-(benzylthio)quinoline-3-carbaldehydes have been synthesized and used as a starting material for the synthesis of new bioactive 1,4-dihydropyridines.

Many catalysts have been used to synthesize 1,4-DHPs such as silica gel/$NaHSO_4$ (Chari and Syamasundar, 2005), $AlCl_3$•$6H_2O$ (Sharma *et al*., 2008), TMSI (Sabitha *et al*., 2003), $HClO_4$-SiO_2 (Maheswara *et al*., 2006), triphenylphosphine (Debache *et al*., 2009), ionic liquid (Li *et al*., 2006), 3,4,5-trifluorobenzeneboronic acid (Sridhar and Perumal, 2005), iodotrimethylsilane (Sabitha *et al*., 2003), $Sc(OTf)_3$ (Donelson *et al*., 2006), HY-Zeolite (Das *et al*., 2006), CAN (Reddy and Raghu, 2008), $Yb(OTf)_3$ (Wang *et al*., 2005) and organocatalysts (Kumar and Maurya, 2007).

Yavari *et al*., 2010 showed a one-pot synthesis of highly functionalized 1,2-dihydropyridines (**5**) from alkyl isocyanide (**1**), acetylenic esters (**2**, **3**) and a primary alkyl amine (**4**). The reaction proceeded smoothly in dichloromethane at room temperature and produced 4-(alkylamino)-1-alkyl(aryl)-1,2-dihydropyridine-2,3,5,6-tetracarboxylates with a 59-95 % yield. The main drawback of the reaction was its long reaction time of 10 h.

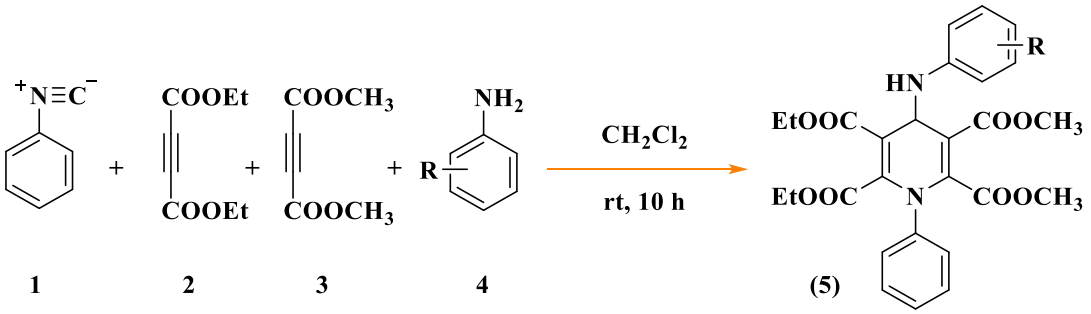

R = 4-OCH_3, 2-Cl, 4-Cl, 4-NO_2

Sridharan *et al*., 2007 developed a one-pot synthesis using cinnamaldehyde (**6**), amines (**7**) and ethyl acetoacetate (**8**) with cerium ammonium nitrate (CAN) in ethanol, which produced 1,4-DHPs (**9**) with a 52-71% isolated yield. However, the recyclability of the catalyst was not elucidated.

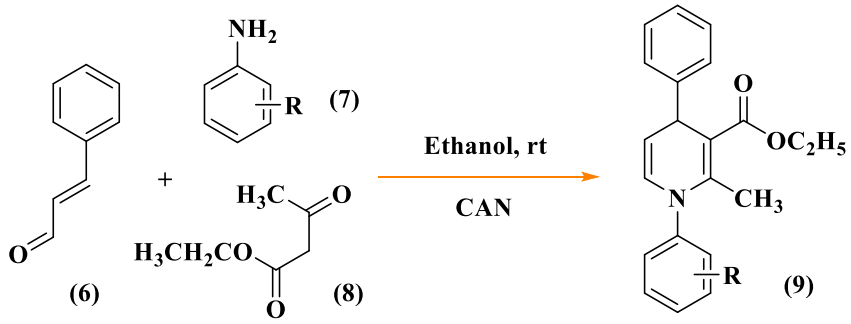

R = H, 3-CH_3, 3-OCH_3, 4-F, 4-Cl, 4-CH_3

Debache *et al*., 2009 synthesized 1,4-DHPs (**12**) by using aromatic aldehydes (**10**), ethyl acetoacetate (**8**) and ammonium acetate (**11**) in triphenylphosphine (PPh_3) with 72-94 % yield. The disadvantage of the reaction was a long reaction time of 5 h.

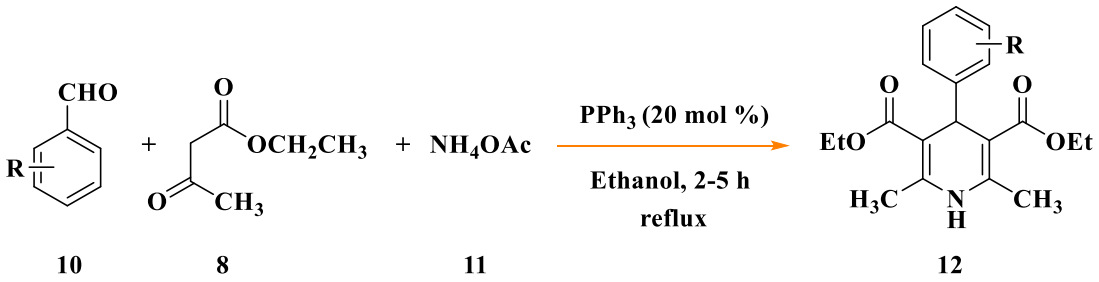

10 **8** **11** **12**

R = H, 4-CH_3, 4-OCH_3, 4-Cl, 4-Br, 2-Furyl

Sabitha *et al*., 2009 developed an efficient one-pot synthesis of 1,4-DHPs (**14**) from aromatic aldehydes (**13**), ethyl acetoacetate (**8**) and ammonium acetate (**11**) within 3-6 h at room temperature. $CeCl_3 \bullet 7H_2O$ was used as a catalyst. The maximum yield obtained was 91 % but it has several drawbacks including long reaction time and non-recyclability of the catalyst.

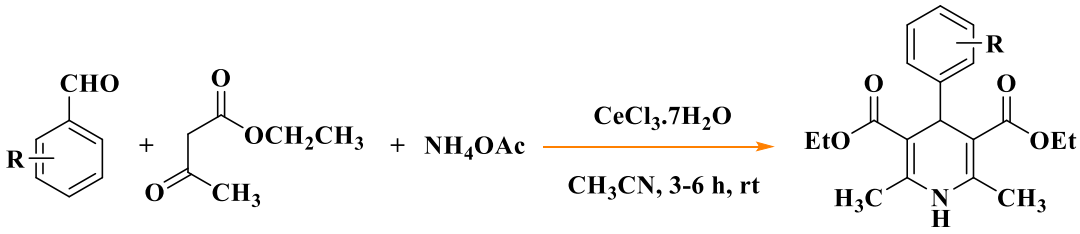

13 **8** **11** **14**

R = H, 4-OCH_3, 4-F, 4-Cl, 4-CH_3, 4-NO_2

Arslan *et al*., 2009 synthesised 1,4-DHPs (**17**) in the presence of alumina-sulphuric acid (ASA) as a catalyst.

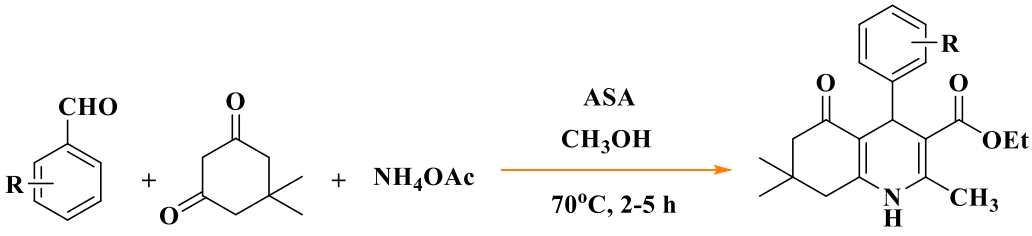

15 **16** **11** **17**

R = H, 4-Br, 4-NO_2, 2-Cl, 3-NO_2, 4-CH_3, 4-OH

Aldehydes (**15**), 1,3-dicarbonyl compounds (**16**) and ammonium acetate (**11**) were used: the product yield was 82-95 %. The disadvantages included the non-reusability of the catalyst and duration of the reaction time of 2-5 h.

All of these syntheses required long reaction times, harsh reaction conditions, tedious work up procedure, unsatisfactory yield due to side products, and the use of large quantities of volatile organic solvents. Therefore, alternate protocols are being sought-after. Ultrasonic irradiation is increasingly being used as a non-traditional technique for accelerating organic reactions. Compared with traditional methods, the salient features and benefits of ultrasonic irradiation includes reduced reaction times, reduced energy consumption, enhanced selectivity and improved product yields (Celle and Stefani, 2009; Cravotto and Cintas, 2006). Often, the reactions under ultrasound irradiation are easier to work-up than those by conventional methods.

Insulating oxides such as SiO_2, Al_2O_3, silica-alumina and zeolites are materials commonly used as catalyst supports (Spivey, 1987). These oxides possess disadvantages such as low thermal conductivity, generates sintering of the assisted metal on hot spots, various acidic and basic sites and the hydrophilic surface of the catalyst with water at low temperatures. Various two dimensional nanomaterials have received considerable attention for heterogeneous catalysis. Among them, boron nitride (BN) has gained attention due to its high elastic modulus, high melting-point, excellent thermal conductivity and a large and direct band gap. Such properties can be of high value for substrates (Liu *et al*., 2014). The graphene like hexagonal boron nitride (h-BN) (Nag *et al*., 2010) is the most stable isomer. It has acid-base resistance, good thermal and electrical conductivity. Moreover, BN is hydrophobic therefore preventing moisture condensation on its surface. Activated BN exhibits an excellent adsorption performance for various metal ions such as Cr^{3+}, Co^{2+}, Ni^{2+}, Ce^{3+}, Pb^{2+}, organic pollutants such as tetracycline, methyl orange and congo red and volatile organic compounds such as benzene (Li *et al*., 2013). BN contains an equal number of boron and nitrogen atoms, isoelectronic with carbon and is analogous to graphite. The strong B-N covalent bonds impart high mechanical, thermal and chemical stability. In view of the above, BN has gained interest in the field of heterogeneous catalysis over the past decade (Primo *et al*., 2015; Wang *et al*., 2011; Molla *et al*., 2013) thus can be used as catalyst support. One of the important features of BN is that it behaves as both a Lewis acid and a Lewis base

(Nag *et al*., 2010). Iodine, as a cheap, less toxic and readily available mild Lewis acid has been used to catalyse various organic transformations (Togo and Iida, 2006; Ren and Cai, 2007; Ren and Cai, 2007; Ren and Cai, 2008). To enhance the ease of separation and Lewis acidity, we incorporated iodine on BN. Due to these facts and interest in the synthesis of 1,4-DHPs with potential biological activities, a convenient ultrasonic-assisted synthesis of benzylthioquinoline-1,4-dihydropyridines (BTQ-DHPs) in the presence of I/BN, is reported.

6.3. Results and discussion

Iodine is used in several organic syntheses (Stowell and Widlanski, 1995; Kitagawa *et al*., 1995; Joseph *et al*., 1995), however several drawbacks exist such as its ease of vaporization and sublimation limits its wide applicability. Therefore, the development of a new catalyst was sought. This study presents the synthesis and characterisation of a new iodine-loaded boron nitride (I/BN) catalyst and its application in the synthesis of new quinolone-based 1,4 DHPs. Briefly, BN was added to a solution of I_2 and the mixture stirred at room temperature for three days. The reaction mixture was filtered, washed with THF and dried to produce a white powder with 98 % yield (**Scheme 1**). I/BN was characterized by XRD, SEM, EDX, TEM, TGA, DSC and FTIR.

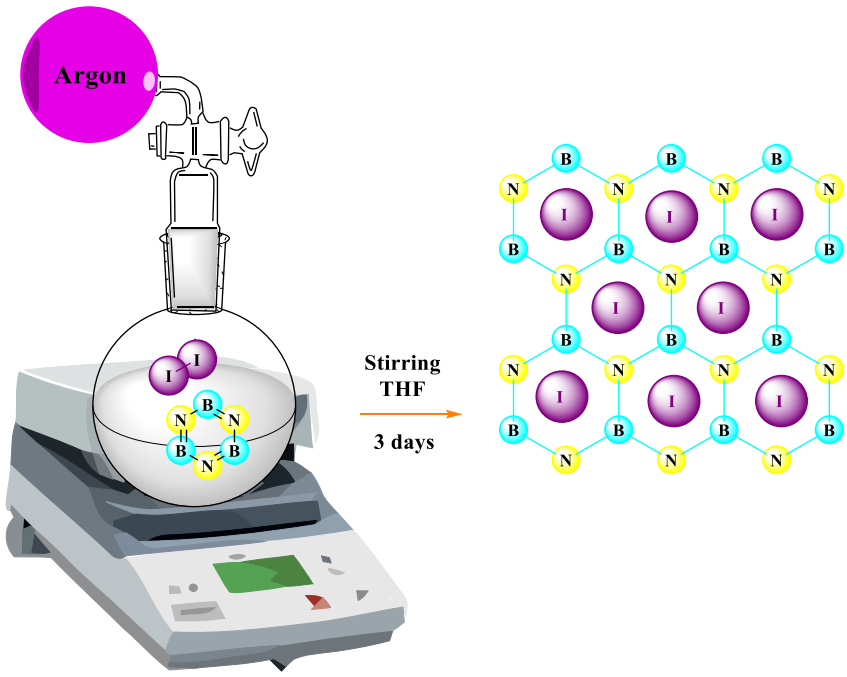

Scheme 1. Synthesis of iodine-loaded boron nitride (I/BN)

The diffraction peaks (**Fig. 1**) which were observed at approximately 41.8°, 50°, 55° and 75.2° were assigned to the crystal planes (101), (200), (211) and (204) of Bragg's reflection for iodine (Hou *et al*., 2011). The diffraction peaks indicated the anatase crystallite structure. The average crystallite size calculated from the full width at half maximum of the main peak (101), based on the Debye-Scherrer formula (d = 0.9 $\lambda/\beta_{1/2}\cos\theta$), was approximately 160 nm, and it was shown to be consistent with the TEM image (**Fig. 4)**. The Bragg's reflection which was observed at approximately 26.3°, 43.4° and 81.8° corresponded to the crystal planes (002), (102) and (004), respectively. These peaks confirmed the hexagonal crystal structure of boron nitride (Trivedi *et al*., 2015).

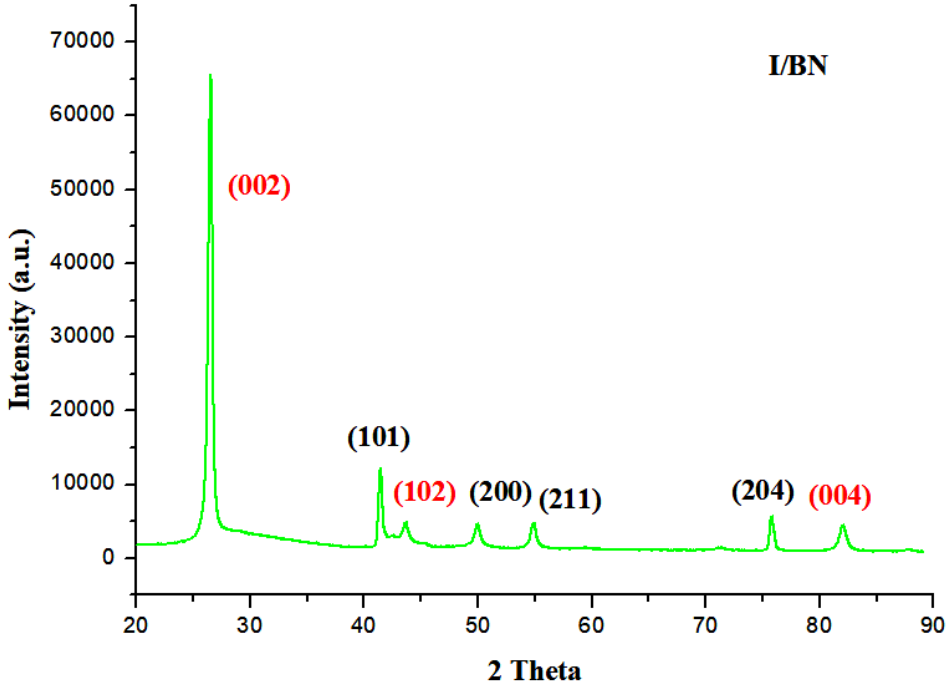

Fig. 1. X-ray diffraction pattern of I/BN

The surface and morphology of I/BN is shown in **Fig. 2 (A-D)**. SEM images, at different scales, showed good spherical morphology with little agglomeration and smooth featureless surfaces **(Fig. 2A-B)**. The spheres had small diameters of approximately 166 nm. The sponge like appearance observed at the surface in the range of 1-2 µm **(Fig. 2C** and **2D)** was probably due to the incorporation of iodine: a similar observation was reported in the literature (Lin *et al*., 2015). **Fig. 2C** and **2D** indicated that I/BN was agglomerated and consisted of irregular shapes and plate-like crystal structures. The

dimensions of these crystals were about 70 and 180 nm and the thickness of sheet was about 25 nm (**Fig. 4A-E,** See: histogram). Also, the average crystalline size calculated from Debye-Scherrer's formula (Scherrer, 1918) was ~24 nm, thus the observed SEM images suggested that h-BN crystals consist of many small crystallites.

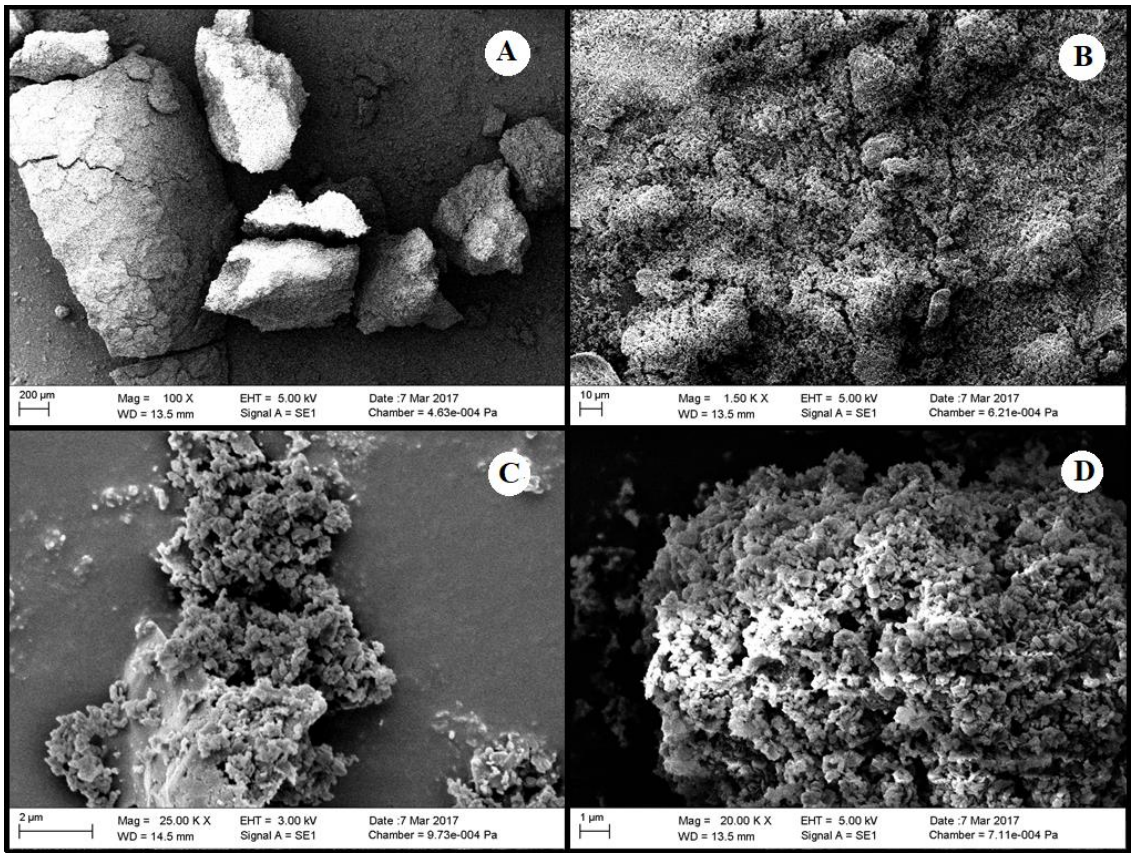

Fig. 2. Scanning electron microscopy images of I/BN

The EDX spectrum **(Fig. 3)** acquired from the SEM images revealed that the elements iodine, boron, nitrogen, carbon and gold were present.

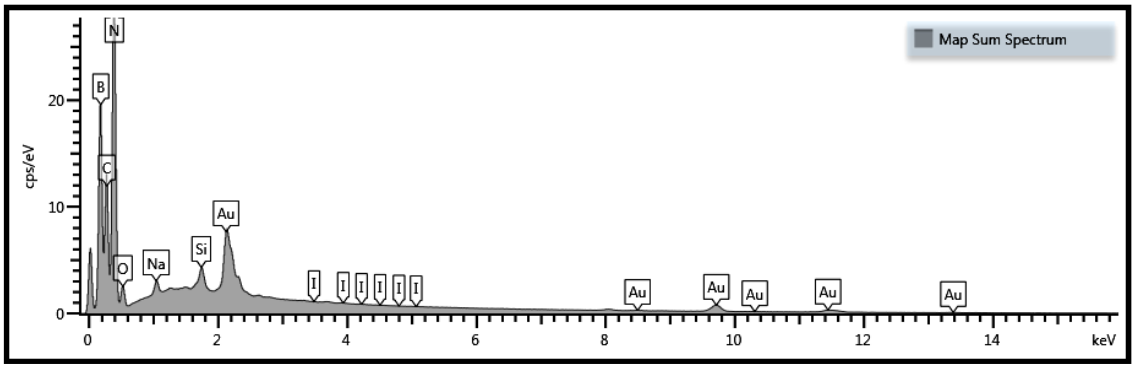

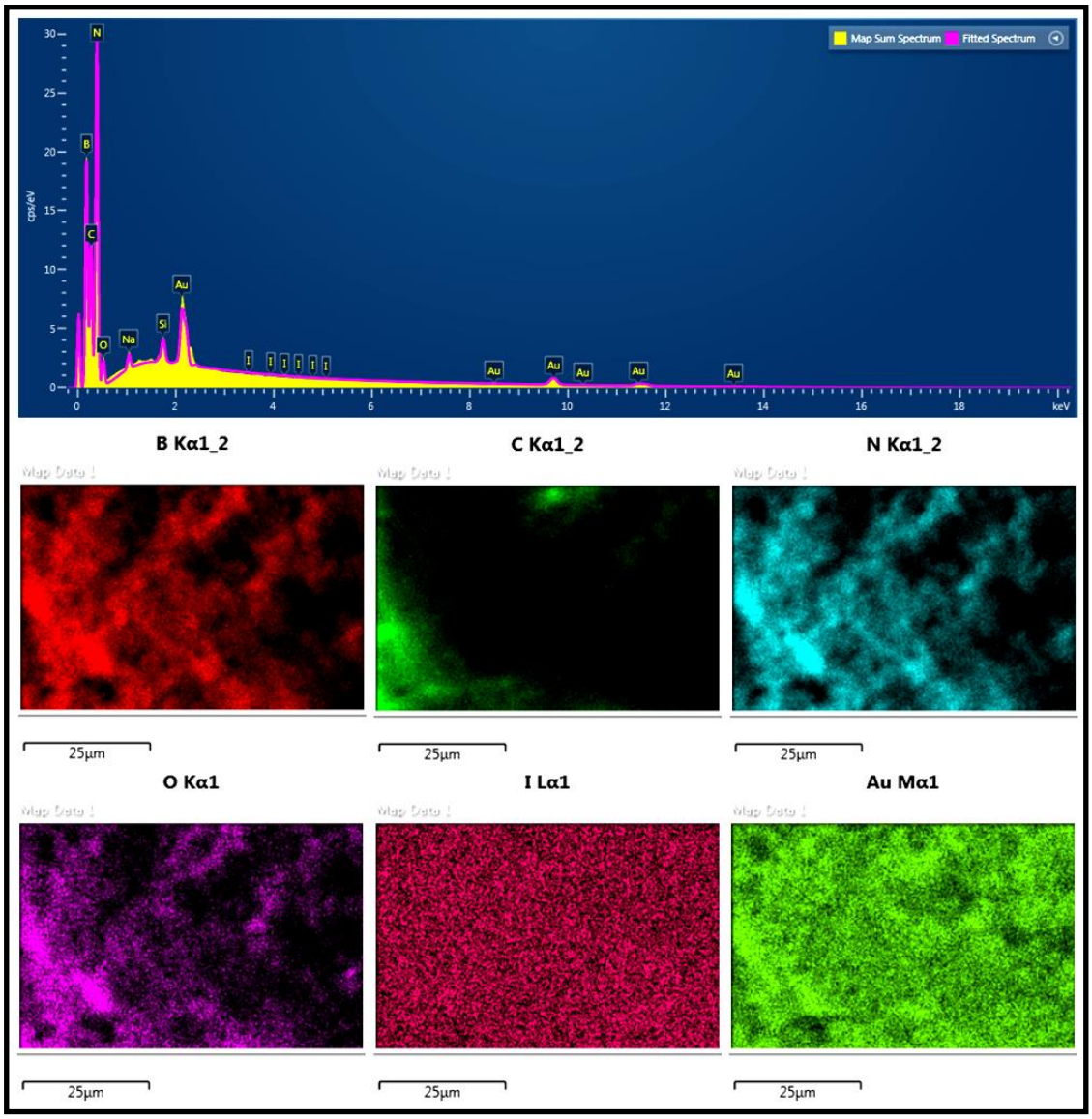

Fig. 3. The energy dispersive X-ray spectrum and elemental mapping of I/BN

The iodine peaks were obtained at 2.75, 3.95, 4.20, 4.35, 4.40 and 4.55. The appearance of gold peaks was due to the coating of the sample with conducting material gold (Au) to reflect electrons (sputter coating).

The particle size and the surface morphology of I/BN was observed as presented in **Fig. 4** (**A-E**). The TEM images showed spindle-like anatase nanocrystals (**Fig. 4B-D**) which confirmed iodine in the samples (Wen *et al*., 2007). The anatase nanocrystals were extended probably due to the incorporation of iodine atoms or by formation of lattice vacancies related to the iodine. Also, irregular and spherical morphologies of h-BN material were observed. The formation of particles with an average size of 166 nm (size variation: ± 19 nm by ImageJ, see: histogram) was observed. The closely packed

aggregated particles arose due to the presence of cavities and the movement of iodine atoms toward the interior sphere of the h-BN material (Wang *et al*., 2009).

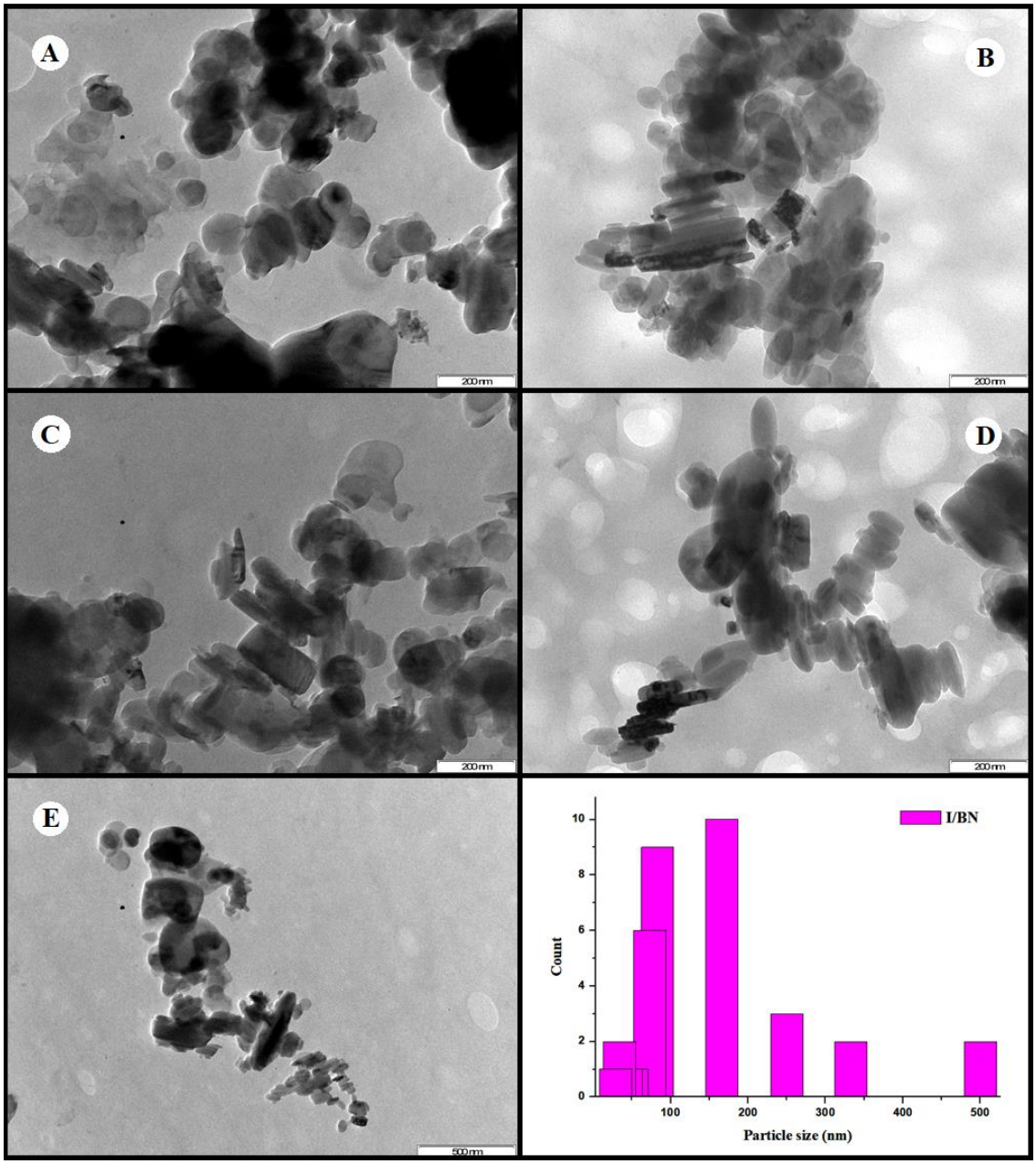

Fig. 4. Transmission electron microscopy images of I/BN

The TGA curve (**Fig. 5**) showed the decomposition of I/BN at the temperature range of 25℃ to 1000℃. The first decomposition of 1.8 % mass loss of the sample was observed at 80℃-90℃ which was due to the loss of absorbed water. The catalyst appeared stabilized from 98℃ to 300℃. Three continuous decomposition peaks were observed at 310℃, 575℃ and 698℃. In the temperature range of 310℃-620℃, there was a mass loss

of approximately 35 % which was due to the thermal degradation of the iodine complex, as reported by Danilovas *et al.*, 2014. During this stage, it is suggested that iodine was released from the complex which further induced thermochemical degradation of the boron nitride material.

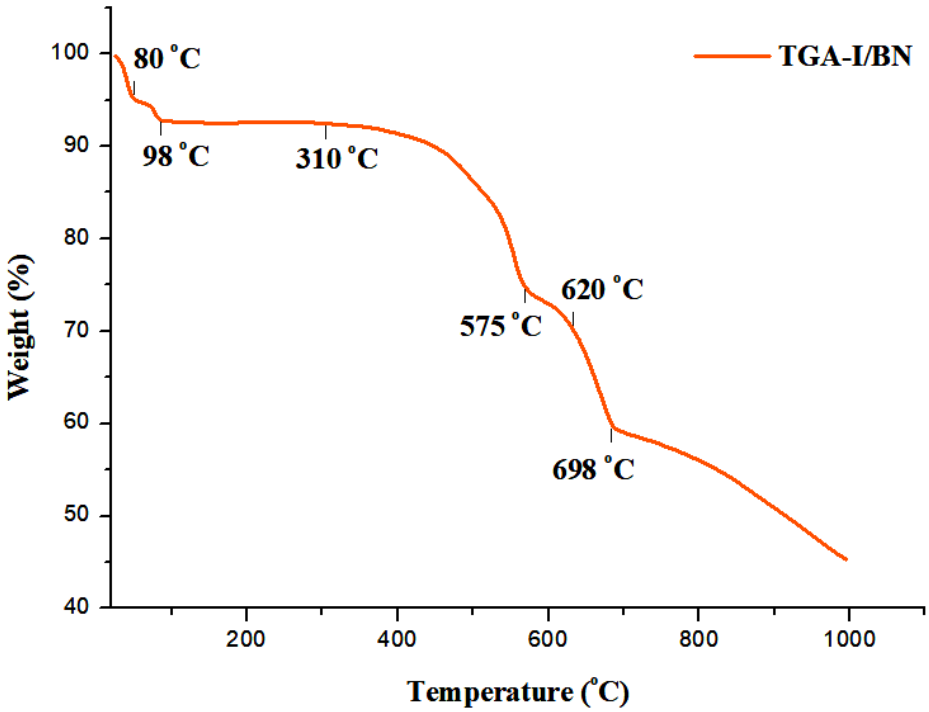

Fig. 5. Thermogravimetric analysis curve of I/BN

The decomposition and subsequent oxidation was observed at 698℃ due to BN oxidation and the subsequent formation of boron trioxide (B_2O_3) on its surface. As the catalyst decomposed, boron reacted with atmospheric oxygen and produced B_2O_3 while nitrogen gas (N_2) was released (Oda and Yoshio, 1993). The process can be explained by the following chemical reaction:

$$2BN + 3/2\ O_2 \longrightarrow B_2O_3 + N_2\uparrow$$

A mass loss of 16 % was observed between the temperature ranges of 698℃ -1000℃ which was due to the loss or degradation of h-BN.

The DSC curve (**Fig. 6**) of I/BN provided the heat flow inside the furnace as a function of temperature, arising from a series of physical and chemical procedures such as decomposition and oxidation. A broad endothermic effect in the temperature ranges of

500℃ - 90℃ was observed which might be connected with the weight decrease and was assigned to partial breaking of B-I bonds (Marinoiu *et al*., 2017). A small exothermic peak appeared at 92℃ which could be associated with atmospheric moisture.

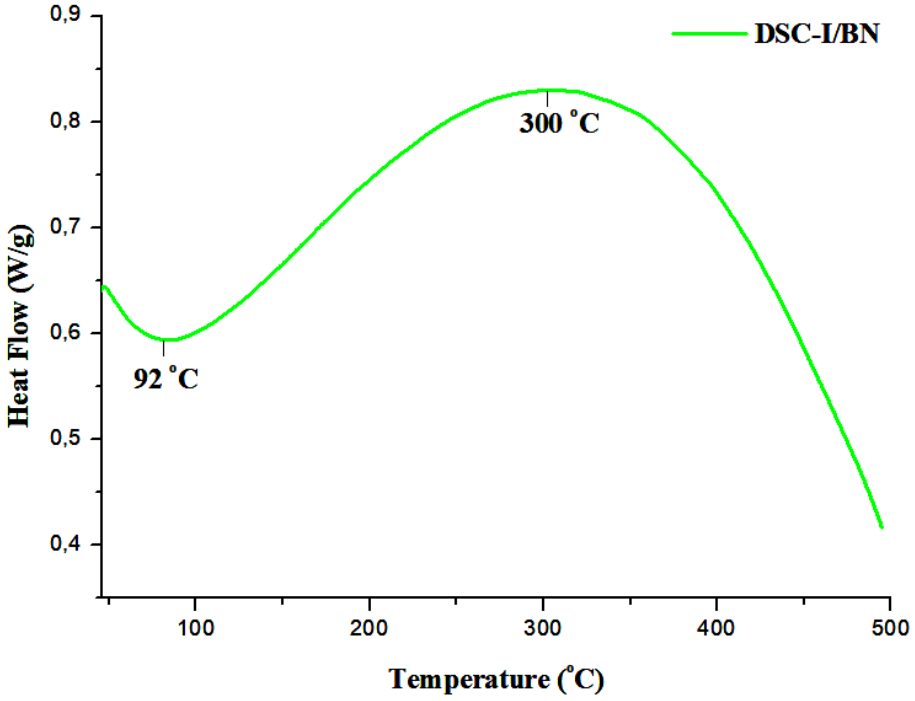

Fig. 6. Differential scanning calorimetry curve of I/BN

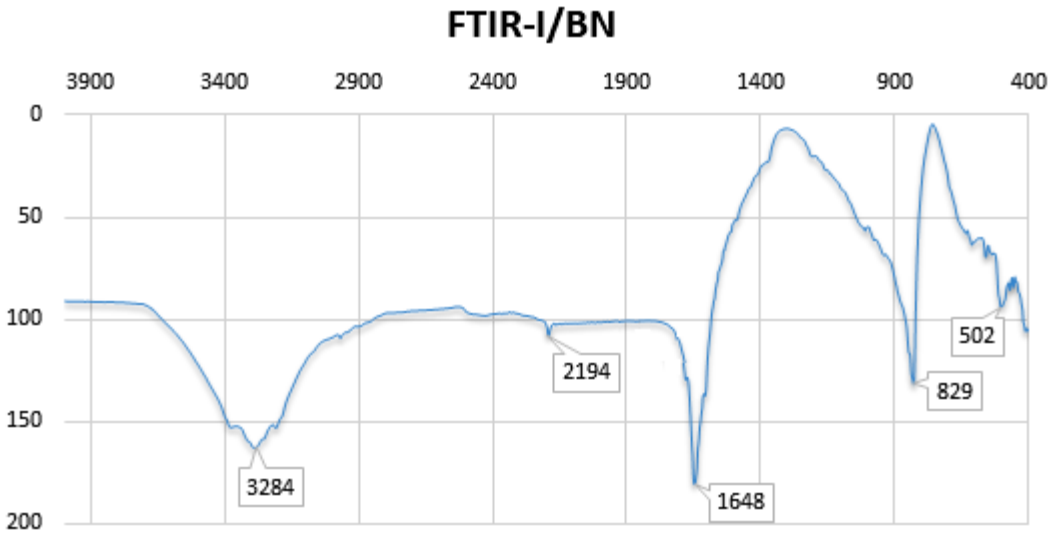

Fig. 7. Fourier transform infrared spectrum of I/BN

Fig. 7 shows the FTIR spectrum of I/BN. The broad absorption peaks at 3284 cm^{-1} and 2194 cm^{-1} corresponded to the hydroxyl group (O-H) and B-H, respectively. Both peaks

were recognized due to the absorbance of water molecules from atmospheric moisture. The peaks at 1648 cm^{-1} and 829 cm^{-1} was assigned to N-B-N and B-N-B, respectively (Muthu *et al*., 2016). The interaction of iodine with h-BN was confirmed by the B-I peak observed at 502 cm^{-1} (Hassanzadeh and Andrews, 1993) (**Fig. 7**).

After the successful characterization of I/BN, the heterogeneous catalytic activity was investigated by a one-pot four-component reaction. The starting compound chloroformylquinoline (CFQ) was synthesized by using the Vilsmeier-Haack reaction as per the procedure (Srivastava and Singh, 2005).

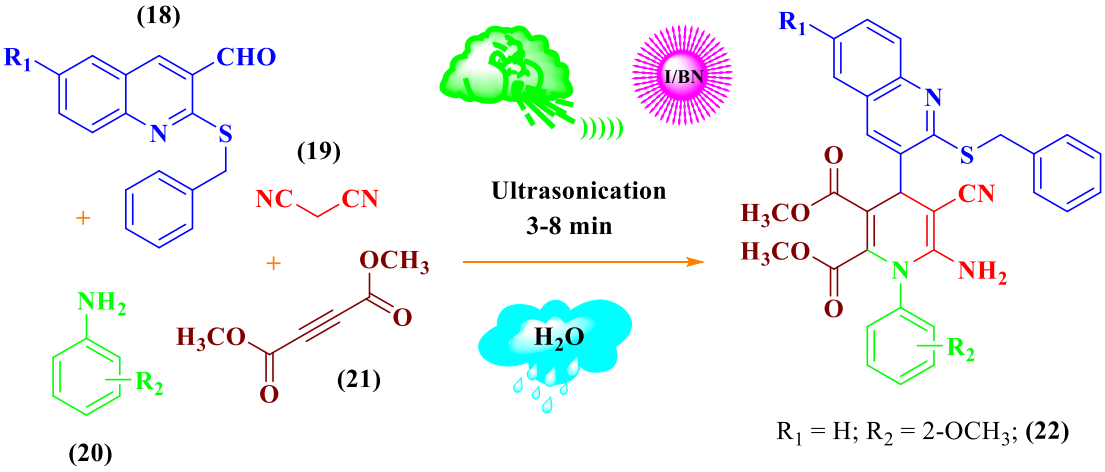

Scheme 2. Synthesis of benzylthioquinoline-1,4-dihydropyridines (**22-35**) via a four-component condensation reaction under ultrasonication by using I/BN

CFQ was used to synthesize the starting material 2-(benzylthio)quinoline-3-carbaldehyde (BTQC) (**18**) via reaction with 2-benzylmercaptan for 2-3 h in the presence of NaH, in DMSO, at 90℃. The mixture was cooled and then separated by a dichloromethane/water mixture (1:3) followed by column chromatography to produce BTQC. In a preliminary investigation, an equimolar mixture (1 mmol) of **18**, malononitrile (**19**), *o*-anisidine and dimethyl acetylene dicarboxylate (DMAD) (**21**) was reacted with triethylamine as a catalyst, in ethanol at ambient temperature for 24 h. The

product was purified by column chromatography. The yield of benzylthioquinoline-1,4-dihydropyridines (BTQ-DHPs) (**22**) was 40 %. When the same reaction was conducted in the presence of I/BN, 53 % yield was obtained within 24 h. The reaction time was too long and therefore ultrasonic irradiation was investigated; the reaction time was reduced to 10 minutes with 71 % yield. The percentage yield increased to 97 %, when the reaction was conducted in water for 3 minutes **(Scheme 2)**.

22 was purified by column chromatography (eluent: ethyl acetate: petroleum ether, 25 %) and characterized by FTIR, ^{1}H-NMR, ^{13}C-NMR, HSQC, HMBC and elemental analysis. The IR spectrum (**Fig. 6.1**, Appendix VI) of **22** showed stretching frequencies (cm^{-1}) at 2187 for C≡N, 1614 for C=N, 1277 for C-N, 2918 for CH, 1652 for C=C, 703 for C-S, 1736 for C=O, 2890 for OCH_3 and 3308 for NH. The ^{1}H-NMR spectrum (**Fig. 6.2**) of **22** showed three singlets at δ 5.03 for (C4'''), δ 5.58 for (C14) and δ 8.19 for (C4).

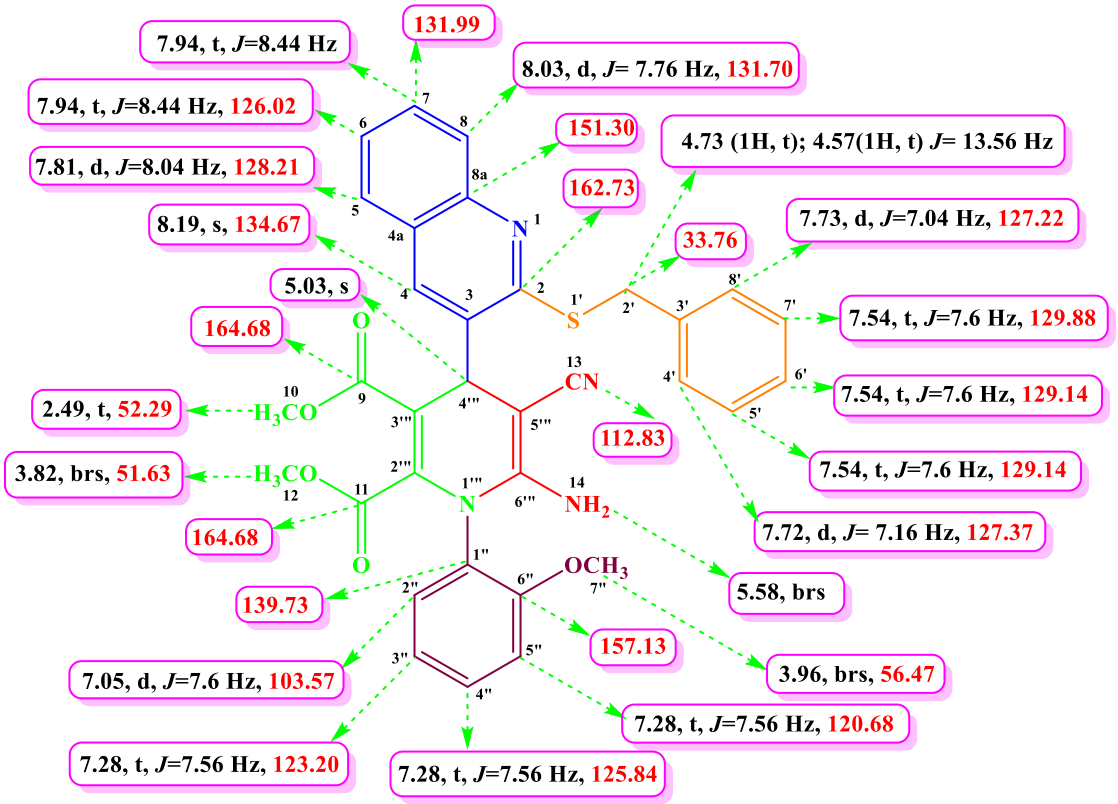

Fig. 8. Selected ^{1}H and ^{13}C-NMR chemical shifts for **22**

The benzyl thio group proton C<u>H</u>$_2$ (C2') showed a triplet at δ 4.73 for one proton with a coupling constant value, *J*=13.6 Hz. Methoxy group, OC<u>H</u>$_3$ (C10) was identified as a triplet at δ 2.49 and the other two OC<u>H</u>$_3$ (C7" and C12) groups showed broad singlets at

δ 3.96 and 3.82. The ^{13}C-NMR spectrum (**Fig. 6.3**) showed two carbonyl groups (C9 and C11) at δ 164.68. The peak observed at δ 45.75 attributed to CH (C4”’). The carbonitrile (C13) carbon showed a peak at δ 112.83. Methoxy carbons (C10, C12 and C7”) showed peaks at δ 52.29, 51.63 and 56.47, respectively. The structure was further confirmed by 2D NMR spectral studies. The selected ^{1}H and ^{13}C-NMR chemical shift for **22** is showed in **Fig. 8**.

The ^{13}C, ^{1}H-COSY correlation of carbon signals at δ 129.14, 128.21, 127.37, 127.22, 125.84, 123.20, 120.68, 112.83, 59.12, 56.47, 51.63 and 33.76 were assigned to C6’, C5, C4’, C8’, C4”, C3”, C5”, C13, C7”, C10 and C2”. The carbon signal at δ 45.75 was due to CH (C4”’) carbon which is shown **(Fig. 6.4)**.

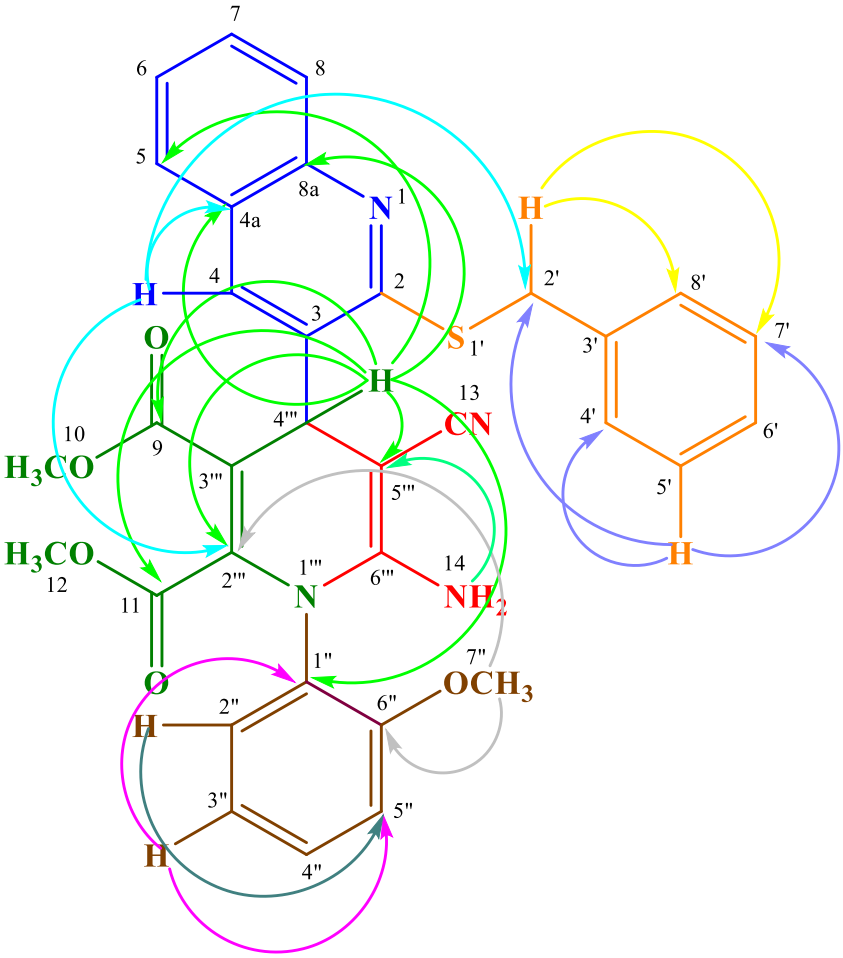

Fig. 9. HMBC correlations and chemical shifts of **22**

The HMBC correlation of protons assigned to the corresponding carbons is showed in **Fig. 9**. The HMBC spectrum (**Fig. 6.5**) of **22** showed the long-range correlations as follows: The C4'''-H of **22** coupled with pyridinyl carbons (C5''') at δ 59.12 and C2''' at δ 156.80, quaternary carbon C1'' at δ 139.73, quinolinyl carbons C5 at δ 128.21, C4a at δ 146.26 and C8a at δ 151.30, carbonyl carbons (C9 and C11) at δ 164.68. This correlation of C4'''-H to the quaternary carbon (C1''), quinolinyl carbons (C4a and C8a), pyridinyl carbons (C5''' and C2''') and carbons (C9) and (C11) of carbonyl group indicated that the four groups were attached to C4''' (CH). Thus it was evident that the four different moieties were bonded to a common carbon (CH) and hence added valuable information to **22**.

The C2'-H proton was coupled with the benzyl mercaptan group carbons, C8' at δ 127.22 and C7' at δ 129.88. The methoxy group C7''-H proton was coupled with C2''' at δ 156.80 and C6'' at δ 157.13. The C14-H proton was coupled with pyridinyl carbon C5''' at δ 59.12. The benzyl mercaptan ring C5'-H proton was coupled with carbons C2' at δ 33.76, C4' at δ 127.32 and C7' at δ 56.47. The proton of C3''-H was coupled with the same *o*-anisidine ring carbon, C1'' at δ 139.73 and C5'' at δ 59.12. The C4-H proton was coupled with C2' at δ 33.76, C4a at δ 146.26 and C2''' at δ 156.80. The C2''-H was correlated with *o*-anisidine ring carbon C5'' at δ 120.68 and thus the selected ^{1}H, ^{13}C-NMR and HMBC chemical shifts of the compound **22** are shown in **Table 1**.

Table 1. HMBC correlation and chemical shifts

Entry	Protons	Correlated carbons
1	C4'''- H (s, 1H) at δ 5.03 ppm	C5''' (59.12), C5 (128.21), C1'' (139.73), C4a (146.26), C8a (151.30), C2''' (156.80), C9 (164.68) and C11 (164.68)
2	C2'-H (d, 2H, *J*=13.56 Hz) at δ 4.73 and 4.57 ppm	C8' (127.22) and C7' (129.88)
3	C7''-H (s, 3H) at δ 3.96 ppm	C2''' (156.80) and C6'' (157.13)
4	C14-H (s 2H) at δ 5.58 ppm	C5''' (59.12)
5	C5'-H (t, 1H, *J*= 7.6 Hz) at δ 7.54 ppm	C2' (33.76), C4' (127.37) and C7' (56.47)
6	C3''-H (t, 1H, *J*= 7.56 Hz) at δ 7.28 ppm	C1'' (139.73) and C5'' (59.12)
7	C4-H (s, 1H) at δ 8.19 ppm	C2' (33.76), C4a (146.26) and C2''' (156.80)
8	C2''-H (t, 1H, *J*=7.6 Hz) at δ 7.05 ppm	C5'' (120.68)

Based on the above spectral details and elemental analysis results: Anal. Calc. for $C_{33}H_{28}N_4O_5S$: C, 66.88; H, 4.76; N, 9.45; %. Found: C, 66.89; H, 4.78; N, 9.47; %, the structure was confirmed as dimethyl 6-amino-4-(2-(benzylthio)quinolin-3-yl)-5-cyano-1-(2-methoxyphenyl)-1,4-dihydropyridine-2,3-dicarboxylate **(22)**.

To determine the optimal reaction medium, different solvents were selected and the results are summarized in **Table 2**. Among the solvents, the reaction in water gave best yield (**Table 2**, entry 5). The yield of **22** decreased to 62 % when the solvent was changed. The low yield was probably due to unreacted substrate **(Table 2**, entry 1). The maximum yield of 97 % was obtained when the reaction was carried out in water with 3 minutes reaction time.

Table 2. The effect of solvents

Entry	Solvent	Time (min)	Yield (%) [b]
1	Acetonitrile	15	62
2	Ethanol	12	77
3	Toluene	13	80
4	Methanol	10	76
5	Water	3	97

[b] Isolated yields

To determine the optimum mole % of I/BN, the reaction was conducted with different mole percentages: 5 mol %, 10 mol %, 15 mol % and 20 mol % (**Table 3**). It was observed that a trace amount of dihydropyridine was obtained when 25 mol % of h-BN used (**Table 3**, entry 1). Among the various mole percentages, the best yield was with 10 mol % of I/BN **(Table 3**, entry 3).

Table 3. Catalyst optimization

Entry	Catalyst	Mol %	Time (min)	Yield (%) [b]
1	BN	25	20	Trace
2	I/BN	5	8	76
3	I/BN	10	3	97
4	I/BN	15	10	90
5	I/BN	20	10	90

[b] Isolated yields

Water has unique physical and chemical properties such as amphiphilicity and hydrogen bonding capability which influence the reactivity of chemicals in addition to the selectivity of reactions (Hayashi *et al*., 2008; Lindström *et al*., 2002; Head-Gordon and Hura, 2002; Bellissent and Dore, 1994). The use of hexagonal boron nitride as a catalyst in water solvent requires a basic understanding of the interaction between water and the h-BN surface and is important in understanding the water-BN interface. Cheng *et al*., 2017 reported that the h-BN showed a strong interaction between O-H bonds of water molecule at 3420 cm^{-1} in the ligand free C-C coupling reaction using h-BN supported palladium (II) as a catalyst. The reactions had high efficiencies with excellent yields when conducted in water (Cheng *et al*., 2017).

The recyclability of a catalyst is usually conducted to determine cost effectiveness. I/BN was recycled for the model reaction (**Fig. 10**). Briefly, after a reaction, I/BN was collected after a simple filtration of the reaction content. The filtered I/BN was washed with a $CHCl_3$: MeOH (1:1) combination followed by acetone. The solid was dried in an oven for 1-2 h and subsequently employed for five successive cycles on the model reaction. There was a loss of only 12 % in catalytic activity after five cycles hence the catalyst is good for possible scale-up.

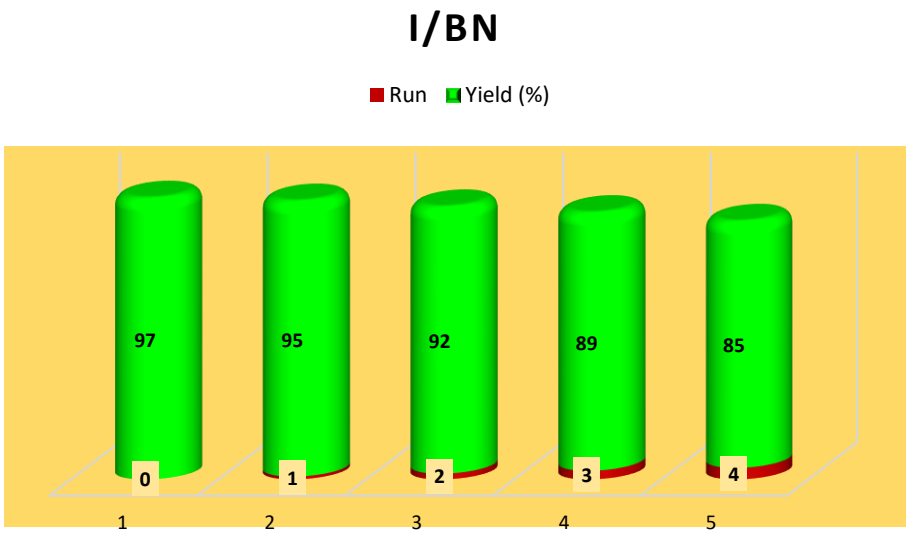

Fig. 10. Recyclability of the catalyst I/BN

Furthermore, the efficiency of I/BN was compared with previously reported catalysts and commercially available catalysts **(Table 4)**.

Table 4. A comparison of catalyst for the synthesis of dihydropyridines

Entry	Catalyst	Condition	Time	Yield (%)	References
1	Silica gel/$NaHSO_4$	CH_3CN/Stirring	6 h	85	Chari *et al*., 2005
2	$AlCl_3.6H_2O$	Heating (60°C)	1 h	83	Sharma, *et al*., 2008
3	TMSI/NaI	CH_3CN/Stirring	2 h	85	Sabitha *et al*., 2003
4	$HClO_4$-SiO_2	Stirring	20 min	95	Maheswara *et al*., 2006
5	PPh_3	EtOH/Reflux	5 h	72	Debache *et al*., 2009
6	$F_3C_6H_2COOH$	Stirring	4 h	90	Sridhar *et al*., 2005
7	I/BN	Sonication	3 min	97	Present work

The reaction time was long and the percentage yield was less for various catalysts (**Table 4**). These catalysts (**Table 4**, entries 7-14) produced 25-39 % yield making them less effective. The procedure for the synthesis of **22** provided a way to compare the effectiveness of I/BN with other reported catalysts and 97 % yield was observed in the current study, in a relatively shorter reaction time of 3 minutes.

Special efforts were made to evaluate and compare the conventional techniques with the ultrasonic irradiation technique: the results are shown in **Table 5**. Without sonication, **22** was obtained with 51 % yield by stirring at room temperature for 24 h. When the same mole ratio of the catalyst was used under reflux conditions for 24 h, 63 % yield was obtained **(Table 5**, entry 2). The effect of ultrasonic irradiation with different power was also investigated **(Table 5**, entries 3-6). It was clearly observed that the ultrasonic irradiation power of 70 W afforded the best yield (97 %) after 3 minutes **(Table 5**, entry 5).

Table 5. Effects of sonication

Entry	Power (W)	Time (min)	Yield (%) [b]
1	Without sonication (r.t)	24 h	51
2	Without sonication (110 °C)	24 h	63
3	40	15	42
4	60	10	70
5	70	3	97
6	80	12	90

[b] Isolated yields

Having established the framework of BTQ-DHP in a one-pot fashion, the reaction scope was profiled for other derivatives. The reaction proceeded smoothly with different

anilines. These compounds were characterised by FTIR, ^{1}H-NMR, ^{13}C-NMR and elemental analysis (**Appendix VI**). A chemical library of fused benzylthioquinoline-1,4-dihydropyridines (**Table 6**) was obtained.

Table 6. Synthesis of BTQ-DHPs by I/BN under ultrasonication

Entry	Aldehyde	Amine	Product	Product	Time (min)	Yield (%) [b]
1	$C_{17}H_{13}NOS$	C_7H_9NO	$C_{33}H_{28}N_4O_5S$	**22**	3	97
2	$C_{17}H_{13}NOS$	C_6H_6FN	$C_{32}H_{25}FN_4O_4S$	**23**	5	90
3	$C_{17}H_{13}NOS$	$C_6H_7N_3O_2$	$C_{32}H_{26}N_6O_6S$	**24**	8	88
4	$C_{17}H_{13}NOS$	C_6H_7N	$C_{32}H_{26}N_4O_4S$	**25**	3	97
5	$C_{17}H_{13}NOS$	C_7H_9N	$C_{33}H_{28}N_4O_4S$	**26**	5	96
6	$C_{17}H_{13}NOS$	C_7H_9N	$C_{33}H_{28}N_4O_4S$	**27**	4	95
7	$C_{17}H_{13}NOS$	$C_6H_6N_2O_2$	$C_{32}H_{25}N_5O_6S$	**28**	5	89
8	$C_{17}H_{13}NOS$	C_7H_9NO	$C_{33}H_{28}N_4O_5S$	**29**	3	97
9	$C_{17}H_{13}NOS$	$C_8H_{11}N$	$C_{34}H_{30}N_4O_4S$	**30**	4	93
10	$C_{17}H_{13}NOS$	$C_6H_8N_2$	$C_{32}H_{27}N_5O_4S$	**31**	5	90
11	$C_{17}H_{13}NOS$	$C_6H_{16}N_4$	$C_{32}H_{35}N_7O_4S$	**32**	6	90
12	$C_{17}H_{13}NOS$	$C_6H_5Cl_2N$	$C_{32}H_{24}Cl_2N_4O_4S$	**33**	8	88
13	$C_{17}H_{13}NOS$	C_6H_6BrN	$C_{32}H_{25}BrN_4O_4S$	**34**	8	87
14	$C_{17}H_{12}FNOS$	$C_8H_{11}N$	$C_{34}H_{29}FN_4O_4S$	**35**	6	92

b Isolated yields

It was determined that the presence of an electron donating group in the amine enabled a faster reaction with higher product yields. The presence of electron withdrawing groups slowed the reaction. Thus the one-pot multi-component synthesis of BTQ-DHPs **(22-35)** was successful.

A plausible mechanism is proposed for the formation of BTQ-DHPs (**Scheme 3**). The isoelectronic nature of boron nitride increased the electrophilicity of the carbonyl carbon of aldehyde groups (Ruifang *et al*., 2016). In the first transformation, aryl aldehyde **1** and malononitrile **2** forms a Knoevenagel condensed product **5a** by removal of a water molecule. Thereafter, the catalyst promoted the formation of an intermediate **5b** with a 1:1 interaction between *o*-anisidine **3** and dimethyl acetylene dicarboxylate **4**. The intermediate **5b** attacked the Knoevenagel adduct **5a** obtained from the initial step and produced a 1,5-dipolar intermediate **6**. The subsequently generated intermediate **7** was transformed into **8** and finally the corresponding product **9** was obtained presumably upon ring closure and a tautomerization processes.

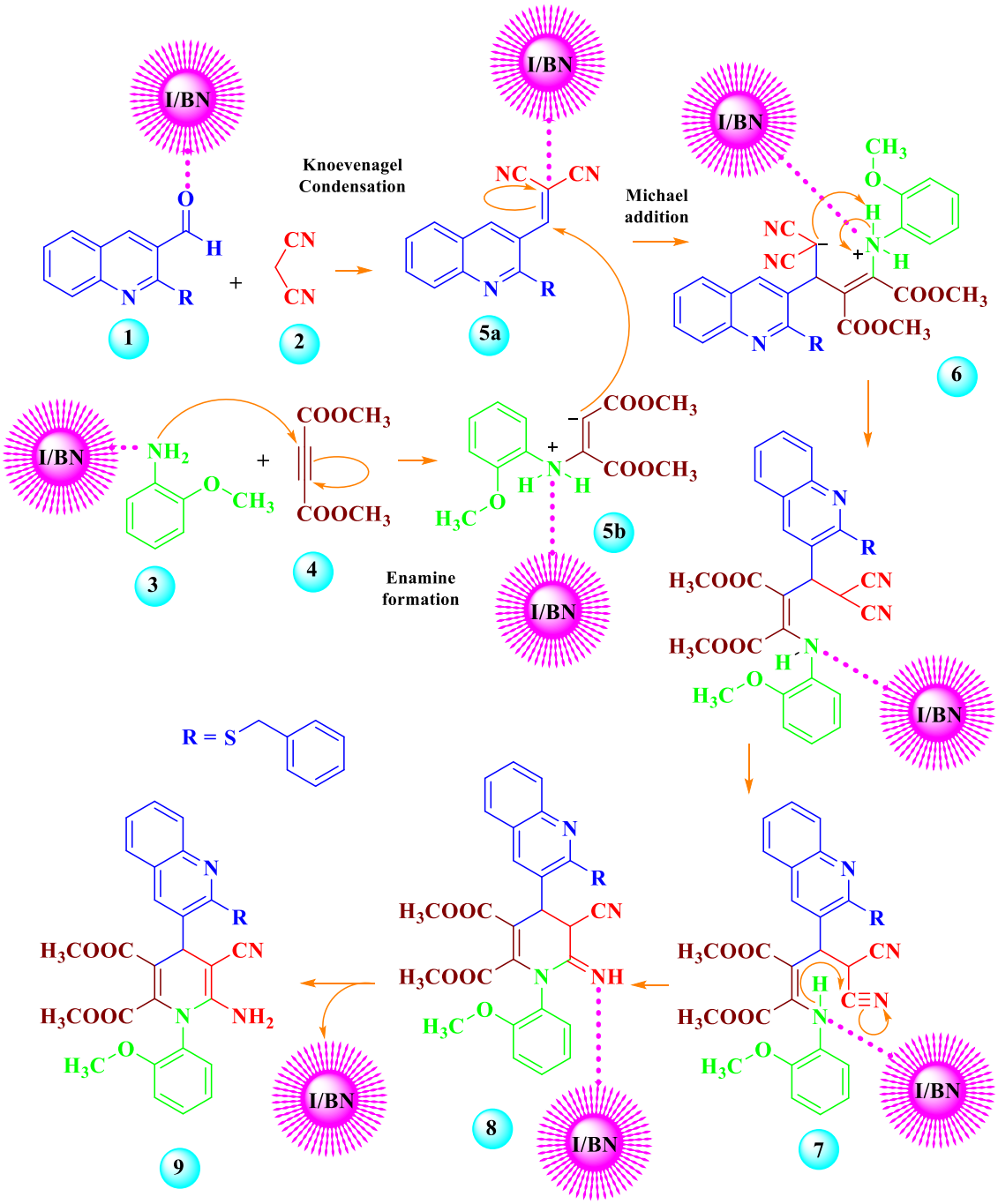

Scheme 3. Plausible mechanism for the formation of BTQ-DHPs

Antibacterial resistance is a challenge that is associated with high morbidity and mortality (Wesgate *et al.*, 2016). Multidrug resistance patterns in Gram-positive and Gram-negative bacteria are difficult to treat and may even be untreatable with conventional antibiotics. There is currently a shortage of effective therapies, lack of successful prevention measures, and only a few new antibiotics available, which require

development of treatment options and alternative antibacterial therapies (Laxminarayan *et al*., 2013). Dihydropyridines were involved in multidrug resistance and can present challenges for infection control.

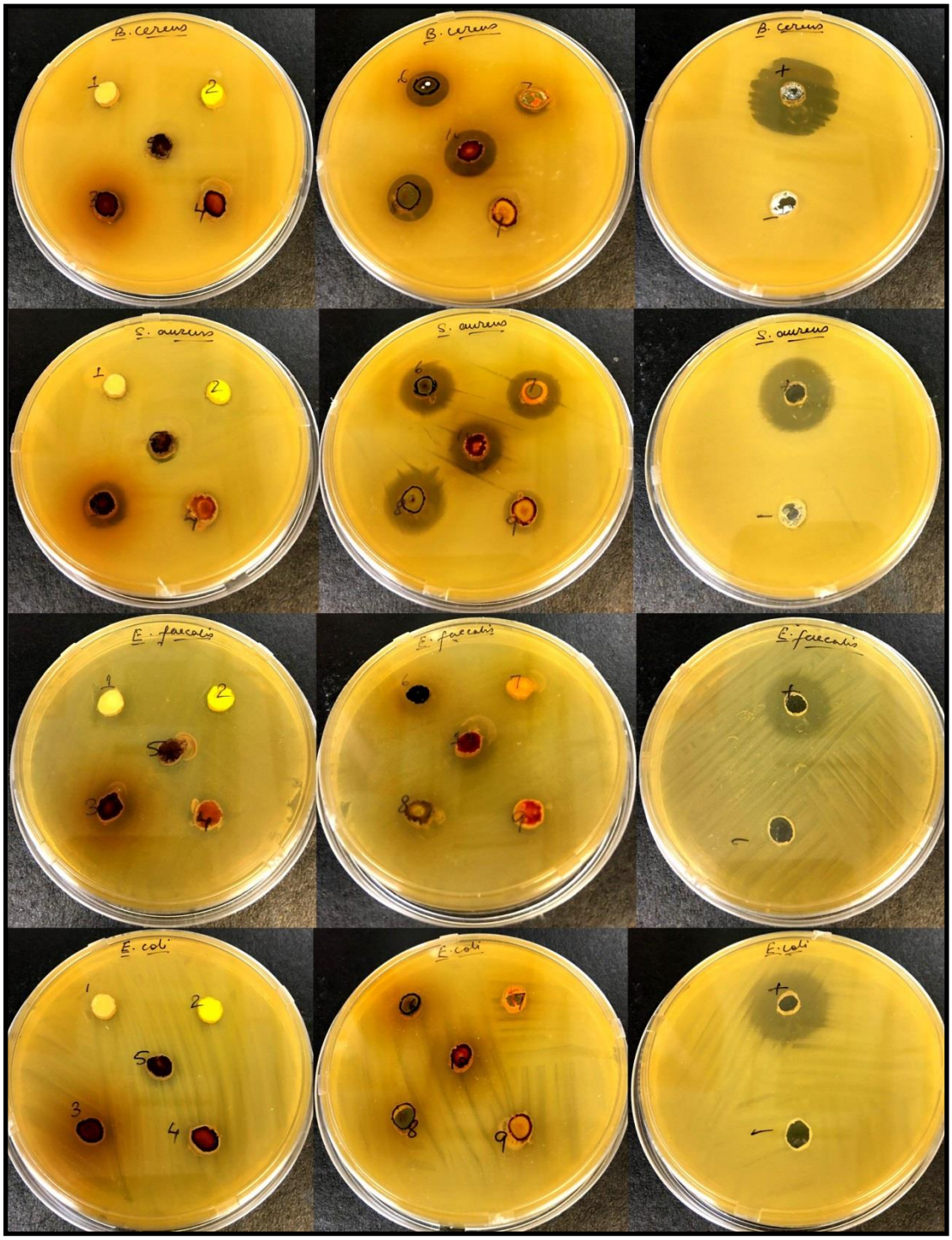

Fig. 11. Antibacterial activity of BTQ-DHPs

1= **22**; 2= **23**; 3= **24**; 4= **25**; 5= **26**; 6= **27**; 7= **28**; 8= **29**; 9= **30**; 10= **31**.

In this present study, a total of 10 benzylthioquinolinyl dihydropyridines (BTQ-DHPs) were screened with pathogenic strains of Gram-positive and Gram-negative bacteria.

The antibacterial activity of benzylthioquinolinyl dihydropyridine derivatives was evaluated by determining the zone of inhibition against a range of bacteria (*Bacillus cereus* (*B. cereus*), *Staphylococcus aureus* (*S. aureus*), *Escherichia coli* (*E. coli*) and *Enterococcus faecalis* (*E. faecalis*)) (**Fig. 11**). The present investigation focused on Gram-positive and Gram-negative bacteria which showed that compounds **24**, **27**, **28**, **29**, **30** and **31** had preferential activity towards Gram-positive species (**Fig. 11**; **Table 7**). Moreover, compounds **28** and **30** showed activity against *S. aureus* only. Among BTQ-DHPs, compound **24** showed potential activity against *E. faecalis*. There were no potential activities obtained against *E.coli* **(Fig. 11**; **Table 7)**. The zone of inhibition by BTQ-DHPs is mentioned in **Table 7**. BTQ-DHPs containing sulfur-based quinoline as the core structure with an amine and nitro group (**24**), methyl groups (**27** and **30**), nitro group (**28**), methoxy group (**29**) and pyridinyl group (**31**) showed potential against Gram-positive species.

Table 7. Antibacterial activity of BTQ-DHP derivatives

Bacteria	Zone of inhibition by benzylthio quinolinyl dihydropyridine (BTQ-DHP) derivatives										Ciprofloxacin (Positive control)
	1	2	3	4	5	6	7	8	9	10	
Bacillus cereus	0	0	0	0	0	14 ± 0.4	0	15 ± 0.3	0	14 ± 0.3	27 ± 0.3
Staphylococcus aureus	0	0	12 ± 0.3	0	0	20 ± 0.3	19 ± 0.4	22 ± 0.4	10 ± 0.3	19 ± 0.3	25 ± 0.4
Escherichia coli	0	0	0	0	0	0	0	0	0	0	25 ± 0.3
Enterococcus faecalis	0	0	12 ± 0.3	0	0	0	0	0	0	0	24 ± 0.4

1= **22**; 2= **23**; 3= **24**; 4= **25**; 5= **26**; 6= **27**; 7= **28**; 8= **29**; 9= **30**; 10= **31**.

The potential activity of BTQ-DHPs against *S. aureus* might be due to the presence of a methyl group (**27**), methoxy group (**29**) and pyridinyl group with a benzylthioquinoline substrate (**31**). The presence of an amine and nitro group (**24**) containing benzylthioquinolinyl-1,4-dihydropyridine showed preferential activity towards *E. faecalis*.

Antioxidants are considered important nutraceuticals due to many health benefits (Valko *et al*., 2007). The antioxidant activity using 2,2-diphenyl-1-picryl-hydrazyl-hydrate (DPPH) assay was investigated. The scavenging assay was used for initial screening of

the compounds for their antioxidant activity. A total of 10 BTQ-DHPs were tested. Among them, BTQ-DHPs containing sulfur-based quinoline as core structure with a methoxy group (**22**), amine and nitro group (**24**), nitro group (**28**) and pyridinyl group (**31**) showed significant DPPH scavenging activities.

Brine shrimp is used for preliminary assessment of toxicity (Rajabi *et al*., 2015). The toxicity was assessed for all BTQPs at different time intervals (24 h and 48 h), which showed activity towards Gram-positive or Gram-negative species. We found that among all compounds tested, **22**, **24**, **27**, **28** and **31** were less toxic, having mortality rates below 50% (**Fig. 12**), which suggested that these compounds are safe for further biological applications (Meyer *et al*., 1982). BTQ-DHPs containing sulfur-based quinoline as core structure with a methoxy group (**22**), amine and nitro group (**24**), methyl group (**27**), nitro group (**28**) and pyridinyl group (**31**) showed mortality rate below than 50%.

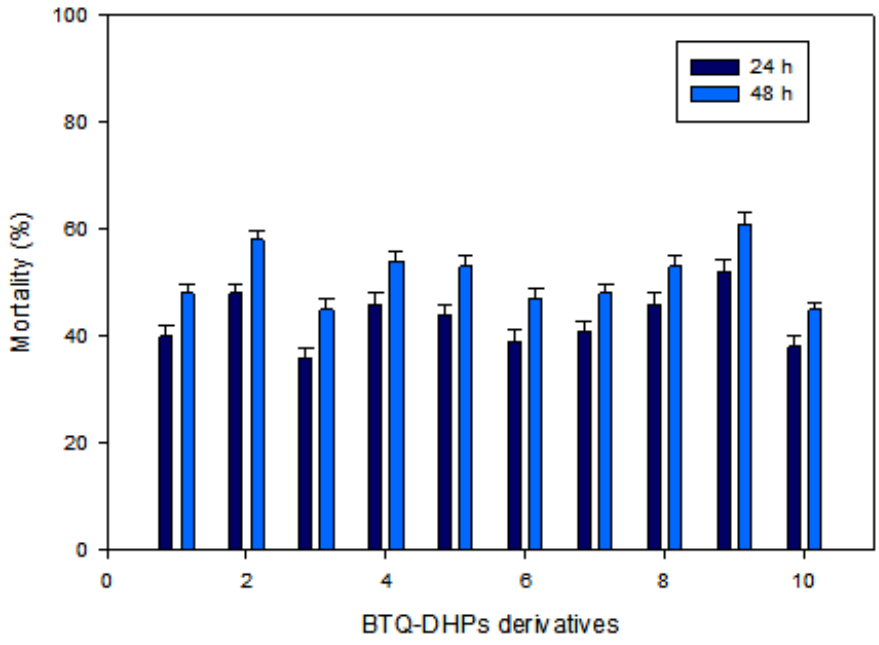

Fig. 12. Toxicity of BTQ-DHPs was assessed using *Artemia salina* (brine shrimp)

1= **22**; 2= **23**; 3= **24**; 4= **25**; 5= **26**; 6= **27**; 7= **28**; 8= **29**; 9= **30**; 10= **31**.

Molecular docking is one of the computational techniques used to identify the ligand-protein interaction. In this study, molecular docking was used for benzylthioquinolinyl-1,4-dihydropyridines to predict the affinity toward *S. aureus* gyrase. The recently reported crystal structure of *S. aureus* gyrase was employed to conduct molecular

docking (PDB ID: 4PLB) (Singh *et al*., 2014). To perform molecular docking, Discovery Studio software was employed (Biovia, 2015). Initially, the ligands were constructed in Chem 3D Biodraw software and then minimized by MM2 method. The minimized 3D structure of the ligands was prepared for the ionization state, stereoisomers, conformation generation etc. in Discovery Studio software. Furthermore, the crystal structure of *S. aureus* gyrase was also prepared in Chimera software (Pettersen *et al*., 2004). During the preparation, the structure was fixed by adding missing hydrogen, removing water molecules etc. Then, molecular docking was conducted in Discovery Studio software using the Libdock module.

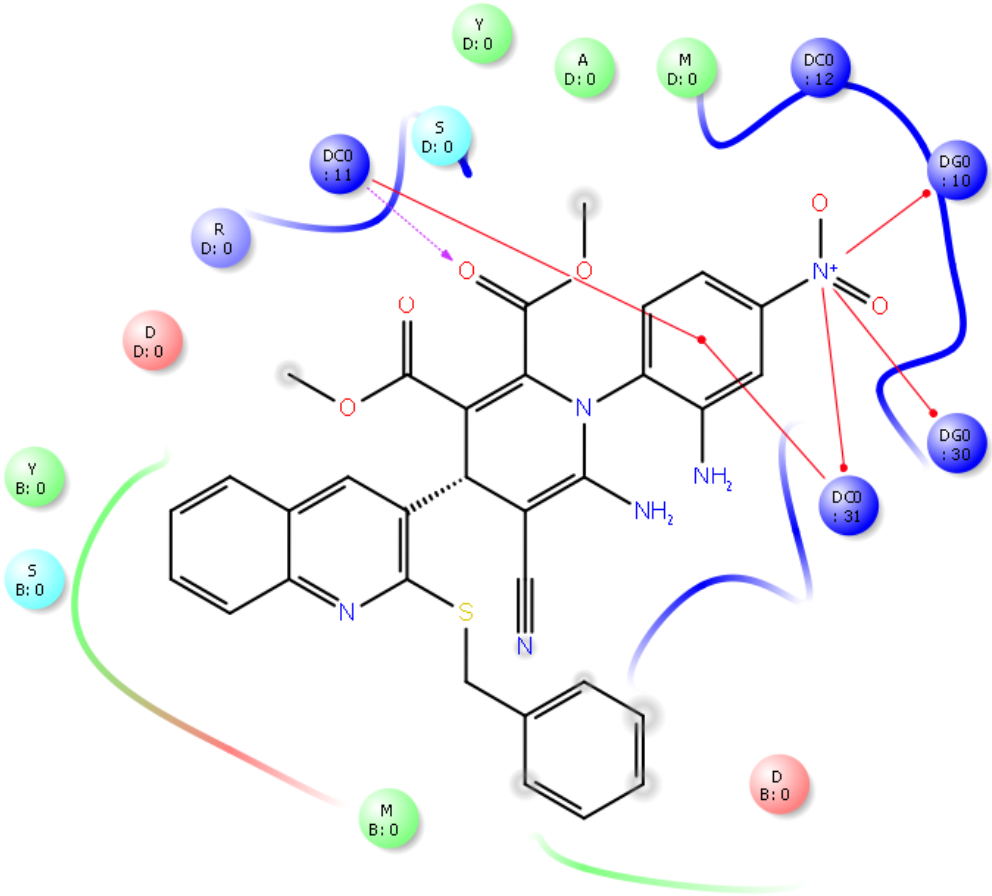

Fig. 13. Ligand-protein bonding interaction of **24** with *Staphylococcus aureus* gyrase enzyme.

The ligands were docked at 15Å sphere which was generated around the bound ligand of *S. aureus* gyrase. The results of molecular docking were analysed to estimate the ligand-protein interactions based on Libdock score.

Table 8. Molecular docking scores of BTQ-DHPs with *Staphylococcus aureus* gyrase

Entry	Molecule	Absolute Energy	LibDock Score
1	**22**	132.43	123.58
2	**23**	115.564	120.31
3	**24**	117.96	125.27
4	**25**	121.08	116.75
5	**26**	126.74	108.90
6	**27**	124.30	106.04
7	**28**	130.25	83.20
8	**29**	119.45	108.7
9	**30**	118.99	118.07
10	**31**	112.467	110.52
11	Reference Ligand AM8191	80.31	193.142

The docked benzylthioquinolinyl-1,4-dihydropyridines have shown Libdock scores ranging from 83.20 to 125.27 kcal/mol. The molecule **24** showed more potency among the series toward *S. aureus* gyrase by forming a strong ligand-protein interaction with the Libdock score of 125.27 kcal/mol (**Fig. 13**). Molecular docking scores of benzylthioquinolinyl-1,4-dihydropyridines toward *S. aureus* gyrase is mentioned in **Table 8.**

6.4. Conclusion

In conclusion, a novel, clean and efficient procedure for the synthesis of benzylthioquinoline-1,4-dihydropyridines via a one-pot four-component condensation reaction was developed. The product yields were excellent when iodine-loaded boron nitride (I/BN) was used as a catalyst. The catalyst was characterized by XRD, SEM with EDX, TEM, TGA, DSC and FTIR analysis. A total of 14 novel BTQ-DHPs were synthesised and characterized by FTIR, ^{1}H-NMR, ^{13}C-NMR and elemental analysis. 10 BTQ-DHP derivatives were evaluated for antibacterial and antioxidant activities: Compounds **24**, **26**, **27**, **28**, **29**, **30** and **31** showed positive results for antibacterial activity and **22**, **24**, **28** and **31** showed positive results for antioxidant activity respectively. Since these BTQ-DHPs showed antibacterial and antioxidant activity and are also safe for biological studies, they could be further investigated for pharmaceutical applications. A series of benzylthioquinolinyl-1,4-dihydropyridines were investigated by the molecular docking approach to estimate their biological importance. Among them, **24** showed stronger potency toward *S. aureus* gyrase. The procedure established in the study has

several advantages including high efficiency, recyclable performance, short reaction times, high yields and using water as solvent, which has the potential application in green synthesis.

6.5. Experimental

Typical procedure for the preparation of iodine-loaded boron nitride

To a solution of iodine (0.10 g, 0.8 mmol), in THF (50 mL), boron nitride (2.66 g, 0.1 mol) was added and the suspension was stirred at room temperature for 3 days. The mixture was filtered and the resultant powder was washed with THF repeatedly and subsequently dried in furnace at 400℃. The iodine-loaded boron nitride I/BN was obtained as a white powder mass of 2.750 g, 98 % yield.

General procedure for the ultrasonicated synthesis of benzylthioquinoline-1,4-dihydropyridines

To a solution of **18** (1 mmol) and **19** (1 mmol) in water (15 mL), I/BN (10 mol %) was added and the reaction mixture was sonicated in an ultrasonic apparatus with 70 W power at room temperature for 1 minute. After the addition of **20** (1 mmol) and **21** (1 mmol), the reaction mixture was sonicated for 2 minutes. The progress of the reaction was monitored by TLC. Following completion, I/BN catalyst was isolated by simple filtration. The residue was purified by column chromatography (eluent: ethyl acetate: petroleum ether, 25 %) followed by EtOAc: H_2O (2:1) separation. Thereafter, recrystallization of the product was performed at 5:1 EtOAc: MeOH to yield the pure desired product.

Bacterial strains

The antibacterial activity of each synthesized compound was assessed using four bacterial strains (*Bacillus cereus, Staphylococcus aureus, Escherichia coli* and *Enterococcus faecalis*) causing diseases. The bacterial strains were provided from the culture collection of Department of Biotechnology and Food Technology, Durban University of Technology, South Africa.

Inoculum preparation

Each bacterial strain was sub-cultured overnight at 37 °C on a Mueller-Hilton agar plate. Further, bacterial cultures were grown in Mueller-Hilton broth at 37 °C, 200 rpm in order to attain the viable count of approximately 10^8 cfu/mL.

Antibacterial activity

The agar well diffusion method was used to evaluate the antibacterial activity of each compound. Hundred microliter of ~ 10^8 cfu/mL bacterial suspension was plated on Mueller-Hinton Agar plates. A well of 6 mm diameter was made using a sterile cork borer and 30 µL of each compound (3 mg/ml) was added in each well and kept at 37 °C for 16 h. The assays were carried out in triplicate. Ciprofloxacin (3 mg/ml) was used as positive control and DMSO (100%) as a negative control.

Antioxidant assays of BTQ-DHP derivatives

The antioxidant activity of BTQ-DHPs were determined by the decolourization of methanol solution of 2,2-diphenyl-1-picrylhydrazyl hydrate (DPPH). Hundred microliter of each compound was added separately to 1 mL of 0.1 mM DPPH solution, and the colour change was observed at regular intervals. Rutin hydrate was used as the positive control and methanol (95%) as negative control.

Toxicity assessment

The brine shrimp larvae (*Artemia salina*) were hatched in sea water for 24-48 h prior to being used. An aliquot of 5 mL sea water containing ten brine shrimp was added to each vial and supplemented with different derivatives of BTQ-DHP. Derivative solution volumes of 300 µg were used in individual vials. Brine shrimp death was observed at regular intervals (24 h and 48 h) in order to determine the toxic nature of each compound.

References

[1] (a) Dömling, A. 2006. Recent developments in isocyanide based multicomponent reactions in applied chemistry. Chemical Reviews, (106) 17-89. (b) Dömling, A., Ugi, I. 2000. Multicomponent reactions with isocyanides. Angewandte Chemie International Edition, (39) 3168-3210. (c) Nair, V., Rajesh, C., Vinod, A. U., Bindu, S., Sreekanth, A. R., Mathen, J. S., Balagopal, L. 2003. Strategies for heterocyclic construction via novel multicomponent reactions based on isocyanides and nucleophilic carbenes. Accounts of Chemical Research, (36) 899-907. (d) Wan, J. P., Liu, Y. 2011. Multicomponent reactions promoted by organosilicon reagents. Current Organic Chemistry, (15) 2758-2773.

[2] Borowicz, K. K., Gasior, M., Kleinrok, Z., Czuczwar, S. J. 1997. Influence of isradipine, niguldipine and dantrolene on the anticonvulsive action of conventional anti epileptics in mice. European Journal of Pharmacology, (323) 45-51.

[3] Loev, B., Goodman, M. M., Snader, K. M., Tedeschi, R., Macko, E. 1974. Hantzsch-type dihydropyridine hypotensive agents. Journal of Medicinal Chemistry, (17) 956-965.

[4] Bossert, F., Meyer, H., Wehinger, E. 1981. 4-Aryldihydropyridines, a new class of highly active calcium antagonists. Angewandte Chemie International Edition in English, (20) 762-769.

[5] Breitenbucher, J. G., Figliozz, G. 2000. Solid-phase synthesis of 4-aryl-1,4-dihydropyridines via the Hantzsch three component condensation. Tetrahedron Letters, (41) 4311-4315.

[6] Boer, R., Gekeler, V. 1995. Chemosensitizers in tumor therapy: new compounds promise better efficacy. Drugs of the Future, (20) 499-510.

[7] Briukhanov, V. M., Zverev, I., Elkin, V. I. 1993. The effect of calcium antagonists on the development of inflammatory edema in rats. Clinics and Pharmacology, (57) 47-49.

[8] Sushilkumar, B., Devanand. S. 2002. Synthesis and anti-inflammatory activity of 1,4-dihydropyridines. Acta Pharmaceutica, (52) 281-287.

[9] Gullapalli, S., Ramarao, P. 2002. L-type Ca^{2+} channel modulation by dihydropyridines potentiates κ-opioid receptor agonist induced acute analgesia and inhibits development of tolerance in rats. Neuropharmacology, (42) 467-475.

[10] Sunkel, C. E., Fau de Casa-Juana, M., Santos, L., Mar Gomez, M., Villarroya, M., Gonzalez-Morales, M. A., Priego, J. G., Ortega, M. P. 1990. 4-Alkyl-1,4-dihydropyridine derivatives as specific PAF-acether antagonists. Journal of Medicinal Chemistry, (33) 3205-3210.

[11] Ono, H., Kimura, M. 1981. Effect of Ca^{2+} antagonistic vasodilators, diltiazem, nifedipine, perhexiline and verapamil, on platelet aggregation in vitro. Arzneimittel-Forschung, (31) 1131-1134.

[12] Vijesh, A. M., Isloor, A. M., Peethambar, S. K., Shivananda, K. N., Arulmoli, T., Isloor, N. A. 2011. Hantzsch reaction: Synthesis and characterization of some new 1, 4-dihydropyridine derivatives as potent antimicrobial and antioxidant agents. European Journal of Medicinal Chemistry, (460) 5591-5597.

[13] Gasparotto, V., Castagliuolo, I., Chiarelotto, G., Pezzi, V., Montanaro, D., Brun, P., Palù, G., Viola, G., Ferlin, M. G. 2006. Synthesis and biological activity of 7-phenyl-6,9-dihydro-3H-pyrrolo [3,2-f] quinolin-9-ones: A new class of antimitotic agents devoid of aromatase activity. Journal of Medicinal Chemistry, (49) 1910-1915.

[14] (a) Alhaider, A. A., Abdelkader, M. A., Lien, E. J. 1985. Design, synthesis and pharmacological activities of 2-substituted 4-phenylquinolines as potential antidepressant drugs. Journal of Medicinal Chemistry, (28) 1394-1398. (b) Segawa, J., Kitano, M., Kazuno, K., Matsuoka, M., Shirahase, I., Ozaki, M., Matsuda, M., Tomii, Y., Kise, M. 1992. Studies on pyridone carboxylic acids. 1. Synthesis and antibacterial evaluation of 7-substituted-6-halo-4-oxo-4H-[1,3] thiazeto [3,2-a] quinoline-3-carboxylic acids. Journal of Medicinal Chemistry, (350) 4727-4738. (c) Jinbo, Y., Kondo, H., Inoue, Y., Taguchi, M., Tsujishita, H., Kotera, Y., Sakamoto, F., Tsukamoto, G. 1993. Synthesis and antibacterial activity of a new series of tetracyclic pyridone carboxylic acids. Journal of Medicinal Chemistry, (36) 2621-2626.

[15] Joseph, B., Darro, F., Béhard, A., Lesur, B., Collignon, F., Decaestecker, C., Frydman, A., Guillaumet, G., Kiss, R. 2002. 3-Aryl-2-quinolone derivatives: Synthesis and characterization of in vitro and in vivo antitumor effects with emphasis on a new therapeutical target connected with cell migration. Journal of Medicinal Chemistry, (45) 2543-2555.

[16] (a) Xavier, J. F. 1958. 2-Mercaptoquinoline (thiocarbostyril) as an analytical reagent for copper and palladium. Fresenius' Zeitschrift für analytische Chemie,

(163) 182-185. (b) Nakano, S., Yoshida, T., Taniguchi, H., Suzuki, N. 1977. Quinoline-2-thiol Derivatives as Organic Reagents. I. Spectrophotometric Investigations on the Coloration with Some Metal Ions. Chemical and Pharmaceutical Bulletin, (25) 1658-1664. (c) Leeaphon, M., Ondracek, A. L., Thomas, R. J., Fanwick, P. E., Walton, R. A. 1995. Reactions of rhenium polyhydrides with internal and terminal alkynes as a route to a new class of hydrido-alkylidyne complexes. Journal of the American Chemical Society, (117) 9715-9724.

[17] (a) Zhang, J., Matteucci, M. D. 1999. A novel thiol protecting group: A 2-thioquinoline sulfide as a masked sulfhydryl moiety. Tetrahedron Letters, (40) 1467-1470. (b) Nakamura, S., Furutani, A., Toru, T. 2002. Highly enantioselective reaction of α-lithio 2-quinolyl sulfide using chiral bis (oxazoline)s: A new synthesis of enantioenriched thiols. European Journal of Organic Chemistry, (10) 1690-1695.

[18] Molina, P., Alajarín, M., Vidal, A. 1989. Ortho-pyrrolyl phenyl heterocumulenes: Preparation and cyclization to fused pyrroles. Tetrahedron Letters, (30) 2847-2850.

[19] Chari, M. A., Syamasundar, K. 2005. Silica gel/$NaHSO_4$ catalyzed one-pot synthesis of Hantzsch 1,4-dihydropyridines at ambient temperature. Catalysis Communications, (6) 624-626.

[20] Sharma, S. D., Hazarika, P., Konwar, D. 2008. A simple, green and one-pot four-component synthesis of 1,4-dihydropyridines and their aromatization. Catalysis Communications, (9) 709-714.

[21] Sabitha, G., Reddy, G. K. K., Reddy, C. S., Yadav, J. S. 2003. A novel TMSI-mediated synthesis of Hantzsch 1,4-dihydropyridines at ambient temperature. Tetrahedron Letters, (44) 4129-4131.

[22] Maheswara, M., Siddaiah, V., Rao, Y. K., Tzeng, Y. M., Sridhar, C. 2006. A simple and efficient one-pot synthesis of 1, 4-dihydropyridines using heterogeneous catalyst under solvent-free conditions. Journal of Molecular Catalysis A: Chemical, (260) 179-180.

[23] Debache, A., Ghalem, W., Boulcina, R., Belfaitah, A., Rhouati, S., Carboni, B. 2009. An efficient one-step synthesis of 1,4-dihydropyridines via a triphenylphosphine-catalyzed three-component Hantzsch reaction under mild conditions. Tetrahedron Letters, (50) 5248-5250.

[24] Li, M., Guo, W. S., Wen, L. R., Li, Y. F., Yang, H. Z. 2006. One-pot synthesis of Biginelli and Hantzsch products catalyzed by non-toxic ionic liquid (BMImSac) and structural determination of two products. Journal of Molecular Catalysis A: Chemical, (258) 133-138.

[25] Sridhar, R., Perumal, P. T. 2005. A new protocol to synthesize 1,4-dihydropyridines by using 3, 4, 5-trifluorobenzeneboronic acid as a catalyst in ionic liquid: Synthesis of novel 4-(3-carboxyl-1H-pyrazol-4-yl)-1, 4-dihydropyridines. Tetrahedron, (61) 2465-2470.

[26] Sabitha, G., Reddy, G. K. K., Reddy, C. S., Yadav, J. S. 2003. A novel TMSI-mediated synthesis of Hantzsch 1,4-dihydropyridines at ambient temperature. Tetrahedron Letters, (44) 4129-4131.

[27] Donelson, J. L., Gibbs, R. A., De, S. K. 2006. An efficient one-pot synthesis of poly hydroquinoline derivatives through the Hantzsch four component condensation. Journal of Molecular Catalysis A: Chemical, (256) 309-311.

[28] Das, B., Ravikanth, B., Ramu, R., Rao, B. V. 2006. An efficient one-pot synthesis of polyhydroquinolines at room temperature using HY-zeolite. Chemical and Pharmaceutical Bulletin, (54) 1044-1045.

[29] Reddy, C. S., Raghu, M. 2008. Cerium (IV) ammonium nitrate catalysed facile and efficient synthesis of poly hydroquinoline derivatives through Hantzsch multicomponent condensation. Chinese Chemical Letters, (19) 775-779.

[30] Wang, L. M., Sheng, J., Zhang, L., Han, J. W., Fan, Z. Y., Tian, H., Qian, C. T. 2005. Facile $Yb(OTf)_3$ promoted one-pot synthesis of poly hydroquinoline derivatives through Hantzsch reaction. Tetrahedron, (61) 1539-1543.

[31] Kumar, A., Maurya, R. A. 2007. Synthesis of poly hydroquinoline derivatives through unsymmetric Hantzsch reaction using organocatalysts. Tetrahedron, (63) 1946-1952.

[32] Yavari, I., Bayat, M. J., Sirouspour, M.. Souri, S. 2010. One-pot synthesis of highly functionalized 1, 2-dihydropyridines from primary alkylamines, alkyl isocyanides, and acetylenic esters. Tetrahedron, (66) 7995-7999.

[33] Sridharan, V., Perumal, P. T., Avendano, C., Menendez, J. C. 2007. A new three-component domino synthesis of 1, 4-dihydropyridines. Tetrahedron, (63) 4407-4413.

[34] Debache, A., Ghalem, W., Boulcina, R., Belfaitah, A., Rhouati, S., Carboni, B. 2009. An efficient one-step synthesis of 1, 4-dihydropyridines via a

triphenylphosphine-catalyzed three-component Hantzsch reaction under mild conditions. Tetrahedron Letters, (50) 5248-5250.

[35] Sabitha, G., Arundhathi, K., Sudhakar, K., Sastry, B. S., Yadav, J. S. 2009. $CeCl_3 \cdot 7H_2O$-catalyzed one-pot synthesis of hantzsch 1, 4-dihydropyridines at room temperature. Synthetic Communications, (39) 2843-2851.

[36] Arslan, M., Faydali, C., Zengin, M., Küçükislamoğlu, M., Demirhan, H. 2009. An efficient one-pot synthesis of 1, 4-dihydropyridines using alumina sulfuric acid (ASA) catalyst. Turkish Journal of Chemistry, (33) 769-774.

[37] Cella, R., Stefani, H. A. 2009. Ultrasound in heterocycles chemistry. Tetrahedron, (65) 2619-2641.

[38] Cravotto, G., Cintas, P. 2006. Power ultrasound in organic synthesis: Moving cavitational chemistry from academia to innovative and large-scale applications. Chemical Society Reviews, (35) 180-196.

[39] Spivey, J. J. 1987. Complete catalytic oxidation of volatile organics. Industrial & Engineering Chemistry Research, (26) 2165-2180.

[40] Liu, F., Mo, X., Gan, H., Guo, T., Wang, X., Chen, B., Chen, J., Deng, S., Xu, N., Sekiguchi, T., Golberg, D., 2014. Cheap, gram-scale fabrication of BN nanosheets via substitution reaction of graphite powders and their use for mechanical reinforcement of polymers. Scientific Reports, (4) 4211.

[41] Nag, A., Raidongia, K., Hembram, K. P., Datta, R., Waghmare, U. V., Rao, C. N. R. 2010. Graphene analogues of BN: Novel synthesis and properties. ACS Nano, (4) 1539-1544.

[42] Li, J., Xiao, X., Xu, X., Lin, J., Huang, Y., Xue, Y., Jin, P., Zou, J., Tang, C. 2013. Activated boron nitride as an effective adsorbent for metal ions and organic pollutants. Scientific Reports, (3) 3208.

[43] (a) Primo, A., Navalón, S., Asiri, A. M., García, H. 2015. Chitosan-templated synthesis of few-layers boron nitride and its unforeseen activity as a Fenton catalyst. Chemistry-A European Journal, (21) 324-330. (b) Wang, L., Sun, C., Xu, L., Qian, Y. 2011. Convenient synthesis and applications of gram scale boron nitride nanosheets. Catalysis Science & Technology, (7) 1119-1123. DOI: 10.1039/C1CY00191D. (c) Molla, A., Hussain, S. 2013. Boron nitride: An efficient reusable heterogeneous catalyst for hetero-Michael reactions under solvent-free condition. Current Catalysis, (2) 88-95.

[44] Nag, A., Raidongia, K., Hembram, K. P., Datta, R., Waghmare, U. V., Rao, C. N. R. 2010. Graphene analogues of BN: Novel synthesis and properties. ACS Nano, (4) 1539-1544.

[45] (a) Togo, H., Iida, S. 2006. Synthetic use of molecular iodine for organic synthesis. Synlett, (14) 2159-2175. (b) Ren, Y. M., Cai, C. 2007. Knoevenagel condensation of aromatic aldehydes with active methylene compounds using a catalytic amount of iodine and K_2CO_3 at room temperature. Synthetic Communications, (37) 2209-2213. (c) Ren, Y., Cai, C. 2007. Iodine catalysis in aqueous medium: An improved reaction system for Knoevenagel and Nitroaldol condensation. Catalysis Letters, (118) 134-138. (d) Ren, Y. M., Cai, C. 2008. A green procedure for the protection of carbonyl compounds catalyzed by iodine in ionic liquid. Tetrahedron Letters, (49) 7110-7112.

[46] Stowell, J. K., Widlanski, T. S. 1995. A new method for the phosphorylation of alcohols and phenols. Tetrahedron Letters, (36) 1825-1826.

[47] Kitagawa, O., Aoki, K., Inoue, T., Taguchi, T. 1995. Diels-Alder reaction of N-allylic enamides and lactam derivatives through iodine mediated activation. Tetrahedron Letters, (36) 593-596.

[48] Joseph, R., Pallan, P. S., Sudalai, A., Ravindranathan, T. 1995. Direct conversion of alcohols into the corresponding iodides. Tetrahedron Letters, (36) 609-612.

[49] Hou, Q., Zheng, Y., Chen, J. F., Zhou, W., Deng, J., Tao, X. 2011. Visible-light-response iodine-doped titanium dioxide nanocrystals for dye-sensitized solar cells. Journal of Materials Chemistry, (21) 3877-3883.

[50] Trivedi, M. K., Patil, S., Nayak, G., Jana, S., Latiyal, O. 2015. Influence of biofield treatment on physical, structural and spectral properties of boron nitride. Materials Science and Engineering: A, (4) 4.

[51] Lin, H., Deng, W., Zhou, T., Ning, S., Long, J., Wang, X. 2015. Iodine-modified nano crystalline titania for photo-catalytic antibacterial application under visible light illumination. Applied Catalysis B: Environmental, (176) 36-43.

[52] Scherrer, P. 1918. Determination of the size and internal structure of colloidal particles using X-rays. Gesellschaft der Wissenschaften zu Göttingen, (2) 98-100.

[53] Wen, P., Itoh, H., Tang, W., Feng, Q. 2007. Single nanocrystals of anatase-type TiO_2 prepared from layered titanate nanosheets: Formation mechanism and characterization of surface properties. Langmuir, (23) 11782–11790.

[54] Wang, Y., Yamamoto, Y., Kiyono, H., Shimada, S. 2009. Effect of ambient gas and temperature on crystallization of boron nitride spheres prepared by vapor phase pyrolysis of ammonia borane. Journal of the American Ceramic Society, (92) 787-792.

[55] Danilovas, P. P., Rutkaite, R., Zemaitaitis, A. 2014. Thermal degradation and stability of cationic starches and their complexes with iodine. Carbohydrate Polymers, (112) 721-728.

[56] Oda K, Yoshio, T. 1993. Oxidation kinetics of hexagonal boron nitride powder. Journal of Materials Science, (28) 6562-6566.

[57] Marinoiu, A., Raceanu, M., Carcadea, E., Varlam, M., Balan, D., Ion-Ebrasu, D., Stefanescu, I., Enachescu, M. 2017. Iodine-doped graphene for enhanced electrocatalytic oxygen reduction reaction in proton exchange membrane fuel cell applications. Journal of Electrochemical Energy Conversion and Storage, (14) 031001.

[58] Muthu, T., Anand, K., Sureshkumar, M., Gengan, R.M. 2016. Eco-friendly approach: Graphene like boron nitride modified calcium material for the synthesis of 2-amino-4H-pyran-3-carbonitrile derivatives. Advanced Materials Letters, (7) 790-794.

[59] Hassanzadeh, P., Andrews, L. 1993. Reaction of halogens with laser-ablated boron: Infrared spectra of BXn (X= F, Cl, Br, I; n= 1, 2, 3) in solid argon. The Journal of Physical Chemistry, (97) 4910-4915.

[60] Srivastava, A., Singh, R. M., 2005. Vilsmeier-Haack reagent: a facile synthesis of 2-chloro-3-formylquinolines from N-arylacetamides and transformation into different functionalities. Indian Journal of Chemistry, (44B) 1868-1875.

[61] (a) Hayashi, Y., Itoh, T., Aratake, S., Ishikawa, H. 2008. A diaryl prolinol in an asymmetric, catalytic, and direct crossed-aldol reaction of acetaldehyde. Angewandte Chemie International Edition, (120) 2112-2114. (b) Lindström, U. M. 2002. Stereoselective organic reactions in water. Chemical Reviews, (102) 2751-2772. (c) Head-Gordon, T., Hura, G. 2002. Water structure from scattering experiments and simulation. Chemical Reviews, (102) 2651-2670. (d) Bellissent, M. C., Dore, F. J. C. 1994. Hydrogen bond networks. Kluwer, Academic Publishers, Boston.

[62] Cheng, X., Li, W., Nie, R., Ma, X., Sang, R., Guo, L., Wu, Y. 2017. Ligand-free c–c coupling reactions promoted by hexagonal boron nitride-supported palladium (II) catalyst in water. Advanced Synthesis & Catalysis, (359) 454-466.

[63] Chari, M. A., Syamasundar, K. 2005. Silica gel/$NaHSO_4$ catalyzed one-pot synthesis of Hantzsch 1, 4-dihydropyridines at ambient temperature. Catalysis Communications, (6) 624-626.

[64] Sharma, S. D., Hazarika, P., Konwar, D. 2008. A simple, green and one-pot four-component synthesis of 1,4-dihydropyridines and their aromatization. Catalysis Communications, (9) 709-714.

[65] Sabitha, G., Reddy, G. K. K., Reddy, C. S., Yadav, J. S. 2003. A novel TMSI-mediated synthesis of Hantzsch 1,4-dihydropyridines at ambient temperature. Tetrahedron Letters, (44) 4129-4131.

[66] Maheswara, M., Siddaiah, V., Rao, Y. K., Tzeng, Y. M., Sridhar, C. 2006. A simple and efficient one-pot synthesis of 1,4-dihydropyridines using heterogeneous catalyst under solvent-free conditions. Journal of Molecular Catalysis A: Chemical, (260) 179-180.

[67] Debache, A., Ghalem, W., Boulcina, R., Belfaitah, A., Rhouati, S., Carboni, B. 2009. An efficient one-step synthesis of 1,4-dihydropyridines via a triphenylphosphine-catalyzed three-component Hantzsch reaction under mild conditions. Tetrahedron Letters, (50) 5248-5250.

[68] Sridhar, R., Perumal, P. T. 2005. A new protocol to synthesize 1,4-dihydropyridines by using 3, 4, 5-trifluorobenzeneboronic acid as a catalyst in ionic liquid: Synthesis of novel 4-(3-carboxyl-1H-pyrazol-4-yl)-1, 4-dihydropyridines. Tetrahedron, (61) 2465-2470.

[69] Ruifang, N., Rui, S., Xiaojun, M., Yang, Z., Xu, C., Weijian, L., Li, G., Hui, J., Yong, W. 2016. Copper-γ-cyclodextrin complexes immobilized on hexagonal boron nitride as an efficient catalyst in the multicomponent synthesis of 1,2,3-triazoles. Journal of Catalysis, (344) 286-292.

[70] Wesgate, R., Grasha, P., Maillard. J. Y. 2016. Use of a predictive protocol to measure the antimicrobial resistance risks associated with biocidal product usage. American Journal of Infection Control, (44) 458-464.

[71] Laxminarayan, R., Duse, A., Wattal, C., Zaidi, A. K. M., Wertheim, H. F. L., Sumpradit, N., Vlieghe, E., Hara, G. L., Gould, I. M., Goossens, H., Greko, C., So, A. D., Bigdeli, M. B., Tomson, G., Woodhouse, W., Ombaka, E., Peralta, A.

Q., Qamar, F. N., Mir, F., Kariuki, S., Bhutta, Z. A., Coates, A., Bergstrom, R., Wright, G. D., Brown, E. D., Cars, O. 2013. Antibiotic resistance- the need for global solutions. The Lancet Infectious Diseases, (130) 1057-1098.

[72] Valko, M., Leibfritz, D., Moncol, J., Cronin, M. T., Mazur, M., Telser. J. 2007. Free radicals and antioxidants in normal physiological functions and human disease. The International Journal of Biochemistry & Cell Biology, (39) 44-84.

[73] Rajabi, S., Ramazani, A., Hamidi, M., Naji, T. 2015. Artemia salina as a model organism in toxicity assessment of nanoparticles. DARU Journal of Pharmaceutical Sciences, (23) 20.

[74] Meyer, B. N., Ferrigni, N. R., Putnam, J. E., Jacobsen, L. B., Nichols, D. E., McLaughlin, J. L. 1982. Brine shrimp: a convenient general bioassay for active plant constituents. Planta Medica, (45) 31-34.

[75] Singh, S. B., Kaelin, D. E., Wu, J., Miesel, L., Tan, C. M., Meinke, P. T., Olsen, D., Lagrutta, A., Bradley, P., Lu, J., Patel, S. 2014. Oxabicyclooctane-linked novel bacterial topoisomerase inhibitors as broad spectrum antibacterial agents. ACS Medicinal Chemistry Letters, (5) 609-614.

[76] Biovia, D.S. 2015. Discovery studio modelling environment. San Diego: Dassault Systemes.

[77] Pettersen, E. F., Goddard, T. D., Huang, C. C., Couch, G. S., Greenblatt, D. M., Meng, E. C., Ferrin, T. E. 2004. UCSF Chimera-a visualization system for exploratory research and analysis. Journal of Computational Chemistry, (25) 1605-1612.

Appendix-VI

6.1. Dimethyl 6-amino-4-(2-(benzylthio)quinolin-3-yl)-5-cyano-1-(2-methoxy phenyl)-1,4-dihydropyridine-2,3-dicarboxylate (22)

Pale yellow solid, m.p = 201-203℃ ; IR ν_{max} (cm^{-1}): 2187 C≡N, 1614 C=N, 1277 C-N, 2918 CH, 1652 C=C, 703 C-S, 1736 C=O, 2890 OCH_3, 3308 NH. ^{1}H-NMR: (400 MHz, $CDCl_3$) δ (ppm) 8.19 (1H, s, Ar-H), 8.03 (1H, d, *J*=7.76 Hz, Ar-H), 7.94 (2H, t, *J*=8.44 Hz, Ar-H), 7.81 (1H, d, *J*=8.04 Hz, Ar-H), 7.73 (2H, d, *J*=7.04 Hz, Ar-H), 7.54 (3H, t, *J*=7.6 Hz, Ar-H), 7.28 (3H, t, *J*=7.56 Hz, Ar-H), 7.05 (1H, d, *J*=7.6 Hz, Ar-H), 5.58 (2H, brs, NH_2), 5.03 (1H, s, CH), 4.73 (1H, t, *J*=13.6 Hz, CH_2), 4.57 (1H, t, *J*= 13.56 Hz, CH_2), 3.96 (3H, brs, OCH_3), 3.82 (3H, brs, OCH_3), 2.49 (3H, t, *J*=1.8 Hz, OCH_3). ^{13}C-NMR: (100 MHz, $CDCl_3$) δ (ppm) 164.88, 164.68, 162.73, 157.13, 156.80, 151.30, 146.26, 139.73, 138.32, 135.15, 134.67, 131.99, 131.70, 129.88, 129.14, 128.21, 127.37, 127.22, 126.81, 126.02, 125.84, 123.20, 120.68, 112.83, 103.57, 59.12, 56.47, 52.29, 51.63, 45.75, 33.76. Elemental Analysis: Anal. Calc. for $C_{33}H_{28}N_4O_5S$: C, 66.88; H, 4.76; N, 9.45; %. Found: C, 66.89; H, 4.78; N, 9.47; %.

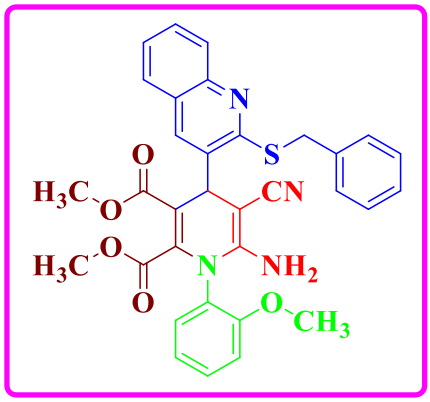

6.2. Dimethyl 6-amino-4-(2-(benzylthio)quinolin-3-yl)-5-cyano-1-(3-fluorophenyl)-1,4-dihydropyridine-2,3-dicarboxylate (23)

Brown solid, m.p = 213-215℃; IR ν_{max} (cm^{-1}): 2163 C≡N, 1219 C=N, 1360 C-N, 2970 CH, 1614 C=C, 705 C-S, 1738 C=O, 2920 OCH_3, 1091 C-F, 3448 NH. ^{1}H-NMR: (400 MHz, DMSO-d_6) δ (ppm) 8.91 (1H, s, Ar-H), 8.31 (2H, d, *J*= 7.68 Hz, Ar-H), 8.10 (1H, d, *J*= 7.32 Hz, Ar-H), 8.00 (1H, d, *J*= 8.32 Hz, Ar-H), 7.91 (1H, td, *J*= 1.36 Hz, Ar-H), 7.61 (1H, td, *J*= 7.04 Hz, Ar-H), 7.49 (2H, d, *J*= 7.16 Hz, Ar-H), 7.42 (2H, s, NH_2), 7.28 (2H, t, *J*= 7.32 Hz, Ar-H), 7.19 (1H, t, *J*= 4.20 Hz, Ar-H), 6.68 (2H, d, *J*=7.08 Hz, Ar-H), 5.89 (1H, s, CH), 4.54 (2H, s, CH_2), 4.31 (3H, s, OCH_3), 4.19 (3H, s, OCH_3). ^{13}C-NMR: (100 MHz, $CDCl_3$) δ (ppm) 159.89, 159.85, 153.12, 150.74, 145.87, 136.85, 136.79,

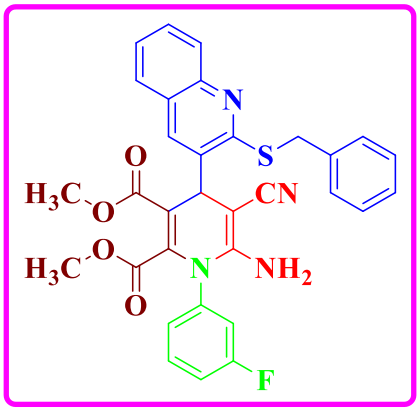

134.43, 134.32, 134.29, 134.18, 129.73, 127.76, 126.78, 125.18, 125.16, 124.55, 124.51, 124.33, 120.81, 118.20, 118.13, 114.80, 114.62, 113.13, 113.10, 63.63, 63.57, 63.30, 63.23, 54.01, 49.37, 47.84, 16.48, 16.42, 16.20, 16.14. Elemental Analysis: Anal. Calc. for $C_{32}H_{25}FN_4O_4S$: C, 66.20; H, 4.34; N, 9.65; %. Found: C, 66.22; H, 4.35; N, 9.67; %.

6.3. Dimethyl 6-amino-1-(2-amino-4-nitrophenyl)-4-(2-(benzylthio)quinolin-3-yl)-5-cyano-1,4-dihydropyridine-2,3-dicarboxylate (24)

Dark yellow, m.p = 231-233℃ ; IR ν_{max} (cm^{-1}): 2155 C≡N, 1642 C=N, 1232 C-N, 3092 CH, 1670 C=C, 659 C-S, 1747 C=O, 2949 OCH_3, 3373 NH. ^{1}H-NMR: (400 MHz, DMSO-d_6) δ (ppm) 11.06 (2H, brs, NH_2), 9.39 (2H, d, *J*= 7.32 Hz, Ar-H), 9.05 (1H, d, *J*= 7.04 Hz, Ar-H), 8.90 (1H, d, *J*= 7.08 Hz, Ar-H), 8.50 (1H, s, Ar-H), 8.09 (1H, s, Ar-H), 7.97 (1H, dd, *J*= 7.68 Hz, Ar-H), 7.85 (2H, s, NH2), 7.54 (1H, t, *J*= 6.76 Hz, Ar-H), 7.24 (1H, s, Ar-H), 7.14 (1H, d, *J*= 8.44 Hz, Ar-H), 6.78 (2H, dd, *J*= 6.44 Hz, Ar-H), 6.48 (1H, t, *J*= 7.00 Hz, Ar-H), 5.57 (1H, s, CH), 4.63 (2H, s, CH_2), 3.69 (3H, s, OCH_3), 2.49 (3H, s, OCH_3). ^{13}C-NMR: (100 MHz, $CDCl_3$) δ (ppm) 159.88, 159.84, 145.96, 145.94, 144.53, 144.39, 136.74, 136.68, 129.71, 129.11, 127.70, 126.87, 125.16, 125.13, 124.32, 123.21, 120.66, 120.64, 114.76, 77.36, 76.72, 63.60, 63.53, 63.40, 63.32, 53.91, 49.68, 48.15, 16.48, 16.43, 16.16, 16.11. Elemental Analysis: Anal. Calc. for $C_{32}H_{26}N_6O_6S$: C, 61.73; H, 4.21; N, 13.50; %. Found: C, 61.53; H, 4.23; N, 13.52; %.

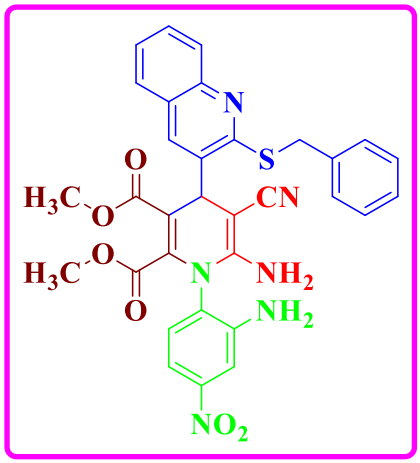

6.4. Dimethyl 6-amino-4-(2-(benzylthio)quinolin-3-yl)-5-cyano-1-phenyl-1,4-dihydropyridine-2,3-dicarboxylate (25)

Brown solid, m.p = 220-222℃ ; IR ν_{max} (cm^{-1}): 2155 C≡N, 1585 C=N, 1329 C-N, 2970 CH, 1615 C=C, 657 C-S, 1738 C=O, 2790 OCH_3, 3463 NH. ^{1}H-NMR: (400 MHz, $CDCl_3$) δ (ppm) 8.39 (1H, s, Ar-H), 7.87 (1H, t, *J*= 8.24 Hz, Ar-H), 7.67 (1H, d, *J*= 8.08 Hz, Ar-H), 7.46 (1H, d, *J*= 6.80 Hz, Ar-H), 7.36 (2H, t, *J*= 6.44 Hz, Ar-H), 7.29 (1H, t, *J*= 7.80 Hz, Ar-H), 7.22 (1H, d, *J*= 2.04 Hz, Ar-H), 7.19 (2H, d, *J*= 7.72 Hz, Ar-H), 7.16

(1H, d, *J*= 8.32 Hz, Ar-H), 7.13 (1H, d, *J*= 7.04 Hz, Ar-H), 6.99 (1H, t, *J*= 7.44 Hz, Ar-H), 6.80 (2H, d, *J*= 7.76 Hz, Ar-H), 6.63 (2H, s, NH_2), 5.30 (1H, s, CH), 4.23 (2H, s, CH_2), 3.64 (3H, s, OCH_3), 3.59 (3H, s, OCH_3). ^{13}C-NMR: (100 MHz, $CDCl_3$) δ (ppm) 150.21, 150.15, 147.00, 146.98, 145.30, 145.16, 139.30, 137.83, 137.78, 130.78, 129.29, 129.12, 129.11, 128.06, 127.90, 127.32, 127.28, 119.92, 114.47, 110.60, 63.99, 63.92, 63.57, 63.49, 52.58, 51.06, 21.55, 16.49, 16.44, 16.14, 16.08. Elemental Analysis: Anal. Calc. for $C_{32}H_{26}N_4O_4S$: C, 68.31; H, 4.66; N, 9.96; %. Found: C, 68.33; H, 4.67; N, 9.98; %.

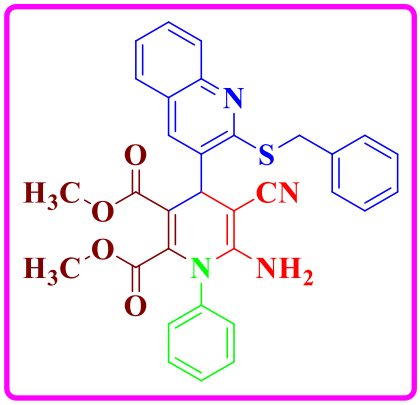

6.5. Dimethyl 6-amino-4-(2-(benzylthio)quinolin-3-yl)-5-cyano-1-(m-tolyl)-1,4-dihydropyridine-2,3-dicarboxylate (26)

Brown solid, m.p = 230-232℃ ; IR ν_{max} (cm^{-1}): 2187 C≡N, 1581 C=N, 1248 C-N, 2980 CH, 1738 C=C, 619 C-S, 1687 C=O, 2804 OCH_3, 3318 NH. ^{1}H-NMR: (400 MHz, $CDCl_3$) δ (ppm) 8.61 (1H, d, *J*= 8.32 Hz, Ar-H), 8.43 (1H, d, *J*= 6.44 Hz, Ar-H), 8.21 (1H, s, Ar-H), 7.86 (1H, d, *J*= 8.20 Hz, Ar-H), 7.65 (2H, d, *J*= 7.56 Hz, Ar-H), 7.58 (1H, t, *J*= 8.28 Hz, Ar-H), 7.38 (2H, d, *J*= 7.08 Hz, Ar-H), 7.16 (3H, t, *J*= 5.40 Hz, Ar-H), 7.11 (1H, t, *J*= 7.00 Hz, Ar-H), 6.99 (1H, d, *J*= 6.24 Hz, Ar-H), 6.60 (2H, s, NH_2), 5.13 (1H, s, CH), 4.56 (2H, s, CH_2), 3.99 (3H, s, OCH_3), 3.56 (3H, s, OCH_3), 2.46 (3H, s, CH_3). ^{13}C-NMR: (100 MHz, $CDCl_3$) δ (ppm) 169.73, 164.64, 150.63, 150.39, 148.30, 147.73, 137.29, 136.26, 129.32, 129.23, 129.17, 128.79, 128.56, 128.40, 127.35, 124.59, 124.47, 124.35, 120.98, 120.56, 120.47, 120.43, 119.90, 118.17, 114.90, 92.37, 53.34, 53.25, 52.70, 52.56, 52.34, 51.70, 14.28, 13.61. Elemental Analysis: Anal. Calc. for $C_{33}H_{28}N_4O_4S$: C, 68.73; H, 4.89; N, 9.72; %. Found: C, 68.74; H, 4.90; N, 9.71; %.

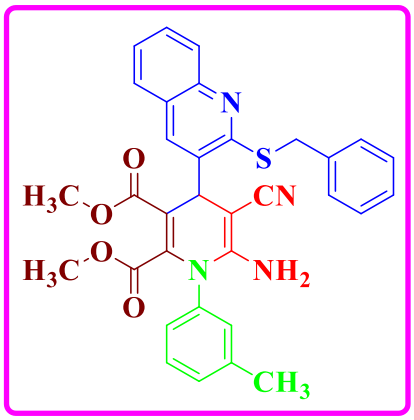

6.6. Dimethyl 6-amino-4-(2-(benzylthio)quinolin-3-yl)-5-cyano-1-(p-tolyl)-1,4-dihydropyridine-2,3-dicarboxylate (27)

Pale yellow solid, m.p = 237-239℃ ; IR ν_{max} (cm^{-1}): 2132 C≡N, 1589 C=N, 1217 C-N, 2970 CH, 1625 C=C, 572 C-S, 1738 C=O, 2948 OCH_3, 3416 NH. ^{1}H-NMR: (400 MHz, DMSO-d_6) δ (ppm) 7.95 (1H, s, Ar-H), 7.66 (2H, d, *J*= 7.76 Hz, Ar-H), 7.48 (2H, t, *J*= 4.08 Hz, Ar-H), 7.31 (2H, d, *J*= 8.24 Hz, Ar-H), 7.13 (2H, t, *J*= 7.52 Hz, Ar-H), 6.84-6.80 (2H, m, *J*= 8.12 Hz, Ar-H), 6.59 (2H, td, *J*= 6.28 Hz, Ar-H), 6.44 (1H, dd, *J*= 6.60 Hz, Ar-H), 5.91 (2H, s, NH_2), 5.24 (1H, s, CH), 4.14-4.07 (2H, m, *J*= 7.20 Hz, CH_2), 3.83 (3H, s, OCH_3), 3.74 (3H, s, OCH_3), 2.40 (3H, s, CH_3). ^{13}C-NMR: (100 MHz, $CDCl_3$) δ (ppm) 195.80, 195.77, 161.31, 160.72, 160.30, 160.24, 159.29, 159.24, 146.56, 145.93, 145.80, 136.83, 136.60, 129.96, 129.86, 128.54, 126.81, 124.58, 122.17, 119.74, 119.70, 119.63, 115.87, 113.84, 113.60, 53.50, 53.24, 49.93, 40.09, 39.88, 39.81, 31.77, 31.64, 28.57, 28.52, 26.39, 26.31. Elemental Analysis: Anal. Calc. for $C_{33}H_{28}N_4O_4S$: C, 68.73; H, 4.89; N, 9.72; %. Found: C, 68.75; H, 4.90; N, 9.73; %.

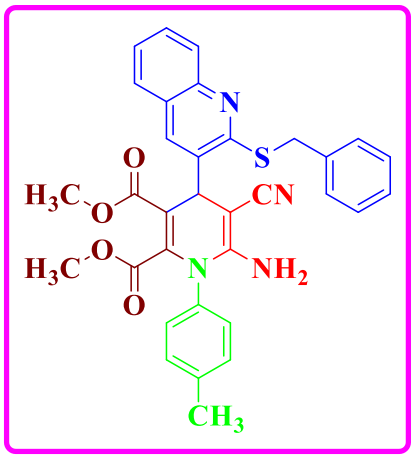

6.7. Dimethyl 6-amino-4-(2-(benzylthio)quinolin-3-yl)-5-cyano-1-(2-nitrophenyl)-1,4-dihydropyridine-2,3-dicarboxylate (28)

Yellow solid, m.p = 194-196℃ ; IR ν_{max} (cm^{-1}): 2163 C≡N, 1556 C=N, 1224 C-N, 2979 CH, 1590 C=C, 701 C-S, 1739 C=O, 2832 OCH_3, 3308 NH. ^{1}H-NMR: (400 MHz, DMSO-d_6) δ (ppm) 8.09 (1H, s, Ar-H), 7.57 (1H, d, *J*= 7.76 Hz, Ar-H), 7.47 (1H, t, *J*= 7.68 Hz, Ar-H), 7.31 (2H, d, *J*= 8.24 Hz, Ar-H), 7.15 (2H, t, *J*= 7.56 Hz, Ar-H), 7.03 (3H, t, *J*= 7.48 Hz, Ar-H), 6.70 (2H, d, *J*= 7.88 Hz, Ar-H), 6.58 (2H, t, *J*= 6.36 Hz, Ar-H), 6.31 (2H, brs, NH_2), 5.32 (1H, s, CH), 4.14-4.07 (2H, m, *J*= 7.08 Hz, CH_2), 3.89 (3H, s, OCH_3), 3.19 (3H, s, OCH_3). ^{13}C-NMR: (100 MHz, DMSO-d_6) δ (ppm) 176.01, 170.29, 144.93, 142.85, 139.04, 136.54, 135.73, 133.99, 131.00,

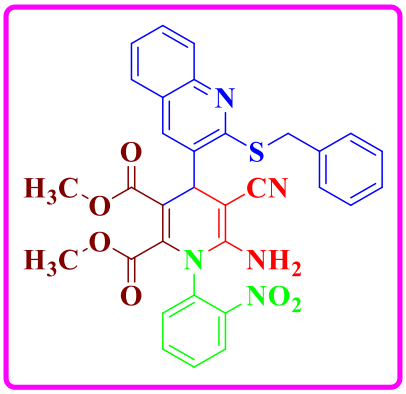

129.99, 128.99, 128.60, 128.35, 128.33, 128.25, 128.00, 127.97, 127.59, 126.59, 125.82, 125.72, 125.28, 125.12, 123.60, 123.49, 123.10, 121.87, 120.82, 119.05, 118.11, 118.02, 112.21, 111.39, 59.71, 20.72, 14.05. Elemental Analysis: Anal. Calc. for $C_{32}H_{25}N_5O_6S$: C, 63.25; H, 4.15; N, 11.53; %. Found: C, 63.27; H, 4.17; N, 11.54; %.

6.8. Dimethyl 6-amino-4-(2-(benzylthio)quinolin-3-yl)-5-cyano-1-(4-methoxy phenyl)-1,4-dihydropyridine-2,3-dicarboxylate (29)

Brown solid, m.p = 220-222℃ ; IR ν_{max} (cm^{-1}): 2253 C≡N, 1588 C=N, 1092 C-N, 2970 CH, 1614 C=C, 702 C-S, 1709 C=O, 2918 OCH_3, 3363 NH. ^{1}H-NMR: (400 MHz, $CDCl_3$) δ (ppm) 8.15 (1H, s, Ar-H), 7.83 (1H, d, *J*= 8.36 Hz, Ar-H), 7.63 (2H, d, *J*= 8.04 Hz, Ar-H), 7.57 (2H, t, *J*= 7.52 Hz, Ar-H), 7.31 (2H, t, *J*= 7.48 Hz, Ar-H), 6.82 (2H, t, *J*= 8.80 Hz, Ar-H), 6.66 (2H, dd, *J*= 2.76 Hz, Ar-H), 6.43 (2H, dt, *J*= 3.20 Hz, Ar-H), 6.19 (2H, s, NH_2), 5.28 (1H, s, CH), 4.19 (3H, s, OCH_3), 3.89 (3H, s, OCH_3), 3.75-3.65 (2H, m, *J*= 7.20 Hz, CH_2), 3.48 (3H, s, OCH_3). ^{13}C-NMR: (100 MHz, $CDCl_3$) δ (ppm) 160.01, 145.90, 145.75, 139.04, 136.84, 136.78, 129.59, 129.13, 127.76, 126.74, 125.26, 125.23, 124.22, 121.36, 121.34, 119.50, 114.54, 110.55, 63.55, 63.49, 63.25, 63.18, 53.95, 49.45, 47.93, 21.57, 16.50, 16.44, 16.18, 16.12. Elemental Analysis: Anal. Calc. for $C_{33}H_{28}N_4O_5S$: C, 66.88; H, 4.76; N, 9.45; %. Found: C, 66.90; H, 4.78; N, 9.47; %.

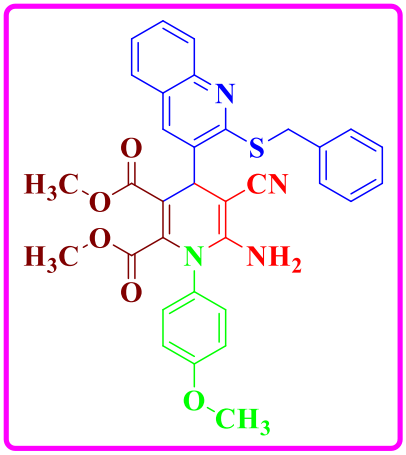

6.9. Dimethyl 6-amino-4-(2-(benzylthio)quinolin-3-yl)-5-cyano-1-(2,4-dimethyl phenyl)-1,4-dihydropyridine-2,3-dicarboxylate (30)

Yellow solid, m.p = 232-234℃ ; IR ν_{max} (cm^{-1}): 2172 C≡N, 1603 C=N, 1216 C-N, 2951 CH, 1666 C=C, 679 C-S, 1740 C=O, 2840 OCH_3, 3017 NH. ^{1}H-NMR: (400 MHz, DMSO-d_6) δ (ppm) 8.36 (2H, s, NH_2), 7.53 (1H, s, Ar-H), 7.25 (3H, t, *J*= 8.32 Hz, Ar-H), 7.00 (2H, q, *J*= 8.04 Hz, Ar-H), 6.38 (1H, dd, 1.28 Hz, Ar-H), 6.36 (1H, dd, *J*= 0.76 Hz, Ar-H), 6.33 (1H, t, *J*= 2.32 Hz, Ar-H), 6.30 (2H, t, *J*= 2.20 Hz, Ar-H), 6.25 (1H, d, *J*= 2.48 Hz, Ar-H), 6.23 (1H, d, *J*= 2.48 Hz, Ar-H), 5.17 (1H, s, CH), 3.99-3.87 (2H, m, *J*= 6.32 Hz, CH_2), 3.69 (3H, s, OCH_3), 2.50 (3H, s, OCH_3), 1.21 (3H, t, *J*= 5.16 Hz, CH_3),

1.20 (3H, t, *J*= 1.47 Hz, CH_3). ^{13}C-NMR: (100 MHz, DMSO-d_6) δ (ppm) 164.44, 162.07, 150.42, 150.32, 138.37, 130.36, 130.22, 130.12, 129.33, 129.16, 129.04, 128.36, 128.23, 127.74, 127.26, 126.92, 110.09, 102.00, 101.79, 100.30, 100.06, 63.08, 60.08, 60.03, 55.99, 40.05, 33.75, 18.49, 16.18, 16.11, 15.86. Elemental Analysis: Anal. Calc. for $C_{34}H_{30}N_4O_4S$: C, 69.13; H, 5.12; N, 9.49; %. Found: C, 69.15; H, 5.14; N, 9.48; %.

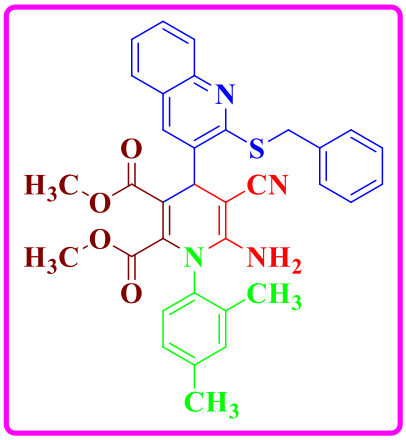

6.10. Dimethyl 6-amino-4-(2-(benzylthio)quinolin-3-yl)-5-cyano-1-(pyridin-2-yl methyl)-1,4-dihydropyridine-2,3-dicarboxylate (31)

Yellow solid, m.p = 198-200℃ ; IR ν_{max} (cm^{-1}): 2252 C≡N, 1615 C=N, 1229 C-N, 2970 CH, 1615 C=C, 708 C-S, 1738 C=O, 2815 OCH_3, 3305 NH. ^{1}H-NMR: (400 MHz, $CDCl_3$) δ (ppm) 8.10 (1H, s, Ar-H), 7.88 (2H, d, *J*= 7.36 Hz, Ar-H), 7.69 (2H, d, *J*= 7.96 Hz, Ar-H), 7.53 (2H, t, *J*= 7.40 Hz, Ar-H), 7.40 (3H, t, *J*= 6.36 Hz, Ar-H), 7.18 (1H, t, *J*= 7.76 Hz, Ar-H), 7.10 (1H, t, *J*= 7.04 Hz, Ar-H), 6.97 (1H, t, *J*= 7.48 Hz, Ar-H), 6.53 (1H, d, *J*= 7.64 Hz, Ar-H), 6.24 (2H, s, NH_2), 4.96 (1H, s, CH), 4.63 (2H, s, CH_2), 4.22-4.08 (2H, m, *J*= 5.64 Hz, CH_2), 3.87 (3H, s, OCH_3), 3.73 (3H, s, OCH_3). ^{13}C-NMR: (100 MHz, $CDCl_3$) δ (ppm) 160.07, 160.02, 147.37, 145.93, 145.91, 136.75, 136.70, 135.82, 135.68, 129.50, 127.76, 126.79, 125.32, 125.29, 124.13, 121.39, 121.37, 121.08, 117.82, 110.83, 109.64, 63.55, 63.49, 63.17, 63.10, 55.50, 53.86, 49.29, 47.76, 16.48, 16.43, 16.21, 16.15. Elemental Analysis: Anal. Calc. for $C_{32}H_{27}N_5O_4S$: C, 66.54; H, 4.71; N, 12.12; %. Found: C, 66.55; H, 4.72; N, 12.14; %.

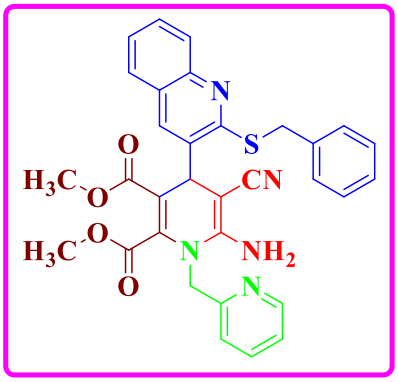

6.11. Dimethyl 6-amino-4-(2-(benzylthio)quinolin-3-yl)-5-cyano-1-((2-(piperazin-1-yl)ethyl)amino)-1,4-dihydropyridine-2,3-dicarboxylate (32)

Brown solid, m.p = 218-220℃ ; IR ν_{max} (cm^{-1}): 2200 C≡N, 1574 C=N, 1217 C-N, 2970 CH, 1666 C=C, 695 C-S, 1756 C=O, 2825 OCH_3, 3288 NH. ^{1}H-NMR: (400 MHz, $CDCl_3$) δ (ppm) 8.17 (2H, brs, NH_2), 7.94 (1H, d, *J*= 8.32 Hz, Ar-H), 7.75 (1H, s, Ar-H),

7.66 (3H, td, *J*= 8.56 Hz, Ar-H), 7.40 (2H, t, *J*= 7.16 Hz, Ar-H), 7.19 (2H, t, *J*= 6.92 Hz, Ar-H), 6.61 (1H, s, Ar-H), 5.30 (2H, s, CH_2), 5.06 (1H, s, CH), 4.68 (1H, s, NH), 3.82 (2H, s, CH_2), 3.79 (2H, s, CH_2), 3.72 (2H, s, CH_2), 3.62 (3H, s, OCH_3), 3.58 (2H, s, CH_2), 3.54 (3H, s, OCH_3), 3.39-3.34 (2H, m, *J*= 5.92 Hz, CH_2), 3.11-3.09 (2H, m, *J*= 4.96 Hz, CH_2), 2.41 (1H, s, NH). ^{13}C-NMR: (100 MHz, $CDCl_3$) δ (ppm) 152.34, 150.84, 147.92, 147.85, 145.68, 137.63, 137.53, 135.64, 130.65, 129.89, 129.29, 128.99, 128.53, 128.46, 128.29, 127.95, 127.91, 127.64, 127.45, 127.25, 127.18, 126.00, 125.89, 125.77, 52.38, 51.84, 50.93, 50.76, 47.09, 46.67, 43.57, 41.51, 37.20, 23.39, 21.42. Elemental Analysis: Anal. Calc. for $C_{32}H_{35}N_7O_4S$: C, 62.62; H, 5.75; N, 15.98; %. Found: C, 62.64; H, 5.77; N, 15.99; %.

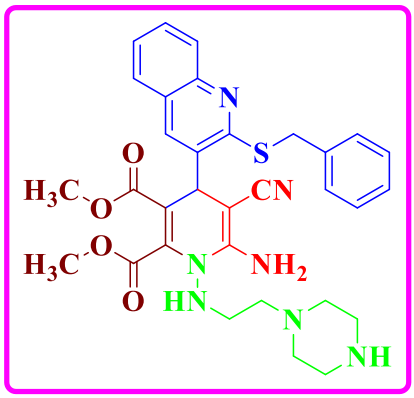

6.12. Dimethyl 6-amino-4-(2-(benzylthio)quinolin-3-yl)-5-cyano-1-(3,4-dichloro phenyl)-1,4-dihydropyridine-2,3-dicarboxylate (33)

Dark yellow solid, m.p = 211-213℃ ; IR ν_{max} (cm^{-1}): 2280 C≡N, 1613 C=N, 1232 C-N, 2917 CH, 1672 C=C, 705 C-S, 1737 C=O, 2829 OCH_3, 789 C-Cl, 3351 NH. ^{1}H-NMR: (400 MHz, $CDCl_3$) δ (ppm) 8.59 (2H, brs, NH_2), 8.30 (1H, s, Ar-H), 8.09 (1H, d, *J*= 8.48 Hz, Ar-H), 7.74 (1H, t, *J*= 8.12 Hz, Ar-H), 7.70 (1H, d, *J* = 7.64 Hz, Ar-H), 7.49 (2H, d, *J*= 7.16 Hz, Ar-H), 7.45 (1H, t, *J*= 7.56 Hz, Ar-H), 7.31 (1H, d, *J*= 3.46 Hz, Ar-H), 7.27 (1H, t, *J*= 4.44 Hz, Ar-H), 7.24 (1H, d, *J*= 7.40 Hz, Ar-H), 6.59 (1H, d, *J*= 8.96 Hz, Ar-H), 6.53 (1H, d, *J*= 8.96 Hz, Ar-H), 6.21 (1H, s, Ar-H), 5.25 (1H, s, CH), 4.28-4.21 (2H, m, *J*= 7.20 Hz, CH_2), 3.91 (3H, s, OCH_3), 3.65 (3H, s, OCH_3). ^{13}C-NMR: (100 MHz, $CDCl_3$) δ (ppm) 197.13, 170.30, 153.65, 147.10, 144.88, 139.77, 137.06, 134.20, 127.85, 127.63, 127.22, 126.78, 124.47, 123.97, 119.07, 111.93, 110.90, 106.56, 34.51, 32.34, 32.11, 31.42, 30.90, 30.18, 29.68, 29.45, 29.39, 29.34, 28.34, 28.21, 28.10, 27.03. Elemental Analysis: Anal. Calc. for $C_{32}H_{24}Cl_2N_4O_4S$: C, 60.86; H, 3.83; N, 8.87; %. Found: C, 60.88; H, 3.84; N, 8.89; %.

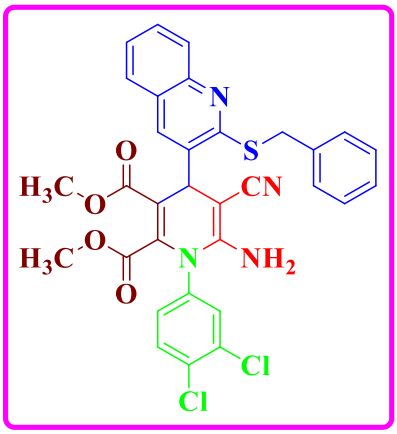

6.13. Dimethyl 6-amino-4-(2-(benzylthio)quinolin-3-yl)-1-(2-bromophenyl)-5-cyano-1,4-dihydropyridine-2,3-dicarboxylate (34)

Brown solid, m.p = 203-205℃ ; IR ν_{max} (cm^{-1}): 2157 C≡N, 1567 C=N, 1233 C-N, 2985 CH, 1614 C=C, 704 C-S, 1729 C=O, 2817 OCH_3, 572 C-Br, 3385 NH. ^{1}H-NMR: (400 MHz, $CDCl_3$) δ (ppm) 8.15 (1H, d, *J*= 6.32 Hz, Ar-H), 8.00 (1H, s, Ar-H), 7.84 (2H, d, *J*= 8.40 Hz, Ar-H), 7.65 (2H, brs, NH_2), 7.56 (2H, t, *J*= 7.20 Hz, Ar-H), 7.31 (2H, t, *J*= 7.08 Hz, Ar-H), 7.17 (3H, t, *J*= 7.52 Hz, Ar-H), 6.66 (1H, t, *J*= 7.20 Hz, Ar-H), 6.60 (2H, d, *J*= 7.72 Hz, Ar-H), 5.32 (1H, s, CH), 4.57-4.46 (2H, m, *J*= 4.68 Hz, CH_2), 4.20 (3H, s, OCH_3), 3.95 (3H, s, OCH_3). ^{13}C-NMR: (100 MHz, $CDCl_3$) δ (ppm) 159.89, 159.84, 145.73, 142.96, 142.82, 136.88, 136.82, 132.54, 129.80, 128.48, 127.81, 126.67, 125.16, 125.14, 124.39, 120.66, 120.63, 119.19, 112.34, 110.51, 63.74, 63.68, 63.38, 63.31, 54.19, 49.93, 48.40, 16.52, 16.46, 16.26, 16.20. Elemental Analysis: Anal. Calc. for $C_{32}H_{25}BrN_4O_4S$: C, 59.91; H, 3.93; N, 8.73; %. Found: C, 59.93; H, 3.95; N, 8.74; %.

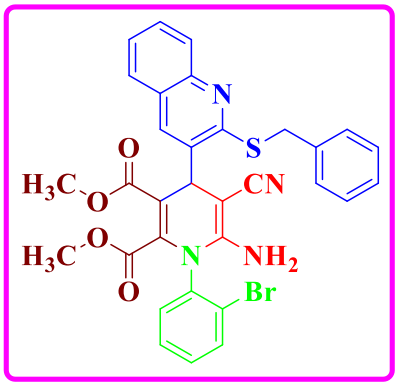

6.14. Dimethyl 6-amino-4-(2-(benzylthio)-6-fluoroquinolin-3-yl)-5-cyano-1-(2,4-dimethylphenyl)-1,4-dihydropyridine-2,3-dicarboxylate (35)

Yellow solid, m.p = 240-242℃ ; IR ν_{max} (cm^{-1}): 2292 C≡N, 1610 C=N, 1218 C-N, 2918 CH, 1671 C=C, 684 C-S, 1738 C=O, 2851 OCH_3, 1360 C-F, 3351 NH. ^{1}H-NMR: (400 MHz, $CDCl_3$) δ (ppm) 9.51 (2H, s, NH_2), 7.86 (1H, s, Ar-H), 7.74 (1H, t, *J*= 8.00 Hz, Ar-H), 7.48 (2H, t, *J*= 7.00 Hz, Ar-H), 7.30 (1H, t, *J*= 7.04 Hz, Ar-H), 6.89 (2H, d, *J*= 8.80 Hz, Ar-H), 6.67 (2H, d, *J*= 8.00 Hz, Ar-H), 6.65 (2H, d, *J*= 7.32 Hz, Ar-H), 6.41 (1H, s, Ar-H), 5.34 (1H, s, CH), 4.71-4.65 (2H, m, *J*= 6.92 Hz, CH_2), 3.73 (3H, s, OCH_3), 3.65 (3H, s, OCH_3), 2.43 (3H, t, *J*= 3.42 Hz, CH_3), 2.26 (3H, t, *J*= 2.08 Hz, CH_3). ^{13}C-NMR: (100 MHz, $CDCl_3$) δ (ppm) 149.34, 147.88, 137.74, 136.35, 136.29, 134.55, 133.39, 132.47, 131.45, 131.38, 131.34, 131.21, 131.17, 130.56, 130.37, 129.34, 128.44, 127.89, 127.82, 127.79, 127.31, 127.12,

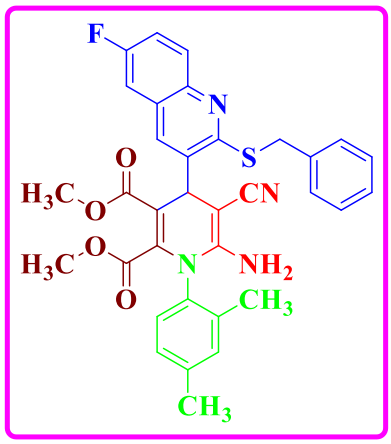

126.98, 126.89, 126.81, 125.81, 125.55, 91.68, 34.98, 20.97, 20.79, 20.48, 17.95, 17.76, 17.26. ^{19}F-NMR: (400 MHz, $CDCl_3$) δ (ppm) -118.37. Elemental Analysis: Anal. Calc. for $C_{34}H_{29}FN_4O_4S$: C, 67.09; H, 4.80; N, 9.20; %. Found: C, 67.08; H, 4.82; N, 9.21; %.

6.1. Dimethyl 6-amino-4-(2-(benzylthio)quinolin-3-yl)-5-cyano-1-(2-methoxy phenyl)-1,4-dihydropyridine-2,3-dicarboxylate (22)

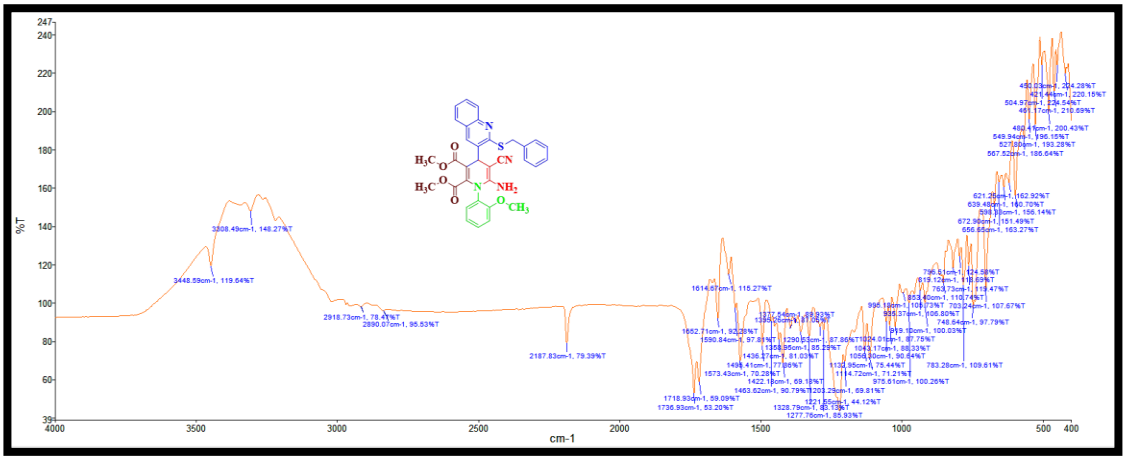

Fig. 6.1. IR spectrum of **22**

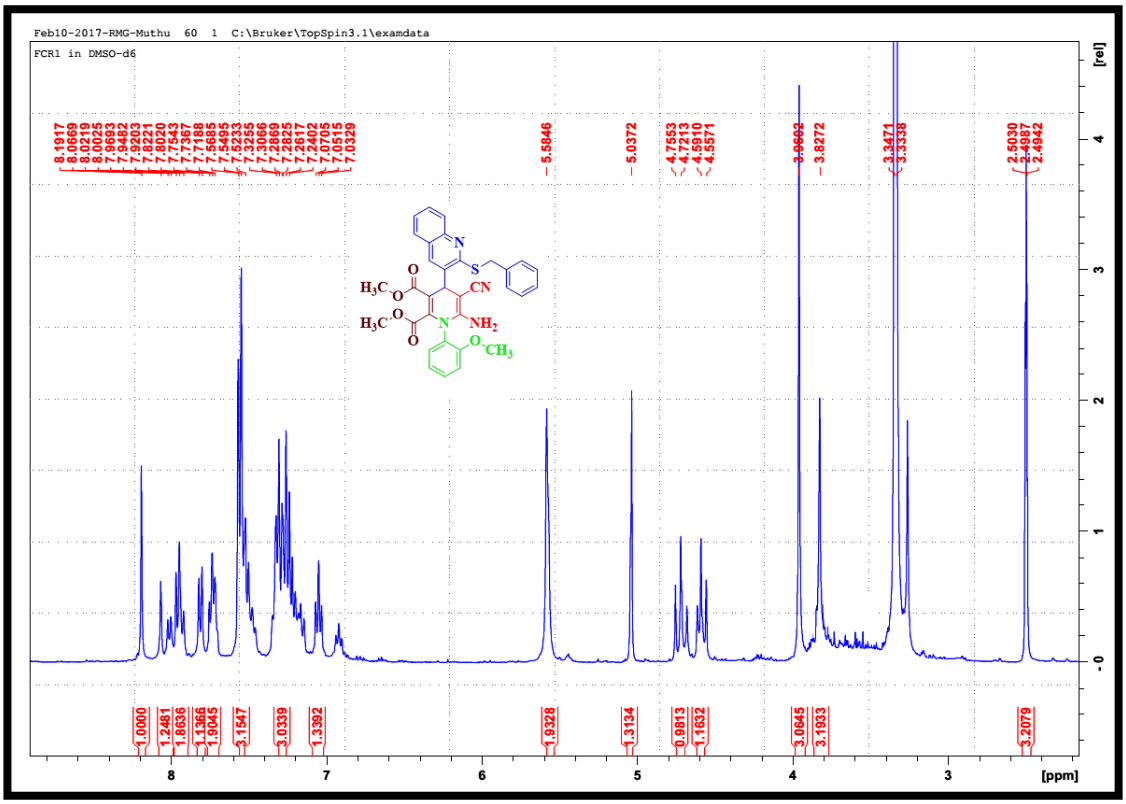

Fig. 6.2. ^{1}H-NMR spectrum of **22**

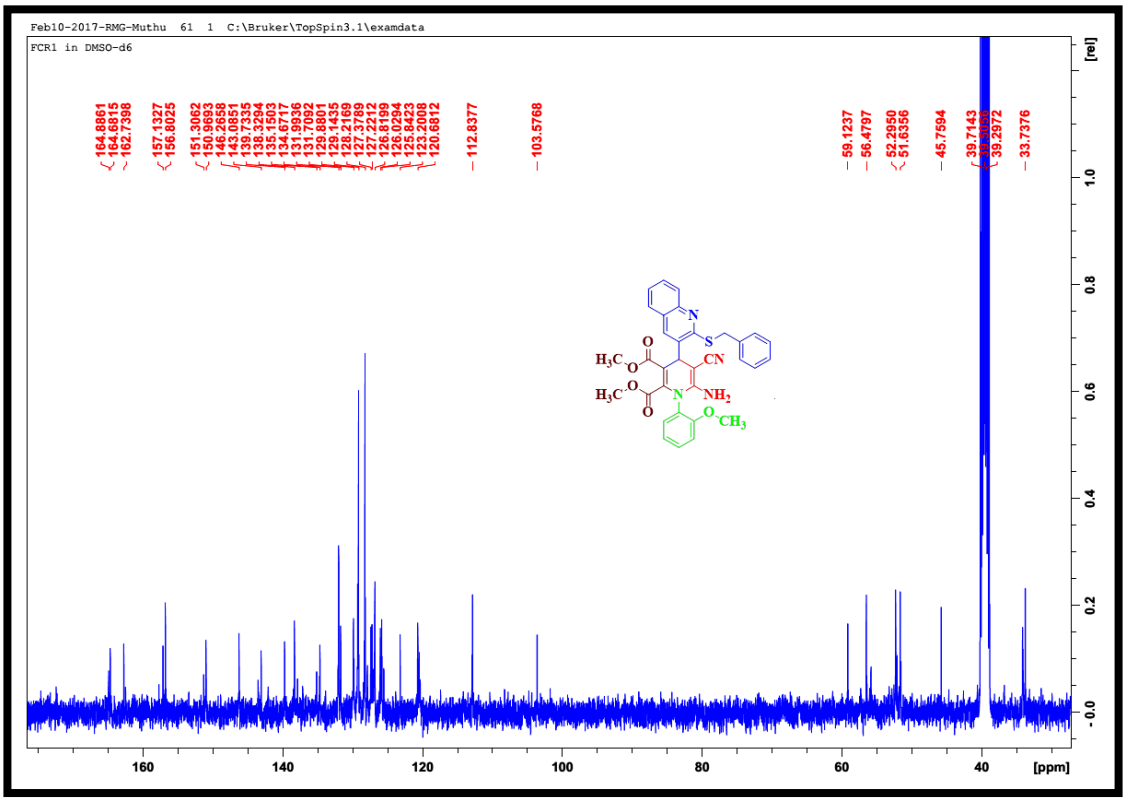

Fig. 6.3. ^{13}C-NMR spectrum of **22**

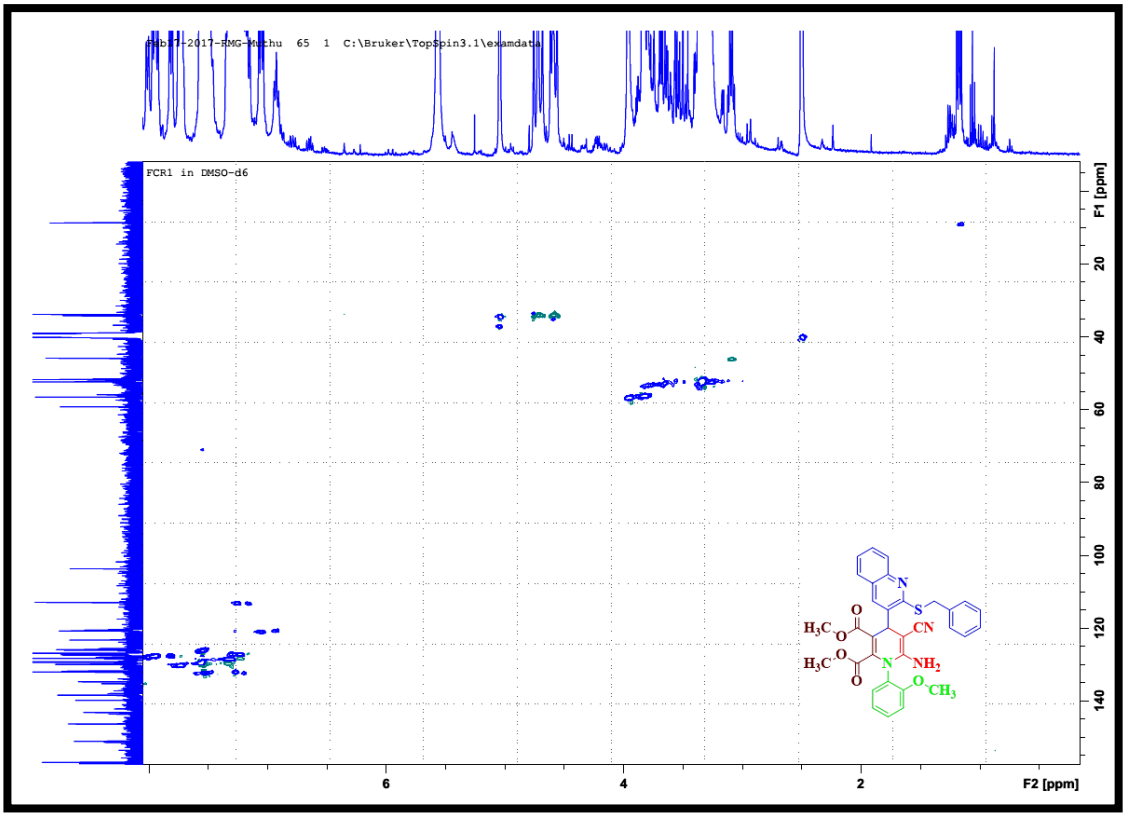

Fig. 6.4. HSQC spectrum of **22**

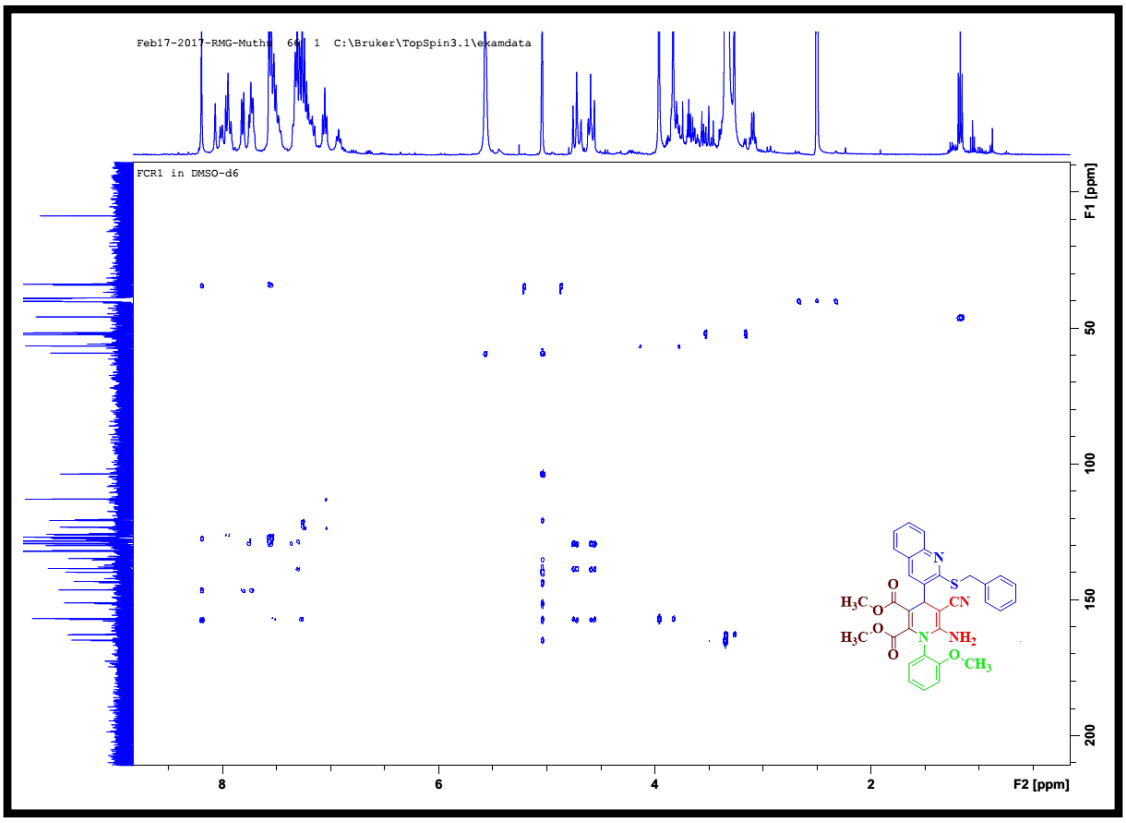

Fig. 6.5. HMBC spectrum of **22**

6.2. Dimethyl 6-amino-4-(2-(benzylthio)quinolin-3-yl)-5-cyano-1-(3-fluorophenyl)-1,4-dihydropyridine-2,3-dicarboxylate (23)

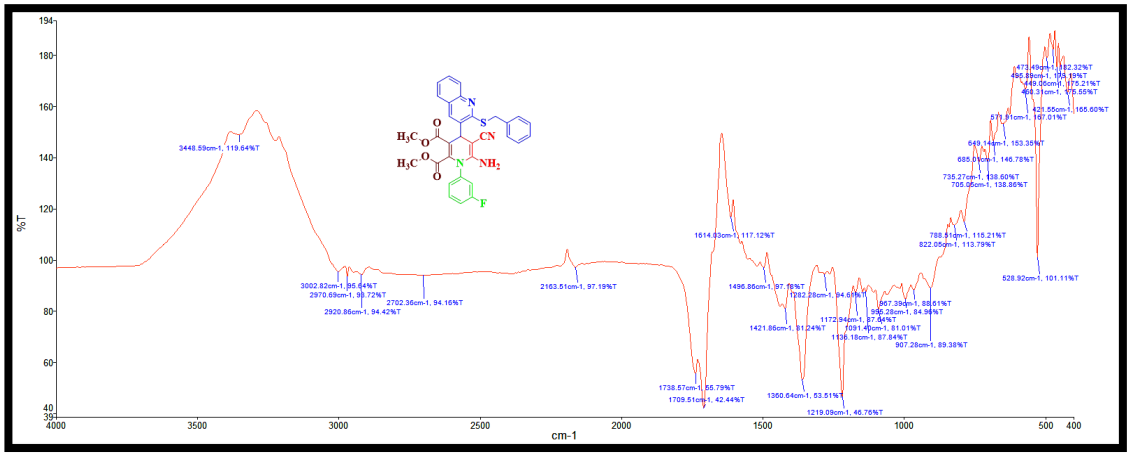

Fig. 6.6. IR spectrum of **23**

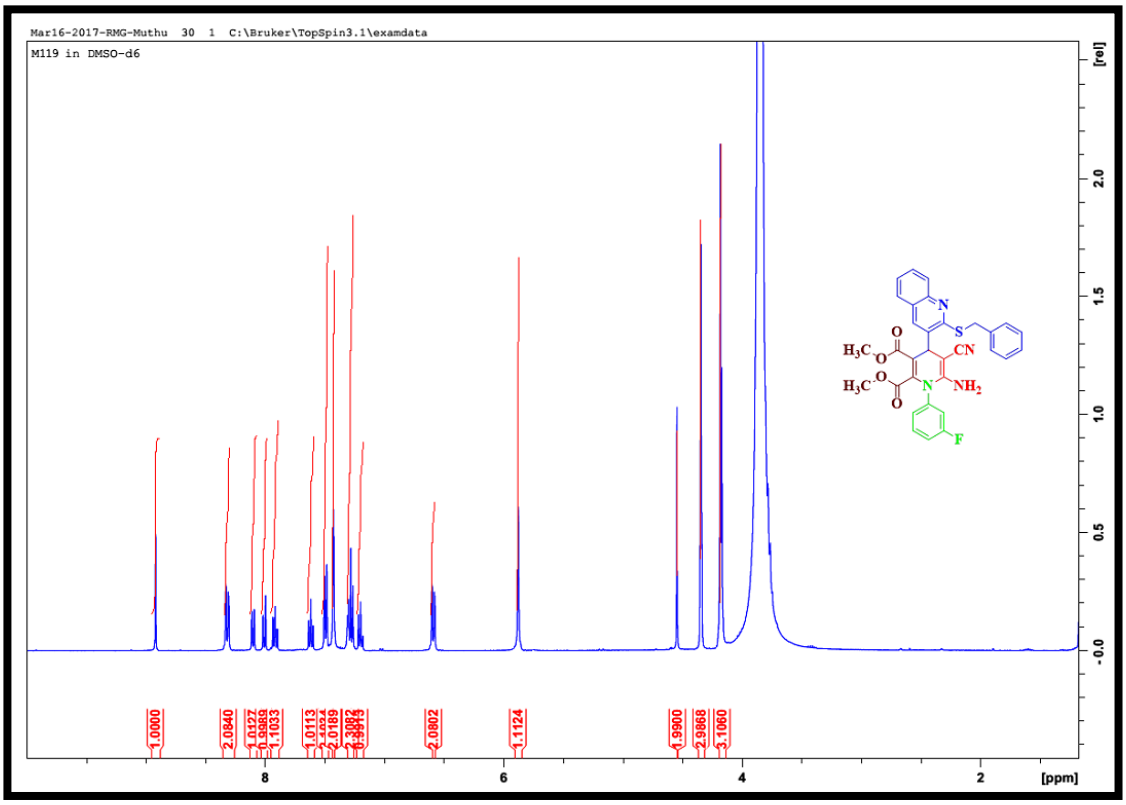

Fig. 6.7. ^{1}H-NMR spectrum of **23**

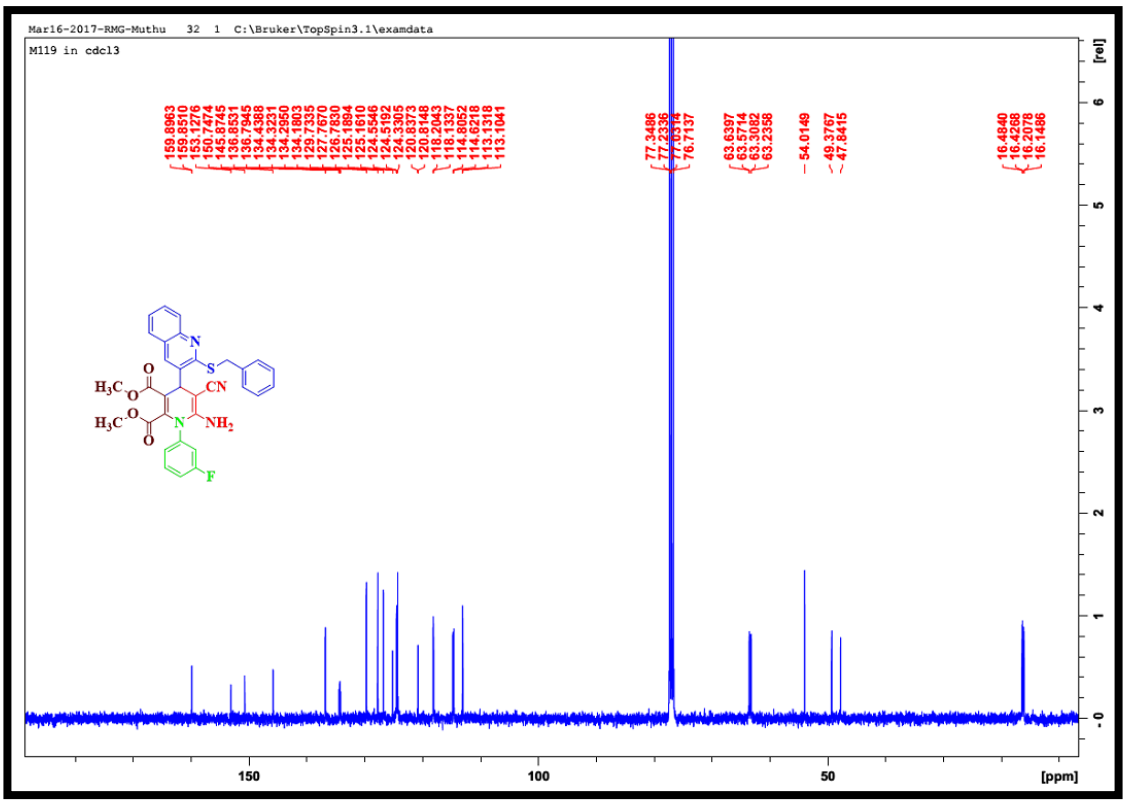

Fig. 6.8. ^{13}C-NMR spectrum of **23**

6.3. Dimethyl 6-amino-1-(2-amino-4-nitrophenyl)-4-(2-(benzylthio)quinolin-3-yl)-5-cyano-1,4-dihydropyridine-2,3-dicarboxylate (24)

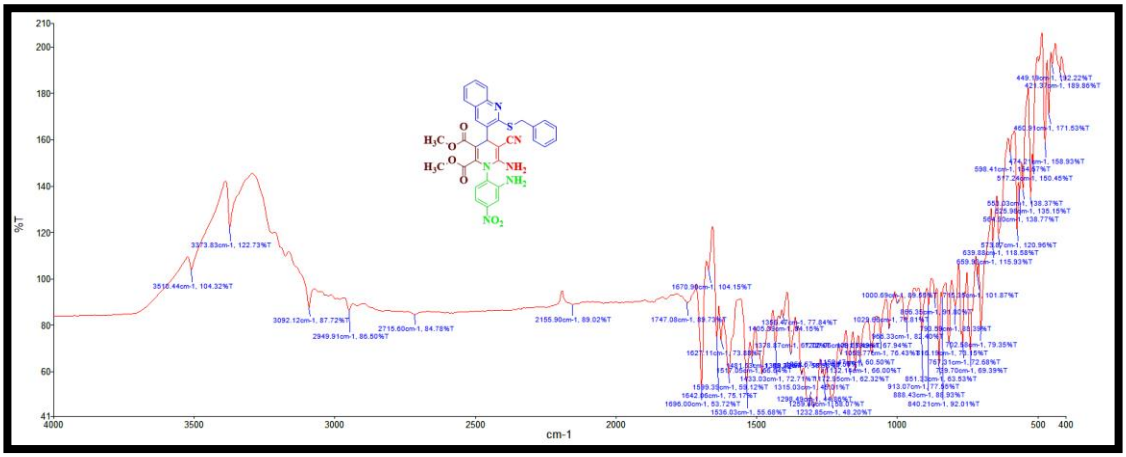

Fig. 6.9. IR spectrum of **24**

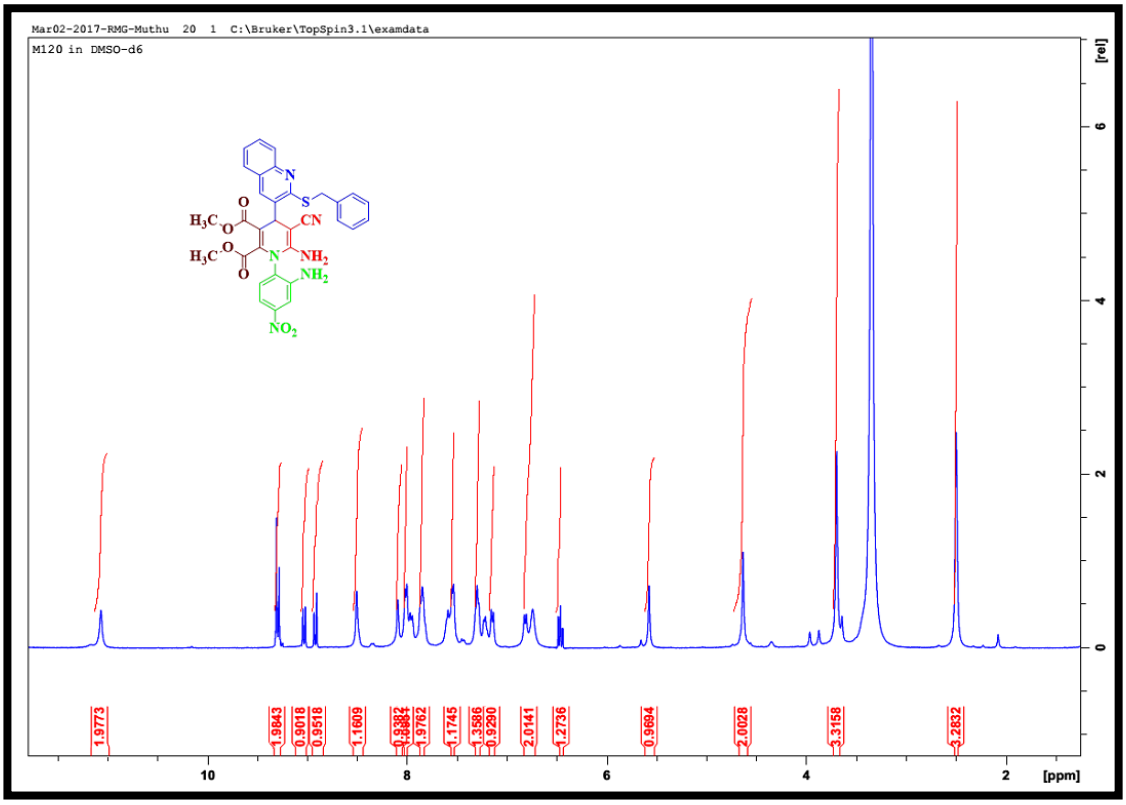

Fig. 6.10. ^{1}H-NMR spectrum of **24**

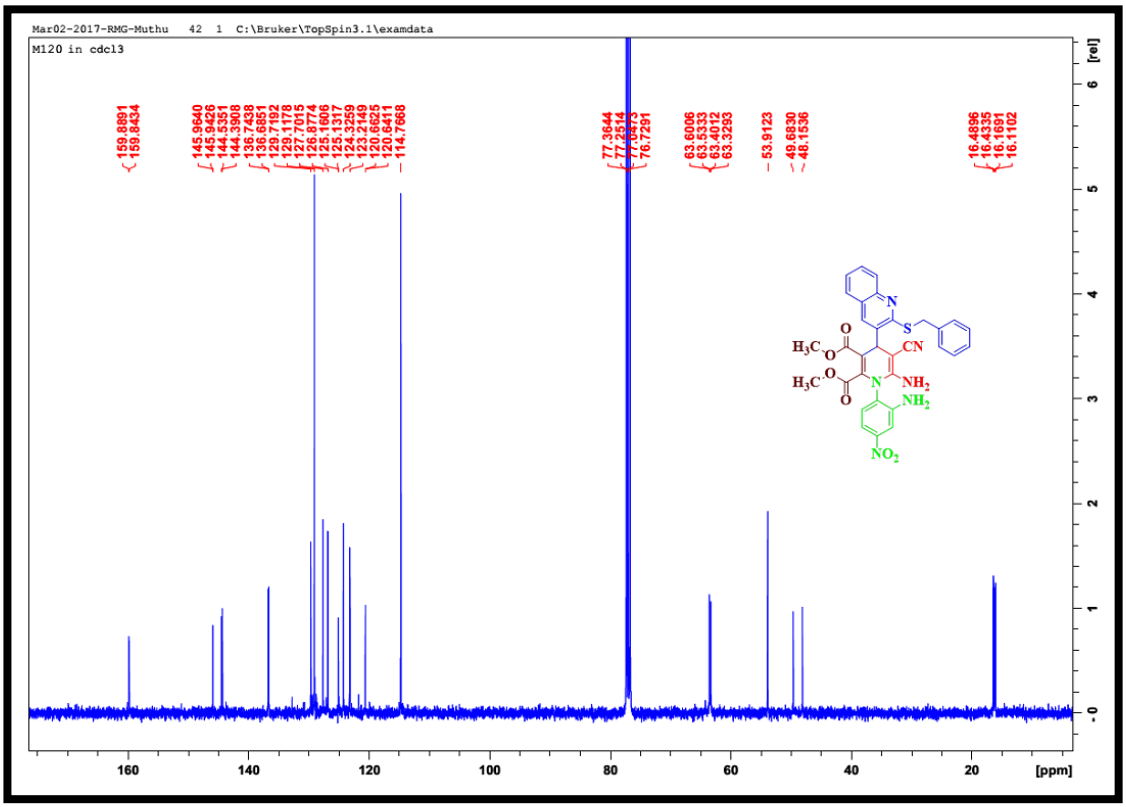

Fig. 6.11. ^{13}C-NMR spectrum of **24**

6.4. Dimethyl 6-amino-4-(2-(benzylthio)quinolin-3-yl)-5-cyano-1-phenyl-1,4-dihydropyridine-2,3-dicarboxylate (25)

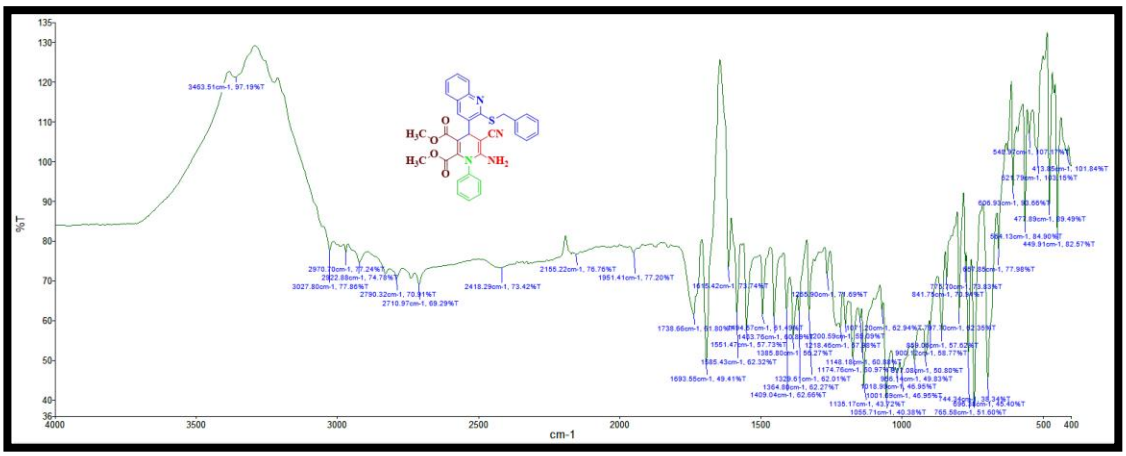

Fig. 6.12. IR spectrum of **25**

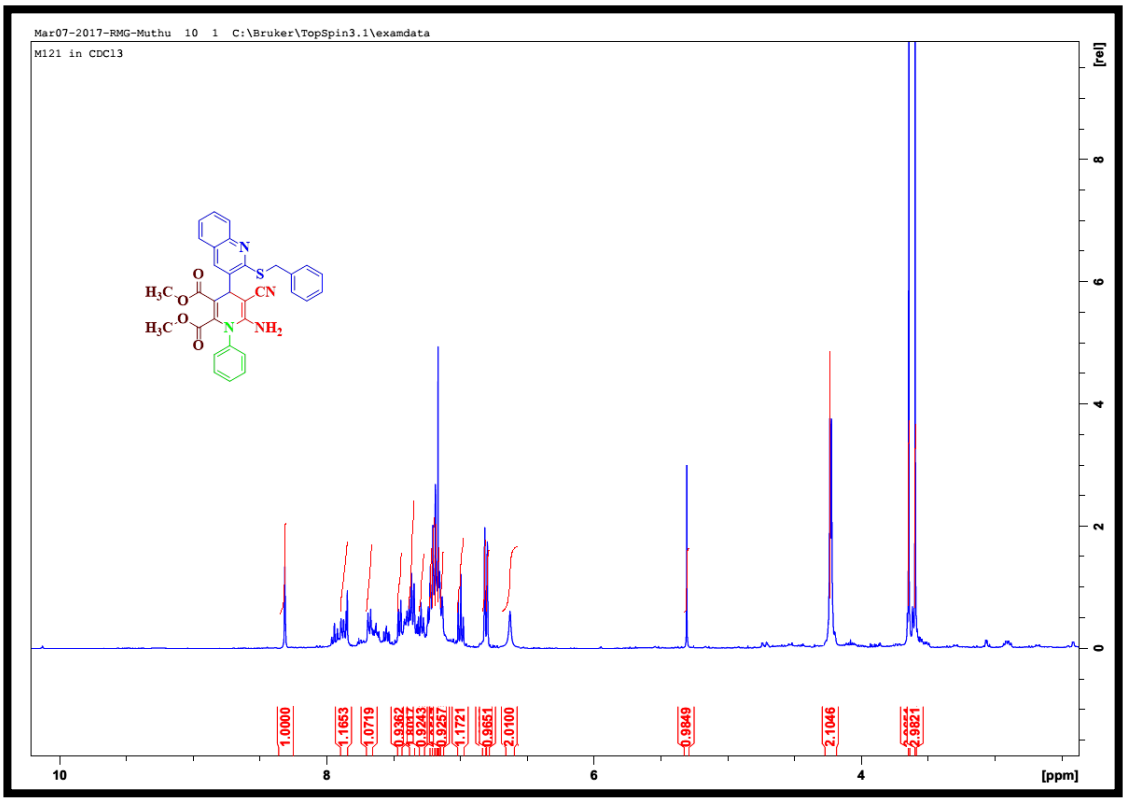

Fig. 6.13. ^{1}H-NMR spectrum of **25**

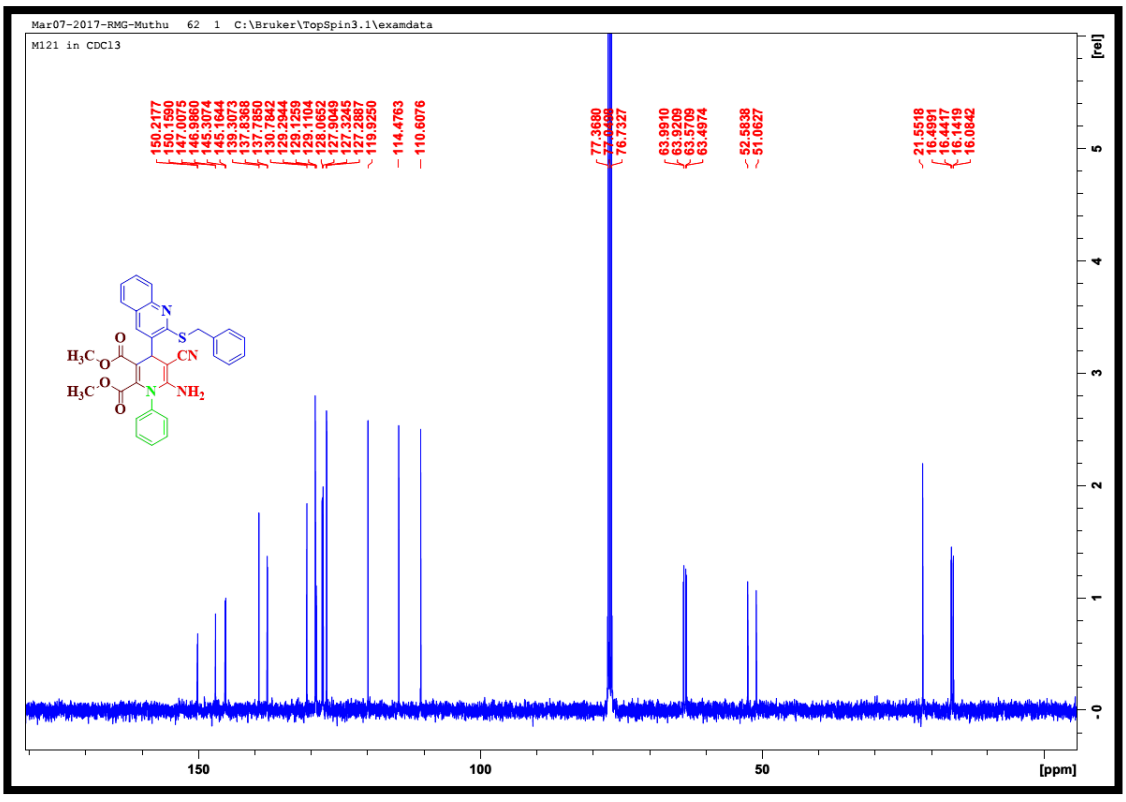

Fig. 6.14. ^{13}C-NMR spectrum of **25**

6.5. Dimethyl 6-amino-4-(2-(benzylthio)quinolin-3-yl)-5-cyano-1-(m-tolyl)-1,4-dihydropyridine-2,3-dicarboxylate (26)

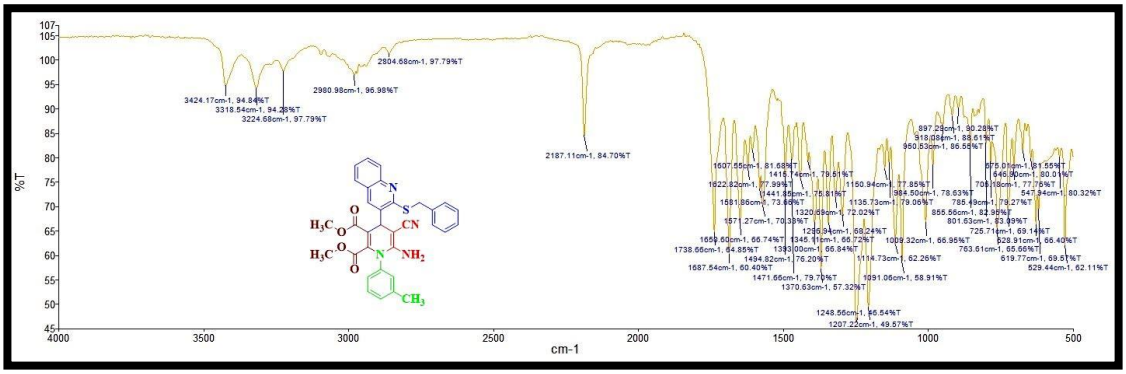

Fig. 6.15. IR spectrum of **26**

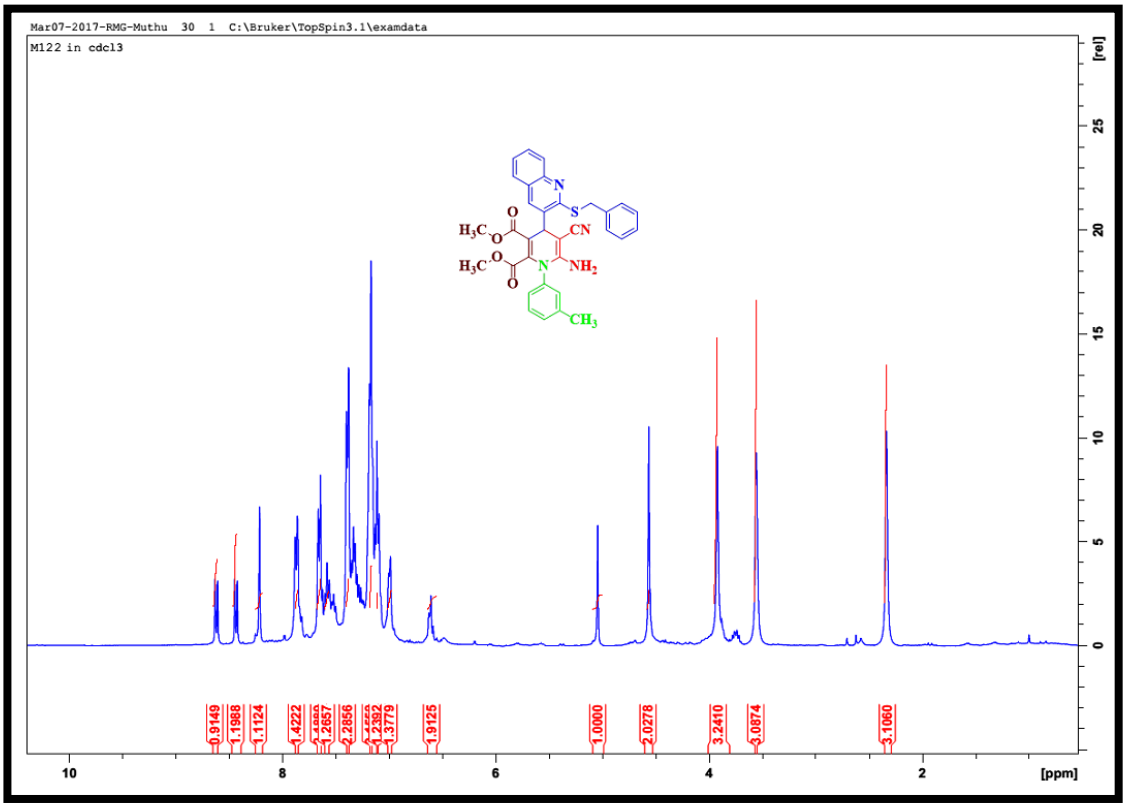

Fig. 6.16. ^{1}H-NMR spectrum of **26**

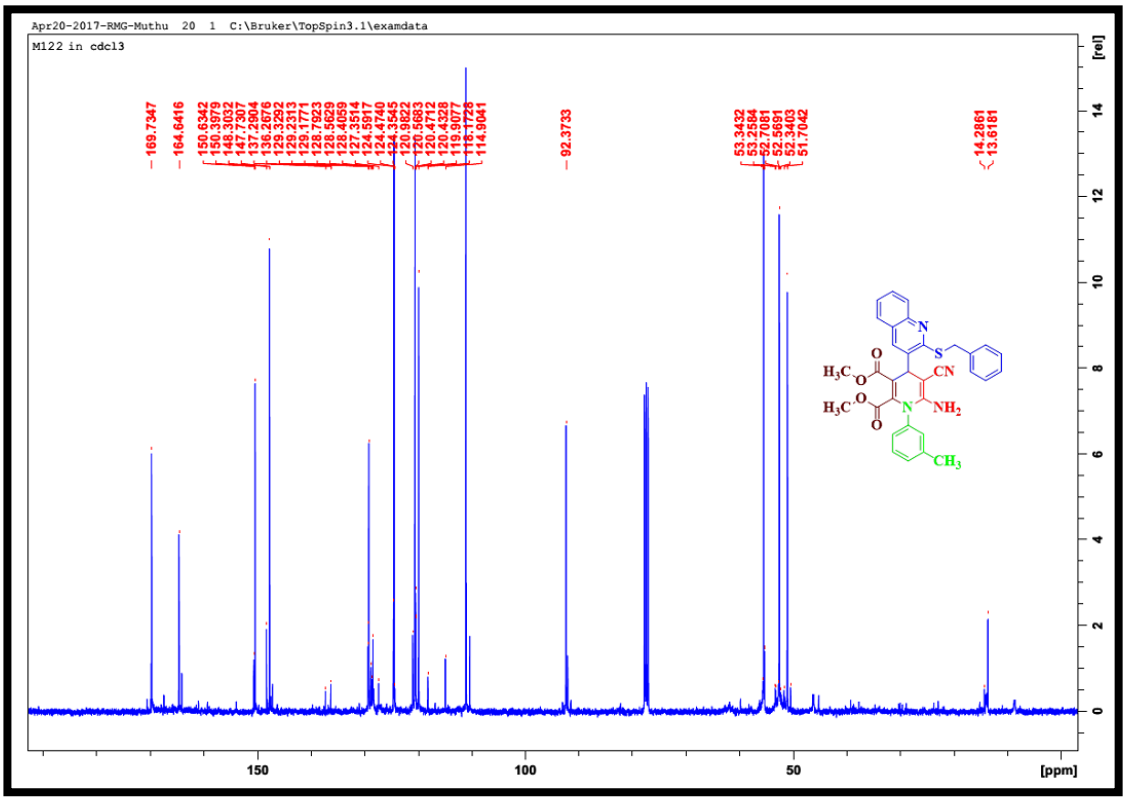

Fig. 6.17. ^{13}C-NMR spectrum of **26**

6.6. Dimethyl 6-amino-4-(2-(benzylthio)quinolin-3-yl)-5-cyano-1-(p-tolyl)-1,4-dihydropyridine-2,3-dicarboxylate (27)

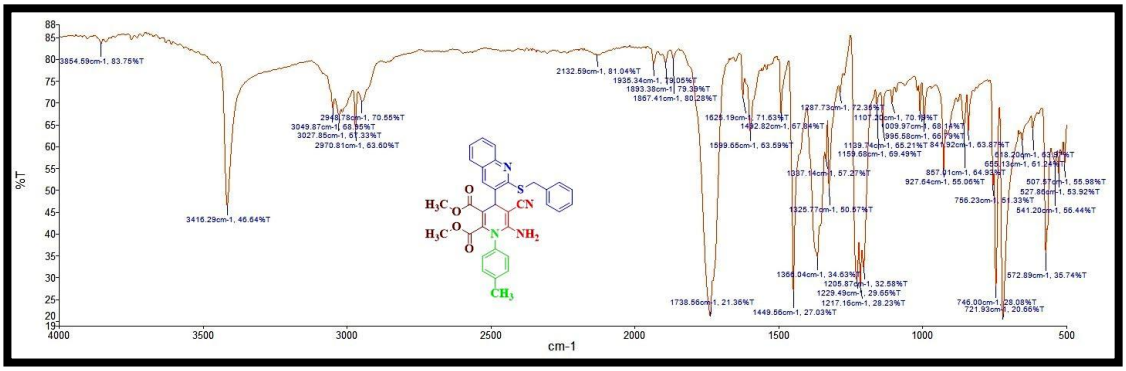

Fig. 6.18. IR spectrum of **27**

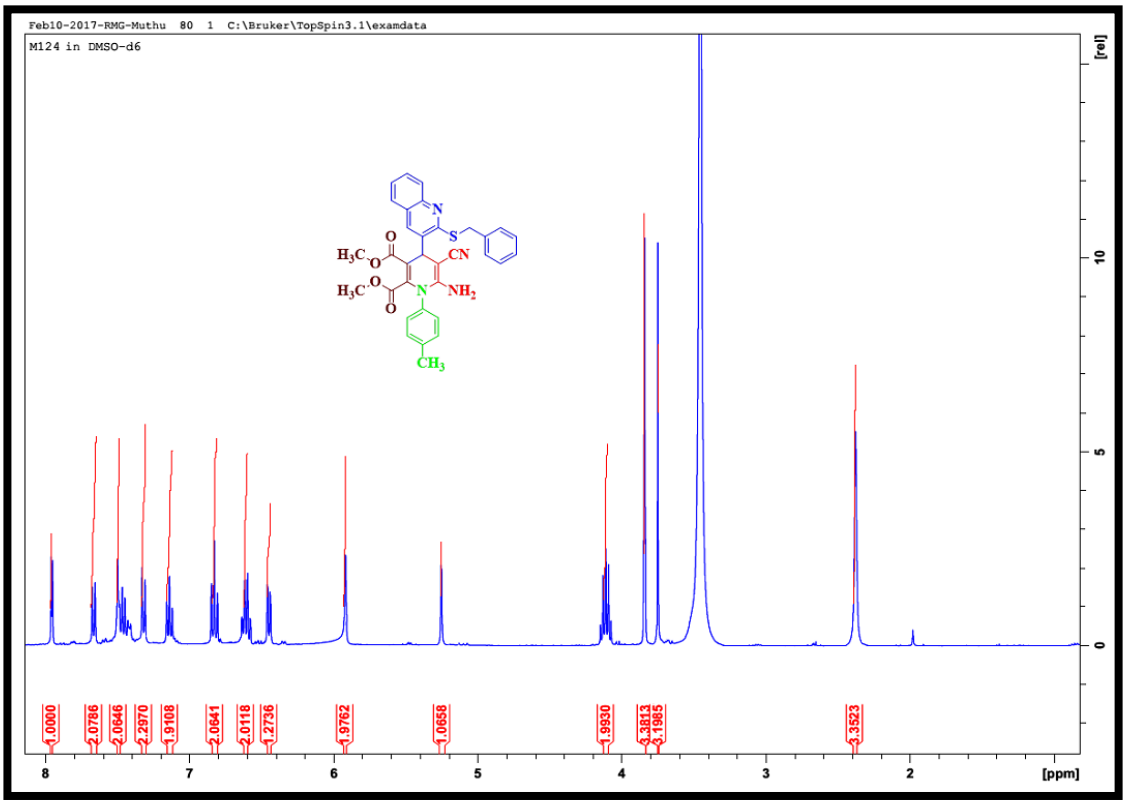

Fig. 6.19. ^{1}H-NMR spectrum of **27**

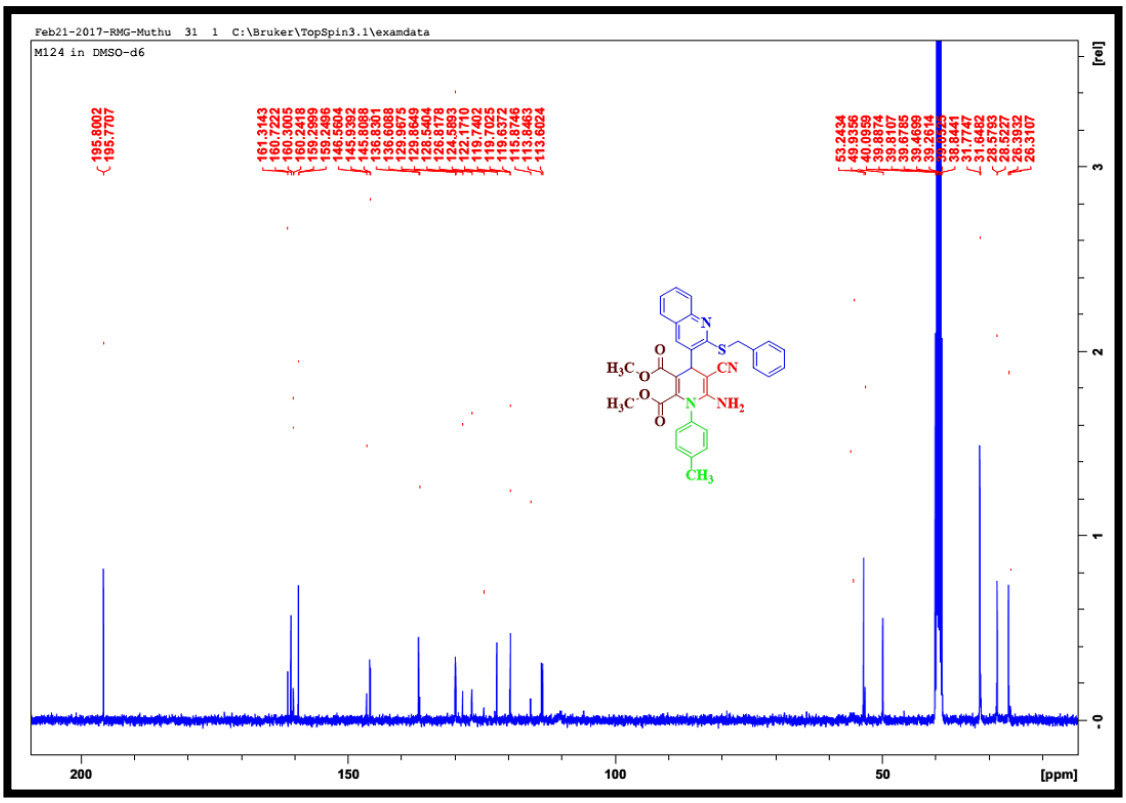

Fig. 6.20. ^{13}C-NMR spectrum of **27**

6.7. Dimethyl 6-amino-4-(2-(benzylthio)quinolin-3-yl)-5-cyano-1-(2-nitrophenyl)-1,4-dihydropyridine-2,3-dicarboxylate (28)

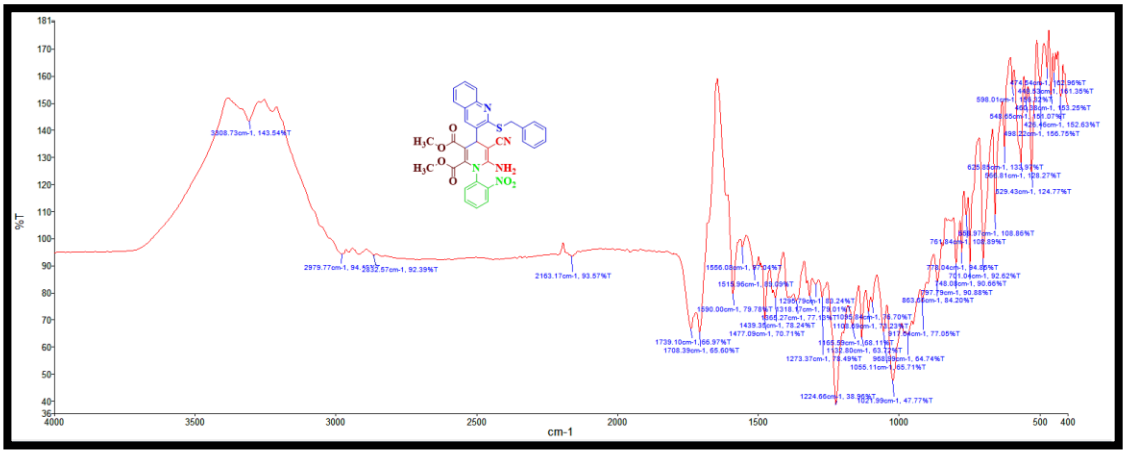

Fig. 6.21. IR spectrum of **28**

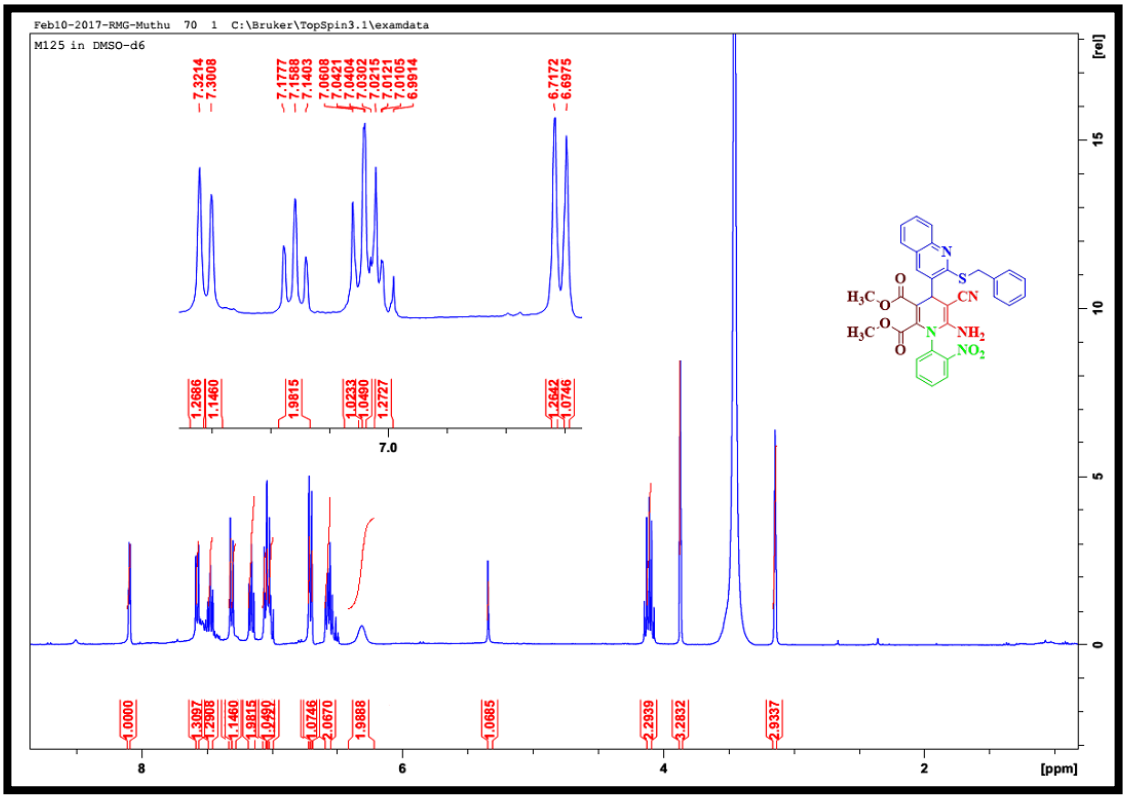

Fig. 6.22. ^{1}H-NMR spectrum of **28**

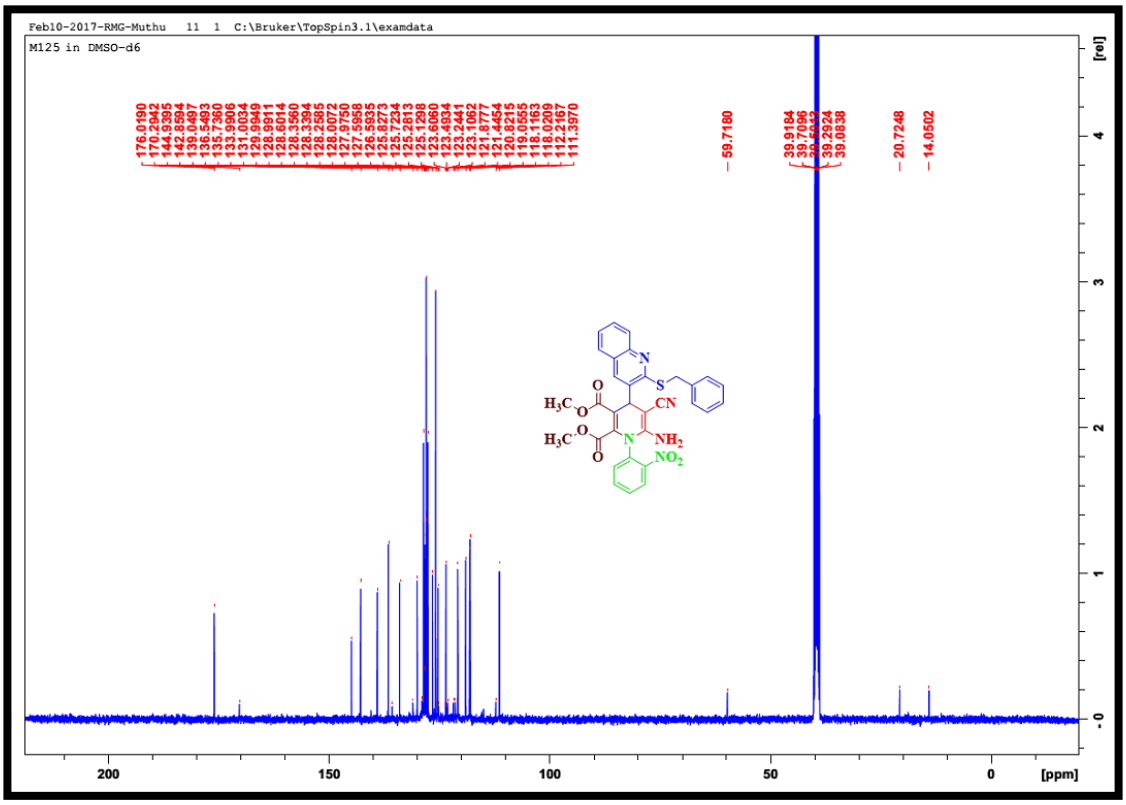

Fig. 6.23. ^{13}C-NMR spectrum of **28**

6.8. Dimethyl 6-amino-4-(2-(benzylthio)quinolin-3-yl)-5-cyano-1-(4-methoxyphenyl)-1,4-dihydropyridine-2,3-dicarboxylate (29)

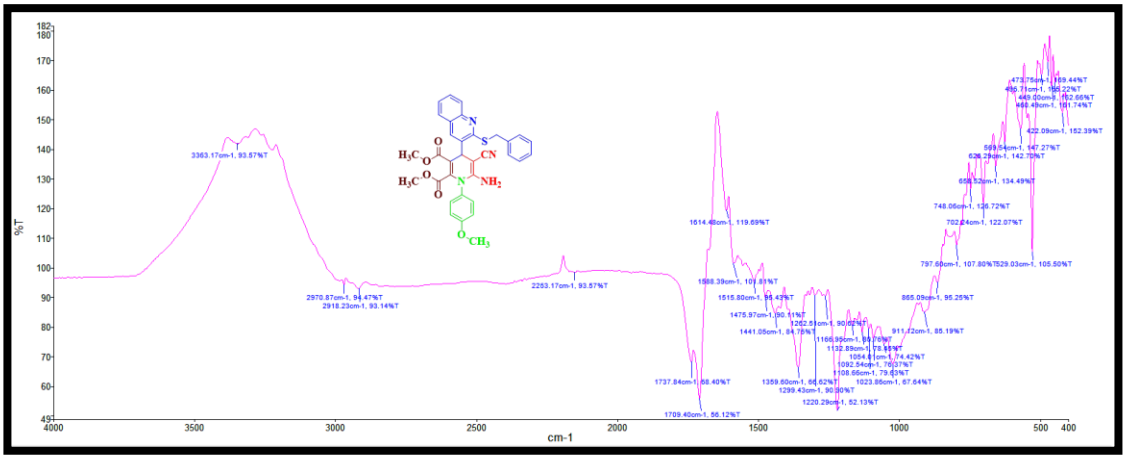

Fig. 6.24. IR spectrum of **29**

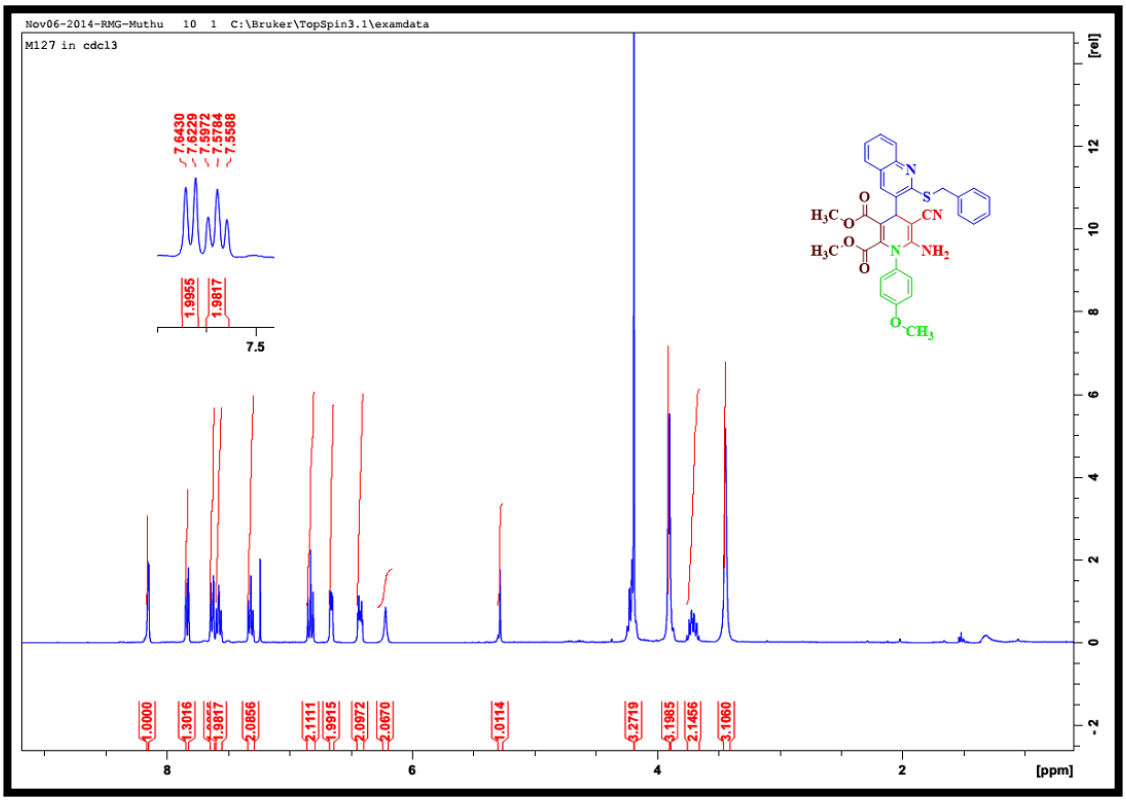

Fig. 6.25. ^{1}H-NMR spectrum of **29**

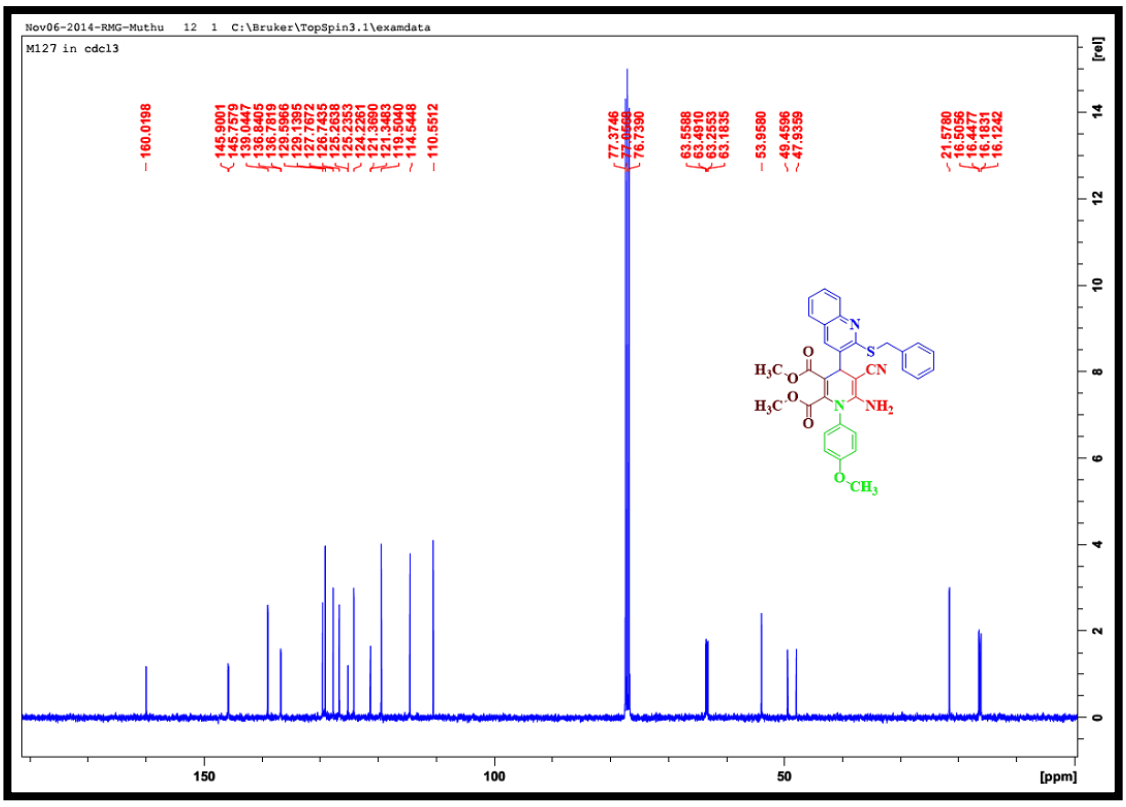

Fig. 6.26. ^{13}C-NMR spectrum of **29**

6.9. Dimethyl 6-amino-4-(2-(benzylthio)quinolin-3-yl)-5-cyano-1-(2,4-dimethylphenyl)-1,4-dihydropyridine-2,3-dicarboxylate (30)

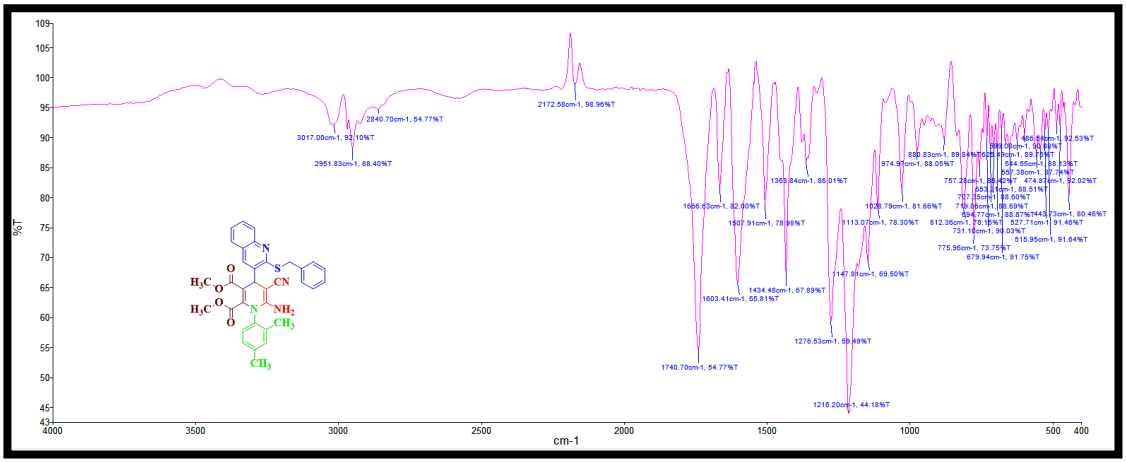

Fig. 6.27. IR spectrum of **30**

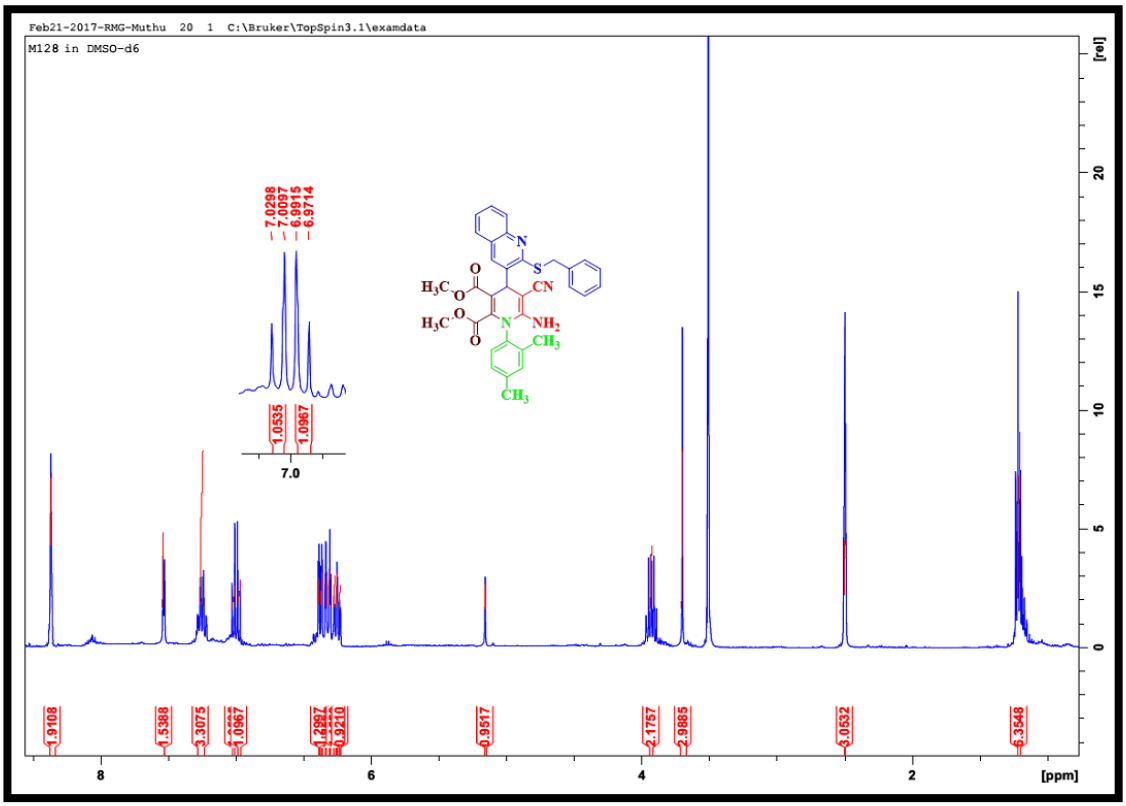

Fig. 6.28. ^{1}H-NMR spectrum of **30**

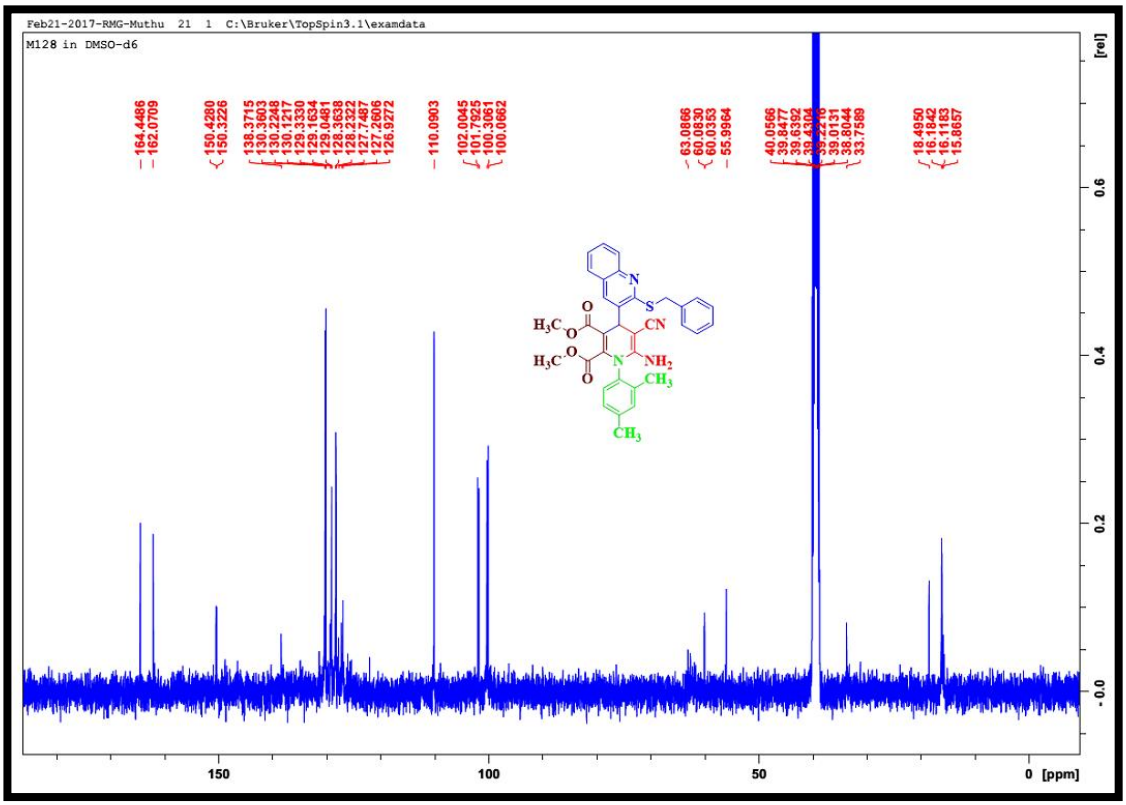

Fig. 6.29. ^{13}C-NMR spectrum of **30**

6.10. Dimethyl 6-amino-4-(2-(benzylthio)quinolin-3-yl)-5-cyano-1-(pyridin-2-ylmethyl)-1,4-dihydropyridine-2,3-dicarboxylate (31)

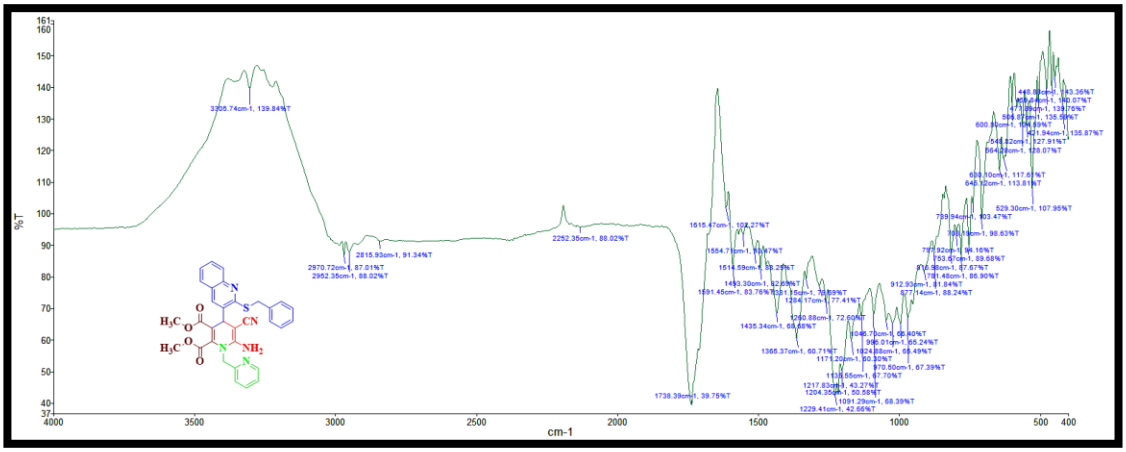

Fig. 6.30. IR spectrum of **31**

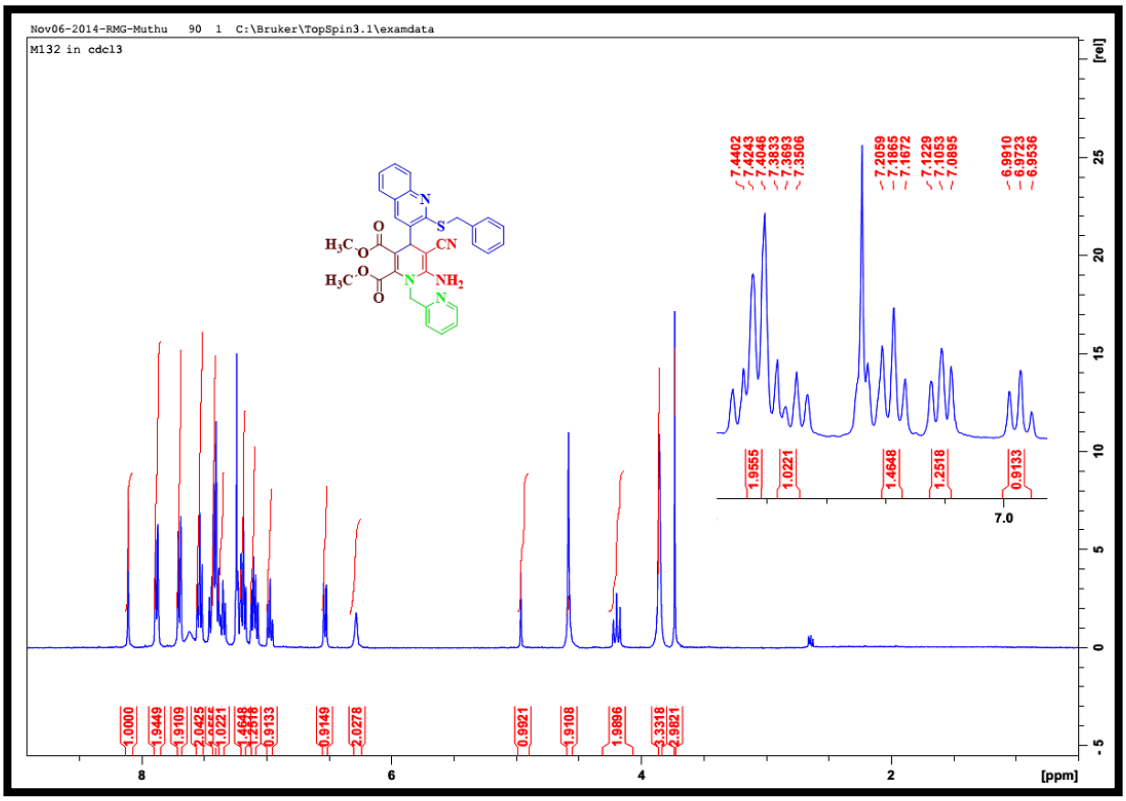

Fig. 6.31. ^{1}H-NMR spectrum of **31**

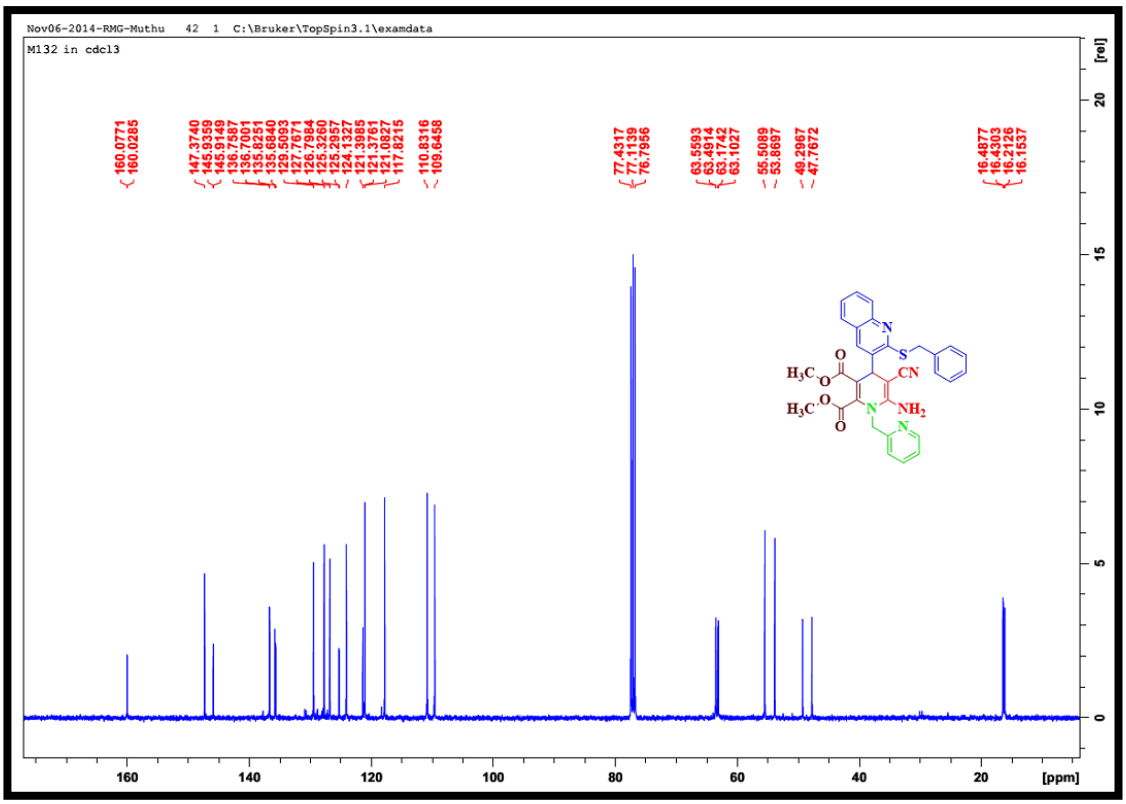

Fig. 6.32. ^{13}C-NMR spectrum of **31**

6.11. Dimethyl 6-amino-4-(2-(benzylthio)quinolin-3-yl)-5-cyano-1-((2-(piperazin-1-yl)ethyl)amino)-1,4-dihydropyridine-2,3-dicarboxylate (32)

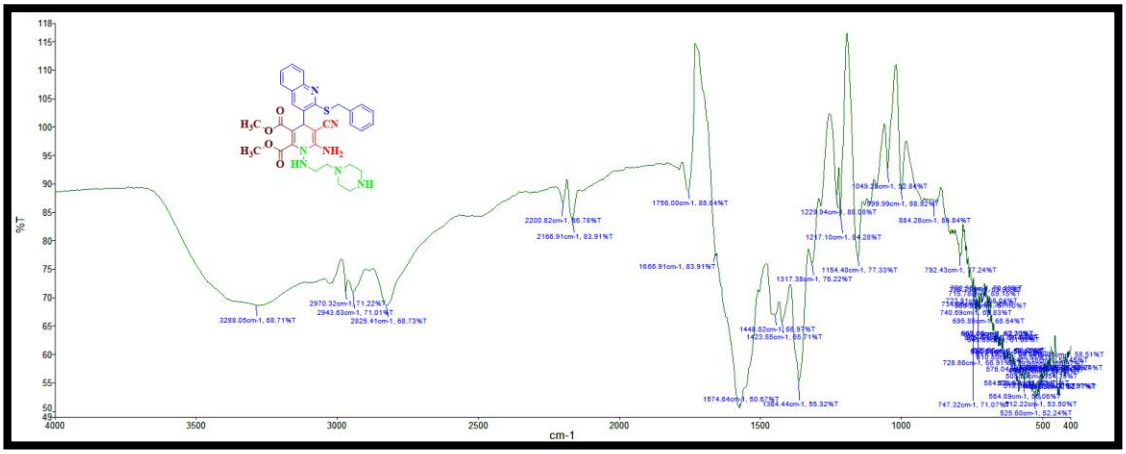

Fig. 6.33. IR spectrum of **32**

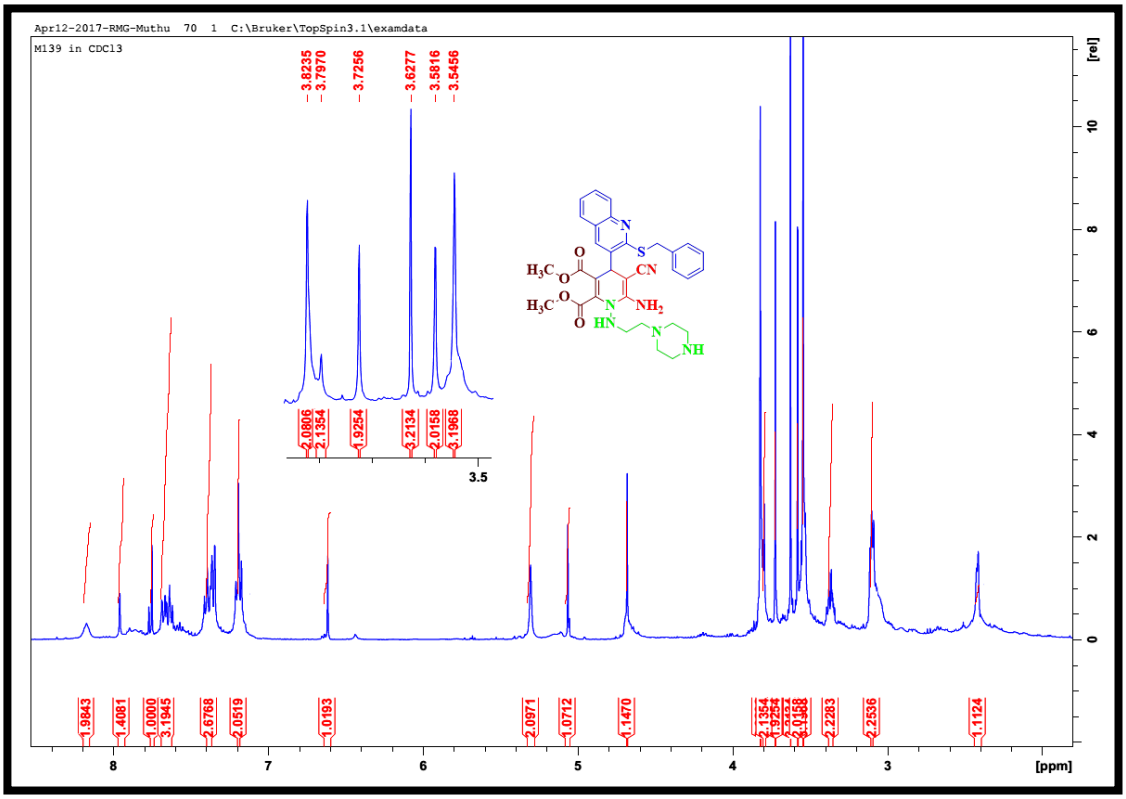

Fig. 6.34. ^{1}H-NMR spectrum of **32**

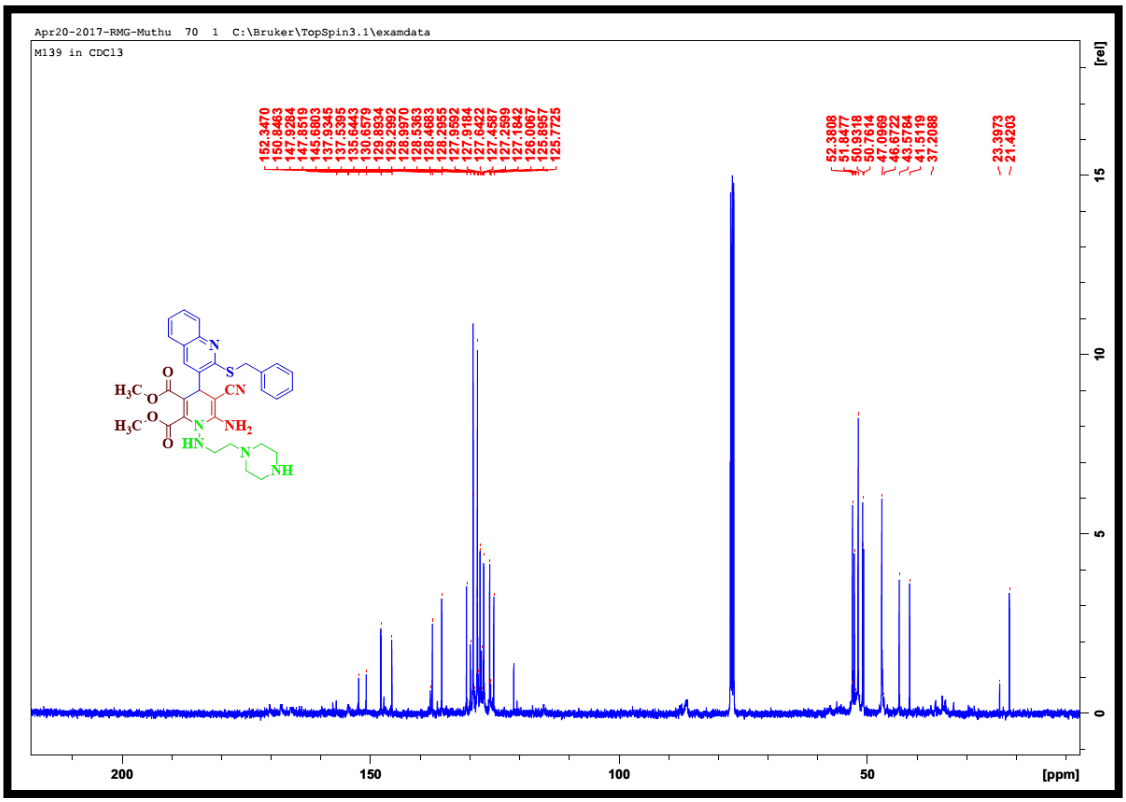

Fig. 6.35. ^{13}C-NMR spectrum of **32**

6.12. Dimethyl 6-amino-4-(2-(benzylthio)quinolin-3-yl)-5-cyano-1-(3,4-dichlorophenyl)-1,4-dihydropyridine-2,3-dicarboxylate (33)

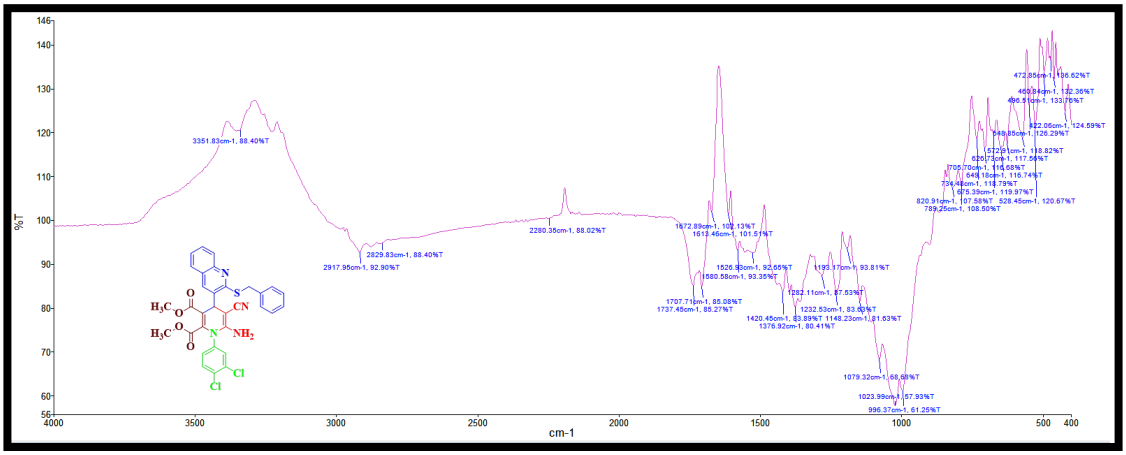

Fig. 6.36. IR spectrum of **33**

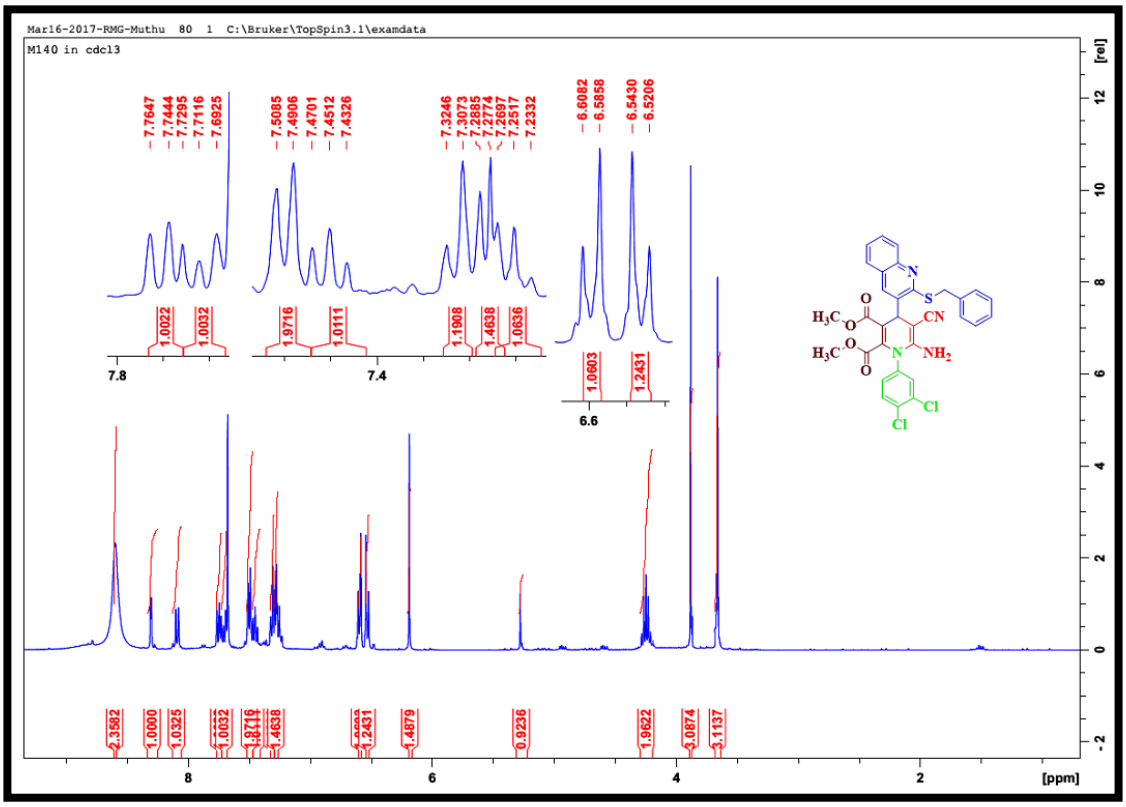

Fig. 6.37. ^{1}H-NMR spectrum of **33**

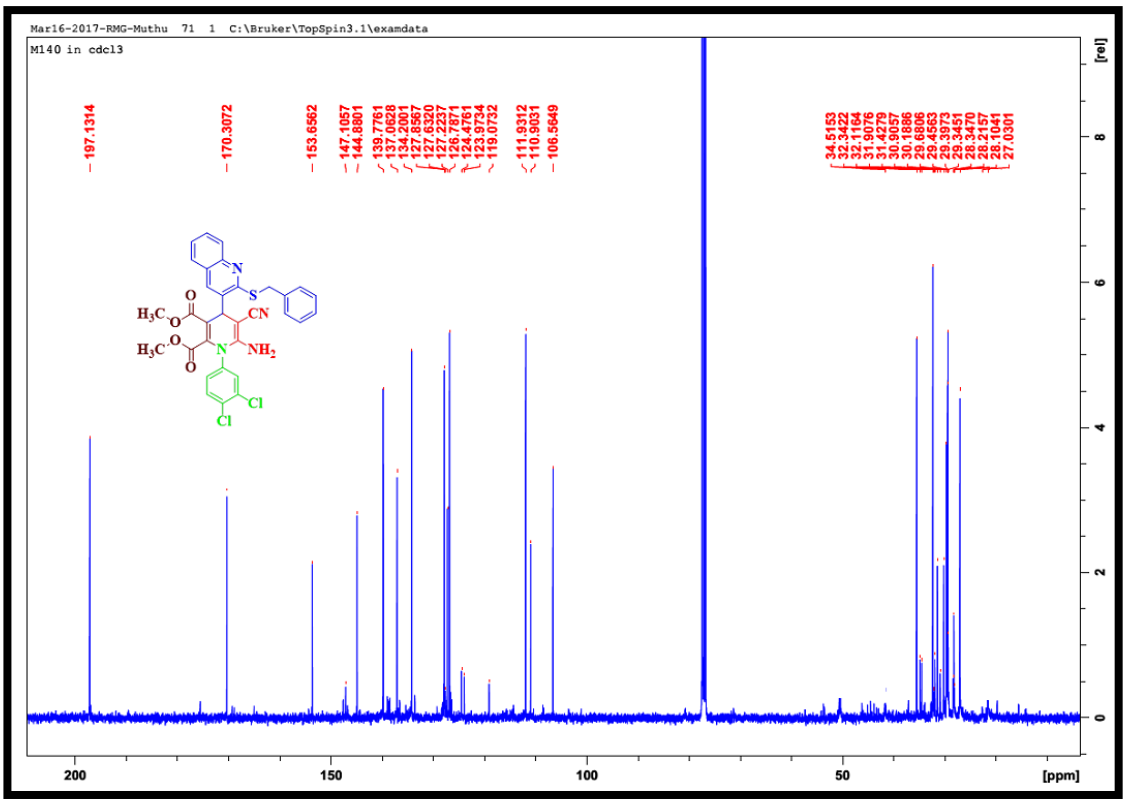

Fig. 6.38. ^{13}C-NMR spectrum of **33**

6.13. Dimethyl 6-amino-4-(2-(benzylthio)quinolin-3-yl)-1-(2-bromophenyl)-5-cyano-1,4-dihydropyridine-2,3-dicarboxylate (34)

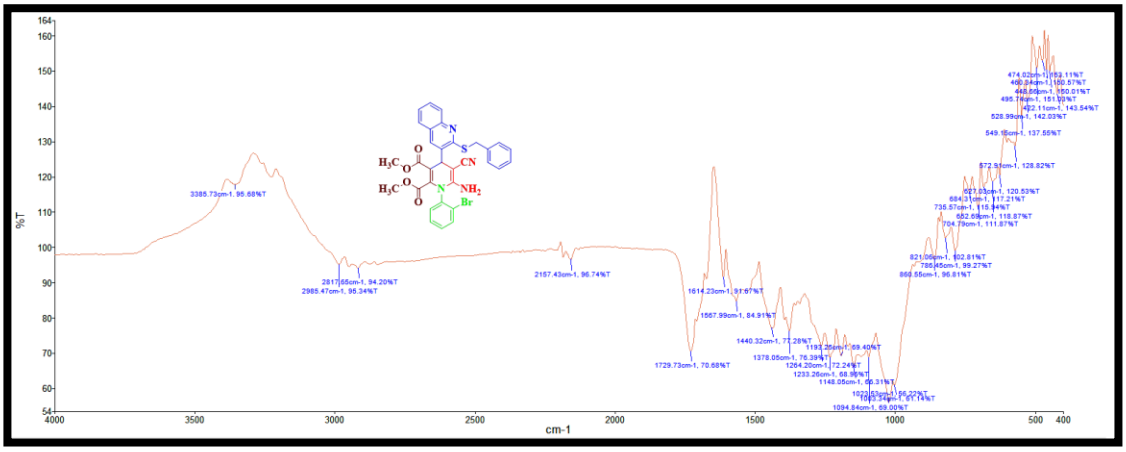

Fig. 6.39. IR spectrum of **34**

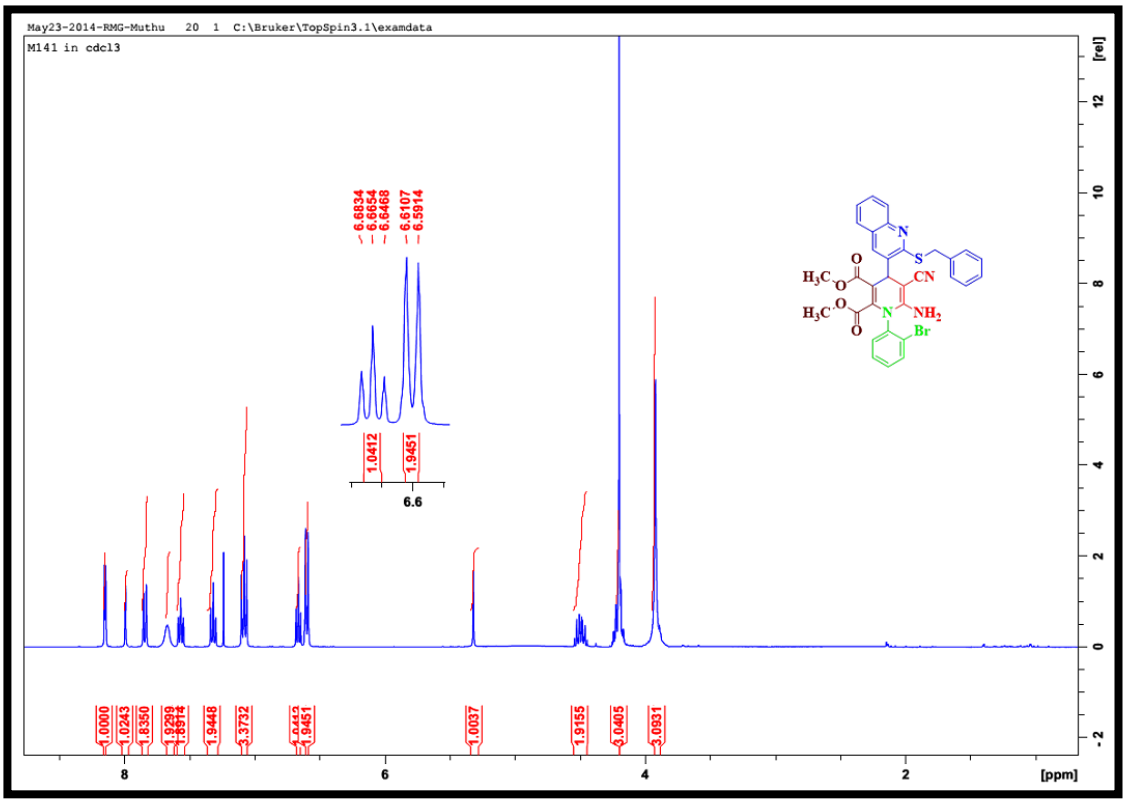

Fig. 6.40. ^{1}H-NMR spectrum of **34**

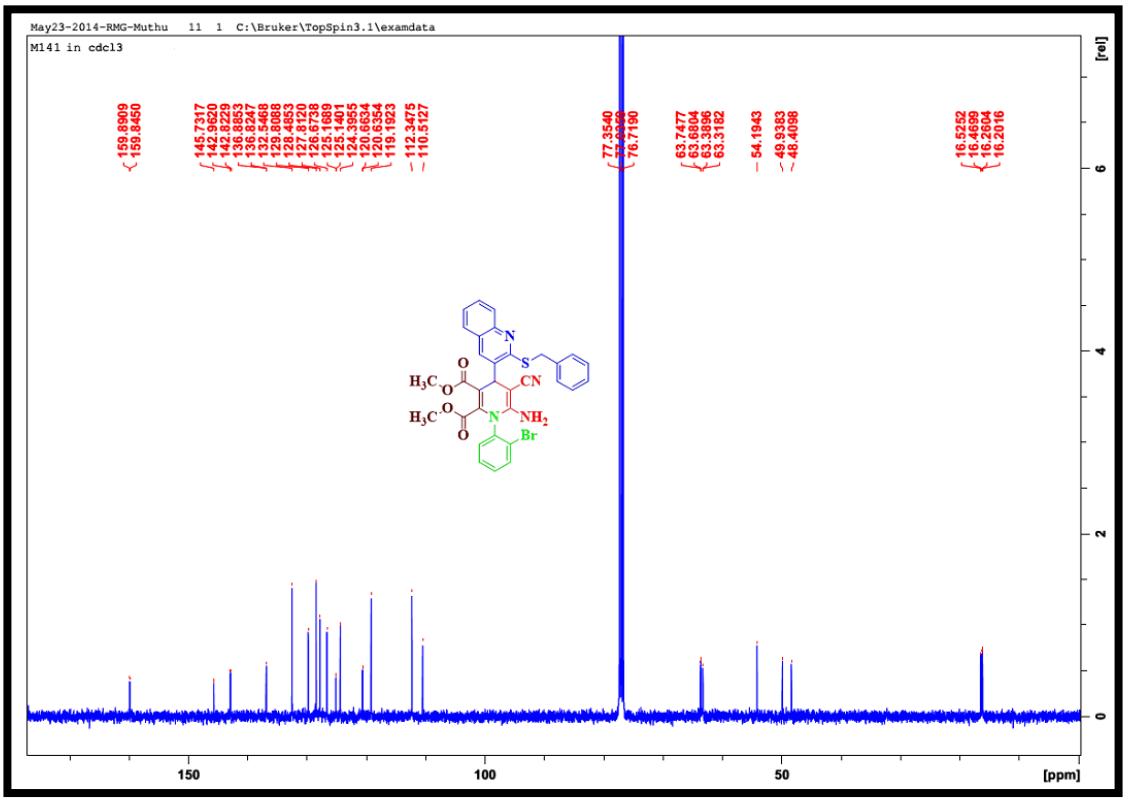

Fig. 6.41. ^{13}C-NMR spectrum of **34**

6.14. Dimethyl 6-amino-4-(2-(benzylthio)-6-fluoroquinolin-3-yl)-5-cyano-1-(2,4-dimethylphenyl)-1,4-dihydropyridine-2,3-dicarboxylate (35)

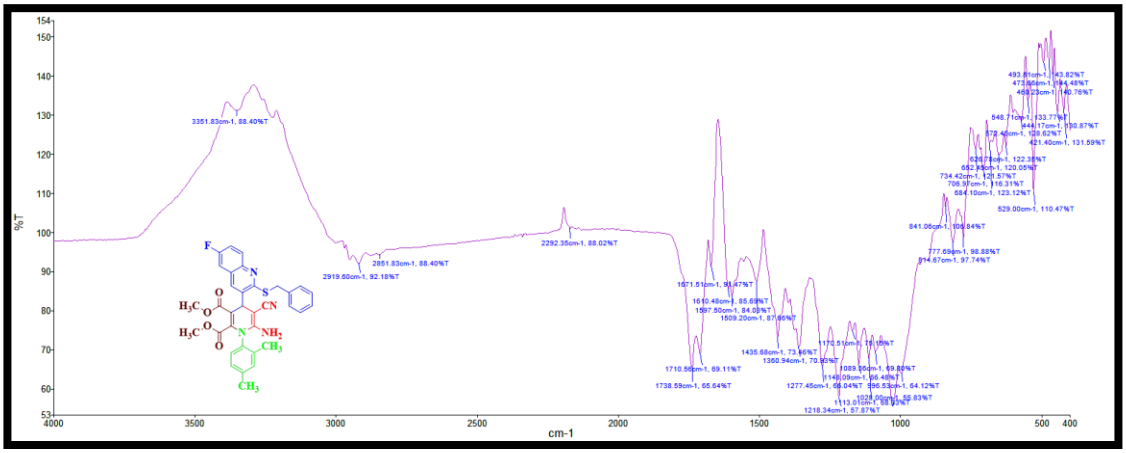

Fig. 6.42. IR spectrum of **35**

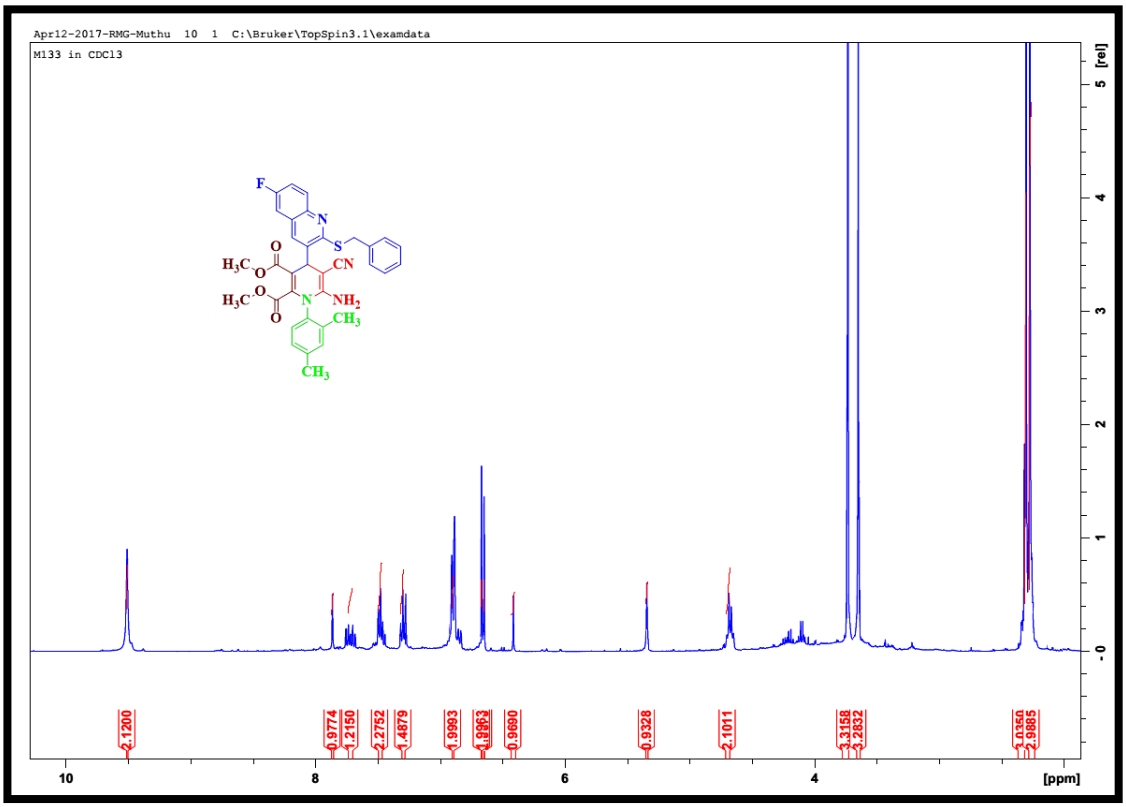

Fig. 6.43. ^{1}H-NMR spectrum of **35**

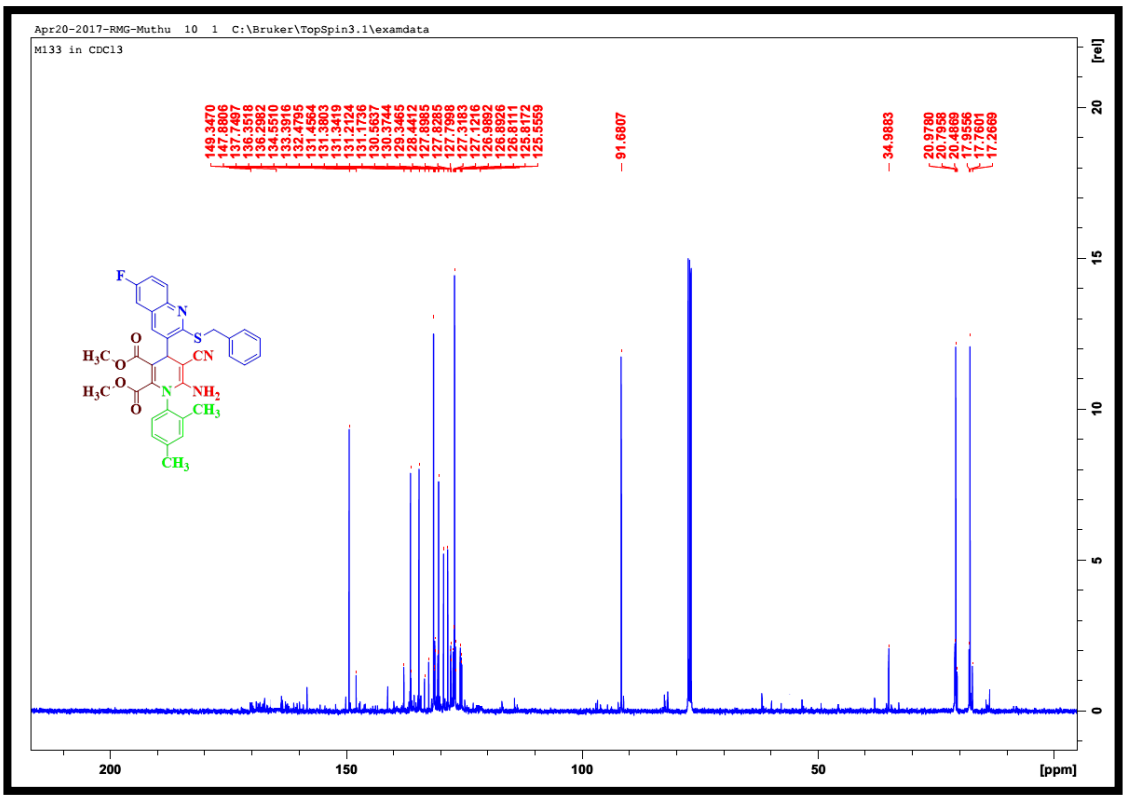

Fig. 6.44. ^{13}C-NMR spectrum of **35**

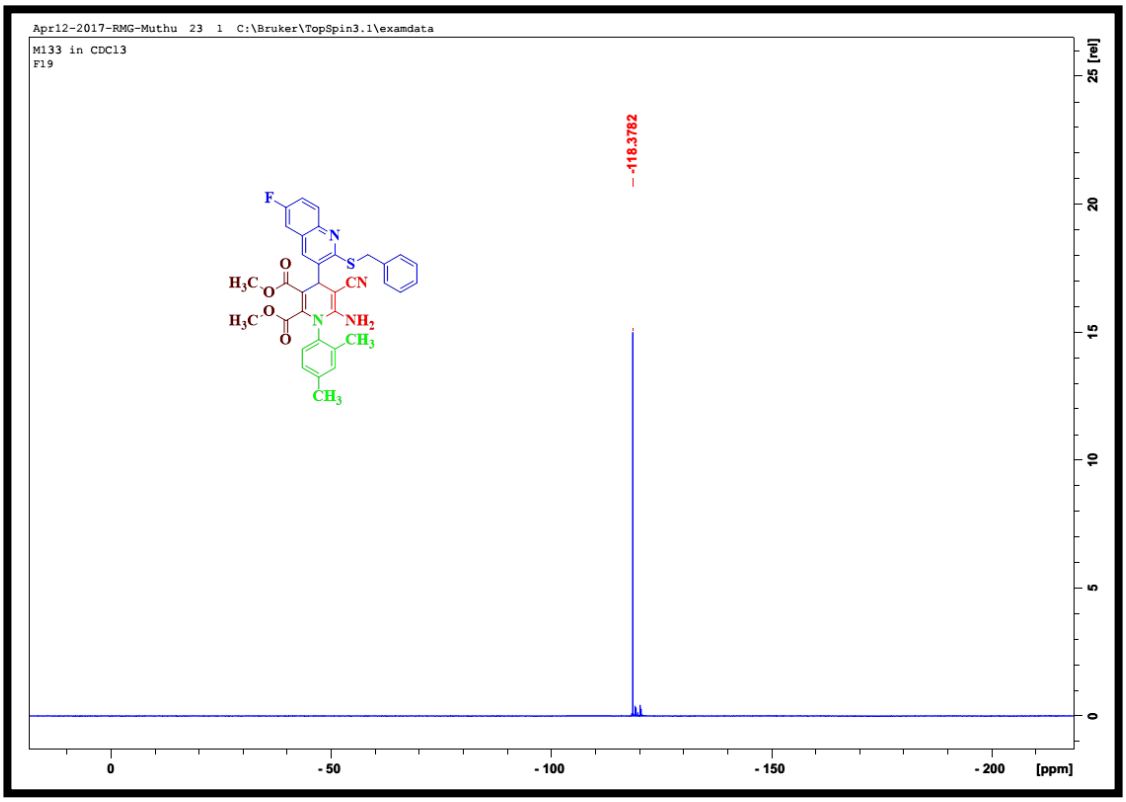

Fig. 6.45. ^{19}F-NMR spectrum of **35**

Chapter-VII

Calcium loaded boron nitride material as a new catalyst for the synthesis of 2-amino-*4H*-pyran-3-carbonitriles and anti-bacterial studies

Chapter Seven

Calcium loaded boron nitride material as a new catalyst for the synthesis of 2-amino-*4H*-pyran-3-carbonitriles and anti-bacterial studies

7.1. Abstract

A new calcium-loaded boron nitride catalyst (Ca/BN) was prepared and characterized fully by XRD, SEM with EDX, Raman spectroscopy, BET, DSC-TGA and FTIR. Then Ca/BN was used in a one-pot multi-component reaction to synthesize 2-amino-*4H*-pyran-3-carbonitrile derivatives (APCs): high yields were obtained. This transformation transpired via a Knoevenagel condensation, Michael addition and intra-molecular cyclization. The APCs were characterised by FTIR, ^{1}H-NMR, ^{13}C-NMR and elemental analysis. Furthermore, Ca/BN was easily separated from the reaction mixture and re-used more than five times with only 10 % loss of activity. A total of five APCs were subjected to antibacterial studies against *Staphylococcus aureus* (*S. aureus*), *Escherichia coli* (*E. coli*) and *Pseudomonas aeruginosa* (*P. aeruginosa*). The minimal inhibitory concentration (MIC) value for the synthesized compounds were obtained. Among them, **29** showed MIC values of 128, 16 and 4 µg/mL towards *E.coli*, *P. aeruginosa* and *S. aureus*, respectively. The methodology used for the synthesis of APCs offers several advantages such as excellent product yields, use of inexpensive solvent and a relatively short reaction time.

7.2. Introduction

One-pot multi-component reactions (MCRs) are simple and efficient synthetic routes for producing diverse heterocycles. These reactions are straight-forward one-step transformations which offer significant advantages over conventional linear type syntheses due to their flexible, convergent and atom efficient nature. Thus, the development of MCRs has attracted considerable attention as an ideal synthesis protocol due to their efficiency, facile implementation and generally high product yield. These reactions are being used to produce elaborate, biologically active compounds hence are an important area of research in organic, combinatorial and medicinal chemistry. The

common MCRs procedure for the synthesis of 2-amino-*4H*-pyran-3-carbonitrile derivatives (APCs) employs a three-component mixture of cyclic 1,3-diketones, aldehydes and malononitrile and is performed under a variety of reaction conditions.

Catalysts such as piperidine/ammonium acetate (Hassanien *et al*., 1999) and triethylamine (Shestopalov *et al*., 2003) were reported with yields of 70-85 %. However, aqueous solutions of alkyl ammonium salts (Balalaie *et al*., 2006) and (S)-proline (Fan *et al*., 2004) resulted in higher yields of 75-95 % but, long reaction times of up to 10 h was a major disadvantage. Other reagents such as benzyltriethylammonium chloride (TEBA) (Shi *et al*., 2003), NaBr (Devi and Bhuyan, 2004), amino functionalized ionic liquid (Peng and Song, 2007), ammonium chloride (Dabiri *et al*., 2009), ethylenediamine diacetate (Hari and Lee, 2010), surfactant metal carboxylates (Wang *et al*., 2010) and β-cyclodextrin (Sridhar *et al*., 2009) were reported.

Insulating oxides such as SiO_2, Al_2O_3, silica-alumina and various zeolites are materials commonly used as catalyst supports (Spivey, 1987). These oxides possess low thermal conductivity, generating sintering of the assisted metal on hot spots, various acidic and basic sites and the coverage of the catalyst with water at low temperature due to its hydrophilic surface. Various two-dimensional (2D) nanomaterials have received considerable attention for developments as heterogeneous catalysis. Among them, boron nitride (BN) is showing potential because of its high elastic modulus, high melting-point, excellent thermal conductivity and a large and direct band gap. Such properties can be of great value for ultraviolet-light emitters, advanced ceramic composites, electrical insulators, solid lubricants and ideal substrates (Liu *et al*., 2014) therefore in this study BN was used as a catalyst support.

The graphene-like hexagonal BN (Nag *et al*., 2010) is the most stable isomer. A giant planar network of hexagonal boron nitride (hBN) provides acid and base resistance, good thermal and electrical conductivity and chemical inertness. BN is hydrophobic preventing the condensation of moisture on its surface. Activated BN exhibits excellent adsorption for various metal ions such as Cr^{3+}, Co^{2+}, Ni^{2+}, Ce^{3+} and Pb^{2+} and for organic pollutants such as tetracycline, methyl orange and Congo red in water, as well as volatile organic compounds such as benzene in air (Li *et al*., 2013).

Wang *et al*., 2004 reported the synthesis of a series of 2-cyano-3-aryl-3-(3,4-dihydro-1(2H)-naphthalene-one-2-yl) propionitrile derivatives from malononitrile, 2-aryl methyl-idene-3,4-dihydro-1(2H)-naphthalenone and 2,6-biarylmethylidene cyclohexanone. This reaction used KF-Al_2O_3 as a catalyst under reflux for 10-14 h. The yield was in the range of 68 to 93 %.

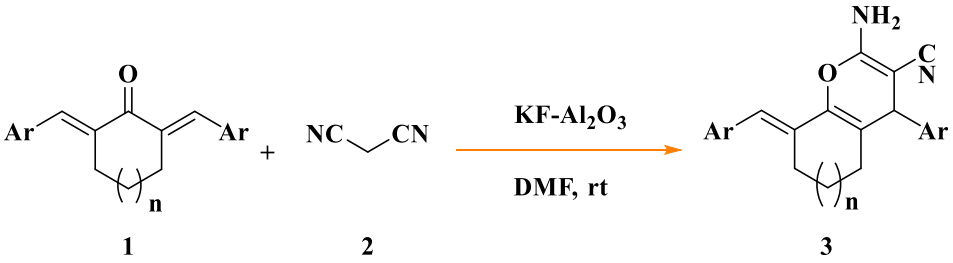

1 2 3

Ar = C_6H_5, 4-$CH_3C_6H_5$, 4-ClC_6H_4, 2,4-ClC_6H_4

Zhou, 2003 synthesized 3-cyano-2-methoxylpyridine and 2-amino-3-cyano-*4H*-pyran derivatives by a one-pot reaction of 2,6-bisarylidene cyclohexanone with malononitrile in sodium hydroxide/piperidine. The yield was 60-80 % within 5-9 h of reflux.

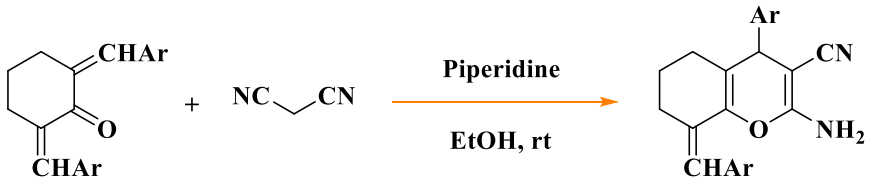

4 2 5

Ar = C_6H_5, 4-ClC_6H_5, 4-$CH_3OC_6H_4$, 3-$O_2NC_6H_4$

Rare earth perfluoro octanoate [RE$(PFO)_3$] was used as a catalyst by Wang *et al*., 2006 for the condensation of dimedone, aldehydes and malononitrile. The corresponding 5-oxo-5,6,7,8-tetrahydro-*4H*-benzo-[b]-pyran derivatives were obtained in 28 to 92 % yield within 5 h.

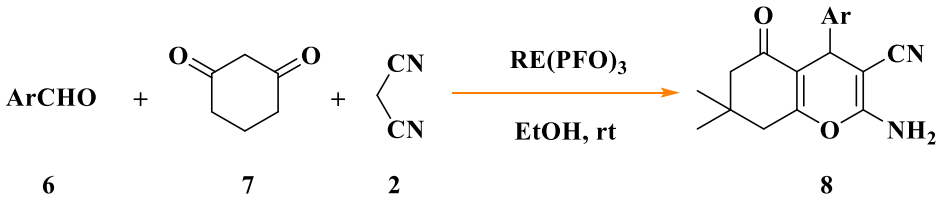

6 7 2 8

Ar = C_6H_5, 4-BrC_6H_4, 4-$OCH_3C_6H_4$, 2,4-$Cl_2C_6H_5$

Khaksar *et al*., 2012 reported a one-pot three-component syntheses of 2-amino-3-cyano-*4H*-chromenes and tetrahydrobenzo[*b*]pyran derivatives by condensation of aldehydes, malononitrile and resorcinol or dimedone in the presence of 2,2,2,-trifluoroethanol as a catalyst. The reaction took 5 h to afford a yield of 80-96 %.

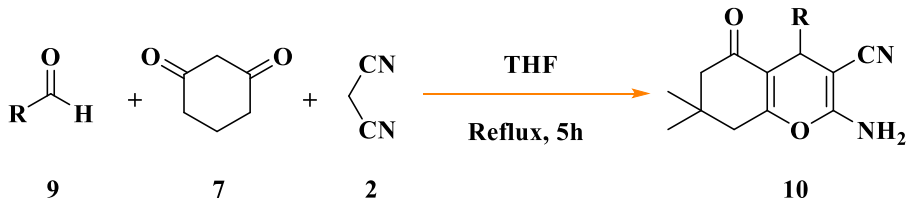

9 7 2 10

R = C_6H_5, 4-ClC_6H_5, 4-FC_6H_5, 4-BrC_6H_5, 4-$NO_2C_6H_5$, 2-FC_6H_5

Elnagdi *et al*., 2012 synthesized pyrans via the multi-component reaction of aromatic aldehydes, malononitrile and active methylenes in the presence of L-proline as a catalyst. The reaction was carried out in 4 h under reflux conditions to afford a yield of 60-90 % in ethanol.

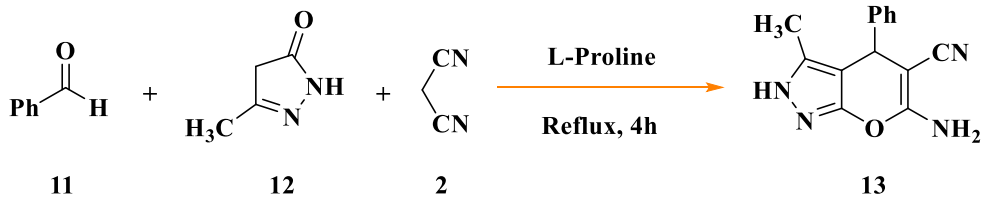

11 12 2 13

Ph = C_6H_5, 2-$CH_3C_6H_5$

Shaabani *et al*., 2009 developed the synthesis of functionalized chromene derivatives through the addition and subsequent cyclization of 2-hydroxynaphthalene-1,4-dione or

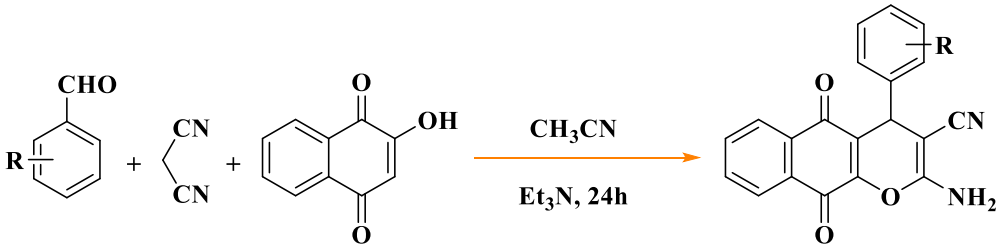

14 2 15 16

R = H, 2-CH_3, 4-Br, 4-NO_2, 4-Cl, 2-OCH_3

2,5-dihydroxy cyclohexa-2,5-dione to the condensation product of an aldehyde with malononitrile in the presence of catalytic amount of Et_3N in acetonitrile at ambient temperature. The products were obtained at 65-82 % yield within 24 h.

Moafi *et al*., 2010 described a three-component method for the synthesis of 2-amino-4-cyano-*4H*-chromenes by reaction of salicylaldehydes, malononitrile or cyanoacetamide and trimethylsilyl cyanide (TMSCN) in the presence of $LiClO_4$ at room temperature. The reaction was achieved within 24 h with a maximum yield of 83-93 %.

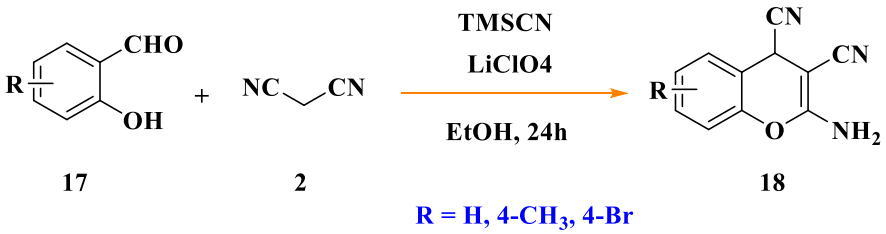

17 2 18

R = H, 4-CH_3, 4-Br

7.3. Results and discussion

A new heterogeneous Ca/BN catalyst containing calcium and BN was prepared by simply stirring a mixture of $Ca(OAc)_2$ and BN in an inert atmosphere for 7 days.

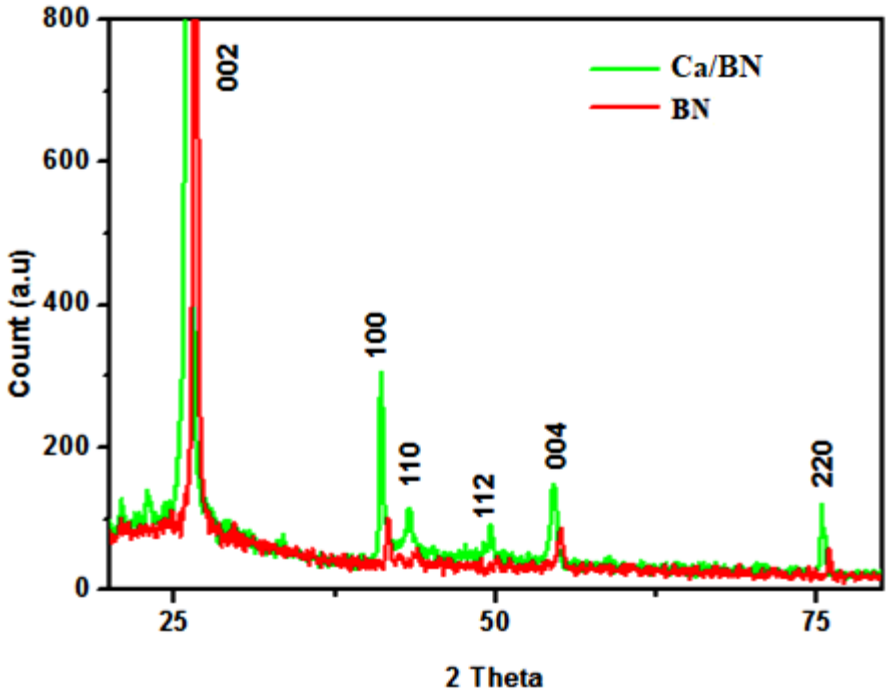

Fig. 1. X-Ray diffraction spectrum of Ca/BN

The Ca/BN was characterized by several techniques such as XRD, SEM with EDX, BET, Raman spectroscopy, DSC-TGA and FTIR. The XRD spectrum of Ca/BN (**Fig. 1**) showed the crystalline nature: the characteristic Bragg's XRD peaks of BN at 26.09, 41.05, 54.43 and 75.34 were indexed to (002), (100), (004) and (220), respectively whilst the Ca peaks at 43.19 and 49.56 were indexed to (110) and (112), respectively.

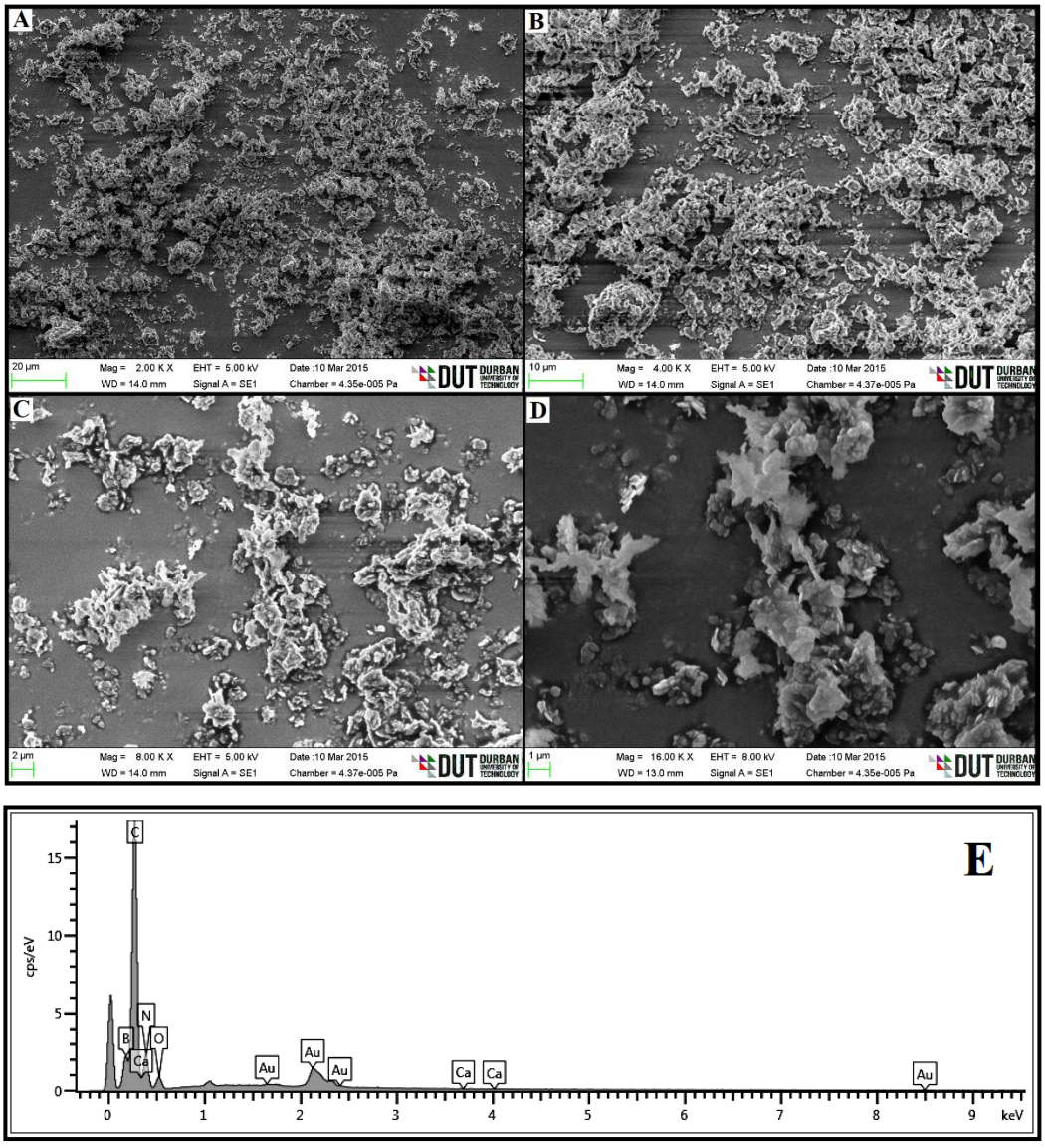

Fig. 2. Scanning electron microscope images of Ca/BN at 20 µm (**A**), 10 µm (**B**), 2 µm (**C**) and 1 µm (**D**) and Energy dispersive X-ray spectrum (**E**)

The SEM images (**Fig. 2A-D)** illustrated the morphologies of Ca/BN at 20 µm, 10 µm, 2 µm and 1 µm. The plate-like particles were clearly visible. The spherical-shaped particles that were observed suggested the presence of B_2O_3 particles (Ertug *et al*., 2007) that explained the presence of moisture during sample analysis.

Fig. 2E shows the Energy Dispersive X-ray (EDX) spectrum of Ca/BN. The Ca peaks were observed at 0.3, 3.7 and 4.0 KeV. The appearance of gold (Au) peaks was due to the coating with Au during sample preparation.

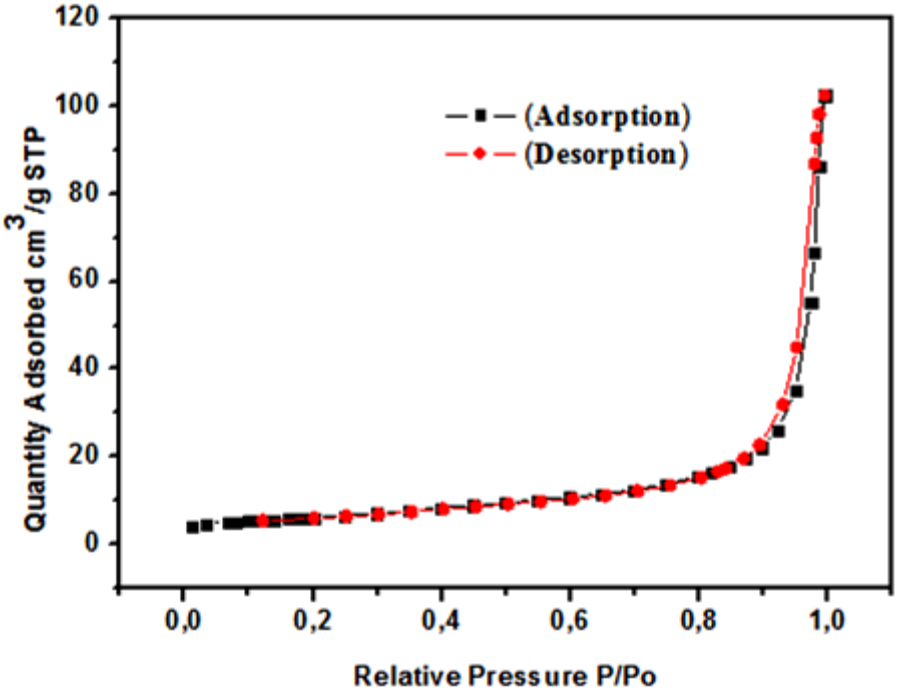

Fig. 3. Brunauer-Emmett-Teller surface area and surface size for Ca/BN

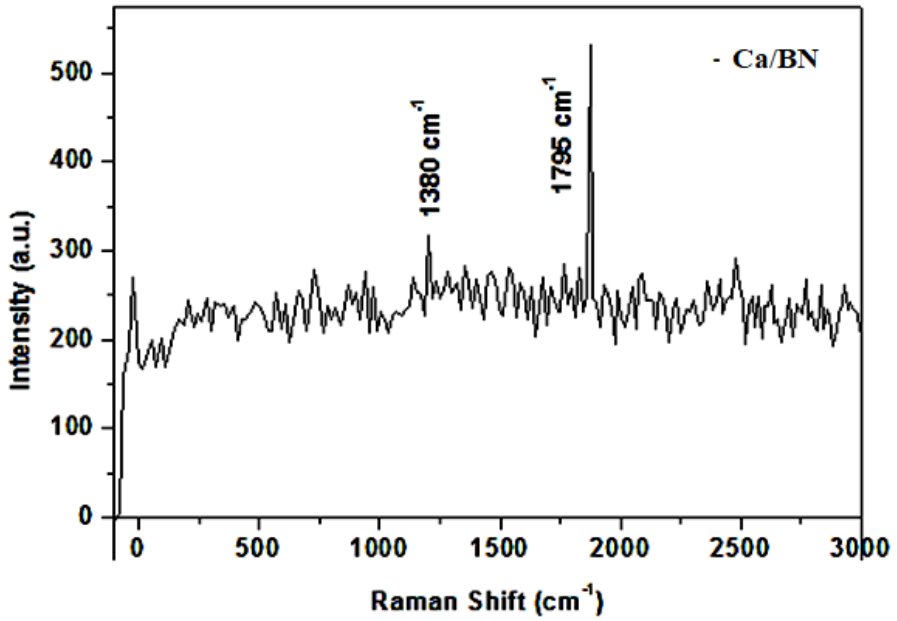

Fig. 4. Raman spectra of Ca/BN

The Brunauer-Emmett-Teller (BET) spectrum showed the specific surface area of Ca/BN by nitrogen multi-layer adsorption **(Fig. 3)**. The nitrogen adsorption and desorption isotherm and the pore size distribution of Ca/BN were determined: the observed BET surface area was 21.52 m^2/g, the pore volume was 0.1028 cm^3/g whilst the pore size was 191.15 A˚.

The Raman Spectrum of Ca/BN **(Fig. 4)** clearly showed three peaks located at approximately 900 cm^{-1}, 1380 cm^{-1} and 1795 cm^{-1}. The peak at 1380 cm $^{-1}$ was aligned to the BN phonon mode (Kalay *et al*., 2013) whilst the peak observed at 1795 cm^{-1} was due to calcium (Antunes *et al*., 2014; Harris *et al*., 2015).

The thermal stability of Ca/BN was measured from room temperature to 800˚C (**Fig. 5**). A broad exothermic peak on the DSC curve was observed at 150 ˚C.

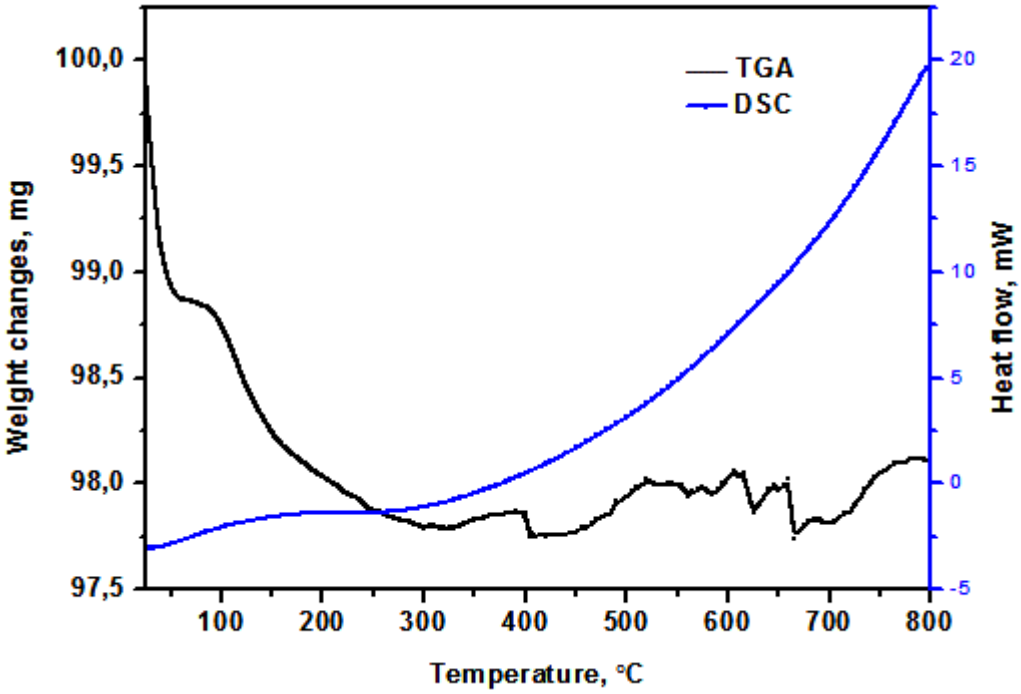

Fig. 5. Differential scanning calorimetry-Thermal gravimetric analysis of Ca/BN

The corresponding TGA curve revealed two mass losses viz., 0.2 wt % in the temperature range of 93 to 95 ˚C and a gradual loss of weight in the temperature range of 102 to 300 ˚C which was probably due to the partial decomposition of Ca/BN. A mass loss of water was observed at 100 ˚C. Above 400 ˚C, the weight was found to increase slightly by ~0.35 wt % which might be associated with the partial formation of Ca_3B_2.

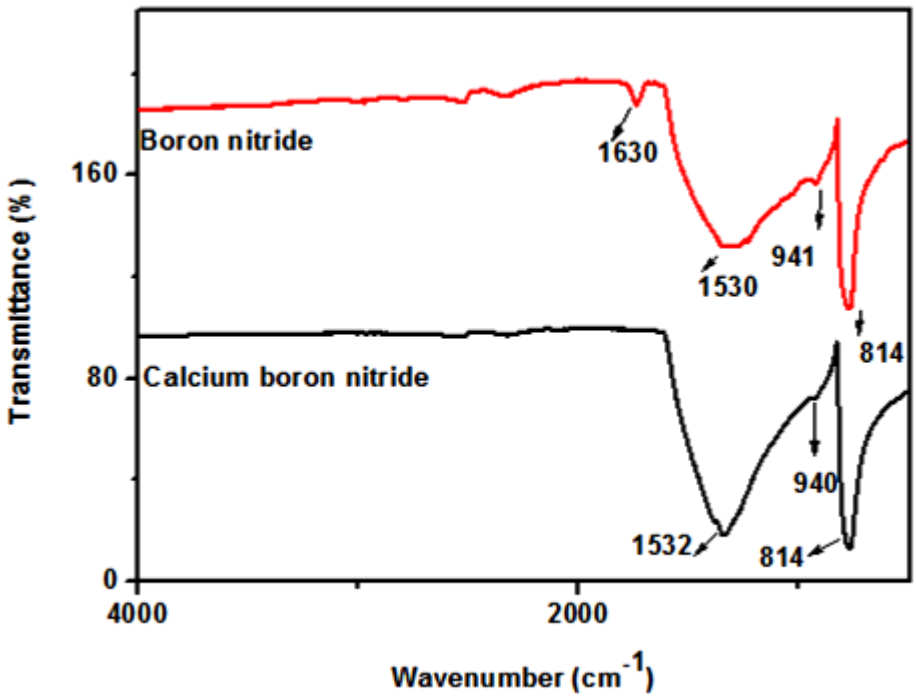

Fig. 6. Fourier transform infrared spectrum of Ca/BN

The FTIR spectrum (**Fig. 6**) of Ca/BN showed BN as N-B-N at 1630 cm^{-1}, B-N at 1530 cm^{-1} and B-N-B at 814 cm^{-1} whilst Ca-N at 940 cm^{-1} was assigned to an asymmetric stretch and 1532 cm^{-1} was assigned as the symmetric stretch. The peak observed at 1630 cm^{-1} for N-B-N was absent after loading calcium to form Ca/BN. Ca/BN was subsequently assessed for catalytic activity for the synthesis of 2-amino-*4H*-pyran-3-carbonitrile (APCs).

In a preliminary experiment, an equivalent quantity (1 mmol) of aromatic aldehyde (**19**), malononitrile (**2)** and dimedone (**7**), in toluene, was refluxed at 110℃ in the presence of pure BN. The reaction was monitored by TLC: after 24 h, trace amount of a new product was observed. However, when the reaction was conducted in the presence of 10 mol % Ca/BN, within 1 h, an intense new spot was observed on the TLC plate. The reflux was continued until all the reactants were used. The reaction took 6 h to afford a 95 % product yield (**Scheme 1**). After the usual work-up of the reaction, and purification by column chromatography, the product was identified as **20** by FTIR, ^{1}H-NMR, ^{13}C-NMR, DEPT 90º, DEPT 135º, HSQC, COSY, NOESY, HMBC and elemental analysis.

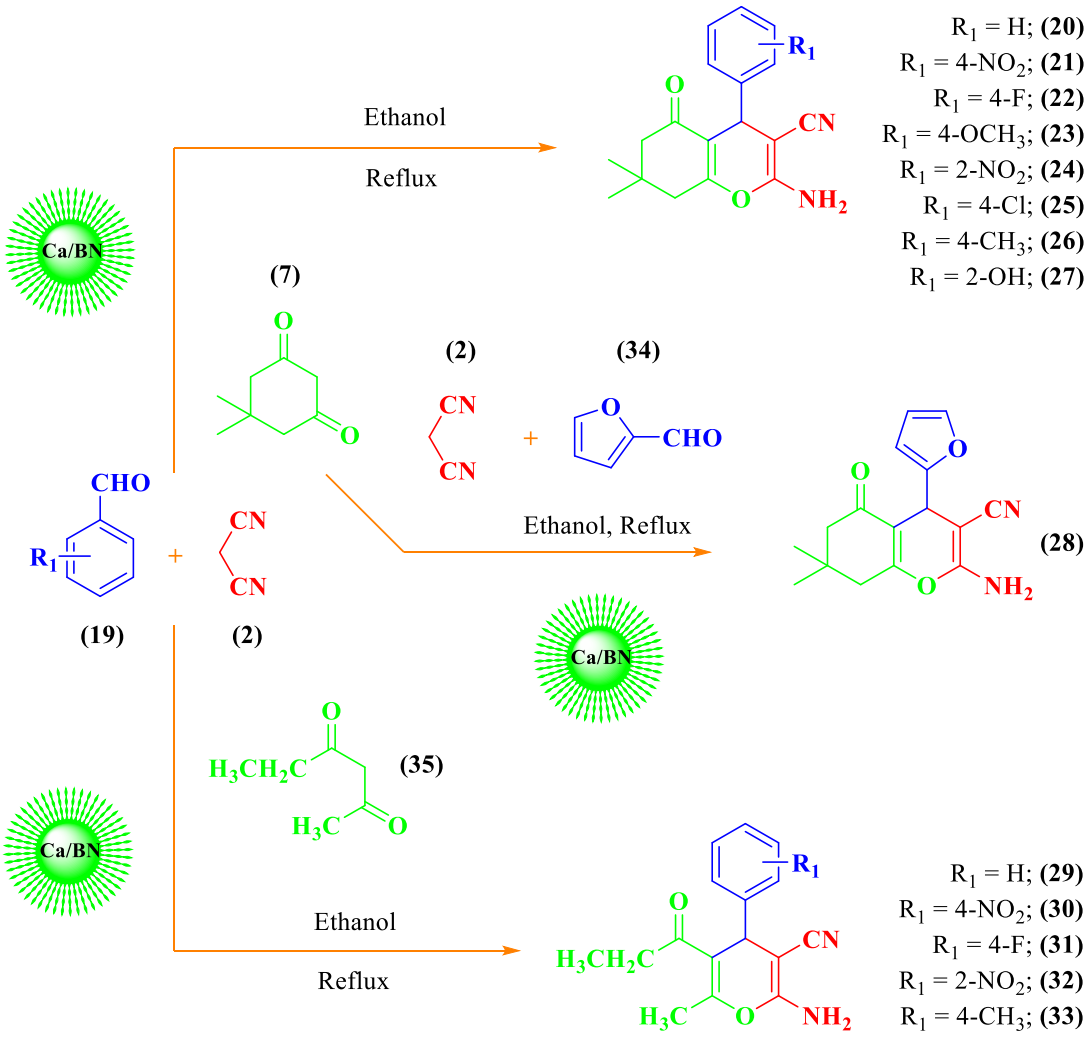

Scheme 1. The synthesis of 2-amino-*4H*-pyran-3-carbonitriles (**20-33**)

The IR spectrum (**Fig. 7.1**, Appendix VII) of **20** showed stretching frequencies (cm^{-1}) at 3394 for NH_2, 1036 for C-N, 2201 for CN, 1456 for C=C, 1642 for C=O, 1036 for C-O and 2963 for CH. The ^{1}H-NMR spectrum (**Fig. 7.2**) of the compound **20** showed four singlets, ie., C<u>H</u> (C4) at δ 4.16, N<u>H</u>$_2$ (C12) broad singlet at δ 6.98 , methyl proton (C<u>H</u>$_3$, C9) broad singlet at δ 0.94 and C<u>H</u>$_3$ (C10) broad singlet δ 1.03 . The (C<u>H</u>$_2$, C6) proton of dimedone, showed a doublet of triplet at δ 2.50. A doublet was observed for one proton (C8 carbon, C<u>H</u>$_2$) at δ 2.25 and a doublet at δ 2.10 which showed the presence of another proton of C8 (C<u>H</u>$_2$). The C2'-<u>H</u> proton at δ 7.13 of the phenyl group was a triplet for one proton with coupling constant, J=11.96 Hz. The C3'-<u>H</u> proton of the phenyl group was a triplet for one proton with coupling constant, J=7.28 Hz, at δ 7.28. The C4'-<u>H</u> proton of the phenyl group was a doublet at δ 7.19 with coupling constant, J=0.96 Hz. The C5'-<u>H</u> proton of the phenyl group at δ 7.28 was a triplet for one proton with coupling constant,

J=7.28 Hz. The C6'-H of the phenyl group was a triplet for one proton at *δ*, 7.13 with coupling constant, *J*=11.96 Hz. The selected ^{1}H and ^{13}C-NMR chemical shifts are shown in **Fig. 7**.

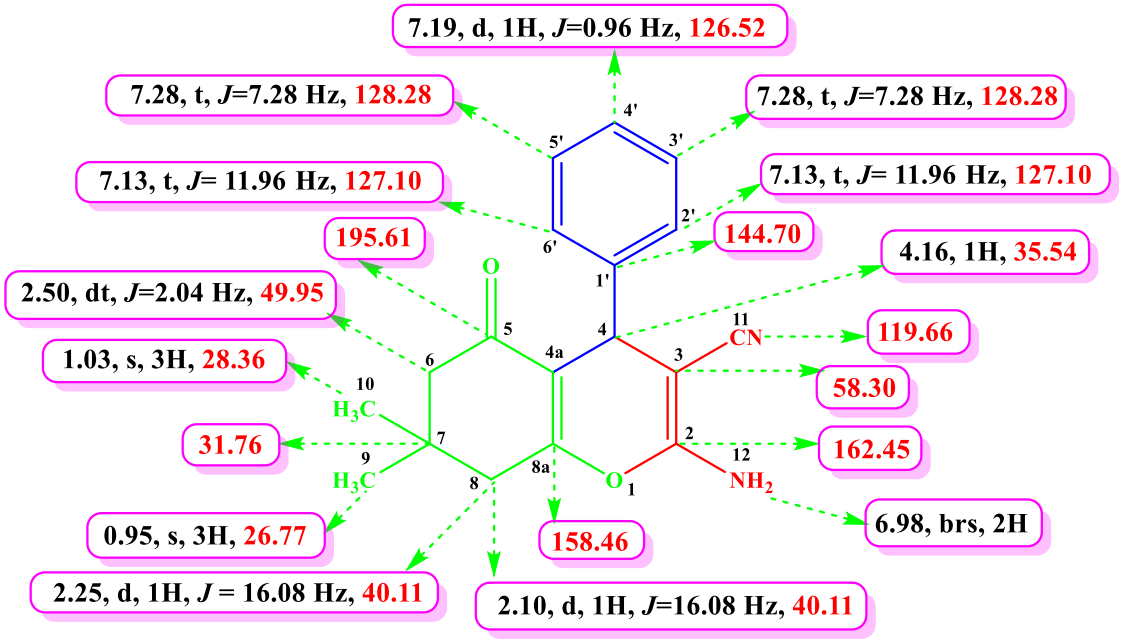

Fig. 7. Selected ^{1}H and ^{13}C-NMR chemical shifts of **20**

The ^{13}C-NMR spectrum (**Fig. 7.3**) showed the carbonyl group C5' at *δ* 195.61. The methyl carbons C9 and C10 were observed at *δ* 26.77 and 28.35. The C7 carbon of the dimedone skeleton showed a peak at *δ* 31.76, C8 showed a peak at *δ* 40.11 and C6 showed a peak at *δ* 49.95. The following *δ* values were observed for the pyran ring and dimedone carbons: C4 at 38.54, C3 at 58.30, C2 at 162.45, C11 at 119.66, C8a at 158.46 and C8 at 40.11. The absorption signals for the phenyl carbons were at the following *δ* values: C1' at 144.70, C2' at 127.10, C3' at 128.28, C4' at 126.52, C5' at 128.28 and C6' at 127.10. Furthermore, CH and CH_2 peaks were confirmed with DEPT 90° and DEPT 135°. The DEPT 90° spectra showed the CH (C4) peak at *δ* 35.54 (**Fig. 7.4**). The DEPT 135° showed the CH_2 peak at *δ* 49.95 for C6 carbon (**Fig. 7.5**).

The structure was further confirmed on the basis of 2D NMR spectral studies. The ^{13}C, ^{1}H-COSY correlation of carbon signals in ppm: *δ* 144.76, 128.28, 127.10, 126.52, 49.95, 35.54, 28.35 and 26.77 which were assigned to carbons C1', C3', C2', C4', C6, C4, C10 and C9, respectively (**Fig. 7.6**).

The ^{1}H, ^{1}H-COSY spectrum (**Fig. 7.7**) of the compound revealed the correlation between the singlet of CH (C4-H) proton at δ 4.16 and doublet of triplet of CH_2 (C6-H) proton at δ 2.50. The C4-H proton was correlated with C4' at δ 126.52 and C3' at δ 128.28. The ^{1}H, ^{1}H-NOESY spectrum (**Fig. 7.8**) of the compound revealed that the singlet of NH_2 at δ 6.98 was coupled with the doublet of triplet of CH_2 (C8-H) at δ 2.50.

The HMBC spectrum (**Fig. 7.9**) of **20** showed the long-range correlations as follows: The proton C4-H, CH group of **20** coupled with pyran ring carbon (C3) at δ 58.30, C2 at δ 162.45 and carbonitrile (C11) carbon at δ 119.66, phenyl ring carbons C1' at δ 144.70 and C6' at δ 127.10, dimedone carbons C4a at δ 112.73 and C8a at δ 158.46. This correlation of C4-H to the quaternary carbon (C1'), dimedone carbons C4a and C8a, pyran ring carbons C3 and C2, carbonitrile (C11) carbon and carbon (C6') of phenyl ring indicated that the three groups were attached to C4 (CH). Thus it was evident the three different moieties were bonded to a common carbon and hence added valuable information to **20**. The selected HMBC correlation chemical shifts are shown in **Fig. 8** below:

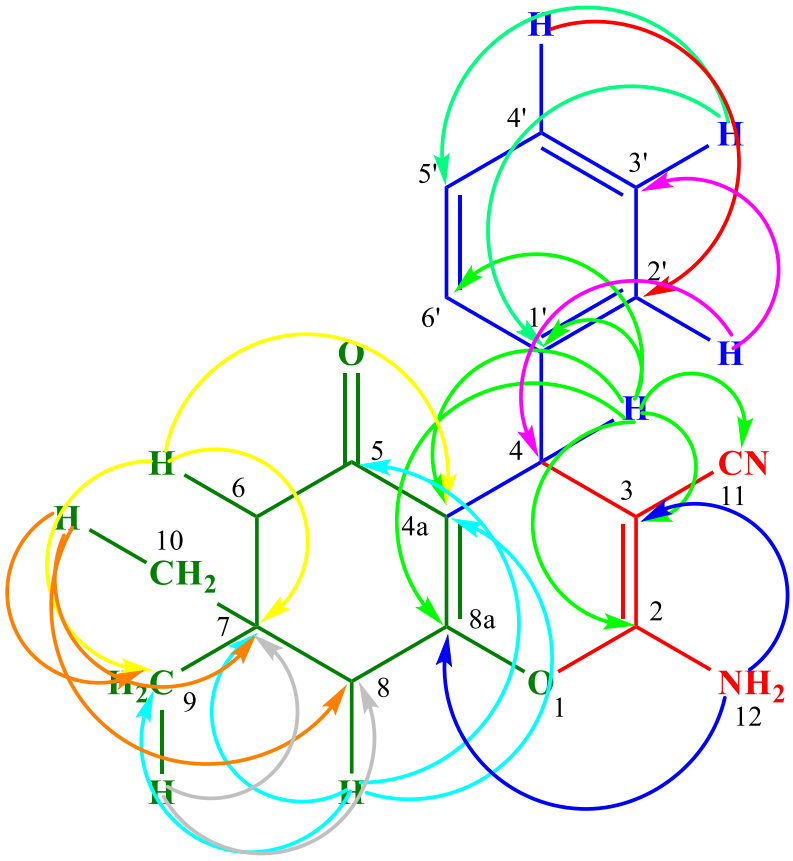

Fig. 8. The selected HMBC correlation for **20**

The phenyl group C3'-H proton coupled with C2' at δ 127.10 and C1' at δ 144.70. The C2'-H phenyl proton was coupled with C4 at δ 35.54 and C3' at δ 128.28. The C6-H, proton was coupled with C9 at δ 26.77, C7 at δ 31.76 and C4a at δ 112.71. The C8-H, proton was coupled with C7 at δ 31.76, C9 at δ 26.77, C5 at δ 195.61 and C4a at δ 112.71. The C9-H was coupled with C7 at δ 31.76 and C8 at δ 40.11. The C10-H was coupled with C9 at δ 26.77, C7 at δ 31.76 and C8 at δ 40.11. The C4'-H was coupled with C2' at δ 127.10. The C12-H (NH_2) was correlated with carbons C3 at δ 58.30 and C8a at δ 158.46. The selected ^{1}H, ^{13}C-NMR and HMBC chemical shifts of the compound **20** is shown in **Table 1**.

Table 1. Selected ^{1}H, ^{13}C-NMR and HMBC chemical shifts

S.No	Protons	Correlated carbons
1	C4-H (s, 1H, CH) at δ 4.16 ppm	C3 (58.30), C4a (112.71), C11 (119.66), C6' (127.10), C1'(144.70), C8a (158.46) and C2 (162.45)
2	C3'-H (t, 1H, J=7.28 Hz) at δ 7.28 ppm	C2' (127.10) and C1' (144.70)
3	C2'-H (t, 1H, J= 7.28 Hz) at δ 7.28 ppm	C4 (35.54) and C3' (128.28)
4	C6-H (d, 2H) at δ 2.25 and 2.10 ppm	C9 (26.77), C7 (31.76) and C4a (112.71)
5	C8-H (dt, 2H) at δ 2.50	C7 (31.76), C9 (26.77), C5 (195.61) and C4a (112.71)
6	C9-H (s, 3H) at δ 0.96 ppm	C7 (31.76) and C8 (40.11)
7	C10-H (s, 3H) at δ 1.03 ppm	C9 (26.77), C7 (31.76) and C8 (40.11)
8	C4'-H (d, 1H, J= 0.96 Hz) at δ 7.19 ppm	C2' (127.10)
9	C12-H (brs, 2H) at δ 6.98 ppm	C3 (58.30) and C8a (158.46)

Based on the above spectral details and elemental analysis: Anal. Calc. for $C_{18}H_{18}N_2O_2$: C, 73.45; H, 6.16; N, 9.52; %. Found: C, 73.47; H, 6.14; N, 9.50; %, the structure was confirmed as 2-amino-7,7-dimethyl-5-oxo-4-phenyl-5,6,7,8-tetrahydro-*4H*-chromene-3-carbonitrile (**20**). The synthesis of **20** was used as a model reaction.

To determine the optimum mole % of Ca/BN, the model reaction was carried with different mole percentages: 5 mol %, 10 mol %, 15 mol % and 20 mol % (**Table 2**).

Table 2. Optimization of Ca/BN catalyst

Entry	Catalyst	Mol %	Time (h)	Yield (%)
1	BN	25	up to 24	Trace
2	Ca/BN	5	6	70
3	Ca/BN	10	6	95
4	Ca/BN	15	6	95
5	Ca/BN	20	6	95

It was observed that on increasing the amount of Ca/BN to either 15 mol% or 20 mol % had no improvement in the yield (**Table 2**, entries 4 and 5). The best yield of **20** was obtained at 10 mol % of Ca/BN.

Also, in the model reaction, the presence of 10 mol % Ca/BN was investigated in different solvents to determine the effect on the reaction yield (**Table 3**). Solvents such as dichloromethane (DCM), ethyl acetate, ethanol, acetonitrile, toluene, methanol and water were used. Ethanol was determined to be the ideal solvent for this reaction which afforded maximum yield (95%) of **20** (**Table 3**, entry 3) for 6 h under reflux at 110 °C. Increasing the reaction time or temperature did not improve the yield.

Table 3. The effect of different solvents on the reaction

Entry	Solvent	Time (h)	Yield (%)
1	DCM	10	80
2	Ethyl Acetate	8	85
3	Ethanol	6	95
4	Acetonitrile	6	80
5	Toluene	8	78
6	Methanol	10	75
7	Water	10	72

To determine the catalytic efficiency of the recycled catalyst, five successive cycles for the synthesis of **20** were investigated under optimal reaction conditions. The procedure was simple: the final reaction mixture was filtered and the solid was washed with solvents, air-dried and then the catalyst was reused. It was observed that the activity of the catalyst did not produce any significant decrease in yield of **20** after five successive runs. The fifth run of the reaction produced 85% yield of **20** (**Fig. 9**).

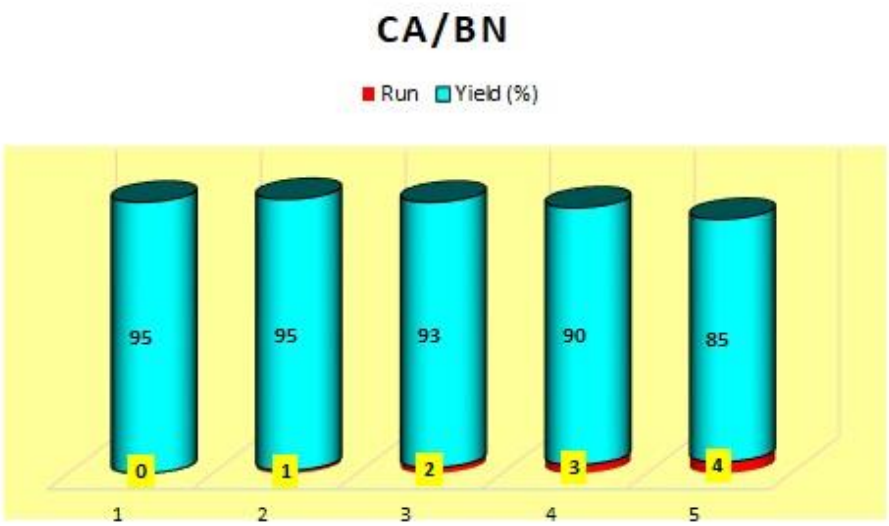

Fig. 9. Recyclability of the calcium loaded boron nitride catalyst

A comparison of the results from our study with previously reported catalysts for the preparation of 2-amino-*4H*-pyran-3-carbonitrile (APC) derivatives **(Table 4)** indicated that some catalysts had longer reaction time which produced lower percentage yields.

Table 4. Comparison of reported catalysts with Ca/BN heterogeneous catalyst

Entry	Catalyst	Condition	Solvent	Time	Yield (%)	Refs
1	NaOH/Piperidine	MW	EtOH	5-9 h	71	Zhou, 2003
2	KF-Al_2O_3	Reflux	DMF	10-14 h	90	Wang *et al*., 2004
3	HTMAB	Reflux	Water	8 h	93	Jin *et al*., 2005
4	L-proline	Reflux	EtOH	4 h	90	Elnagdi *et al*., 2015
5	$RE(PFO)_3$	Reflux	EtOH	5 h	90	Wang *et al*., 2006
6	Trifluoroethanol	Reflux	EtOH	5 h	90	Khaksar *et al*., 2012
7	I_2	Reflux	DMSO	4 h	86	Tahmassebi *et al*., 2011
8	Ca/BN	Reflux	EtOH	6 h	95	This work

The catalysts such as KF-Al_2O_3, HTMAB, L-proline, $RE(PFO)_3$, and trifluoroethanol gave 90 % of yield in shorter reaction time. The major advantage of Ca/BN over other catalysts was the maximum yield of APCs and the recyclability potential.

After optimising the reaction condition for the synthesis of **20**, the protocol was used with the appropriate starting compounds to synthesize **21-33** (**Table 5**). The 13 new derivatives were easily characterized from the spectroscopic data because there was only a minor change in their structure from **20**. It was concluded that the one-pot MCR synthesis of APCs was successful. The FTIR, ^{1}H-NMR, ^{13}C-NMR and elemental analysis is presented in **Appendix-VII**.

Table 5. Synthesis of 2-amino-*4H*-pyran-3-carbonitrile derivatives under reflux conditions in the presence of 10 mol % Ca/BN.

Entry	Ar-CHO	1,3-diketone	Product	Yield (%)	Melting Point (°C)	
					Observed	Reported
1	H	$C_8H_{12}O_2$	**20**	95	233-235	234-235 (Gao *et al*., 2008)
2	4-NO_2	$C_8H_{12}O_2$	**21**	95	176-178	177-178 (Nemouchi *et al*., 2012)
3	4-F	$C_8H_{12}O_2$	**22**	85	199-201	200 (Oskooie *et al*., 2011)
4	4-MeO	$C_8H_{12}O_2$	**23**	80	199-201	199-200 (Oskooie *et al*., 2011)
5	2-NO_2	$C_8H_{12}O_2$	**24**	94	223-226	224-226 (Jin *et al*., 2004)
6	4-Cl	$C_8H_{12}O_2$	**25**	94	208-210	209-210 (Katkar *et al*., 2011)
7	4-Me	$C_8H_{12}O_2$	**26**	90	219-222	220-222 (Rong *et al*., 2006)
8	2-OH	$C_8H_{12}O_2$	**27**	75	175-177	No literature
9	Furfural	$C_8H_{12}O_2$	**28**	94	215-217	216 (Lian *et al*., 2008)
10	H	$C_6H_{10}O_2$	**29**	95	194-196	No literature
11	4-NO_2	$C_6H_{10}O_2$	**30**	94	177-179	No literature
12	4-F	$C_6H_{10}O_2$	**31**	83	159-161	No literature
13	2-NO_2	$C_6H_{10}O_2$	**32**	94	176-178	No literature
14	4-Me	$C_6H_{10}O_2$	**33**	75	171-173	No literature

A plausible mechanism for the formation of APCs is presented in **Scheme 2**. In this mechanism BN increased the electrophilicity of the carbonyl carbon of C-H activated compounds as well as aryl aldehydes and efficiently catalysed Michael addition (Molla and Hussain, 2013). In the first transformation, aryl aldehyde **1** and malononitrile **2** formed a Knoevenagel product **3**. The methine carbon of **3** was activated by BN and reacted with the C-H activated compound of 1,3-diketone **4** in a Michael fashion, producing intermediate **5**. Finally, the intermediate **5**, underwent intramolecular cyclization followed by the formation of pyran derivatives **6**.

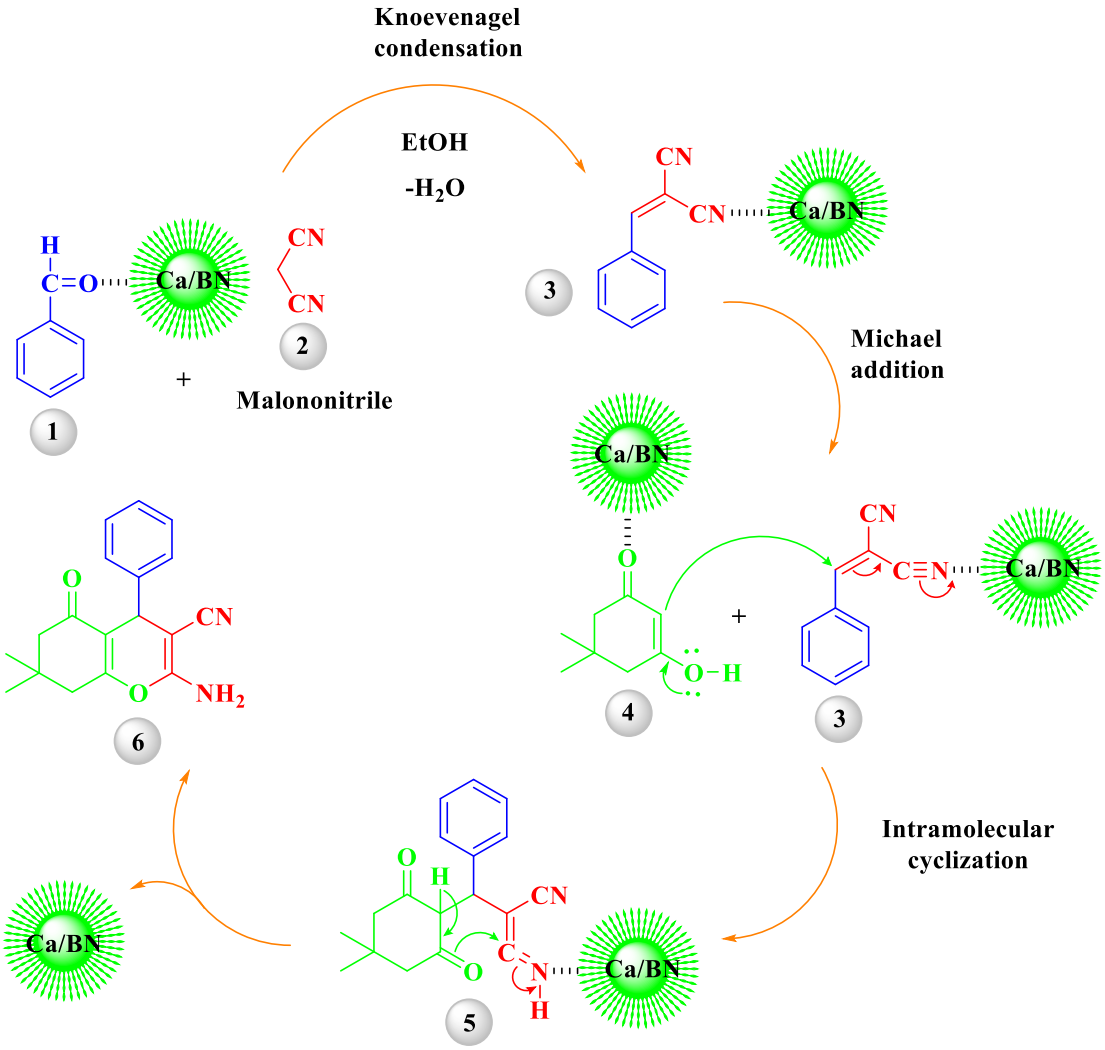

Scheme 2. Plausible mechanism of the synthesis of 2-amino-*4H*-pyran-3-carbonitriles

Due to pathogenic bacteria developing resistance against antibiotics, there is a need to identify new compounds/drugs that could be used as alternate to these antibiotics. Therefore, research into medicinal raw material which can be used to identify new compounds that may have antibiotic action is imperative (Andrews, 2001). Various heterocyclic compounds have shown antimicrobial potential and pyran is one of the promising heterocyclic moieties. The incorporation of the pyran nucleus is an important synthetic strategy in drug discovery. As discussed in Chapter Two, several pyrans have been used as precursors for the synthesis of pharmacologically active compounds such as HIV protease inhibitors, antifungals, cardiotonics, anticonvulsants, antimicrobials, pheromones, natural pigments, antitumor agents and plant growth regulators. Pyran derivatives can be used for medicinal applications therefore these compounds were investigated for their antibacterial properties. In this investigation, we reported that some

pyran derivatives showed significant antibacterial activities against *Staphylococcus aureus* (*S. aureus*), *Escherichia coli* (*E. coli*) and *Pseudomonas aeruginosa* (*P. aeruginosa*).

The minimal inhibitory concentration (MIC) was determined by serially diluting the extracts using nutrient broth. A series of five APCs **(29-33)** were evaluated for antibacterial activity against two Gram-negative bacteria, *E. coli* (ATCC 25922) and *P. aeruginosa* (ATCC 27853) and one Gram-positive bacterium, *S. aureus* (ATCC 29213), **Fig. 10**, **Fig. 11** and **Fig. 12**.

Table 6. Antibacterial activities of APCs: Minimal Inhibitory Concentration

Entry	APCs	*E. coli* (µg/mL)	*P. aeruginosa* (µg/mL)	*S. aureus* (µg/mL)
1	**29**	128	16	4
2	**30**	256	-	-
3	**31**	256	256	-
4	**32**	256	256	-
5	**33**	256	-	256

Standard antibacterial drugs: Ciprofloxacin and Nalidixic acid.

(-): has no bacterial effect.

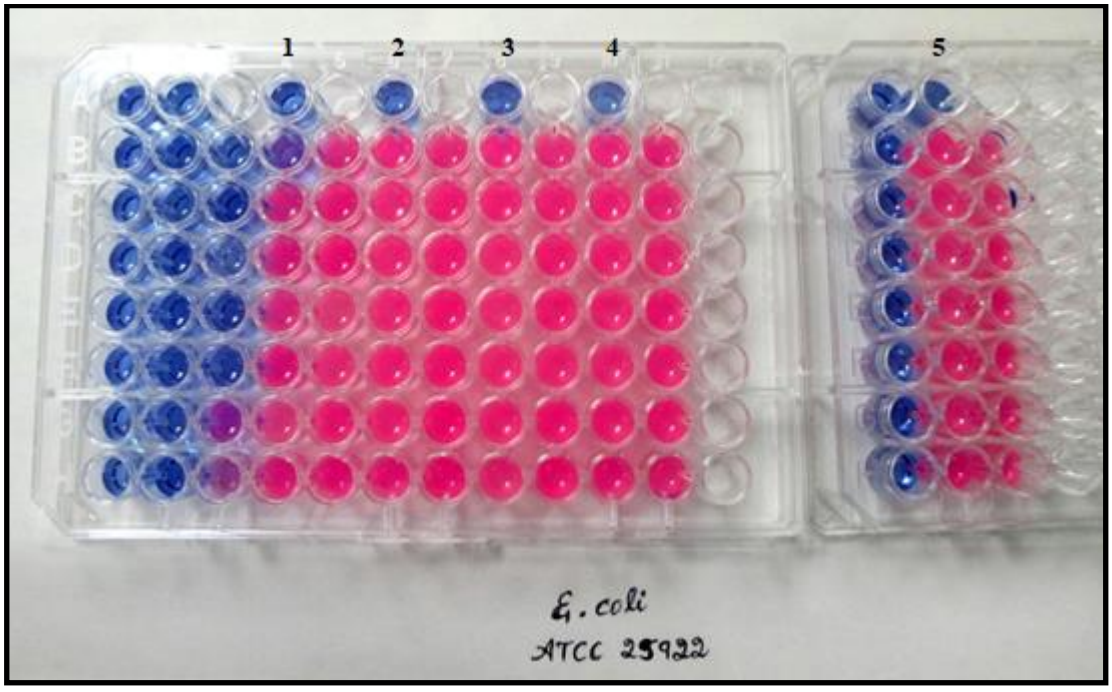

Fig. 10. Antibacterial activity of 2-amino-*4H*-pyran-3-carbonitriles against *E. coli*

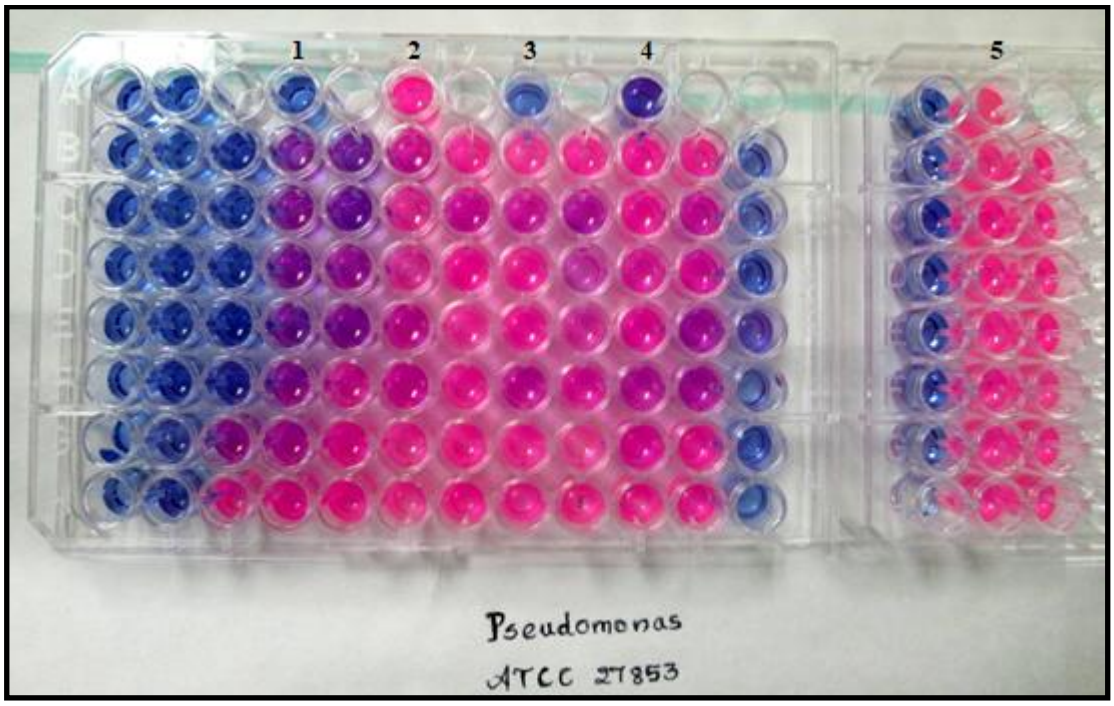

Fig. 11. Antibacterial activity of 2-amino-*4H*-pyran-3-carbonitriles against *P. aeruginosa*

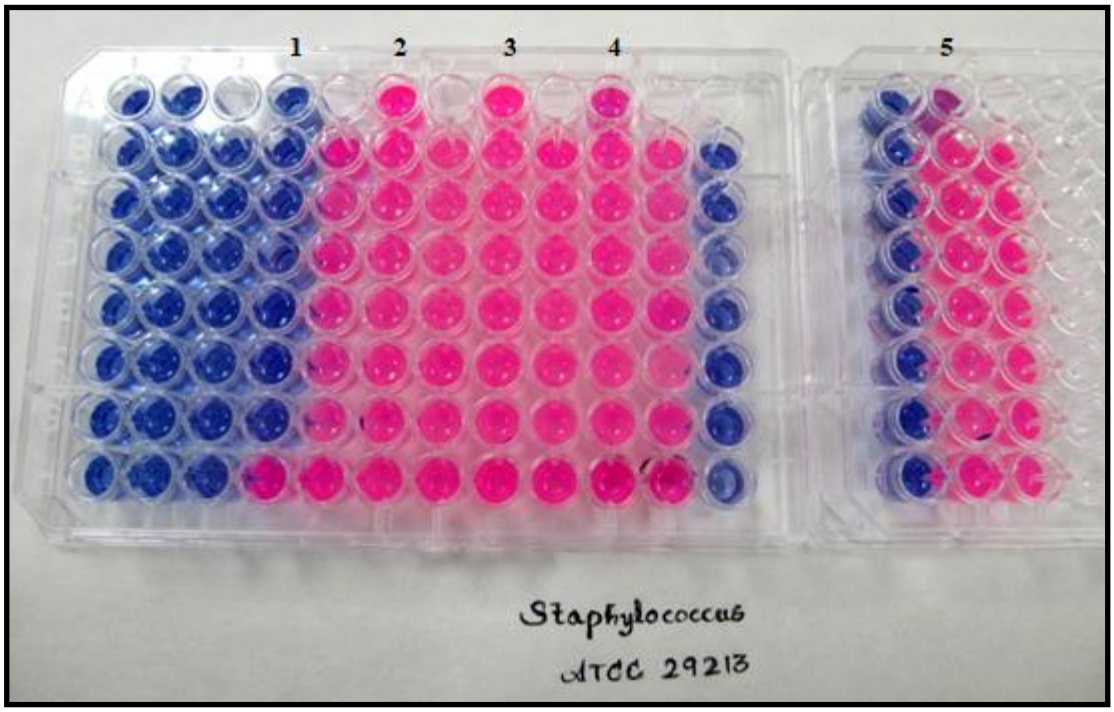

Fig. 12. Antibacterial activity of 2-amino-*4H*-pyran-3-carbonitriles against *S. aureus*

1= **29;** 2= **30;** 3= **31;** 4= **32;** 5= **33**

Standard antibiotics, ciprofloxacin and nalidixic acid were used as positive controls and DMSO used as negative control. DMSO had no effect on the bacteria. The antibacterial activity results are presented in **Table 6.** The results indicate that the APCs showed moderate to good activity against the bacterial strains. It is interesting that compound **29** showed very good activity against all strains. Compounds **30** and **33** showed no inhibitory effect against *P. aeruginosa*. Furthermore, compounds **30**, **31** and **32** showed no activity against *S. aureus*.

These results indicate that the APCs had good antibacterial activity against the strains used. The pyran nucleus is one of the active constituents present in many standard drugs and is known to increase the pharmacological activity of the molecule. The presence of substituents like fluorine, nitro and methyl groups in the APCs contributed to the net biological activity (Shah and Westwell, 2007; Chauvière *et al*., 2003; Deckers *et al*., 2000). Overall, these synthesized compounds showed moderate to promising activity as compared to standard drugs, although not against all tested bacterial strains.

7.4. Conclusion

In conclusion, a facile and convenient practical method for easy access to a wide range of pharmaceutically functionalized 2-amino-*4H*-pyran-3-carbonitriles in the presence of Ca/BN via a one-pot tandem Knoevenagel-cyclocondensation of aldehydes, malononitrile and 1,3-diketone in ethanol at room temperature was developed. Mild reaction conditions, excellent yields, operational simplicity, clean reaction profiles as well as the use of inexpensive solvent and catalysts are the key advantages of the present method. Moreover, reusability of the catalyst is an added advantage to this protocol. A total of five APCs were subjected to antibacterial studies against *S. aureus, E. coli* and *P. aeruginosa*. The MIC value for the synthesized 2-amino-*4H*-pyran-3-carbonitriles showed moderate to promising activity against the bacteria tested. Among them, compound **29** showed MIC values of 128, 16 and 4 µg/mL towards *E.coli*, *P. aeruginosa* and *S. aureus*. The synthesis of biologically relevant pyran-annulated heterocyclic scaffolds is important for medicinal research hence, the present methodology with mild reaction conditions and operational simplicity offers the possibility of its use in a cost-effective way for large-scale industrial syntheses.

7.5. Experimental

Preparation of calcium loaded boron nitride catalyst

To a solution of $Ca(OAc)_2$ (19.7 mg, including 7.6 % mg of Ca metal; 0.5 wt % of Ca metal vs. BN) in methanol (50 mL), boron nitride (2.66 g) was added and the mixture was stirred at room temperature for a week. The resulting suspension was filtered and the solid was washed with MeOH, dried under reduced pressure to yield 0.3 % Ca/BN catalyst as a white powder; yield: 2.679 g.

General Procedure for the preparation of 2-amino-*4H*-pyran-3-carbonitrile derivatives

A 100 mL round bottom flask containing the selected aryl aldehyde (1 mmol), malononitrile (1 mmol) and Ca/BN (0.10 g, 10 mol % of the substrate), in ethanol (15 mL), was set up for reflux, with stirring, on an oil bath. After one h of reflux, 5,5-dimethylcyclohexane-1,3-dione was slowly added with stirring. Reflux was continued whilst the progress of the reaction was intermittently monitored by TLC. Following completion of the reaction, the mixture was filtered, the filtrate was collected and the solvent was removed *in vacuo*. The product was purified by column chromatography with an eluent system of ethyl acetate: petroleum ether, 50 % (1:1). The products were characterized by IR, ^{1}H-NMR and ^{13}C-NMR and elemental analysis. The solid in the filtration process was collected, washed with $CHCl_3$: MeOH mixture followed by acetone and kept aside for further use.

Antibacterial studies

The preparation of Media

Fresh Nutrient Agar, Oxoid Ltd (Hampshire, England) was prepared according to the manufacturer's guidelines as follow:

- 28 g was weighed out into each of 3 separate one litre glass bottles
- 1L of distilled water was added to each bottle
- The solution was mixed until the powder completely dissolved.
- Bottles were sterilized by autoclaving for 15 minutes at 121℃.
- The agar was poured into plates to solidify.

The preparation of the Nutrient Broth

Fresh Mueller Hinton Broth (Sigma-Aldrich) was made up according to manufacturer's guidelines as follows:

- 23 g of Nutrient Broth powder was weighed into a one litre glass bottle
- 1L of distilled water was added The solution was mixed until the powder completely dissolved
- This was dispensed into bijou bottles before autoclaving
- Bijou bottles were sterilized by autoclaving for 15 minutes at 121℃

Bacterial cultures

The cultures of *Staphylococcus aureus, Escheriachia coli* and *Pseudomonas aeruginosa* were maintained on nutrient agar slopes at 4℃ and sub-cultured on to blood agar plates for 24 h before use.

Preparation of reagent: Microplate Alamar Blue Assay (MABA)

0.2 g of Resazurin powder was dissolved in 10 mL autoclaved distilled water. The dye solution was vortexed vigorously. The solution was immediately covered with aluminium foil as it was light sensitive. Each well was inoculated with a bacterial suspension containing $1x10^6$ CFU/mL and incubated at 37℃ for 24 h. The MIC was regarded as lowest concentration of the extract which would not permit any visible growth when compared with extract free broths inoculated with each of the bacterial suspensions. They were incubated at 37℃ for 24 h and then examined for growth. The antibacterial activities of the synthesized compounds were studied by MABA using 96-wells microplates including positive control (containing standard antibiotic) and growth control (containing culture broth without testing materials). 20 µL of each concentration of the synthesized compounds were added in duplicate except for positive and growth control wells. After adding Alamar Blue (20 µL) to all 96 wells the total volume in each well reached 200 µL. The final concentrations of the tested compounds were 256, 128, 64, 32, 16, 8, 4, 2, 1 µg/mL. After incubation, the results were recorded and MIC was determined.

References

[1] Hassanien, A. A., Zahran, M. A., El-Gaby, M. S. A., Ghorab, M. M., 1999. Utility of 2-Amino-4, 5, 6, 8-tetrahydro-7H-chromene-3-carbonitriles in Synthesis of Chromeno [2, 3-d] pyrimidine and Chromeno [3, 2-e][1, 2, 4] triazolo [1, 5-c] pyrimidine Derivatives of Pharmaceutical Interest. ChemInform, (42).

[2] Shestopalov, A. M., Emelianova, Y. M., Nesterov, V. N. 2003. One-step synthesis of substituted 2-amino-5, 6, 7, 8-tetrahydro-4H-benzo [b] pyrans. Molecular and crystal structure of 2-amino-3-(2-methoxyethoxycarbonyl)-4-(2-nitrophenyl)-5-oxo-5, 6, 7, 8-tetrahydro-4H-benzo [b] pyran. Russian Chemical Bulletin, (52) 1164-1171.

[3] Balalaie, S., Bararjanian, M., Amani, A. M., Movassagh, B. 2006. (S)-Proline as a neutral and efficient catalyst for the one-pot synthesis of tetrahydrobenzo [b] pyran derivatives in aqueous media. Synlett, (2) 263-266.

[4] Fan, X., Hu, X., Zhang, X., Wang, J. 2004. Ionic liquid promoted Knoevenagel and Michael reactions. Australian Journal of Chemistry, (57) 1067-1071.

[5] Shi, D. Q., Zhang, S., Zhuang, Q. Y., Tu, S. J., Hu, H. W. 2003. Clean synthesis of 2-amino-3-cyano-4-aryl-7, 7-dimethyl-5-oxo-4H-5, 6, 7, 8-tetrahydrobenzo [b] pyran in water. Chinese Journal of Organic Chemistry, (23) 877-879.

[6] Devi, I., Bhuyan, P. J. 2004. Sodium bromide catalysed one-pot synthesis of tetrahydrobenzo [b] pyrans via a three-component cyclocondensation under microwave irradiation and solvent free conditions. Tetrahedron Letters, (45) 8625-8627.

[7] Tu, S. J., Gao, Y., Guo, C., Shi, D., Lu, Z. 2002. A convenient synthesis of 2-amino-5, 6, 7, 8-tetrahydro-5-oxo-4-aryl-7, 7-dimethyl-4H-benzo-[b]-pyran-3-carbonitrile under microwave irradiation. Synthetic communications, (32) 2137-2141.

[8] Peng, Y., Song, G. 2007. Amino-functionalized ionic liquid as catalytically active solvent for microwave-assisted synthesis of 4H-pyrans. Catalysis Communications, (8) 111-114.

[9] Dabiri, M., Bahramnejad, M., Baghbanzadeh, M. 2009. Ammonium salt catalyzed multicomponent transformation: Simple route to functionalized spirochromenes and spiroacridines. Tetrahedron, (65) 9443-9447.

[10] Hari, G. S., Lee, Y. R. 2010. Efficient one-pot synthesis of spirooxindole derivatives by ethylenediamine diacetate catalyzed reactions in water. Synthesis, (3) 453-464.

[11] Wang, L. M., Jiao, N., Qiu, J., Yu, J. J., Liu, J. Q., Guo, F. L., Liu, Y. 2010. Sodium stearate-catalyzed multicomponent reactions for efficient synthesis of spirooxindoles in aqueous micellar media. Tetrahedron, (66) 339-343.

[12] Sridhar, R., Srinivas, B., Madhav, B., Reddy, V. P., Nageswar, Y. V. D., Rao, K. R. 2009. Multi-component supramolecular synthesis of spirooxindoles catalyzed by β-cyclodextrin in water. Canadian Journal of Chemistry, (87) 1704-1707.

[13] Spivey, J. J. 1987. Complete catalytic oxidation of volatile organics. Industrial & Engineering Chemistry Research, (26) 2165-2180.

[14] Liu, F., Mo, X., Gan, H., Guo, T., Wang, X., Chen, B., Chen, J., Deng, S., Xu, N., Sekiguchi, T., Golberg, D. 2014. Cheap, gram-scale fabrication of BN nanosheets via substitution reaction of graphite powders and their use for mechanical reinforcement of polymers. Scientific Reports, (4) 4211.

[15] Nag, A., Raidongia, K., Hembram, K. P., Datta, R., Waghmare, U. V., Rao, C. N. R. 2010. Graphene analogues of BN: Novel synthesis and properties. ACS Nano, (4) 1539-1544.

[16] Li, J., Xiao, X., Xu, X., Lin, J., Huang, Y., Xue, Y., Jin, P., Zou, J., Tang, C. 2013. Activated boron nitride as an effective adsorbent for metal ions and organic pollutants. Scientific Reports, (3) 3208.

[17] Wang, X. S., Shi, D. Q., Du, Y., Zhou, Y., Tu, S. J. 2004. Synthesis of 2-Aminopyran derivatives and 3-arylpropionitrile derivatives catalyzed by KF/AL_2O_3. Synthetic Communications, (34) 1425-1432.

[18] Zhou, J. F. 2003. One-step synthesis of pyridine and 4 H-pyran derivatives from bisarylidene cyclohexanone and malononitrile under microwave irradiation. Synthetic Communications, (33) 99-103.

[19] Wang, L. M., Shao, J. H., Tian, H., Wang, Y. H., Liu, B. 2006. Rare earth perfluorooctanoate $[RE(PFO)_3]$ catalyzed one-pot synthesis of benzopyran derivatives. Journal of Fluorine Chemistry, (127) 97-100.

[20] Khaksar, S., Rouhollahpour, A., Talesh, S. M. 2012. A facile and efficient synthesis of 2-amino-3-cyano-4H-chromenes and tetrahydrobenzo [b] pyrans using 2, 2, 2-trifluoroethanol as a metal-free and reusable medium. Journal of Fluorine Chemistry, (141) 11-15.

[21] Elnagdi, N. M. H., Al-Hokbany, N. S. 2012. Organocatalysis in synthesis: L-proline as an enantioselective catalyst in the synthesis of pyrans and thiopyrans. Molecules, (17) 4300-4312.

[22] Shaabani, A., Ghadari, R., Ghasemi, S., Pedarpour, M., Rezayan, A. H., Sarvary, A., Ng, S. W. 2009. Novel one-pot three-and pseudo-five-component reactions: Synthesis of functionalized benzo [g]-and dihydropyrano [2, 3-g] chromene derivatives. Journal of Combinatorial Chemistry, (11) 956-959.

[23] Moafi, L., Ahadi, S., Bazgir, A. 2010. New HA 14-1 analogues: Synthesis of 2-amino-4-cyano-4H-chromenes. Tetrahedron Letters, (51) 6270-6274.

[24] Ertug, B., Boyraz, T., Addemir, O. 2007. Microstructural aspects of the hot-pressed hexagonal boron nitride ceramics with limited content of boron oxide. Materials Science Forum, (554) 197-200.

[25] Kalay, S., Yilmaz, Z., Çulha, M. 2013. Synthesis of boron nitride nanotubes from unprocessed colemanite. Beilstein Journal of Nanotechnology, (4) 843.

[26] Antunes, V., Oliveira, M. J., Vargas, H., Serrão, V., Candeias, A., Carvalho, M. L., Coroado, J., Mirão, J., Dias, L., Longelin, S., Seruya, A. I. 2014. Characterization of glue sizing under calcium carbonate ground layers in Flemish and Luso-Flemish painting–analysis by SEM-EDS, μ-XRD and μ-Raman spectroscopy. Analytical Methods, (6) 710-717.

[27] Harris, J., Mey, I., Hajir, M., Mondeshki, M., Wolf, S. E. 2015. Pseudomorphic transformation of amorphous calcium carbonate films follows spherulitic growth mechanisms and can give rise to crystal lattice tilting. CrystEngComm, (17) 6831-6837.

[28] Zhou, J. F. 2003. One-step synthesis of pyridine and 4 H-pyran derivatives from bisarylidenecyclohexanone and malononitrile under microwave irradiation. Synthetic Communications, (33) 99-103.

[29] Wang, X. S., Shi, D. Q., Du, Y., Zhou, Y., Tu, S. J. 2004. Synthesis of 2-aminopyran derivatives and 3-arylpropionitrile derivatives catalyzed by KF/Al_2O_3. Synthetic Communications, (34) 1425-1432.

[30] Jin, T. S., Liu, L. B., Zhao, Y., Li, T. S. 2005. Clean, one-pot synthesis of 4 h-pyran derivatives catalyzed by hexa decyltrimethyl ammonium bromide in aqueous media. Synthetic Communications, (35) 1859-1863.

[31] Elnagdi, M. H., Moustafa, M. S., Al-Mousawi, S. M., Mekheimer, R. A., Sadek, K. U. 2015. Recent developments in utility of green multi-component reactions

for the efficient synthesis of poly substituted pyrans, thiopyrans, pyridines, and pyrazoles. Molecular Diversity, (19) 625-651.

[32] Wang, L. M., Shao, J. H., Tian, H., Wang, Y. H., Liu, B. 2006. Rare earth perfluorooctanoate [$RE(PFO)_3$] catalyzed one-pot synthesis of benzopyran derivatives. Journal of Fluorine Chemistry, (127) 97-100.

[33] Khaksar, S., Rouhollahpour, A., Talesh, S. M. 2012. A facile and efficient synthesis of 2-amino-3-cyano-4H-chromenes and tetrahydrobenzo [b] pyrans using 2, 2, 2-trifluoroethanol as a metal-free and reusable medium. Journal of Fluorine Chemistry, (141) 11-15.

[34] Tahmassebi, D., Bryson, J. A., Binz, S. I. 2011. 1,4-Diazabicyclo [2.2.2] octane as an efficient catalyst for a clean, one-pot synthesis of tetrahydrobenzo [b] pyran derivatives via multicomponent reaction in aqueous media. Synthetic Communications, (41) 2701-2711.

[35] Gao, S., Tsai, C. H., Tseng, C., Yao, C. F. 2008. Fluoride ion catalyzed multicomponent reactions for efficient synthesis of 4H-chromene and N-aryl quinoline derivatives in aqueous media. Tetrahedron, (64) 9143-9149.

[36] Nemouchi, S., Boulcina, R., Carboni, B., Debache, A. 2012. Phenyl boronic acid as an efficient and convenient catalyst for a three-component synthesis of tetrahydrobenzo [b] pyrans. Comptes Rendus Chimie, (15) 394-397.

[37] Oskooie, H. A., Heravi, M. M., Karimi, N., Zadeh, M. E. 2011. Caro's acid–silica gel: an efficient and versatile catalyst for the one-pot synthesis of tetrahydrobenzo [b] pyran derivatives. Synthetic Communications, (41) 436-440.

[38] Jin, T. S., Wang, A. Q., Wang, X., Zhang, J. S., Li, T. S. 2004. A clean one-pot synthesis of tetrahydrobenzo [b] pyran derivatives catalyzed by hexa decyltrimethyl ammonium bromide in aqueous media. Synlett, (5) 0871-0873.

[39] Katkar, S. S., Lande, M. K., Arbad, B. R., Gaikwad, S. T. 2011. A recyclable and highly effective ZnO-beta zeolite as a catalyst for one-pot three-component synthesis of tetrahydrobenzo [b] pyrans. Chinese Journal of Chemistry, (29) 199-202.

[40] Rong, L., Li, X., Wang, H., Shi, D., Tu, S., Zhuang, Q. 2006. Efficient synthesis of tetrahydrobenzo [b] pyrans under solvent-free conditions at room temperature. Synthetic Communications, (36) 2363-2369.

[41] Lian, X. Z., Huang, Y., Li, Y. Q., Zheng, W. J. 2008. A green synthesis of tetrahydrobenzo [b] pyran derivatives through three-component condensation

using N-methylimidazole as organocatalyst. Monatshefte für Chemie-Chemical Monthly, (139) 129-131.

[42] Molla, A., Hussain, S. 2013. Boron nitride: An efficient reusable heterogeneous catalyst for hetero-Michael reactions under solvent-free condition. Current Catalysis, (2) 88-95.

[43] Andrews, J. M. 2001. Determination of minimum inhibitory concentrations. Journal of Antimicrobial Chemotherapy, (48) 5-16.

[44] Shah, P., Westwell, A. D. 2007. The role of fluorine in medicinal chemistry. Journal of Enzyme Inhibition and Medicinal Chemistry, (22) 527-540.

[45] Chauvière, G., Bouteille, B., Enanga, B., de Albuquerque, C., Croft, S. L., Dumas, M., Périé, J. 2003. Synthesis and biological activity of nitro heterocycles analogous to Megazol, a trypanocidal lead. Journal of Medicinal Chemistry, (46) 427-440.

[46] Deckers, G. H., Schoonen, W. G. E. J., Kloosterboer, H. J. 2000. Influence of the substitution of 11-methylene, Δ 15, and/or 18-methyl groups in norethisterone on receptor binding, transactivation assays and biological activities in animals. The Journal of Steroid Biochemistry and Molecular Biology, (74) 83-92.

Appendix-VII

7.1. 2-Amino-7,7-dimethyl-5-oxo-4-phenyl-5,6,7,8-tetrahydro-*4H*-chromene-3-carbonitrile (20)

White solid, m.p = 233-235℃; IR (ATR, cm^{-1}): 3394 NH_2, 1036 C-N, 2201 CN, 1456 C=C, 1642 C=O, 1036 C-O, 2963 CH. ^{1}H-NMR (400 MHz, DMSO-d_6): δ (ppm) 7.28 (t, 2H, *J*=7.28 Hz, Ar-H). 7.19 (d, 1H, *J*=0.96 Hz, Ar-H), 7.13 (t, 2H, *J*= 11.96 Hz, Ar-H), 6.98 (brs, 2H, NH_2), 4.16 (s, 1H, CH), 2.50 (dt, 2H, *J*=2.04 Hz, CH_2), 2.25 (d, 1H, *J*=16.08 Hz, CH_2), 2.10 (d, 1H, *J*=16.08 Hz, CH_2), 1.03 (s, 3H, CH_3), 0.94 (s, 3H, CH_3). ^{13}C-NMR (100 MHz, DMSO-d_6): δ (ppm) 195.61, 162.45, 158.46, 144.70, 128.28, 127.10, 126.52, 119.66, 112.71, 58.30, 49.95, 40.11, 35.54, 31.76, 28.35, 26.77. Elemental Analysis: Anal. Calc. for $C_{18}H_{18}N_2O_2$: C, 73.45; H, 6.16; N, 9.52; %. Found: C, 73.47; H, 6.14; N, 9.50; %.

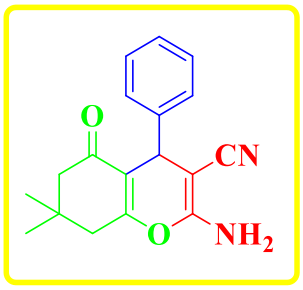

7.2. 2-Amino-7,7-dimethyl-4-(4-nitrophenyl)-5-oxo-5,6,7,8-tetrahydro-*4H*-chromene-3-carbonitrile (21)

Yellow solid, m.p = 185-187℃; IR (ATR, cm^{-1}): 3314 NH_2, 1043 C-N, 2191 CN, 1514 C=C, 1603 C=O, 1112 C-O, 2971 CH. ^{1}H-NMR (400 MHz, DMSO-d_6): δ (ppm) 8.15-8.17 (d, *J* =7.12 Hz, 2H, Ar-H). 7.43-7.45 (d, *J* = 5.36, 2H, Ar-H), 7.16 (brs, 2H, NH_2), 4.36 (s, 1H, CH), 2.49-2.53 (t, *J* = 3.52 Hz, 2H, CH_2), 2.23 (d, *J* = 16.08 Hz, 1H, CH_2), 2.01 (d, *J* = 16.04 Hz, 1H, CH_2), 1.03 (s, 3H, CH_3), 0.95 (s, 3H, -CH_3). ^{13}C-NMR (100 MHz, $CDCl_3$): δ (ppm) 163.27, 149.80, 148.53, 142.27, 134.89, 130.75, 130.20, 130.08, 127.35, 125.94, 125.90, 125.86, 120.13, 104.46, 62.12, 52.66, 5216, 38.49. Elemental Analysis: Anal. Calc. for $C_{18}H_{17}N_3O_4$: C, 63.71; H, 5.05; N, 12.38; %. Found: C, 63.72; H, 5.08; N, 12.39; %.

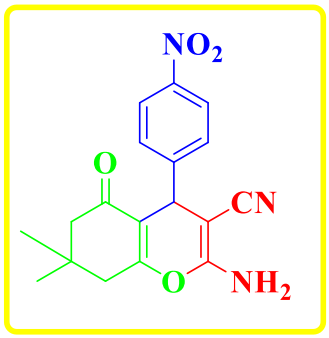

7.3. 2-Amino-4-(4-fluorophenyl)-7,7-dimethyl-5-oxo-5,6,7,8-tetrahydro-*4H*-chromene-3-carbonitrile (22)

White solid, m.p = 130-132℃; IR (ATR, cm^{-1}): 3408 NH_2, 1063 C-N, 2234 CN, 1508 C=C, 1594 C=O, 938 C-O, 3049 CH. ^{1}H-NMR (400 MHz, $CDCl_3$): δ (ppm) 11.85 (brs, 2H, NH_2), 7.00-7.03 (m, 2H, Ar-H), 6.90-6.94 (m, 2H, Ar-H), 5.46 (s, 1H, CH), 2.31-

2.41 (m, 4H, CH_2), 1.19 (s, 3H, CH_3), 1.07 (s, 3H, -CH_3). ^{13}C-NMR (100 MHz, DMSO-d_6): δ (ppm) 146.09, 143.92, 130.02, 129.96, 129.82, 128.24, 123.92, 123.40, 119.43, 116.34, 116.34, 116.10, 114.36, 114.30, 97.07, 62.05, 40.10, 38.85, 15.10. Elemental Analysis: Anal. Calc. for $C_{18}H_{17}FN_2O_2$: C, 69.22; H, 5.49; N, 8.97; %. Found: C, 69.25; H, 5.47; N, 8.99; %.

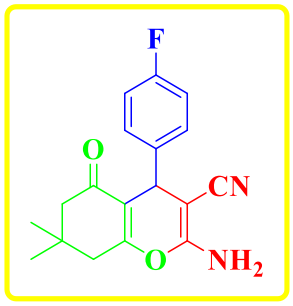

7.4. 2-Amino-4-(4-methoxyphenyl)-7,7-dimethyl-5-oxo-5,6,7,8-tetrahydro-*4H*-chromene-3-carbonitrile (23)

Pale yellow solid, m.p = 212-214℃; IR (ATR, cm^{-1}): 3334 NH_2, 1075 C-N, 2197 CN, 1456 C=C, 1641 C=O, 1036 C-O, 2962 CH. ^{1}H-NMR (400 MHz, $CDCl_3$): δ (ppm) 7.11-7.13 (dd, J = 4.56 Hz, 2H, Ar-H). 6.78-6.80 (dd, J = 4.60 Hz, 2H, Ar-H), 4.48 (brs, 2H, NH_2), 4.33 (s, 1H, CH), 3.75 (s, 3H, OCH_3), 2.41 (s, 2H, CH_2), 2.18-2.19 (d, J = 5.08 Hz, 2H, CH_2), 1.08 (s, 3H, CH_3), 1.01 (s, 3H, -CH_3). ^{13}C-NMR (100 MHz, $CDCl_3$): δ (ppm) 195.94, 161.21, 158.61, 157.32, 135.45, 128.62, 118.70, 114.24, 113.98, 77.33, 76.70, 63.90, 55.21, 50.69, 40.67, 34.74, 32.19, 28.88, 27.68. Elemental Analysis: Anal. Calc. for $C_{19}H_{20}N_2O_3$: C, 70.35; H, 6.21; N, 8.64; %. Found: C, 70.37; H, 6.20; N, 8.66; %.

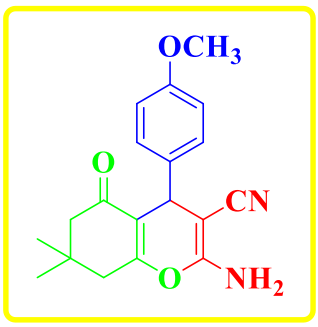

7.5. 2-Amino-7,7-dimethyl-4-(2-nitrophenyl)-5-oxo-5,6,7,8-tetrahydro-*4H*-chromene-3-carbonitrile (24)

Dark yellow solid, m.p = 234-236℃; IR (ATR, cm^{-1}): 3324 NH_2, 1145 C-N, 2195 CN, 1521 C=C, 1602 C=O, 1042 C-O, 2959 CH. ^{1}H-NMR (400 MHz, DMSO-d_6): δ (ppm) 7.80-7.82 (d, J = 8.04 Hz, 1H, Ar-H), 7.63-7.67 (t, J = 7.56 Hz, 1H, Ar-H), 7.34-7.36 (t, J = 7.76 Hz, 2H, Ar-H), 0.87 (s, 3H, -CH3), 7.34-7.35 (d, J = 7.8 Hz, 2H, NH_2), 4.93 (s, 1H, CH), 1.00 (s, 3H, CH_3), 2.50 (m, 2H, CH_2), 2.17-2.21 (d, J = 16.12 Hz, 1H, CH_2), 1.99-2.03 (d, J = 16.12 Hz, 1H, CH_2), ^{13}C-NMR (100 MHz, DMSO-d_6): δ (ppm) 196.27, 163.19, 159.65, 149.43, 139.42, 133.82, 130.74, 128.33, 124.18, 119.52, 112.78, 56.82,

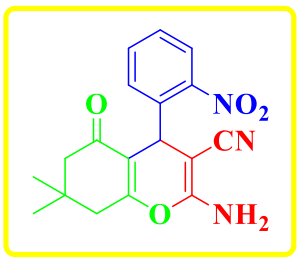

50.02, 39.35, 32.30, 30.40, 28.75, 27.16. Elemental Analysis: Anal. Calc. for $C_{18}H_{17}N_3O_4$: C, 63.71; H, 5.05; N, 12.38; %. Found: C, 63.73; H, 5.08; N, 12.40; %.

7.6. 2-Amino-4-(4-chlorophenyl)-7,7-dimethyl-5-oxo-5,6,7,8-tetrahydro-*4H*-chromene-3-carbonitrile (25)

White solid, m.p = 217-219℃; IR (ATR, cm^{-1}): 3330 NH_2, 1091 C-N, 2195 CN, 1607 C=C, 1643 C=O, 1038 C-O, 2969 CH. ^{1}H-NMR (400 MHz, $CDCl_3$): δ (ppm) 7.33-7.35 (d, J = 8.16 Hz, 2H, Ar-H), 7.16-7.18 (d, J = 8.2 Hz, 2H, Ar-H), 7.05 (brs, 2H, NH_2), 4.19 (s, 1H, CH), 2.50 (m, 2H, CH_2), 2.22-2.26 (d, J = 16.08 Hz, 1H, CH_2), 2.08-2.12 (d, J = 16.04 Hz, 1H, CH_2), 1.02 (s, 3H, CH_3), 0.94 (s, 3H, CH_3), ^{13}C-NMR (100 MHz, $CDCl_3$): δ (ppm) 196.12, 163.07, 158.90, 144.20, 131.58, 129.57, 128.74, 120.00, 112.81, 58.27, 55.34, 50.42, 40.61, 39.36, 35.57, 32.25, 28.77, 27.33. Elemental Analysis: Anal. Calc. for: $C_{18}H_{17}ClN_2O_2$: C, 65.75; H, 5.21; N, 8.52; %. Found: C, 65.77; H, 5.23; N, 8.54; %.

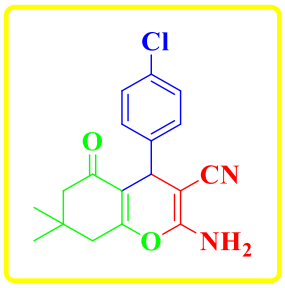

7.7. 2-Amino-7,7-dimethyl-5-oxo-4-(p-tolyl)-5,6,7,8-tetrahydro-*4H*-chromene-3-carbonitrile (26)

White solid, m.p = 222-224℃; IR (ATR, cm^{-1}): 3333 NH_2, 1143 C-N, 2194 CN, 1512 C=C, 1603 C=O, 1037 C-O, 2961 CH. ^{1}H-NMR (400 MHz, DMSO-d_6): δ (ppm) 7.09-7.07 (d, J = 7.84, 2H, Ar-H), 7.00-7.02 (d, J = 7.8, 2H, Ar-H), 6.95 (brs, 2H, NH_2), 4.12 (s, 1H, CH), 2.45-2.55 (m, J =4.4 Hz, 3H, Ar-CH_3), 2.22-2.26 (t, J= 6.92, 4H, CH_2), 1.03 (s, 3H, CH_3), 0.94 (s, 3H, -CH_3), ^{13}C-NMR (100 MHz, DMSO-d_6): δ (ppm) 196.10, 162.75, 158.90, 142.27, 136.08, 129.33, 127.53, 120.21, 113.34, 58.94, 50.46, 40.59, 39.75, 39.34, 35.64, 32.24, 28.88, 27.22, 21.04. Elemental Analysis: Anal. Calc. for $C_{19}H_{20}N_2O_2$: C, 74.00; H, 6.54; N, 9.08; %. Found: C, 74.03; H, 6.56; N, 9.06; %.

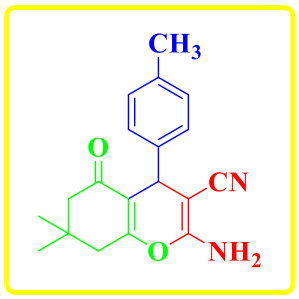

7.8. 2-Amino-4-(2-hydroxyphenyl)-7,7-dimethyl-5-oxo-5,6,7,8-tetrahydro-*4H*-chromene-3-carbonitrile (27)

Dark brown solid, m.p = 175-177℃; IR (FTIR, cm^{-1}): 2958 NH_2, 1147 C-N, 2201 CN, 1579 C=C, 1642 C=O, 1025 C-O, 2900 CH. ^{1}H-NMR (400 MHz, $CDCl_3$): δ (ppm) 10.50

(s, 1H, OH), 7.10-7.11 (m, 1H, Ar-H), 6.99-7.00 (m, 3H, Ar-H), 7.11 (brs, 2H, NH_2), 4.64 (s, 1H, CH), 2.47 (s, 2H, CH_2), 1.15 (s, 2H, CH_2), 1.00 (s, 3H, CH_3), 0.98 (s, 3H, -CH_3). ^{13}C-NMR (100 MHz, $CDCl_3$): δ (ppm) 200.92, 169.17, 151.03, 127.98, 127.52, 124.58, 124.29, 118.32, 115.74, 111.03, 49.92, 41.55, 32.29, 30.95, 29.69, 29.16, 27.76, 27.18. Elemental Analysis: Anal. Calc. for $C_{18}H_{18}N_2O_3$: C, 69.66; H, 5.85; N, 9.03; %. Found: C, 69.68; H, 5.87; N, 9.05; %.

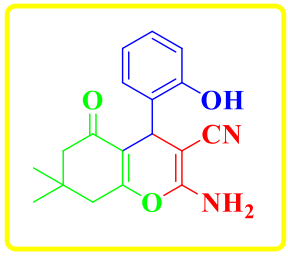

7.9. 2-Amino-4-(furan-2-yl)-7,7-dimethyl-5-oxo-5,6,7,8-tetrahydro-*4H*-chromene-3-carbonitrile (28)

Brown solid, m.p = 220-222℃; IR (FTIR, cm^{-1}): 2925 NH_2, 1174 C-N, 2224 CN, 1465 C=C, 1613 C=O, 1082 C-O, 2852 CH. ^{1}H-NMR (400 MHz, CD_3OD): δ (ppm) 7.32-7.33 (d, J = 4.0, 1H, Ar-H), 6.28-6.30 (m, 1H, Ar-H), 6.10 (d, J = 3.16 Hz, 1H, Ar-H), 7.32 (brs, 2H, NH_2), 4.44 (s, 1H, CH), 2.47-2.55 (q, 2H, CH_2), 2.22-2.36 (q, 2H, CH_2), 1.08 (s, 3H, CH_3), 1.05 (s, 3H, CH_3). ^{13}C-NMR (100 MHz, $CDCl_3$): δ (ppm) 164.77, 163.00, 141.64, 137.84, 129.69, 128.60, 122.46, 120.47, 115.13, 111.49, 50.87, 40.99, 32.18, 31.18, 29.28, 27.04. Elemental Analysis: Anal. Calc. for $C_{16}H_{16}N_2O_3$: C, 67.59; H, 5.67; N, 9.85; %. Found: C, 67.60; H, 5.69; N, 9.87; %.

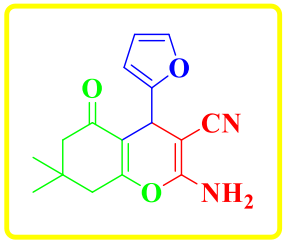

7.10. 2-Amino-6-methyl-4-phenyl-5-propionyl-*4H*-pyran-3-carbonitrile (29)

White solid, m.p = 194-196℃; IR (ATR, cm^{-1}): 3395 NH_2, 1061 C-N, 2190 CN, 1411 C=C, 1693 C=O, 1121 C-O, 2970 CH. ^{1}H-NMR (400 MHz, DMSO-d_6): δ (ppm) 7.22-7.32 (t, J = 7.28, 2H, Ar-H). 7.18-7.22 (t, J = 8.08 Hz, 1H, Ar-H), 7.13-7.15 (d, J = 7.04 Hz, 2H, Ar-H), 6.89 (brs, 2H, NH_2), 4.28 (s, 1H, CH), 3.94-3.97 (m, 2H, CH_2),), 2.12 (s, 3H, CH_3), 1.00-1.03 (t, J = 7.08, 3H, CH_3), ^{13}C-NMR (100 MHz, DMSO-d_6): δ (ppm) 206.48, 165.40, 158.43, 156.55, 144.83, 128.39, 127.14, 126.77, 119.68, 107.20, 60.10, 57.21, 38.82, 30.62, 18.07 13.66. Elemental Analysis: Anal. Calc. for $C_{16}H_{16}N_2O_2$: C, 71.62; H, 6.01; N, 10.44; %. Found: C, 71.64; H, 6.03; N, 10.46; %.

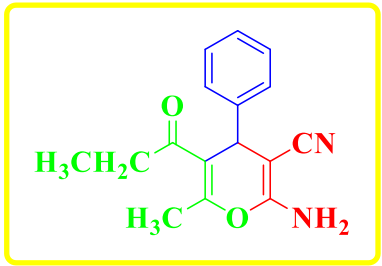

7.11. 2-Amino-6-methyl-4-(4-nitrophenyl)-5-propionyl-*4H*-pyran-3-carbonitrile (30)

Yellow solid, m.p = 177-179℃; IR (ATR, cm^{-1}): 3406 NH_2, 1120 C-N, 2201 CN, 1519 C=C, 1682 C=O, 1055 C-O, 2985 CH. ^{1}H-NMR (400 MHz, DMSO-d_6): δ (ppm) 8.17-8.20 (d, J = 8.67 Hz, 2H, Ar-H). 7.42-7.44 (d, J = 8.63 Hz, 2H, Ar-H), 7.06 (brs, 2H, NH_2), 4.46 (s, 1H, CH), 3.92-3.97 (m, 2H, CH_2), 2.34 (s, 3H, CH_3), 0.99-1.02 (t, J = 7.12, 3H, -CH_3), ^{13}C-NMR (100 MHz, DMSO-d_6): δ (ppm) 165.05, 158.52, 157.90, 152.51, 146.35, 128.50, 123.77, 119.29, 105.95, 60.33, 56.10, 39.99, 39.78, 38.73, 18.27, 13.64. Elemental Analysis: Anal. Calc. for $C_{16}H_{15}N_3O_4$: C, 61.34; H, 4.83; N, 13.41; %. Found: C, 61.36; H, 4.85; N, 13.43; %.

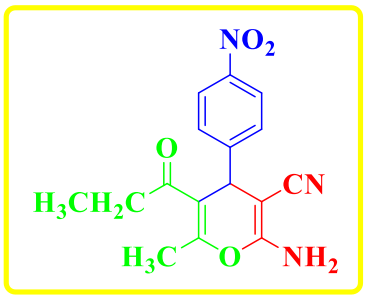

7.12. 2-Amino-4-(4-fluorophenyl)-6-methyl-5-propionyl-*4H*-pyran-3-carbonitrile (31)

White solid, m.p = 159-161℃; IR (ATR, cm^{-1}): 3407 NH_2, 1094 C-N, 2194 CN, 1508 C=C, 1605 C=O, 1057 C-O, 2985 CH. ^{1}H-NMR (400 MHz, $CDCl_3$): δ (ppm) 7.32-7.35 (m, 2H, Ar-H), 7.13-7.18 (t, J = 8.52 Hz, 2H, Ar-H), 7.24 (brs, 2H, NH_2), 3.91-3.96 (m, 1H, CH), 2.59 (s, 3H, CH_3), 2.14 (s, 2H, CH_2), 0.85-089 (t, J = 7.12, 3H, CH_3). ^{13}C-NMR (100 MHz, $CDCl_3$): δ (ppm) 164.96, 163.05, 160.31, 127.41, 126.80, 125.40, 124.09, 120.32, 117.08, 116.85, 103.83, 61.52, 53.63, 33.70, 13.86, 13.54. Elemental Analysis: Anal. Calc. for $C_{16}H_{15}FN_2O_2$: C, 67.12; H, 5.28; N, 9.78; %. Found: C, 67.14; H, 5.30; N, 9.79; %.

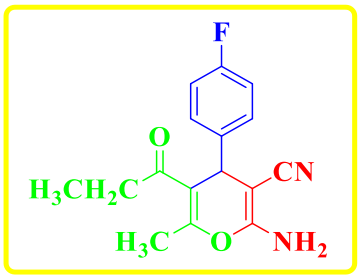

7.13. 2-Amino-6-methyl-4-(2-nitrophenyl)-5-propionyl-*4H*-pyran-3-carbonitrile (32)

Dark yellow solid, m.p = 176-178℃; IR (ATR, cm^{-1}): 3455 NH_2, 1127 C-N, 2209 CN, 1525 C=C, 1602 C=O, 1064 C-O, 2987 CH. ^{1}H-NMR (400 MHz, $CDCl_3$): δ (ppm) 7.67-7.69 (t, J = 6.72, 1H, Ar-H), 7.47-7.48 (m, 1H, Ar-H), 7.43-7.47 (m, 2H, Ar-H), 7.42 (brs, 2H,

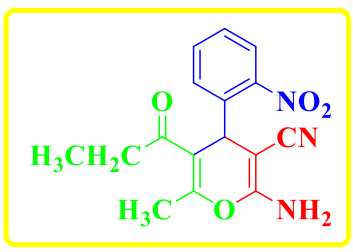

NH_2), 5.01 (s, 1H, CH), 3.85-3.90 (m, *J* =6.92, 2H, CH_2), 2.84 (s, 3H, OCH_3), 0.89-0.92 (t, *J* = 7.08, 3H, -CH_3), ^{13}C-NMR (100 MHz, $CDCl_3$): δ (ppm) 164.79, 158.93, 158.25, 148.47, 139.55, 133.73, 130.41, 128.06, 123.70, 118.91, 106.30, 60.25, 55.8532.83, 18.27, 13.43. Elemental Analysis: Anal. Calc. for $C_{16}H_{15}N_3O_4$: C, 61.34; H, 4.83; N, 13.41; %. Found: C, 61.36; H, 4.85; N, 13.44; %.

7.14. 2-Amino-6-methyl-5-propionyl-4-(p-tolyl)-*4H*-pyran-3-carbonitrile (33)

White solid, m.p = 121-123℃; IR (FTIR, cm^{-1}): 3049 NH_2, 1133 C-N, 2229 CN, 1575 C=C, 1615 C=O, 1046 C-O, 2979 CH. ^{1}H-NMR (400 MHz, $CDCl_3$): δ (ppm) 7.95-7.97 (t, *J* = 8.92, 2H, Ar-H) 7.15-7.18 (t, *J* = 7.08, 2H, Ar-H), 4.48 (brs, 2H, NH_2), 4.38 (s, 1H, CH), 4.01- 4.03 (m, 2H, CH_2), 2.33 (s, 3H, Ar-CH_3), 2.27 (s, 3H, CH_3), 1.01-1.07 (t, *J* = 7.16, 3H, -CH_3), ^{13}C-NMR (100 MHz, $CDCl_3$): δ (ppm) 207.46, 165.99, 157.61, 156.58, 140.87, 136.71, 129.69, 129.24, 127.38, 119.14, 108.13, 62.21, 60.64, 38.29, 30.90, 21.04, 18.38. Elemental Analysis: Anal. Calc. for $C_{17}H_{18}N_2O_2$: C, 72.32; H, 6.43; N, 9.92; %. Found: C, 72.34; H, 6.46; N, 9.93; %.

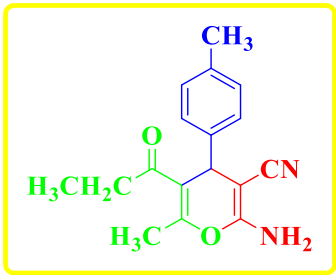

7.1. 2-Amino-7,7-dimethyl-5-oxo-4-phenyl-5,6,7,8-tetrahydro-*4H*-chromene-3-carbonitrile (20)

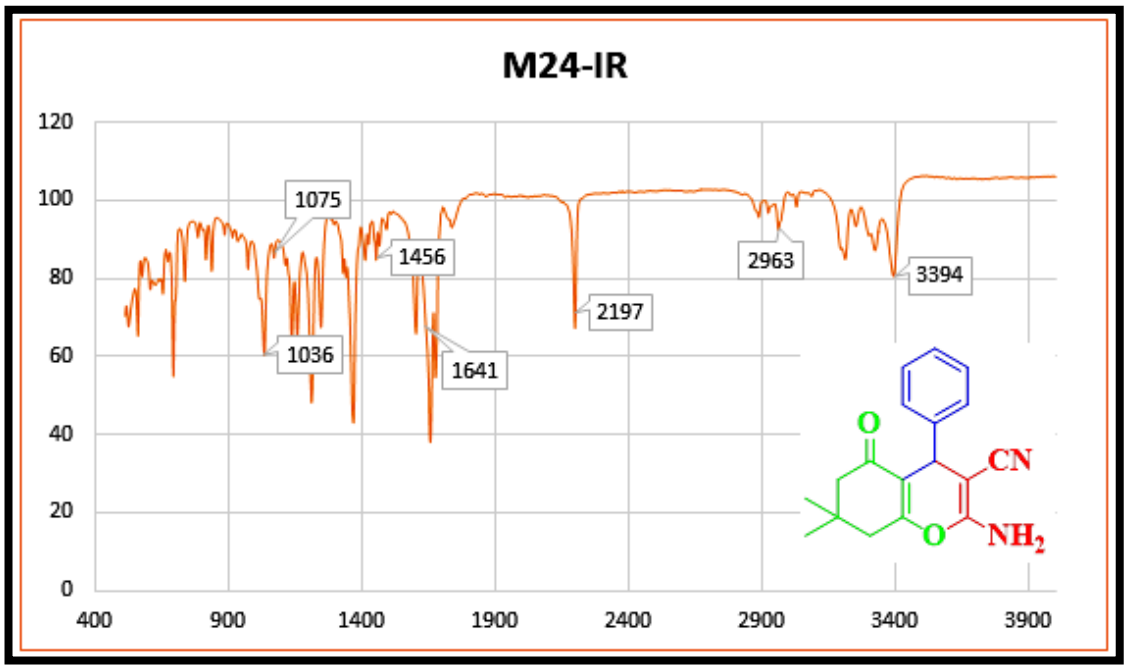

Fig. 7.1. IR spectrum of **20**

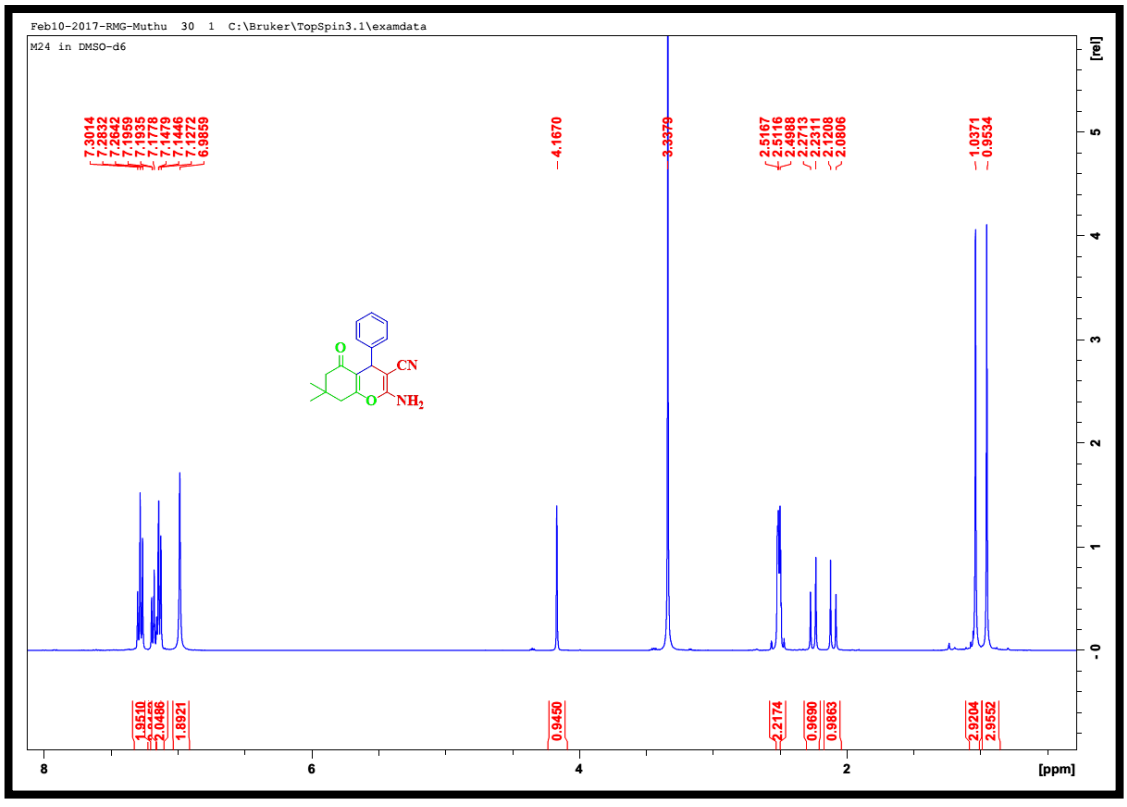

Fig. 7.2. ^{1}H-NMR spectrum for **20**

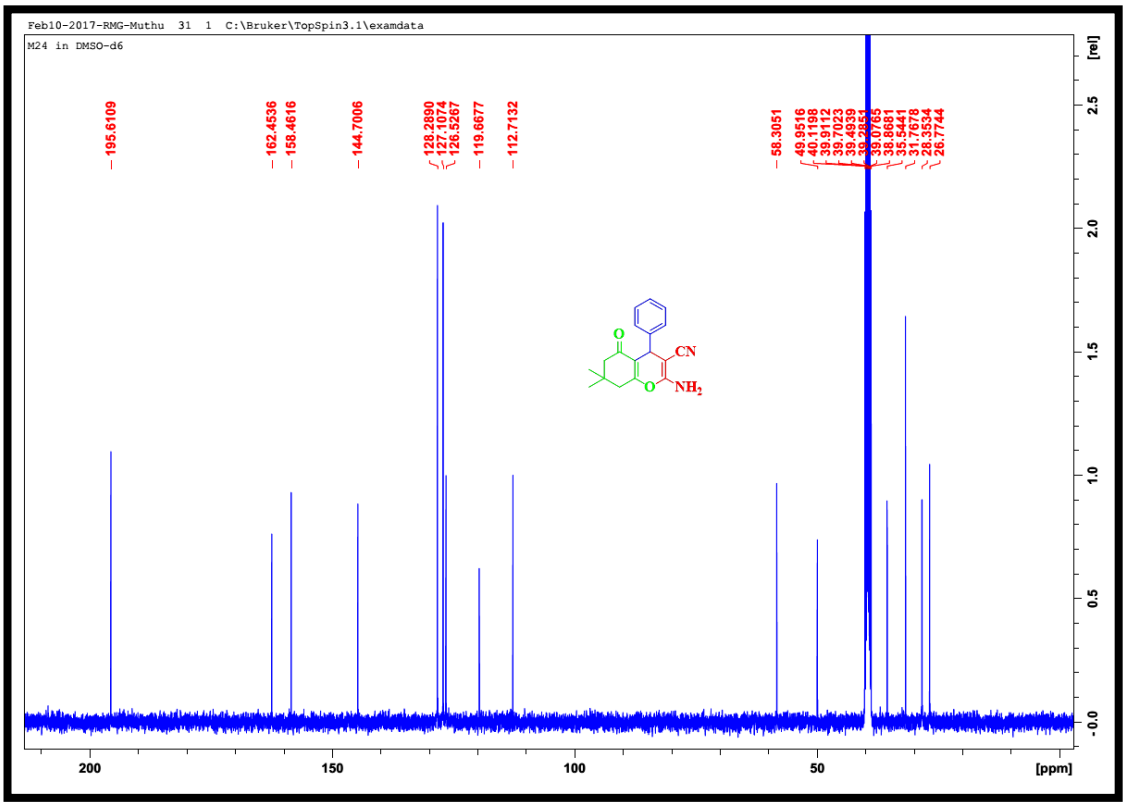

Fig. 7.3. ^{13}C-NMR spectrum for **20**

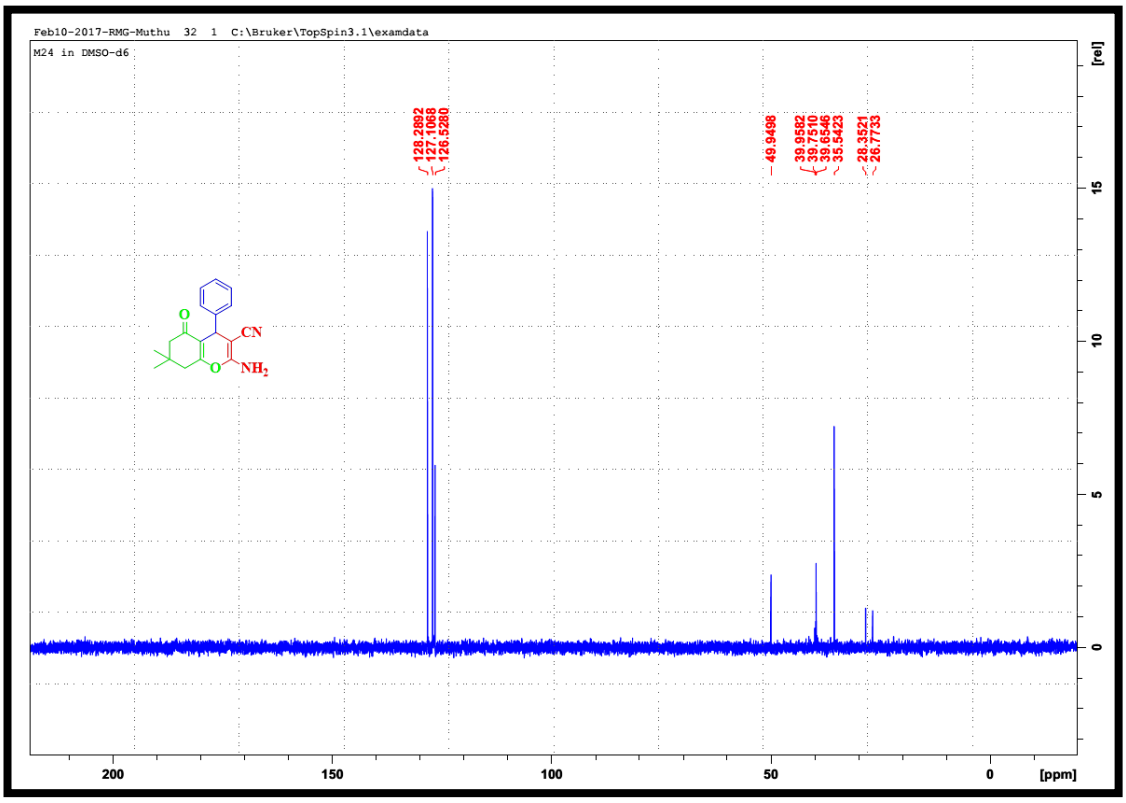

Fig. 7.4. DEPT 90º spectrum for **20**

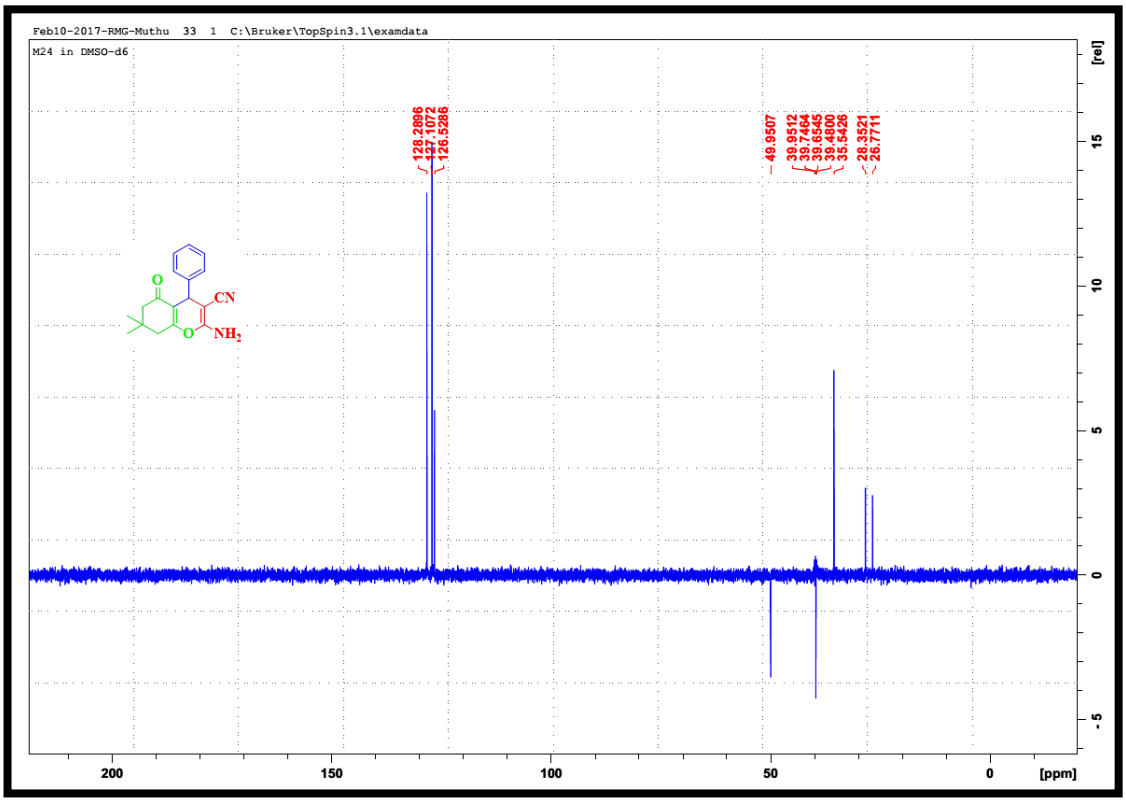

Fig. 7.5. DEPT 135º spectrum for **20**

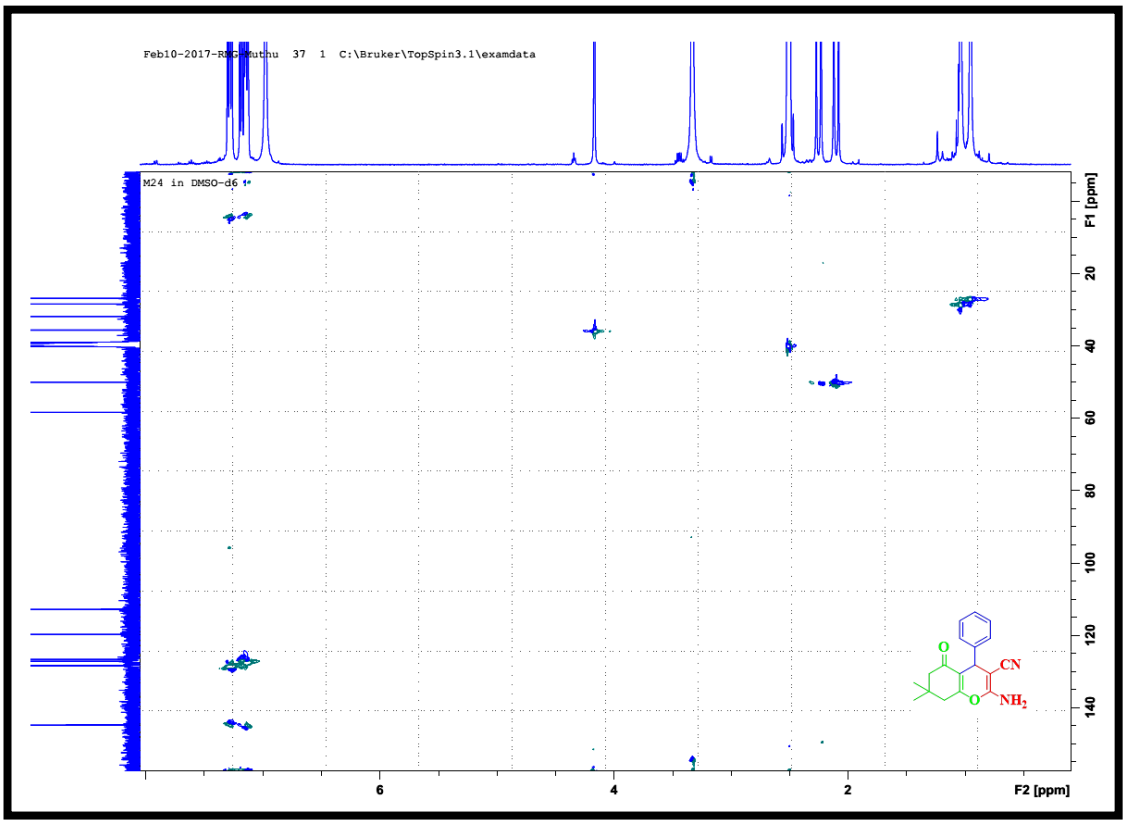

Fig. 7.6. HSQC spectrum for **20**

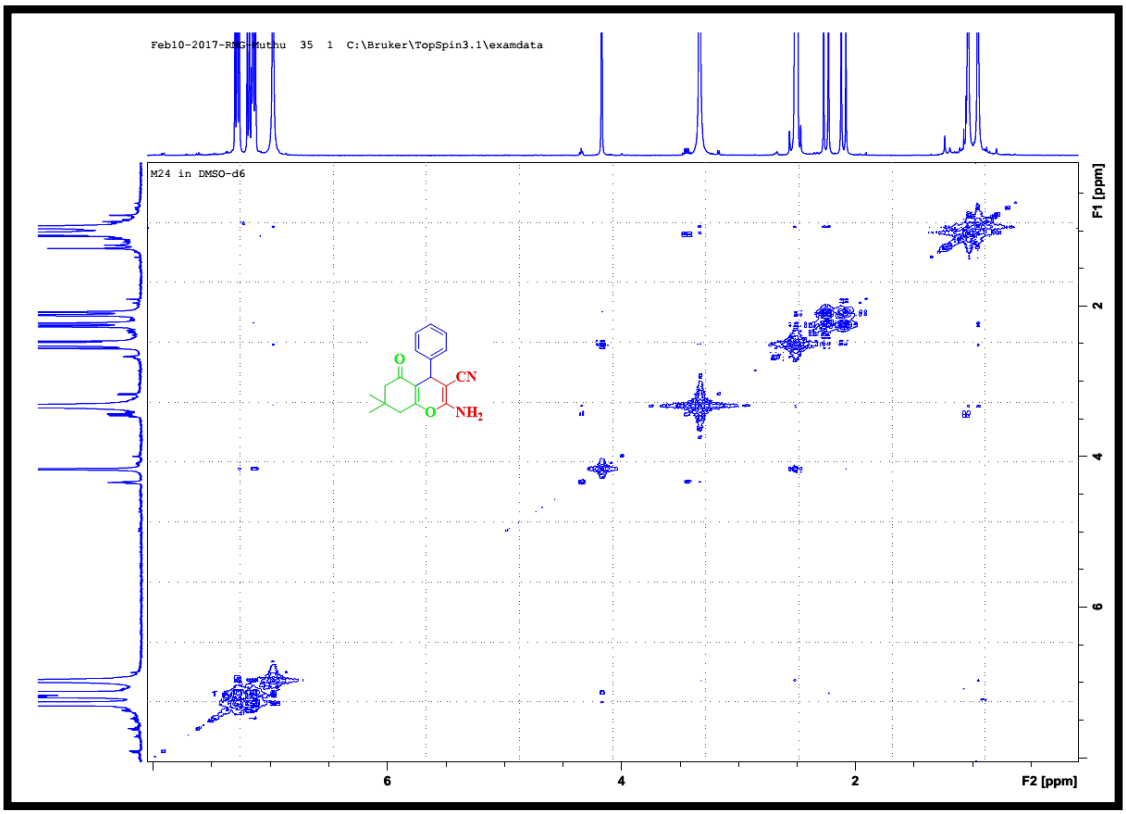

Fig. 7.7. COSY spectrum for **20**

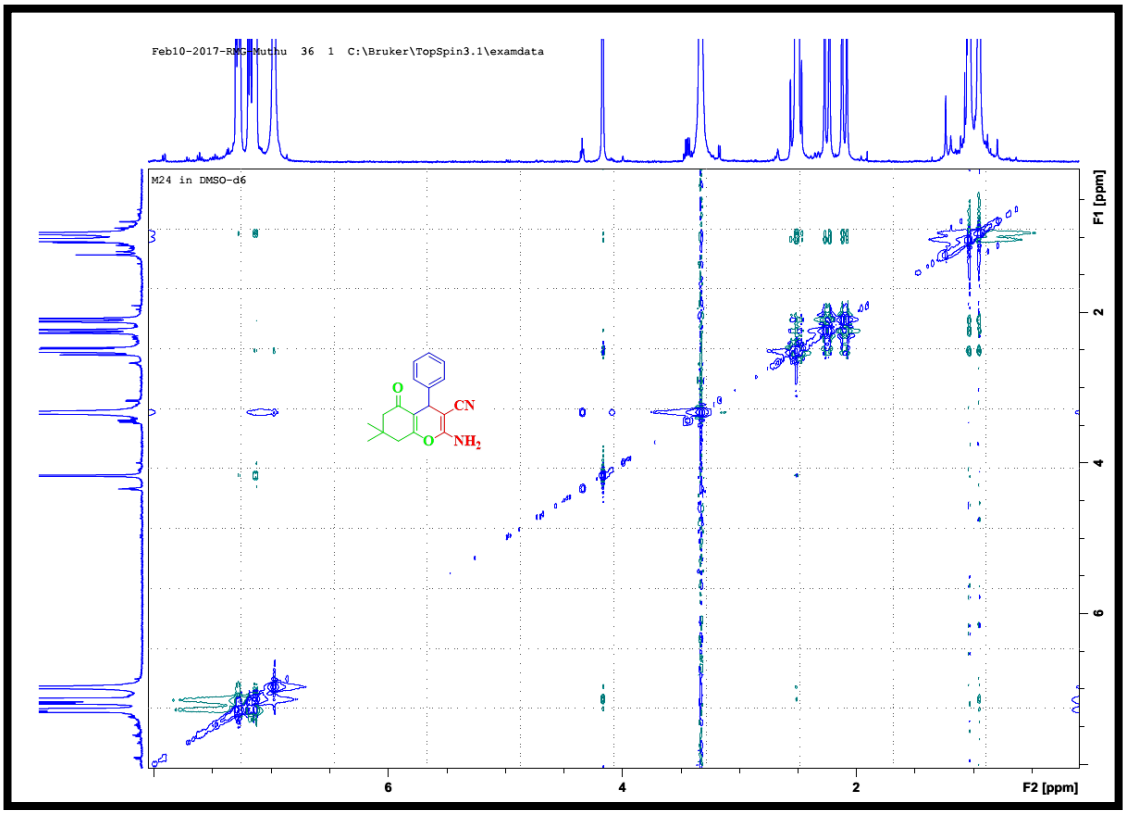

Fig. 7.8. NOESY spectrum for **20**

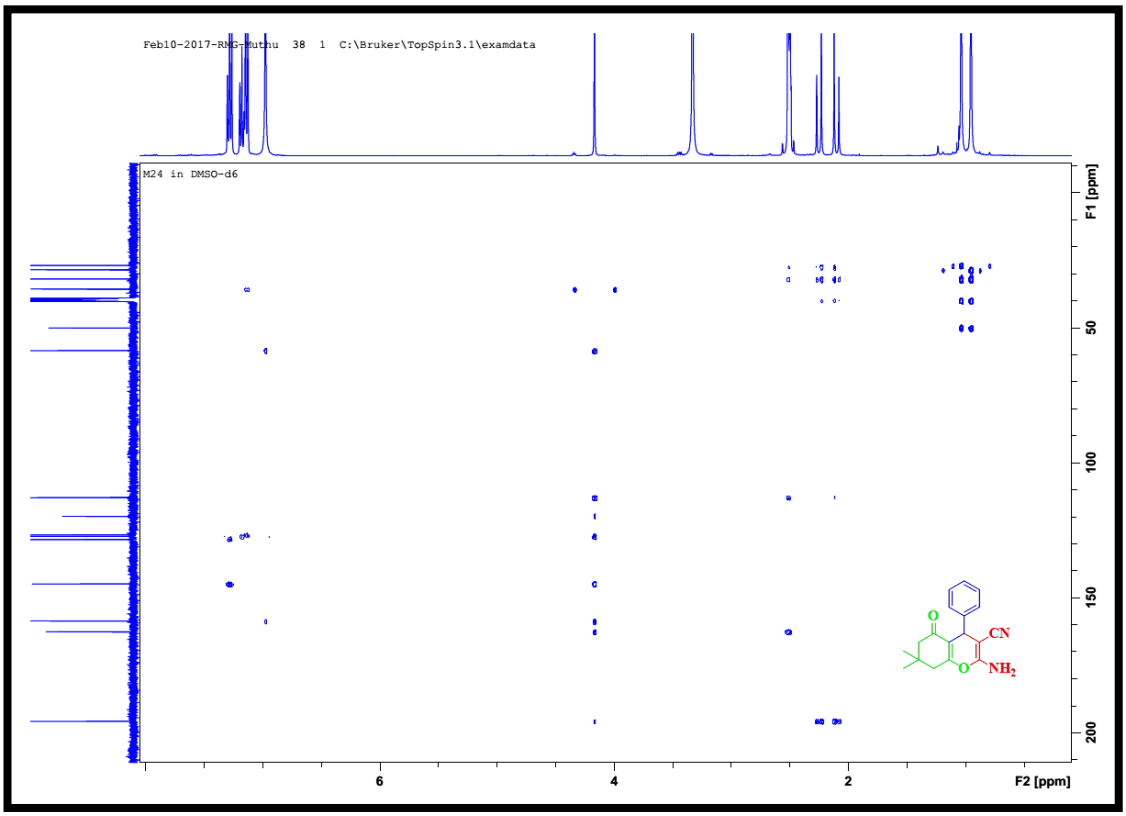

Fig. 7.9. HMBC spectrum for **20**

7.2. 2-Amino-7,7-dimethyl-4-(4-nitrophenyl)-5-oxo-5,6,7,8-tetrahydro-*4H*-chromene-3-carbonitrile (21)

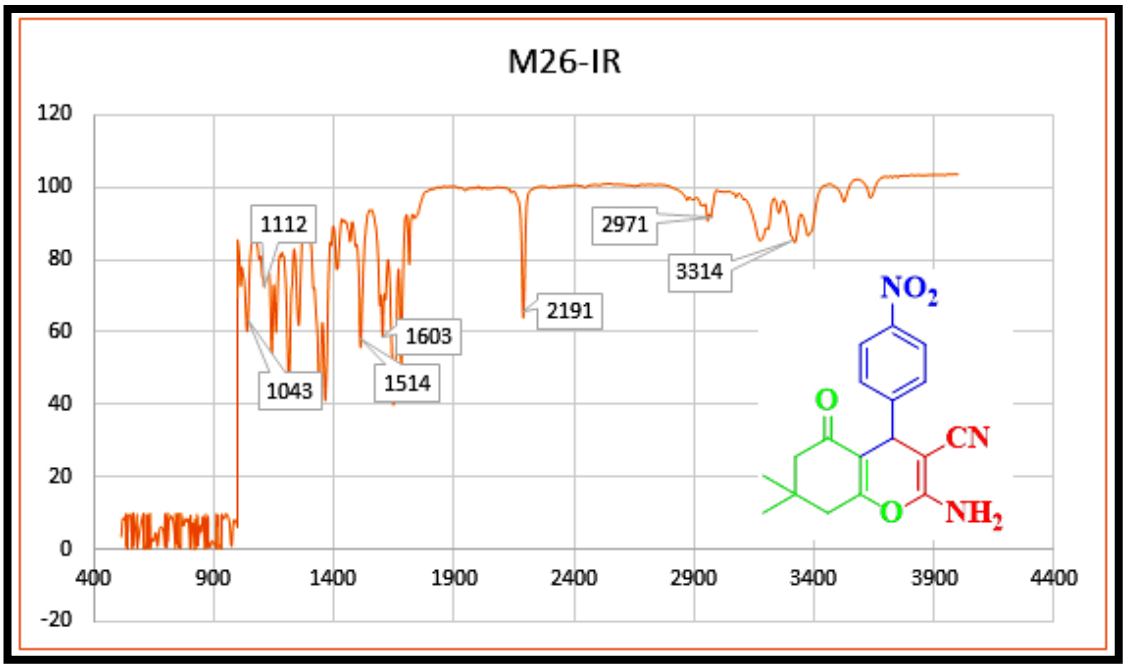

Fig. 7.10. IR spectrum of **21**

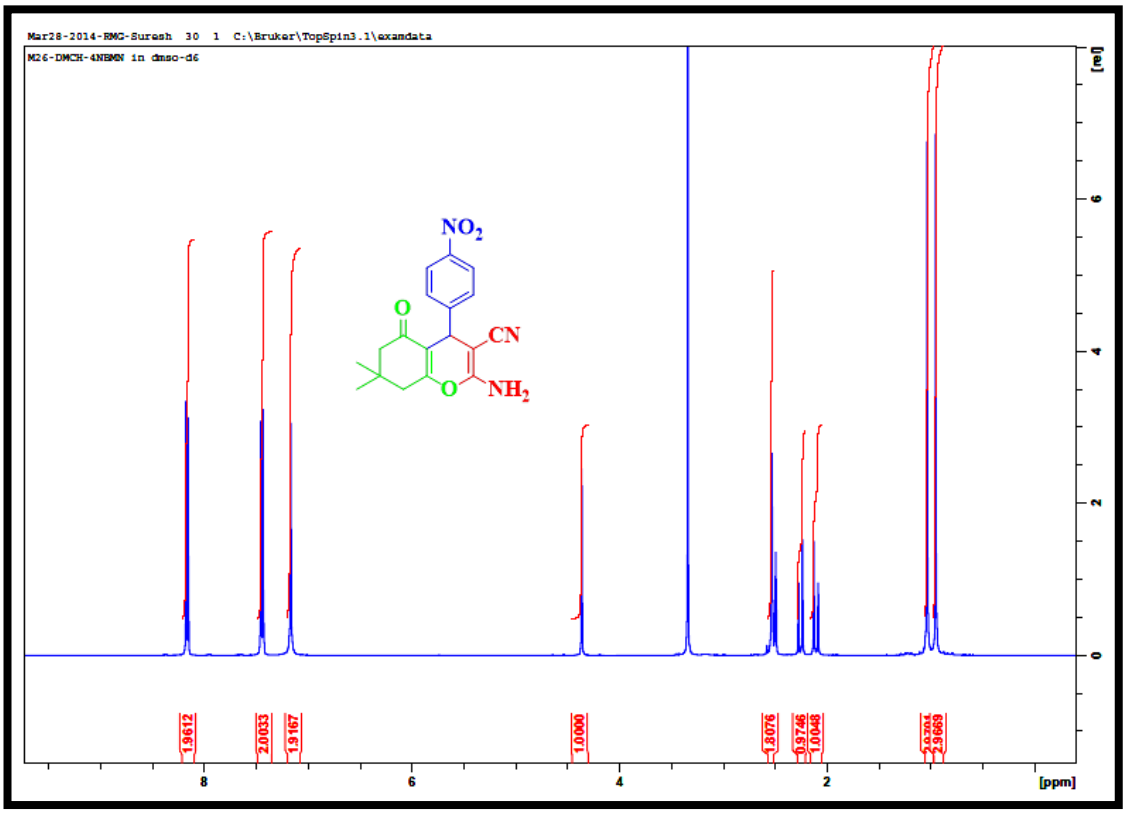

Fig. 7.11. ^{1}H-NMR spectrum for **21**

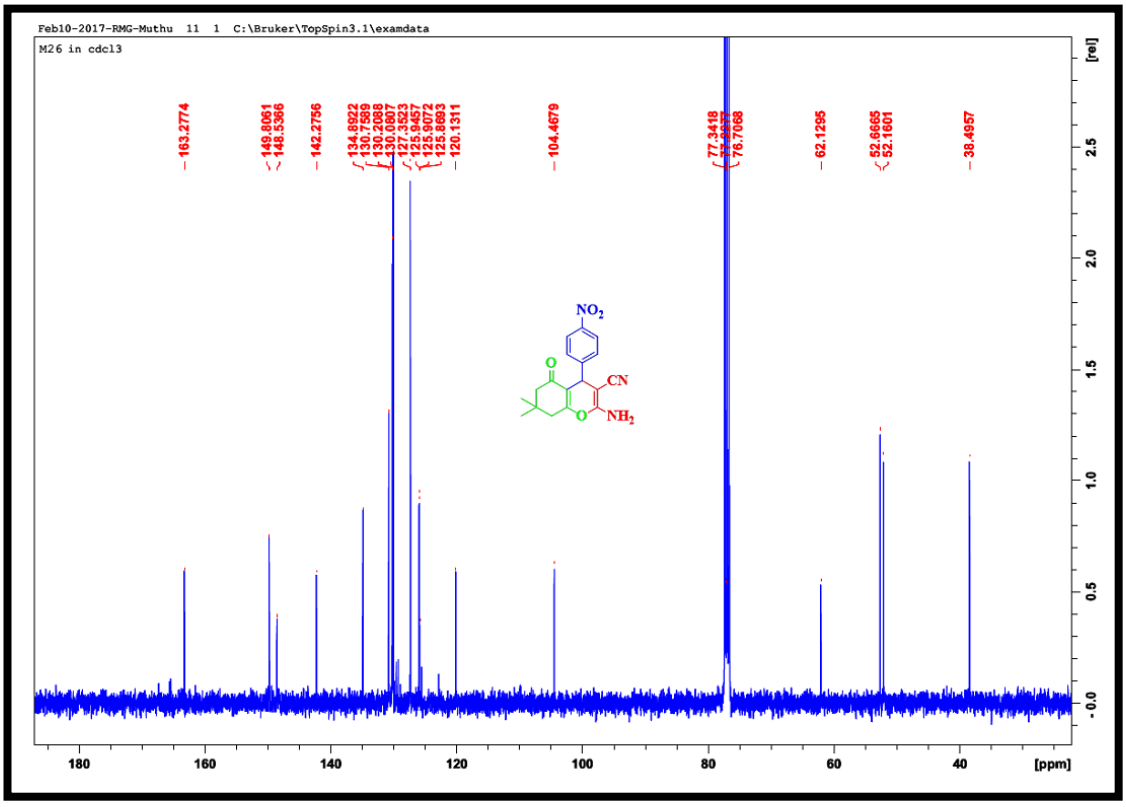

Fig. 7.12. ^{13}C-NMR spectrum for **21**

7.3. 2-Amino-4-(4-fluorophenyl)-7,7-dimethyl-5-oxo-5,6,7,8-tetrahydro-*4H*-chromene-3-carbonitrile (22)

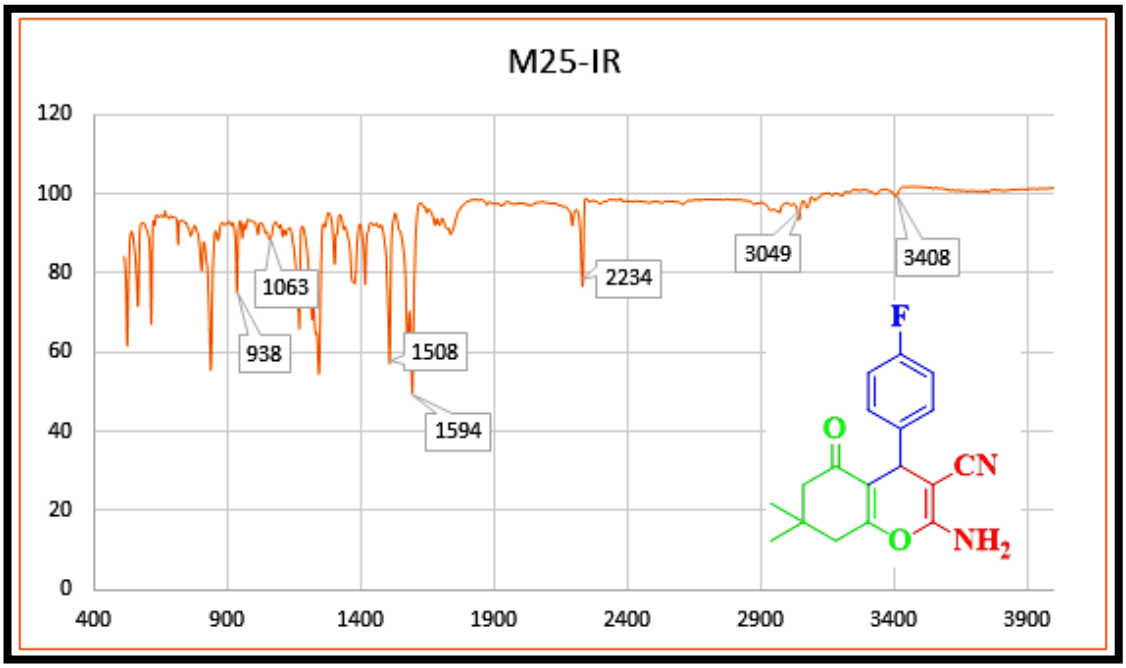

Fig. 7.13. IR spectrum of **22**

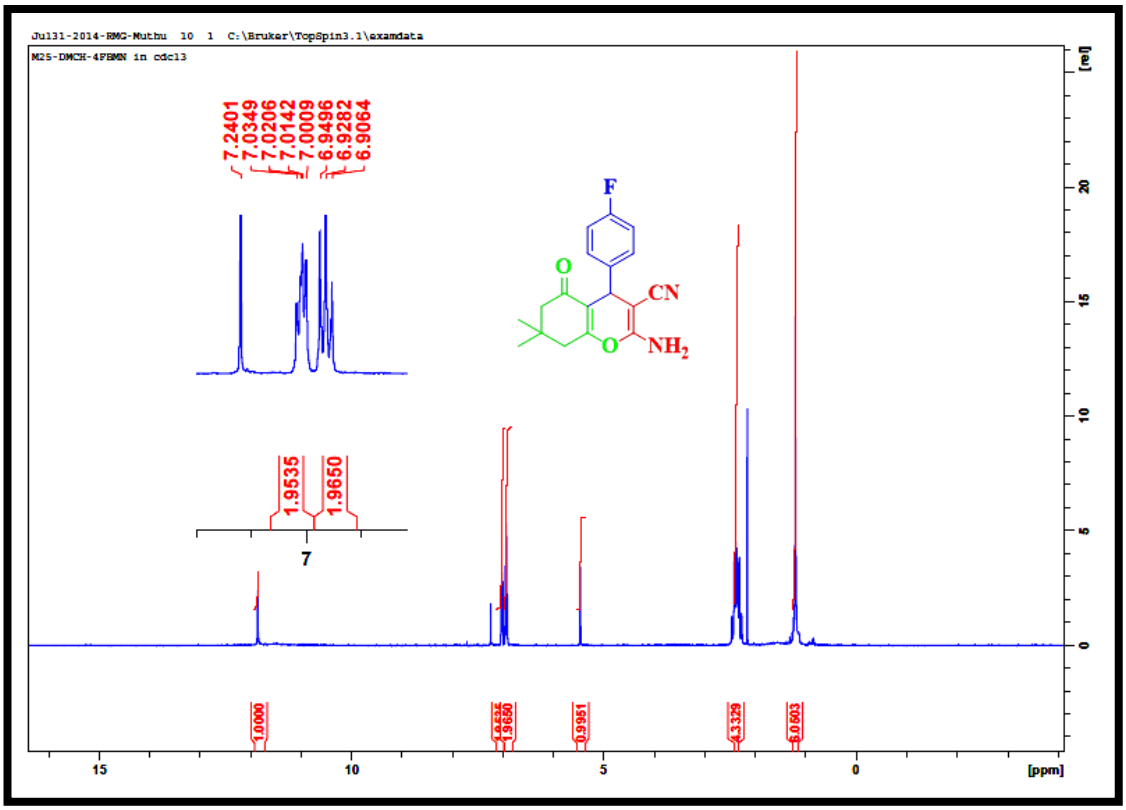

Fig. 7.14. ^{1}H-NMR spectrum for **22**

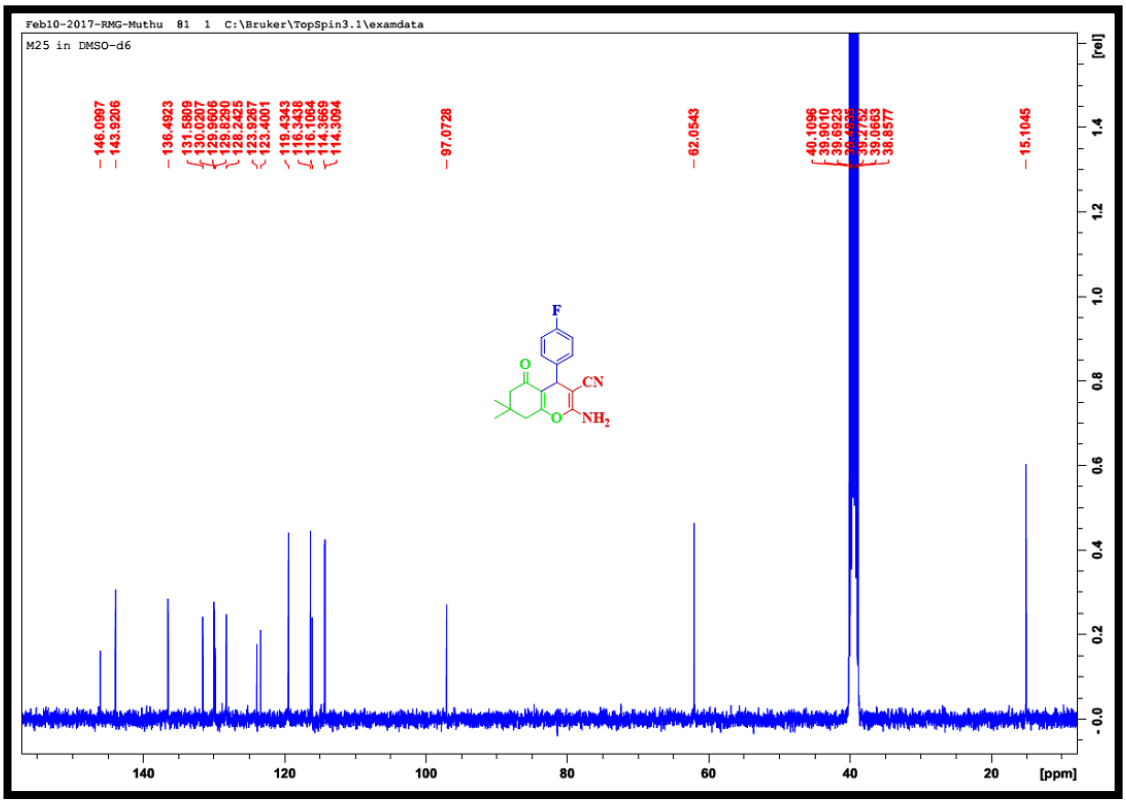

Fig. 7.15. ^{13}C-NMR spectrum for **22**

7.4. 2-Amino-4-(4-methoxyphenyl)-7,7-dimethyl-5-oxo-5,6,7,8-tetrahydro-*4H*-chromene-3-carbonitrile (23)

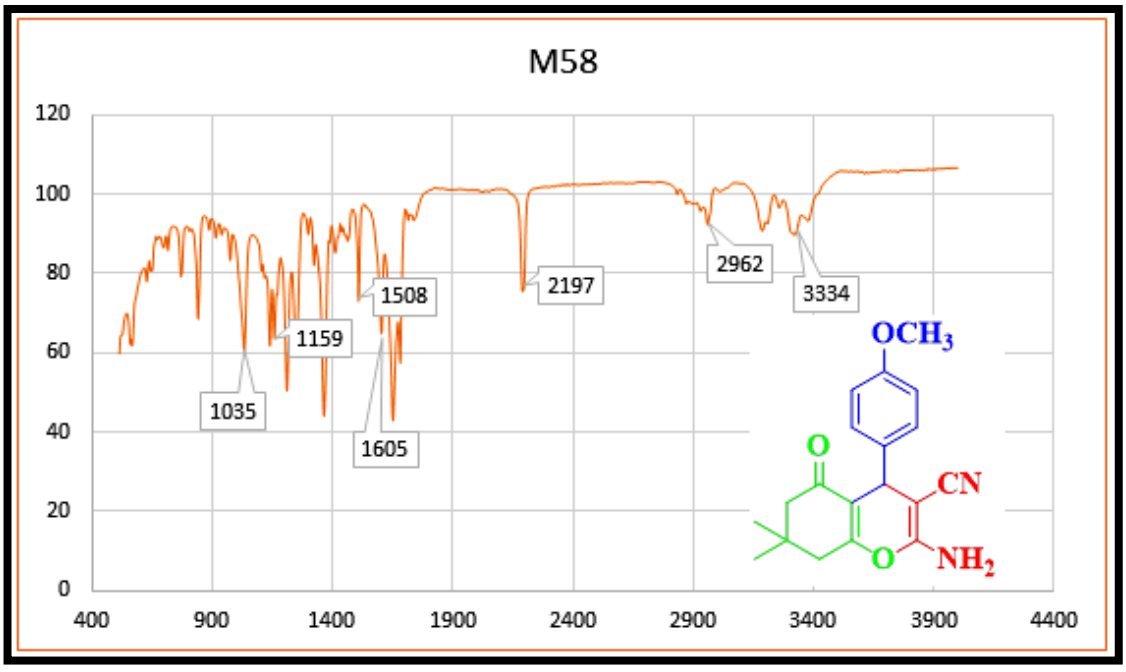

Fig. 7.16. IR spectrum of **23**

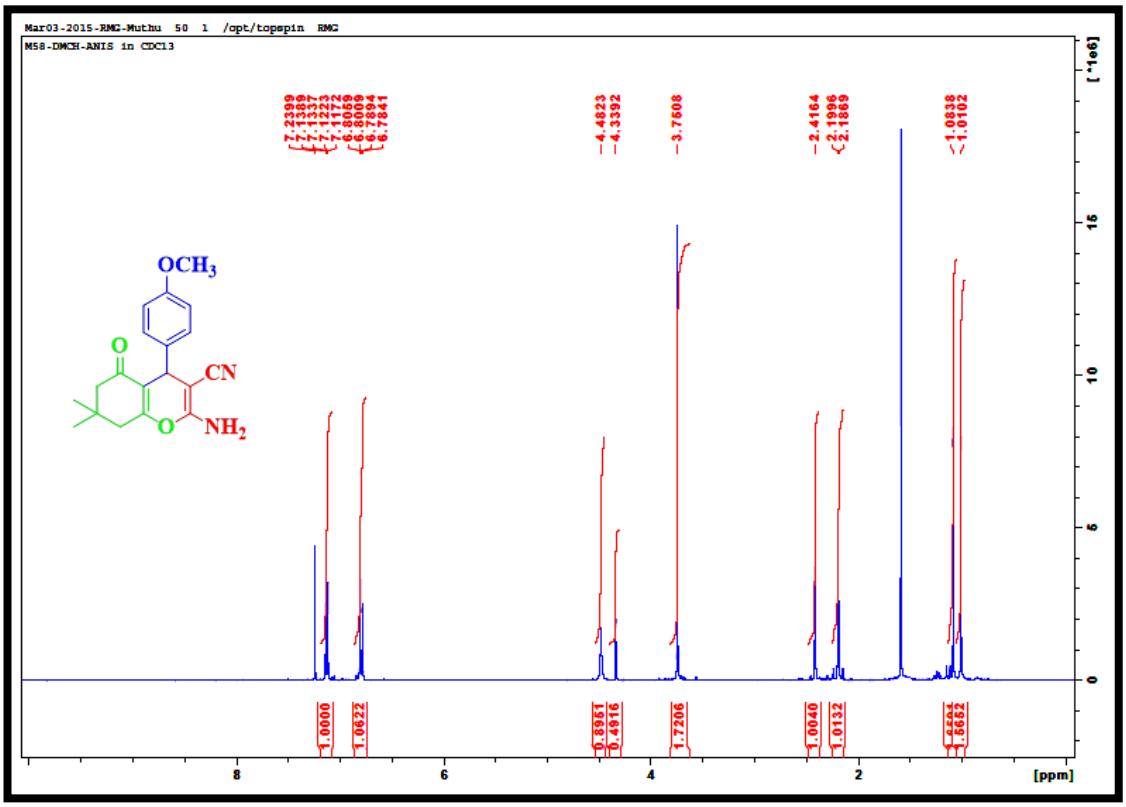

Fig. 7.17. ^{1}H-NMR spectrum for **23**

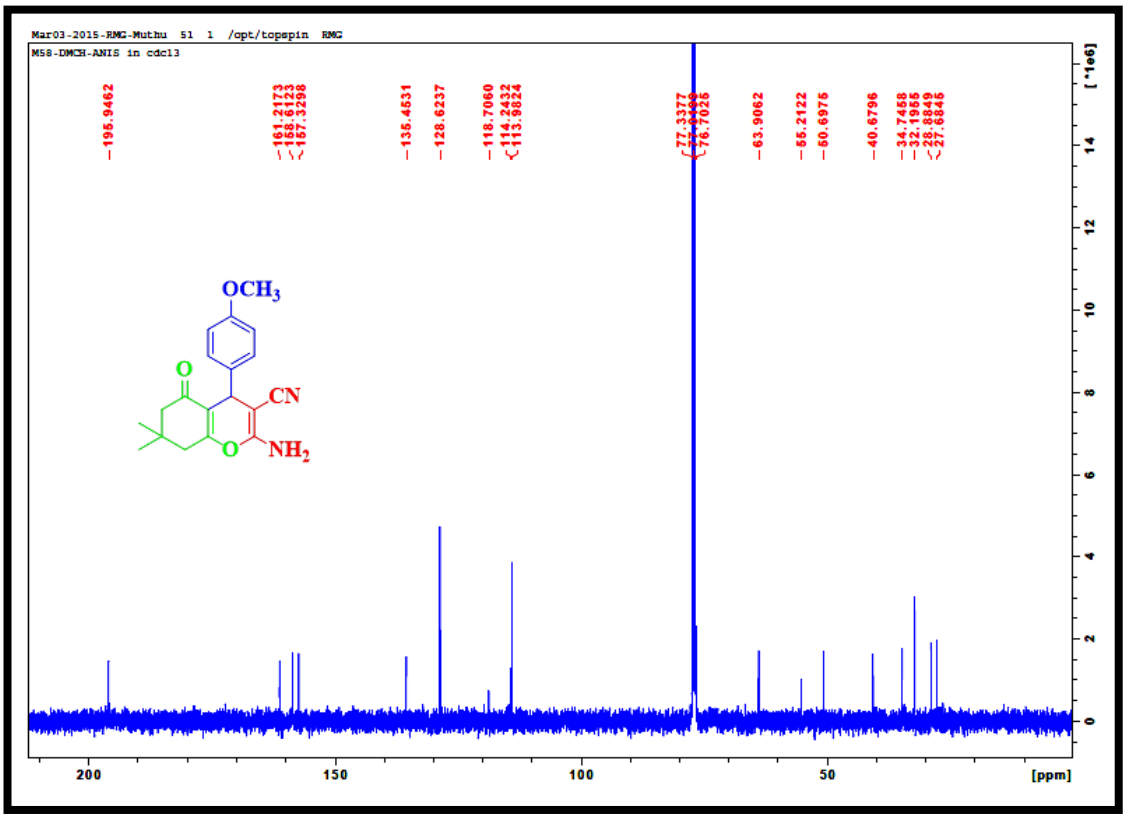

Fig. 7.18. ^{13}C-NMR spectrum for **23**

7.5. 2-Amino-7,7-dimethyl-4-(2-nitrophenyl)-5-oxo-5,6,7,8-tetrahydro-*4H*-chromene-3-carbonitrile (24)

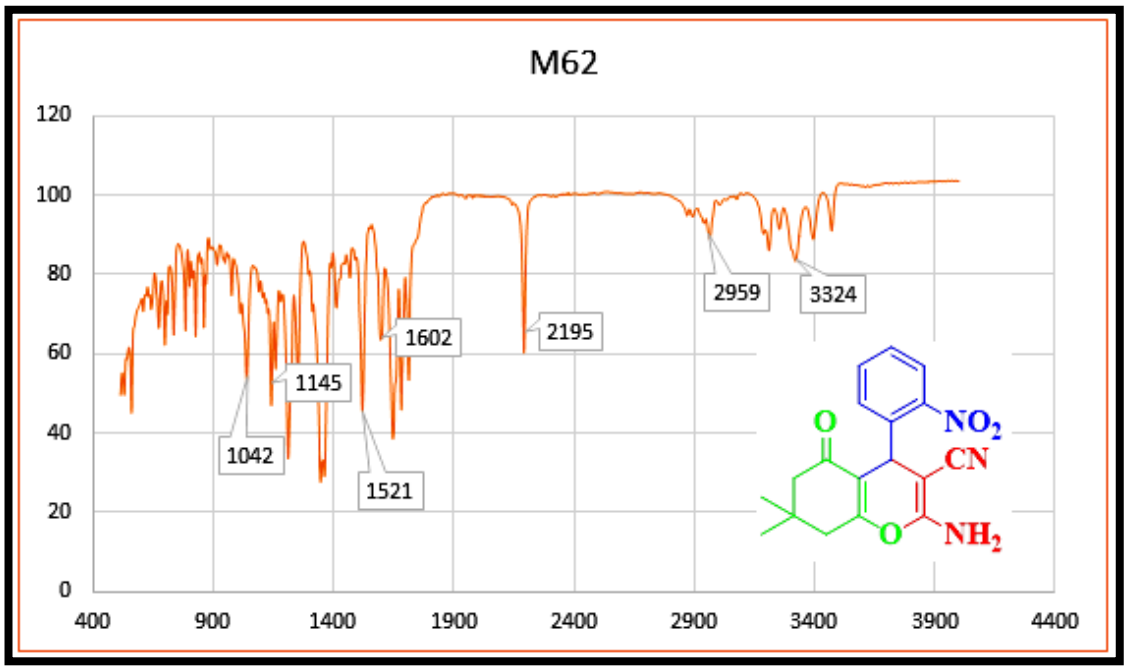

Fig. 7.19. IR spectrum of **24**

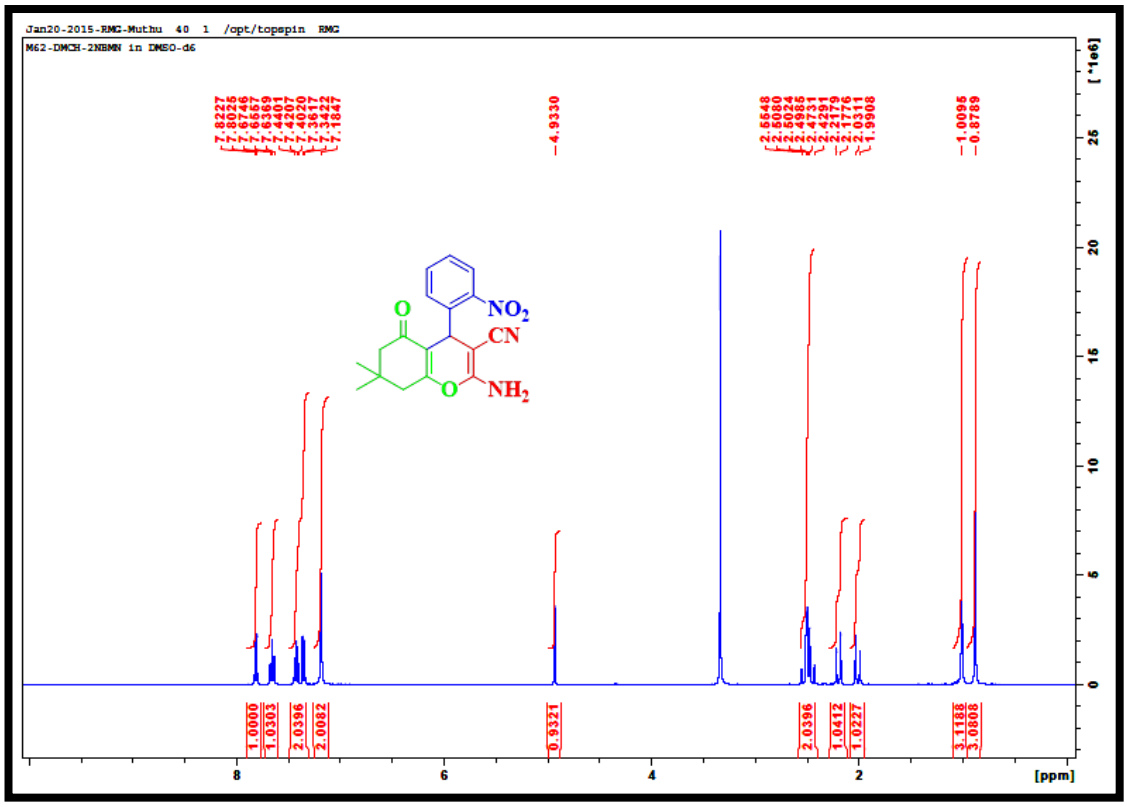

Fig. 7.20. ^{1}H-NMR spectrum for **24**

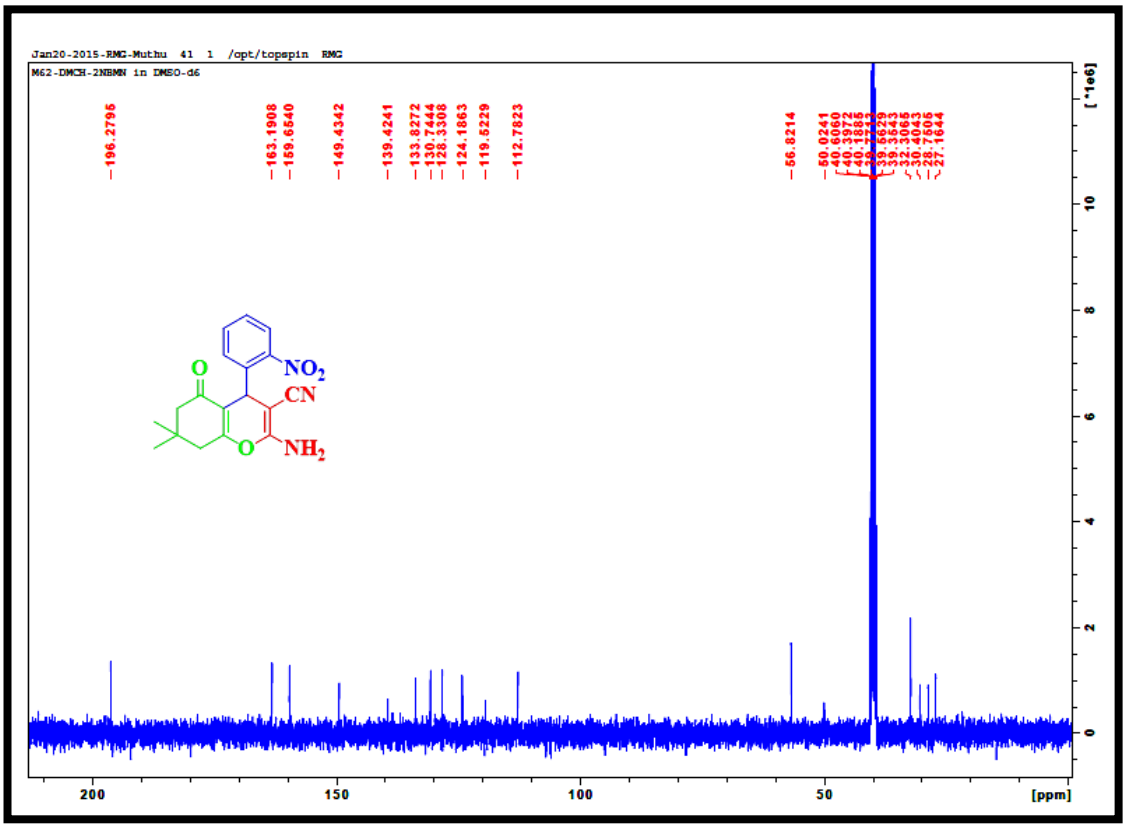

Fig. 7.21. ^{13}C-NMR spectrum for **24**

7.6. 2-Amino-4-(4-chlorophenyl)-7,7-dimethyl-5-oxo-5,6,7,8-tetrahydro-*4H*-chromene-3-carbonitrile (25)

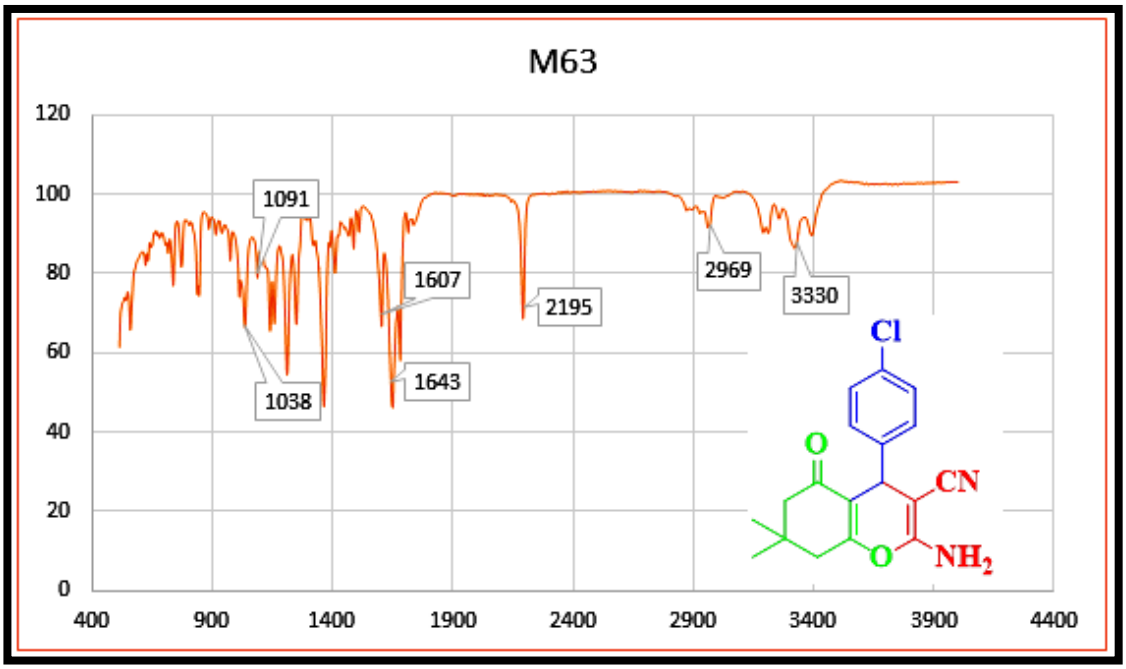

Fig. 7.22. IR spectrum of **25**

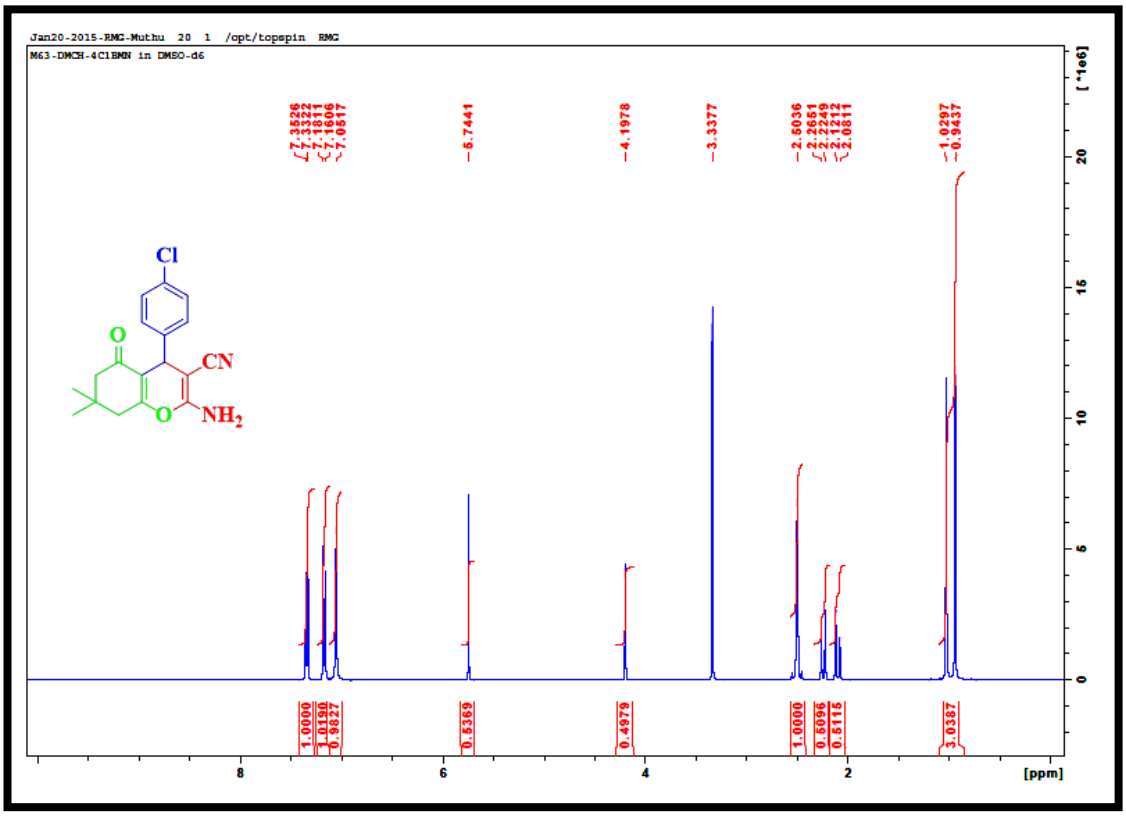

Fig. 7.23. ^{1}H-NMR spectrum for **25**

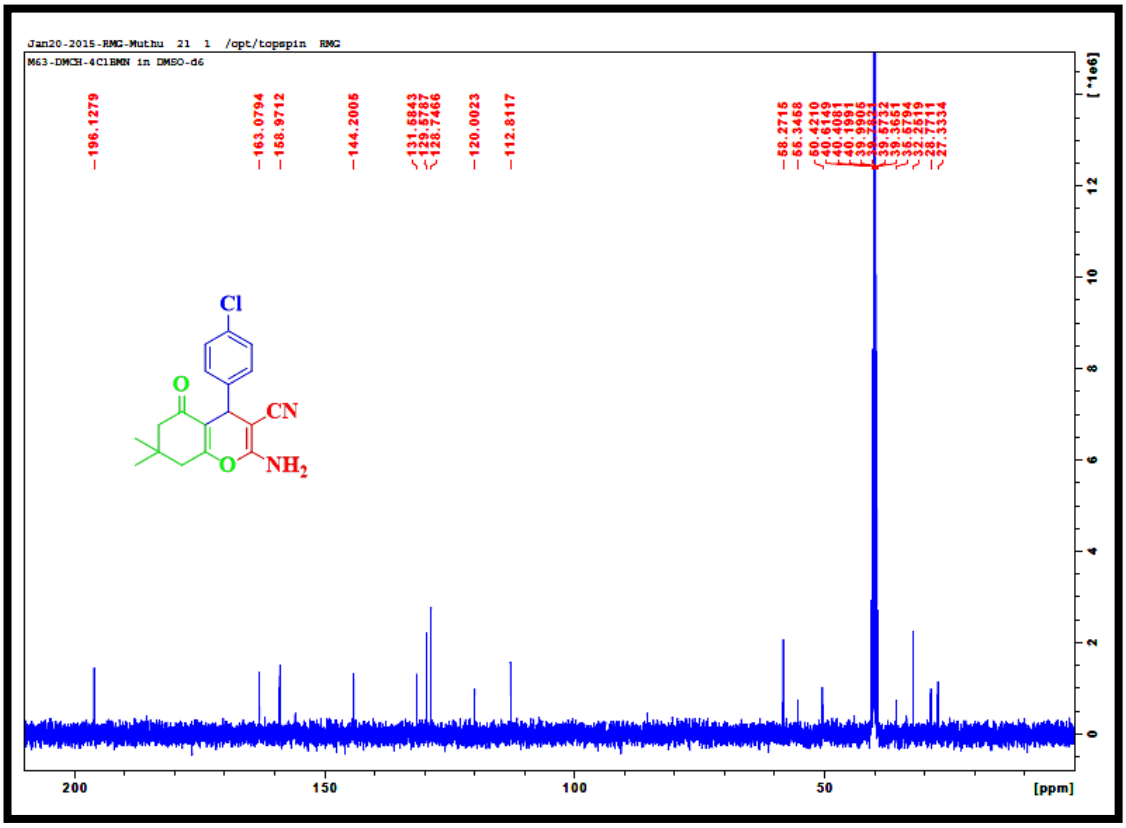

Fig. 7.24. ^{13}C-NMR spectrum for **25**

7.7. 2-Amino-7,7-dimethyl-5-oxo-4-(p-tolyl)-5,6,7,8-tetrahydro-*4H*-chromene-3-carbonitrile (26)

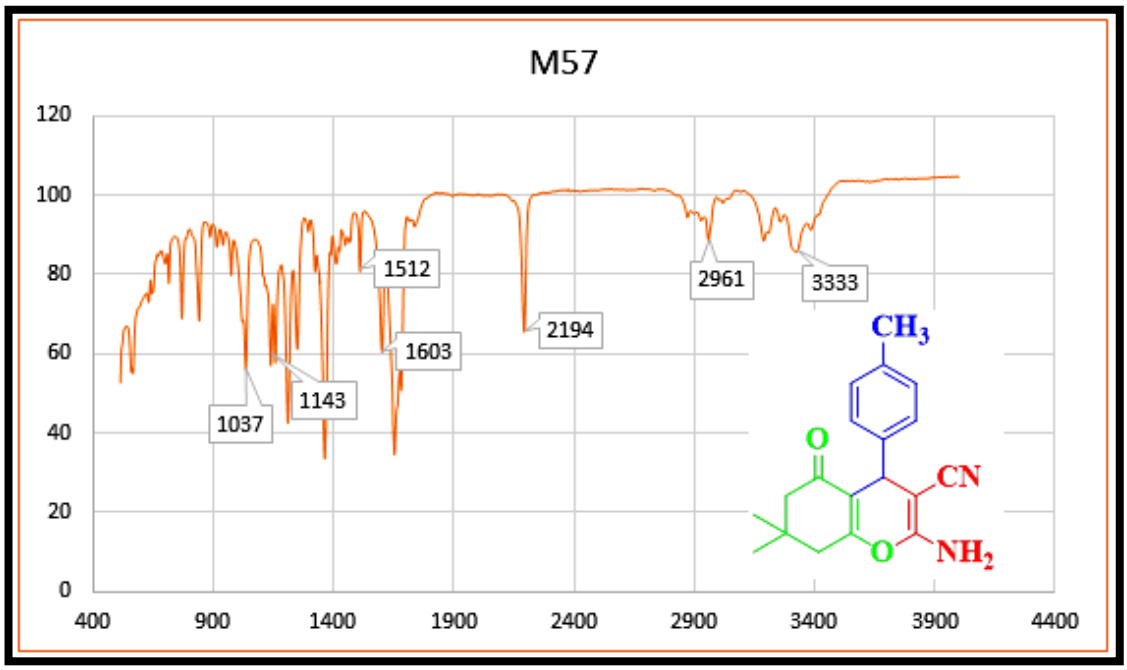

Fig. 7.25. IR spectrum of **26**

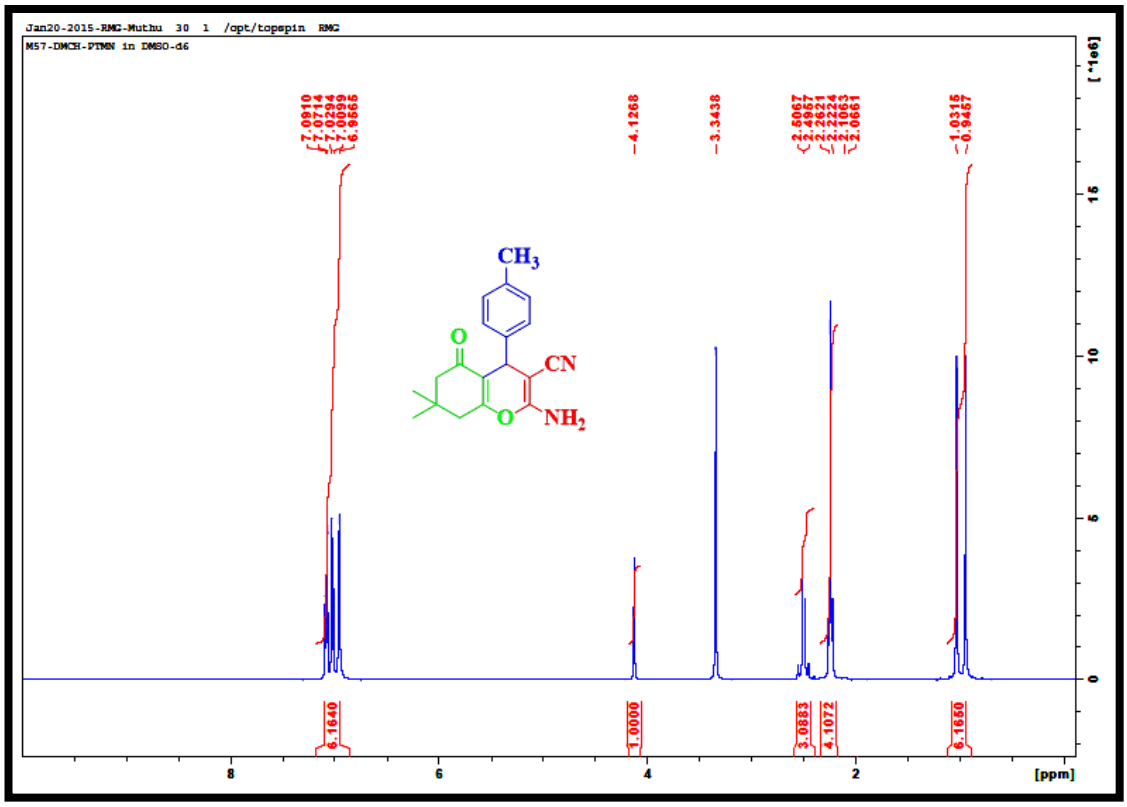

Fig. 7.26. ^{1}H-NMR spectrum for **26**

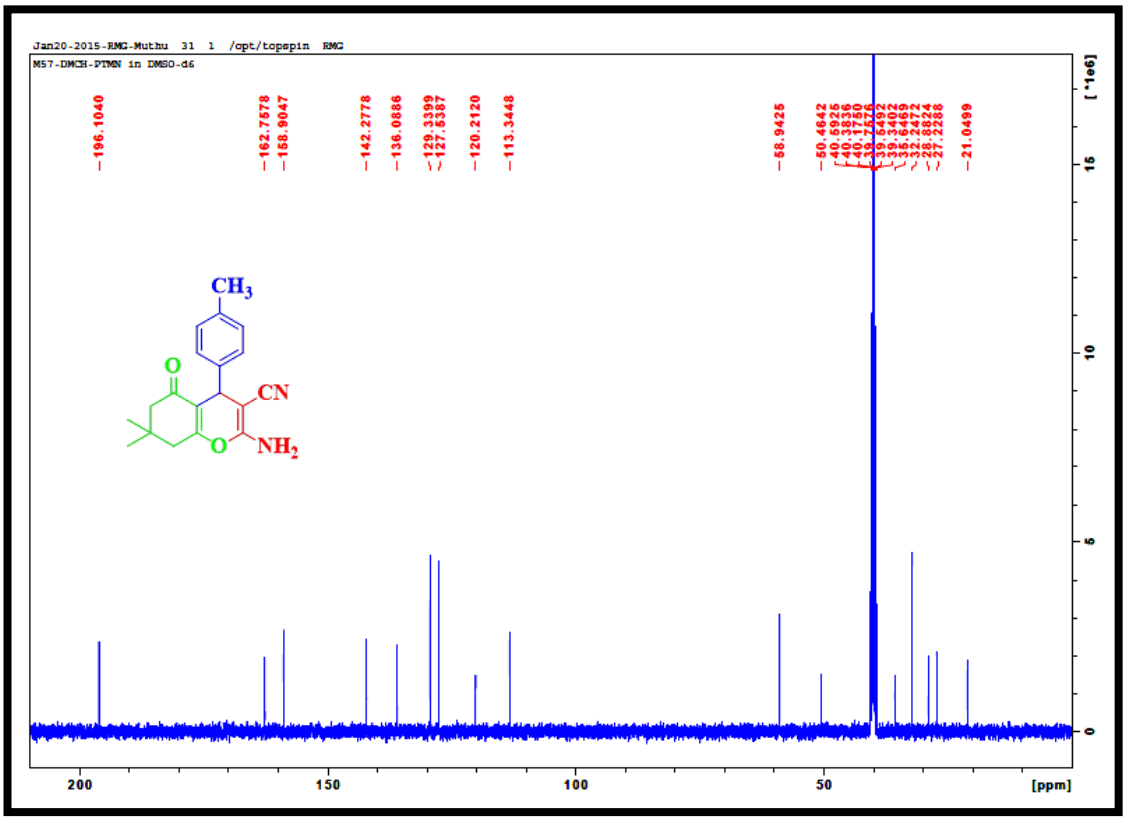

Fig. 7.27. ^{13}C-NMR spectrum for **26**

7.8. 2-Amino-4-(2-hydroxyphenyl)-7,7-dimethyl-5-oxo-5,6,7,8-tetrahydro-*4H*-chromene-3-carbonitrile (27)

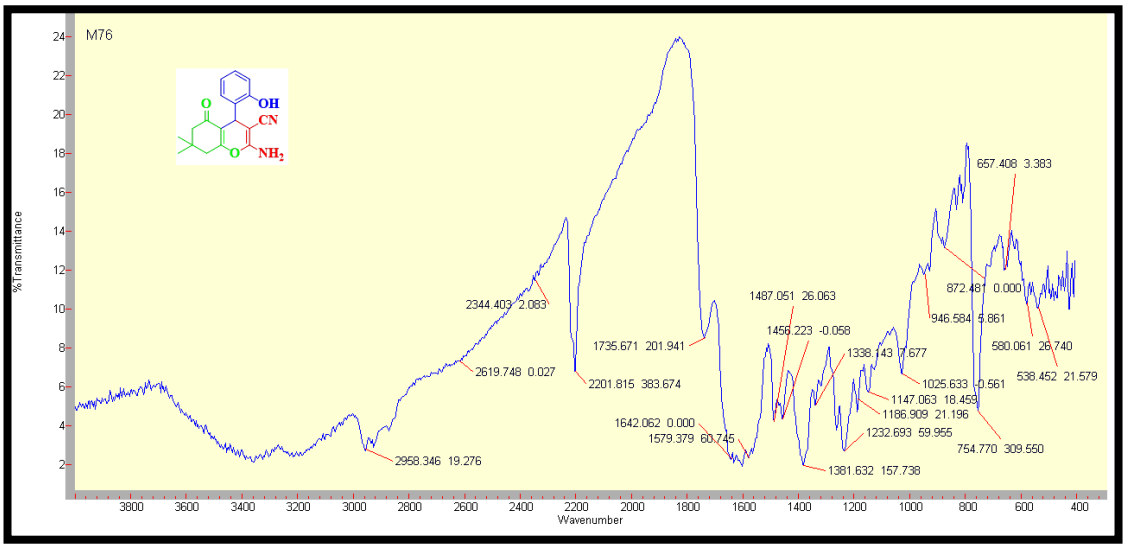

Fig. 7.28. IR spectrum of **27**

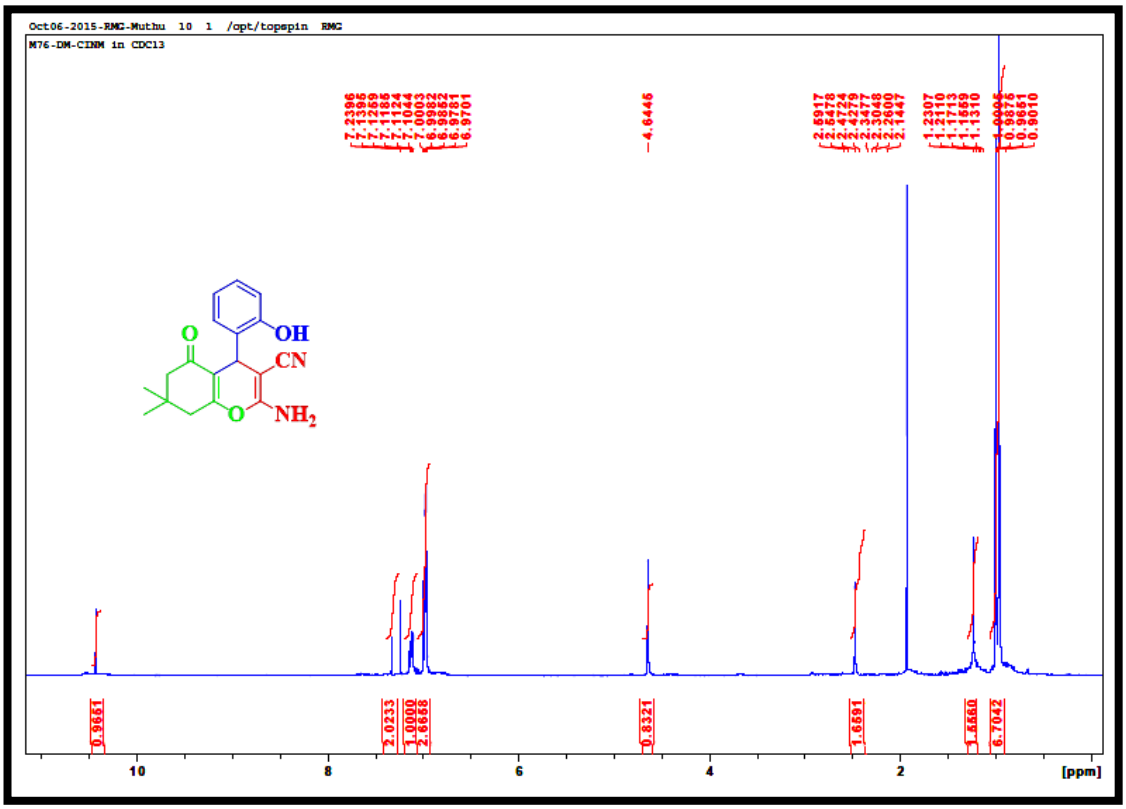

Fig. 7.29. ^{1}H-NMR spectrum for **27**

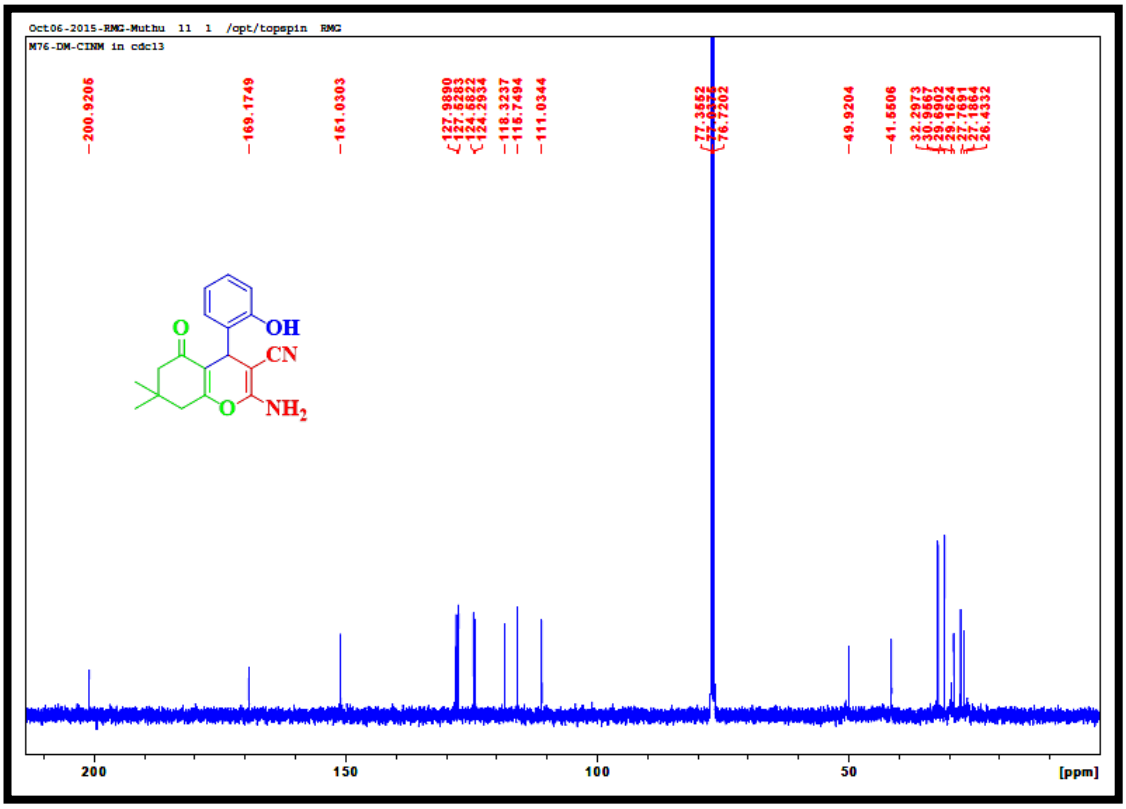

Fig. 7.30. ^{13}C-NMR spectrum for **27**

7.9. 2-Amino-4-(furan-2-yl)-7,7-dimethyl-5-oxo-5,6,7,8-tetrahydro-*4H*-chromene-3-carbonitrile (28)

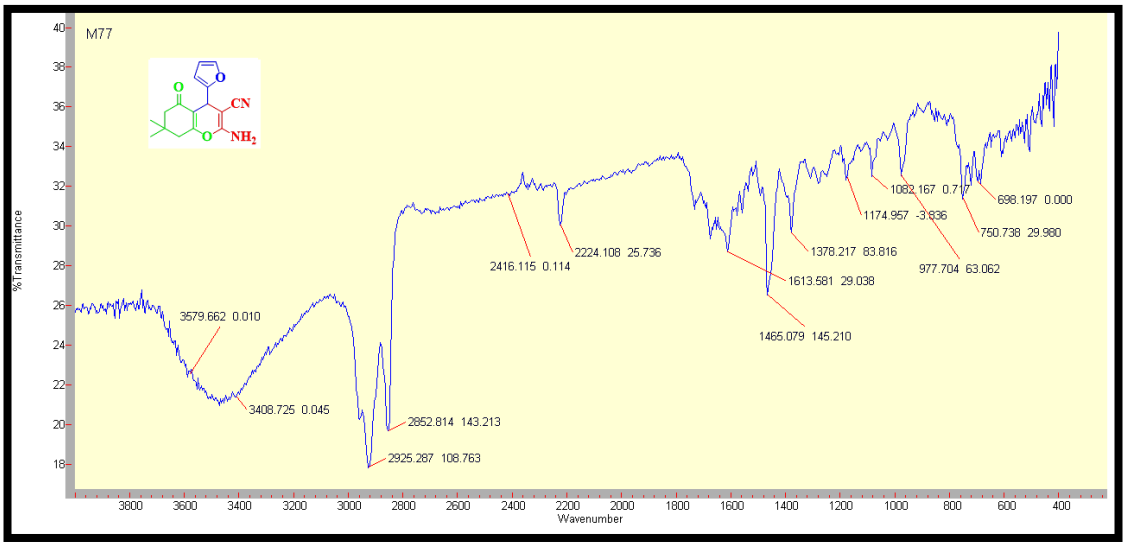

Fig. 7.31. IR spectrum of **28**

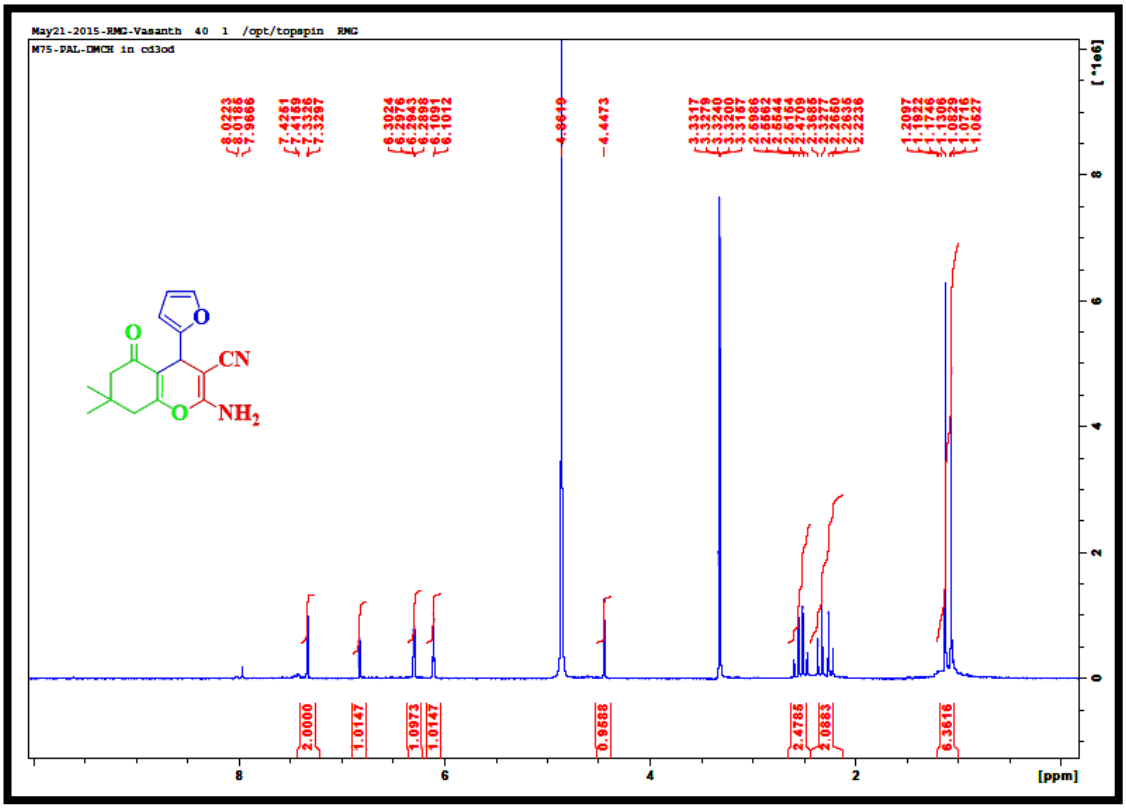

Fig. 7.32. ^{1}H-NMR spectrum for **28**

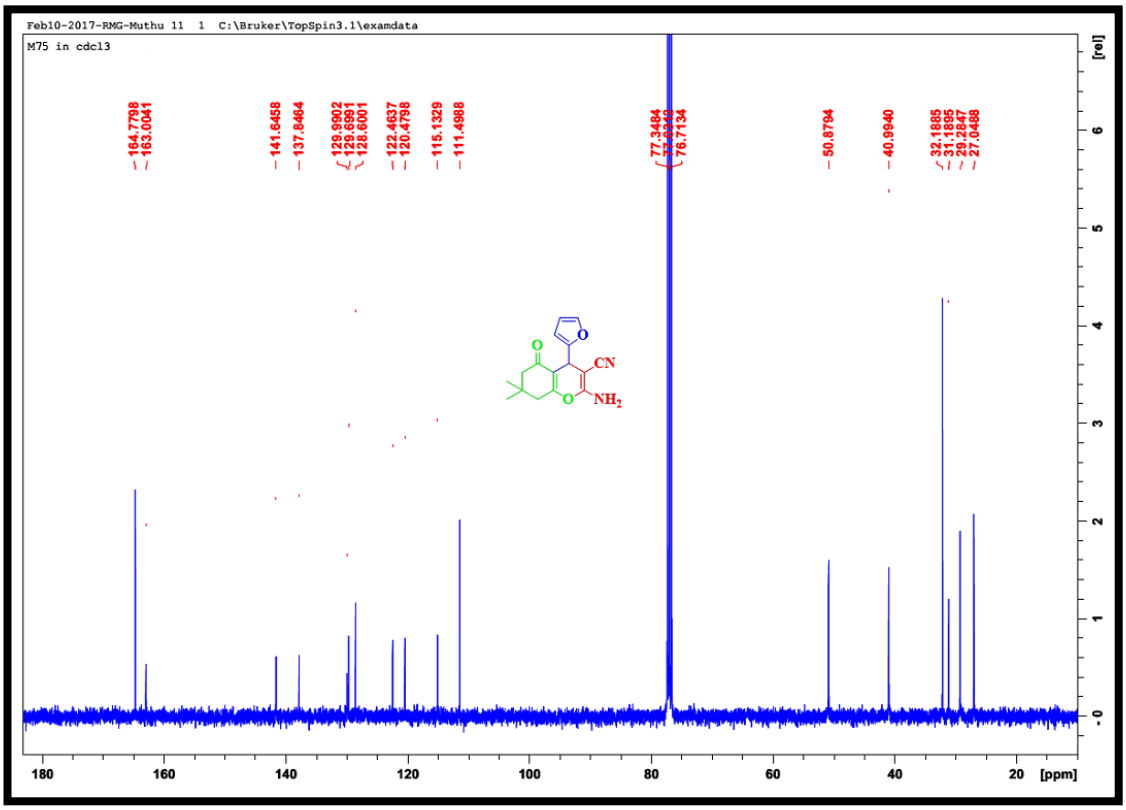

Fig. 7.33. ^{13}C-NMR spectrum for **28**

7.10. 2-Amino-6-methyl-4-phenyl-5-propionyl-*4H*-pyran-3-carbonitrile (29)

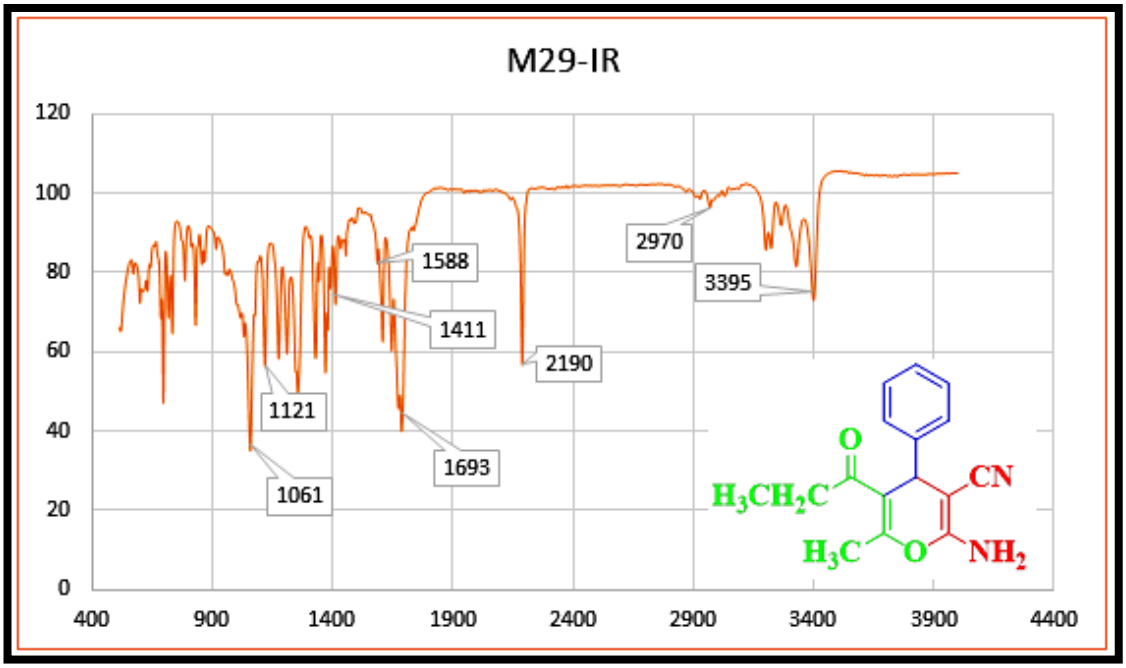

Fig. 7.34. IR spectrum of **29**

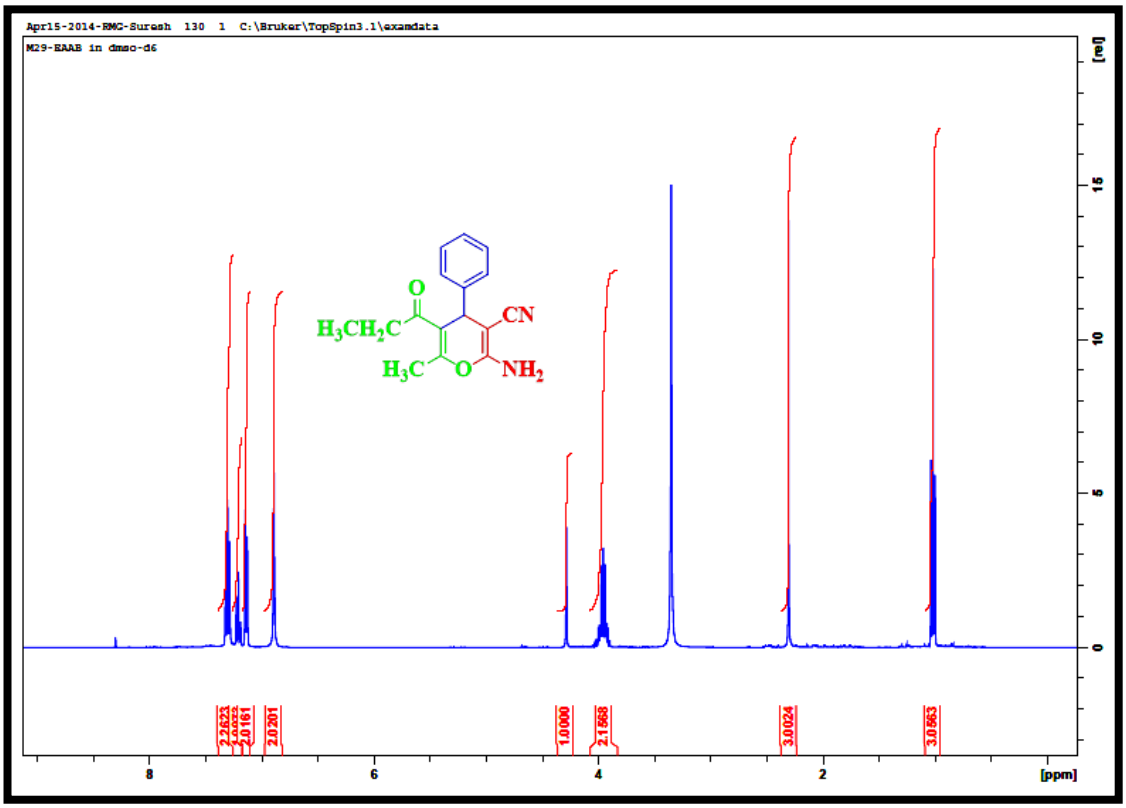

Fig. 7.35. ^{1}H-NMR spectrum for **29**

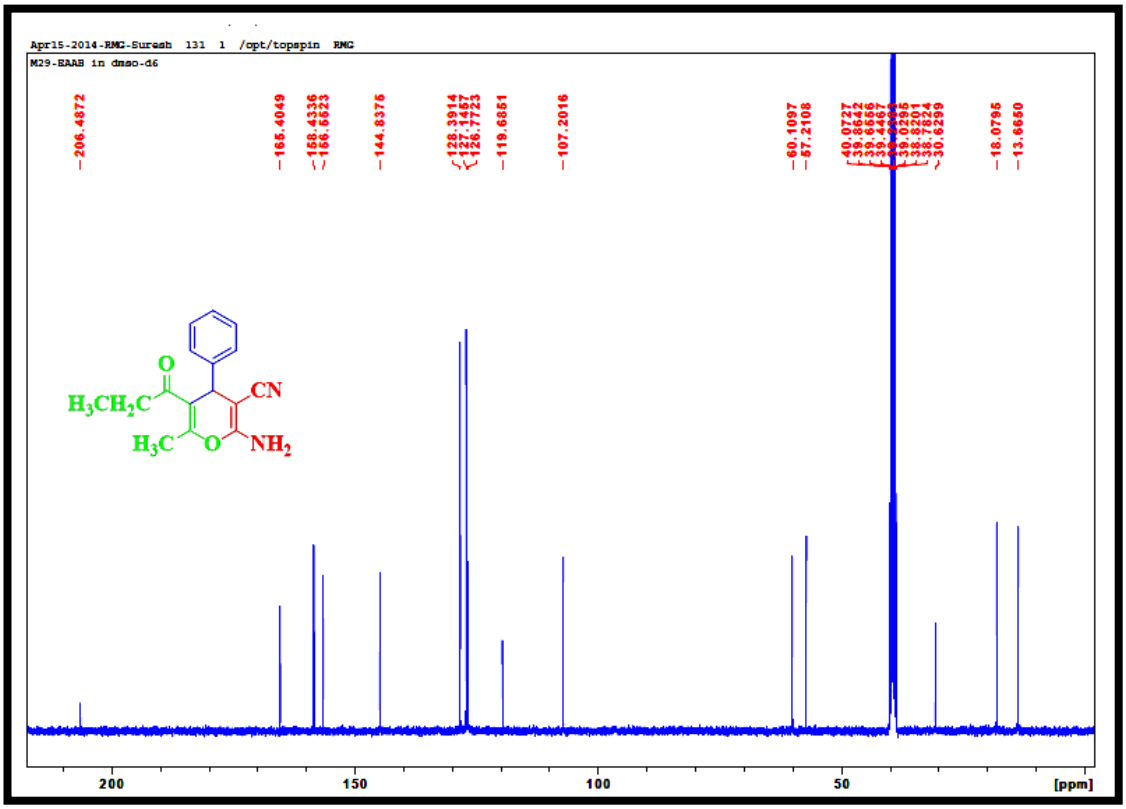

Fig. 7.36. ^{13}C-NMR spectrum for **29**

7.11. 2-Amino-6-methyl-4-(4-nitrophenyl)-5-propionyl-*4H*-pyran-3-carbonitrile (30)

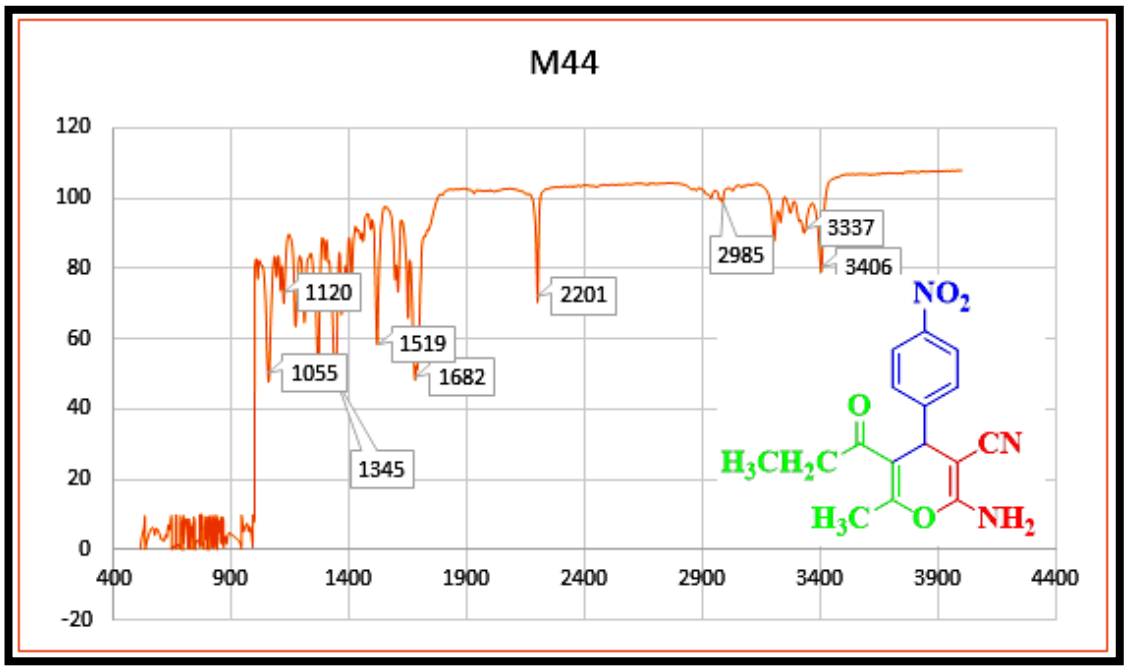

Fig. 7.37. IR spectrum of **30**

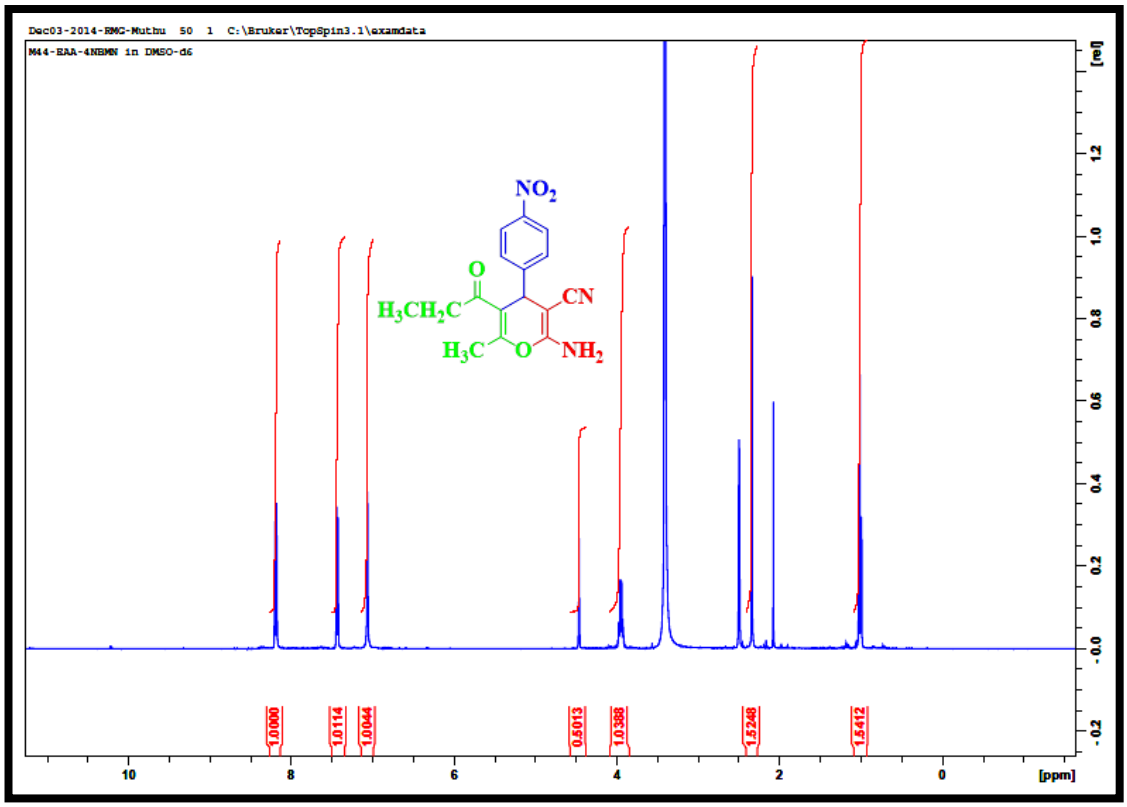

Fig. 7.38. ^{1}H-NMR spectrum for **30**

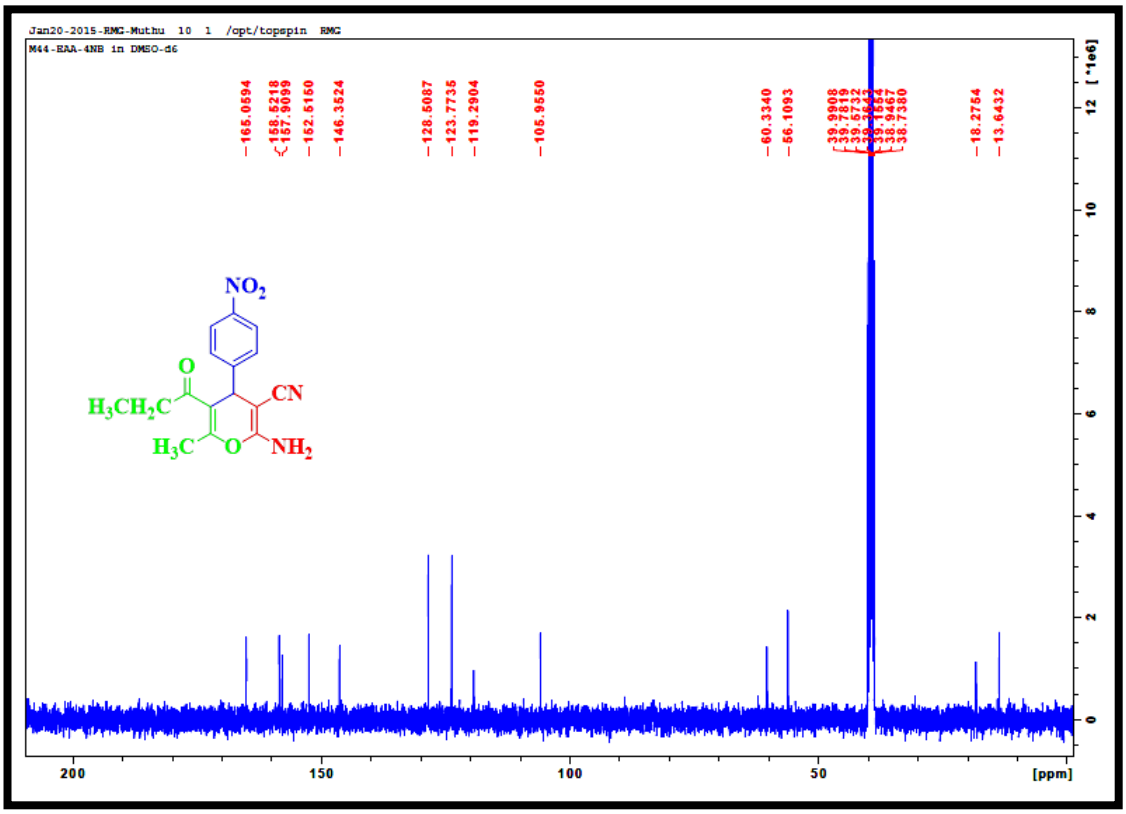

Fig. 7.39. ^{13}C-NMR spectrum for **30**

7.12. 2-Amino-4-(4-fluorophenyl)-6-methyl-5-propionyl-*4H*-pyran-3-carbonitrile (31)

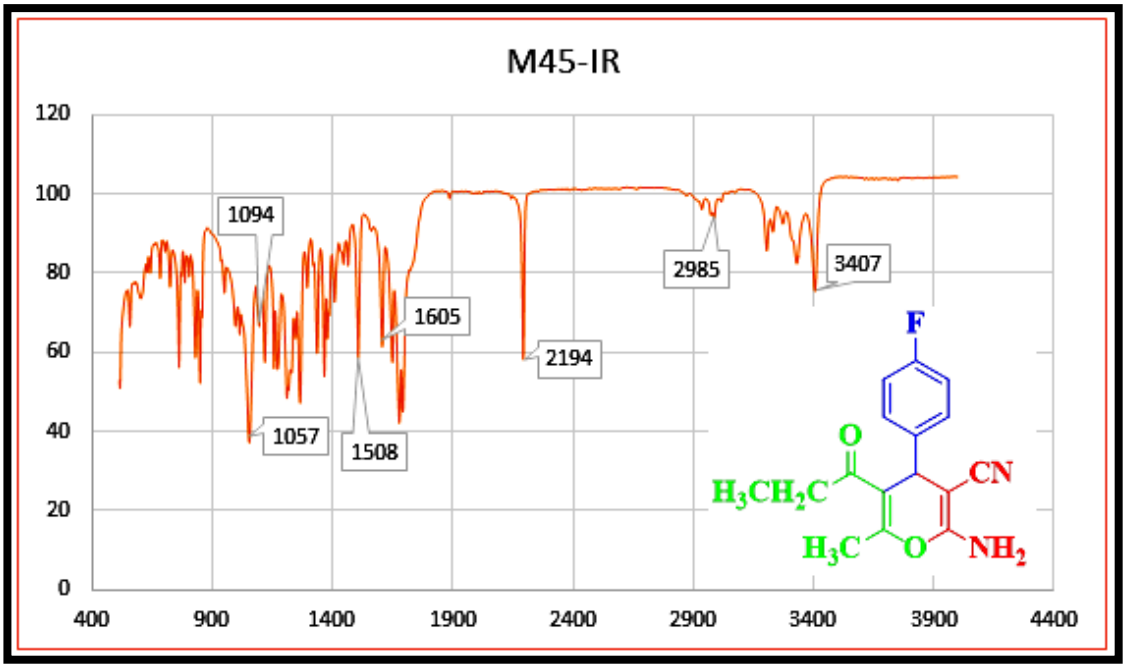

Fig. 7.40. IR spectrum of **31**

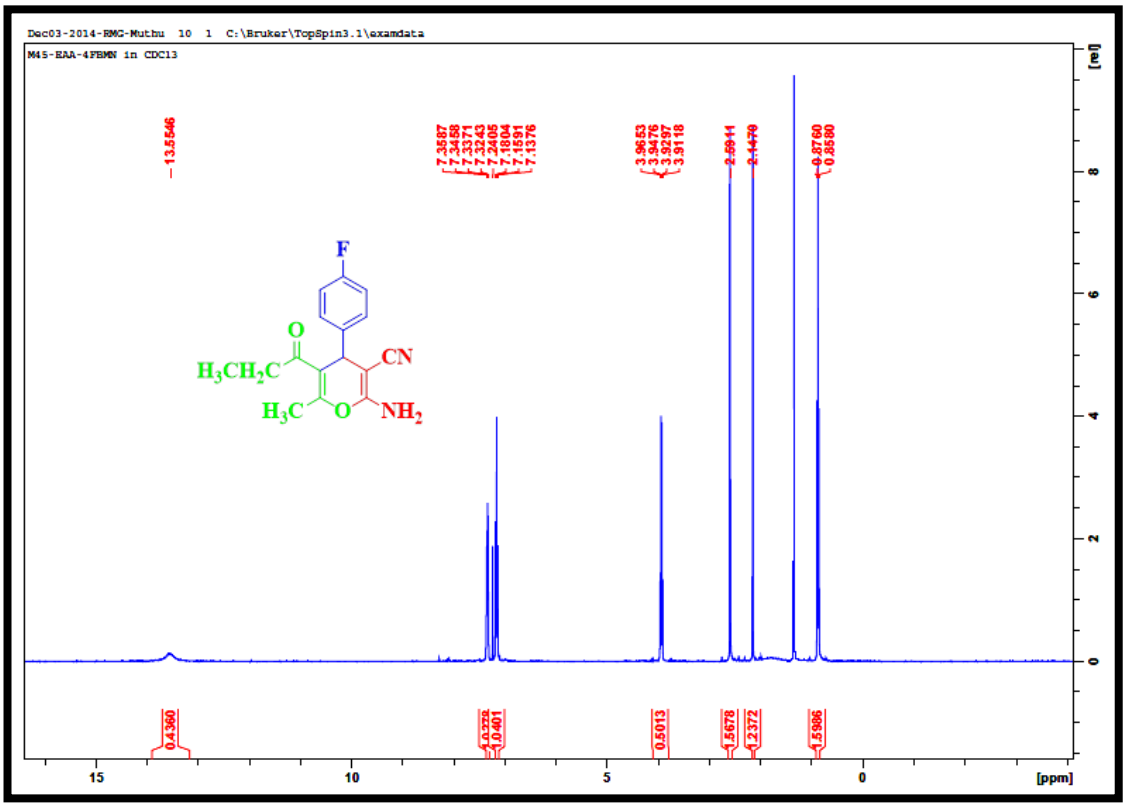

Fig. 7.41. ^{1}H-NMR spectrum for **31**

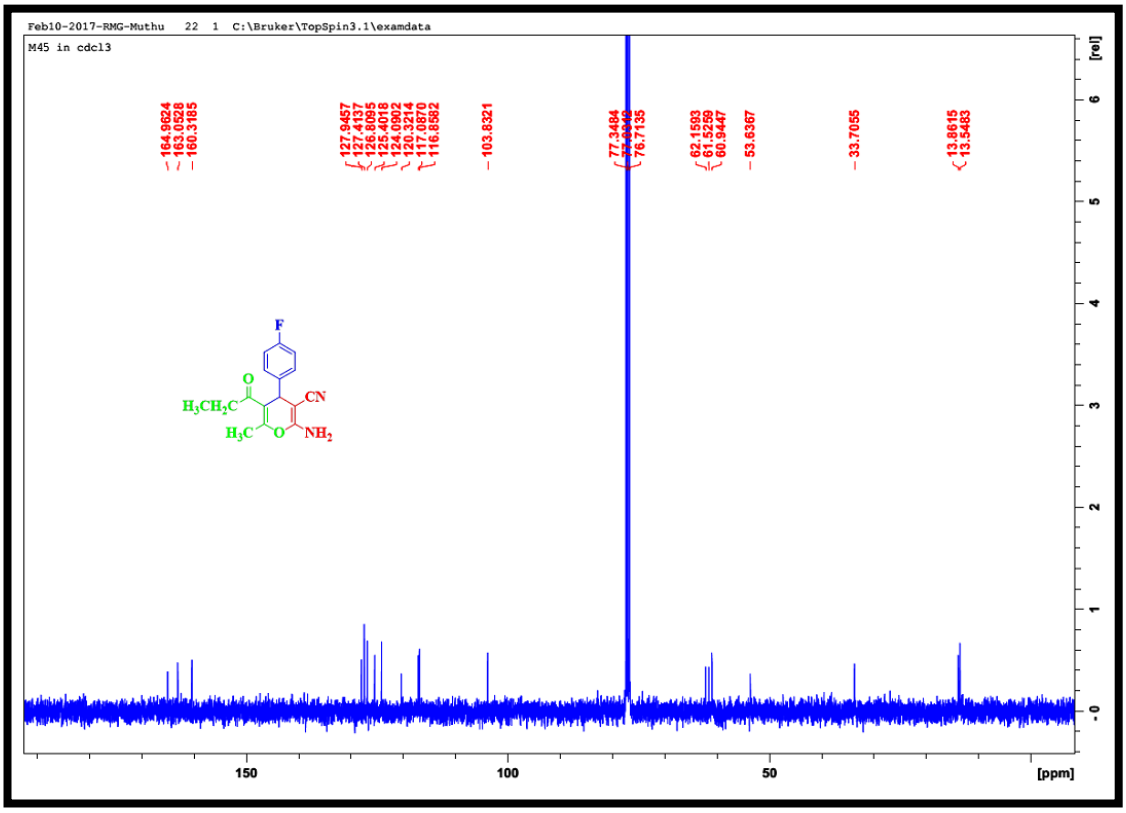

Fig. 7.42. ^{13}C-NMR spectrum for **31**

7.13. 2-Amino-6-methyl-4-(2-nitrophenyl)-5-propionyl-*4H*-pyran-3-carbonitrile (32)

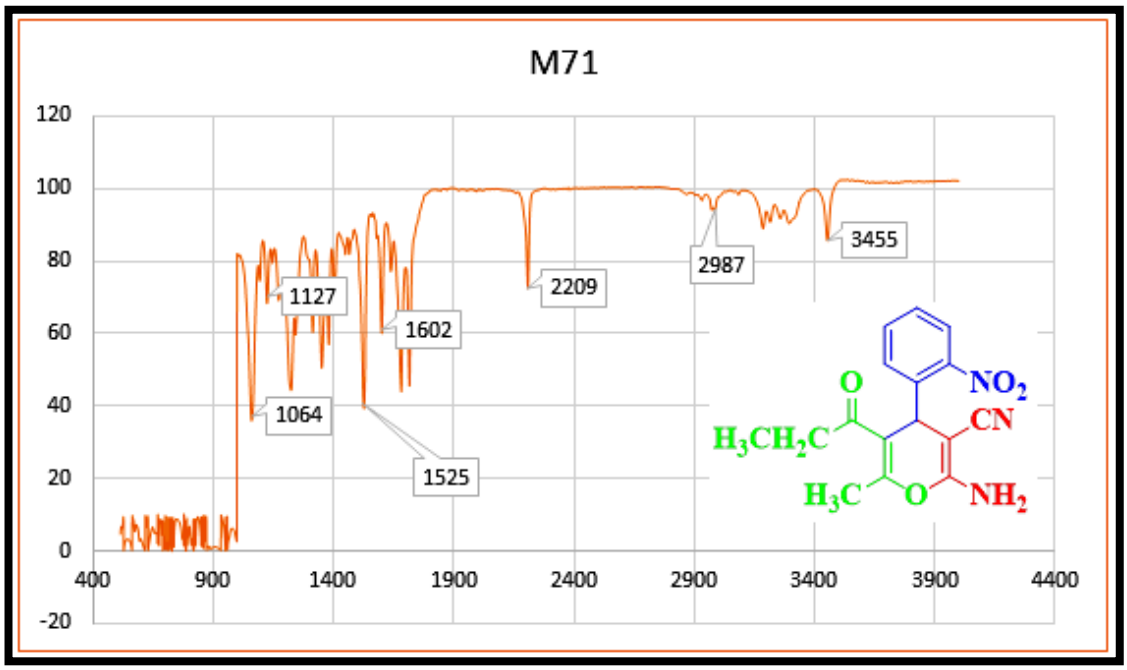

Fig. 7.43. IR spectrum of **32**

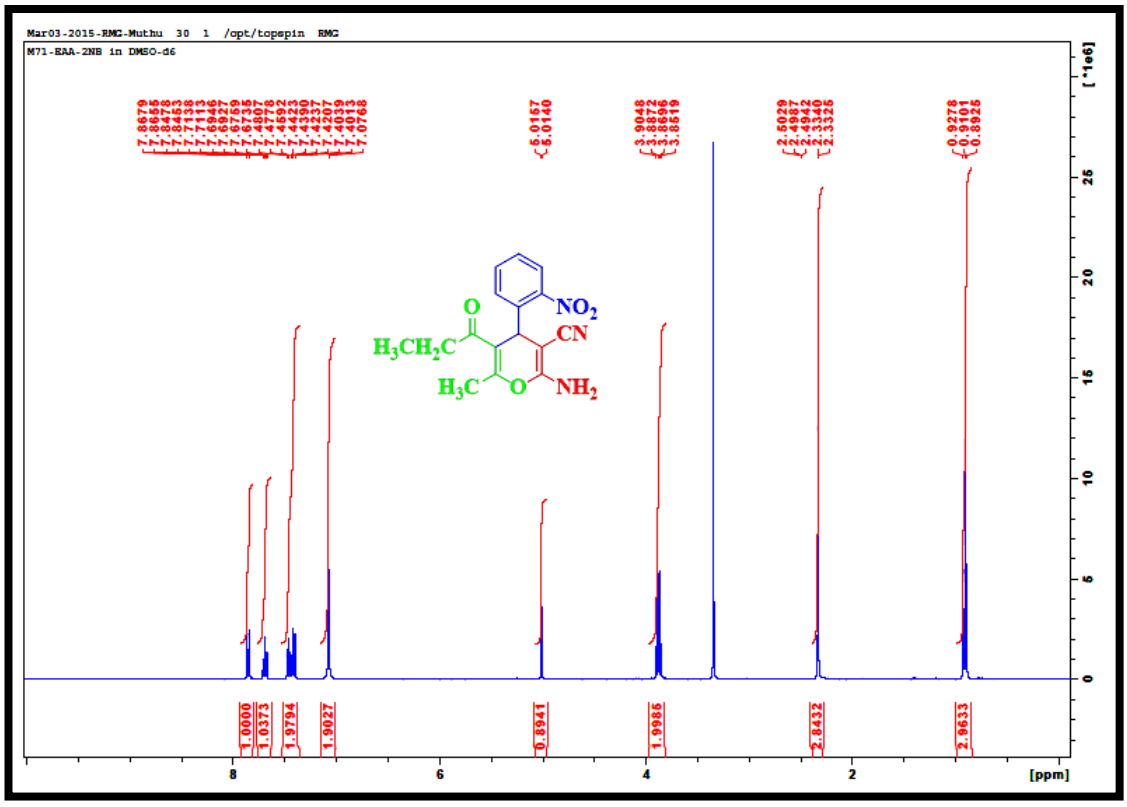

Fig. 7.44. ^{1}H-NMR spectrum for **32**

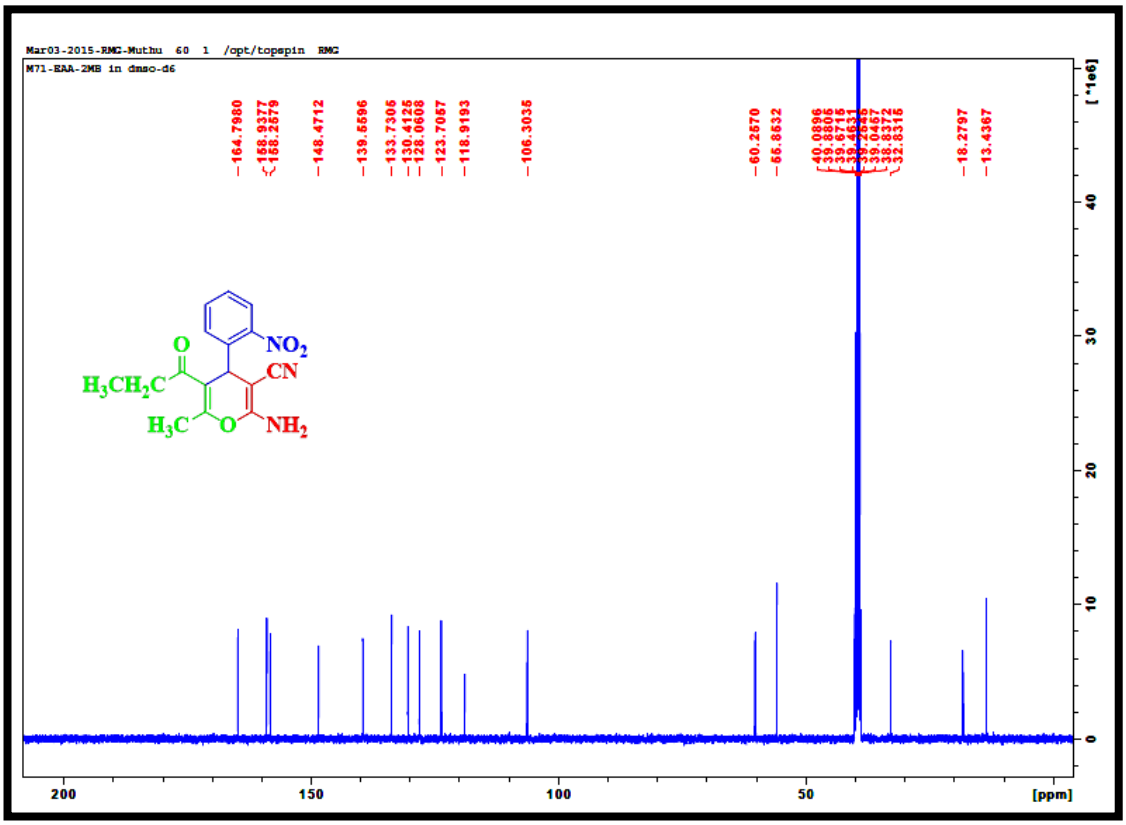

Fig. 7.45. ^{13}C-NMR spectrum for **32**

7.14. 2-Amino-6-methyl-5-propionyl-4-(p-tolyl)-*4H*-pyran-3-carbonitrile (33)

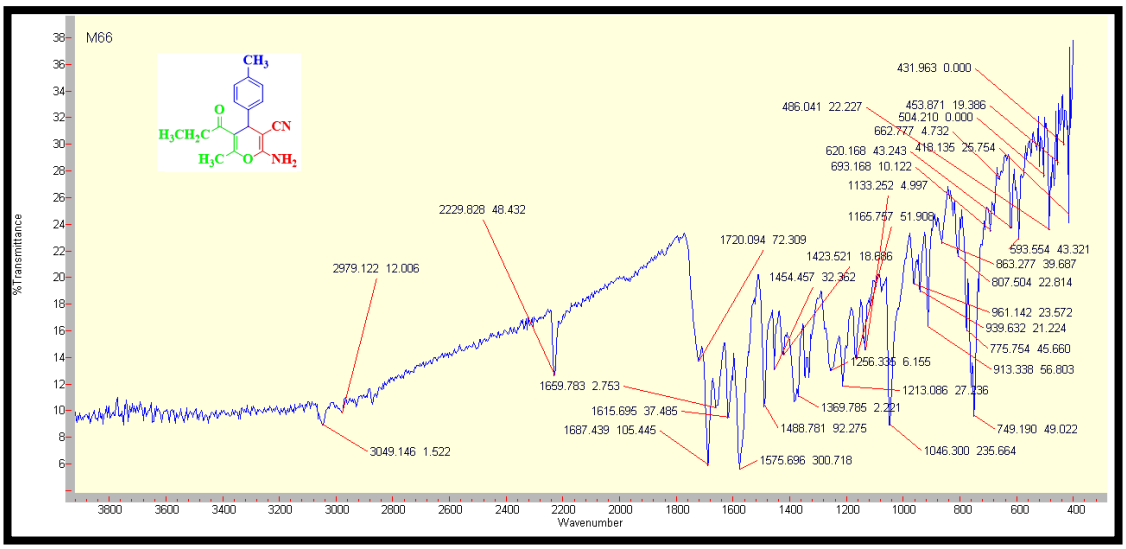

Fig. 7.46. IR spectrum of **33**

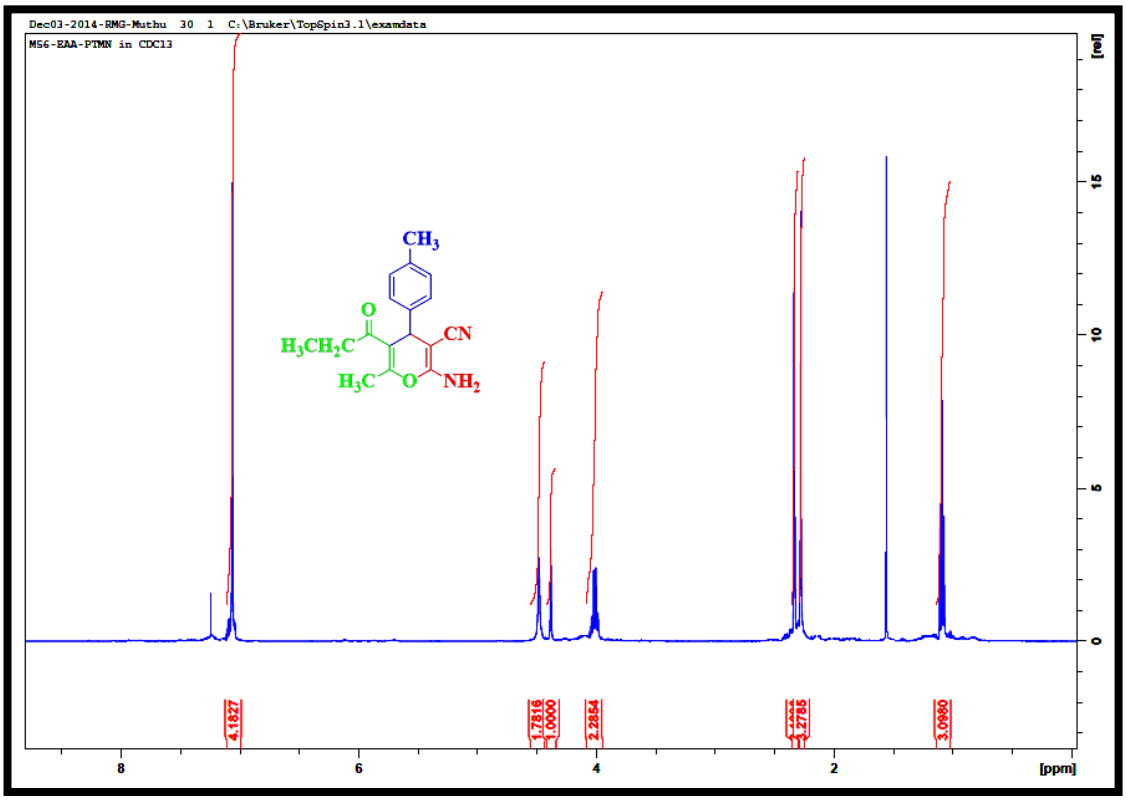

Fig. 7.47. ^{1}H-NMR spectrum for **33**

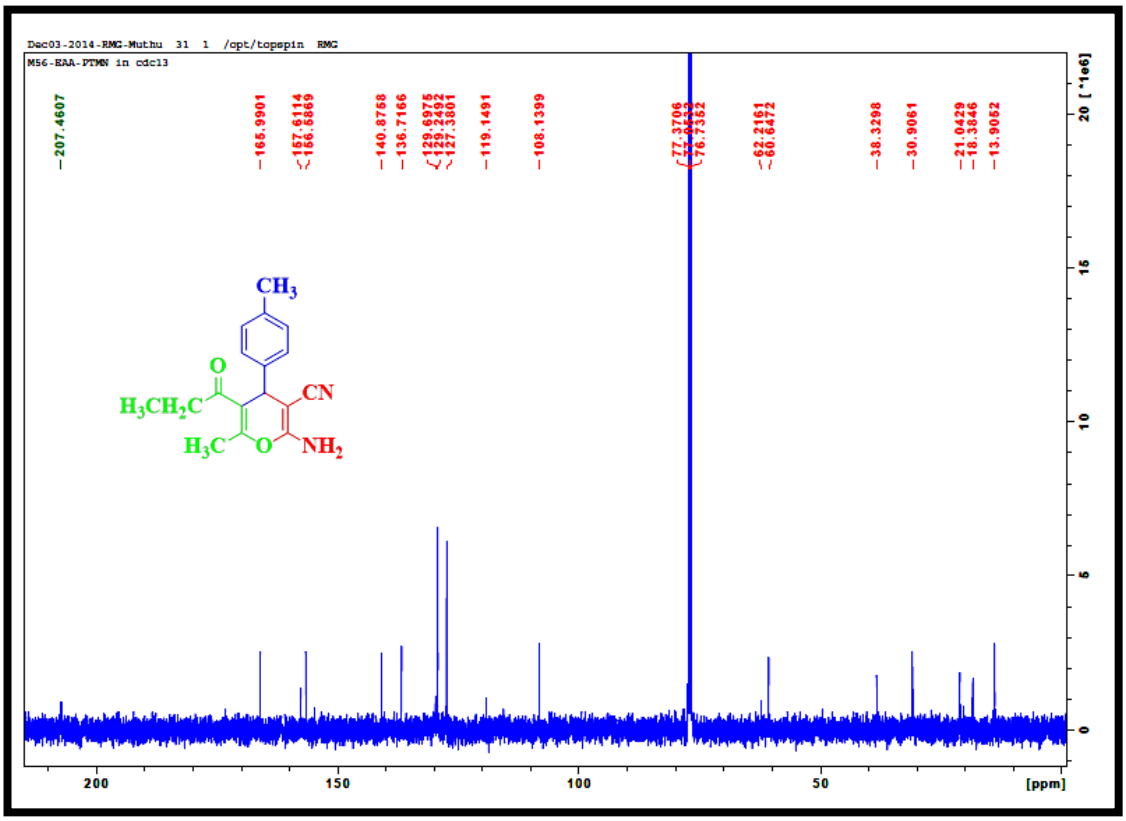

Fig. 7.48. ^{13}C-NMR spectrum for **33**

Conclusion and recommendation for future studies

An efficient synthesis of a library of biologically active oxygen, nitrogen and sulfur based heterocyclic scaffolds were successfully reported. A total of 71 small molecules were prepared by using multi-component reactions by using new catalysts.

- In chapter III, a total of new 14 quinoline and quinolone based peptides were synthesised by Ugi four-component reaction under the action of microwave irradiation. A total of eight peptides were subjected to antimicrobial, antioxidant and toxicity evaluation; compounds **41**, **43**, **46**, **47** showed positive results for antimicrobial activity and **41**, **46**, **47** showed positive results for antioxidant activity. Molecular docking studies of **41** and **43** showed a higher binding affinity (183.24 kcal/mol and 165.01 kcal/mol) towards DNA gyrase than ciprofloxacin based on Libdock score.
- In chapter IV, a total of 15 new quinoline, quinolone and indole based pyrans were synthesized by a three-component reaction under the action of microwave irradiation in the presence of a new catalyst: humic acid supported 1-butyl-3-methylimidazolium thiocyanate ionic liquid. All the compounds were subjected to antimicrobial, antioxidant and toxicity evaluation. Seven QPs (**31**, **34**, **37**, **38**, **42**, **43** and **44**) and one QOP (**40**) showed good potential against *B. cereus, S. aureus, E. coli* and *E. faecalis* whilst nine (**32**, **34**, **35**, **36**, **37**, **38**, **42**, **43** and **44**) QPs showed antioxidant activity. The brine shrimp test showed five QPs (**34**, **37**, **42**, **43** and **44**) with mortality rate less than 50 % up to 48 h. Molecular docking showed higher binding affinity of 96.96 kcal/mol for **42** based on Libdock score with Mtb DNA gyrase.
- In chapter V, a total of 14 new BTQP derivatives were synthesized in the presence of new catalyst: iron loaded boron nitride by using water as medium under microwave irradiation. A total of 10 BTQPs evaluated for antibacterial and antioxidant activities: compounds **24**, **25**, **27**, **28**, **29**, **31**, **32** and **36** showed positive results for antibacterial activity and **23**, **24**, **26**, **27**, **29** and **36** showed positive results for antioxidant potential, respectively. Among these compounds, **31** exhibited potential binding affinity with *Staphylococcus aureus* gyrase based on *in-silico* molecular docking studies.

- In chapter VI, a total of 14 novel BTQ-DHP derivatives were synthesized in the presence of new catalyst: iodine loaded boron nitride by using water as solvent under ultrasonic irradiation. A total of 10 BTQ-DHPs were subjected to antimicrobial, antioxidant, toxicity assessment and molecular docking studies. Among them, compounds **24**, **26**, **27**, **28**, **29**, **30** and **31** showed positive results for antibacterial activity and **22**, **24**, **28** and **31** showed positive results for antioxidant activity respectively. Compound **24** showed stronger potency toward *Staphylococcus aureus* gyrase on molecular docking studies.
- In chapter VII, a total of 14, 2-amino-*4H*-pyran-3-carbonitriles in the presence of calcium loaded boron nitride catalyst via a one-pot tandem Knoevenagel-cyclocondensation reaction were synthesized in ethanol. A total of five APCs were subjected to antibacterial studies against *S. aureus, E. coli* and *P. aeruginosa*. The MIC value for the synthesized 2-amino-*4H*-pyran-3-carbonitriles showed moderate to promising activity against the bacteria tested. Among them, compound **29** showed MIC values of 128, 16 and 4 µg/mL towards *E.coli*, *P. aeruginosa* and *S. aureus*.

All the synthesized molecules (QLPs, QOLP, QPs, QOPs, IP, BTQPs, BTQ-DHPs and APCs) were confirmed by FTIR, ^{1}H-NMR, ^{13}C-NMR and elemental analysis. Moreover, ^{19}F-NMR, ^{31}P-NMR and TOF-MS analysis were included for some selected compounds. The advantages of the synthetic methodology of this project are its green approach, easy work up, mild reaction conditions, the use of an inexpensive solvent, short reaction times with higher yields and recyclability of the catalyst.

Recommendation for future studies

Since all the synthesized new compounds showed good antibacterial and antioxidant activity and are also safe for biological studies, they could be further investigated for pharmaceutical applications. Peptides, pyrans, aminophosphonates and dihydropyridines are involved in a variety of physiological and pathological processes and play very important roles in modulating various cell functions. Also, O, N and S based heterocyclic drugs have been successfully applied in treating human diseases. By keeping this in mind, the synthesized new quinoline based O, N and S heterocycles with different functional groups will be studied with the following applications: NR8383 and ESAT-6 tuberculosis cell lines, secretory protein and potent T cell antigen for *M.tuberculosis*.

Also, the compounds will be investigated for breast cancer application and targeted with the following cell lines: MCF-7, MDA-MB-231, SKBr3 and T47D. A549 lung cancer cell lines will also be used to find the cytotoxicity of the synthesized compounds. Effective synthesized drugs are planned to do human lymphoblastic T cell lines, Sup T1, Jurkat and CEM and the human embryonic kidney (HEK) 293T. All the synthesized compounds aimed to screen twice with antibacterial, antifungal, antioxidant (DPPH), toxicity assessment (*Artemia larvae*) and molecular docking studies to continue their studies on cancer applications.

List of conferences attended

Presentation

International & National

"Efficient one-pot synthesis of 2-amino-*4H*-pyran-3-carbonitriles catalyzed by calcium-boron nitride frame works" at Second International conference on Composites, Biocomposites and Nanocomposites conducted by Composite Research Group, Department of mechanical Engineering, Durban University of Technology, Durban.

"Eco-friendly approach: graphene like boron nitride modified calcium material for the synthesis of 2-amino-*4H*-pyran-3-carbonitrile derivatives" at SACI national conference, Durban University of Technology, Durban.

"Calcium loaded boron nitride catalyst for the ultrasonicated synthesis of quinolinyl-lipoyl peptides", at Institutional Research day-2017, ICC, Durban.

Participation in conferences

Participated an international conference on "Current Trends in Chemistry", conducted by School of Chemical Sciences, Bharathiyar University sponsored by UGC XI plan, UGC, SAP, DRS –II, India.

Participated a national level workshop on "SPECTROSCOPY" held at School of Chemical Sciences, Bharathiyar University, India.

List of publications

[1] **Muthu, T.,** Anand, K., Sureshkumar, M., Gengan, R. M. 2016. Eco-friendly approach: graphene like boron nitride modified calcium material for the synthesis of 2-amino-*4H*-pyran-3-carbonitrile derivatives. Advanced Materials Letters, (7) 790-794.
DOI: 10.5185/amlett.2016.6850

[2] **Muthu, T.,** Gengan, R. M., Bibhuti, R., Ramesh, M. 2018. Synthesis, molecular docking, antimicrobial, antioxidant and toxicity assessment of quinoline peptides. Journal of Photochemistry & Photobiology, B: Biology, (178) 287-295.
https://doi.org/10.1016/j.jphotobiol.2017.11.019

[3] Sureshkumar, M., Anand, K., **Muthu, T.,** Gengan, R. M. 2016. Cobalt boron nitride: a novel heterogeneous catalyst for the synthesis of medicinally important α-amino quinoline phosphonates. Phosphorus, Sulfur, and Silicon and the Related Elements, (191) 1022-1029.
https://doi.org/10.1080/10426507.2015.1130046

[4] **Muthu, T.,** Gengan, R. M., Bibhuti, R., Ramesh, M. Microwave synthesis of quinolinyl, quinolonyl and indolyl pyrans by humic acid supported ionic liquid catalyst and their antimicrobial, antioxidant, toxicity assessment and molecular docking studies. Materials Chemistry and Physics. Manuscript number: MATCHEMPHYS-D-18-00067. (Under review)

[5] **Muthu, T.,** Gengan, R. M., Bibhuti, R., Ramesh, M. Microwave assisted synthesis of α-aminobenzylthioquinolinyl phosphonates by using Fe/BN and their antimicrobial, antioxidant, toxicity assessment and molecular docking studies. Journal of Photochemistry & Photobiology, B: Biology. Manuscript number: JPHOTOBIOL_2018_53. (Under review)

[6] **Muthu, T.,** Gengan, R. M., Bibhuti, R., Ramesh, M. Synthesis of benzylthio quinolinyl-1,4-dihydropyridines using I/BN and their antimicrobial, antioxidant, toxicity assessment and molecular docking studies. Journal of Molecular Structure. Manuscript number: MOLSTRUC-D-18-00652. (Under review)

[7] **Muthu, T.,** Ramesh, M., Madhan, V., Lin, C.H., Gengan, R. M. Synthesis and characterization of 6-methoxy-2-methyl-3-formyl quinoline carboxaldehyde and its crystal confirmation. (To be communicated).

Journal of Photochemistry & Photobiology, B: Biology 178 (2018) 287–295

Contents lists available at ScienceDirect

Journal of Photochemistry & Photobiology, B: Biology

journal homepage: www.elsevier.com/locate/jphotobiol

Synthesis, molecular docking, antimicrobial, antioxidant and toxicity assessment of quinoline peptides

Muthu Thangaraj[a], Robert Moonsamy Gengan[a,*], Bibhuti Ranjan[b], Ramesh Muthusamy[c]

[a] Department of Chemistry, Faculty of Applied Sciences, Durban University of Technology, Durban 4001, South Africa
[b] Department of Biotechnology & Food Technology, Faculty of Applied Sciences, Durban University of Technology, Durban 4001, South Africa
[c] Department of Medicinal/Pharmaceutical Chemistry, Akal College of Pharmacy & Technical Education, Mastuana Sahib, Sangrur 148001, Punjab, India

ARTICLE INFO

Keywords:
Quinoline
Ugi reaction
Peptides
Antimicrobial
Antioxidant
Libdock

ABSTRACT

A series of quinoline based peptides were synthesized by a one-pot reaction through Ugi-four component condensation of lipoic acid, cyclohexyl isocyanide, aniline derivatives and 2-methoxy quinoline-3-carbaldehyde derivatives under microwave irradiation. The products were obtained in excellent yields and high purity. Solvent optimization and the effect of microwave irradiation with various powers were also observed. All the synthesized compounds were characterized by FTIR, NMR spectral data and elemental analysis. A total of eight peptides were subjected to antimicrobial, antioxidant and toxicity evaluation. Among them, four peptides showed potential towards antibacterial screening with *Bacillus cereus*, *Staphylococcus aureus*, *Escherichia coli*, *Enterococcus faecalis* and *Candida albicans*, *Candida utilis* and three peptides showed antioxidant test positive (DPPH). Besides, toxicity of all the peptides were evaluated by using brine shrimp and it was observed that four peptides showed mortality rate less than 50% up to 48 h. Molecular docking studies revealed that the higher binding affinity of the two peptides toward DNA gyrase than ciprofloxacin based on Libdock score. The described chemistry represents a facile tool to synthesize complex heterocycles of pharmaceutical relevance in a highly efficient and one-pot fashion. The advantages of this method are its green approach, inexpensive solvent, shorter reaction times and excellent yields.

1. Introduction

Microbial infections are one of the leading diseases which are responsible for millions of deaths every year because of lack of effective antimicrobial therapy and this situation becomes more complicated because of microbial resistance towards conventional antibiotics [1]. Occurrence of the antibiotic resistance pathogen has become a severe health issue and thus, numerous studies have been stated to improve the current antimicrobial therapies. It is known that over 70% of bacterial infections are resistant to one or more of the antibiotics that are generally used to eradicate the infection [2]. Recently, bioactive peptides have received close scientific attention for their broad scope of bioactivities, mainly including antioxidation, antihypertensive, anticancer, and antimicrobial properties. Peptides open up new perspectives in drug design by providing an entire range of highly selective and nontoxic pharmaceuticals. With growing applications of their synthesis and bioactivity, considerable attention has been focused on the research of peptide-based derivatives [3].

One-pot multi-component reactions (MCRs) are simple and efficient synthetic routes for sustaining diverse heterocycles. These reactions are straight forward one-step transformations which offer significant advantages over conventional linear type synthesis due to its flexible, convergent and atom efficient nature [4]. Among multicomponent condensation reactions, the Ugi reaction [5] is a highly convergent for the rapid generation of organic druglike molecule libraries and many different types of biologically active targets [6]. The Ugi four component reaction (Ugi-4CR) in which an amine, an aldehyde or ketone, a carboxylic acid and an isocyanide combine to yield α-N-acylaminoamide [7] is particularly attractive because of the wide range of products obtainable through variation of the starting materials.

Quinoline is an important class of heterocyclic compounds found in many synthetic and natural products with a wide range of pharmacological activities such as anti-inflammatory [8], antimalarial [9], antimicrobial [10], anticonvulsant [11], antineoplastic [12], vasorelaxing [13], antiproliferative [14] and platelet derived growth factor receptor tyrosine kinase inhibiting agents [15] which can be well illustrated by the large number of drugs in the market. Ugi four-component derivatives have also been found to have various applications (viz., anesthetics, antibiotics, natural product isolation, HIV protease inhibitor crixivan, [16–18] etc.). Therefore, it is of significance to develop novel

* Corresponding author.
E-mail address: genganrm@dut.ac.za (R.M. Gengan).

https://doi.org/10.1016/j.jphotobiol.2017.11.019
Received 2 March 2017; Received in revised form 14 November 2017; Accepted 15 November 2017
Available online 16 November 2017
1011-1344/

Research Article Adv. Mater. Lett. 2016, **7**(10), 790-794 Advanced Materials *Letters*

www.vbripress.com/aml, DOI: 10.5185/amlett.2016.6850 Published online by the VBRI Press in 2016

Eco-friendly approach: Graphene like boron nitride modified calcium material for the synthesis of 2-amino-4H-pyran-3-carbonitrile derivatives

T. Muthu, K. Anand, M. Sureshkumar, R. M. Gengan*

Department of Chemistry, Faculty of Applied Sciences, Durban University of Technology, Durban 4001, South Africa

*Corresponding author. Tel: (+27) 31 3732309; Fax: (+27) 31 2022671; E-mail: genganrm@dut.ac.za

Received: 09 April 2016, Revised: 06 June 2016 and Accepted: 17 June 2016

ABSTRACT

An efficient one-pot multi-component synthesis of medicinally important 2-amino-4H-pyran-3-carbonitrile derivatives using a new heterogeneous calcium loaded boron nitride (CaBNT) catalyst is described herein. This transformation transpires by Knoevenagel condensation, Michael addition and intramolecular cyclization. Alkaline earth metal-based green catalyst was successfully prepared and characterized by XRD, SEM with EDX, Raman spectroscopy, BET, DSC-TGA and FT-IR. The reaction works up is facile and CaBNT catalyst can easily be separated from the reaction mixture and re-used more than five times in subsequent reactions. This methodology offers several advantages such as excellent yields, use of inexpensive solvent and relatively shorter reaction time. Copyright © 2016 VBRI Press.

Keywords: Heterogeneous catalyst; calcium; boron nitride; multi-component synthesis.

Introduction

One-pot multi-component reactions (MCRs) are simple and efficient synthetic routes for sustaining diverse heterocycles. These reactions are a straight forward one-step transformation which offers significant advantages over conventional linear type synthesis due to its flexible, convergent and atom efficient nature. Thus, the development of multi-component reactions has attracted considerable attention from the view of ideal synthesis by virtue of their efficiency, facile implementation and generally high yield of the products. These reactions are designed to produce elaborate biologically active compounds hence are an important area of research in organic, combinatorial and medicinal chemistry.

The known multi-component procedures for the synthesis of 2-amino-4H-pyran-3-carbonitriles employ a three-component condensation of cyclic 1,3-diketones, aldehydes and malononitrile and is performed under a variety of reaction conditions. Catalysts such as piperidine/ammonium acetate [**1**], triethylamine [**2**] are reported and the yields are in the range of 70-85 %. Alkyl ammonium salts in water [**3**], (S)-proline in aqueous media [**4**] afford the corresponding carbonitriles in higher yields (75-95 %), however they suffer from long reaction times up to 10 hours. As a consequence, reagents such as benzyltriethylammonium chloride (TEBA) [**5**], NaBr [**6**], microwave irradiation [**7**] and amino functioned ionic liquid [**8**] are reported to catalyze these reactions including ammonium chloride [**9**], ethylenediamine diacetate [**10**], surfactant metal carboxylates [**11**] and b-cyclodextrin [**12**]. However, some of the reporting procedures have drawbacks such as tedious work-up, use of expensive reagents, long reaction times and low yields of products.

Insulating oxides such as SiO_2, Al_2O_3, silica-alumina and various zeolites are the materials commonly used as catalyst supports [**13**]. These oxides possess low thermal conductivity, generating sintering of the assisted metal on hot spots, various acidic and basic sites and the coverage of the catalyst with water at low temperature due to its hydrophilic surface. Various two-dimensional (2D) nanomaterials have received considerable developments for heterogeneous catalysis. Among them, boron nitride has attracted more attention because of its high elastic modulus, high melting-point, excellent thermal conductivity and a large and direct band gap. Such properties can be of high value for ultraviolet-light emitters, advanced ceramic composites, electrical insulators, solid lubricants and ideal substrates [**14**] so we have fixed boron nitride (BNT) as catalyst support. The graphene like hexagonal boron nitride [**15**] is a most stable isomer. A giant planar network of hexagonal boron nitride has an acid-base resistance, good thermal and electrical conductivity and chemically very inert. Moreover, BNT is hydrophobic, hence preventing moisture condensation on its surface. Activated BNT exhibits an excellent adsorption performance for various metal ions such as Cr^{3+}, Co^{2+}, Ni^{2+}, Ce^{3+}, Pb^{2+} and organic pollutants (tetracycline, methyl orange and congo red) in water, as well as volatile organic compounds (benzene) in air [**16**].

Herein we report the synthesis and characterization of a new calcium loaded boron nitride catalyst which is subsequently used for a one-pot three component synthesis of 2-amino-4H-pyran-3-carbonitrile derivatives.

PHOSPHORUS, SULFUR, AND SILICON
2016, VOL. 191, NO. 7, 1022–1029
http://dx.doi.org/10.1080/10426507.2015.1130046

Taylor & Francis
Taylor & Francis Group

Cobalt boron nitride: A novel heterogeneous catalyst for the synthesis of medicinally important α-amino quinoline phosphonates

M. Sureshkumar, K. Anand, T. Muthu, and R. M. Gengan

Department of Chemistry, Durban University of Technology, Durban, South Africa

ABSTRACT

A novel cobalt supported on boron nitride (CoBNT) heterogeneous catalyst for the synthesis of α-amino quinoline phosphonates (AQPs) is reported in the present work. The CoBNT was synthesised by simply mixing boron nitride in a solution of cobalt acetate, under an inert atmosphere for 7 d followed by filtration; the yield was 94%. It exhibited excellent catalytic properties for the synthesis of 16 novel AQPs in a one pot mixture containing 2-methoxy 3-formyl quinoline, aniline derivatives and diethyl phosphite. Reactions were rapid, products were easily worked-up and were obtained in more than 90% yield. The CoBNT also exhibited higher catalytic activity than conventional catalysts and was re-used five times without significant decrease in catalytic activity.

ARTICLE HISTORY
Received 17 August 2015
Accepted 6 December 2015

KEYWORDS
2-Methoxy 3-formyl quinoline; diethyl phosphite; boron nitride; cobalt; heterogeneous catalyst

GRAPHICAL ABSTRACT

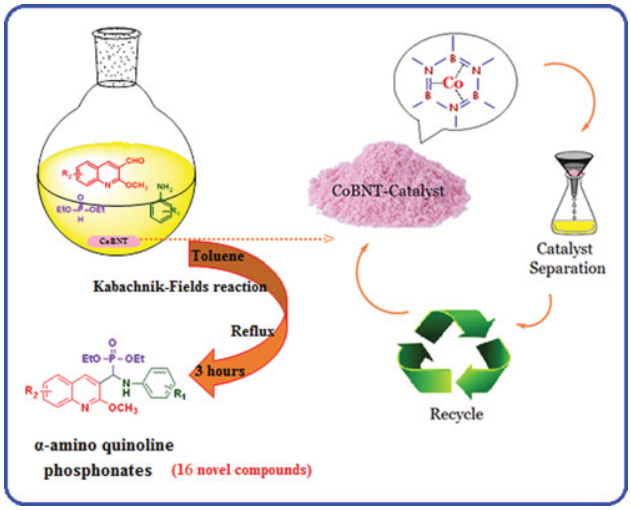

1. Introduction

Over the next few decades, the synthesis of more effective drugs will increase all over the world owing to the outbreak of new diseases and illnesses. Therefore, more efforts are expected by the scientific community to address this dilemma by designing, synthesizing, and assessing new drugs for their biological potency. In particular, the synthesis of α-amino phosphonates (APS) has attracted significant interest in recent years because they exhibit useful biological activities such as the mimicking of peptides,[1,2] and acting as enzyme inhibitors,[3] antibiotics,[4] pharmacological,[5] and anticancer agents.[6,7]

Although several methods are reported for the synthesis of α-amino phosphonates,[8] the Kabachnik–Fields (KF) and Pudovik reactions are commonly used. In the KF reaction, a carbonyl substrate and an amine are reacted with dialkyl or trialkyl phosphites in the presence of a catalyst (Scheme 1). Various catalysts are reported such as Bronsted–Lewis acids and heterogeneous catalysts such as $SnCl_4$,[9] $ZnCl_2$,[10] scandium tris (dodecyl sulfate),[11] samarium diiodide,[12] bismuth nitrate pentahydrate,[13] bmim BF_4,[14] lithium perchlorate,[15] montmorillonite KSF,[16] and $ZrCl_4$.[17] These protocols however suffer from drawbacks such as long reaction time, low yield of the products, and formation of large amount of waste, while some catalysts are expensive,[18–20] require relatively high amounts and display limited reusability. Hence, our aim was to synthesize novel α-amino quinoline phosphonates (AQPs) but with the aid of an alternative novel heterogeneous catalysts. Also, we decided to

CONTACT R. M. Gengan genganrm@dut.ac.za Department of Chemistry, Durban University of Technology, PO Box 1334, Durban, South Africa.
Color versions of one or more of the figures in the article can be found online at www.tandfonline.com/gpss.
Supplemental data for this article can be accessed on the publisher's website at http://dx.doi.org/10.1080/10426507.2015.1130046